Characterization of Vadose Zone Sediments Below the TX Tank Farm: Boreholes C3830, C3831, C3832 and RCRA Borehole 299-W10-27

RJ Serne
BN Bjornstad
DG Horton
DC Lanigan
CW Lindenmeier

MJ Lindberg
RE Clayton
VL LeGore
RD Orr
IV Kutnyakov

SR Baum
KN Geiszler
MM Valenta
TS Vickerman

September 2008

Pacific Northwest
NATIONAL LABORATORY

DISCLAIMER

This report was prepared as an account of work sponsored by an agency of the United States Government. Neither the United States Government nor any agency thereof, nor Battelle Memorial Institute, nor any of their employees, makes **any warranty, express or implied, or assumes any legal liability or responsibility for the accuracy, completeness, or usefulness of any information, apparatus, product, or process disclosed, or represents that its use would not infringe privately owned rights**. Reference herein to any specific commercial product, process, or service by trade name, trademark, manufacturer, or otherwise does not necessarily constitute or imply its endorsement, recommendation, or favoring by the United States Government or any agency thereof, or Battelle Memorial Institute. The views and opinions of authors expressed herein do not necessarily state or reflect those of the United States Government or any agency thereof.

Characterization of Vadose Zone Sediments Below the TX Tank Farm: Boreholes C3830, C3831, and C3832 and RCRA Borehole 299-W10-27

R. J. Serne	M. J. Lindberg	S. R. Baum
B. N. Bjornstad	R. E. Clayton	K. N. Geiszler
D.G. Horton	V. L. LeGore	M. M. Valenta
D. C. Lanigan	R. D. Orr	T. S. Vickerman
C. W. Lindenmeier	I. V. Kutnyakov	

September 2008

Pacific Northwest National Laboratory
Richland, Washington 99352

Executive Summary

This report was revised in September 2008 to remove acid-extractable sodium data from Tables 4.8, 4.28, 4.43, and 4.59. The sodium data was removed due to potential contamination introduced during the acid extraction process. The rest of the text remains unchanged from the original report issued in April 2004.

The overall goal of the Tank Farm Vadose Zone Project, led by CH2M HILL Hanford Group, Inc., is to define risks from past and future single-shell tank farm activities at Hanford. To meet this goal, CH2M HILL Hanford Group, Inc. tasked scientists from Pacific Northwest National Laboratory to perform detailed analyses on vadose zone sediments from within Waste Management Area (WMA) T-TX-TY. This report is the first of two reports written to present the results of these analyses. Specifically, this report contains all the geologic, geochemical, and selected physical characterization data collected on vadose zone sediment recovered from boreholes C3830, C3831, and C3832 in the TX Tank Farm, and from borehole 299-W-10-27 installed northeast of the TY Tank Farm.

Sediments from borehole 299-W-10-27 were considered to be background uncontaminated sediments against which to compare contaminated sediments for the TX characterization effort. This report also presents our interpretation of the data in the context of sediment types, the vertical extent of contamination, the migration potential of the contaminants, and the likely source of the contamination in the vadose zone and groundwater below the TX Tank Farm. The information presented in this report supports the T-TX-TY Waste Management Area field investigation report[a] in preparation by CH2M HILL Hanford Group, Inc.

Sediment samples from the boreholes were analyzed and characterized in the laboratory for the following parameters: moisture content, gamma-emitting radionuclides, one-to-one water extracts (which provide soil pH, electrical conductivity, cation, trace metal, and anion data), total carbon and inorganic carbon content, and 8 M nitric acid extracts (which provide a measure of the total leachable sediment content of contaminants). Two key radiocontaminants, technetium-99 and uranium-238, along with other trace metals were determined in acid and water extracts by inductively coupled plasma mass spectrometry.

Overall, our analyses showed that common ion exchange is a key mechanism that influences the distribution of contaminants within that portion of the vadose zone affected by tank liquor. Past characterization at WMA B-BX-BY did not show significant indications of caustic alteration of the sediment mineralogy or porosity, but did show slightly elevated pH values between the depths of 79 and 141 feet (ft) below ground surface (bgs). At WMA S-SX, some indication of mineral alteration was found directly below tank SX-108, and elevated pH zones were found in the vadose zone sediments at two boreholes near SX-108 and SX-109 tanks. Unlike the vadose zone sediments at the SX and BX Tank Farms, we did not observe significant indications of caustic alteration of the sediment mineralogy or porosity, or significant zones of elevated pH values in samples from the three boreholes (C3830, C3831, and C3832) at WMA T-TX-TY.

Sediments from the three TX tank farm boreholes show that sodium-, nitrate-, and sulfate-dominated fluids are present below tanks TX-104, TX-105, and TX-107 and have formed three salt plumes. The fluids are more dilute than tank fluids observed below tanks at the SX and BX Tank Farms. Most of the chemical data for contaminants intercepted by boreholes C3831 and C3832 suggest that fluid leaked from Tank TX-107 and may have percolated deeper into the sediments and traveled southwest to C3832.

(a)   *Field Investigation Report for Waste Management Areas T and TX-TY,* by FJ Anderson (CH2M HILL Hanford Group, Inc., Richland, Washington), under preparation.

However, more uranium is present in the sediments and water extracts at C3832. This confounds the hypothesis that TX-107 is the sole source of fluids that were intercepted by both boreholes. Therefore, we hypothesize that a small-volume leak with elevated uranium also occurred from TX-104. Borehole C3830 suggests another small-volume leak occurred from TX-105.

The conceptual model of the geology between core samples is based on our interpretation of the geophysical log and blow-count data. Three primary stratigraphic units were encountered in each of the three boreholes: 1) backfill material, 2) the Hanford formation, and 3) the Cold Creek unit. At C3830, we infer that there are four thin fine-grained layers in the Hanford formation H2 stratigraphic unit. At C3831, we infer that there are at least eight fine-grained layers in the H2 unit. Also at C3831, a clastic dike was observed within the Hanford formation H2 unit at about 60 ft bgs. Contamination at this borehole starts at the depth where the clastic dike was intercepted, suggesting that the dike may represent a preferred pathway for fluids that leaked from Tank TX-107. There are at least eight thin, fine-grained interbeds in the Hanford formation H2 unit at C3832. These thin fine-grained lenses within sands of the Hanford formation H2 unit may impact the flow of leaked fluids and affect irregular and horizontal flow.

The boreholes could not penetrate below the calcium-carbonate-rich strata of the Cold Creek lower subunit (CCU_l) (refusal was met at about 115 ft bgs at all three holes); therefore, we did not identify the maximum vertical penetration of the tank-related plumes. However, the more elevated portions of the electrical conductivity (EC) profile at C3830 currently reside at the bottom of a fine-grained thin lens in the Hanford formation H2 unit at 87 ft bgs. At C3831, we lack good sample coverage in the fine-grained CCU_u subunit and the caliche unit to ascertain whether the salt plume has significantly descended into the Cold Creek unit sediments. There is strong indication that at C3832 the saline plume has descended into the Cold Creek unit to the bottom of the borehole. The EC, nitrate, and technetium-99 profiles versus depth do not identify the leading edge of the plume with any certainty. The profiles do collectively suggest that the deepest penetration of tank-related fluids is found in C3832 and that the plume has reached the caliche material in the Cold Creek lower subunit at least to a depth of 116 ft bgs.

Despite the evidence that elevated EC values may be present in all three boreholes to their depth of refusal, the concentrations are not large. For example, the maximum dilution-corrected EC at C3832 is 6.27 milliSieverts per centimeter (mS/cm). At C3830, the maximum is 12.5 mS/cm, and at C3831 the maximum is 43.3 mS/cm. The leaks near the SX108-109 and BX-102 tanks had peak vadose zone porewater concentrations that were much more concentrated waste fluids: 524 to 1774 and 77 mS/cm, respectively.

The water potential data from 299-W10-27's Hanford formation H2 unit, the unit where most of the contaminants reside in the TX boreholes, are consistent with a draining profile. The inventories as a function of depth of potential contaminants of concern (nitrate, technetium-99, uranium, and chromium) are provided. In addition, in situ desorption K_d (distribution coefficient or sorption partition coefficient) values for these potential contaminants are provided based on the difference between acid and water extracts of the contaminated sediments. For conservative modeling purposes, we recommend using K_d values of 0 milliliters/gram (mL/g) for nitrate and technetium-99, a value of 1 mL/g for uranium, and 10 mL/g for chromium to represent the entire vadose zone profile from the bottoms of the tanks to the water table. These conservative K_d values, along with the provided inventories in the vadose zone sediments obtained from the three boreholes, can be used in long-term risk projections that rely on estimates of water recharge and vadose zone and aquifer transport calculations.

In summary, there is no current similarity between the present or past groundwater contamination and current porewater compositions from the contaminated borehole sediments. Therefore, we cannot link the contaminants in the groundwater, currently or during the era of contaminant introduction into the vadose zone, to the porewaters currently in the borehole sediments, which are known to be derived from liquids that leaked from tank TX-107. Thus, we cannot identify the TX tank leaks as the sole source of the contamination present in the groundwater in the past or currently.

Acknowledgments

Acronyms and Abbreviations

ASA — American Society of Agronomy
ASTM — American Society for Testing and Materials
bgs — below ground surface
CCU_u — Cold Creek unit, upper subunit
CCU_l — Cold Creek unit, lower subunit; also referred to as Cold Creek caliche subunit
EC — electrical conductivity
EPA — United States Environmental Protection Agency
FIR — Field Investigation Report
g — gram
GEA — gamma energy analysis
GPS — global positioning system
H1 — Hanford formation – H1 unit
H2 — Hanford formation – H2 unit
HPGe — High-Purity Germanium
IC — ion chromatography
ICP — inductively coupled plasma (also called inductively coupled plasma – optical emission spectroscopy
ICP-MS — inductively coupled plasma mass spectrometer
ICP-OES — inductively coupled plasma – optical emission spectroscopy
K_d — distribution coefficient, or sorption partition coefficient, in units of mL/g
KUT — potassium, uranium, and thorium
MPa — megapascal
mS — millisiemen
MSL — mean sea level
PNNL — Pacific Northwest National Laboratory
QA — quality assurance
QC — quality control
RCRA — *Resource Conservation and Recovery Act*
REDOX — Reduction Oxidation Process (the second fuel reprocessing process used at the Hanford Site to extract plutonium)
R_{tf} — Ringold Formation – Member of Taylor Flat
R_{wi} — Ringold Formation – Member of Wooded Island
SEM — scanning electron microscope
TEM — transmission electron microscopy
UFA — unsaturated flow apparatus (ultracentrifuge for squeezing porewater out of sediment)
UV — ultraviolet
WMA — Waste Management Area
wt% — weight percent
XRD — X-ray diffraction
XRF — X-ray fluorescence (a technique to measure total element mass in solids)

Contents

Figures

Tables

1.0 Introduction

The overall goals of the of the Tank Farm Vadose Zone Project, led by CH2M HILL Hanford Group, Inc., are 1) to define risks from past and future single-shell tank farm activities, 2) to identify and evaluate the efficacy of interim measures, and 3) to aid, via collection of geotechnical information and data, the future decisions that must be made by the Department of Energy (DOE) regarding the near-term operations, future waste retrieval, and final closure activities for the single-shell tank Waste Management Areas (WMA). For a more complete discussion of the goals of the Tank Farm Vadose Zone Project, see the overall work plan, Phase 1 RCRA Facility Investigation/Corrective Measures Study Work Plan for the Single-Shell Tank Waste Management Areas (DOE 1999). Specific details on the rationale for activities performed at WMA T-TX-TY are found in Crumpler (2002). To meet these goals, CH2M HILL Hanford Group, Inc. tasked scientists from Pacific Northwest National Laboratory (PNNL) to perform detailed analyses of vadose zone sediment, both uncontaminated and contaminated, in the vicinity of WMA T-TX-TY.

Specifically, this report contains all the geologic, geochemical, and selected physical characterization data collected on vadose zone sediment recovered from two sources: 1) a new RCRA monitoring well, 299-W10-27, located just outside the WMA fenceline to the east and in the northern quadrant of tank TY tank farm, and 2) three boreholes that extended from ground surface down to refusal in the Cold Creek unit caliche. Drill locations for the boreholes were selected to evaluate possible leaks from tanks 241-TX-105 (C3830), TX-107 (C3831), and TX-104 (C3832), respectively. Location maps are presented in Section 2. We have also provided our interpretation of the data in the context of determining the appropriate hydrogeologic model, the vertical extent of contamination, the migration potential of the contaminants that still reside in the vadose zone, and the correspondence of the contaminant distribution in the borehole sediment to groundwater plumes in the aquifer proximate and downgradient from the TX tank farm.

This report is the first of two reports written to present recent data collected on vadose zone sediments, both uncontaminated and contaminated, from within WMA T-TX-TY. The second PNNL report will discuss the characterization of 1) uncontaminated sediment from a *Resource Conservation and Recovery Act* (RCRA) borehole (299-W11-39) that provides baseline against information from contaminated sediment, and 2) contaminated sediment obtained from two boreholes near tank T-106, a confirmed leaker (~115,000 gallons) in 1973. The two documents contain preliminary interpretations to identify the distribution of key contaminants within the vadose zone and to determine what their future migration potential could be. The two PNNL reports will be incorporated into Appendix B of the WMA T-TX-TY field investigation report (FIR) (scheduled for publication in 2005).

This document describes the characterization data collected and interpretations assembled by the Applied Geology and Geochemistry Group within the PNNL Environmental Technology Division. Based on a review of all available historical information on tank farm operations and vadose zone gross and spectral gamma monitoring of dry wells around the TX tanks (see Crumpler 2002 and Wood et al. 2001), three areas of interests were identified. The historical data analysis did not uncover any explicit documentation that there were fluid losses at the TX tank farm, which was quite active during the early 1970s during the bismuth phosphate metals waste recovery activity, used to obtain uranium for reuse in

making fuel. However, vadose zone monitoring data show a uranium plume between tanks TX-101 and TX-105 with the higher concentrations closer to tank TX-105. Therefore, borehole C3830 was drilled to the southwest of Tank TX-105.

The second area of interest is the region between tanks TX-107 and TX-103 where historical vadose zone spectral gamma monitoring data indicate there is cobalt-60 and europium-152/154 in the vadose zone below the tanks. There are about six drywells concentrated in the area between these two tanks but no paper trail was found as to why these holes were drilled. These signs suggest that there was a loss of tank fluids from one of these tanks. Further, tank TX-107 was used for transferring wastes to the T Evaporator and thus there were very large volumes of fluids moved through this tank. For these reasons, borehole C3831 was drilled to the southwest of tank TX-107 in the region between tanks TX-107/103. The third borehole, C3832, was placed to the southeast of tank TX-104 in the hopes that it would capture the migration of more mobile contaminants in the down dip direction from a tank leak at TX-107 and to evaluate whether there were separate and distinct leaks from TX-107 and TX-104. If the mobile contaminant profile at C3832 differed significantly from the nature of the profile at C3831, two distinct leaks, one from TX-107 and one from TX-104, would be a more plausible explanation. It is also possible that the two leaks might have commingled.

This report is divided into sections that describe the geology, geochemical characterization methods employed, geochemical results and contaminant migration potential, and correlation between the existing vadose zone porewater with current and past groundwater contamination characteristics, as well as summary and conclusions, references, and appendixes with additional geology details and sediment photographs.

English units are used in this report for descriptions and discussions of drilling activities and samples because that is the system of units used by drillers to measure and report depths and well construction details. To convert feet to meters, multiply by 0.3048; to convert inches to centimeters, multiply by 2.54. The metric system is used in this report for all other purposes.

2.0   Geology

The geology of the vadose zone underlying the 241-TX Tank Farm (TX Tank Farm) forms the framework through which contaminants that leaked from the single-shell tanks or their ancillary piping and junction boxes move, and is fundamental to the understanding of migration and distribution of the contamination in the vadose zone. Of particular interest are the interrelationships between the coarser and finer-grained strata, and the degree of contrast in their physical and geochemical properties.

This section presents a discussion of the regional geologic setting and the geology of the TX Tank Farm, followed by a discussion of the geohydrologic characterization methods and background information on four recently completed boreholes sampled for physical and geochemical characterization.

2.1   Regional Geologic Setting

The Hanford Site is located within the Columbia Plateau of southeastern Washington State. This broad plain, situated between the Cascade Mountains to the west and the Rocky Mountains to the east, is underlain by a thick sequence of Miocene age tholeiitic basalt flows (the Columbia River Basalt Group). The Columbia River Basalt Group (composed of approximately 50 basalt flows) is more than 3,000-m thick and forms the bedrock beneath southeastern Washington. Sedimentary interbeds are sandwiched between the basalt flows, particularly in the uppermost Saddle Mountains Basalt. These interbeds along with the porous basalt flow tops and flow bottoms form confined aquifers that extend across the Pasco Basin (DOE 1988).

The basalt flows have been folded and faulted creating broad structural and topographic basins, separated by asymmetric anticlinal ridges. Sediments of late Miocene, Pliocene, and Pleistocene age have accumulated up to 520-m thick in some of these basins. The Hanford Site lies within one of the larger of these basins, the Pasco Basin. This basin is partially bisected by the Umtanum-Gable Mountain anticline creating two subordinate synclinal basins. The largest of these is the Cold Creek syncline, which is further subdivided into two basins, the Wye Barricade depression and the Cold Creek depression. The Cold Creek depression underlies the principal waste management areas (200 East and 200 West Areas) of the Hanford Site, including the TX Tank Farm.

The generalized stratigraphy beneath the Hanford Site consists of, in ascending order, the Columbia River Basalt Group, the Ringold Formation, the Cold Creek unit (CCU) (formerly called the Plio-Pleistocene unit), and the Hanford formation. A geologic cross section showing the stratigraphic relationships of these units in the western Pasco Basin is presented in Figure 2.1. Thin veneers of Holocene alluvium, colluvium, and/or eolian sediments discontinuously overlie these principal geologic units. The regional suprabasalt stratigraphy is described in more detail elsewhere (Lindsey 1995; DOE 1988; DOE 2002a).
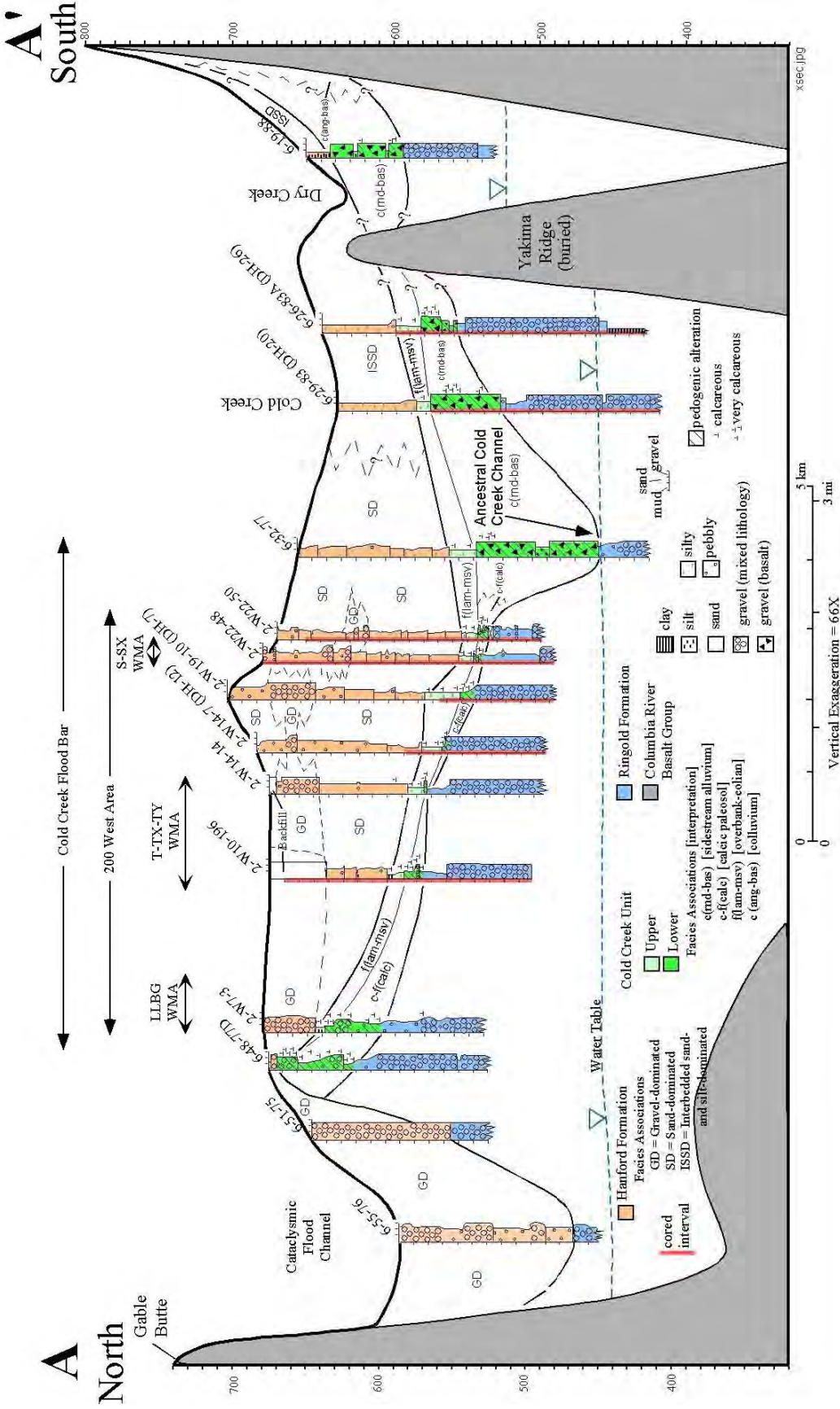
Figure 2.1. **Stratigraphic Cross Section of the Vadose Zone Within the Central Pasco Basin.** *The study area (TX Tank Farm) is located left of center along this cross section. The cross section is located in Figure 2.2.*

2.2

2.1.1 Ringold Formation

The Ringold Formation records fluvial-lacustrine deposition associated with the ancestral Columbia River drainage system, following the last eruption of basalt at the Hanford Site about 10.5 million years (m.y.) ago (Tallman et al. 1981; DOE 1988; Lindsey et al. 1994a, Lindsey 1996). Deformation of the Yakima folds, which began in the middle Miocene Epoch, concurrent with the Columbia River basalt volcanism, continued into Ringold Formation time so the centers of downwarped basins received more sediments than the margins. The Ringold Formation is up to 185-m (600 ft) thick in the center of the basin and pinches out against the basin-bounding basalt ridges.

The Ringold Formation consists of semi-indurated clay, silt, fine- to coarse-grained sand, and variably cemented granule to cobble gravel. Ringold Formation sediments have been classified into five sediment facies associations: 1) fluvial gravel, 2) fluvial sand, 3) overbank deposits, 4) lacustrine deposits, and 5) alluvial fan deposits. See Lindsey (1996) and Lindsey et al. (2001) for more detailed descriptions of these facies.

2.1.2 Cold Creek Unit

After a period of post-Ringold Formation incision, the eroded surface of the Ringold Formation was locally weathered and/or covered with deposits of the Cold Creek unit (CCU). These deposits consist of fluvial, eolian and/or colluvial deposits, often pedogenically altered (DOE 2002a). The Cold Creek unit includes those deposits formerly referred to as the "Plio-Pleistocene unit" and "pre-Missoula Gravels," as well as the "early Palouse soil" and "caliche layer" within the 200 West Area. The new name, Cold Creek unit, was given to these deposits because recent studies suggest this unit is all of late Pliocene age. The Cold Creek unit is a more appropriate name choice since it is independent of age and geographically better describes the unit, which is generally confined to the boundaries of the Cold Creek syncline within the west central Pasco Basin (DOE 2002a).

Five different facies of the CCU have been differentiated based on grain size, sedimentary structure, sorting, roundness, fabric, and mineralogic composition (DOE 2002a). These facies include: 1) fluvial-overbank and/or eolian, 2) calcic paleosol, 3) mainstream alluvium, 4) colluvium, and 5) sidestream alluvium.

2.1.3 Hanford Formation

The Hanford formation is an informal name used within the Pasco Basin to describe Pleistocene cataclysmic flood deposits (Tallman et al. 1979, 1981; DOE 1988, 2002a). Ice Age floods originated from outbursts of glacial Lake Missoula, as well as other ice-dammed lakes (Baker and Bunker 1985), pluvial lake Bonneville (O'Connor 1993), or possible sub-glacial floods (Shaw et al. 1999) associated with the Cordilleran Ice Sheet. The Hanford formation may include some minor fluvial, colluvial, and/or eolian deposits interbedded with flood deposits.

Recently, the possibility of converting the Hanford formation into a formalized stratigraphic unit was investigated (Bjornstad et al. 2002; DOE 2002a). However, the consensus is that the Hanford formation cannot be formalized as a stratigraphic unit at this time, even though it is a mappable unit, for several reasons as specified in the International Stratigraphic Guide (Salvador 1994). These include 1) the Hanford formation, as defined, is based on a common time period and depositional environment, which

are invalid formalization criteria; 2) the Hanford formation is very diverse lithologically (i.e., facies range from bouldery gravels to silts); geologic formations, as defined in the stratigraphic code, should have similar lithologic properties; and 3) there is lack of complete reference sections with which to define and characterize the Hanford formation. For example, the range of internal variability within the Hanford formation often exceeds that between adjacent stratigraphic units (e.g., CCU and Ringold Formation). Therefore, for the present, the Hanford formation should continue to be used informally to describe cataclysmic flood deposits within the Pasco Basin.

As mentioned above, the Hanford formation consists predominantly of unconsolidated sediments that cover a wide range in grain size, from boulder-size gravel to sand, silty sand, and silt. The sorting ranges from poorly sorted (for gravel facies) to well-sorted (for fine sand to silt facies). Traditionally the Hanford formation has been subdivided into three lithofacies (gravel-, sand-, and silt-dominated), which grade into one another, both vertically and laterally (DOE 1988; Baker et al. 1991; Lindsey et al. 1994a). These lithofacies may interfinger with or grade from gravel-dominated to sand-dominated facies, or sand-dominated to silt-dominated facies, but rarely from gravel-dominated to silt-dominated facies.

An interbedded sand- and silt-dominated facies (DOE 2002a) is stratigraphically equivalent to Touchet Beds, which were first formally recognized by R. F. Flint in 1938 (Flint 1938). Beginning in the late 1980s, these deposits were called by a variety of other informal names, including slackwater facies (Moody 1987; Lindsey et al. 1992b; Connelly et al. 1992a; Last et al. 1989; Smith 1993), silt-dominated facies (Lindsey et al. 1992a, 1994b; Connelly et al. 1992b), silty facies (Lindsey et al. 1994a), and rhythmite facies (Baker et al. 1991). Interbedded sand- and silt-dominated facies occur as sequences of rhythmic, graded beds that range from 0.1 to 1 m (0.3 to 3.3 ft) in thickness and are characterized by loose, horizontal- to ripple-laminated, coarse to medium sand, grading up into cohesive fine sand to silt. The silt-sized fractions consist predominantly of quartz, feldspar, and mica (Tallman et al. 1979).

Sand-dominated facies of the Hanford formation (Lindsey et al. 1992a, 1992b, 1994a, 1994b; Connelly et al. 1992a, 1992b) consist of relatively thick ($\geq$ 1 m), predominantly horizontally laminated, loose, basalt-rich, fine- to coarse-grained sand, sometimes grading upward into a thinner sequence of ripple-laminated fine sand to silt. The sand-dominated facies have also been referred to as the transitional sand facies (Reidel et al. 1992; Fecht and Weekes 1996) and the plane-laminated sand facies (Baker et al. 1991). Typically, sand-dominated facies average about 50% mafic rock fragments (i.e., basalt) and 50% quartz-feldspar (Tallman et al. 1979). This composition gives the Hanford formation its characteristic "salt and pepper" appearance that is frequently noted in drillers' and geologists' logs.

The gravel-dominated facies have been variously named Pasco gravels (Brown 1970; Myers and Price 1979; Tallman et al. 1979, 1981; DOE 1984), Missoula flood gravels (Webster and Crosby 1982), coarse-grained main-channel facies (DOE 1988; Last et al. 1989), coarse-grained flood gravels (Moody 1987; Baker et al. 1991), and gravel-dominated facies (Lindsey et al. 1992a, 1992b, 1994b; Connelly et al. 1992a, 1992b). The gravel-dominated facies of the Hanford formation consist of loose, massive, horizontal and large-scale, planar-tabular cross-bedded, poorly sorted mixtures of gravel, sand, and silt. Gravel clasts in flood gravels generally consist of 50% to 75% subangular to subrounded basalt (DOE 2002a).

Below an elevation of approximately 300 m (1,000 ft) within the Pasco Basin, the Hanford formation unconformably overlies the Cold Creek unit and, where the CCU is eroded, lies directly on the Ringold Formation or Columbia River basalt. Within the central Pasco Basin up to 100 m of flood deposits

accumulated along Priest Rapids, Cold Creek and Gable Mountain bars, which developed downstream of constrictions or obstructions in floodwater flow through the basin (Figure 2.2).

Figure 2.2. **Thickness and Distribution of Cataclysmic Flood Deposits (i.e., Hanford formation) Within the Central Pasco Basin.** *Cross section A-A' is shown in Figure 2.1.*
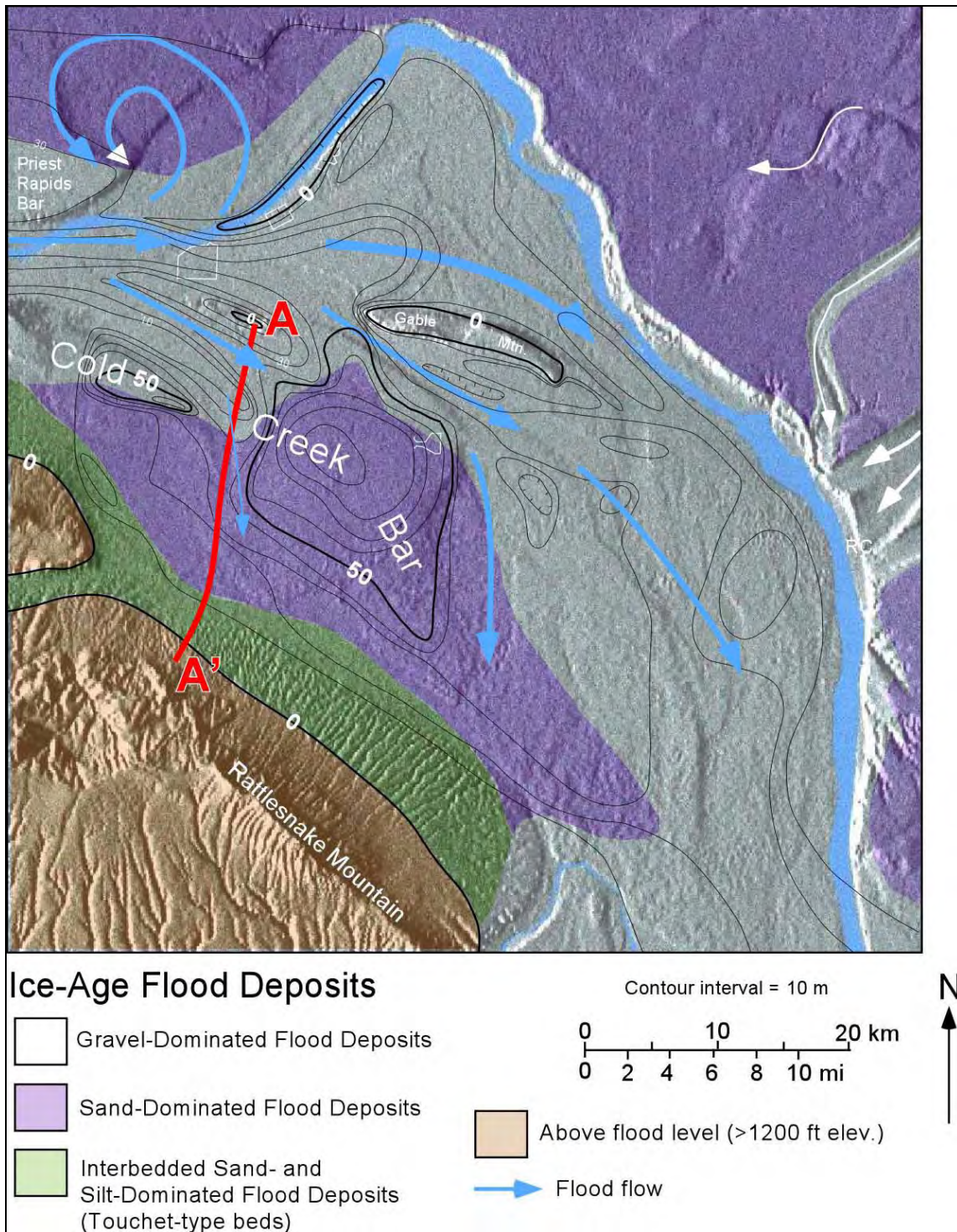
2.2   Geologic Setting of the TX Tank Farm

The geology in the vicinity of the TX Tank Farm has been described in numerous reports (Price and Fecht 1976; Tallman et al. 1979; Last et al. 1989; Bjornstad 1990; Connelly et al. 1992a; DOE-GJO 1997; Lindsey et al. 2001; Wood et al. 2001). A generalized stratigraphic column for the TX Tank Farm is presented in Figure 2.3.

More detailed descriptions of the vadose zone units, the focus of this report, are presented in Table 2.1. The stratigraphic terminology for the post-Ringold-Formation units used in this report may be different than that used in previous reports but reflects the standardized stratigraphic nomenclature recommended by DOE (2002a).

The subsurface geology of the TX Tank Farm is interpreted from dozens of boreholes drilled in the area. A total of 94 dry wells were constructed between 1952 and 1978 to monitor for leaks from the 18 single-shell tanks of the TX Tank Farm (DOE-GJO 1997). These shallow vadose-zone holes served as primary and secondary leak-detection devices. In addition, 9 deeper groundwater monitoring wells are located around the perimeter of the TX Tank Farm. The key boreholes used in this study are shown in Figure 2.4.

2.2.1   Stratigraphy and Lithology

Stratigraphic terminology of the vadose zone used in this report is presented in Table 2.1. The tank farm was excavated into the Pleistocene-age Hanford formation and Holocene eolian deposits that mantle the central portion of the Cold Creek flood bar. The depth to groundwater in the vicinity of the TX Tank Farm is about 220 ft (67 m). Stratigraphic units that make up the vadose-zone units beneath the tank farm include (in descending order) 1) recent deposits, 2) Hanford formation, 3) Cold Creek unit, and 4) Ringold Formation.

Two additional detailed cross sections are presented in Figures 2.5 and 2.6 for the TX Tank Farm. Additional information on the stratigraphic and facies relationships among the different stratigraphic units in the vicinity of the TX Tank Farm is presented in Wood et al. (2001) and Lindsey et al. (2001).

2.2.2   Holocene Deposits

Holocene deposits within the TX Tank Farm consist of backfill material emplaced around the tanks. This backfill material is composed of mostly gravel-dominated H1 unit of the Hanford formation perhaps mixed with eolian materials, which blanketed the area with 1-2 m of windblown sand and silt prior to construction of TX Tank Farm. Up to 52 ft of the Hanford formation H1 unit, perhaps extending down into the Hanford formation H2 unit, were removed during construction of the tank farm and stockpiled for placement later around and over the underground storage tanks. The backfill has been described as poorly sorted gravelly sand to sandy gravel (Price and Fecht 1976; Caggiano and Goodwin 1991). Fine-grained sand and silt was occasionally placed at and toward the base of the backfill within the TX Tank Farm, apparently to improve traction for construction vehicles (DOE-GJO 1997).

STRATIGRAPHIC COLUMN FOR 241-TX TANK FARM

LITHOLOGY

Interstratified basaltic gravel, sand, and minor silt.

Silt, silty sand, and sand with local gravel.

Unconsolidated, massive to laminated and stratified fine sand and silt.

Calcic paleosol(s) developed on clay, silt, sand, and minor gravel; variably cemented.

Sand with minor interbedded silt.

Gravel with intercalated sand and silt.

Paleosols and lacustrine silts and clays.

Gravel with intercalated sand and silt.

Basalt

STRATIGRAPHY

Gravel-Dominated Flood Sequence (H1) — Hanford formation

Sand-Dominated Flood Sequence (H2)

Upper Subunit — Cold Creek Unit
Lower Subunit

Member of Taylor Flat (Rtf) (Upper Ringold Unit)

Unit E [Rwi(e)]

Member of Wooded Island — Ringold Formation

Lower Mud Unit [Rwi(lm)]

Unit A [Rwi(a)]

Elephant Mountain Member Saddle Mountains Basalt, Columbia River Basalt Group

Legend:
Silt
Gravel
Cemented Calcium Carbonate (Caliche)
Sand
Basalt
Groundwater Table

2002/DCL/TX-TY/021 (12/16)

Figure 2.3. Generalized, Composite Stratigraphy for the Late-Cenozoic Sediments Overlying the Columbia River Basalt Group at the TX Tank Farm (Modified After Wood et al. 2001)

Table 2.1.   Stratigraphic Terminology for the Vadose Zone Beneath the TX Tank Farm

Stratigraphic Symbol	Formation	Facies / Subunit	Description	Genesis
Backfill	NA	Backfill	**Gravel-dominated sequence** consisting of poorly to moderately sorted cobbles, pebbles, and coarse to medium sand with some silt derived from coarse-grained Hanford formation (H1 Unit) excavated around tanks (Price and Fecht 1976; Wood et al. 2001); occasional layers of sand to silty sand occur near the base of the backfill sequence.	Anthropogenic
H1	Hanford formation	Unit H1 (Gravel-dominated facies association)	**Gravel-dominated flood sequence** composed of mostly poorly sorted, basaltic, sandy gravel to silty sandy gravel. Equivalent to the upper gravel sequence discussed by Last et al. (1989), the Qfg documented by Reidel and Fecht (1994), Hanford Gravel Unit A of Johnson et al. (1999), coarse-grained sequence (H1 unit) of Wood et al. (2001) and gravel facies of unit H1 of Lindsey et al. (2001), and gravel-dominated facies association of DOE (2002a). The majority of this unit was excavated out and is missing from beneath TX Tank Farm.	Cataclysmic flood deposits (high-energy)
H2		Unit H2 (Sand-dominated facies association)	**Sand-dominated flood sequence** composed of mostly horizontal to tabular cross-bedded sand to gravelly sand. Some sand beds capped with thin layers of silty sand to sandy silt. Equivalent to Hanford Sands of Johnson et al. (1999), Fine-Grained Sequence (H2 unit) of Wood et al. (2001) and unit H2 of Lindsey et al. (2001), the sandy sequence of Last et al. (1989) and Lindsey et al. (1992a), and to Qfs documented by Reidel and Fecht (1994), and sand-dominated facies association of DOE (2002a).	Cataclysmic flood deposits (moderate energy)
CCU$_u$	Cold Creek unit	Upper subunit	**Silty sequence** consisting of interstratified well-sorted silt and fine sand. Uncemented but may be moderately to strongly calcareous from detrital CaCO$_3$. Equivalent to the "early Palouse soil" (Brown 1970; Tallman et al. 1979; DOE 1988; and DOE-GJO 1997) and the Hanford Formation(?)/Plio-Pleistocene (?) deposits (H/PP) of Wood et al. (2001). Also equivalent to the upper Plio-Pleistocene unit in Lindsey et al. (2001) and the fine-grained, laminated to massive [CCUf (lam-msv)] lithofacies of the Cold Creek unit DOE (2002a).	Post-Ringold Fm. eolian and/or overbank alluvial deposits
CCU$_l$		Lower subunit	**Calcic paleosol sequence,** consisting of interbedded layers of pedogenically altered to unaltered gravel, sand, silt, and/or clay, cemented together with one or more layers of secondary CaCO$_3$, originally referred to as "caliche" (Brown 1959). Since then the name has evolved from the Plio-Pleistocene unit (Bjornstad 1984; DOE 1988; DOE-GJO 1997; Slate 2000)**,** the Plio-Pleistocene calcrete facies (DOE 1988; Wood et al. 2001), the lower Plio-Pleistocene unit (Lindsey et al. 2001), and the coarse- to fine-grained, CaCO$_3$-cemented lithofacies [CCUc-f(calc)] of the Cold Creek unit (DOE 2002a).	Calcic paleosols developed on eroded Ringold Fm. or post-Ringold Fm. eolian and/or fluvial deposits

Table 2.1. **(contd)**

Stratigraphic Symbol	Formation	Facies / Subunit	Description	Genesis
R_{tf}	Ringold Formation	Member of Taylor Flat	**Fine-grained Ringold Formation sequence** consisting of interstratified, well bedded fine to coarse sand to silt. Equivalent to the upper Ringold Formation unit (DOE 1988). This unit is not present beneath most of the TX Tank Farm.	Ancestral Columbia River System fluvial channel, crevasse splay, and overbank deposits
R_{wi}		Member of Wooded Island	**Coarse-grained Ringold Formation sequence** consisting of mostly moderately sorted, quartzitic sandy gravel to silty sandy gravel. Equivalent to middle Ringold Formation unit (DOE 1988) and the Ringold Formation Unit E gravels (Wood et al. 2001; Lindsey et al. 2001)**.**	Ancestral Columbia River System braided-stream deposits
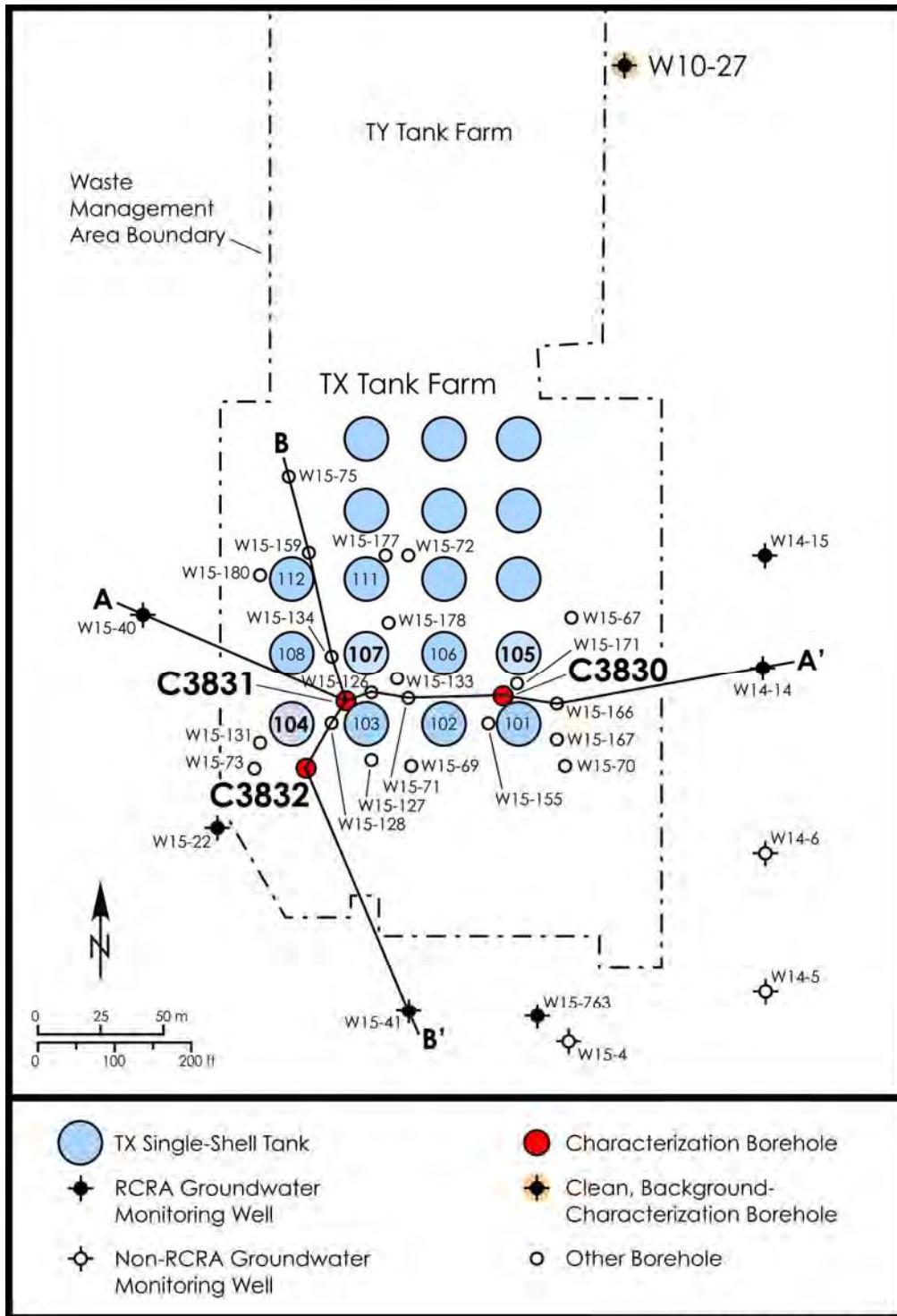
Figure 2.4. **Selected Borehole Location Map for the TX Tank Farm.** *Cross sections A-A' and B-B' are shown in Figures 2.5 and 2.6, respectively.*

Figure 2.5. **East-West Hydrogeologic Cross Section A-A' Across the TX Tank Farm.** *Located in Figure 2.4.*

2.11
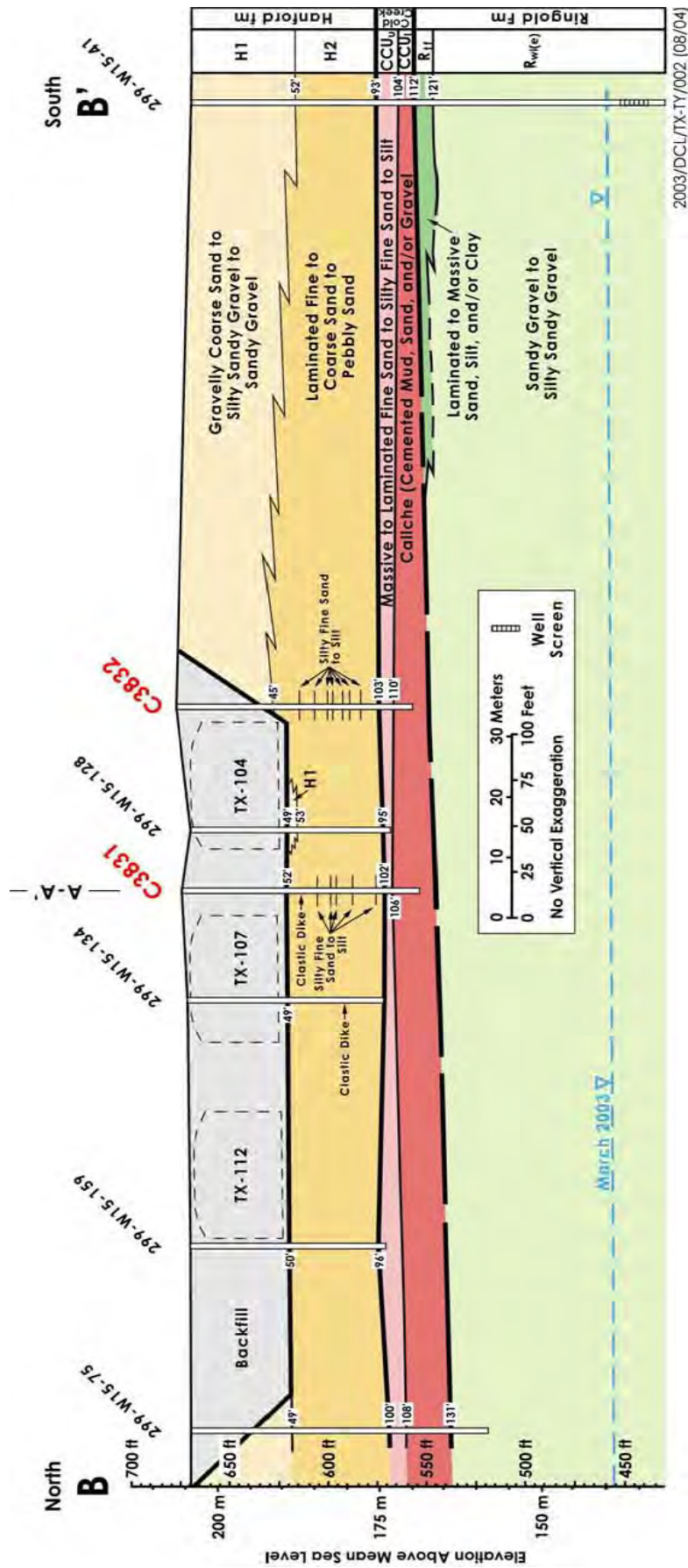
Figure 2.6. North-South Hydrogeologic Cross Section B-B' Across the TX Tank Farm. *Located in Figure 2.4.*

2.12

2.2.2.1 Hanford Formation

The Hanford formation in the TX Tank Farm consists of two informal subunits: the H1 and H2 units. The H2 unit belongs to the sand-dominated facies association, while the H1 is gravel-dominated (DOE 2002a). However, during excavation of the TX Tank Farm, most of the Hanford formation H1 unit was removed so that only the H2 unit occurs beneath backfill material emplaced around the tanks.

2.2.2.1.1 Gravel-Dominated Sequence (H1 Unit).

The gravel-dominated Hanford formation H1 unit is generally not present in the TX Tank Farm, having been completely removed during tank-farm excavation. However, much of the material used for backfill around the tanks consists of the Hanford formation H1 unit.

2.2.2.1.2 Sand-Dominated Sequence (H2 Unit)

The H2 unit consists of predominantly sand-dominated facies of the Hanford formation. Cementation is very minor or absent, and total calcium carbonate- ($CaCO_3$) content is generally only a few weight percent (wt%) or less.

The Hanford formation H2 unit is continuous beneath the TX Tank Farm; the base is well-defined by a change from well-stratified fine-coarse-grained "salt and pepper"-like sands to silt-dominated facies of the upper CCU. There is also usually an increase in total natural gamma activity and moisture along this contact.

2.2.2.2 Cold Creek Unit

The Cold Creek unit lies unconformably on the tilted and truncated Ringold Formation that formed following incision and downcutting by the ancestral Columbia River toward the end of the Pliocene Epoch about 2.5 to 3.4 m.y. ago. Two distinctive subunits of the Cold Creek unit are present beneath the TX Tank Farm and most of the 200 West Area (DOE 2002a). The lower subunit consists of a variably cemented calcic paleosol sequence, while the upper subunit consists of unconsolidated, fine-grained, fluvial-overbank and/or eolian facies sediments.

2.2.2.2.1 Upper Cold Creek Subunit

The unconsolidated, silt-rich sediments of the upper Cold Creek unit consist of cohesive, compact, massive to laminated and stratified, fine-grained sand and silt. This brown- to yellow-colored unit is also characterized as micaceous, very well sorted, and moderately to strongly calcareous, with relatively high natural background-gamma activity (DOE 2002a). It is equivalent to the "early Palouse soil" (Brown 1960; Tallman et al. 1979, 1981; Bjornstad 1984, 1990; DOE 1988, Last et al. 1989; Lindsey et al. 1992b, Delaney et al. 1991; DOE-GJO 1997) and the "Hanford Formation (?)/Plio-Pleistocene (?) deposits" of Wood et al. (2001), and most recently identified as the CCUf(lam-msv) facies of the Cold Creek unit by DOE (2002a). Similar to the lower CCU, the upper CCU ranges from 10–15-ft thick and dips to the southwest beneath the TX Tank Farm (Wood et al. 2001).

While the upper CCU was originally interpreted as an eolian deposit, which was derived from the reworking of the underlying Ringold Formation and/or caliche (Brown 1960), more recent investigations indicate this facies may contain other fine-grained deposits besides eolian silt and fine sand (Lindsey et al.

1994b, 2000; Slate 1996). For example, recent studies in the S-SX WMA (Lindsey et al. 2000; Serne et al. 2002a) indicate that the upper CCU is composed of mostly intercalated layers of fine sand and silt, with some weakly developed paleosols, which is more characteristic of overbank-type alluvial deposits than eolian deposits (Lindsey et al. 2000). Regardless of its exact stratigraphic relationship and origin, the upper CCU is a distinctive lithostratigraphic unit has a significant influence on the moisture and contaminant distribution within the vadose zone.

2.2.2.2.2 Lower Cold Creek Subunit

Diagnostic features of the lower CCU include 1) advanced induration with pedogenic calcium carbonate, 2) white color, 3) presence of pedogenic structures (e.g., root traces, animal burrows, or soil horizonation), as well as an erratic geophysical log (i.e., natural gamma and neutron moisture) response (DOE 1988; Bjornstad 1990; DOE 2002a).

The upper boundary is usually sharp and distinct in contrast to the lower boundary, which is commonly gradational and overprinted onto the underlying Ringold Formation within the west central Pasco Basin. The upper CCU is easily distinguished from the lower CCU based on a contrast in color, degree of cementation (Figure 2.7), as well as natural-gamma activity. Furthermore, while the upper CCU may be compact and cohesive, it is generally uncemented, in contrast to the underlying pedogenically altered lower CCU. Even though the upper CCU may contain moderate to high concentrations of calcium carbonate, the carbonate is evenly disseminated as detrital grains. The bulk of the detrital calcium carbonate in the upper CCU is likely derived from the disintegration and mechanical reworking/redeposition of the underlying lower CCU, where discrete calcium carbonate-rich zones developed diagenetically as a result of pedogenesis. The top of the lower CCU is well defined by a coincident significant increase in calcium-carbonate content and decrease in mud content and sorting, accompanied by a sudden drop in total gamma activity (i.e., potassium-40 [K-40]) on borehole geophysical logs (Bjornstad 1990; DOE-GJO 1997).

Figure 2.7. **Sharp Contact Between the Upper and Lower Cold Creek Subunits in Borehole 299-W10-27.** *The upper unit consists of unconsolidated, yellowish-brown, silt and fine sand (mS), in sharp contrast to the white, CaCO₃-cemented lower unit. The top of this 1-foot core is to the right.*

The lower CCU represents a highly weathered paleosurface that developed unconformably on top of the Ringold Formation (Brown 1959, 1960) following a period of downcutting and degradation within the central Pasco Basin. Other names used to describe this facies have included "caliche" (Brown 1959) and "calcrete" (DOE 1988). The lower CCU consist of basaltic to quartzitic gravels, sands, silt, and clay that are cemented with one or more layers of secondary, pedogenic calcium carbonate. The concentration of calcium carbonate within the lower CCU is generally 20 to 30 wt% but can range from 5 to 70 wt%. The overall thickness of the lower CCU beneath the TX Tank Farm is generally 10 to 20 ft and dips to the southwest about one degree (Wood et al. 2001).

Considerable variability may exist internally within the lower CCU because of natural heterogeneity inherent in soils and soil-forming processes, which vary under different physical, chemical, and biological conditions (e.g., moisture, grain size, aspect, mineralogy, bioturbation, and microbial activity). An additional complicating factor is that the land surface during late Pliocene time was locally undergoing changes via fluvial and eolian activity, which resulted in variable rates of aggradation, degradation, and soil development (Bjornstad 1984, 1990; DOE 1988; Slate 1996, 2000; Wood et al. 2001). The calcium-carbonate overprint is superimposed onto a variety of rock types, including silt, quartz-feldpsar-rich sand and gravel, and locally derived basaltic sand and gravel (Slate 1996, 2000; Lindsey et al. 2000). In the vicinity of the TX Tank Farm, multiple, calcic-rich zones may be separated by relatively noncalcareous, uncemented material indicating some rapid accumulations occurred periodically between periods of soil development.

2.2.2.3　Ringold Formation

Generally, only fluvial gravel and sand facies are represented in the Ringold Formation vadose zone beneath the TX Tank Farm. A thick sequence of fluvial gravel facies occurs in the vadose zone beneath the TX Tank Farm; these belong to the Ringold Formation member of Wooded Island, Unit E. Fluvial sands, which locally overlie Unit E adjacent to the TX Tank Farm, are considered part of Ringold Formation member of Taylor Flat (Lindsey et al. 2001).

2.2.2.3.1　Member of Taylor Flat (R_{tf})

The Ringold Formation member of Taylor Flat within the T-TX-TY WMA (previously referred to as the upper Ringold Formation unit) consists of interstratified, well-bedded fine to coarse sand to silt belonging to a mixture of fluvial-sand and overbank facies associations. Post-Ringold Formation erosion has locally stripped away this member, including all the area beneath TX Tank Farm. In areas adjacent to the TX Tank Farm, up to 10 m (30 ft) of R_{tf} lies sandwiched between the Cold Creek unit and gravels of the Ringold Formation member of Wooded Island (Wood et al. 2001).

Weathering and soil development associated with the overlying Cold Creek unit is often overprinted onto the member of Taylor Flat and/or the member of Wooded Island, Unit E. Because the degree of post-Ringold Formation pedogenesis decreases with depth, the contact with the overlying Cold Creek unit is gradational and generally defined by an upward decrease in natural-gamma activity, increase in calcium carbonate content, and/or decrease in mud content (indicative of more cementation).

2.2.2.3.2　Member of Wooded Island (R_{wi}, Unit E)

Unit E consists predominantly of the fluvial-gravel facies association with occasional thin beds of the fluvial-sand and/or the overbank facies associations. Unit E within the TX Tank Farm averages about 85 m (275 ft) thick and the top of the unit dips very gently to the southwest (Wood et al. 2001), consistent with the top of basalt and underlying Ringold Formation units. There exists about 10 ft (3 m) of structural relief on top of the Ringold Formation Unit E beneath the TX Tank Farm. The water table lies within Unit E gravels at about 220-ft (67 m) depth, about half-way between basalt bedrock and the ground surface.

2.2.3　Clastic Dikes

Clastic dikes are vertical to sub-vertical sedimentary structures that crosscut normal sedimentary layering that are common to ice-age flood deposits, especially in the sand- and silt-dominated facies of the Hanford formation (Black 1979; Fecht and Weekes 1996; Fecht et al. 1999). Some clastic dikes were noted during excavation of the T-TX-TY Tank Farms (Price and Fecht 1976) and clastic dikes were previously reported for two boreholes (299-W15-134 and 299-W15-180) within the TX Tank Farm (Wood et al. 2001). Of the four new boreholes documented here, two of boreholes intersected clastic dikes. One of the boreholes (C3831) intersected a dike in the Hanford formation H2 unit; the other borehole (299-W10-27) appears to have intersected two dikes, one in the Hanford formation H2 unit and another in the Ringold Formation member of Taylor Flat. These dikes are discussed further in subsequent sections of this report.

Where clastic dikes intersect the ground surface and are not covered with younger deposits, a feature known as "patterned ground" can be observed (Fecht et al. 1999). Well-developed "patterned ground" exists just south of the 200 West Area. Within the 200 West Area and the T-TX-TY WMA, however, "patterned ground" is scarce due to the many man-made surface disturbances and/or because it is buried under a thin cover of recent eolian sand. Clastic dikes occur in swarms and form four types of networks: 1) regular-shaped polygonal-patterns, 2) irregular-shaped, polygonal-patterns, 3) pre-existing fissure fillings, and 4) random occurrences. Clastic dikes in the T-TX-TY Tank Farm area probably occur randomly in the gravel-dominated facies of the Hanford formation (H1 unit) and as regular-shaped polygons in the finer-grained facies (H2 unit). Regular polygonal networks resemble 4- to 8-sided polygons and typically range from 3 cm to 1 m in width, from 2 m to greater than 20 m in depth and from 1.5 to 100 m along strike. Smaller dikelets, sills, and small-scale faults and shears are commonly associated with master dikes that form the polygons.

2.3   Summary of Recent Characterization Activities Within TX Tank Farm

Four boreholes were recently drilled and sampled within or near the TX Tank Farm (Table 2.2). Boreholes C3830, C3831, and C3832 were drilled via the closed-end probe method within the TX Tank Farm for the specific purpose of collecting core samples for physical and chemical characterization as outlined in Crumpler (2002). Core samples, 1.25-ft-long by 2.5-in.-diameter, were collected at predetermined intervals within these boreholes (Gardner et al 2002a, 2002b; Reynolds 2003). Drill locations were selected to evaluate possible leaks from tanks 241-TX-105 (C3830), TX-107 (C3831), and TX-104 (C3832), respectively.

In addition, almost continuous, 2.5-ft-long by 4-in.-diameter splitspoon core samples were collected in well 299-W10-27 (C3125) from 50 to 132 ft bgs. Well 299-W10-27 is a RCRA groundwater monitoring well about 200 m northeast of the TX Tank Farm (Figure 2.4). Located outside of the tank farm, this well is considered generally free of contamination and was chosen as a background control for the other three boreholes suspected of having possible chemical and radiological contamination. A geologic and hydrologic summary, based on the information collected from these boreholes, is presented below.

2.3.1   Hydrogeologic Characterization

Field hydrogeologic characterization for the four new boreholes in Table 2.2 included geophysical logging and penetration resistance measured via hammer blow counts. Additional hydrogeologic characterization was performed in the laboratory, including photography as well as geologic logging and gravimetric moisture measurements on the splitspoon core samples.

Table 2.2. Four Borings Used for Recent Geochemical Characterization in the Vicinity of TX Tank Farm

| Hanford Well ID | Borehole Number | Washington State Plane Coordinates | | Total Depth (ft bgs) | Purpose | Drill Method | Surface Elevation (ft) | Length/ Inside Diameter of Splitspoon | Date Cores Collected | Date Cores Logged/ Sampled | Percent of Hole Cored | Geologist Performing Logging |
		Northing	Easting									
2-W10-27	C3125	136442	566844	268.7	RCRA Ground-water Monitoring	Cable Tool	672.2	2.5 ft/ 4 in.	1/22-3/13/01	5/16/01- 11/21/02	89.8% (between 50-132 ft bgs)	Kevin Lindsey (Kennedy/Jenks), Bruce Bjornstad (PNNL)
	C3830	136167	566795	116.8	Vadose-Zone Core Sampling	Push Probe	675.9	1.25 ft/ 2.5 in.	8/20-9/5/02	10/16/02	22%	Bruce Bjornstad (PNNL), Victoria Johnson (Kennedy/Jenks)
	C3831	136167	566733	115.4	Vadose-Zone Core Sampling	Push Probe	674.6	1.25 ft/ 2.5 in.	7/1-8/7/02	8/14- 8/15/02	23%	Bruce Bjornstad (PNNL), Victoria Johnson (Kennedy/Jenks)
	C3832	136137	566718	115.9	Vadose-Zone Core Sampling	Push Probe	676.6	1.25 ft/ 2.5 in.	5/2-6/3/02	6/11- 6/12/02	23%	Bruce Bjornstad (PNNL), Victoria Johnson (Kennedy/Jenks)

2.3.1.1   Geophysical Logging

Geophysical logging was performed by Duratek Federal Services on all four boreholes using high-purity germanium (HPGe) spectral gamma and neutron-moisture tools (Lindsey et al. 2001; Gardner et al. 2002a, 2002b; Reynolds 2003). The neutron-moisture log is generally used to depict the relative moisture content within a 20-30-cm (8-12 in.) radius around the borehole. However, the neutron-moisture logging tool was not calibrated for the casing conditions; therefore, absolute moisture values cannot be obtained directly from the neutron-moisture log. Generally, where there is no radiological contamination, the total gamma count rate increases in finer-grained sediments with a corresponding increase in moisture content due the moisture-retaining properties of these sediments.

Processing of the spectral gamma log data allows the identification of gamma-emitting man-made radionuclides (if present) and the naturally occurring radionuclides potassium, uranium, and thorium (KUT) that are present in earth materials (Lindsey et al. 2001). As expected, man-made radiological contaminants were detected in the three boreholes within the TX Tank Farm, while no man-made contaminants were detected outside the tank farm in borehole 299-W10-27. More detailed descriptions of the logging tools and data analysis for 299-W10-27 are presented in Lindsey et al. (2001). Additional information on the geophysical logging results on the three TX boreholes is presented below under the more detailed discussions for these holes, as well as in Gardner et al. (2002a, 2002b) and Reynolds (2003).

2.3.1.2   Sample Handling

Because there was no man-made contamination in 299-W10-27, sample handling was slightly different for this clean background borehole compared to the three boreholes sampled within the TX Tank Farm. Two, 4-in.-diameter, 1-ft-long, lexan-lined core samples were recovered from each 2.5-ft splitspoon in 299-W10-27. Upon recovery, any open spaces in the ends of the liners were stuffed with aluminum foil in the field and plastic end caps were secured with duct tape. The outside of the liner was labeled with the borehole number, depth interval, and an "up" arrow. Alternatively, potentially contaminated core samples from the three TX boreholes were collected in two, 2.5-in.-diameter, 0.5-ft long stainless-steel liners (Gardner et al. 2002a, 2002b; Reynolds 2003). The liners were sealed with plastic end caps and the outsides labeled with chain-of-custody or borehole ID number, an "up" arrow, and the letter "A" or "B". The letter "A" was assigned to the deeper of the two cores in the core run.

Once received at the PNNL 3720 Building, the core samples were stored in a refrigerator to maintain the sample temperatures between 2 and 4°C. Core samples from the clean 299-W10-27 borehole were opened, sampled, and described within a non-radiologically controlled PNNL laboratory (Lindsey et al. 2001). Because of the potential for radiological contamination, more precautions were taken processing the cores from within the tank farms.

Within a month of collection, the core samples from the boreholes were sequentially taken to a fume hood for sample processing. Initially, the liner end caps were removed and the contents of the liner were placed in a plastic tray, one plastic tray per liner. Material within the plastic tray was then subsampled for physical and geochemical analysis, photographed, and described geologically. A complete set of core photographs for all four boreholes documented in this report are presented in Appendixes A.1 through A.4. Sediment within the sample liners was extracted using either a hammer to tap out the contents of the liner or a specially constructed hydraulic "extruder." Efforts were made to keep the sample materials as

intact as possible. In the coarser-grained facies however, the internal sedimentary structures could generally not be preserved because of the unconsolidated, friable nature of these materials.

2.3.1.3　Subsampling and Geologic Description

Geologic description for the 299-W10-27 borehole was performed in May 2001 by Kevin Lindsey of Kennedy / Jenks Consultants, Inc. Geologic descriptions and logs for this hole are presented in Lindsey et al. (2001).

Moisture samples were collected immediately upon extracting material from the core liner within the three TX Tank Farm boreholes. An attempt was made to sample the finer-grained and/or wetter materials as well as any distinct hydrogeologic units, while at the same time trying to avoid slough and/or other unrepresentative portions. The remaining sample was used for a brief visual geologic evaluation. Geologic logs of the opened cores from the three boreholes (C3830, C3831, and C3832) are presented in Appendixes B.1, B.2, and B.3, respectively.

A visual geologic evaluation of cores from the TX Tank Farm boreholes was conducted in accordance with the following procedures: ASTM D2488 (ASTM 1993), PNL-DO-1 (PNL 1990a), and PNL-D9T81-99-GVL-1 (PNNL 1999). Throughout the subsampling and geologic evaluation activities, the PNNL geologist made continual visual observations regarding the mineralogy, structure, grain-size distribution (and sorting), maximum particle size, grain-shape (e.g., roundness), color, moisture, consolidation, and reaction to dilute hydrochloric acid [HCl] (used to test for the presence of calcium carbonate). Particular attention was given to visually estimate the percentage (by weight) of gravel, sand, and mud (silt+clay), and to visually classify the samples based on the modified Folk (1968)-Wentworth (1922) classification scheme historically used at the Hanford Site. This sediment classification scheme uses a ternary diagram to categorize the sediment into one of 19 textural classes based on the relative proportions of gravel, sand, and mud (Figure 2.8).
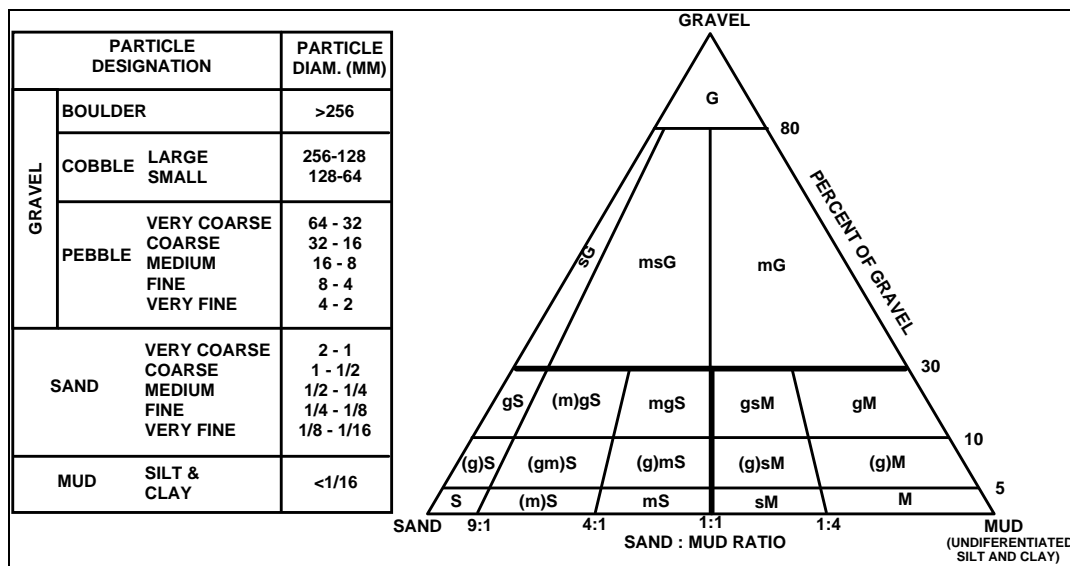
Figure 2.8.　**Sediment Textural Classification [modified after Folk (1968) and Wentworth (1922)]**

The tops of some cores contained several inches or more of sloughed material in the core liners. Slough is recognizable by its loose, darker, more massive, and poorly sorted nature, and is always at the top of the core. The sloughed material represents sediment that either fell back into the hole or was not completely removed between core runs. Re-coring of sloughed materials was more common in coarser and looser sediments found in backfill and the Hanford formations; it was generally not a problem in the finer-grained and/or higher moisture intervals, which have a greater tendency to hold together between core runs. Whenever possible, sampling of sloughed material was intentionally avoided during the collection of physical- and chemical-characterization samples in the laboratory.

2.3.2   Hydrogeology of Borehole 299-W10-27 (Background Well)

Borehole 299-W10-27 (C3125) was drilled using the cable-tool method between January 22 and March 13, 2001. The borehole is located approximately 650 ft (200 m) northeast of TX Tank Farm (Figure 2.4). The total depth of the borehole is 268.7 ft (81.9 m) bgs; the hole terminated within the Ringold Formation Unit E gravels at 81 ft (25 m) below the groundwater table.

Near continuous core sampling was performed between 50 to 132 ft bgs (Lindsey et al. 2001), for a total of 33 splitspoon core runs. Two, 1.0-ft-long plastic (i.e., lexan) core liners were collected for each 2.5-ft-splitspoon run. The extra 0.5 ft collected in the shoe of the splitspoon was used for geologic description in the field geologist's log. Generally, after performing a geologic description, the core material in the shoe was discarded. Accounting for the loss of the 0.5-ft shoe samples and slough atop many of the cores, the total recovery for the 50 to 132 ft interval in 299-W10-27 is estimated at 89.8% (Lindsey et al. 2001). Sampling above 50 ft was limited to core-barrel grab samples every 5 ft, while below 132 ft bgs grab samples were collected every 5 ft from the hard-tool drill cuttings. An additional three splitspoon cores were collected between hard-tooled intervals from the saturated zone within Ringold Formation Unit E gravels.

Core logging was performed by K.A. Lindsey of Kennedy / Jenks Consultants, Inc. at PNNL's 3720 Building laboratory on May 16, 2001. Core logs are presented in Lindsey et al. (2001 [Appendix A]). Geologic logging and sampling for gravimetric moisture occurred after each core segment was cut and split open, logged, and photographed. During logging, PNNL staff also collected 20 samples for paleomagnetic analysis (Table 2.3). Core photos taken during logging of this hole are presented in Appendix A.1 of this report. After geologic logging, moisture sampling, and photographing, the plastic-lined cores were resealed with duct tape and placed into cold storage for archival purposes.

Selected cores from 299-W10-27 were reopened 20 months later and nine subsamples were collected for physical and chemical characterization (Table 2.4).

Table 2.3. Core Samples Collected from 299-W10-27 for Paleomagnetic Analysis - May 16, 2001

Depth (ft bgs)	Stratigraphic Unit	Sample Description
50.8	H2	Medium sand, loose, well-sorted
53.3	H2	Fine sand, compact, v. well-sorted, moist
54.0	H2	Fine to medium sand, laminated
58.0	H2	Medium to coarse sand, loose, well-sorted
61.2	H2	Fine to medium sand, compact, moderately sorted
64.0	H2	Fine to coarse sand, loose, moderately sorted
68.3	H2	Fine to coarse sand, compact, moderately sorted
70.7	H2	Silty fine sand, weak lamination, compact, dipping $\geq 45^{\circ}$ (clastic dike)
74.0	H2	Fine to coarse sand, compact, moderately sorted
78.0	H2	Fine to medium sand, moderately sorted, weakly laminated
80.8	H2	Fine to medium sand, moderately sorted, weakly laminated
83.0	H2	Silty fine to medium sand, compact, poorly sorted, laminated
85.7	H2	Silty fine to medium sand, compact, poorly sorted, laminated
88.3	H2	Silty v. fine sand, well laminated, well-sorted
90.7	CCU$_u$	Fine sandy silt, compact, laminated, v. well-sorted
93.3	CCU$_u$	Silty v. fine sand, weakly laminated, compact, v. well-sorted
95.5	CCU$_u$	Silty v. fine sand, massive to weakly mottled, well-sorted
97.8	CCU$_u$	Silty fine sand, massive, few $CaCO_3$ nodules (just above caliche)
105.6	CCU$_l$	Fine pebbly silty sand, massive, v. poorly sorted, crumbly, mottled
108.1	CCU$_l$	Fine pebbly silty sand, massive, v. poorly sorted, crumbly, mottled

Table 2.4. **Splitspoon Samples Selected for Physical and Chemical Characterization from the Vadose Zone in 299-W10-27.** *One physical and chemical characterization sample was collected from each of the depths indicated.*

Core Sample ID	Discrete Sample Depth (ft)	Lithology	Stratigraphic Unit	Comments
C3125-52.5	53.3	Silty fine sand	H2	
C3125-53.5	54.2	Silty fine-medium sand	H2	
C3125-61	61.2	Silty fine-coarse sand	H2	
C3125-87.5	88.2	Silty fine sand	H2	
C3125-92.5	93.0	Silty fine sand	CCU_u	
C3125-100	100.5	Sandy caliche	CCU_l	
C3125-113.5	114.0	Fine-medium sand	R_{tf}	
C3125-117.5	118.5	Silt and sand	R_{tf}	Clastic dike within R_{tf}
C3125-130	130.2	Muddy sandy gravel	R_{wi}	

Figure 2.9 presents a summary geologic log for borehole 299-W10-27 based on a compilation of field geologists' logs, core log notes (Lindsey et al. 2001 [Appendix A]), geophysical logs (PNNL 2004), gravimetric moisture measurements, and core photographs (Appendix A.1 of this report). Four primary stratigraphic units were encountered in this borehole: 1) recent backfill/eolian materials, 2) the Hanford formation, 3) the Cold Creek unit, and 4) the Ringold Formation. A brief description of the sampled materials from each of these major stratigraphic units is presented below.

Based on the results of geophysical logging, no man-made contaminants were detected in borehole 299-W10-27 (Lindsey et al. 2001). Geophysical logging (Figure 2.9) shows a sharp increase in total gamma and neutron-moisture activity at a depth of 56 ft where the casing telescopes down from a double to a single string of temporary steel casing. These casings were advanced during drilling of the hole and used to keep it open for geophysical logging and subsequent well installation. At depth, the total gamma count rate increases again between 90-96 ft bgs within the silts and fine sands of the upper CCU before dropping very sharply at the contact with the lower CCU (i.e., top of the calcic paleosol sequence).

Zones of elevated moisture occur within the CCU and R_{tf} units between 90-120 ft bgs in 299-W10-27 (Figure 2.9). Moisture ranged from as low as 2.2 wt% in pebbly sand facies of the Hanford formation H2 unit up to 23.7 wt% in fine-grained facies of the lower CCU (Table 2.5).

2.23

Table 2.5.   Gravimetric Moisture Content Measured in Core Samples. *Units are wt% water.*

Strat. Unit	W10-27					C3830					C3831					C3832				
	#	Mean	Min.	Max.	S.D.	#	Mean	Min.	Max.	S.D.	#	Mean	Min.	Max.	S.D.	#	Mean	Min.	Max.	S.D.
Backfill	0					10	6.07	5.16	9.20	1.28	10	7.09	3.05	16.54	4.04	8	7.07	4.05	15.91	4.19
H_1	0					0					0					0				
H_2	30	4.78	2.23	14.80	3.05	17	5.74	2.46	12.42	3.08	26	8.70	4.47	18.06	4.13	21	9.23	3.80	18.54	3.75
CCU_u	5	11.92	8.66	15.53	3.01	6	11.01	6.83	14.72	2.67	1	10.49	NA	NA	NA	3	10.14	9.35	11.03	0.84
CCU_l	6	10.62	6.87	23.74	6.54	2	11.94	9.98	13.91	2.78	1	12.94	NA	NA	NA	5	10.83	9.27	13.79	1.73
R_{tf}	9	4.30	1.95	11.84	3.06	0					0					0				
R_{wi}	0					0					0					0				

S.D. = Standard Deviation of the Mean Value.

Blank Cells = In general, blank cells mean no samples were taken in this strata.

NA = Not Applicable. No statistics are possible when only one sample was obtained in a given strata.

More specifically, highest moisture occurs 1) toward the top of the upper CCU between 90-95 ft, 2) along the contact between the upper and lower CCU at ~98 ft, 3) at the base of the lower CCU at ~110 ft, and 4) within a fine-grained clastic dike at 120 ft.

2.3.2.1 Recent Backfill/Eolian Materials

Less than 2 ft of sandy gravel surface-construction material covers the surface at 299-W10-27. This material lies over about 3 ft of eolian silty sand that exists to a depth of 4.5 ft bgs.

2.3.2.2 Hanford Formation

Pleistocene cataclysmic flood deposits of the Hanford formation underlie the recent sediments to a depth of 89.4 ft in borehole 299-W10-27. Both units of the Hanford formation in the area (Wood et al. 2001) are represented, including a coarse-grained, gravel-dominated sequence (H1 unit) and an underlying finer, sand-dominated sequence (H2). The H1 unit, which extends from 4.5 to 41.5 ft bgs, consists of mostly poorly sorted, clast-supported sandy gravel to silty sandy gravel. The H2 unit, on the other hand, is predominantly medium- to coarse-grained sand to slightly pebbly sand, which extends to a depth of 89.4 ft bgs. The term "salt and pepper" is often used to describe sands of the H2 unit on geologic logs due to the roughly equal amounts of dark- (basaltic) and light-colored (quartz and feldspar) grains. These beds show occasional weak horizontal laminations and are generally non-calcareous to weakly calcareous. A few, relatively thin, low permeability, well-sorted, fine-grained layers of laminated fine to silty fine sand are interspersed within the H2 unit (Figure 2.10).

No samples were analyzed for physical and chemical characterization from the Hanford formation H1 unit since no splitspoon samples were collected from this unit. Four characterization samples were obtained from the Hanford formation H2 unit, however (Table 2.4, see Figure 2.10 for example). These were selected from finer-grained lenses within the H2 unit, since these typically contain more moisture (Bjornstad et al. 2003), and thus may have a higher probability for carrying contaminants. The clastic dike showed relatively high moisture (~15 wt%) compared to adjacent strata (Figure 2.9).

A thin zone of steeply dipping (>45°) beds (Table 2.3) of silty fine sand, which occurs between 70-71 ft, is suggestive of a clastic dike within the H2 unit in 299-W10-27. A clastic dike at this depth was reported in association with sampling for paleomagnetism (Table 2.3).
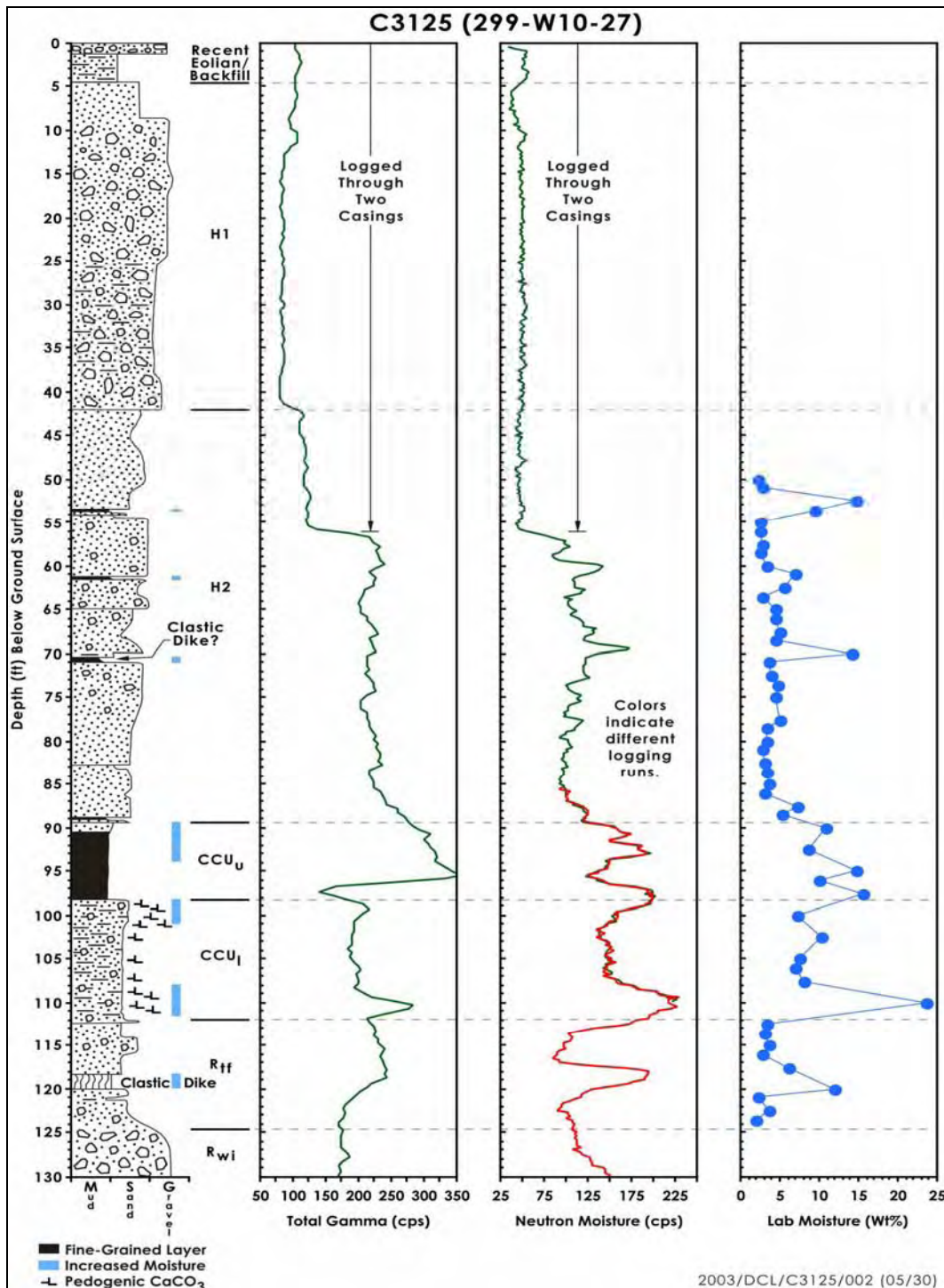
Figure 2.9. **Summary Hydrogeologic Log for Borehole 299-W10-27.** *Zones of increased moisture are indicated as those with >15 wt% water in core samples and/or show as distinct spikes on neutron-moisture log. Fine-grained layers are defined as those consisting predominantly of particles ≤ 0.25 mm in diameter (i.e., fine sand and smaller).*

Figure 2.10. Hanford Formation H2 Unit in Borehole 299-W10-27. *A thin (0.2 ft) layer of well-laminated silty very fine sand (mS) lies between beds of medium- to coarse-grained "salt and pepper" sand (S). One of the nine characterization samples from this borehole was collected from the silty sand layer at 54.2 ft. The top of the core is to the right. Notice the drilling-induced drag folding along the sides of the core.*

2.3.2.3   Cold Creek Unit

The Cold Creek unit is subdivided into the upper and lower subunits within the TX Tank Farm as well as the greater 200 West Area (DOE 2002a). The upper Cold Creek subunit consists of a brownish, well-sorted, unconsolidated fine-grained unit, which sharply overlies the lower subunit, characterized as a whitish calcic paleosol or sequence of paleosols. A distinct contact occurs between these two highly contrasting units (Figure 2.7).

2.3.2.3.1   Upper Cold Creek Subunit (CCU$_u$)

The upper CCU, 2.6-m (8.6 ft) thick, underlies the basalt-rich, "salt and pepper" sands of the Hanford formation in borehole 299-W10-27 between 27.2 m (89.4 ft) and 29.9 m (98 ft) bgs. This unit consists of a brownish, laminated to massive, compacted and very well sorted, silty fine sand to fine sandy silt. This unit is also relatively unconsolidated and moderately to strongly calcareous. The uncemented nature of this unit suggests the calcium carbonate is probably of detrital origin instead of that forming pedogenically in situ, as did carbonate in the underlying lower Cold Creek unit. Also characteristic of this unit is its relatively high natural-gamma activity and increased moisture on the neutron-moisture log, compared to adjacent units. Core photographs (Appendix A.1) show the upper half of this unit to be mostly laminated, while the lower half is mostly massive. The average moisture content (~ 12 wt%) for the upper CCU is significantly greater than that of the overlying Hanford formation (Table 2.5).

A single sample was collected for laboratory characterization from near the top of the upper CCU at 100.5 ft bgs (Table 2.4, Figure 2.9).

2.3.2.3.2   Lower Cold Creek Subunit (CCU$_l$)

The lower Cold Creek unit, also referred to as "caliche," "calcrete," or "calcic paleosol" (Table 2.1), extends from 98 to 112 ft bgs in 299-W10-27. Characteristics of the lower CCU are the abundance of white, secondary calcium carbonate cement, massive to mottled structures with evidence for bioturbation, and low to erratic natural-gamma activity on geophysical logs (DOE 1988; Bjornstad 1990; Wood et al. 2001). Two highly cemented calcic horizons are present within the 14-ft-thick calcic paleosol sequence in 299-W10-27 (Lindsey et al. 2001). One highly cemented zone (Stage III-IV as described in DOE [2002a]) occurs from the top at 98 ft (Figure 2.7) to 112 ft bgs; the other lies at the base of lower Cold Creek unit between 109.3 to 111 ft bgs. In between these two zones are more weakly developed Stage I-II calcic horizons (Figure 2.11).

Figure 2.11.   Lower Cold Creek Subunit (CCU$_l$) in 299-W10-27. *Massive to mottled, poorly sorted, sand and silt [(g)mS] with white stringers and nodules of secondary, pedogenic, calcium carbonate. The top of the core is to the right.*

A single sample, near the top of the lower CCU (100.5 ft bgs), was collected from the lower Cold Creek unit in 299-W10-27 for laboratory characterization (Table 2.4). Moisture content within the upper CCU is relatively high, similar to the upper CCU, but is more variable (Table 2.5).

2.3.2.4   Ringold Formation

The Ringold Formation is present from about 112 ft bgs to the bottom of 299-W10-27 (268.7 ft bgs). Predominantly sand to pebbly sand makes up the upper 12 ft of the Ringold Formation, which is considered part of the Ringold Formation member of Taylor Flat (R_{tf}), or upper Ringold (Table 2.1). The remaining 144 ft of 299-W10-27 is predominantly clast-supported sandy gravel to silty sandy gravel, considered part of the member of Wooded Island (R_{wi}), unit E (Lindsey et al. 2001).

Three characterization samples were collected from the Ringold Formation. These included one each from the R_{tf} member (114.0 ft bgs), a clastic dike within the R_{tf} member (118.5 ft bgs), and the R_{wi} member (130.2 ft bgs) (Table 2.4, Figure 2.9). Except for the clastic dike, moisture content within the R_{tf} member is relatively low, averaging about 4 wt% (Table 2.5).

2.3.3   Borehole C3830 (TX-105)

Borehole C3830 was drilled and sampled using a driven-probe technique between August 20 and September 5, 2002 (Table 2.2). The borehole is located approximately 40 ft (12.2 m) southwest of single-shell tank 241-TX-105 (Figure 2.4). The total depth of the borehole was 116.75 ft (35.6 m) bgs; the hole was terminated when refusal was encountered near the top of the caliche within the lower Cold Creek unit. Borehole C3830 was decommissioned on September 19, 2002 by back-pulling the casing while filling the annulus with dry bentonite. During decommissioning, four sets of in situ tensiometers were placed within the hole at depths of 96.25 ft, 49.95 ft, 7.45 ft, and 2.9 ft bgs. The surface elevation of the boring was 675.9 ft (206 m) and geographic coordinates were N136167 and E566795 (Reynolds 2003).

During drilling, a total of 18, 1.25-ft long, 2.5-inch-diameter splitspoon core samples were collected intermittently starting at a depth of 15 ft bgs (Table 2.6, Figure 2.12). Two, 0.5-ft-long stainless-steel core liners were collected during each core run. A separate sample was collected in the laboratory from each of the two liners for physical and chemical characterization, making a total of 36 characterization samples collected from this hole. In all, about 25 ft of core was obtained from C3830, or about 22% of the total length of the hole (Table 2.2). No samples or drill cuttings were collected between the 18 core runs since the hole was advanced in a closed configuration using a solid, removable tip (Reynolds 2003).

All cores were extracted, sampled, photographed, and geologically logged on October 16, 2002 in a radiologically controlled PNNL laboratory. Geologic logs of the material within the core liners were generated by geologists Victoria Johnson (Kennedy / Jenks Consultants, Inc.) and Bruce Bjornstad (PNNL); the core logs for these two geologists are presented in Reynolds (2003) and Appendix B.1 of this report, respectively. Geologic logging occurred after the contents of each 0.5-ft stainless-steel core liner was emptied into an open plastic container, followed by photographing and subsampling for physical and chemical characterization. Upon completion of these activities, the contents in the plastic containers were sealed shut and placed into cold storage for archival purposes.

The hole was advanced using a solid probe such that no grab samples were collected between core runs; thus no near-continuous geologic field log is available for this hole unlike the background hole (299-W10-27). Figure 2.12 presents a summary log for C3830 based on available geologic descriptions, core photographs, geophysical logs, laboratory derived gravimetric moisture and blow-count data. The geology between core runs is inferred and interpreted based on the geophysical log and blow-count data. Four primary stratigraphic units were encountered by this borehole: 1) recent backfill material, 2) the

Hanford formation, 3) the Cold Creek unit, and 4) the Ringold Formation. A brief description of the sampled materials from each of these major stratigraphic units is presented below.

Table 2.6. **Splitspoon Core Samples from C3830.** *Two characterization samples, labeled "A" and "B" were collected from each of the cores for a total of 36 samples.*

Core Sample ID	Top Depth (ft)	Bottom Depth (ft)	Mid Depth (ft)	Sampled Interval Thickness (ft)	Lithology	Stratigraphic Unit	Comments
C3830-14.96	14.96	16.31	15.64	1.35	Sand	backfill	
C3830-27.91	27.91	29.25	28.58	1.34	Gravelly sand	backfill	
C3830-40.93	40.93	42.49	41.71	1.56	Gravelly sand	backfill	
C3830-46.2	46.20	47.50	46.85	1.30	Gravelly sand	backfill	
C3830-47.5	47.50	49.00	48.25	1.50	Slightly gravelly sand	backfill	
C3830-52.98	52.98	54.36	53.67	1.38	Sand	H2	
C3830-56.99	56.99	58.37	57.68	1.38	Sand	H2	
C3830-58.29	58.29	59.70	59.00	1.41	Sand to silty sand	H2	0.08 ft of overlap with sample above
C3830-66.06	66.06	67.46	66.76	1.40	Sand	H2	
C3830-71.95	71.95	73.30	72.63	1.35	Sand	H2	
C3830-76.98	76.98	78.35	77.67	1.37	Sand	H2	
C3830-80.91	80.91	82.21	81.56	1.30	Sand	H2	
C3830-86.11	86.11	87.41	86.76	1.30	Sand to silty sand	H2	
C3830-98.97	98.97	100.36	99.67	1.39	Sand	H2	
C3830-100.32	100.32	101.72	101.02	1.40	Silty sand to sandy silt and silt	CCU$_u$	0.04 ft of overlap with sample above
C3830-102.99	102.99	104.44	103.72	1.45	Sandy silt	CCU$_u$	
C3830-107.89	107.89	109.19	108.54	1.30	Sandy silt	CCU$_u$	
C3830-113.55	113.55	115.00	114.28	1.45	Calcareous, pebbly sand and mud	CCU$_l$	Cemented caliche
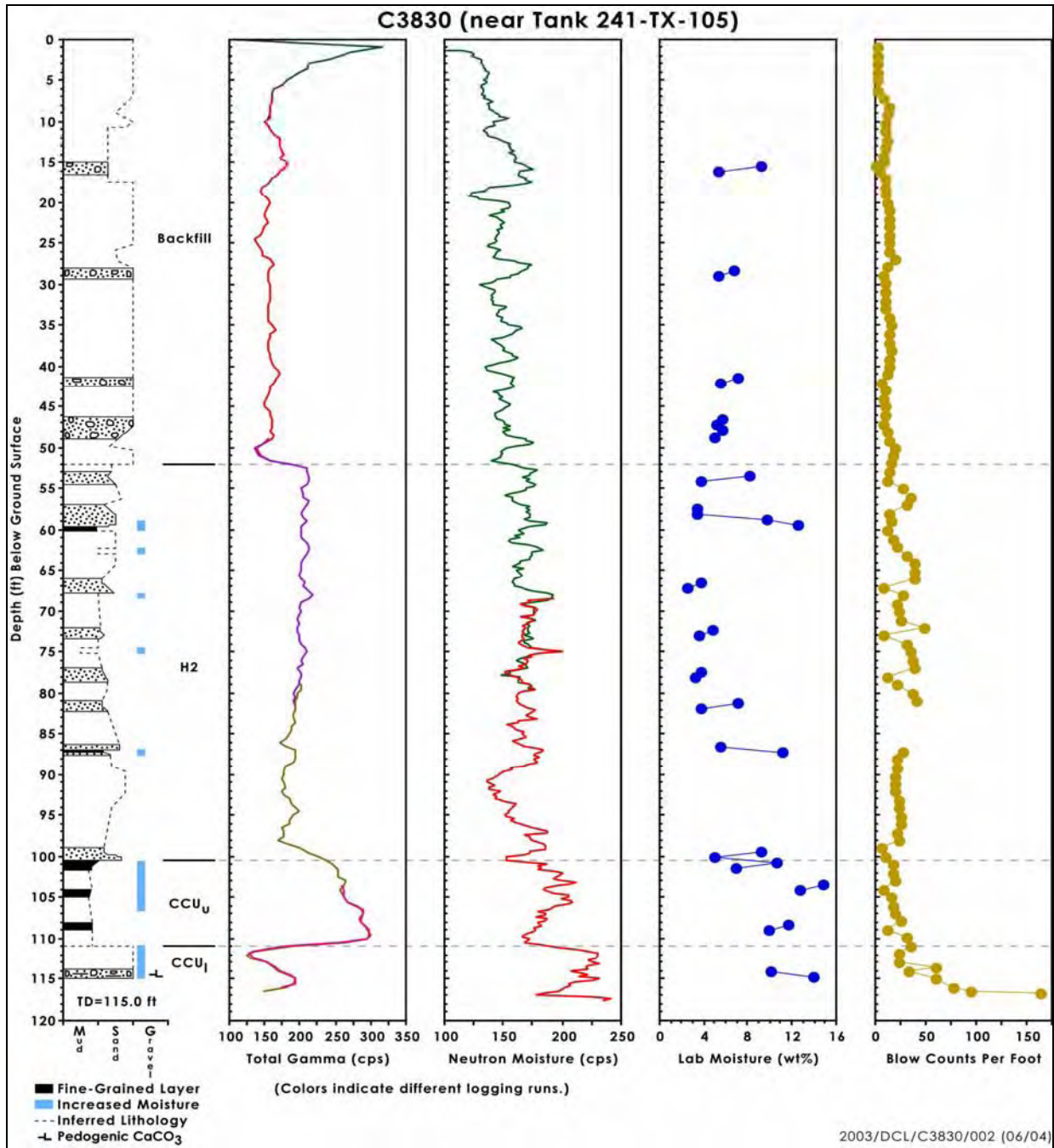
Figure 2.12. Summary Hydrogeologic Log for Borehole C3830. *Zones of increased moisture are indicated as those with >15 wt% water in core samples and/or show as distinct spikes on neutron-moisture log. Fine-grained layers are defined as those consisting predominantly of particles ≤ 0.25 mm in diameter (i.e., fine sand and smaller).*

2.3.3.1 Backfill

The backfill extends from the ground surface to a depth of 15.8 m (52 ft) where it lies in contact with the Hanford formation (Figure 2.12). This depth is consistent with a minimum depth of 45 ft required to completely bury tanks used at TX Tank Farm (Crumpler 2002). A total of 10 physical/chemical characterization samples were collected in backfill material (Table 2.6). Backfill material (Figure 2.13) consists of predominantly grayish brown, poorly to moderately sorted, massive, gravelly sand to slightly gravelly sand, which is unconsolidated and weakly to strongly calcareous (see Appendix B.1 for more detailed descriptions). A sharp increase in total gamma activity in the upper few feet of this hole is associated with near-surface cesium-137 contamination at this location (Reynolds 2003). This unit appears to be rather homogeneous and lacks lithologic variation suggested by relatively uniform geophysical logs and blow-count data (Figure 2.12). Moisture content is also relatively low, averaging about 6 wt% (Table 2.5).

Figure 2.13. Typical Backfill from Borehole C3830. *Core sample C3830-27.91A, described as a slightly moist, dark grayish brown, poorly sorted, pebbly, fine to coarse sand (gS), weakly to moderately calcareous. The top of the 0.5-ft core is to the right. Considerable pulverization of the sample occurred during drilling, as indicated by the abundance of angular gravel clasts.*

2.3.3.2 Hanford Formation

Pleistocene cataclysmic flood deposits of the Hanford formation underlie backfill materials to a depth of 100.4 ft in borehole C3830. Only the sand-dominated Hanford formation H2 unit is represented; all of the coarse-grained Hanford formation H1 unit was removed during tank-farm construction, to be used later as backfill around the tanks.

2.3.3.2.1 Hanford Formation H2 Unit

The Hanford formation H2 unit is present between 52.0 to 100.4 ft bgs. The H2 unit consists of predominantly fine-to-coarse-grained, gray to brownish-gray "salt and pepper" sand (Figure 2.14). H2 unit strata show occasional weak horizontal laminations and are weakly to strongly calcareous. Dispersed within the Hanford formation H2 unit are at least two separate, relatively thin (≤ 0.5 ft), brown to yellow, compact, well-sorted, silty fine sand beds (Figure 2.15). These occur at depths starting at 59.3 and 86.8 ft bgs (Figure 2.12). Other coincident peaks in total gamma and neutron moisture logs suggest additional fine-grained beds are probably present between cored intervals. Zones with increased moisture, both within the sampled cores as well as those interpreted from the geophysical logs, are illustrated together on Figure 2.12. There appears to be a significant increase in penetration resistance (i.e., blow counts) within portions of the Hanford formation H2 unit, relative to the overlying backfill material.

Figure 2.14. **Fine to Medium Sand Recovered from the Hanford Formation H2 Unit in Borehole C3830.** *Core C3830-76.98A, described as slightly moist, light gray, well-sorted, fine to medium sand (S), moderately calcareous. The core separated along natural, well-developed laminations. The top of the 0.5-ft core is to the right.*

Figure 2.15. **Interbedded Sand and Silty Sand Within the Hanford Formation H2 Unit.** *Core C3830-58.29A, described as two lenses of slightly moist, cohesive, brown, well-sorted and laminated silty fine sand (mS), interbedded with loose, grayish-brown, medium-grained sand (S). The top of the 0.5-ft core is to the right.*

A total of 18 characterization samples were obtained from the Hanford formation H2 unit (Table 2.5). Most of the samples are composed of medium- to coarse-grained sand while two of the samples are silty fine sand.

2.3.3.3   Cold Creek Unit

The top of the CCU in C3830 lies at 100.4 ft bgs; the bottom of the hole terminates within the lower CCU. A total of eight characterization samples were collected from the CCU, six from the upper and two from the lower Cold Creek subunits (Table 2.6). The average moisture content (Table 2.5) is significantly greater in the CCU, compared to other stratigraphic units.

2.3.3.3.1   Upper Cold Creek Unit (CCU_u)

The contact between the Cold Creek unit and the overlying Hanford formation H2 unit is at 100.4 ft bgs (Figure 2.16). The upper CCU is 10.6-ft thick.

Figure 2.16. **Contact Between Hanford Formation H2 and Cold Creek Units.** *Contact was encountered in the nose cone of the splitspoon sampler in core #3830-98.7. The contact is well-defined based on the sudden textural, color, and moisture change at 100.4 ft bgs. The Hanford formation H2 unit is described as slightly moist, laminated, moderately sorted, light brownish-gray, fine to coarse sand (S). The underlying CCU$_u$ unit is described as moist, well-sorted, yellowish-brown, silty fine sand (mS). The top of the core is to the right.*

Six samples of the upper CCU were collected for physical and chemical characterization at three different depths within the upper CCU (Table 2.6). Sediments from this unit are compact and well-sorted silt to silty fine sand, which range from laminated to massive and moderately to strongly calcareous. An example of one of the cores is shown in Figure 2.17.

Figure 2.17. **Upper Cold Creek Unit (CCU$_u$) in C3830.** *Core C3830-102.99A, described as moist, laminated to massive, compact, yellowish-brown, fine sandy silt (sM), moderately to strongly calcareous. The top of the 0.5-ft core is to the right.*

2.35

2.3.3.3.2 Lower Cold Creek Unit (CCU$_l$)

Only a single core was obtained from a caliche layer within the lower CCU (Figure 2.18). The hole was abandoned at 115 ft depth after this core sample was collected. Two characterization samples were collected, one from the lower "A" liner and another from the "B" liner.

Figure 2.18. Lower Cold Creek Unit (CCU$_l$) in C3830. *Core C3830-113.55A, described as slightly moist, mottled and cemented, pinkish-gray, very poorly sorted sand, silt, and clay, with a few small pebbles of angular basalt ([g]mS), and very strongly calcareous. Material in this photo is highly fragmented because it had to be manually broken apart to be removed from the core liner. The top of the 0.5-ft core is to the right.*

2.3.4   Borehole C3831 (TX-107)

Borehole C3831 was drilled and sampled using a driven-probe technique between July 1 and August 7, 2002 (Gardner et al. 2002a). The borehole is located approximately 40 ft (12 m) southwest of single-shell tank 241-TX-107 (Figure 2.4). Total depth of the borehole was 115.37 ft (35.2 m) bgs; the hole terminated within the vadose zone about 100 ft (30 m) above the groundwater table. During drilling, a total of 20, 1.25-ft long by 2.5-in.-diameter splitspoon core samples were collected intermittently starting at a depth of 15 ft bgs (Table 2.7, Figure 2.19). Many of the samples were overdriven beyond the 1.25-ft length of the splitspoon, which resulted in over-compaction of some samples. In all, 26.74 ft of core was drilled in C3831, which accounts for about 23% of the total length of the hole. No samples or drill cuttings were collected between the 20 core runs because the hole was advanced in a closed configuration using a solid, removable tip. The surface elevation of the since abandoned borehole was 674.63 ft above mean sea level and geographic coordinates were N136167.19 m and E566732.93 m (Gardner et al. 2002a). Borehole C3831 was decommissioned on August 13-14, 2002 by back-pulling the casing while filling the annulus with dry bentonite (Gardner et al. 2002a).

The same as the other boreholes documented in this report, each splitspoon contained two 0.5-ft-long stainless-steel core liners. A separate subsample was collected from each of the two liners for physical and chemical characterization, making a total of 40 characterization samples collected within this borehole. All but three of the 40 liners were completely full (Gardner et al. 2002a).

All cores were extracted, sampled, photographed, and geologically logged on August 14-15, 2002 in a radiologically controlled PNNL laboratory. Geologic logs of the material within the core liners were generated by geologists Victoria Johnson (Kennedy / Jenks) and Bruce Bjornstad (PNNL); the core logs for these two geologists are presented in Gardner et al. (2002a) and Appendix B.2 of this report, respectively. Geologic logging occurred after the contents of each 0.5-ft stainless-steel core liner was emptied into an open plastic container, followed by photographing and subsampling for physical and chemical characterization. Upon completion of these activities the contents in the plastic containers were sealed shut and placed into cold storage for archival purposes.

No radiological contamination was detected with field instrumentation during the driving and sampling of borehole C3831; however, HPGe spectral logging did detect cobalt-60 from 52 ft (near the base of the backfill and tanks) to total depth (Gardner et al. 2002a). Because of contamination with radionuclides, the total gamma signal is significantly greater than natural background and therefore not useful for interpreting lithology, especially between 52-77 ft bgs (Figure 2.19).

Table 2.7. Splitspoon Core Samples from C3831. Two characterization samples (labeled "A" and "B") were collected from each of the cores for a total of 40 samples.

Core Sample ID	COC#	Top Depth (ft)	Bottom Depth (ft)	Mid Depth (ft)	Sampled Interval Thickness (ft)	Lithology	Strati-graphic Unit	Comments
C3831-15	S02057-01	14.93	16.31	15.62	1.38	Silty sandy gravel	backfill	
C3831-21	S02057-02	20.80	22.30	21.55	1.50	Silty sandy gravel	backfill	
C3831-28	S02057-03	27.96	29.21	28.59	1.25	Silty sandy gravel	backfill	
C3831-45	S02057-04	45.06	46.39	45.73	1.33	Silty sand to gravelly sand	backfill	
C3831-51	S02057-05	51.01	52.36	51.69	1.35	Silty gravelly sand to silty sandy gravel to silty sand	backfill/H2	Contact between backfill and H2 at 52.3 ft bgs
C3831-52	S02057-06	52.16	53.51	52.84	1.35	Sand	H2	
C3831-59	S02057-07	59.04	60.24	59.64	1.20	Sand to silty sand	H2	
C3831-60	S02057-08	60.08	61.50	60.79	1.42	Sand, silt and clay (clastic dike) to sand	H2	Excess free water observed while sampling; ^{60}Co contamination (Gardner et al. 2002a); upper half of this core is a clastic dike; 0.16 ft of overlap with sample above
C3831-67	S02057-09	67.19	68.54	67.87	1.35	Sand to silty sand	H2	
C3831-69	S02057-10	68.43	69.98	69.21	1.55	Sand to silty sand	H2	^{60}Co contamination (Gardner et al. 2002a); 0.11 ft of overlap with sample above
C3831-74	S02057-11	74.04	75.30	74.67	1.26	Sand to silty sand	H2	
C3831-77	S02057-12	76.73	77.98	77.36	1.25	Sand to silty sand	H2	

Table 2.7.   (contd)

Core Sample ID	COC#	Top Depth (ft)	Bottom Depth (ft)	Mid Depth (ft)	Sampled Interval Thickness (ft)	Lithology	Strati-graphic Unit	Comments
C3831-78	S02057-13	77.76	79.04	78.40	1.28	Sand to silty sand	H2	0.22 ft of overlap with sample above
C3831-85	S02057-14	85.05	86.30	85.68	1.25	Sand to silty sand to sandy silt	H2	
C3831-88	S02057-15	88.30	89.75	89.03	1.45	Sand	H2	
C3831-93	S02057-16	93.05	94.30	93.68	1.25	Sand	H2	
C3831-97	S02057-17	97.11	98.38	97.75	1.27	Sand to silty sand and silt	H2	
C3831-100	S02057-18	100.20	101.65	100.93	1.45	Sand to silty sand	H2	
C3831-102	S02057-19	101.63	102.98	102.31	1.35	Silty sand	CCU$_u$	0.02 ft of overlap with sample above
C3831-114	S02057-20	114.12	115.37	114.75	1.25	Slightly gravelly muddy sand	CCU$_l$	Borehole refuses to advance through cemented caliche

The hole was advanced via a solid probe so no grab samples were collected between core runs; thus no geologic field log is available for this hole. Figure 2.19 presents a summary log for C3831 based on available geologic descriptions, core photographs, geophysical logs, laboratory measured gravimetric moisture, and blow-count data. The geology between core runs is inferred and interpreted based on these data. Four primary stratigraphic units were encountered by this borehole: 1) recent backfill materials, 2) the Hanford formation, 3) the Cold Creek unit, and 4) the Ringold Formation. A brief description of the sampled materials from each of these stratigraphic intervals is presented in Sections 2.3.4.1−2.3.4.3.2.
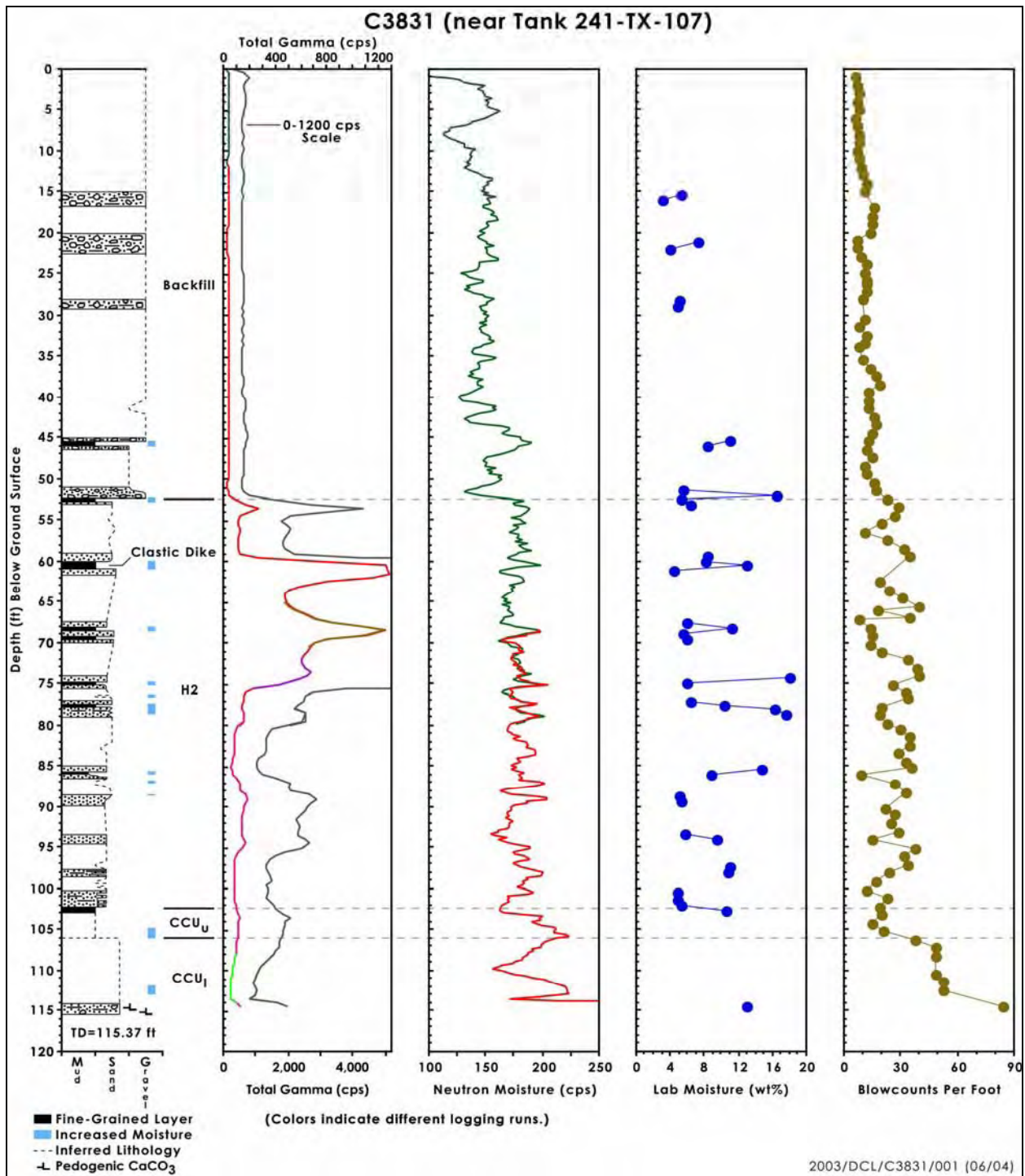
Figure 2.19. Summary Hydrogeologic Log for Borehole C3831. *Penetration resistance (i.e., blow-count) data is from Gardner et al. (2002a). Zones of increased moisture are indicated as those with >15 wt% water in core samples and/or show as distinct spikes on neutron-moisture log. Fine-grained layers are defined as those consisting predominantly of particles ≤ 0.25 mm in diameter (i.e., fine sand and smaller).*

2.3.4.1   Backfill

The backfill extends from the ground surface to a depth of 15.9 m (52.3 ft) where it lies in contact with the Hanford formation (Figure 2.19). This depth is consistent with a minimum depth of 45 ft required to completely bury tanks used at the TX Tank Farm (Crumpler 2002). Five of the 20 splitspoons contained backfill materials. The backfill material consisted of predominantly dark gray to brown, poorly to very poorly sorted, silty sandy gravel, which was unconsolidated and moderately calcareous. A finer-grained layer of laminated silty sand, about one ft thick, occurred within the backfill at about 46 ft bgs (Figure 2.20). Rust-coated fragments of metal (nails?) at the base of this layer prove a backfill origin.

Figure 2.20.   Rusted Metal Fragments from Backfill Material in C3831. *Metal fragments came from 46 ft depth. The top of the 0.5-ft core is to the right.*

The total gamma and neutron-moisture activity is generally low in the backfill materials. Blow counts are also lower in the backfill, compared to the underlying Hanford formation (Figure 2.19). Because of subsurface contamination with radionuclides below the backfill, background gamma activity appears washed out through the backfill in Figure 2.19 and therefore not very useful for interpreting lithology.

2.3.4.2   Hanford Formation

About 50 ft of Pleistocene cataclysmic flood deposits of the Hanford formation underlie backfill materials in C3831. Only the sand-dominated Hanford formation H2 is represented; all of the coarser-grained Hanford formation H1 unit was removed during tank-farm construction and later used as backfill around the tanks.

2.3.4.2.1   Hanford Formation H2 Unit

The Hanford formation H2 unit is present between 52.3 to 102.2 ft bgs. A total of 27 physical and chemical characterization samples were collected from within this unit (Table 2.7). The Hanford formation H2 sediments consist of mostly fine to coarse sand, sometimes capped or interbedded with thin beds of silty fine sand to silt (Figures 2.21 and 2.22). The fine to coarse sand beds are loose, massive to laminated, brownish-gray to olive-brown, moderately to well-sorted, and weakly to moderately calcareous. Finer-grained beds are generally very well sorted, cohesive, massive to laminated, yellowish- to olive-brown, and moderately to strongly calcareous.

Figure 2.21.   Hanford Formation H2 Unit in C3831 - Core C3831-69A. *Mostly a slightly moist, loose, well-sorted, laminated, moderately calcareous, medium to coarse, "salt and pepper"-like, grayish-brown sand (S). A few thin lenses of brownish, silty fine sand (mS) are interspersed. The top of the 0.5-ft-long core is to the right.*

The base of the Hanford formation in C3831 contains a number of fine-grained layers of silty fine sand to silt interbedded with coarser sands (Figure 2.22). Two types of soft-sediment deformation were observed within the Hanford formation H2 unit of C3831: 1) a clastic dike, and 2) load structures (Figure 2.23). A single clastic dike was observed within the Hanford formation H2 unit at about 60 ft bgs. The clastic dike is characterized by compact and cohesive, sub-vertically laminated, grayish brown sand to dark gray silt and clay. A few small pebbles are also present within the dike, which is moderately calcareous. The clastic dike shows a higher moisture content compared to adjacent strata, probably as a

Figure 2.22. **Interbedded, Laminated Sand and Silt Near Base of the Hanford Formation H2 Unit - Core 3831-97A.** *Slightly moist, loose, fine to medium sand (S) is interbedded with more cohesive silty fine sand (mS) to silt (M) layers.*

Figure 2.23. **Soft-Sediment Deformation Within the Hanford Formation H2 Unit.** *Left Photo: Core C3831-60B, 0.5-ft long. Moist clastic dike, with alternating sub-vertical layers of sand, silt, and clay. Right Photo: C3831-85B, 0.3-ft long. Syndepositional loading and deformation occurred along the contact between slightly moist, fine to medium sand (above) and moist silt (below). The tops of the cores are to the right.*

result of the presence of more fine-grained material, which tends to retain more moisture. Discordant clastic dikes, which are common to the Hanford formation, probably formed during or soon after Ice-Age flood episodes (Fecht et al. 1999).

"Ball and pillow" and flame structures (right photo in Figure 2.23) are a type of soft sediment deformation related to the differential loading of rapidly deposited sediment (Reineck and Singh, 1975). The mechanism involves rapid flood deposition onto a saturated and fine-grained substrate, which is unable to support the sudden added weight and loading of the overlying bed. As a result, material from the underlying bed is squeezed upward and protrudes into the overlying bed, creating flame structures. Where the underlying fine-grained material became completly enveloped within the coarser overlying material, "ball and pillow" structures formed.

2.3.4.3   Cold Creek Unit

The contact between the Cold Creek unit and the overlying Hanford formation H2 unit lies at about 102.2 ft bgs (Figure 2.19). Two samples each were collected for characterization from the upper and lower Cold Creek units, respectively.

2.3.4.3.1   Upper Cold Creek Unit (CCU$_u$)

Sediments from this unit are compact and well-sorted silt to silty fine sand, which range from laminated to massive and moderately to strongly calcareous. An image of one of the cores collected from the top of the upper CCU in C3831 is shown in Figure 2.24. The upper CCU in C3831 is relatively thin (only 3.8 ft-thick) compared to other nearby boreholes. As in most other holes through the upper CCU, the neutron moisture and total gamma activity are slightly elevated on geophysical logs (Figure 2.19).

Figure 2.24.   Upper Cold Creek Unit in C3831 - Core 3831-102A. *Described as slightly moist, weakly laminated, well-sorted, strongly calcareous, yellowish-brown, silty fine sand (mS). The top of the 0.5-ft core is to the right.*

2.3.4.3.2   Lower Cold Creek Unit (CCU$_l$).

The top of the lower CCU lies at a depth of about 106 ft, where there is a sudden increase in penetration resistance (Figure 2.19) and extends to the bottom of the hole at 115.37 ft. The casing met refusal between 113.9 and 114.1 ft bgs. The hard, cemented nature of the formation was corroborated by the permanent damage to the shoe, as observed upon removal of the casing (Gardner et al. 2002a). Only a single core was obtained from the lower CCU; this came from the bottom of the borehole (Figure 2.25).

Figure 2.25.   Lower Cold Creek Unit Within C3831 - Core 3831-114A. *Described as slightly moist, poorly sorted, strongly to very strongly calcareous, moderately to strongly consolidated, yellowish brown, slightly gravelly silty sand ([g]zS), mottled with gray to brownish-gray, pedogenic, calcium-carbonate cemented caliche nodules and stringers. Includes about 5% small, angular, matrix-supported basalt pebbles. The sample in the tray had to be broken up in order to be removed from the core liner. The top of the 0.5-ft core is to the right.*

2.3.5   Hydrogeology of Borehole C3832 (TX-104)

Borehole C3832 was drilled and sampled using a driven-probe technique between May 2 and June 3, 2002 (Gardner et al. 2002b). The borehole is located about 20 ft (6 m) south-southeast of single-shell tank 241-TX-104 (Figure 2.4). Total depth of the borehole was 115.89 ft (35.3 m) bgs; casing refusal (blow counts in excess of 120 blows per foot) occurred at 113.77 ft bgs (Gardner et al. 2002b). Soon afterwards, the hole was terminated about 100 ft (30 m) above the groundwater table.

During drilling, a total of 19, 1.25-ft-long by 2.5-in.-diameter splitspoon core samples were collected intermittently starting at a depth of about 16 ft bgs (Table 2.8, Figure 2.26). Two, 0.5-ft-long stainless-steel core liners were collected during each core run. One characterization sample was obtained from each 0.5-ft liner, for a total of 38 characterization samples. In all, 27.09 ft of core was drilled, which accounts for about 23% of the total length of the hole (Table 2.2). Most of the samples were driven beyond the 1.25-ft length of the splitspoon, suggesting most cores were over-compacted during drilling. While over-compaction can destroy the sedimentary structure and alter hydraulic properties (i.e., density and porosity), it does not adversely affect chemical or radiological analysis. No samples or drill cuttings

were collected between the 19 core runs since the hole was advanced in a closed configuration using a solid, removable tip. Borehole C3832 was decommissioned on June 12-13, 2002 by back-pulling the casing while filling the hole with dry bentonite. The surface elevation of the abandoned borehole was 676.57 ft above mean sea level and the geographic coordinates were N136137.32 m and E566717.68 m (Gardner et al. 2002b).

Core extraction, logging and sampling were performed later in a radiologically controlled PNNL laboratory between June 11-12, 2002. A geologic log of the material within the core liners was compiled by geologists Victoria Johnson (Kennedy / Jenks Consultants, Inc.) and Bruce Bjornstad (PNNL); the core logs for these two geologists are presented in Gardner et al. (2002b) and, for Bjornstad, in Appendix B.3 of this report, respectively. Geologic logging occurred after each 0.5-ft core segment was emptied into an open plastic container, followed by photographing and subsampling for physical and chemical characterization. Upon completion of these activities, the contents in the plastic containers were sealed shut and placed into cold storage for archival purposes.

Between core runs, the hole was advanced using a closed-end probe so no grab samples were collected between core runs; thus no geologic field log is available for this hole. Figure 2.26 presents a summary log for C3832 based on geologic descriptions, core photographs, laboratory-derived gravimetric moisture, blow counts, and geophysical logs. The geology between core runs is inferred and interpreted based on the geophysical log and blow-count data. Four primary stratigraphic units were encountered in this borehole: 1) recent backfill material, 2) the Hanford formation, 3) the Cold Creek unit, and 4) the Ringold Formation. The description and photographs of the sampled materials from each of these major stratigraphic units is presented below.

Table 2.8. Splitspoon Core Samples from C3832. Two characterization samples, labeled "A" and "B" were collected from each of the cores for a total of 38 samples.

Core Sample ID	COC#	Top Depth (ft)	Bottom Depth (ft)	Mid Depth (ft)	Sampled Interval Thickness (ft)	Lithology	Strati-graphic Unit	Comments
C3832-15	S02046-02	16.21	17.61	16.91	1.40	Silty sandy gravel	backfill	
C3832-28	S02046-03	28.09	29.49	28.79	1.40	Silty sandy gravel	backfill	
C3832-37	S02046-04	36.09	37.49	36.79	1.40	Sandy gravel	backfill	
C3832-44	S02046-05	44.14	45.54	44.84	1.40	Silty sand	backfill	Free water present during sampling
C3832-52	S02046-06	51.18	52.28	51.73	1.10	Sand	H2	
C3832-53	S02046-07	53.08	54.43	53.76	1.35	Sand to silty sand	H2	
C3832-61	S02046-08	60.12	61.52	60.82	1.40	Sand	H2	
C3832-62	S02046-09	61.76	63.36	62.56	1.60	Silty sand to sand	H2	
C3832-69	S02046-10	69.01	70.31	69.66	1.30	Sand to silty sand	H2	
C3832-76	S02046-11	75.99	77.39	76.69	1.40	Sand to silty sand	H2	
C3832-79	S02046-12	78.29	80.31	79.30	2.02	Sand to silty sand/sandy silt	H2	
C3832-83	S02046-13	82.99	84.34	83.67	1.35	Sand to silty sand	H2	^{60}Co contamination along contact between sand/silt (Gardner et al. 2002c)
C3832-87	S02046-14	86.99	88.41	87.70	1.42	Sand to silty sand	H2	
C3832-93	S02046-15	92.99	94.40	93.70	1.41	Sand to silty sand	H2	
C3832-96	S02046-16	95.64	97.04	96.34	1.40	Sand	H2	
C3832-104	S02046-17	103.94	105.36	104.65	1.42	Silty sand to silt	CCU$_u$	
C3832-110	S02046-18	109.91	111.38	110.65	1.47	Silty sand to calcic pebbly muddy sand	CCU$_u$/CCU$_l$	Contact between upper and lower Cold Creek unit at 110.4 ft
C3832-114	S02046-19	113.77	115.20	114.49	1.43	Pebbly sandy mud	CCU$_l$	
C3832-121	S02046-20	114.47	115.89	115.18	1.42	Pebbly sandy mud	CCU$_l$	0.73 ft of overlap with sample above
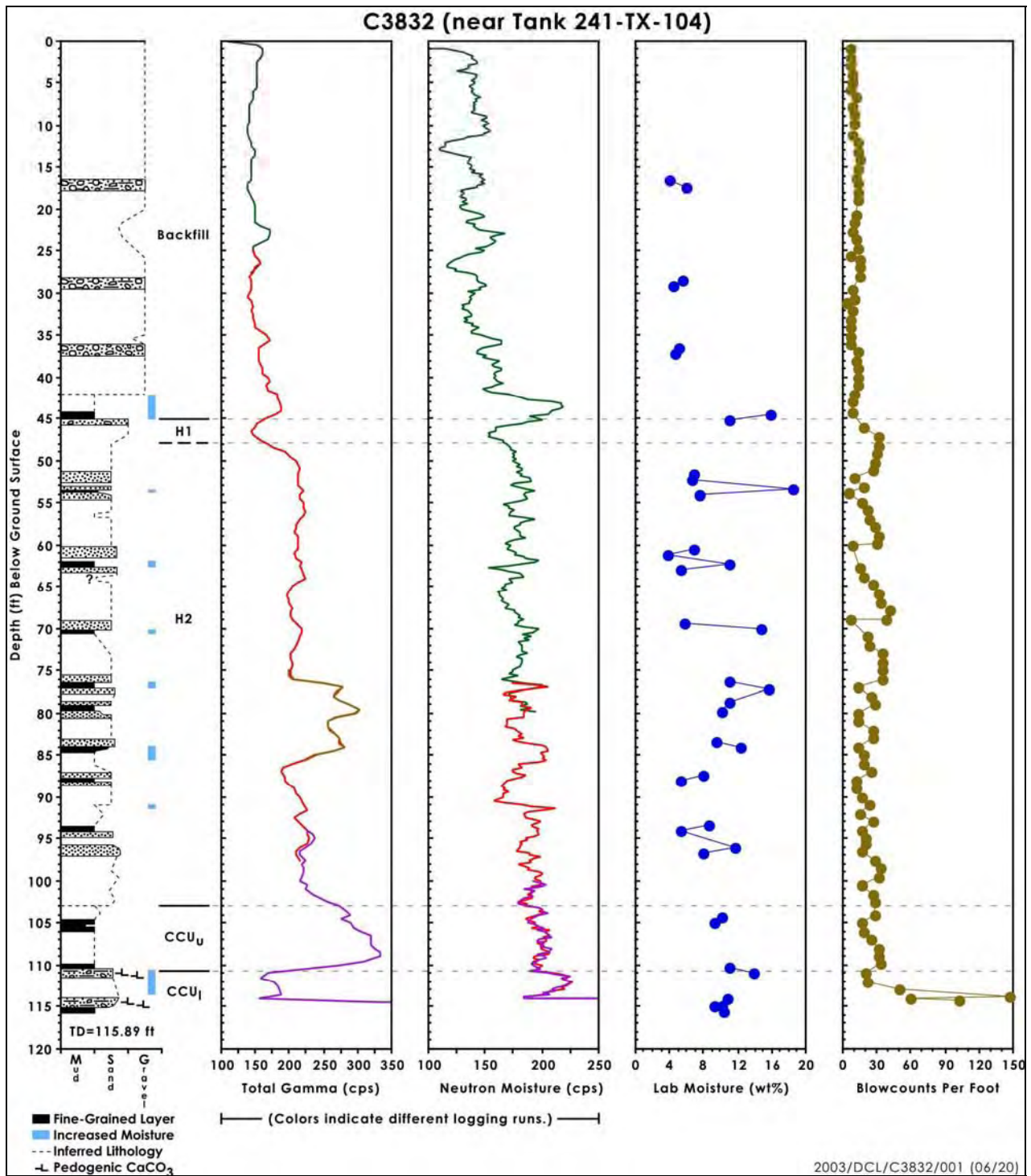
Figure 2.26. Summary Hydrogeologic Log for Borehole C3832. *Penetration resistance (i.e., blow-count) data is from Gardner et al. (2002b). Zones of increased moisture are indicated as those with >15 wt% water in core samples and/or show as distinct spikes on the neutron-moisture log. Fine-grained layers are defined as those consisting predominantly of particles ≤ 0.25 mm in diameter (i.e., fine sand and smaller).*

2.3.5.1 Backfill

The backfill extends from the ground surface to a depth of 45 ft (13.7 m) where it lies in contact with the Hanford formation (Figure 2.26). This depth is exactly the height of the tanks buried in the TX Tank Farm (Crumpler 2002). Four of the 19 splitspoons contained backfill materials. The backfill material consisted of mostly loose, dark gray to brown, very poorly sorted, sandy gravel to silty sandy gravel, which was slightly moist and weakly to moderately calcareous (Figure 2.27). Several feet or more of wet to moist, cohesive, well-sorted, strongly calcareous, dark grayish-brown, silty fine sand is present at the base of the backfill sequence (Figure 2.28). This material appears to be from a compacted zone at the bottom of the tank-farm excavation; free water was reported in this material during core sampling (Gardner et al. 2002b). Fine-grained sand and silt was occasionally placed at and toward the base of the backfill within the TX Tank Farm, apparently to improve traction for construction vehicles (DOE-GJO 1997).

The total gamma and neutron-moisture activity is generally low in the backfill materials of C3832. Blow counts are also uniformly lower in the backfill, compared to the underlying Hanford formation (Figure 2.26).

Figure 2.27. Backfill from C3832 - Core C3832-28A. *Described as slightly moist, loose, very poorly sorted, weakly to moderately calcareous, dark grayish-brown, silty sandy gravel (msG). The top of the 0.5-ft core is to the right.*

Figure 2.28. Fine-Grained Sediments at Base of Backfill Sequence - Core C3832-44A. *Described as a moist, consolidated, well-sorted, strongly calcareous, dark grayish-brown, felsic, silty fine to very fine sand (mS). The top of the 0.5-ft core is to the right.*

2.3.5.2   Hanford Formation

A total of 58 ft of Pleistocene cataclysmic flood deposits of the Hanford formation underlie backfill materials in C3832. Only the sand-dominated Hanford formation H2 is represented; all of the coarser-grained Hanford formation H1 unit was removed during tank-farm construction.

2.3.5.2.1   Hanford Formation H2 Unit

The Hanford formation H2 unit is present between 45 to 103 ft bgs. A total of 22 physical and chemical characterization samples were collected from within this unit (Table 2.8). The Hanford formation H2 sediments consist of mostly fine to coarse sand, sometimes capped or interbedded with thin beds of silty fine sand to silt (Figure 2.29). The fine to coarse sand beds are loose, massive to laminated, brownish-gray to olive-brown, moderately to well-sorted, and weakly to moderately calcareous. Finer grained beds are generally well-sorted, cohesive, massive to laminated, yellowish- to olive-brown, and moderately to strongly calcareous.

Figure 2.29. Hanford Formation H2 Unit in C3832 - Core C3832-83A. *Alternating layers of slightly moist, well laminated, moderately to well-sorted, loose, grayish-brown, medium sand (S), and moist, compact, strongly calcareous, light olive-brown, silty fine sand (mS). The top of the 0.5-ft-long core is to the right.*

2.3.5.3   Cold Creek Unit

The contact between the Cold Creek unit and the overlying Hanford formation H2 unit lies at about 103 ft bgs (Figure 2.26). Three characterization samples were collected from the upper CCU while five came from the calcic paleosol sequence of the lower CCU (Table 2.8).

2.3.5.3.1   Upper Cold Creek Subunit (CCU$_u$)

The upper CCU in C3832 is 7.4 ft-thick and consists of compacted and well-sorted, mottled to laminated, moderately to strongly calcareous, yellowish-brown to olive-brown, silt to silty fine sand (Figure 2.30). The top of the upper CCU is defined by a dramatic decrease in grain size and an increase in the total gamma activity, as demonstrated in Figure 2.26. The base of the upper CCU lies in sharp contact with the caliche of the underlying lower CCU.

Figure 2.30. Upper Cold Creek Unit in C3832 - Core 3832-110B. *Described as slightly moist, laminated, well-sorted, strongly calcareous, olive-brown, silty fine sand (mS). Whitish CaCO$_3$-cemented nodules to the left are associated with the underlying caliche of the lower CCU. The top of the 0.5-ft core is to the right.*

2.3.5.3.2   Lower Cold Creek Unit (CCU$_l$).

The lower CCU extends from a depth of 100.4 ft to the bottom of hole at 115.89 ft bgs. The uppermost few feet of the lower CCU are relatively soft compared to deeper depths where there is a sharp increase in penetration resistance (Figure 2.26). The casing met refusal at 114.29 ft bgs. The resistant bottom of the borehole consisted of mostly olive-colored clay and silt mottled with pedogenic calcium carbonate stringers and nodules (Figure 2.31).

Figure 2.31. Lower Cold Creek Unit Within C3832 - Core C3832-121A. *Described as slightly moist, very poorly sorted, mottled to massive, strongly to very strongly calcareous, strongly consolidated, olive, pebbly sandy mud (gsM), mottled with gray to brownish-gray, pedogenic, calcium-carbonate-cemented caliche nodules and stringers. Includes about 10% small pebbles. The sample in the tray was broken apart during removal from the core liner. The top of the 0.5-ft core is to the right.*

2.4 Discussion of Increased Moisture Zones

Zones of increased moisture in the vadose zone may be determined indirectly using the downhole, neutron moisture geophysical log and/or, when available, gravimetric moisture may be measured directly from core samples in the laboratory. As discussed previously, borehole 299-W10-27 (Figure 2.9) was continuously cored and sampled between 50-125 ft bgs. Lab moisture results in Figure 2.9 show a close correlation with the neutron moisture log. Therefore, the neutron moisture log appears to accurately reflect the relative moisture content, and can confidently be used as a substitute to estimate relative moisture conditions when core samples are unavailable.

The moisture distribution for three boreholes C3830, C3831, and C3832 are shown in Figures 2.12, 2.19, and 2.26, respectively. Similarly, moisture distribution for the background well (299-W10-27) is shown in Figure 2.9. Zones with relatively high moisture (>15 wt%) are illustrated via a light blue bar immediately to the right of the lithologic log in these diagrams.

Increased moisture appears to be associated with the boundary between sudden, large contrasts in grain size. Commonly, a lower-permeability fine-grained silty layer may be present along the boundary, but is not required for a high-moisture zone to develop. Depending on the flux rate, moisture may collect and move laterally 1) within finer-grained layers, 2) along interfaces between highly contrasting facies, or 3) along primary sedimentary structures (Bjornstad et al. 2003). Moisture may also move vertically along discordant clastic dikes. During high flux rates moisture moves preferentially within the coarser units in contrast to fine-grained layers, which transmit relatively more moisture under a low flux rate.

Generally <10 wt% moisture content is associated with backfill materials, except where fine-grained sand and/or silt occurs within backfill deposits, such as near the base of the backfill sequence in C3831 (Figure 2.19) and C3832 (Figure 2.26). Figure 2.32 shows a statistical analysis of moisture conditions at different stratigraphic levels for each of the four borings documented in this report. Conclusions that can be drawn from this table include:

There is relatively higher moisture for the Cold Creek unit in all holes, especially for the lower CCU (i.e., caliche), although it is variable.

- Gravelly backfill materials have relatively little moisture, generally <10 wt%, except for fine-grained zones that occasionally occur at the base of this unit.

- Average moisture content for the Hanford formation H2 unit in the background hole is significantly less than C3830, C3831, and C3832. This may be attributed to either:

  1. sample bias. Moisture samples from 299-W10-27 were collected at regular 1-ft intervals, whereas the C3830, C3831, and C3832 borehole intervals were pre-selected based on suspected contamination (i.e., high moisture), or

  2. higher natural recharge beneath the tank farms due to the removal of surface vegetation. In exchange for vegetation, a cover of gravel was placed, which significantly reduces or eliminates near-surface transpiration of moisture back to the atmosphere.
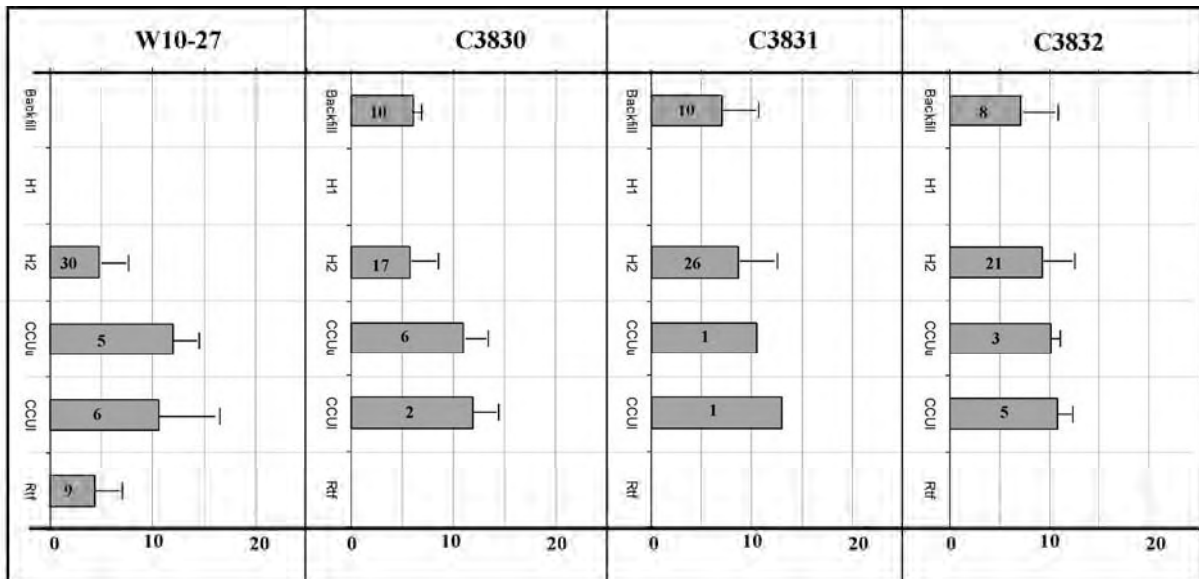
Figure 2.32.   Average Moisture Content (wt% water) from Different Stratigraphic Units in the Vicinity of the TX Tank Farm. *Numbers in shaded boxes are the number of analyses; lines to the right of the boxes are one standard deviation from the mean.*

3.0 Geochemical Methods and Materials

This section discusses the methods and philosophy used to determine which borehole samples would be characterized and the parameters that would be measured and analyzed in the laboratory. It also describes the materials and methods used to conduct analyses of the physical, geochemical, and radioanalytical properties of the sediments, and the water potential (suction) measurements of the core liners in each sequential splitspoon sample from borehole 299-W10-27.

3.1   Sample Inventory

Samples were identified using a project-specific prefix, in this case, C3125 (for the background borehole 299-W10-27), C3830 (for the borehole southwest of TX-105), C3831 (for the borehole southwest of TX-107), and C3832 (for the borehole south of TX-104), followed by a specific sample identification suffix such as -01, for each splitspoon. As noted in Section 2.3, the cores contained two liners identified by the letters A and B, where the A Liner was always in the deeper position closest to the drive shoe (i.e., the protective end attached to the bottom of the drive casing).

3.2   Approach

During a past investigation at WMA SX, a significant finding was that changes in sediment type and contaminant concentrations occurred within a distance of a few inches within a given liner. It was concluded that a more methodical scoping approach would be necessary to provide the technical justification for selecting samples for detailed characterization as defined in the data quality objectives process (DOE 1999). Subsequently, a method was developed that considered depth, geology (e.g., lithology, grain-size composition, and carbonate content, etc.), individual liner contaminant concentration (e.g., radionuclides, nitrate), moisture content, and overall sample quality. Inexpensive analyses and certain key parameters (i.e., moisture content, gamma energy analysis) were performed on sediment from each liner. More complicated and costly analyses were performed on sediment from selected depths.

The objective of the TX characterization was to quantify the extent of penetration of mobile contaminants into the vadose zone sediment. Because of the potential for slough material in the upper liner, only the sediment from the A Liner was analyzed for most constituents except moisture and gamma energy. Measurable or significant drag-down effects (i.e., the process of moving contaminants down through the sediment column via pushing the casing) for contaminants were not noted, perhaps because the borehole was installed by pile driving closed end casing with periodic sampling through the retractable nose cone, and the main contaminants (i.e., uranium-238 and technetium-99) are associated mainly with the porewater (technetium-99) or not exclusively concentrated on the sediment particles (uranium-238). Because drag-down is dominated by highly contaminated sediment particles, the contaminants in these boreholes had less chance of concentrating on particles.

During the geologic examination, the liner contents were subsampled for moisture content, gamma-emission radiocounting, 1:1 water extracts (which provide soil pH, electrical conductivity (EC), cation, and anion data), total carbon and inorganic carbon content, and 8 M nitric acid extracts (which provide a measure of the total leachable sediment content of contaminants). The remaining sediment from each

liner was then sealed and placed in cold storage. Later, additional aliquots of selected liners from clean borehole 299-W10-27 were removed to measure particle size distribution and total chemical composition.

3.3   Materials and Methods

During subsampling of the selected core liner, every effort was made to minimize moisture loss and prevent cross contamination between samples. Depending on the sample matrix, very coarse pebble and larger material (i.e., >32 millimeter [mm]) was avoided during subsampling. Larger substrate was excluded to provide moisture contents representative of counting and 1:1 sediment:water extract samples. Therefore, the results from the subsample measurements may contain a possible bias toward higher concentrations for some analytes that would be preferentially associated with the smaller sized sediment fractions. The sediment in the lower Cold Creek unit (silt-dominated facies) contained no large pebbles or cobbles.

Procedures ASTM D2488-93 (1993) and PNL-MA-567-DO-1 (PNL 1990a) were followed for visual descriptions and geologic description of all splitspoon samples. The sediment classification scheme used for geologic identification of the sediment types is based on the modified Folk/Wentworth classification scheme described earlier (Section 2.3.1.3 and Figure 2.8). However, the particle size distribution for samples from the background well was also performed where further separation of the mud into discrete silt and clay size fractions was performed.

3.3.1   Moisture Content

Gravimetric water contents of the sediment samples from each liner were determined using PNNL procedure PNL-MA-567-DO-1 (PNL 1990a). This procedure is based on the American Society for Testing and Materials procedure *Test Method for Laboratory Determination of Water (Moisture) Content of Soil and Rock by Mass* (ASTM D2216-98 [ASTM 1998]). One representative subsample of at least 15 to 70 grams (g) was taken from each liner. Sediment samples were placed in tared containers, weighed, and dried in an oven at 105°C (221°F) until constant weight was achieved, which took at least 24 hours. The containers then were removed from the oven, sealed, cooled, and weighed. At least two weighings, each after a 24-hour heating, were performed to ensure that all moisture was removed. All weighings were performed using a calibrated balance. A calibrated weight set was used to verify balance performance before weighing samples. The gravimetric water content was computed as the percentage change in soil weight before and after oven drying.

3.3.2   1:1 Sediment:Water Extracts

The water-soluble inorganic constituents were determined using a 1:1 sediment:deionized-water extract method. This method was chosen because the sediment was too dry to easily extract vadose zone porewater. The extracts were prepared by adding an exact weight of deionized water to approximately 60 to 80 g of sediment subsampled from each liner. The weight of deionized water needed was calculated based on the weight of the field-moist samples and their previously determined moisture contents. The sum of the existing moisture (porewater) and the deionized water was fixed at the mass of the dry sediment. The appropriate amount of deionized water was added to screw cap jars containing the sediment samples. The jars were sealed and briefly shaken by hand, then placed on a mechanical orbital shaker for one hour. The samples were allowed to settle until the supernatant liquid was fairly clear. The supernatant was carefully decanted and separated into unfiltered aliquots for conductivity and pH

determinations, and filtered aliquots (passed through 0.45 μm membranes) for anion, cation, carbon, and radionuclide analyses. More details can be found in Rhoades (1996) and within *Methods of Soils Analysis - Part 3* (ASA 1996a).

3.3.2.1   pH and Conductivity

Two approximately 3-mL aliquots of the unfiltered 1:1 sediment:water extract supernatant were used for pH and conductivity measurements. The pHs for the extracts were measured with a solid-state pH electrode and a pH meter calibrated with buffers 4, 7, and 10. Electrical conductivity was measured and compared to potassium chloride standards with a range of 0.001 M to 1.0 M.

3.3.2.2   Anions and Small Organic Acids

The 1:1 sediment:water extracts were analyzed for anions using an ion chromatograph. Fluoride, acetate, formate, chloride, nitrite, bromide, nitrate, carbonate, phosphate, sulfate, and oxalate were separated on a Dionex AS17 column with a gradient elution of 1 mM to 35 mM sodium hydroxide and measured using a conductivity detector. This methodology is based on U.S. Environmental Protection Agency (EPA) Method 300.0A (EPA 1984) with the exception of using the gradient elution of sodium hydroxide. Only small carbon chained organic acids elute with the inorganic anions using this procedure, and no attempts were made to measure other soluble organic components. Water extract chromatograms were visually scanned to assure there were no unidentified peaks caused by other constituents. No unexpected peaks were found in the water extracts from the background or contaminated sediments.

3.3.2.3   Cations and Trace Metals

Major cation analysis was performed using an inductively coupled plasma-optical emission spectrometry (ICP-OES) unit using high-purity calibration standards to generate calibration curves and verify continuing calibration during the analysis run. Dilutions of 100x, 50x, 10x, and 5x were made of each 1:1 water extract for analysis to investigate and correct for matrix interferences. Details of this method are found in EPA Method 6010B (EPA 2000b). The second instrument used to analyze trace metals, including technetium-99 and uranium-238, was an inductively coupled plasma-mass spectrometer (ICP-MS) using PNNL-AGG-415 method (PNNL 1998). This method is quite similar to EPA Method 6020 (EPA 2000c).

3.3.2.4   Alkalinity and Carbon

The alkalinity and inorganic/organic carbon content of several of the 1:1 sediment:water extracts were measured using standard titration with acid and a carbon analyzer, respectively. The alkalinity procedure is equivalent to the U.S. Geological Survey (USGS) *National Field Manual* (USGS 2001) method. Inorganic and organic carbon in the water extracts were determined using a carbon analyzer and ASTM Method D4129-88 (ASTM 1988), *Standard Test Method for Total and Organic Carbon in Water by High Temperature Oxidation and by Coulometric Detection.*

3.3.3 Radioanalytical Analysis

3.3.3.1 Gamma Energy Analysis

Gamma energy analysis (GEA) was performed on sediment from either the A or the B core liners for the three TX boreholes. For C3831, sediment from both the A and the B liners was counted. All samples for gamma energy analysis were analyzed using 60%-efficient intrinsic germanium gamma detectors. All germanium counters were efficiency calibrated for distinct geometries using mixed gamma standards traceable to the National Institute of Standards and Technology. Field-moist samples were placed in 150-cm^3 counting containers and analyzed for 100 minutes in a fixed geometry. All spectra were background-subtracted. Spectral analysis was conducted using libraries containing most mixed fission products, activation products, and natural decay products. Control samples were run throughout the analysis to ensure correct operation of the detectors. The controls contained isotopes with photo peaks spanning the full detector range and were monitored for peak position, counting rate, and full-width half-maximum. Details are found in *Gamma Energy Analysis, Operation, and Instrument Verification using Genie2000™ Support Software* (PNNL 1997).

3.3.3.2 Total Beta and Total Alpha Measurements on Water and Acid Extracts

Gross alpha and beta measurement were made on both the water and acid extracts. For each extract, an ~ 1-mL sample volume was placed in a 20-mL tared liquid scintillation and weighed. Fifteen mL of scintillation cocktail were then added and the samples were mixed and counted on a Wallac Model 1415 Liquid Scintillation Counter as prescribed in procedure AGG-RRL-002, *Liquid Scintillation Counting and Instrument Verification Using the 1400 DSA™Support Software* (PNNL 2000). Results were converted to picocuries (pCi) per gram of dry sediment by using the known solution-to-solid ratios used to extract aliquots of the sediment.

3.3.4 Carbon Content of Sediment

The carbon content of borehole sediment samples was determined using ASTM Method D4129-88, *Standard Methods for Total and Organic Carbon in Water by High Temperature Oxidation and by Coulometric Detection* (ASTM 1988). Total carbon in all samples was determined using a Coulometrics, Inc. Model 5051 Carbon Dioxide Coulometer with combustion at approximately 980°C (1796°F). Ultrapure oxygen was used to sweep the combustion products through a barium chromate catalyst tube for conversion to carbon dioxide. Evolved carbon dioxide was quantified through coulometric titration following absorption in a solution containing ethanolamine. Equipment output reported carbon content values in micrograms per sample. Soil samples for determining total carbon content were placed into pre-combusted, tared platinum combustion boats and weighed on a four-place analytical balance. After the combustion boats were placed into the furnace introduction tube, a one-minute waiting period was allowed so that the ultrapure oxygen carrier gas could remove (i.e., sparge) any carbon dioxide introduced to the coulometric system from the atmosphere during sample placement. After this system sparge, the sample was moved into the combustion furnace and the titration was begun. Sample titration readings were performed at 3 minutes after combustion began and again once stability was reached, usually within the next 2 minutes. The system background was determined by performing the entire process using an empty, pre-combusted platinum boat. Adequate system performance was confirmed by analyzing for known quantities of a calcium carbonate standard.

Inorganic carbon contents for borehole sediment samples were determined using a Coulometrics, Inc., Model 5051 Carbon Dioxide Coulometer. Soil samples were weighed on a four-place analytical balance, and then placed into acid-treated glass tubes. Following placement of sample tubes into the system, a one-minute waiting period allowed the ultrapure oxygen carrier gas to remove any carbon dioxide introduced to the system from the atmosphere. Inorganic carbon was released through acid-assisted evolution (50% hydrochloric acid) with heating to 200°C (392°F). Samples were completely covered by the acid to allow full reaction to occur. Ultrapure oxygen gas swept the resultant carbon dioxide through the equipment to determine inorganic carbon content by coulometric titration. Sample titration readings were performed 5 minutes following acid addition and again once stability was reached, usually within 10 minutes. Known quantities of calcium carbonate standards were analyzed to verify that the equipment was operating properly. Background values were determined. Inorganic carbon content was determined through calculations performed using the microgram per-sample output data and sample weights. Organic carbon was calculated by subtracting inorganic carbon from total carbon and using the remainder.

3.3.5   8 M Nitric Acid Extract

Approximately 20 g of oven-dried sediment was contacted with 8 M nitric acid at a ratio of ~ 5 parts acid to one part sediment. The slurries were heated to about 80°C (176°F) for several hours and then the fluid was separated by centrifugation and filtration through 0.2 µm membranes. The acid extracts were analyzed for major cations and trace metals using ICP and ICP-MS techniques, respectively. The acid digestion procedure is based on EPA SW-846 Method 3050B (EPA 2000a).

3.3.6   Elemental Analysis

The elemental composition of the bulk sediment from nine liners from the clean borehole, 299-W10-27, was determined by a commercial analytical laboratory using total fusion (using lithium metaborate/tetraborate) and inductively coupled plasma (ICP) and ICP-MS. The commercial lab used was ACTLAB-Skyline in Tucson, Arizona. Sample preparation involved grinding and mixing the sample in a Coors high-density alumina (Al_2O_3) mortar and pestle. Fifty-six elements (i.e., beryllium, sodium through phosphorous, potassium through arsenic, rubidium through molybdenum, silver, indium through antimony, cesium through tungsten, thallium, lead , bismuth, thorium, and uranium) were analyzed on each sample. Nine geologic material standards that represent a wide range of geologic materials were fused and run along with the unknown sediments. Results for each element for the nine standards were reported along with the certified values from NIST, USGS, and other institutions that provide certified standards. We were satisfied with the accuracy on reported results for the standards and also found that the total oxide composition of the sediments from 299-W10-27 summed to close to 100%, suggesting that the results were acceptable.

No elemental analyses were performed on the three contaminated borehole sediments because the commercial laboratory cannot test radioactive samples. We also have found that bulk elemental analysis of moderately radionuclide-contaminated sediments, such as the three TX borehole samples, do not vary significantly from uncontaminated samples.

3.3.7 Particle Size Distribution

The wet sieving/hydrometer method was used to determine the particle size distribution of selected samples from the background borehole, 299-W10-27. No particle size measurements were made on samples from C3830, C3831, and C3832. The technique is described in ASA (1986a), Part 1, Method 15-5, "Hydrometer Method." It concentrates on quantifying the relative amounts of silt and clay. The silt and clay separates were saved for later mineralogical analyses. Samples from the borehole that were used for the hydrometer method were never air- or oven-dried to minimize the effects of particle aggregation that can affect the separation of clay grains from the coarser material.

3.3.8 Particle Density

The particle density of bulk grains from the background borehole are usually determined using pychnometers as described in ASA (1986b) Part 1, Method 14-3, "Pychnometer Method," and oven-dried material. The particle density is an input needed to determine the particle size when using the hydrometer method. For the 299-W10-27 particle size analyses reported in this document, the quartz default value of 2.65 g/cm^3 was assumed and no direct particle density measurements were performed.

3.3.9 Water Potential (Suction) Measurements

Suction measurements were made on the core liners in each splitspoon sampler from borehole 299-W10-27 using the filter paper method PNL-MA-567-SFA-2 (PNL 1990b), which is essentially the same as ASTM (2002). This method relies on three filter papers folded together into a small sandwich that rapidly equilibrates with the sediment sample. The middle filter paper does not contact sediment that might stick to the paper and bias the mass measurements. At equilibrium, the matric suction in the filter paper is the same as the matric suction of the sediment sample. The dry filter paper sandwiches were placed in the liners while still filled with the sediment and remained there for three weeks to allow sufficient time for the matric suction in the sediment to equilibrate with the matric suction in the filter paper. The mass of the wetted middle filter paper that has had no direct contact with the sediment was subsequently determined, and the suction of the sediment was determined from a calibration relationship between filter paper water content and matric suction. The filter paper method provides a good estimate of water potentials over the range from -0.01 to -2 MPa (1 to 200 m [3.3 to 656 ft] suction head) (Deka et al. 1995).

The relationships used for converting the water content of filter paper to matric suction for Whatman #42 filter paper have been determined by Deka et al. (1995) and can be expressed as:

$$Sm = 10^{(5.144 - 6.699\,w)}/10 \text{ for } w < 0.5$$
$$Sm = 10^{(2.383 - 1.309\,w)}/10 \text{ for } w > 0.5$$

where
Sm is the matric suction (m) and
w is the gravimetric water content (g/g).

Fifty-one core liner samples from borehole 299-W10-27 were analyzed for soil matric suction. The matric potential samples covered the borehole profile from 50 to 123.5 ft bgs (15.2 to 37.6 m).

4.0   Results and Discussion

This section presents the geochemical and physical characterization data collected on sediment from the background borehole 299-W10-27 and the three boreholes C3830 (near tank TX105), C3831 (near tank TX107), and C3832 (near tank TX104). The results for 299-W10-27 are presented in Section 4.1, and those for C3830, C3831, and C3832 are given in Sections 4.2, 4.3, and 4.4, respectively.

The first activities emphasized tests that were inexpensive or that were key to determining the vertical distribution of mobile contaminants in the vadose zone sediments. Information on the borehole sediments presented in this section includes moisture content and total and inorganic carbon content of the sediments, pH, and electrical conductivity (EC) of 1:1 sediment:water extracts, and measurements of major cations, anions, trace metals, and radionuclides in both the sediment and 1:1 sediment:water extracts. A gamma energy analysis (GEA) of the sediments was also performed to search for any detectable man-made gamma emitting radionuclides. The particle size and bulk chemical composition of selected sediment samples were measured in the second phase of characterization to aid in selecting contacts between major geologic units and to attempt to better define the background composition of the uncontaminated sediments with the intent of aiding in determining the vertical extent of mobile contaminants in the other boreholes.

4.1   Vadose Zone Sediment from Borehole 299-W10-27

4.1.1   Moisture Content

The moisture content of the sediment from the sleeves from the section of borehole 299-W10-27 that was continuously cored (50 to 132 ft bgs) is listed in Table 4.1 and presented as a graph in Section 2.0 Geology (see Figure 2.9). Figure 2.9 shows both the field volumetric moisture obtained via neutron logging and the gravimetric moisture content of small aliquots of sediment taken during the geologic description activities. The moisture content profile correlates with the lithology described in Section 2.3.2 and shown in Figure 2.9. The first region with elevated moisture in the Hanford formation H2 unit is the thin mud lens at 52 to 54 ft bgs. There is one other elevated moisture content spot in the Hanford formation H2 unit that appears to be a clastic dike at 70 ft bgs. The rest of the Hanford formation H2 unit is rather dry, with a mean gravimetric moisture content of 3.9 wt%. Both the Cold Creek upper (fine-grained) and the lower (carbonate-rich) units are wetter than the Hanford formation unit and the Ringold Formation units that lie below the Cold Creek unit. Both Cold Creek subunits have moisture contents that average between 11 and 12 wt%. The wettest sediment is found at the bottom of the Cold Creek lower subunit at 110 ft bgs with 23.74 wt% water (Table 2.5). As discussed in Section 2, there appears to be a deep clastic dike manifesting itself in the Ringold Formation – Member of Taylor Flat (R_{tf}) at 120 ft bgs with a moisture content of 12 wt%. Excluding this wet sample, the R_{tf} unit has an average moisture content of 3.4 wt%.

4.1.2   1:1 Sediment:Water Extracts for Borehole 299-W10-27

No subsampling of the background sediment from borehole 299-W10-27 – aside from moisture content determination – was performed immediately after core opening. When cores were selected for geochemical characterization several months later, it was found that the samples had dried significantly.

Table 4.1. Gravimetric Moisture Content of Core Samples Obtained Between 50 and 125 ft bgs in Borehole 299-W10-27

Depth (ft bgs)	Stratigraphic Unit	MC % Wt	Depth (ft bgs)	Stratigraphic Unit	MC % Wt
	H1	no samples	83.5	**H2**	3.41
50	**H2**	2.23	85	**H2**	3.67
51	**H2**	2.75	86	**H2**	3.07
52.5	**H2**	*14.80*	87.5	**H2**	7.35
53.5	**H2**	*9.61*	88.5	**H2**	5.31
55	**H2**	2.52	90	**CCU$_u$**	*10.81*
56	**H2**	2.43	92.5	**CCU$_u$**	*8.66*
57.5	**H2**	2.92	95	**CCU$_u$**	*14.66*
58.5	**H2**	2.44	96	**CCU$_u$**	*9.94*
60	**H2**	3.27	97.5	**CCU$_u$**	*15.53*
61	**H2**	6.88	100	**CCU$_l$**	7.25
62.5	**H2**	5.60	102.5	**CCU$_l$**	*10.27*
63.5	**H2**	2.83	105	**CCU$_l$**	7.48
65	**H2**	4.58	106	**CCU$_l$**	6.87
66	**H2**	4.61	107.5	**CCU$_l$**	8.09
67.5	**H2**	5.05	110	**CCU$_l$**	*23.74*
68.5	**H2**	4.48	112.5	**R$_{tf}$**	3.40
70	**H2**	*14.12[a]*	113.5	**R$_{tf}$**	3.08
71	**H2**	3.52	115	**R$_{tf}$**	3.63
72.5	**H2**	3.78	116	**R$_{tf}$**	2.71
73.5	**H2**	4.67	117.5	**R$_{tf}$**	6.05
75	**H2**	4.57	120	**R$_{tf}$**	*11.84*[a]
77.5	**H2**	5.00	121	**R$_{tf}$**	2.37
78.5	**H2**	3.34	122.5	**R$_{tf}$**	3.66
80	**H2**	3.37	123.5	**R$_{tf}$**	1.95
81	**H2**	2.93		**R$_{wi}$**	no samples
82.5	**H2**	3.12			

Italics connote wet sediment.
(a) Designates samples where clastic dikes appear to be intercepted.
MC = moisture content.

Unlike past comparisons between background and contaminated sediments at the S-SX and B-BX-BY waste management areas (WMA), no attempt is made to estimate the chemical composition of uncontaminated vadose zone porewater from the 1:1 sediment:water extracts. Instead, the data from the 1:1 water extracts for the background borehole (299-W10-27) and the three boreholes around suspected leaking tanks in the TX Tank Farm were compared on a per gram of dry soil basis. The following sections discuss the results of the analyses for the 1:1 sediment:water extracts on the background sediment.

4.1.2.1 pH and Electrical Conductivity

The pH and EC for the water extracts are shown in Table 4.2 and Figure 4.1. The pH is plotted as measured in the 1:1 sediment:water extracts but the EC is corrected for dilution and plotted as if it was actual porewater.

The pH profile shows the highest values [~7.5] at the bottom of the lower Cold Creek subunit (caliche) and in the gravel facies of the Ringold Formation-Member of Wooden Island (R_{wi}). These two water extracts also show the highest values for EC. The sample in the R_{tf} at 113 ft bgs shows the lowest pH and EC values. During the SX Tank Farm characterization two uncontaminated boreholes, 299-W22-48 and 299-W22-50, were cored and fully characterized. The pH and EC data for 299-W10-27 sediments agree more closely with the data for 299-W22-48 than 299-W22-50 (see Tables 5.15 and 5.38 in Serne et al. 2002a). The R_{wi} unit 1:1 sediment:water extract at 299-W10-27 (only one sample characterized) has a higher EC (0.227 mS/cm) than the uncontaminated samples characterized at the SX Tank Farm (EC ranges from 0.08 to 0.12 mS/cm). This may suggest that there is more leachable salts in the R_{wi} unit further north in the T-TX-TY WMA.

Table 4.2.   pH and EC Values for 1:1 Sediment:Water Extracts from 299-W10-27

Depth (ft)	Stratigraphic Unit	pH	Conductivity mS/cm
53.3	H2	7.18	0.156
53.5	H2	7.08	0.137
61	H2	7.16	0.149
88.3	H2	7.27	0.165
92.5	CCU_u	7.33	0.154
100	CCU_l	7.47	0.184
113.5	R_{tf}	6.82	0.066
113.5(dup)	R_{tf}	6.95	0.084
117.5	R_{tf}	7.37	0.170
130	R_{wi}	7.40	0.227
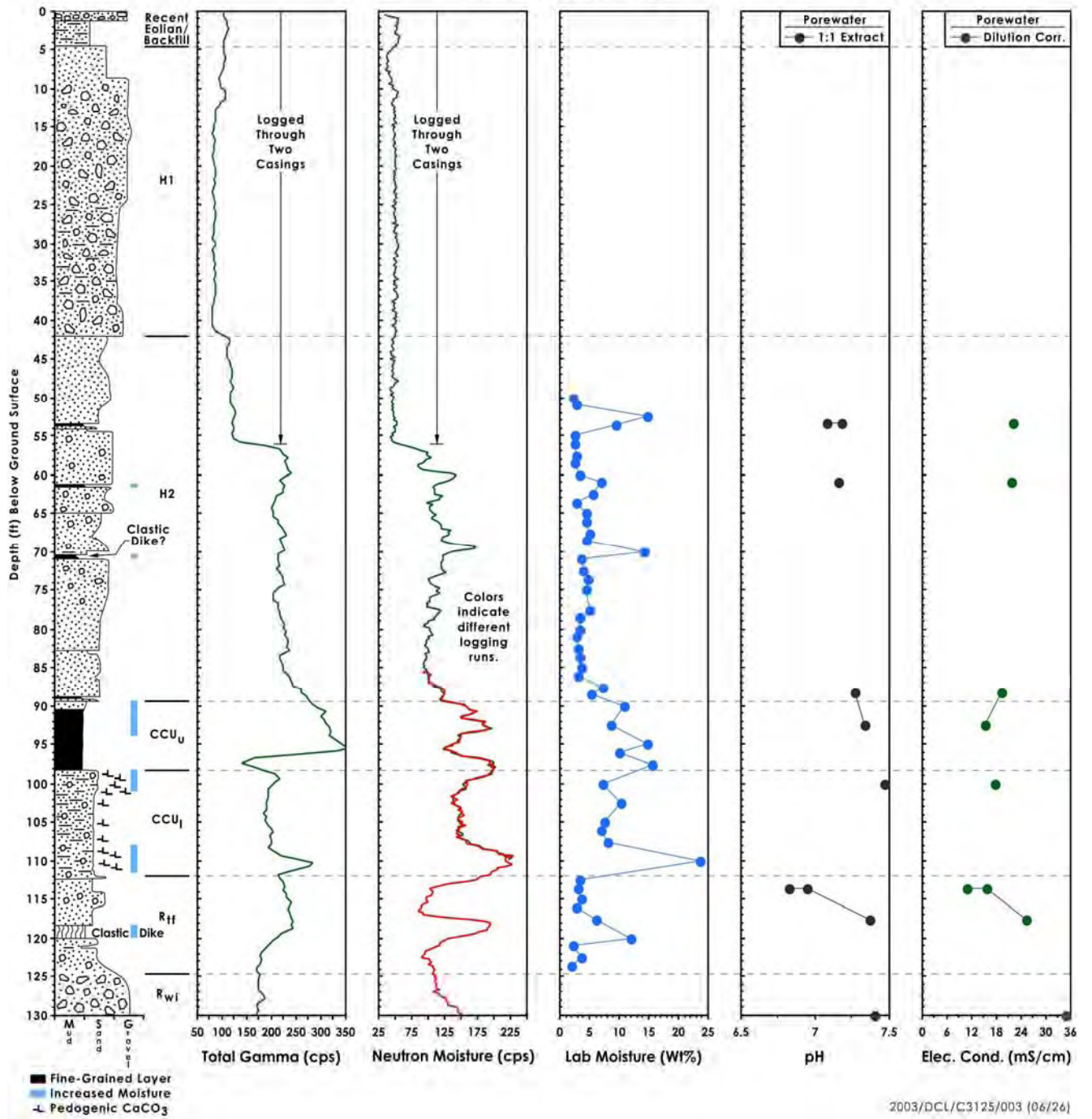
Figure 4.1. pH and Electrical Conductivity Calculated (from Sediment:Water Extracts) for Borehole 299-W10-27

4.1.2.2   Water Extract Composition or the 1:1 Sediment:Water Extract for 299-W10-27

The 1:1 sediment:water extract anion composition from 299-W10-27 samples, in units of µg per g of dry sediment, is shown in Table 4.3 and Figure 4.2a and Figure 4.2b. We are assuming that the values represent background values that can be compared to values for water extracts from the three boreholes near TX tanks that were suspected as having leaked in the past. Values in Table 4.3 that appear to be elevated compared to the others are shown in bold type and values that are low compared to the others are shown in italics. Two samples show high water-leachable fluoride, the calcium-carbonate-rich CCU_l sediment at 100 ft bgs and the R_{wi} gravel at 130 ft bgs. At the SX tank farm we also observed sediments enriched in calcium carbonate contained numerous other water-leachable solutes (see Serne et al. 2002a). The CCU_l stratum is an old near-surface soil zone that translocated solutes during periods of active precipitation-evaporation. Thus, this stratum would be expected to contain larger quantities of leachable salts. We have no explanation as to why the R_{wi} gravel sample should contain high water-leachable fluoride. This sample also contains high water-leachable chloride and sulfate compared to all the other sediment samples that were water-leached. In general, the water extracts for both Cold Creek unit samples show slightly elevated concentrations of water-leachable carbonates, likely signifying the higher calcium carbonate contents in sediments in these two units. Figure 4.2b shows two measurements of inorganic carbon (IC) in the 1:1 sediment:water extracts. We find that the IC values reported as carbonate are biased high compared to the values measured by standard alkalinity titration. None of the water extracts contain measurable amounts of phosphate, nitrite, or bromide.

Table 4.4 and Figure 4.2c show the water-leachable composition for small organic molecules. In general, the Hanford formation sediments geologically have slightly lower water-leachable concentrations of formate, acetate, and oxalate than the Cold Creek unit and Ringold Formation sediments. One possible cause for the differing concentrations of water-leachable organic molecules is the fact that the Hanford formation was deposited very rapidly and large volumes of sediment diluted any near surface organic matter that was present.

Table 4.5 shows the water-leachable concentrations of divalent and monovalent cations, in units of µg per gram of dry sediment for the background borehole 299-W10-27. Table 4.6 shows the water-leachable concentrations of aluminum (Al), silicon (Si), iron (Fe), manganese (Mn), zinc (Zn), and phosphorous (P) and sulfur (S). The latter two were converted to their respective anions, phosphate and sulfate, and the data are compared to the ion chromatograph measured anion data in Figure 4.2a. The comparison is quite good. The distributions of several of the major cations versus depth are shown in Figure 4.3. The depth profiles for the divalent alkaline earth cations magnesium (Mg), barium (Ba), and strontium (Sr) show higher values leach from the carbonate-rich CCU_l sediment. This is to be expected as these cations form moderately soluble carbonates. The Ringold Formation sediments from both the deeper R_{tf} and R_{wi} units show slightly elevated water-leachable divalent cations with the exception of calcium, suggesting that carbonate coatings on the grains or detrital carbonates are present in these older sediments. The shallow R_{tf} sample shows the lowest water-leachable divalent and monovalent cations but the highest water-leachable iron and manganese, suggesting that this sample may contain Fe- and Mn-oxide coatings instead of carbonates. The fine-grained upper Cold Creek subunit at 92.5 ft bgs appears to contain some water-leachable phosphorous and the R_{wi} contains elevated levels of soluble sulfate, perhaps indicating the presence of gypsum.

Table 4.3. Anion Composition of Water Extracts of 299-W10-27 Sediment (units µg/g dry sediment)

Depth (ft bgs)	Stratigraphic Unit	Fluoride	Chloride	Nitrate	Alk as CO$_3$	Sulfate	Phosphate	Nitrite	Bromide
53.3	H2	0.44	0.64	2.89	32.97	13.07	<0.25	<0.08	<0.14
53.5	H2	0.26	0.90	2.16	29.35	10.40	<0.24	<0.08	<0.14
61	H2	0.25	0.90	2.54	28.04	11.56	<0.24	<0.08	<0.14
88.3	H2	0.53	1.66	1.31	40.07	8.30	<0.25	<0.08	<0.14
92.5	CCU$_u$	0.31	0.48	1.10	43.03	8.04	0.43	<0.08	<0.14
100	CCU$_l$	**1.16**[a]	0.37	0.66	48.15	6.70	<0.24	<0.08	<0.14
113.5	R$_{tf}$	0.43	0.56	1.00	*13.28*[b]	4.70	<0.24	<0.08	<0.14
113.5(dup)	R$_{tf}$	0.51	0.65	0.77	26.65	5.39	<0.24	<0.08	<0.14
117.5	R$_{tf}$	0.64	*0.22*	*0.33*	45.35	*3.89*	<0.24	<0.08	<0.14
130	R$_{wi}$	**1.45**	**2.57**	2.33	36.00	**39.67**	<0.24	<0.08	<0.14

(a) Bold values are higher than others for given constituent.
(b) Italicized values are lower than others for a given constituent.

Table 4.4. Small Molecular Weight Organic Content of Water Extracts of 299-W10-27 Sediment (units µg/g dry sediment)

Depth (ft)	Stratigraphic Unit	Formate	Acetate	Oxalate
53.3	H2	0.12	0.29	0.54
53.5	H2	*<0.13*[b]	0.43	0.60
61	H2	*<0.11*	*<0.16*	0.53
88.3	H2	0.28	0.41	0.48
92.5	CCU$_u$	0.18	0.54	0.68
100	CCU$_l$	0.14	0.51	0.76
113.5	R$_{tf}$	0.39	0.47	0.58
113.5(dup)	R$_{tf}$	0.48	0.68	0.55
117.5	R$_{tf}$	**0.80**[a]	**0.85**	0.66
130	R$_{wi}$	0.42	0.61	**0.94**
(a) Bold values are higher than others for given constituent.				
(b) Italicized values are lower than others for a given constituent.				

Table 4.7 and Figures 4.4 and 4.5 show the water-leachable concentrations of some metals that are present in tank leak fluids and, in the case of Figure 4.5, metals that have been found to be relatively mobile under some tanks in the S-SX and B-BX-BY WMAs (see Serne et al. 2002b, 2002c, 2002d, 2002e, 2002f for more discussion). The lower Cold Creek subunit (CCU$_l$) contains the highest water-leachable chromium (Cr) in this background borehole and the R$_{wi}$ sample contains the highest concentration water-leachable molybdenum (Mo) (Figure 4.5). The technetium-99 (Tc-99) data are all below or very near to our detection limit as expected for a background borehole (Table 4.7).

The values presented in Tables 4.2 through Table 4.7 will be compared to similar data for the three TX boreholes C3830, C3831, and C3832, to evaluate whether significantly higher values are found in any borehole that would suggest tank fluids had percolated into the vadose zone where the boreholes were pushed.
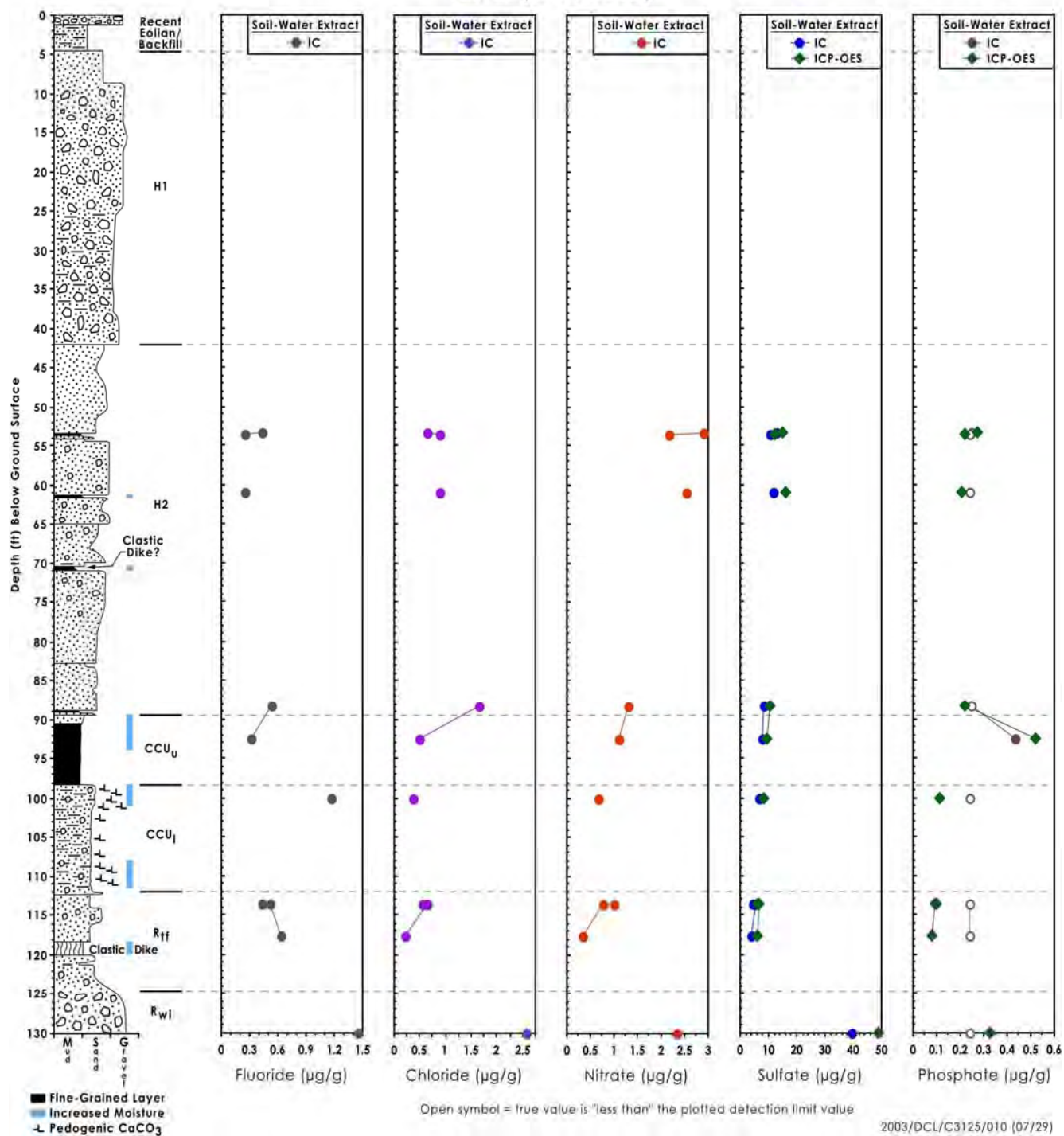
Figure 4.2a. Major Anions in 1:1 Sediment:Water Extracts from Borehole 299-W10-27
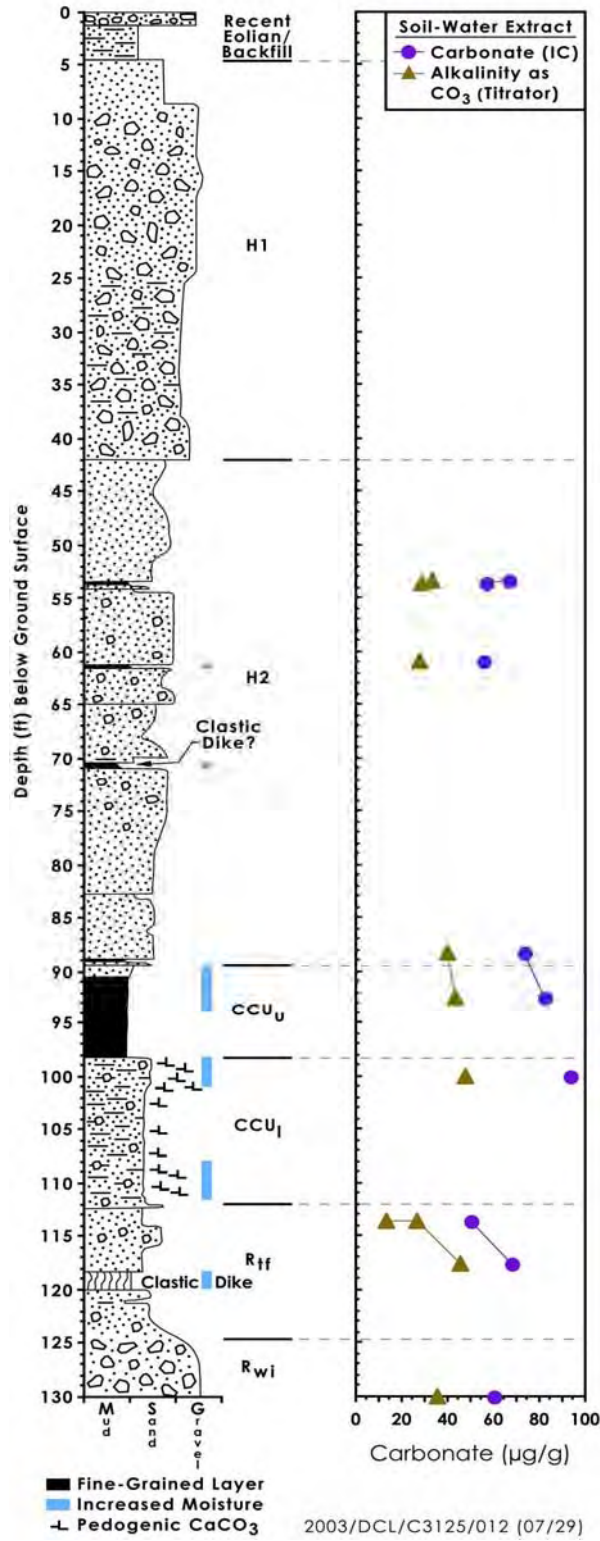
Figure 4.2b. 1:1 Sediment:Water Extract Carbonate and Alkalinity (as Carbonate) Contents from Borehole 299-W10-27 (units µg per g dry sediment)

4.9
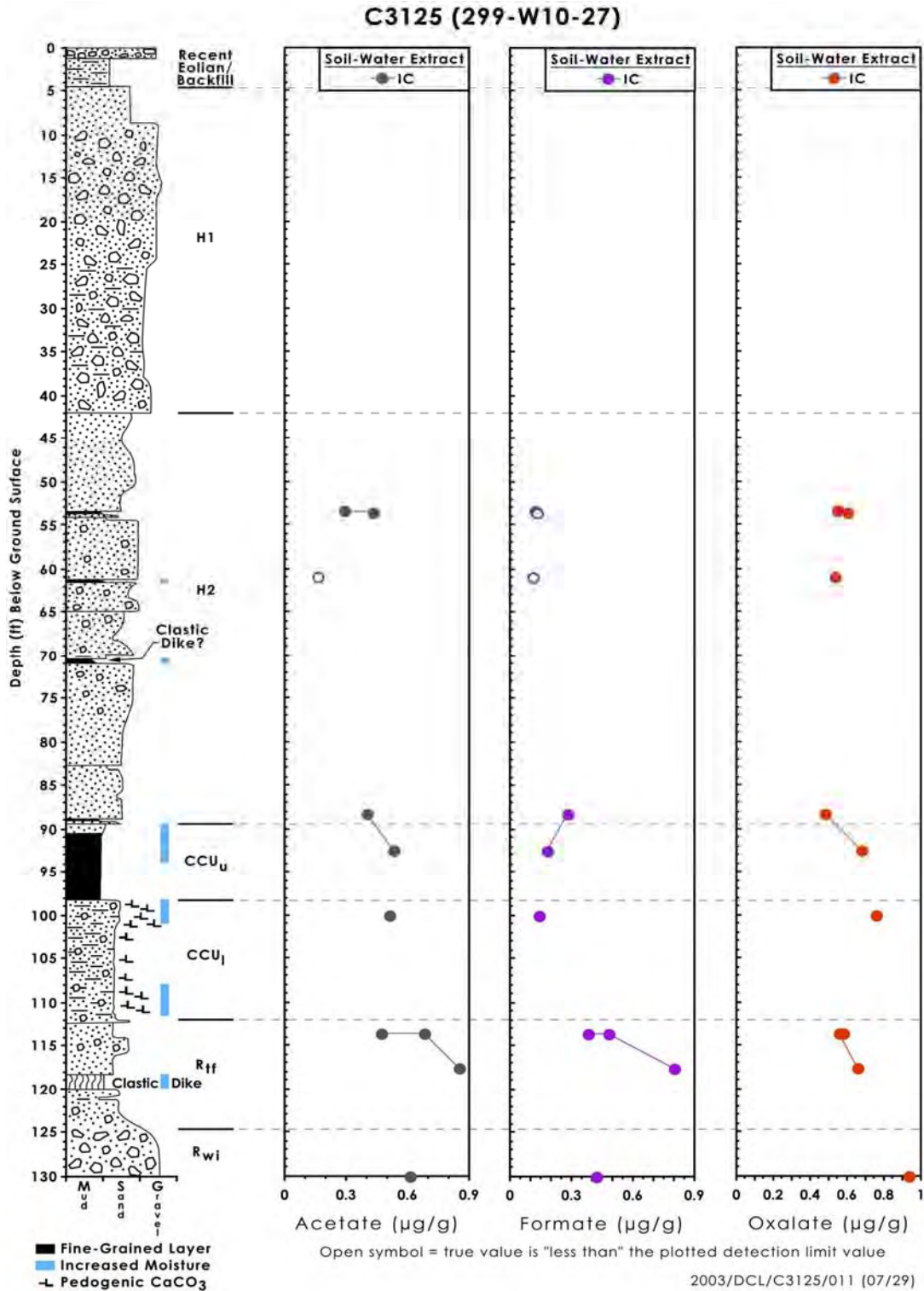
Figure 4.2c. 1:1 Sediment:Water Extract Small Organic Molecule Contents from Borehole 299-W10-27 (units μg per g dry sediment)

Table 4.5.   Water-Extractable Cations in Borehole 299-W10-27 Sediments (µg/g dry soil)

Depth (ft bgs)	Stratigraphic Unit	Mg	Ca	Sr	Ba	Na	K
53.3	H2	3.11E+00	1.38E+01	6.11E-02	1.79E-02	7.29E+00	3.44E+00
53.5	H2	2.35E+00	1.09E+01	5.57E-02	2.48E-02	6.66E+00	2.85E+00
61	H2	2.80E+00	1.26E+01	6.28E-02	1.78E-02	7.25E+00	4.18E+00
88.3	H2	2.95E+00	1.34E+01	6.72E-02	2.60E-02	1.08E+01	3.78E+00
92.5	CCU$_u$	2.88E+00	1.32E+01	6.55E-02	3.79E-02	9.34E+00	3.30E+00
100	CCU$_l$	**6.71E+00**[a]	1.36E+01	**1.06E-01**	**4.55E-02**	9.19E+00	2.46E+00
113.5	R$_{tf}$	*1.48E+00*[b]	*2.46E+00*	*2.51E-02*	1.60E-02	*4.32E+00*	*1.46E+00*
113.5(dup)	R$_{tf}$	2.36E+00	*4.05E+00*	*3.95E-02*	1.76E-02	*5.01E+00*	*1.87E+00*
117.5	R$_{tf}$	**6.54E+00**	1.25E+01	**1.09E-01**	3.22E-02	7.55E+00	2.51E+00
130	R$_{wi}$	4.26E+00	1.08E+01	**1.06E-01**	**4.60E-02**	**2.53E+01**	**6.13E+00**

(a) Bold values are higher than others for given constituent.
(b) Italicized values are lower than others for a given constituent.

Table 4.6.   Other Water-Extractable Cations in Borehole 299-W10-27 Sediments (µg/g dry soil)

Depth (ft bgs)	Strati-graphic Unit	Al	Si	Fe	Mn	Zn	P as PO$_4$	S as SO$_4$
53.3	H2	(1.29E-02)[c]	1.11E+01	(9.62E-03)	(8.13E-04)	2.91E-02	2.72E-01	1.48E+01
53.5	H2	2.64E-02	1.13E+01	(1.93E-02)	(5.82E-04)	2.89E-02	2.19E-01	1.22E+01
61	H2	(1.97E-02)	1.31E+01	(1.56E-02)	(6.16E-04)	(2.09E-02)	2.05E-01	1.60E+01
88.3	H2	(1.30E-02)	1.54E+01	(1.15E-02)	(5.71E-04)	3.41E-02	2.22E-01	1.06E+01
92.5	CCU$_u$	2.69E-02	1.20E+01	(6.30E-03)	<2.60E-03	3.58E-02	**5.23E-01**	9.38E+00
100	CCU$_l$	*<1.27E-02*[b]	**2.53E+01**[a]	*(5.42E-03)*	(5.72E-04)	3.07E-02	(1.15E-01)	8.13E+00
113.5	R$_{tf}$	3.24E-02	1.95E+01	**5.29E-02**	**(3.53E-03)**	(2.30E-02)	(9.75E-02)	*6.08E+00*
113.5 (dup)	R$_{tf}$	2.89E-02	1.92E+01	**5.03E-02**	**(3.43E-03)**	2.51E-02	(9.34E-02)	*6.45E+00*
117.5	R$_{tf}$	(2.51E-03)	**2.95E+01**	(9.94E-03)	(8.40E-04)	3.08E-02	(8.36E-02)	*6.41E+00*
130	R$_{wi}$	**5.82E-02**	1.44E+01	(3.12E-02)	(2.98E-03)	(2.33E-02)	3.27E-01	**4.88E+01**

(a) Bold values are higher than others for given constituent.
(b) Italicized values are lower than others for a given constituent.
(c) Parentheses signify values below level of quantitation but considered valid.

Table 4.7. **Water-Extractable Mobile Trace Contaminants in Borehole 299-W10-27 Sediments (μg per gram dry soil)**

Depth (ft bgs)	Stratigraphic Unit	Tc-99	U-238	Cr	Mo (ICP-MS)	Mo (ICP)
53.3	H2	<4.39E+00	1.07E-03	8.19E-04	7.99E-03	9.15E-03
53.5	H2	(2.58E-01)	4.98E-04	(4.65E-04)	3.35E-03	(4.30E-03)
61	H2	<1.70E+00	6.41E-04	5.41E-04	4.32E-03	4.57E-03
88.3	H2	<4.36E+00	1.46E-03	1.01E-03	4.37E-03	5.64E-03
92.5	CCU_u	<1.77E+00	9.58E-04	**1.60E-03**[a]	8.62E-03	1.05E-02
100	CCU_l	<1.72E+00	2.89E-03	(2.52E-04)	*9.05E-04*	*<2.53E-03*
113.5	R_{tf}	<1.69E+00	*(4.39E-05)*[b]	(4.03E-04)	1.76E-03	(2.32E-03)
113.5(dup)	R_{tf}	<1.70E+00	1.13E-04	(3.86E-04)	1.84E-03	(8.46E-04)
117.5	R_{tf}	(2.36E-01)[c]	1.60E-03	5.90E-04	9.49E-03	9.66E-03
130	R_{wi}	<1.69E+00	6.86E-04	(4.25E-04)	**1.05E-02**	**1.15E-02**

(a) Bold values are higher than others for given constituent.
(b) Italicized values are lower than others for a given constituent.
(c) Parentheses signify values below level of quantitation but considered valid.
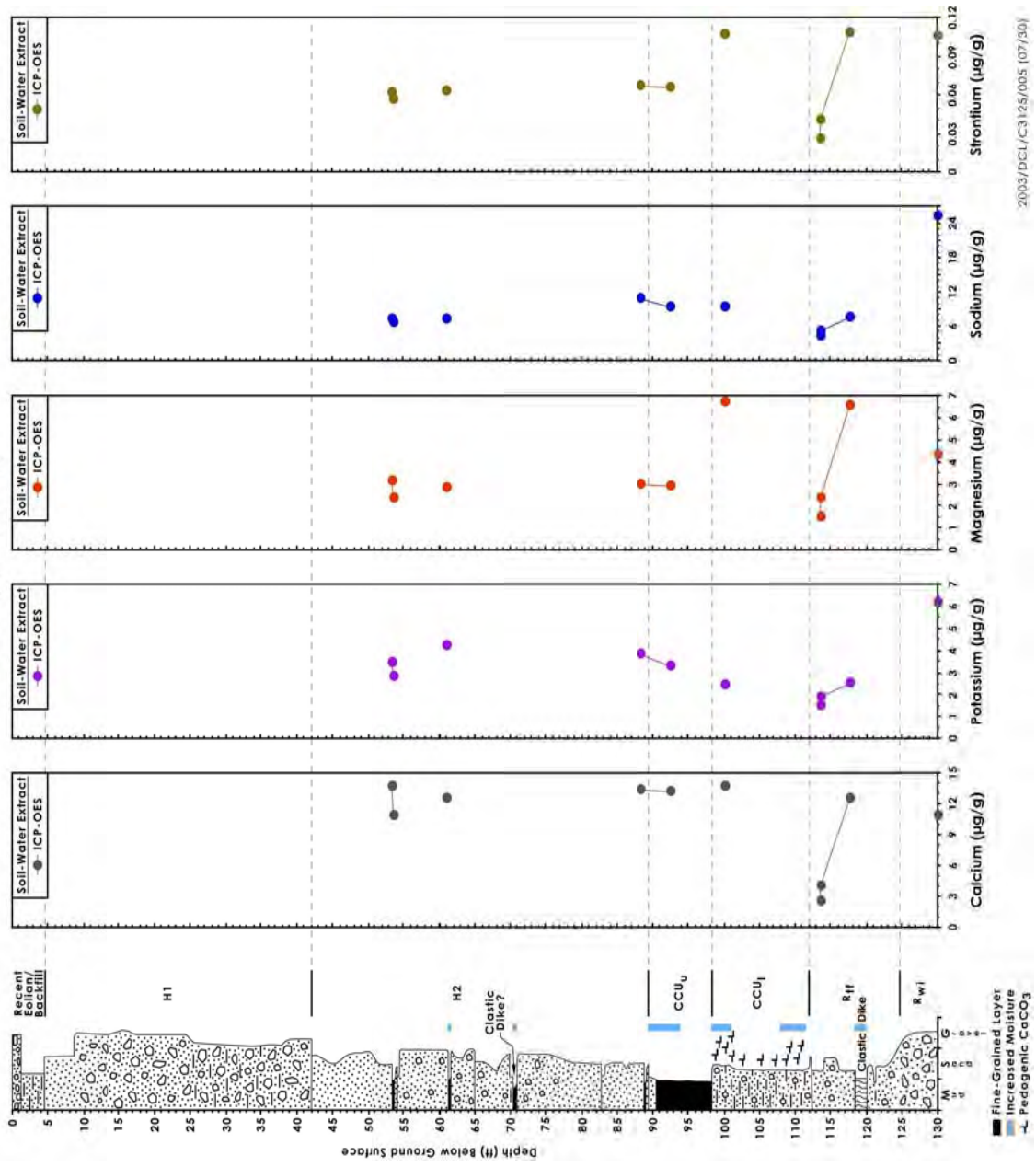
Figure 4.3. Cations in 1:1 Sediment:Water Extracts for Borehole 299-W10-27
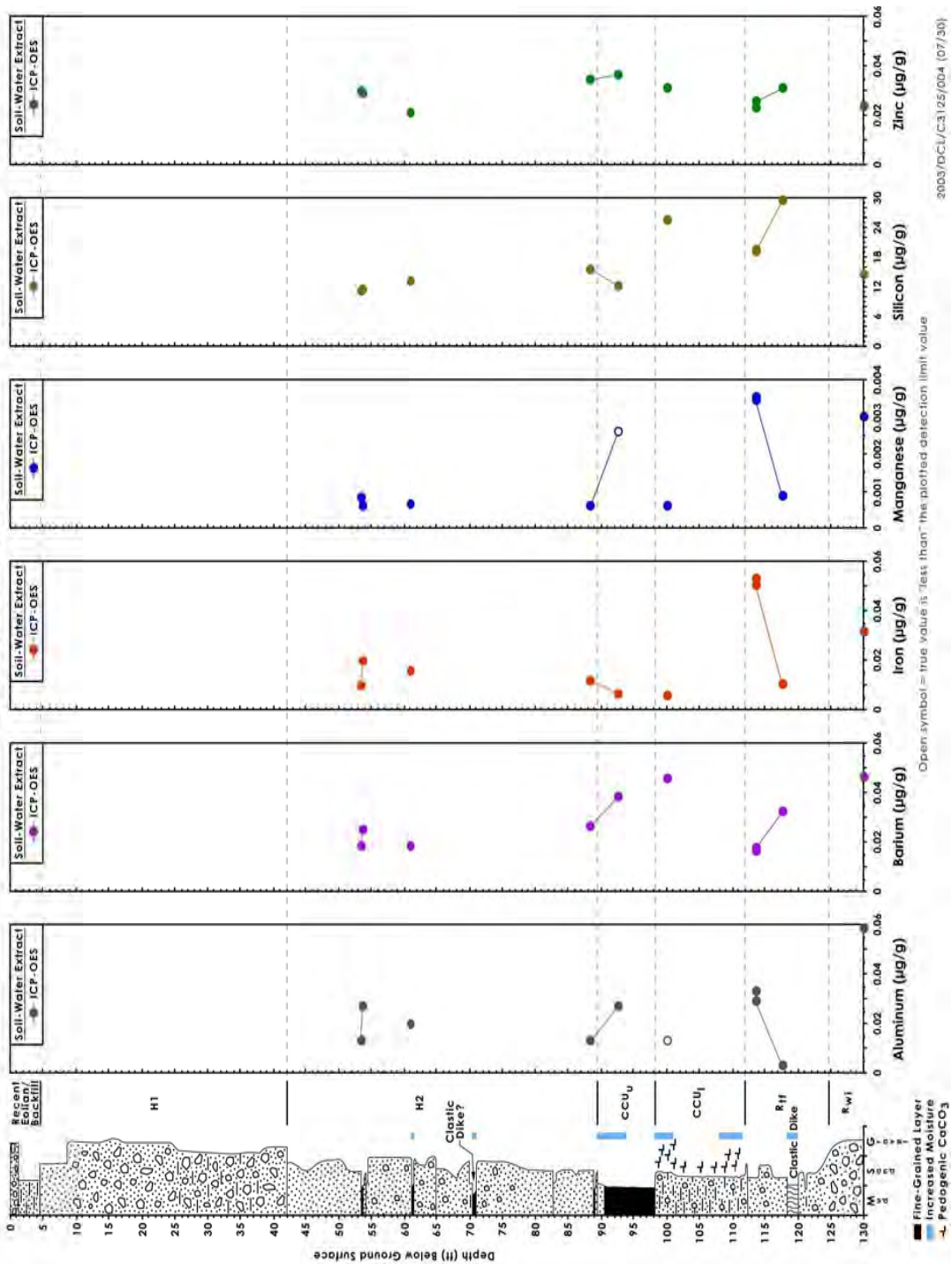
Figure 4.4. Aluminum, Barium, Iron, Manganese, Silicon, and Zinc in 1:1 Sediment:Water Extracts from Borehole 299-W10-27
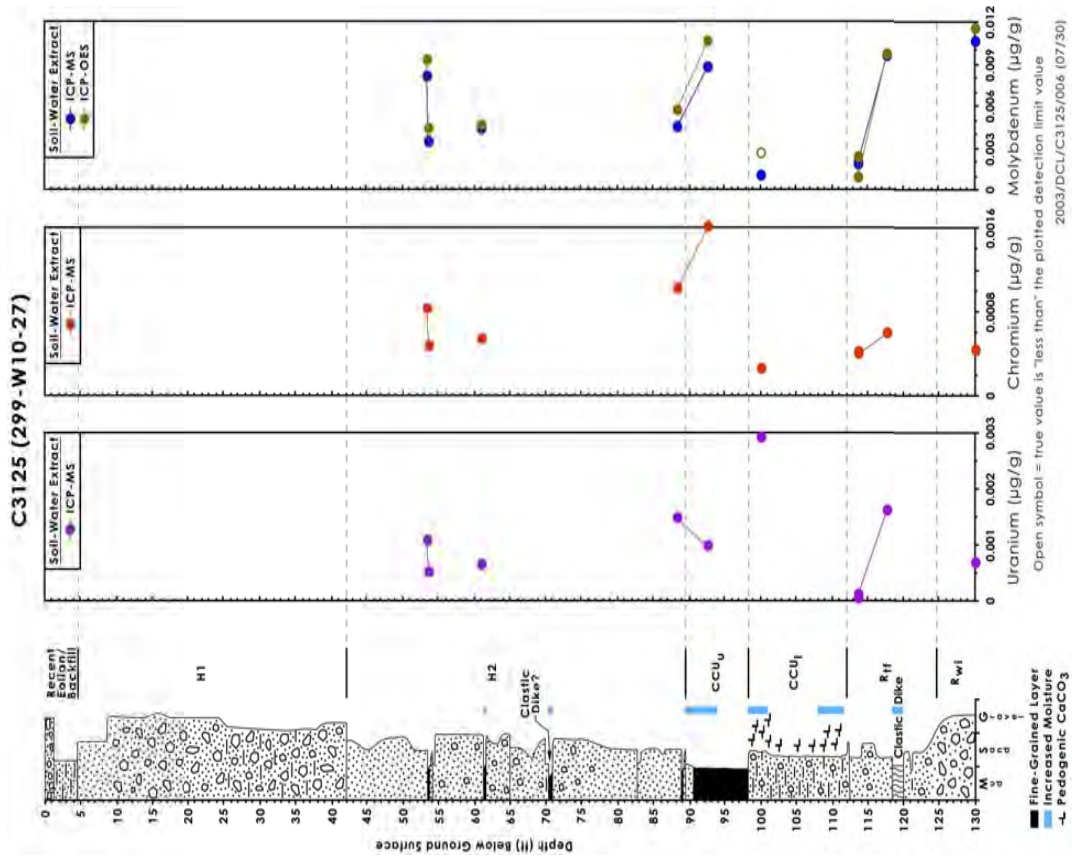
Figure 4.5. Trace Metals in 1:1 Sediment:Water Extracts Borehole 299-W10-27

4.1.3 8 M Nitric Acid-Extractable Amounts of Selected Elements

The amount of material that could be extracted from the vadose zone sediment into 8 M nitric acid is shown in Tables 4.8 through 4.10 and Figures 4.6 through 4.9. The 8 M nitric acid extraction is a protocol used by the U.S. Environmental Protection Agency to estimate the maximum concentrations of regulated metals in contaminated sediment that would be biologically available. Aliquots of uncontaminated sediment from borehole 299-W10-27 were subjected to the acid extraction to establish baseline values to compare with acid extracts of potentially contaminated sediments from the three boreholes, C3830, C3831, and C3832.

The acid extract data show high values for barium in the fine-grained CCU_u subunit, and high values for calcium (Ca), strontium (Sr), manganese (Mn), sodium (Na), uranium (U) and sulfate (SO_4^{2-}) in the two sediment types with high calcium-carbonate content, CCU_l at 100 ft bgs and R_{tf} at 117 ft bgs. The acid-extractable magnesium content of the R_{tf} sample at 117 ft bgs is also high. All these high values suggest that these elements are associated with readily acid-soluble carbonates. Similar results were found for background sediments near the SX tank farm (Serne et al. 2002a). Conversely, the acid-extractable chromium content of the caliche enriched sample at 100 ft bgs is low compared to the other sediments. Chromium is also low but molybdenum and sulfur are relatively high in the acid extract from the gravelly R_{wi} unit sample at 130 ft bgs. Acid-leachable potassium (K) is also low in this coarse sample as one might expect seeing as higher potassium is generally associated with certain clay and fine-grained materials.

A comparison of the water-leachable and acid-leachable contents of the uncontaminated sediments from borehole 299-W10-27 (see data shown in Tables 4.3 to 4.7 versus 4.8 to 4.10) shows that less than 0.1% of the acid-extractable quantities of the following elements are water leachable: Al, Ba, Fe, Mn, Zn, Cr, and P as phosphate. Less than 0.2% of the acid-extractable quantities of the following elements are water leachable: Ca, K, Mg, Sr, and U. Less than 5% of the acid-extractable sodium and molybdenum are water soluble and less than 20% of the acid-extractable sulfur as sulfate is water extractable. The sulfur in the sediments may be predominately present as slightly soluble gypsum and the phosphorous may be present predominantly as rather insoluble apatite-like minerals. The comparison of water- to acid-soluble sulfur and phosphorous are shown in Figure 4.9.

4.1.4 Bulk Chemical Composition of Sediment from 299-W10-27

Nine core samples were selected from this borehole and sent to a commercial analytical lab for bulk chemical composition analyses using fusion, followed by dissolution of the fused beads and analysis by ICP and ICP-MS. The carbon content of the samples was determined with a carbon analyzer as discussed in Section 4.1.6. The total chemical composition of the samples is shown in Table 4.11 and total trace element compositions are shown in Table 4.12.

As found for most Hanford Site sediments, the bulk chemistry is dominated by silicon and aluminum oxides, with calcium and iron being next in abundance. Calcium from $CaCO_3$ is evident in several of the samples (100 and 117.5 ft bgs). There is also several percent of sodium, potassium, and magnesium present in all the sediments. The relatively high iron-oxide contents in the R_{tf} and R_{wi} samples from 117.5 and 130 ft bgs (see Table 4.11) likely are caused by ferric oxide coatings or cement. Trace metals are often used to differentiate different lithologic units but the data in Table 4.12 only suggest that the fine-grained Cold Creek upper subunit is distinguishable from all other units by the presence of elevated

4.16

lanthanide series elements. The other elements do not show striking differences in trace element concentrations with lithology.

4.1.5 Radionuclide Content in Vadose Zone Sediment from 299-W10-27

The sediment cores from borehole 299-W10-27 did not contain any man-made gamma radioactivity. The radioanalytical analyses performed on the sediment included direct gamma energy analysis and technetium-99 and uranium-238 analysis of the 1:1 sediment:water extracts and the sediment:acid extracts. The uranium and technetium water-extractable contents of the background sediments that were characterized are shown in Table 4.7 and the acid-extractable amounts are shown in Table 4.10. Both data sets suggest no elevated amounts are present. As mentioned above, the sediments with high concentrations of calcium-carbonate-equivalent carbonate contain slightly higher concentrations of acid-leachable uranium, one part per million (ppm). The gamma energy analysis data are not reported because there is nothing significant to report.

4.1.6 Total Carbon, Calcium Carbonate, and Organic Carbon Content of Vadose Zone Sediment from Borehole 299-W10-27

Table 4.13 shows the total carbon, inorganic carbon, and organic carbon contents of the vadose zone sediment at selected depths. The inorganic carbon was also converted to the equivalent calcium-carbonate content. The sediment in the Hanford formation H2 unit is relatively low in calcium carbonate (<2 wt%) and organic carbon. The three shallow H2 unit samples show a fairly uniform distribution for inorganic carbon between 1.6 and 1.8% as calcium carbonate. At depth, the H2 unit shows slightly more calcium carbonate. The fine-grained CCU_u sample contains ~2.6 wt% calcium carbonate.

The coarser-grained CCU_l contains significant quantities (~25 wt%) of calcium carbonate and low organic carbon content. The R_{tf} unit samples show highly variable calcium-carbonate contents as a function of depth. The coarse-grained R_{wi} gravel has very little calcium carbonate and organic carbon. The calcium-carbonate content of the CCU_l unit at 299-W10-27 is less than at 299-W22-48 (contained 38 to 39 wt%) but larger than sediments at 299-W22-50, which contained only 2 to 8 wt% (Serne et al. 2002a).

4.1.7 Particle Size Measurements on Vadose Zone Sediment

Both the hydrometer and wet sieving methods were used to determine the particle size distributions of the selected samples from borehole 299-W10-27. Wet sieving results are shown in Table 4.14. The four samples of the Hanford formation H2 unit that were chosen for particle-size characterization represent zones with atypically high contents of fines. Samples for geochemical characterization were biased in favor of the fine-grained strata since these tend to contain more moisture and are more likely to have contaminants associated with them. Therefore, the values in Table 4.14 should not be used as representative of the bulk of the Hanford H2 unit. The Cold Creek upper subunit is predominantly silt. In contrast, the Cold Creek lower subunit (caliche) is very poorly sorted and has a wide range of particle sizes from gravel to silt and clay, as has been described previously for sediments below the SX tank farm (Serne et al. 2002a, 2002b, 2002c, 2002d). The two grain size samples from the R_{tf} unit show great variability as described in Section 2.3.2.4. One is a well-sorted sand; the other, a well-sorted silt.

Table 4.8. Acid-Extractable Major Cations in Borehole 299-W10-27 Sediments (µg/g dry sediment)

Depth (ft bgs)	Stratigraphic Unit	Ba	Ca	K	Mg	Sr	Zn	Na
53.3	H2	6.71E+01	1.01E+04	2.45E+03	6.19E+03	4.17E+01	4.89E+01	- - - - -
53.5	H2	9.57E+01	8.66E+03	2.15E+03	5.55E+03	3.46E+01	4.43E+01	- - - - -
61	H2	7.15E+01	8.91E+03	1.92E+03	5.15E+03	3.37E+01	4.21E+01	- - - - -
88.3	H2	6.18E+01	1.21E+04	2.14E+03	5.91E+03	4.08E+01	4.72E+01	- - - - -
92.5	CCU$_u$	**1.07E+02**[a]	1.38E+04	2.75E+03	7.15E+03	4.00E+01	5.31E+01	- - - - -
100	CCU$_l$	9.40E+01	**9.05E+04**	1.30E+03	6.44E+03	**1.70E+02**	3.09E+01	**- - - - -**
113.5	R$_{tf}$	7.15E+01	3.20E+03	1.34E+03	5.47E+03	3.17E+01	4.13E+01	- - - - -
113.5(dup)	R$_{tf}$	7.48E+01	3.17E+03	1.35E+03	5.47E+03	3.39E+01	4.14E+01	- - - - -
117.5	R$_{tf}$	8.49E+01	**3.91E+04**	2.07E+03	**8.88E+03**	**7.32E+01**	5.97E+01	- - - - -
130	R$_{wi}$	6.43E+01	5.50E+03	*8.92E+02*[b]	3.79E+03	3.80E+01	3.86E+01	**- - - - -**

(a) Bold values are higher than others for given constituent.
(b) Italicized values are lower than others for a given constituent.

4.18

Table 4.9. Acid-Extractable Content for Major Constituents in Borehole 299-W10-27 Sediments (μg/g dry sediment)

Depth (ft bgs)	Stratigraphic Unit	Al	Fe	Mn	Si	P	S
53.3	H2	1.10E+04	1.68E+04	3.50E+02	(5.41E+01)[b]	6.90E+02	(3.43E+01)
53.5	H2	8.69E+03	1.55E+04	3.35E+02	(9.17E+01)	4.98E+02	(5.06E+01)
61	H2	8.33E+03	1.56E+04	3.49E+02	(5.14E+01)	5.83E+02	5.15E+01
88.3	H2	9.39E+03	1.56E+04	3.45E+02	(3.88E+01)	7.42E+02	(3.85E+01)
92.5	CCU_u	1.34E+04	1.81E+04	**4.07E+02**[a]	(8.62E+00)	6.52E+02	(3.63E+01)
100	CCU_l	9.09E+03	1.33E+04	2.16E+02	(9.34E+00)	5.20E+02	**(1.91E+02)**
113.5	R_{tf}	9.35E+03	1.62E+04	2.92E+02	(1.80E+01)	3.90E+02	(2.88E+01)
113.5(dup)	R_{tf}	9.40E+03	1.63E+04	2.93E+02	(2.00E+01)	3.98E+02	(2.54E+01)
117.5	R_{tf}	1.28E+04	1.94E+04	**4.61E+02**	(9.88E+00)	6.08E+02	(5.12E+01)
130	R_{wi}	7.16E+03	1.93E+04	2.62E+02	(8.58E+00)	8.89E+02	**9.40E+01**

(a) Bold values are higher than others for given constituent.
(b) Parentheses signify values below level of quantitation but considered valid.

Table 4.10. Acid-Extractable Mobile Trace Metals in Borehole 299-W10-27 Sediments (µg per gram dry sediment)

Depth (ft bgs)	Stratigraphic Unit	Tc-99	U-238	Cr (ICP-MS)	Cr (ICP)	Mo (ICP-MS)
53.3	H2	(1.26E+01)[c]	7.55E-01	2.21E+01	1.78E+01	2.58E-01
53.5	H2	<5.58E+01	5.18E-01	1.71E+01	1.39E+01	2.16E-01
61	H2	<5.25E+01	4.88E-01	1.43E+01	1.20E+01	2.28E-01
88.3	H2	(7.65E+00)	7.40E-01	1.69E+01	1.38E+01	2.12E-01
92.5	CCU$_u$	<5.21E+01	6.57E-01	1.95E+01	1.65E+01	2.58E-01
100	CCU$_l$	<5.75E+01	**1.01E+00**[a]	*9.89E+00*[b]	*7.98E+00*	2.68E-01
113.5	R$_{tf}$	<5.46E+01	5.54E-01	1.35E+01	1.13E+01	2.00E-01
113.5 (dup)	R$_{tf}$	<5.51E+01	5.58E-01	1.38E+01	1.13E+01	2.05E-01
117.5	R$_{tf}$	(2.32E+01)	**1.01E+00**	1.95E+01	1.67E+01	3.51E-01
130	R$_{wi}$	<5.42E+01	5.26E-01	*7.80E+00*	*6.58E+00*	**4.36E-01**

(a) Bold values are higher than others for given constituent.
(b) Italicized values are lower than others for a given constituent.
(c) Parentheses signify values below level of quantitation but considered valid.
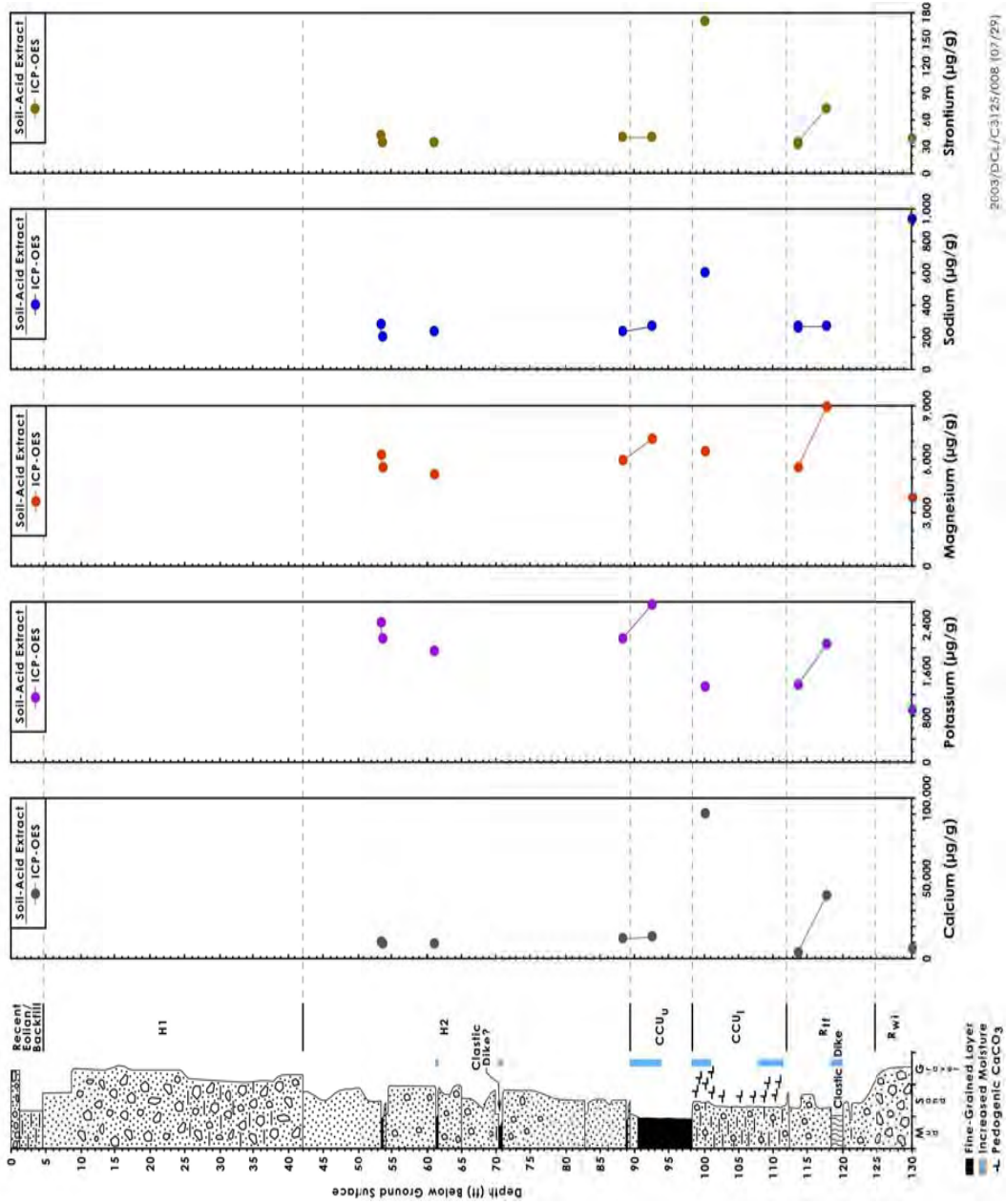
Figure 4.6. Acid-Extractable Concentrations of Major Cations in Borehole 299-W10-27 Sediment
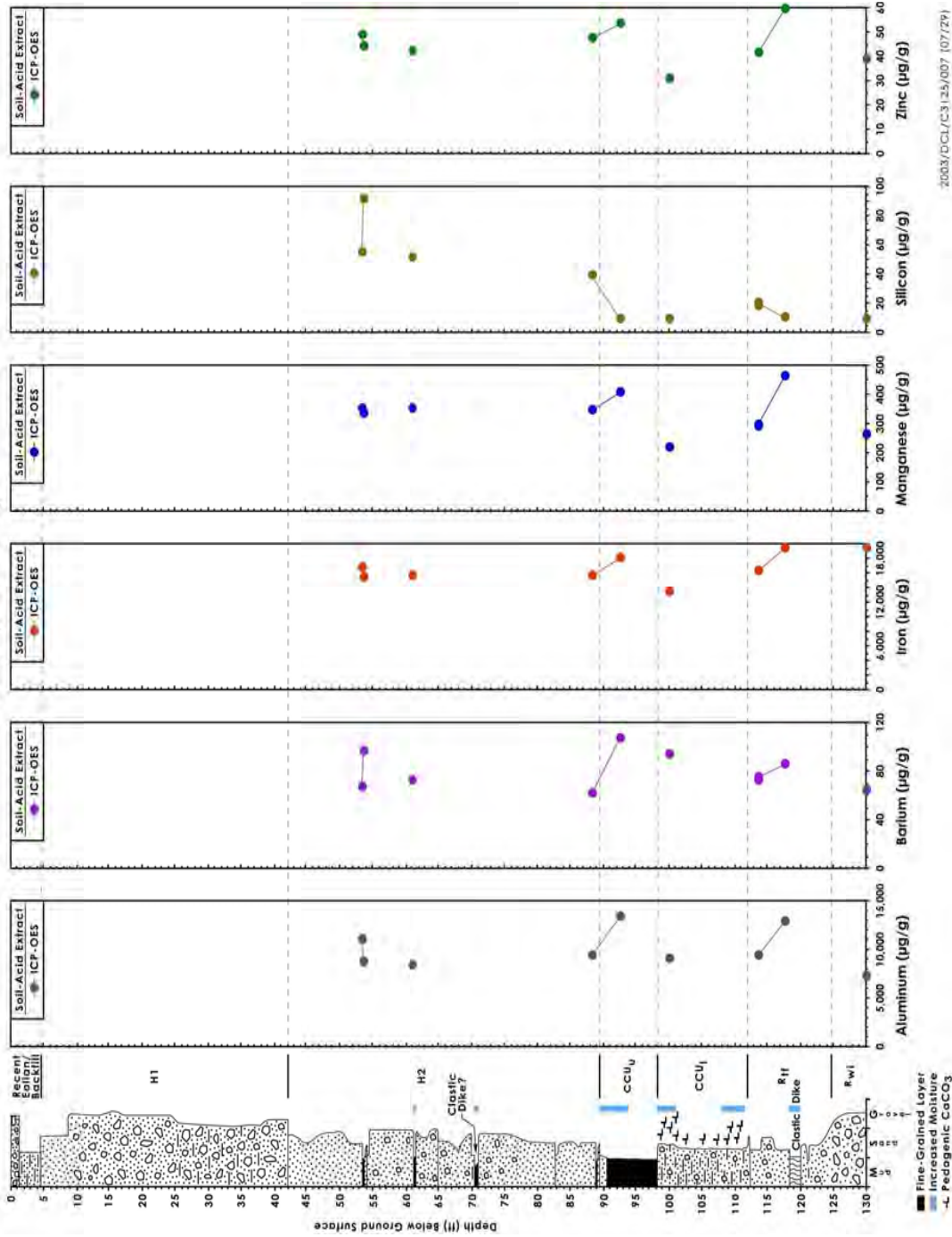
Figure 4.7. Acid-Extractable Concentrations of Aluminum, Barium, Iron, Manganese, Silicon and Zinc from Borehole 299-W10-27 Sediments
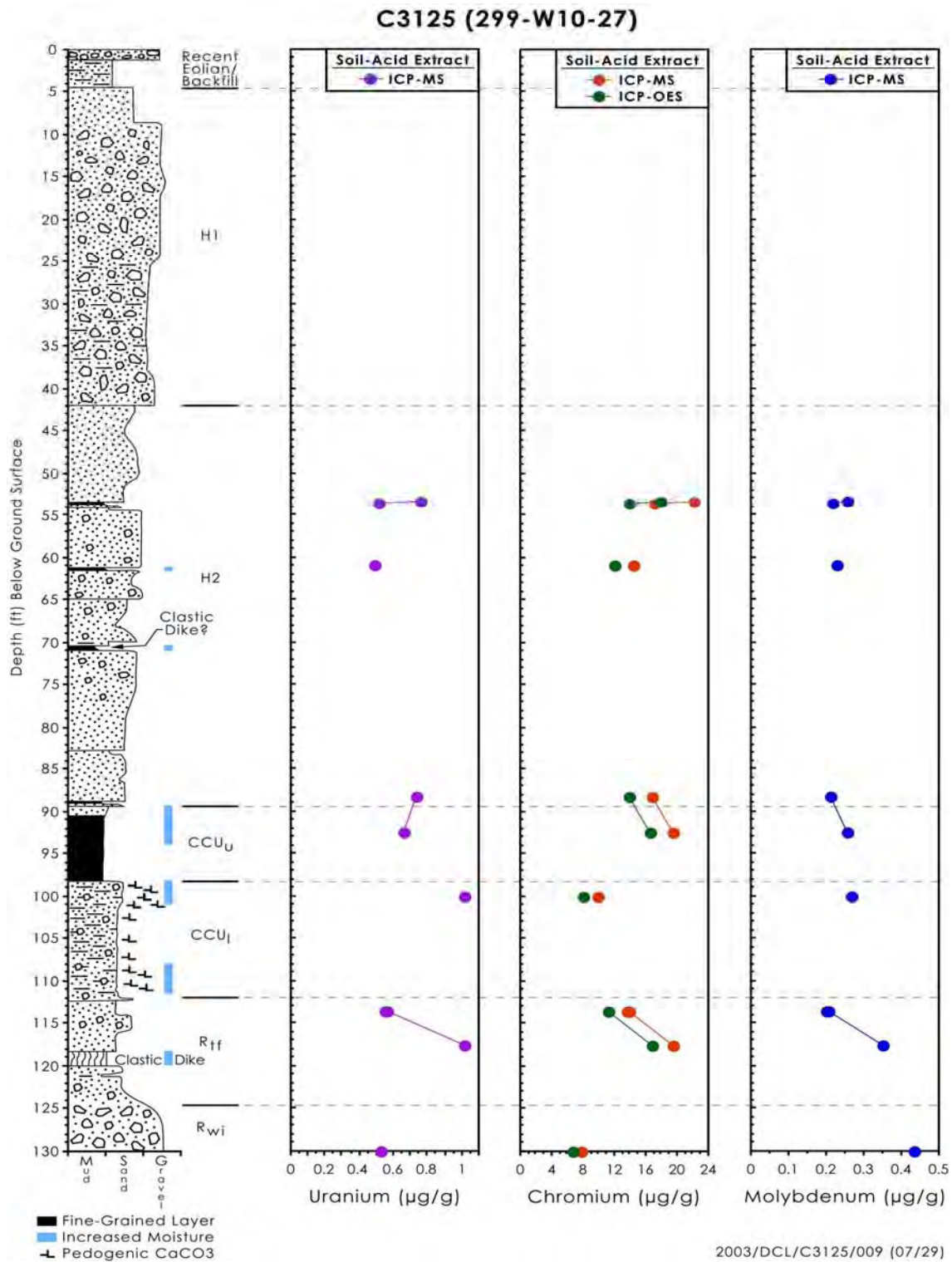
Figure 4.8. Concentration of Uranium-238, Chromium, and Molybdenum in 299-W10-27 Borehole Sediment that is Acid-Extractable. (Technetium-99 and Ruthenium were not detected in clean sediments; thus, they are not plotted).
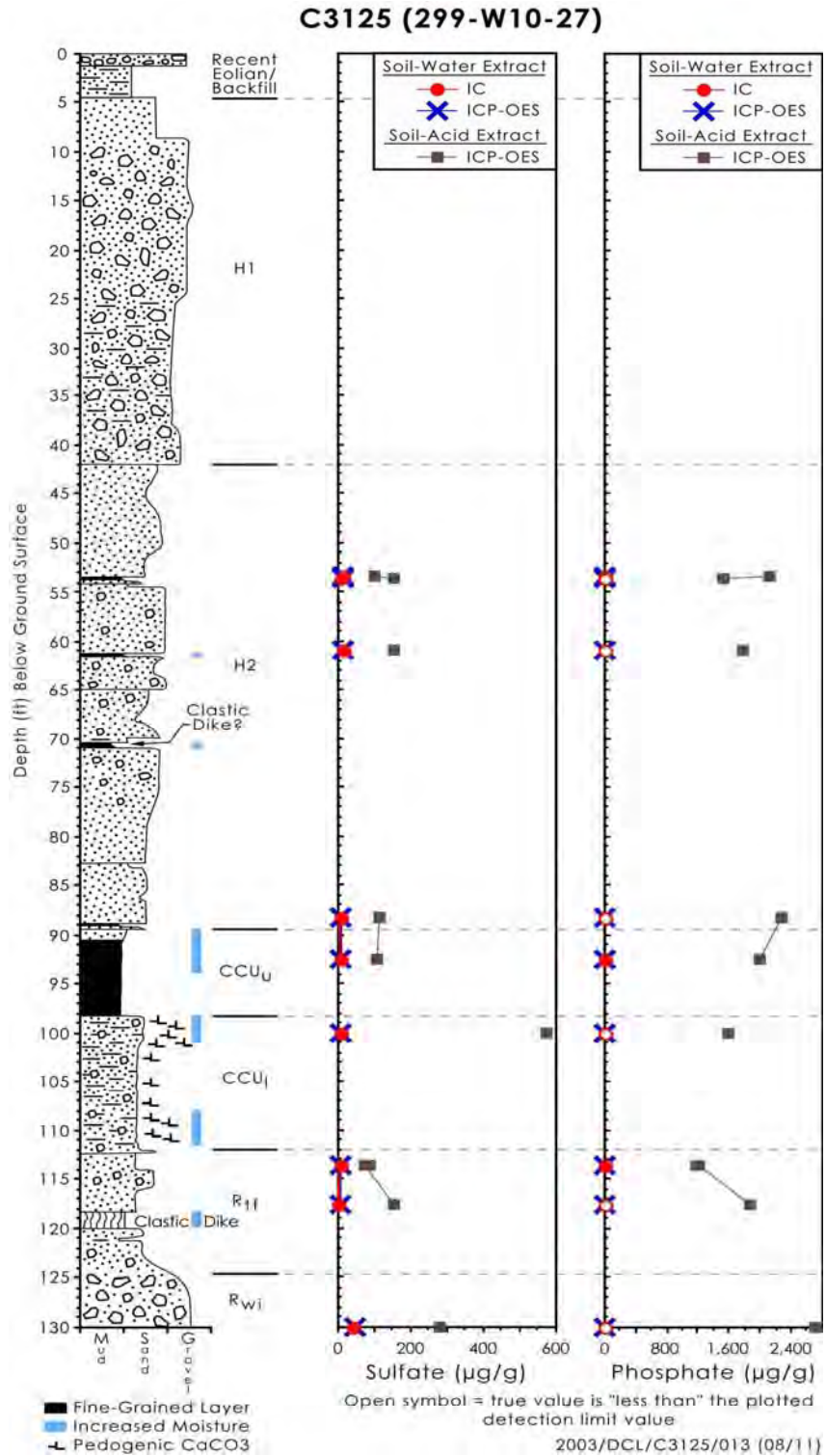
Figure 4.9. Comparison between Acid-and Water-Extractable Sulfate and Phosphate in Vadose Zone Sediments from Borehole 299-W10-27

Table 4.11.   Total Chemical Composition of Borehole 299-W10-27 Sediments (as wt% Oxides)

Depth (ft bgs)	53.3	53.5	61	88.3	92.5	100	113.5	113.5 DUP	117.5	130
Unit	H2	H2	H2	H2	CCU_u	CCU_l	R_{tf}	R_{tf}	R_{tf}	R_{wi}
CO_2	0.81	0.73	0.77	1.17	1.17	9.71	0.22	0.04	3.85	0.29
Na_2O	2.56	2.60	2.52	2.42	2.02	1.97	2.56	2.60	2.16	2.95
MgO	1.82	1.54	1.87	1.66	1.79	2.85	1.36	1.35	1.53	2.70
Al_2O_3	12.40	12.17	12.37	11.83	11.58	9.74	12.08	12.21	11.13	12.28
SiO_2	66.32	68.41	66.59	66.53	66.39	48.91	69.59	69.27	63.73	60.08
P_2O_5	0.17	0.14	0.17	0.15	0.16	0.15	0.10	0.10	0.12	0.30
SO_3	NA[1]	NA	NA	NA	NA	NA	NA	NA	NA	NA
Cl	NA	NA	NA	NA	NA	NA	NA	NA	NA	NA
K_2O	2.25	2.43	2.23	2.26	2.23	1.10	2.41	2.38	2.29	1.67
CaO	3.37	3.13	3.67	3.65	3.23	15.67	1.95	1.90	4.97	5.26
TiO_2	0.670	0.575	0.784	0.654	0.658	1.193	0.520	0.532	0.530	1.465
V_2O_5	1.67E-02	1.42E-02	2.01E-02	1.54E-02	1.32E-02	2.82E-02	1.29E-02	1.34E-02	1.36E-02	3.77E-02
Cr_2O_3	1.05E-02	7.60E-03	1.08E-02	1.23E-02	8.04E-03	6.72E-03	7.89E-03	7.45E-03	9.06E-03	1.08E-02
MnO	0.105	0.086	0.101	0.094	0.103	0.100	0.089	0.084	0.103	0.152
Fe_2O_3	8.92	6.11	8.13	7.38	9.15	7.14	8.94	8.69	11.05	12.75
CoO	1.53E-03	1.14E-03	1.65E-03	1.27E-03	1.27E-03	1.53E-03	1.14E-03	8.90E-04	1.27E-03	2.80E-03
NiO	4.20E-03	2.55E-03	1.86E-02	2.11E-02	3.82E-03	3.82E-03	3.18E-03	1.78E-03	4.07E-03	4.58E-03

Table 4.11.   (contd)

Depth (ft bgs)	53.3	53.5	61	88.3	92.5	100	113.5	113.5 DUP	117.5	130
Unit	$H2$	$H2$	$H2$	$H2$	CCU_u	CCU_l	R_{tf}	R_{tf}	R_{tf}	R_{wi}
ZnO	7.72E-03	7.22E-03	7.84E-03	7.84E-03	1.24E-03	8.59E-03	7.84E-03	-3.73E-03	6.72E-03	9.09E-03
Rb_2O	8.31E-03	8.42E-03	8.75E-03	8.75E-03	9.08E-03	3.17E-03	9.08E-03	8.75E-03	9.41E-03	4.81E-03
SrO	4.27E-02	4.28E-02	4.19E-02	4.27E-02	3.19E-02	4.93E-02	4.00E-02	4.12E-02	3.74E-02	3.98E-02
YO_2	3.21E-03	2.58E-03	3.05E-03	3.18E-03	3.82E-03	2.79E-03	2.50E-03	2.51E-03	2.94E-03	3.67E-03
ZrO_2	2.69E-02	2.02E-02	2.33E-02	3.41E-02	4.46E-02	2.33E-02	1.78E-02	1.76E-02	2.20E-02	2.38E-02
BaO	8.457E-02	8.932E-02	8.558E-02	8.284E-02	7.386E-02	5.387E-02	8.189E-02	8.245E-02	7.681E-02	8.898E-02
ThO_2	9.69E-04	8.45E-04	7.97E-04	9.61E-04	1.15E-03	7.08E-04	6.91E-04	6.60E-04	8.45E-04	6.76E-04
UO_3	3.00E-04	2.22E-04	2.61E-04	3.39E-04	3.82E-04	3.30E-04	2.03E-04	2.02E-04	3.37E-04	2.03E-04
Total	**99.60**	**98.12**	**99.43**	**98.03**	**98.68**	**98.72**	**100.01**	**99.33**	**101.65**	**100.13**

(1) NA = Not analyzed.

Table 4.12. Trace Element Composition of Borehole 299-W10-27 Sediments (as µg per g dry sediment)

Depth (ft bgs)	53.3	53.5	61	88.3	92.5	100	113.5	113.5 DUP	117.5	130
Unit	H2	H2	H2	H2	CCU_u	CCU_l	R_{tf}	R_{tf}	R_{tf}	R_{wi}
Be	2	2	2	2	2	1	2	2	2	2
Sc	11	10	12	10	10	15	8	8	9	22
Ga	15	14	16	15	15	12	14	13	14	17
Ge	1.6	1.2	1.5	1.3	1.4	1	1.4	1.2	1.6	0.9
As	9	6	8	7	7	6	7	<5	10	<5
Se	NA[1]	NA	NA	NA	NA	NA	NA	NA	NA	NA
Nb	11.5	8.8	10.1	11.3	12.6	9.4	7.7	7.7	9.1	11.9
Mo	3	<2	2	3	<2	<2	3	<2	4	0
Ag	<0.5	<0.5	<0.5	<0.5	<0.5	<0.5	<0.5	<0.5	<0.5	<0.5
In	<0.1	<0.1	<0.1	<0.1	<0.1	<0.1	<0.1	<0.1	<0.1	<0.1
Sn	4	3	4	4	3	2	5	4	5	3
Sb	1.2	0.8	0.9	0.8	1	0.4	1.3	0.9	1.6	0.4
Cs	3.3	3	3.3	3.2	4.1	1	3.4	3.3	3.9	1.1
La	33.1	27.5	26.9	32.5	38.1	26.3	22.1	23.4	27.7	24.9
Ce	61.8	53.9	51.9	62.1	74.4	49.3	45.3	45.2	53.2	49.9
Pr	6.9	5.82	6.18	6.98	8.6	5.49	5.03	5.02	6.11	5.77
Nd	27.8	22	24.9	28.1	33.3	22.2	18.9	19.6	24.4	23.4
Sm	5.35	4.33	4.74	5.23	6.07	4.64	3.74	3.87	4.61	5.17
Eu	1.27	1.08	1.18	1.14	1.31	1.25	0.967	0.980	1.04	1.70
Gd	3.98	3.23	3.98	3.97	5.33	3.54	3.04	3.18	3.66	4.60
Tb	0.75	0.54	0.72	0.74	0.88	0.62	0.53	0.55	0.66	0.80
Dy	4.38	3.27	4.00	4.16	4.94	3.86	3.18	3.30	3.85	4.96
Ho	0.83	0.65	0.78	0.80	0.97	0.74	0.65	0.63	0.79	1.00
Er	2.52	1.87	2.44	2.54	2.98	2.08	1.92	1.89	2.35	2.86
Tm	0.373	0.275	0.353	0.374	0.457	0.306	0.282	0.281	0.356	0.419
Yb	2.53	1.86	2.30	2.44	2.89	2.02	1.80	1.89	2.26	2.65
Lu	0.373	0.289	0.350	0.371	0.460	0.304	0.288	0.282	0.335	0.407

Table 4.12 (contd)

Depth (ft bgs)	53.3	53.5	61	88.3	92.5	100	113.5	113.5 DUP	117.5	130
Unit	H2	H2	H2	H2	CCU_u	CCU_l	R_{tf}	R_{tf}	R_{tf}	R_{wi}
Hf	5.5	3.8	4.6	6.6	8.2	4.4	3.4	3.3	4.5	4.4
Ta	0.96	0.71	0.78	0.94	1.03	0.70	0.59	0.64	0.77	0.79
W	1.5	1.0	1.1	1.9	1.6	0.6	1.2	1.2	1.6	0.1
Tl	0.48	0.46	0.42	0.46	0.32	0.19	0.49	0.29	0.51	0.26
Pb	13	13	11	12	2	8	10	<5	13	0
Bi	0.3	0.2	0.2	0.3	0.1	0.1	0.3	<0.1	0.4	<0.1

(1) NA = Not analyzed.

Table 4.13. Total, Inorganic, and Organic Carbon Content of Vadose Zone Sediments from Borehole 299-W10-27

Depth (ft bgs)	Stratigraphic Unit	Total Carbon %	Inorganic Carbon %	IC as CaCO$_3$ %	Organic Carbon (by difference)
53.3	H2	0.26	0.22	1.84	0.04
53.5	H2	0.22	0.20	1.64	0.02
61	H2	0.22	0.21	1.75	0.01
88.3	H2	0.35	0.32	2.68	0.03
92.5	CCU$_u$	0.41	0.32	2.63	0.09
100	CCU$_l$	2.75	2.65	22.05	0.10
113.5	R$_{tf}$	0.08	0.06	0.48	0.02
113.5(dup)	R$_{tf}$	0.05	0.01	0.09	0.04
117.5	R$_{tf}$	1.16	1.05	8.79	0.11
130	R$_{wi}$	0.05	0.08	0.69	0.03

Shaded data indicates high concentrations of calcium carbonate.

The sample from the R_{wi} unit is a poorly sorted mixture of gravel, sand, and mud. The hydrometer results and wet sieving results are combined in Figures 4.10 through Figure 4.12 as plots of cumulative percent finer than versus particle size in microns. The data for the two particle size methods are shown in Table 4.15.

Within the Hanford formation H2 unit the samples from 53.3 and 88.3 ft bgs are more fine-grained than the samples from 53.5 and 61 ft bgs. The median grain size of these H2 unit samples are ~150, 260, 250, and 75 microns for the 53.3, 53.5, 61, and 88.3 ft bgs samples.

The sample from the Cold Creek upper subunit is well-sorted, based on the steep slope in Figure 4.11, and has a fine texture with the median grain size, ~57 microns. The sample from the Cold Creek lower subunit is less sorted and has a median grain size of ~110 microns. The two samples of R_{tf} have significantly different particle size distributions with the 113.5 ft bgs sample being medium sand (median particle size ~300 microns) but well-sorted, and the 117.5 ft bgs sample being rather mostly silt (median particle size ~ 45 microns) but less well sorted. The R_{wi} sample is poorly sorted with a median grain size of ~200 microns.

Table 4.14.   Wet Sieve Particle Size Results for Borehole 299-W10-27 Sediments

Depth (ft bgs)	Stratigraphic Unit	Weight Percent		
		Gravel	Sand	Silt/Clay
53.3	H2	0.61	83.94	15.45
53.5	H2	0.39	88.58	11.03
61	H2	4.16	73.86	21.98
88.3	H2	0.14	52.28	47.58
92.5	CCU_u	0.00	27.11	72.89
100	CCU_l	10.5	68.44	21.07
113.5	R_{tf}	0.00	88.78	11.22
117.5	R_{tf}	0.91	11.77	87.32
130	R_{wi}	15.68	48.23	36.09

Table 4.15. Particle Size Data for Borehole 299-W10-27 Sediments Using Two Techniques-Reported as Cumulative Percent Finer Than

Stratigraphic Unit	H2		H2		H2		H2	
Sample	53.3		53.5		61		88.3	
	μm	% finer than	μm	% finer than	μm	% finer than	μm	% finer than
Wet Sieve								
	2000	99.39	2000	99.61	2000	95.84	2000	99.86
	1000	97.79	1000	97.69	1000	89.18	1000	99.37
	500	88.86	500	81.41	500	69.38	500	96.21
	250	56.95	250	43.21	250	49.92	250	86.63
	105	25.14	105	18.93	105	30.23	105	66.59
	74	20.14	74	14.66	74	26.16	74	57.95
	53	15.45	53	11.03	53	21.98	53	47.58
Hydrometer								
	86.65	47.19	80.98	11.88	83.79	20.63	85.30	43.24
	59.83	35.86	56.76	8.91	58.64	17.41	59.35	35.00
	33.41	20.76	32.55	6.68	33.35	12.89	33.55	24.71
	18.06	15.10	17.75	5.20	18.11	10.31	18.14	16.47
	10.33	9.44	10.22	4.45	10.41	9.03	10.38	12.35
	7.27	6.61	7.23	4.45	7.31	7.09	7.31	9.27
	5.94	5.66	5.90	4.45	5.96	6.45	5.97	8.24
	5.14	5.66	5.11	4.45	5.16	6.45	5.17	8.24
	1.48	5.66	1.47	2.97	1.48	3.87	1.48	6.18

Table 4-15.   (contd)

Stratigraphic Unit	CCU_u		CCU_l		R_{tf}		R_{tf}		R_{wi}	
Sample	92.5		100		113.5		117.5		130	
	μm	% finer than	μm	% finer than	μm	% finer than	μm	% finer than	μm	% finer than
Wet Sieve										
	2000	100	2000	89.5	2000	100	2000	99.09	2000	84.32
	1000	100	1000	83.36	1000	99.68	1000	99.09	1000	73.91
	500	99.98	500	76.85	500	96.43	500	98.92	500	61.3
	250	99.98	250	65.1	250	39	250	98.38	250	53.21
	105	97.32	105	39.2	105	6.01	105	98.28	105	42.87
	74	90.82	74	29.37	74	2.58	74	96.53	74	39.49
	53	72.89	53	21.07	53	0.06	53	87.32	53	36.09
Hydrometer										
	83.10	71.35	80.83	25.85	90.75	10.19	89.17	78.65	86.20	37.61
	57.52	53.99	56.77	16.62	62.11	8.15	61.78	65.13	60.24	32.71
	32.92	32.78	32.63	12.93	34.35	6.79	34.36	41.78	34.43	28.62
	17.95	21.21	17.79	11.08	18.35	5.43	18.43	29.49	18.63	23.71
	10.32	15.43	10.25	9.23	10.45	4.75	10.46	19.66	10.60	17.99
	7.28	12.53	7.23	8.31	7.34	4.07	7.31	13.52	7.43	14.72
	5.93	11.57	5.90	7.39	5.98	4.07	5.96	12.29	6.05	13.90
	5.13	10.61	5.11	7.39	5.17	4.07	5.14	9.83	5.23	13.08
	1.48	5.79	1.47	7.39	1.48	2.72	1.47	4.92	1.48	6.54

4.1.8 Matric Suction Potential Measurements

Water potential measurements have been included in the Hanford Tank Farm Vadose Zone Characterization Program to document the energy state of porewaters in the tank farm sediments. At the tank farms, vegetation is absent, surface soils are coarse-textured, and the potential for drainage (recharge) is high (Gee 1987; Gee et al. 1992). However, actual drainage rates are generally unknown. Attempts are currently being made to status the soil water matrix potential and use the analysis to confirm the occurrence of recharge within the Hanford Site tank farms.

The status of soil water can be defined by either the amount of water in the soil (water content) or by the force that holds water to the soil matrix (i.e., the matric potential or suction) (Or and Wraith 2002). In recent studies, Serne et al. (2002b, 2002d, 2002e, and 2002f) measured both water content (gravimetrically) and matric water potential (filter paper method, ASTM 2002) on core samples obtained from boreholes in the SX and B-BX tank farm environs. The same measurements were made at borehole 299-W10-27 near to the TX tank farm. All cores from the Hanford formation H2 unit that were obtained were analyzed. Unfortunately, at 299-W10-27 continuous coring was not performed all the way to the water table so that the entire profile of matric potential is not available.

Table 4.16 and Figure 4.13 show the matric potentials as a function of depth. Also plotted in Figure 4.13 is the gravity head expressed in pressure units (MPa). The gravity head is zero at the water table and increases linearly with height to the soil surface. For the core samples available from 299-W10-27, the water potentials are generally much less than the gravity potential from the shallowest core at 50 ft bgs down to the deepest core taken at 123.5 ft bgs all within the Hanford formation H2 unit. The last sample taken at 123.5 ft bgs appears to have a matric potential larger than the theoretical line but all other measurements are lower than the theoretical line. The green line labeled "theoretical value" in Figure 4.13 is the theoretical line that represents the steady state unit gradient condition, which represents the profile for matric potential in a sediment profile that is neither draining nor drier than (actively evapotranspiring) equilibrium. Matric potential values to the left of the unit gradient line suggest a draining profile. The general trend for the data from 299-W10-27 is that the water potentials are consistent with a draining profile.
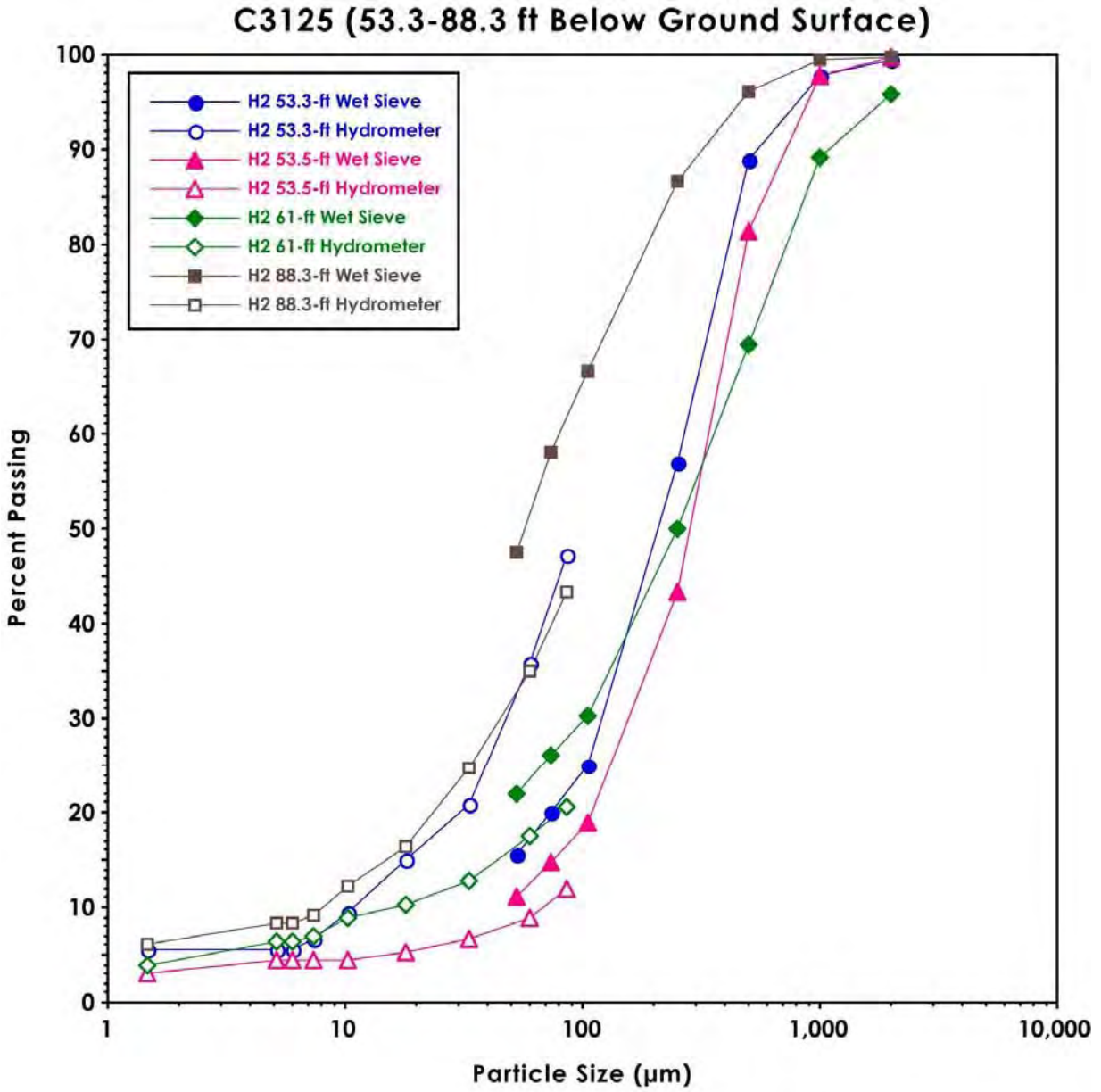
Figure 4.10. Particle Size Distribution of Hanford Formation H2 Unit Subsamples from Borehole 299-W10-27
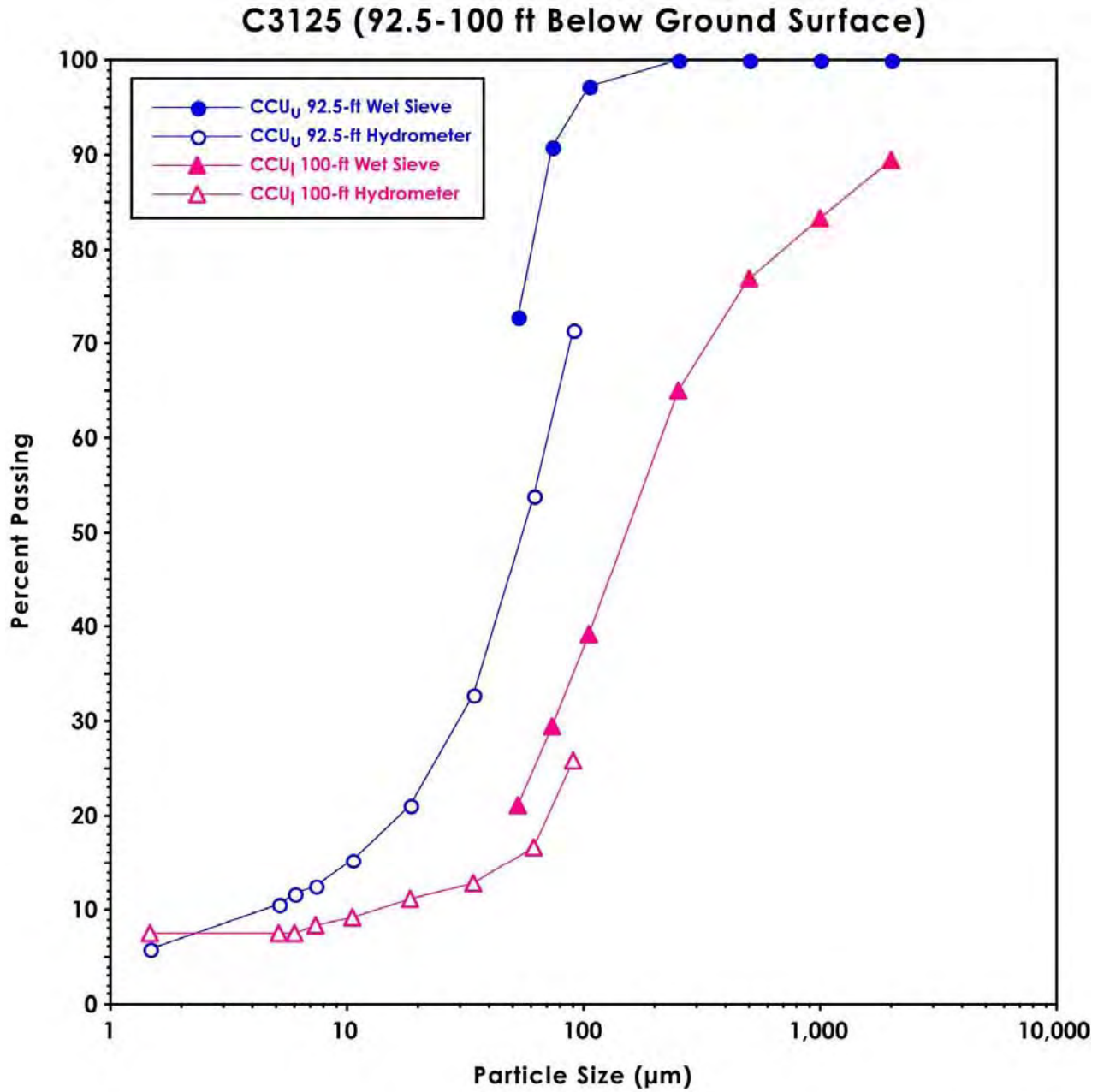
Figure 4.11. Particle Size Distribution of Cold Creek Unit Subsamples from Borehole 299-W10-27
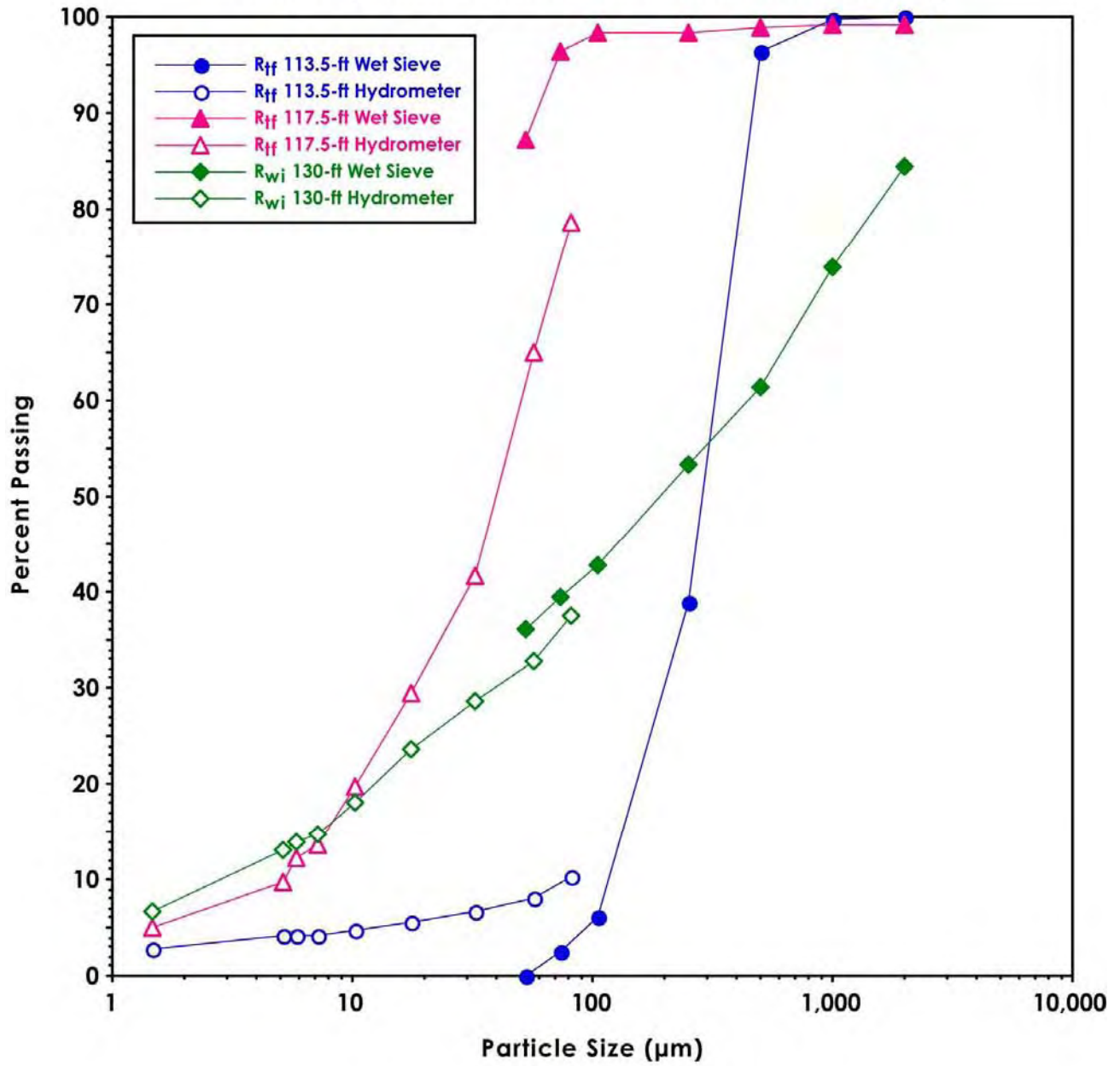
Figure 4.12. Particle Size Distribution of Ringold Formation Subsamples from Borehole 299-W10-27

Table 4.16.   Matric Potential as Measured by Filter Paper Method for Borehole 299-W10-27 Core Sediments

Depth (ft bgs)	Stratigraphic Unit	Matric Potential (MPa)	Theoretical Potential (MPa)	Depth (ft bgs)	Stratigraphic Unit	Matric Potential (MPa)	Theoretical Potential (MPa)
	H1	no samples	no samples	83.5	H2	0.1678	0.4306
50	H2	0.0936	0.5327	85	H2	0.2659	0.4260
51	H2	0.0901	0.5297	86	H2	0.2442	0.4230
52.5	H2	0.0105	0.5251	87.5	H2	0.2542	0.4184
53.5	H2	0.0250	0.5221	88.5	H2	0.3339	0.4154
55	H2	0.1107	0.5175	90	CCU_u	0.1667	0.4108
56	H2	0.1449	0.5144	92.5	CCU_u	0.0944	0.4032
57.5	H2	0.0948	0.5099	95	CCU_u	0.0416	0.3956
58.5	H2	0.1094	0.5068	96	CCU_u	0.0486	0.3925
60	H2	0.0797	0.5022	97.5	CCU_u	0.1300	0.3879
61	H2	0.0143	0.4992	100	CCU_l	0.1040	0.3803
62.5	H2	0.0519	0.4946	102.5	CCU_l	0.1356	0.3727
63.5	H2	0.1447	0.4916	105	CCU_l	0.2160	0.3651
65	H2	0.1053	0.4870	106	CCU_l	0.1703	0.3620
66	H2	0.1506	0.4840	107.5	CCU_l	0.0708	0.3575
67.5	H2	0.2371	0.4794	110	CCU_l	0.0676	0.3498
68.5	H2	0.1567	0.4763	112.5	R_{tf}	0.1365	0.3422
70	H2	0.0415	0.4718	113.5	R_{tf}	0.1944	0.3392
71	H2	0.1212	0.4687	115	R_{tf}	0.2668	0.3346
72.5	H2	0.2565	0.4641	116	R_{tf}	0.2362	0.3316

Table 4.16. (contd)

Depth (ft bgs)	Stratigraphic Unit	Matric Potential (MPa)	Theoretical Potential (MPa)	Depth (ft bgs)	Stratigraphic Unit	Matric Potential (MPa)	Theoretical Potential (MPa)
73.5	**H2**	0.2663	0.4611	117.5	$\mathbf{R_{tf}}$	0.0716	0.3270
75	**H2**	0.1670	0.4565	120	$\mathbf{R_{tf}}$	0.0052	0.3194
77.5	**H2**	0.2442	0.4489	121	$\mathbf{R_{tf}}$	0.1281	0.3163
78.5	**H2**	0.3129	0.4459	122.5	$\mathbf{R_{tf}}$	0.2083	0.3117
80	**H2**	0.2056	0.4413	123.5	$\mathbf{R_{tf}}$	0.4030	0.3087
81	**H2**	0.1937	0.4382		$\mathbf{R_{wi}}$	no samples	no samples
82.5	**H2**	0.3691	0.4337	224.78	water table		0.0000
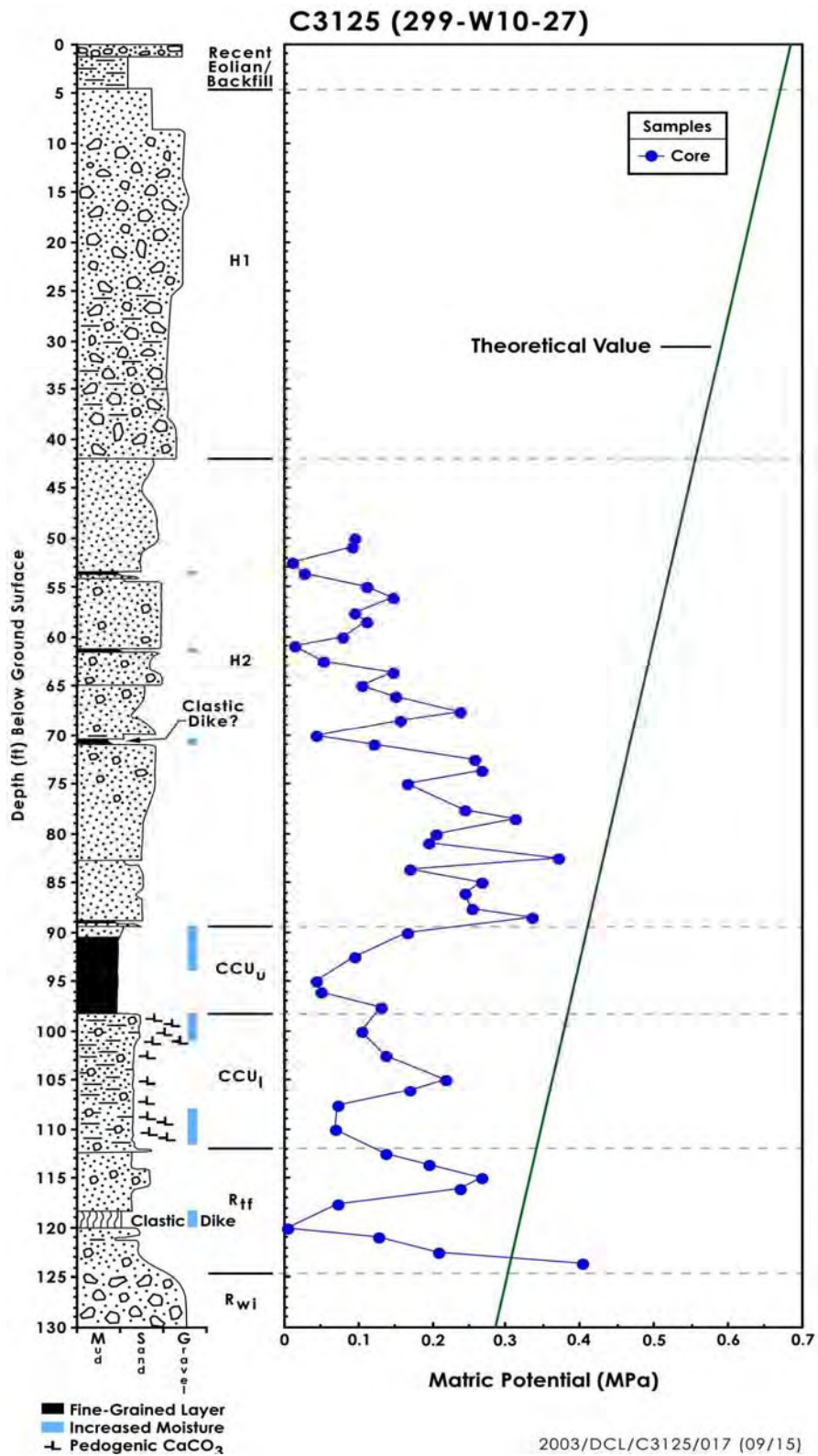
Figure 4.13. **Matric Water Potential Measured by Filter Paper Technique on Core Samples from Borehole 299-W10-27**

4.2 Vadose Zone Sediment from Borehole C3830

Borehole C3830 was pushed into the vadose zone sediment approximately 40 ft southwest of tank TX-105 to evaluate whether there is evidence to support designating tank TX-105 as having leaked in the past. The borehole reached a depth of 116.8 ft bgs at which point it met refusal.

4.2.1 Moisture Content

The moisture content of the 36 core liners as a function of depth and lithology are shown in Table 4.17 and Figure 2.12. The backfill samples have a mean moisture content of 6.1% by weight with little variation. The Hanford formation H2 samples have a mean moisture content of 5.7% by weight with more variation that tracks variations in particle size (finer-grained samples have slightly higher moisture contents). The Cold Creek subunits have higher moisture with averages for the two subunits of 11.0% and 11.9% by weight. Both show about the same variability as the H2 unit. The average moisture content of the H2 unit samples measured in C3830 is about one percent by weight larger than the average for the same stratigraphic unit at the uncontaminated borehole 299-W10-27. Whether this is significant and an indication of the various tank farm operations that encourage higher moisture infiltration cannot be determined because of the small sample population obtained. The moisture content of the C3830 borehole and 299-W10-27 Cold Creek unit sediments is about the same, and this does not suggest any excess tank fluids in the Cold Creek unit sediments at C3830.

Table 4.17.   Moisture Content of Borehole C3830 Cores

Sample No.	Depth (ft bgs)	Stratigraphic Unit	Lithology	Moisture Content % Wt
C3830-14.96B	15.30	Bkfl	Sand	9.20%
C3830-14.96A	15.98	Bkfl		5.37%
C3830-27.91B	28.25	Bkfl	Gravelly sand	6.74%
C3830-27.91A	28.92	Bkfl		5.37%
C3830-40.93B	41.32	Bkfl	Gravelly sand	6.97%
C3830-40.93A	42.10	Bkfl		5.50%
C3830-46.20B	46.53	Bkfl	Gravelly sand	5.71%
C3830-46.20A	47.18	Bkfl		5.16%
C3830-47.50B	47.88	Bkfl	Slightly gravelly sand	5.71%
C3830-47.50A	48.63	Bkfl		4.96%
C3830-52.98B	53.33	H2	Sand	8.11%
C3830-52.98B DUP	53.33	H2		6.94%
C3830-52.98A	54.02	H2	Sand	3.70%
C3830-52.98A DUP	54.02	H2		4.36%

Table 4.17. (contd)

Sample No.	Depth (ft bgs)	Stratigraphic Unit	Lithology	Moisture Content % Wt
C3830-56.99B	57.34	H2	Sand	3.31%
C3830-56.99A	58.03	H2		3.41%
C3830-58.29B	58.65	H2	Sand to silty sand	9.62%
C3830-58.29A	59.35	H2		12.42%
C3830-66.06B	66.41	H2	Sand	3.63%
C3830-66.06A	67.11	H2		2.46%
C3830-71.95B	72.29	H2	Sand	4.74%
C3830-71.95A	72.63	H2		3.45%
C3830-76.98B	77.33	H2	Sand	3.63%
C3830-76.98A	78.01	H2		3.14%
C3830-80.91B	81.24	H2	Sand	7.10%
C3830-80.91A	81.89	H2		3.70%
C3830-86.11B	86.44	H2	Sand to silty sand	5.53%
C3830-86.11A	87.09	H2		11.18%
C3830-98.97B	99.32	H2	Sand	9.19%
C3830-98.97A	100.02	H2		4.95%
C3830-100.32B	100.67	CCU_u	Silty sand to sandy silt and silt	10.53%
C3830-100.32A	101.37	CCU_u		6.83%
C3830-100.32A DUP	101.37	CCU_u		7.08%
C3830-102.99B	103.36	CCU_u	Sandy silt	14.72%
C3830-102.99A	104.08	CCU_u		12.59%
C3830-107.89B	108.22	CCU_u	Sandy silt	11.57%
C3830-107.89A	108.87	CCU_u		9.80%
C3830-113.55B	113.92	CCU_l	Calcareous, pebbly sand and mud	9.98%
C3830-113.55A	114.64	CCU_l		13.91%

4.2.2 1:1 Sediment:Water Extracts for Borehole C3830

The A liners (the deeper of two liners) from the 18 cores were characterized by performing 1:1 sediment:water extracts. The following tables present the mass of a given constituent leached per gram of sediment as measured in the water extracts to allow direct comparison to the same data for the background sediments from borehole 299-W10-27. Other figures show dilution-corrected values that represent concentrations in vadose zone porewater. As discussed in several other Vadose Zone Characterization Project reports, the dilution-corrected 1:1 sediment:water extracts are a reasonable estimate of the actual vadose zone porewater (see Serne et al. 2002b, 2002c, 2002e, 2002f).

4.2.2.1   pH and Electrical Conductivity

The 1:1 sediment:water extract pH and EC data are shown in Table 4.18. Both the measured value and dilution-corrected EC values are shown. Figure 4.14 shows the 1:1 sediment:water extract pH value and dilution-corrected EC as a function of depth and stratigraphy. A comparison of the data in Table 4.18 with the pH and EC of the 299-W10-27 extracts suggests that there is slightly elevated EC in the C3830 borehole sediments from 59.4 ft bgs to the bottom of the borehole samples. This suggests the presence of some higher than normal salinity fluids in the porewaters, such as tank liquors. Although the dilution-corrected porewater EC is above the background values, the highest values between 67 and 87 ft bgs are equivalent to a pore solution of 0.12 M KCl, the salt solution used to calibrate the conductivity probe. The leaks near the SX108-109 and BX-102 tanks had peak vadose zone porewater concentrations that were equivalent to much more concentrated waste fluids, 7 to 17 and 0.7 to 1 M KCl solutions, respectively. The maximum dilution-corrected EC at C3830 is 12.5 mS/cm, slightly lower than the dilution-corrected EC at 299-E33-46 near tank B-110 that contained 15.1 mS/cm (Serne et al. 2002f).

The slightly elevated electrical conductivities are evident in Figure 4.14 from about 65 to 87 ft bgs. The figure also shows that there are elevated values for sodium and nitrate in this range. The sodium peak value occurs at 65 ft bgs and the peak nitrate and EC value occurs at ~77 ft bgs.

Table 4.18.   pH and EC Data for Sediment:Water Extracts from Borehole 3830

Sample No.	Depth (ft bgs)	Stratigraphic Unit	pH	Conductivity mS/cm	Dilution-Corrected Conductivity (mS/cm)
C3830-14.96A	15.98	Bkfl	7.93	0.171	3.19
C3830-27.91A	28.92	Bkfl	8.39	0.166	3.09
C3830-40.93A	42.10	Bkfl	8.02	0.163	3.01
C3830-46.20A	47.18	Bkfl	8.15	0.158	3.14
C3830-47.50A	48.63	Bkfl	8.09	0.218	4.40
C3830-52.98A	54.02	H2	8.03	0.178	4.81
C3830-52.98A DUP	54.02	H2	8.13	0.165	3.79
C3830-56.99A	58.03	H2	7.92	0.166	4.88
C3830-58.29A	59.35	H2	7.97	0.218	1.76
C3830-66.06A	67.11	H2	8.24	0.307	12.51
C3830-71.95A	72.63	H2	7.93	0.259	7.51
C3830-76.98A	78.01	H2	7.94	0.358	11.40
C3830-80.91A	81.89	H2	7.97	0.205	5.74
C3830-86.11A	87.09	H2	8.02	0.365	3.54
C3830-98.97A	100.02	H2	7.93	0.246	4.97
C3830-100.32A	101.37	CCU_u	8.00	0.243	3.56
C3830-100.32A DUP	101.37	CCU_u	7.98	0.256	3.62
C3830-102.99A	104.08	CCU_u	7.96	0.253	2.66
C3830-107.89A	108.87	CCU_u	8.07	0.205	2.09
C3830-113.55A	114.64	CCU_l	8.00	0.332	2.39
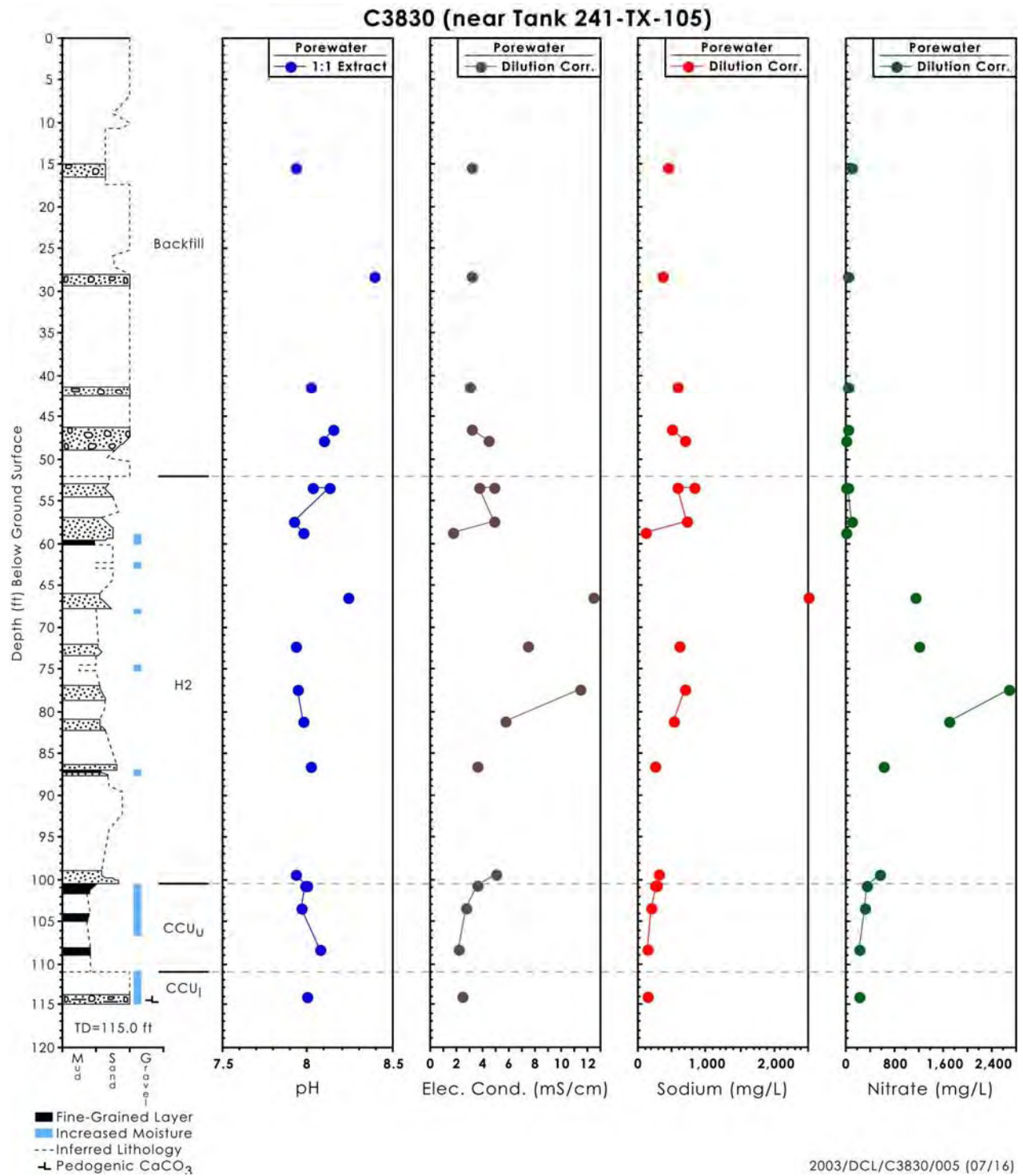
Figure 4.14. Borehole 3830 Sediment: Water Extract pH and Calculated Porewater Electrical Conductivity, Sodium, and Nitrate

4.2.2.2   Water Extract Composition or the 1:1 Sediment:Water Extract for C3830

The water extract values for the major cations and anions and several trace constituents are discussed in this section. The anion data are tabulated in Tables 4.19 and 4.20 and Figure 4.15 in units of mass per gram of dry sediment. The data for the water extracts of borehole C3830 for fluoride, phosphate, nitrite, and bromide do not differ significantly from the same data for the uncontaminated sediments from borehole 299-W10-27. However, there are obvious signs of elevated chloride, nitrate, and sulfate in the water extracts of C3830 sediments. The chloride values from 78 ft bgs to the deepest sample obtained at 114.6 ft bgs are elevated by a factor of ~8 to 20 when compared to water extracts of uncontaminated sediment. The nitrate water extract values for the C3830 borehole are elevated from 67 ft bgs to the deepest sample obtained. The nitrate water extract values are 10 to 50 times larger than for the background sediments in similar uncontaminated lithologies in borehole 299-W10-27. The sulfate water extracts from C3830 are elevated from about 59.4 ft bgs to the deepest sample obtained and the values exceed the background sediment values by a factor of 2 to 8. There is one very large value for water-extractable carbonate in the Cold Creek upper subunit in the C3830 borehole sediments at 104 ft bgs. As shown in Figure 4.15, a direct analysis of carbonate using the ion chromatograph does not show a similar very high value, however. So we attribute the very large alkalinity value to analytical vagaries and conclude that dissolvable carbonates in the C3830 sediments are not significantly different than values in the background borehole 299-W10-27. The agreement between measuring the water extracts for phosphate and sulfate directly with the ion chromatograph and indirectly by converting the ICP measurements for phosphorous and sulfur is very good. Besides validating the ion chromatography data, we can state that the water-extractable sulfur and phosphorous species are in fact sulfate and phosphate.

The water-extractable small organic molecules in the C3830 borehole sediments are shown in Table 4.20. The values are not significantly different than for the uncontaminated sediments from borehole 299-W10-27.

The water-extractable major cations in the C3830 borehole sediments are tabulated in Table 4.21 and the distribution with depth is shown in Figure 4.16. The distribution of the divalent alkaline earth cations (Mg, Ca, and Sr but not Ba) and the monovalent cation potassium, show low water-extractable quantities between 54 and 58 ft bgs and the lowest values of all at 67 ft bgs. The water-extractable mass of these cations at the 59.35 ft bgs sample is very similar to uncontaminated background sediments. Conversely, the distribution of water-extractable sodium is higher than the mass that is water-leachable from uncontaminated sediments in the whole profile, excepting at the 59.35 ft depth. These trends suggest that tank fluids that are high in sodium and nitrate did seep into the vadose zone near this borehole. The sodium pushed the natural divalent cations and some of the natural potassium off the sediment cation exchange sites in the sediments between 54 and at least 67 ft bgs, excepting a zone near 59.35 ft bgs. There is a fine-grained lens near this depth that may have forced tank fluids to percolate horizontally around this zone. We have observed the same cation distribution and ion exchange fronts where divalent cations and sometimes potassium are depleted in the shallow sediments and high levels of water-extractable sodium are present at both the SX and BX tank farms where tank fluids have been confirmed as being present (see Serne et al. 2002b, 2002c, 2002e, 2002f for details). Right below the leading edge of the sodium plume one finds elevated levels of the divalent cations that were displaced. We observe the high levels of divalent cations in the samples between 78 and 87 ft bgs. But there are also elevated masses of water-leachable calcium and strontium at 104.8 and 114.64 ft bgs, both in the Cold Creek unit.

Table 4.19. Water-Extractable Anions in Borehole C3830 Vadose Zone Sediments (µg/g dry sediment)

Depth (ft bgs)	Stratigraphic Unit	Fluoride	Chloride	Nitrate	Alk as CO$_3$	Sulfate	Phosphate	Nitrite	Bromide
15.98	Bkfl	0.48	0.34	4.91	47.54	2.09	4.03	<0.08	<0.14
28.92	Bkfl	0.79	0.49	1.58	31.85	7.21	0.28	<0.08	<0.14
42.10	Bkfl	0.96	0.32	1.18	14.48	9.61	<0.24	<0.08	<0.14
47.18	Bkfl	0.56	0.62	1.57	42.89	10.97	0.25	<0.08	<0.14
48.63	Bkfl	0.54	1.58	0.80	50.47	25.63	0.44	<0.08	<0.14
54.02	H2	0.38	0.17	0.59	52.28	5.13	<0.24	<0.08	<0.14
54.02	H2	0.45	0.51	1.91	48.96	6.29	<0.24	<0.08	<0.14
58.03	H2	0.44	0.80	2.94	41.46	9.23	<0.24	<0.08	<0.14
59.35	H2	0.46	1.75	1.46	52.27	21.19	<0.24	<0.08	0.17
67.11	H2	0.42	2.83	28.24	26.15	28.36	<0.24	<0.08	<0.14
72.63	H2	0.32	3.86	41.87	29.97	25.00	<0.24	<0.08	<0.14
78.01	H2	0.33	9.31	84.13	32.79	34.64	<0.24	0.08	<0.14
81.89	H2	0.47	7.98	62.17	35.95	31.58	0.27	0.08	<0.14
87.09	H2	0.38	11.64	69.28	41.78	50.04	0.31	0.44	<0.15
100.02	H2	0.42	11.03	27.97	36.12	22.82	<0.24	<0.08	<0.14
101.37	CCU$_u$	0.30	10.76	22.84	25.67	28.83	0.29	0.10	<0.14
101.37	CCU$_u$	0.30	11.45	24.21	20.44	30.77	<0.17	<0.07	<0.14
104.08	CCU$_u$	0.46	16.94	37.25	207.55	46.83	0.31	0.17	<0.18
108.87	CCU$_u$	0.12	2.64	20.21	34.68	13.40	0.57	<0.08	<0.14
114.64	CCU$_l$	1.19	2.92	31.75	47.06	48.18	0.24	0.21	0.15
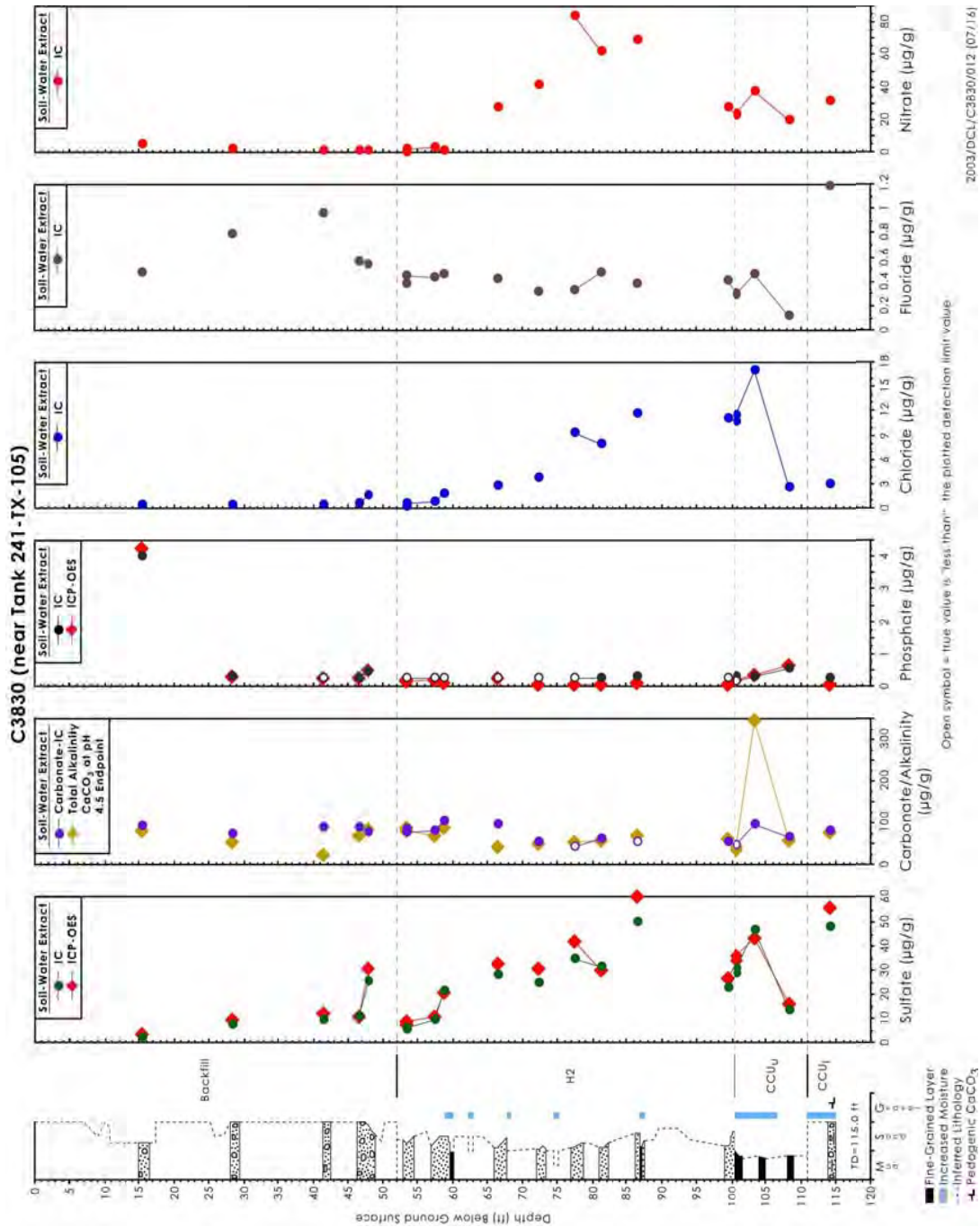
Figure 4.15. Borehole C3830 Water-Extractable Anions (μg/g dry sediment)

It is possible that some of the elevated divalent cations in these deeper samples reflect water-leachable carbonate minerals. The lowest values for water-leachable divalent cations occur at 67 ft bgs and this depth is also the position of the highest water-leachable sodium.

The water-extractable aluminum, silicon, iron, manganese, zinc, phosphorous, and sulfur in the C3830 borehole sediments are shown in Table 4.22 and Figure 4.17. The phosphorous and sulfur data were converted to water-extractable phosphate and sulfate and plotted with the anion data in Figure 4.15. In general, the agreement between direct measurement of the two anions by ion chromatography and the converted ICP measurements is very good. The water-soluble aluminum and iron data show elevated values between the depths of 54 and 67 to 72 ft bgs, excepting the sample at 59.35 ft bgs. We speculate that these elevated values indicate some chemical reaction between alkaline tank fluids and native sediments that formed precipitates of aluminum and iron that are more water soluble than the native sediments. There are also elevated water-leachable aluminum and iron in the upper Cold Creek subunit. The water-extractable S values between the depths of 67 ft bgs and the bottom of the borehole at 114.6 ft bgs also appear to be elevated in comparison with the S that is water extractable from background sediments in borehole 299-W10-27.

The water-extractable data for potentially mobile metals such as technetium-99, uranium-238, chromium, molybdenum and ruthenium (Ru) are shown in Table 4.23 and Figure 4.18. There appears to be some technetium-99 present in the sediment in the zone between 67 and 87 ft bgs and perhaps as shallow as 59 ft bgs and as deep as 100 ft bgs. There is only one indication of uranium-238 contamination in the sample at 67 ft bgs. This sample also shows the highest value found in borehole C3830 sediments for chromium. The molybdenum and ruthenium data do not suggest any elevated values compared to uncontaminated sediments. The technetium-99 data suggest that tank fluids may have percolated down through the entire Hanford formation H2 unit and then stopped on top of the fine-grained CCU_u mud contact at 100.4 ft bgs.

4.2.3   Derivation of Vadose Zone Porewater Chemical Composition

The 1:1 water extract data was recalculated to derive the porewater composition of the vadose zone sediments. From knowledge of the moisture content of the sediment samples taken from the A liners of each core, we calculated the amount of deionized water that would be needed to make the water extract exactly one part water (total of native porewater and added deionized water) to one part by weight dry sediment. The ratio of the total volume of water in the extract to the native mass of porewater is the dilution factor. We assume that the deionized water acts solely as a diluent of the existing porewater and that the deionized water does not dissolve any of the solids in the sediments. Thus by correcting for the dilution, we can estimate the actual chemical composition of the native porewater in the partially saturated vadose zone sediments. The assumption that none of the solid is dissolved during the water extraction process is simplistic. In comparisons of actual porewater that was obtained via ultracentrifugation of vadose zone sediments to the dilution-corrected calculated porewaters from both contaminated and uncontaminated sediments from the SX and B-BX Tank Farms (see Serne et al. 2002b, 2002c, 2002d, 2002e, 2002f), we have found that for highly contaminated sediments that the comparison is quite good. For slightly contaminated or uncontaminated sediments the dilution-corrected water extract data is biased high by a factor of 2 to 7 for many constituents such that the true porewater is less saline.

Tables 4.24 through 4.27 and Figures 4.19 through 4.22 show the derived porewater composition of key constituents as a function of depth and stratigraphy. The most concentrated porewater — on a total

dissolved salts basis — is found at ~78 ft bgs and has a total concentration of 102 meq/L cations and 102 meq/L anions. The calculated most saline porewater composition consists of 42 meq/L Ca, 32 meq/L Na, 18 meq/L Mg and 10 meq/L K. The cation charge is compensated by the following mixture of anions: 40 meq/L nitrate, 34 meq/L bicarbonate, 20 meq/L sulfate and 8 meq/L chloride. This concentration is very dilute compared to the vadose zone porewaters found at the SX and BX tank farms where the total ionic strength of the porewaters were as high as 7,000 to 17,000 and 1,000 meq/L, respectively. At the borehole emplaced near tank B-110 the most saline porewater was 150 to 160 meq/L.

There appears to be a thin lens of technetium-99 in the porewaters between the depths of 67 and 87 ft bgs that has maximum concentrations of 1 to 4 x 10^{+05} pCi/L. On a per gram of dry sediment basis, these porewater concentrations are 3 to 11 pCi/g. Because the water content of the H2 unit sediments is so small, when equated to porewater concentrations this small mass of technetium-99 reaches concentrations about 400 times larger than the drinking water standard in the thin zone where technetium-99 was found.

The calculated porewater uranium concentration for the sample at 67 ft bgs is 0.1 g/L and about 1000 times larger than any other measurements. As mentioned, this water extract also shows high values for technetium-99, chromium, silicon, aluminum, iron, and sulfate besides the uranium. Thus we conclude that there is tank-related contamination concentrated at this location.

4.2.4   8 M Nitric Acid-Extractable Amounts of Selected Elements in C3830 Sediments

The same cores that were characterized for water-extractable constituents were also characterized to see how much of various constituents could be leached with hot 8 M nitric acid. A comparison between the quantities that were acid extractable with those that are water extractable often indicates the relative mobility of a given constituent and can sometimes differentiate man-disposed from naturally occurring constituents. Finally, a comparison of the acid-extractable quantities in suspected contaminated sediments with acid-extractable amounts in uncontaminated sediments can be used to delineate the presence of less mobile contaminants.

The quantities of various constituents in the C3830 vadose zone sediments that were acid extractable are shown in Tables 4.28 through 4.30 and Figures 4.23 through 4.26. Upon comparing the acid extract data for borehole C3830 with similar lithologies in the uncontaminated borehole 299-W10-27, most of the variation in mass leached per gram of sediment versus depth is found to be lithology-related. That is, for most constituents there is no sign of elevated values of acid-leachable constituents in borehole C3830 sediments with the exception of acid-extractable sulfur (assumed to represent sulfate) and technetium-99. The acid-extractable sulfate profile in borehole C3830 sediments averages about 4 to 7 times higher than in comparable uncontaminated sediments from borehole 299-W10-27. The acid-extractable technetium-99 profile in the C3830 borehole sediments is elevated from 42 ft bgs to 109 ft bgs by a factor of 4 over the distribution of acid-extractable technetium-99 in the background sediment, which was a measure of our detection limit. The deepest sample obtained in borehole C3830 within the lower Cold Creek (caliche) subunit does not have this slight elevated acid-extractable technetium-99. We are not sure how to interpret the acid-extractable data for technetium-99 in borehole C3830. If the differences are real, it would appear that some technetium-99 is present in the backfill at 42 ft bgs, which is above the base of

Table 4.20.   Water-Extractable Organics in C3830 Vadose Zone Sediments (µg/g)

Depth (ft bgs)	Stratigraphic Unit	Formate	Acetate	Oxalate
15.98	Bkfl	<0.11	<0.16	0.28
28.92	Bkfl	<0.11	<0.16	0.34
42.10	Bkfl	<0.11	0.30	0.33
47.18	Bkfl	<0.12	0.47	<0.22
48.63	Bkfl	<0.11	<0.16	0.72
54.02	H2	<0.11	0.34	0.52
54.02	H2	<0.11	0.32	0.30
58.03	H2	<0.11	0.21	<0.21
59.35	H2	<0.11	0.22	0.28
67.11	H2	<0.11	0.90	<0.21
72.63	H2	<0.11	0.21	0.45
78.01	H2	0.11	<0.16	<0.21
81.89	H2	0.12	<0.17	0.36
87.09	H2	<0.12	<0.17	<0.23
100.02	H2	<0.11	<0.16	<0.21
101.37	CCU$_u$	<0.11	<0.16	<0.21
101.37	CCU$_u$	<0.11	<0.16	<0.21
104.08	CCU$_u$	<0.15	<0.21	<0.28
108.87	CCU$_u$	0.24	0.36	0.37
114.64	CCU$_l$	0.40	0.75	0.41

Table 4.21. Water-Extractable Cations in C3830 Vadose Zone Sediments (µg/g dry sediment)

Depth (ft bgs)	Stratigraphic Unit	Mg	Ca	Sr	Ba	Na	K
15.98	Bkfl	1.49	4.90	2.21E-02	1.21E-02	24.30	7.70
28.92	Bkfl	1.56	6.45	3.39E-02	1.84E-02	19.86	5.49
42.10	Bkfl	1.43	4.03	2.58E-02	2.89E-02	31.63	5.28
47.18	Bkfl	0.68	3.37	1.92E-02	2.13E-02	26.07	4.39
48.63	Bkfl	1.18	4.98	2.69E-02	1.69E-02	33.74	6.57
54.02	H2	0.64	3.01	1.67E-02	2.11E-02	30.20	4.46
54.02	H2	0.82	3.96	2.27E-02	2.25E-02	24.69	4.19
58.03	H2	1.01	3.69	2.03E-02	1.57E-02	24.76	4.21
59.35	H2	3.31	17.72	8.08E-02	5.59E-02	13.06	5.29
67.11	H2	0.32	1.63	7.69E-03	2.03E-02	61.43	4.34
72.63	H2	3.82	14.03	7.05E-02	3.22E-02	21.40	8.87
78.01	H2	6.46	25.09	1.26E-01	3.70E-02	21.40	11.31
81.89	H2	4.32	17.01	8.70E-02	3.09E-02	19.03	9.17
87.09	H2	6.30	27.42	1.34E-01	2.01E-02	26.97	10.93
100.02	H2	3.71	16.93	8.28E-02	2.08E-02	15.14	6.06
101.37	CCU$_u$	3.38	15.57	7.28E-02	2.15E-02	17.06	5.04
101.37	CCU$_u$	3.61	17.18	7.99E-02	2.49E-02	19.18	5.35
104.08	CCU$_u$	4.80	22.04	1.11E-01	6.78E-02	24.08	8.26
108.87	CCU$_u$	3.66	13.65	6.89E-02	2.72E-02	13.33	5.24
114.64	CCU$_l$	11.03	22.48	1.95E-01	5.13E-02	17.69	5.27

Table 4.22. Water-Extractable Concentrations of Other Metals in C3830 Vadose Zone Sediments (µg/g dry sediment)

Depth (ft bgs)	Stratigraphic Unit	Al	Si	Fe	Mn	Zn	P as PO₄	S as SO₄
15.98	Bkfl	3.49E-02	12.90	4.96E-02	(1.81E-03)	3.72E-02	4.25E+00	3.24
28.92	Bkfl	(2.20E-02)[a]	13.34	(3.60E-02)	(1.26E-03)	4.06E-02	2.78E-01	9.52
42.10	Bkfl	2.70E-02	13.73	(3.56E-02)	(1.07E-03)	3.28E-02	2.49E-01	11.94
47.18	Bkfl	3.52E-02	11.64	(3.54E-02)	(6.82E-04)	2.99E-02	2.75E-01	10.81
48.63	Bkfl	5.09E-02	9.86	6.07E-02	(2.48E-03)	3.52E-02	4.95E-01	30.96
54.02	H2	8.46E-02	7.26	5.31E-02	(1.58E-03)	4.01E-02	(1.84E-01)	7.16
54.02	H2	9.23E-02	8.50	8.14E-02	(2.09E-03)	3.56E-02	(1.76E-01)	8.63
58.03	H2	8.24E-02	8.16	5.67E-02	(1.17E-03)	3.16E-02	(1.83E-01)	10.98
59.35	H2	3.03E-02	7.18	(4.40E-02)	(2.18E-02)	2.87E-02	(9.32E-02)	20.68
67.11	H2	1.16E-01	9.17	5.42E-02	(1.14E-03)	4.32E-02	2.60E-01	32.47
72.63	H2	5.51E-02	7.21	(1.87E-02)	3.09E-03	5.59E-02	(4.64E-02)	30.44
78.01	H2	3.44E-02	7.56	(2.46E-02)	(1.54E-03)	3.96E-02	(5.45E-02)	41.93
81.89	H2	6.02E-02	8.55	(3.05E-02)	(1.17E-03)	3.42E-02	(5.20E-02)	30.13
87.09	H2	(1.65E-02)	11.19	(3.21E-02)	(1.18E-03)	3.80E-02	(1.07E-01)	60.68
100.02	H2	(2.18E-02)	10.47	(2.25E-02)	(6.89E-04)	2.83E-02	(4.91E-02)	26.93
101.37	CCUᵤ	2.04E-01	11.06	2.34E-01	(1.61E-03)	4.18E-02	2.06E-01	33.91
101.37	CCUᵤ	5.28E-02	10.54	(3.44E-02)	(5.30E-04)	1.05E-01	(1.91E-01)	36.10
104.08	CCUᵤ	(2.10E-02)	12.61	(2.70E-02)	ND[b]	5.14E-02	3.39E-01	43.40
108.87	CCUᵤ	(1.57E-02)	6.59	(1.39E-02)	(1.77E-03)	2.96E-02	6.26E-01	16.13
114.64	CCUₗ	(1.19E-03)	27.16	8.93E-02	(9.64E-04)	4.82E-02	(3.83E-02)	56.37

(a) Parentheses signify values below level of quantitation but considered valid.
(b) ND = Not determined.

Table 4.23. Water-Extractable Concentrations of Mobile Metals in C3830 Vadose Sediments (µg/g dry sediment)

Depth (ft bgs)	Stratigraphic Unit	Tc-99[a]	U-238	Cr	Mo (ICP-MS)	Mo (ICP)	Ru
15.98	Bkfl	**<4.24E+00**[b]	8.05E-04	6.79E-04	5.76E-03	6.88E-03	(6.50E-05)
28.92	Bkfl	**<4.24E+00**	1.72E-03	(2.94E-04)	1.20E-02	1.53E-02	(5.40E-05)
42.10	Bkfl	**<4.31E+00**	7.44E-03	1.16E-03	9.26E-03	1.07E-02	(4.37E-05)
47.18	Bkfl	(3.48E-01)[a]	2.09E-03	(3.91E-04)	5.57E-03	8.51E-03	(4.21E-05)
48.63	Bkfl	**<4.25E+00**	1.58E-03	(4.34E-04)	8.52E-03	9.36E-03	(2.40E-05)
54.02	H2	**<4.24E+00**	1.83E-03	5.06E-04	1.02E-02	1.04E-02	(5.55E-05)
54.02	H2	**<4.24E+00**	1.12E-03	2.98E-03	1.66E-02	1.77E-02	(5.10E-05)
58.03	H2	**<4.25E+00**	4.61E-04	5.48E-04	1.37E-02	1.63E-02	(3.91E-05)
59.35	H2	(1.70E-01)[c]	1.07E-03	(4.37E-04)	4.94E-02	5.49E-02	(4.30E-05)
67.11	H2	(2.88E+00)	2.79E+00	8.39E-03	1.00E-02	1.25E-02	(6.30E-05)
72.63	H2	(4.08E+00)	8.21E-04	1.27E-03	9.37E-03	1.35E-02	(4.98E-05)
78.01	H2	1.14E+01	2.09E-04	1.55E-03	8.81E-03	1.20E-02	(9.75E-05)
81.89	H2	6.19E+00	1.49E-03	1.05E-03	1.21E-02	1.46E-02	(6.53E-05)
87.09	H2	5.60E+00	5.77E-04	2.02E-03	3.59E-02	4.30E-02	(5.64E-05)
100.02	H2	(3.39E-01)	5.67E-04	1.86E-03	7.50E-03	1.07E-02	(3.10E-05)
101.37	CCU$_u$	**<4.24E+00**	3.12E-04	2.45E-03	1.14E-02	1.52E-02	(3.60E-05)
101.37	CCU$_u$	**<4.24E+00**	3.52E-04	2.62E-03	1.28E-02	1.79E-02	(2.40E-05)
104.08	CCU$_u$	**<5.61E+00**	6.26E-04	5.49E-03	3.16E-02	3.73E-02	(3.44E-05)
108.87	CCU$_u$	**<4.24E+00**	1.35E-03	8.52E-04	2.08E-02	2.44E-02	(2.70E-05)
114.64	CCU$_l$	**<4.24E+00**	2.89E-03	1.28E-03	1.97E-02	2.45E-02	(3.60E-05)

(a) Technetium-99 data are in units of pCi/g while all others are µg/g of dry sediment.
(b) Values in bold are below detection limit and no attempt to optimize detection limit was performed.
(c) Parentheses signify values below level of quantitation but considered valid.

Figure 4.16. Water-Extractable Cations in C3830 Vadose Zone Sediments (μg/g)

2003/DCL/C3830/015 (07/23)

4.54
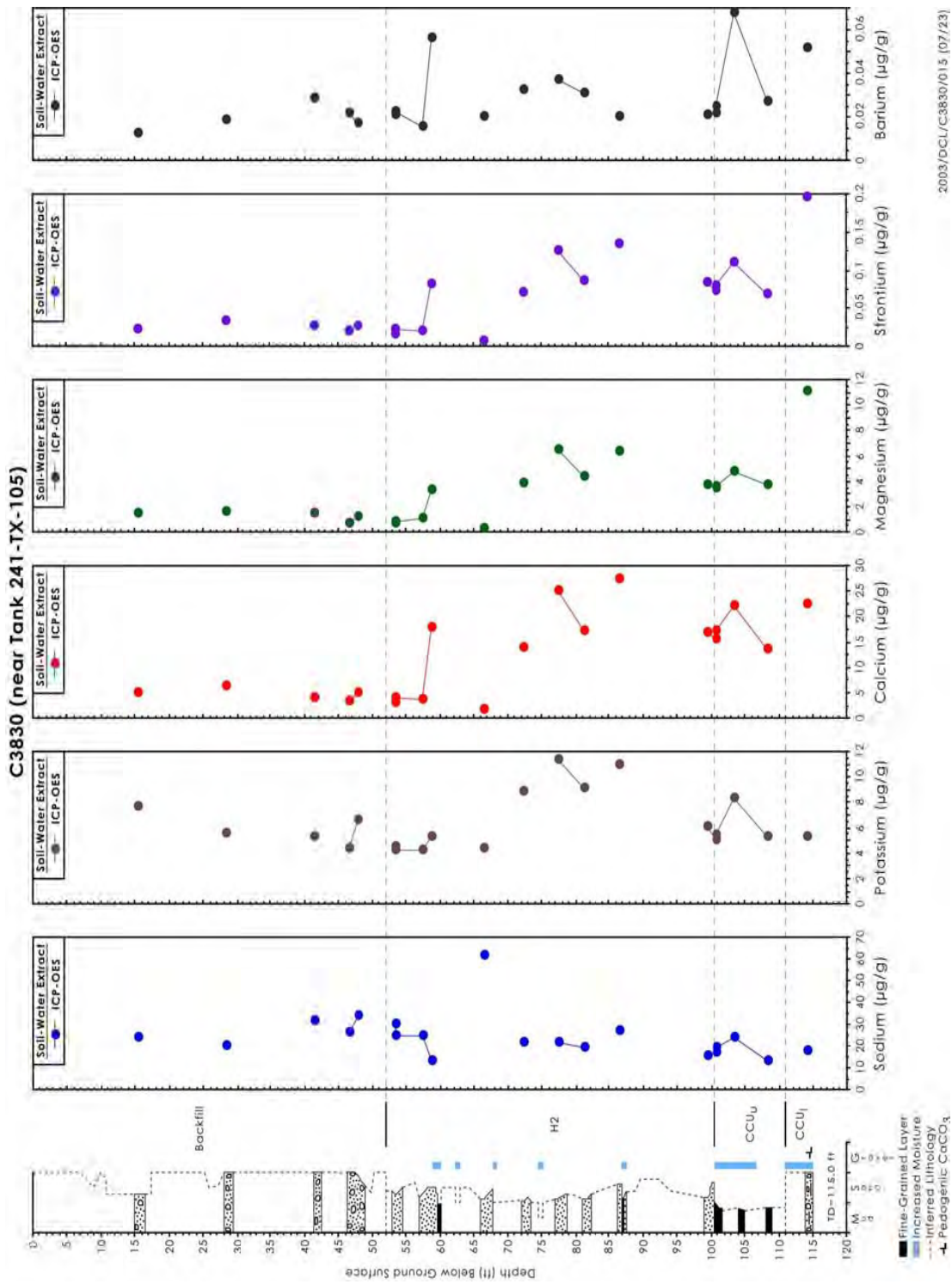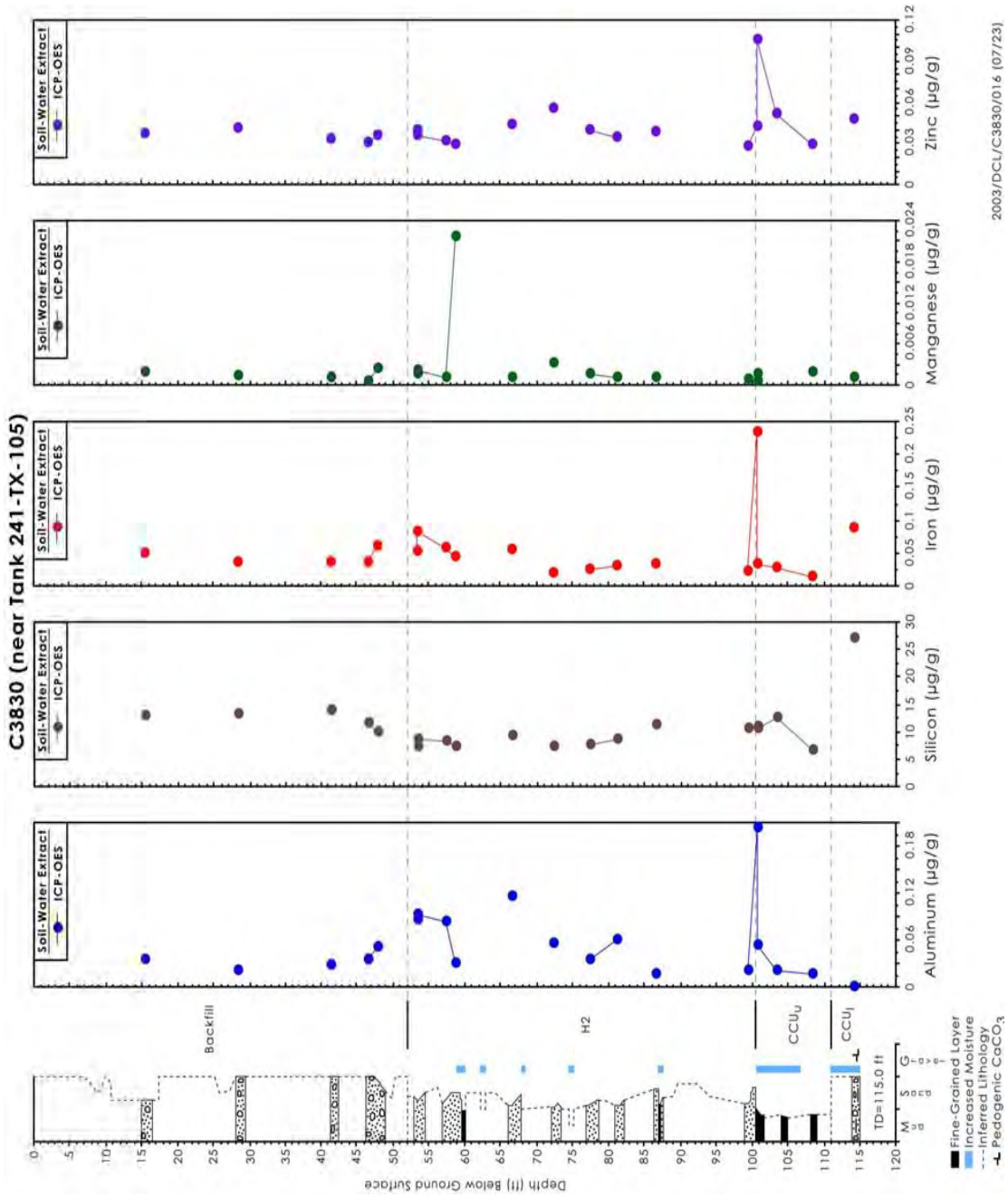
Figure 4.17. Water-Extractable Metals in C3830 Vadose Sediments (μg/g dry sediment)
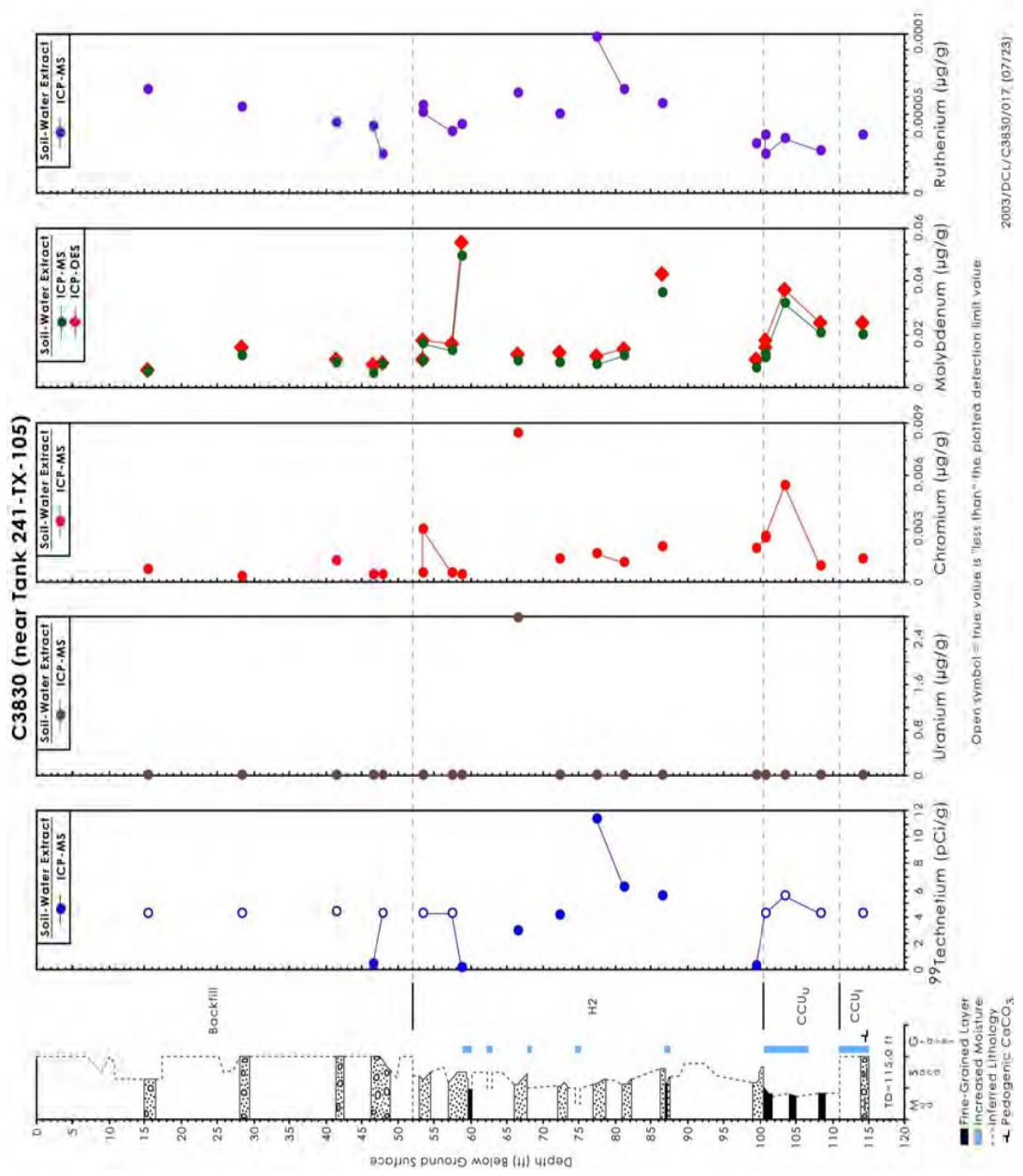
Figure 4.18. Distribution of Mobile Metals in Water Extracts of C3830 Vadose Zone Sediments

Table 4.24. Calculated Porewater Cation Concentrations in C3830 Vadose Zone Sediments

	Units	mg/L	mg/L	mg/L	µg/L	mg/L	mg/L
Depth (ft bgs)	Stratigraphic Unit	Mg	Ca	Sr	Ba	Na	K
15.98	Bkfl	2.78E+01	9.14E+01	4.12E-01	2.26E+02	4.53E+02	1.44E+02
28.92	Bkfl	2.90E+01	1.20E+02	6.31E-01	3.42E+02	3.70E+02	1.02E+02
42.10	Bkfl	2.60E+01	7.32E+01	4.70E-01	5.24E+02	5.75E+02	9.59E+01
47.18	Bkfl	1.31E+01	6.53E+01	3.72E-01	4.13E+02	5.05E+02	8.52E+01
48.63	Bkfl	2.37E+01	1.00E+02	5.43E-01	3.41E+02	6.80E+02	1.32E+02
54.02	H2	1.73E+01	8.13E+01	4.51E-01	5.72E+02	8.17E+02	1.21E+02
54.02	H2	1.89E+01	9.09E+01	5.21E-01	5.17E+02	5.67E+02	9.62E+01
58.03	H2	2.94E+01	1.08E+02	5.93E-01	4.58E+02	7.25E+02	1.23E+02
59.35	H2	2.67E+01	1.43E+02	6.51E-01	4.50E+02	1.05E+02	4.26E+01
67.11	H2	1.28E+01	6.66E+01	3.13E-01	8.25E+02	2.50E+03	1.77E+02
72.63	H2	1.11E+02	4.07E+02	2.04E+00	9.34E+02	6.20E+02	2.57E+02
78.01	H2	2.06E+02	7.99E+02	4.02E+00	1.18E+03	6.82E+02	3.60E+02
81.89	H2	1.17E+02	4.60E+02	2.35E+00	8.36E+02	5.14E+02	2.48E+02
87.09	H2	5.63E+01	2.45E+02	1.20E+00	1.80E+02	2.41E+02	9.77E+01
100.02	H2	7.49E+01	3.42E+02	1.67E+00	4.20E+02	3.06E+02	1.22E+02
101.37	CCU$_u$	4.95E+01	2.28E+02	1.07E+00	3.14E+02	2.50E+02	7.37E+01
101.37	CCU$_u$	5.10E+01	2.43E+02	1.13E+00	3.52E+02	2.71E+02	7.57E+01
104.08	CCU$_u$	3.81E+01	1.75E+02	8.81E-01	5.39E+02	1.91E+02	6.56E+01
108.87	CCU$_u$	3.73E+01	1.39E+02	7.04E-01	2.77E+02	1.36E+02	5.35E+01
114.64	CCU$_l$	7.93E+01	1.62E+02	1.40E+00	3.69E+02	1.27E+02	3.79E+01

Table 4.25. Calculated Porewater Anion Concentrations in C3830 Vadose Zone Sediments

	Units	mg/L	mg/L	mg/L	mg/L	mg/L	mg/L
Depth (ft bgs)	Stratigraphic Unit	Fluoride	Chloride	Nitrate	Alk as CO$_3$	Sulfate	Phosphate
15.98	Bkfl	8.96	6.41	91.52	885.94	38.97	75.18
28.92	Bkfl	14.65	9.06	29.48	592.86	134.24	5.26
42.10	Bkfl	17.40	5.80	21.36	263.12	174.55	**<4.43**[a]
47.18	Bkfl	10.90	12.04	30.45	831.43	212.63	4.77
48.63	Bkfl	10.89	31.77	16.14	1016.53	516.32	8.94
54.02	H2	10.41	4.58	15.91	1413.45	138.60	**<6.49**
54.02	H2	10.35	11.80	43.82	1123.28	144.19	**<5.51**
58.03	H2	12.90	23.45	86.15	1214.14	270.33	**<7.05**
59.35	H2	3.74	14.08	11.77	420.89	170.67	**<1.93**
67.11	H2	17.11	115.37	1150.19	1065.09	1155.12	**<9.78**
72.63	H2	9.15	111.91	1213.38	868.55	724.58	**<6.96**
78.01	H2	10.43	296.38	2679.25	1044.43	1103.04	**<7.64**
81.89	H2	12.79	215.65	1680.36	971.71	853.70	7.36
87.09	H2	3.41	104.08	619.53	373.65	447.48	2.73
100.02	H2	8.42	222.97	565.15	729.96	461.17	**<4.85**
101.37	CCU$_u$	4.45	157.43	334.17	375.54	421.86	4.18
101.37	CCU$_u$	4.19	161.84	342.22	288.83	434.87	**<2.36**
104.08	CCU$_u$	3.68	134.49	295.83	1648.13	371.84	2.46
108.87	CCU$_u$	1.27	26.92	206.27	354.02	136.75	5.77
114.64	CCU$_l$	8.54	21.02	228.21	338.28	346.38	1.73

(a) Values in bold are below instrument detection limit.

4.58

Table 4.26. Calculated Porewater Concentrations of Selected Constituents in C3830 Vadose Zone Sediments

Depth (ft bgs)	Stratigraphic Unit	Al µg/L	Si mg/L	Fe µg/L	Mn µg/L	Zn µg/L	PO$_4$ (ICP) mg/L	SO$_4$ (ICP) mg/L
15.98	Bkfl	6.50E+02	2.40E+02	9.24E+02	(3.38E+01)	6.92E+02	7.91E+01	6.04E+01
28.92	Bkfl	(4.10E+02)[a]	2.48E+02	(6.71E+02)	(2.35E+01)	7.56E+02	5.18E+00	1.77E+02
42.10	Bkfl	4.90E+02	2.50E+02	(6.48E+02)	(1.94E+01)	5.95E+02	4.52E+00	2.17E+02
47.18	Bkfl	6.83E+02	2.26E+02	(6.86E+02)	(1.32E+01)	5.80E+02	5.34E+00	2.10E+02
48.63	Bkfl	1.02E+03	1.99E+02	1.22E+03	(4.99E+01)	7.09E+02	9.97E+00	6.24E+02
54.02	H2	2.29E+03	1.96E+02	1.44E+03	(4.27E+01)	1.08E+03	4.98E+00	1.94E+02
54.02	H2	2.12E+03	1.95E+02	1.87E+03	(4.79E+01)	8.16E+02	4.04E+00	1.98E+02
58.03	H2	2.41E+03	2.39E+02	1.66E+03	(3.43E+01)	9.25E+02	5.36E+00	3.22E+02
59.35	H2	2.44E+02	5.78E+01	(3.54E+02)	(1.75E+02)	2.31E+02	7.50E-01	1.67E+02
67.11	H2	4.72E+03	3.74E+02	2.21E+03	(4.63E+01)	1.76E+03	1.06E+01	1.32E+03
72.63	H2	1.60E+03	2.09E+02	(5.43E+02)	8.96E+01	1.62E+03	1.34E+00	8.83E+02
78.01	H2	1.09E+03	2.41E+02	(7.83E+02)	(4.90E+01)	1.26E+03	1.74E+00	1.34E+03
81.89	H2	1.63E+03	2.31E+02	(8.24E+02)	(3.16E+01)	9.23E+02	1.41E+00	8.16E+02
87.09	H2	(1.48E+02)	1.00E+02	(2.87E+02)	(1.05E+01)	3.40E+02	9.57E-01	5.43E+02
100.02	H2	(4.40E+02)	2.12E+02	(4.55E+02)	(1.39E+01)	5.73E+02	9.92E-01	5.45E+02
101.37	CCU$_u$	2.99E+03	1.62E+02	3.43E+03	(2.35E+01)	6.11E+02	3.01E+00	4.97E+02
101.37	CCU$_u$	7.46E+02	1.49E+02	(4.86E+02)	(7.49E+00)	1.49E+03	2.70E+00	5.11E+02
104.08	CCU$_u$	(1.67E+02)	1.00E+02	(2.14E+02)	ND[b]	4.08E+02	2.69E+00	3.45E+02
108.87	CCU$_u$	(1.60E+02)	6.72E+01	(1.42E+02)	(1.81E+01)	3.02E+02	6.38E+00	1.65E+02
114.64	CCU$_l$	(8.59E+00)	1.95E+02	6.42E+02	(6.93E+00)	3.46E+02	2.75E-01	4.06E+02

(a) Parentheses signify values below level of quantitation but considered valid.
(b) ND = Not determined.

Table 4.27. Calculated Porewater Concentrations of Potentially Mobile Constituents in C3830 Vadose Sediments

	Units	pCi/L	µg/L	µg/L	µg/L	µg/L	µg/L
Depth (ft bgs)	Stratigraphic Unit	Tc-99[a]	U-238	Cr (ICP-MS)	Mo	Mo (ICP-MS)	Ru
15.98	Bkfl	**<7.90E+04**[b]	1.50E+01	1.27E+01	1.28E+02	1.07E+02	(1.21E+00)
28.92	Bkfl	**<7.90E+04**	3.20E+01	(5.47E+00)	2.85E+02	2.24E+02	(1.01E+00)
42.10	Bkfl	**<7.83E+04**	1.35E+02	2.10E+01	1.94E+02	1.68E+02	(7.94E-01)
47.18	Bkfl	(6.74E+03)[c]	4.06E+01	(7.57E+00)	1.65E+02	1.08E+02	(8.15E-01)
48.63	Bkfl	**<8.56E+04**	3.19E+01	(8.74E+00)	1.88E+02	1.72E+02	(4.84E-01)
54.02	H2	**<1.15E+05**	4.95E+01	1.37E+01	2.80E+02	2.76E+02	(1.50E+00)
54.02	H2	**<9.73E+04**	2.57E+01	6.85E+01	4.07E+02	3.81E+02	(1.17E+00)
58.03	H2	**<1.25E+05**	1.35E+01	1.60E+01	4.76E+02	4.01E+02	(1.15E+00)
59.35	H2	(1.37E+03)	8.62E+00	(3.52E+00)	4.42E+02	3.98E+02	(3.46E-01)
67.11	H2	(1.17E+05)	1.13E+05	3.42E+02	5.09E+02	4.09E+02	(2.57E+00)
72.63	H2	(1.18E+05)	2.38E+01	3.68E+01	3.93E+02	2.72E+02	(1.44E+00)
78.01	H2	3.62E+05	6.66E+00	4.95E+01	3.82E+02	2.81E+02	(3.11E+00)
81.89	H2	1.67E+05	4.03E+01	2.85E+01	3.93E+02	3.28E+02	(1.76E+00)
87.09	H2	5.00E+04	5.16E+00	1.81E+01	3.85E+02	3.21E+02	(5.05E-01)
100.02	H2	(6.86E+03)	1.15E+01	3.76E+01	2.15E+02	1.51E+02	(6.27E-01)
101.37	CCU$_u$	**<6.21E+04**	4.57E+00	3.58E+01	2.23E+02	1.67E+02	(5.27E-01)
101.37	CCU$_u$	**<5.99E+04**	4.97E+00	3.71E+01	2.53E+02	1.80E+02	(3.39E-01)
104.08	CCU$_u$	**<4.46E+04**	4.97E+00	4.36E+01	2.96E+02	2.51E+02	(2.73E-01)
108.87	CCU$_u$	**<4.33E+04**	1.38E+01	8.69E+00	2.49E+02	2.12E+02	(2.76E-01)
114.64	CCU$_l$	**<3.05E+04**	2.08E+01	9.23E+00	1.76E+02	1.41E+02	(2.59E-01)

(a) Technetium-99 data are in units of pCi/g while all others are µg/g of dry sediment.
(b) Values in bold are below detection limit and no attempt to optimize detection limit was performed.
(c) Parentheses signify values below level of quantitation but considered valid.
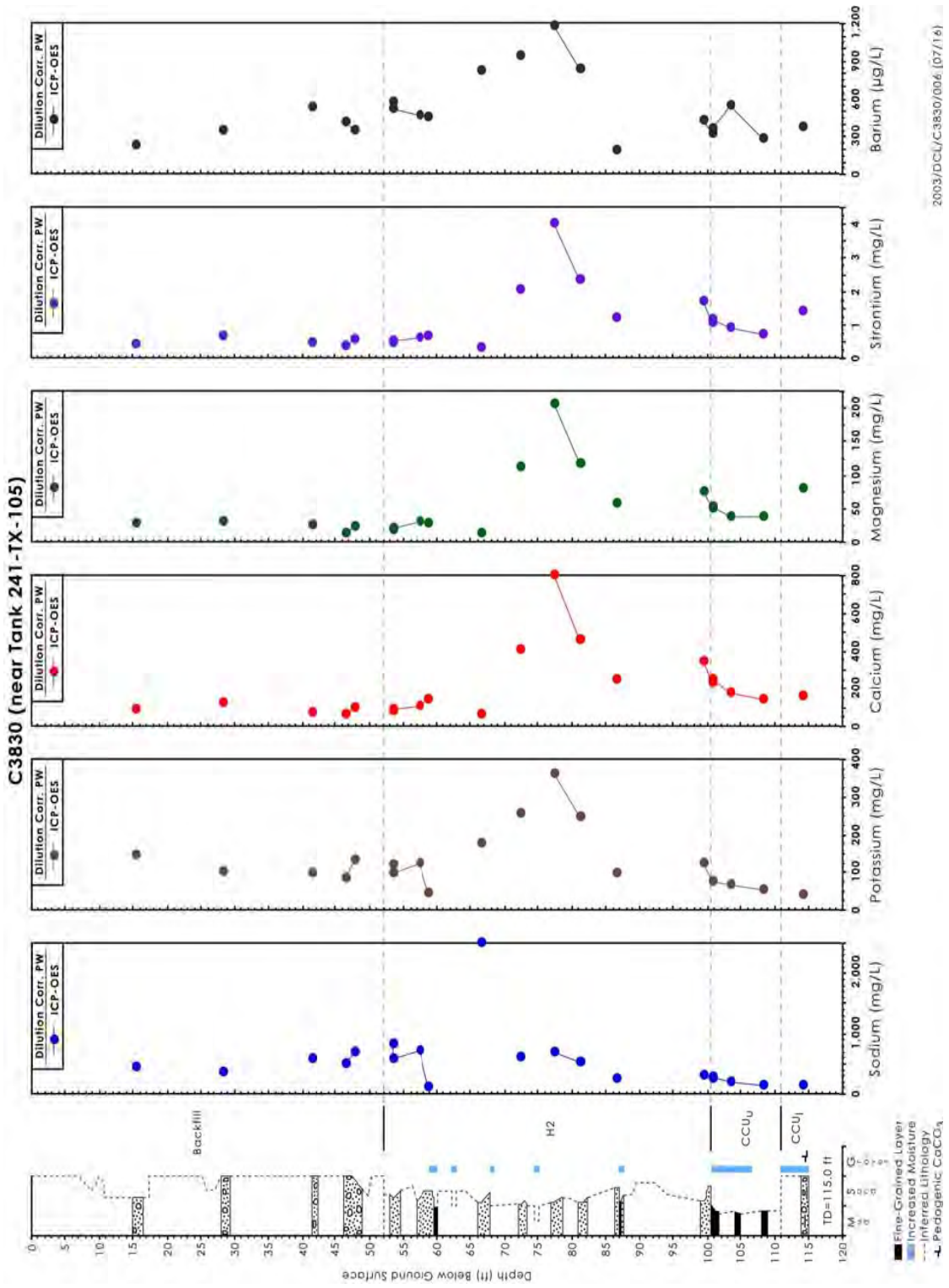
Figure 4.19. Derived Porewater Composition of Major Cations in C3830 Vadose Zone Sediments

2003/DCL/C3830/006 (07/16)

4.61
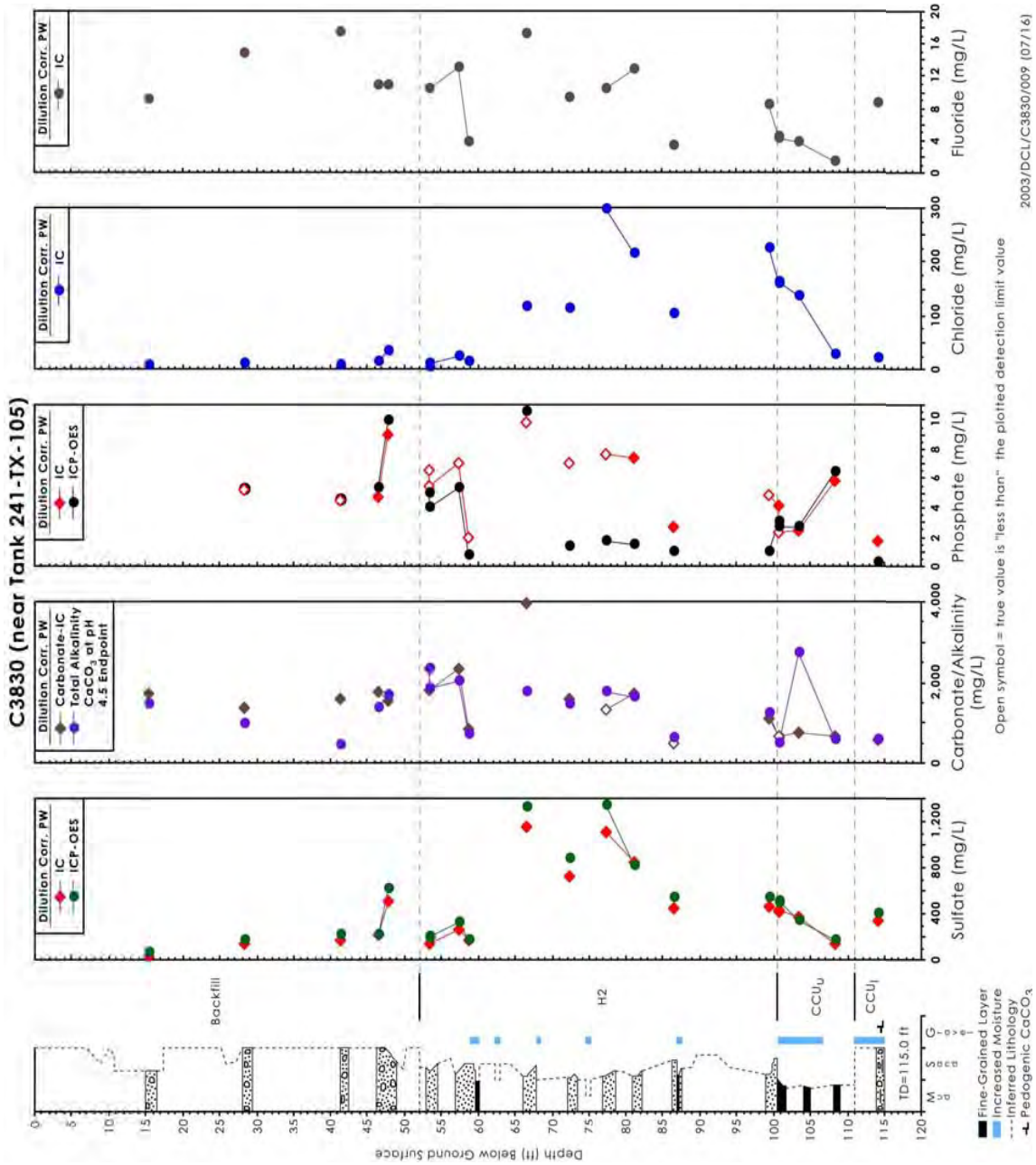
Figure 4.20. Derived Porewater Anion Composition in C3830 Vadose Zone Sediments
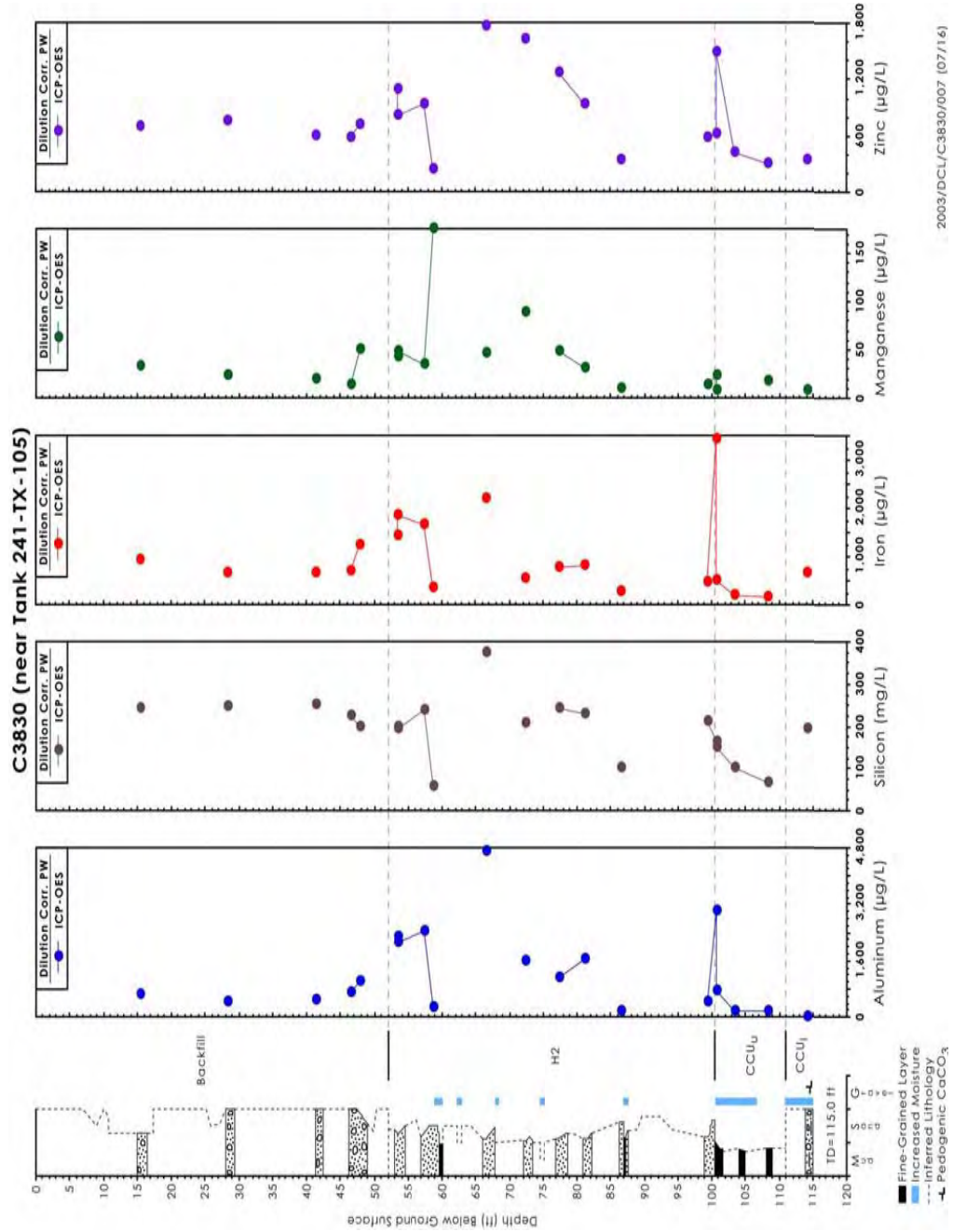
Figure 4.21. Derived Porewater Composition for Selected Metals in C3830 Vadose Zone Sediments

2003/DCL/C3830/007 (07/16)
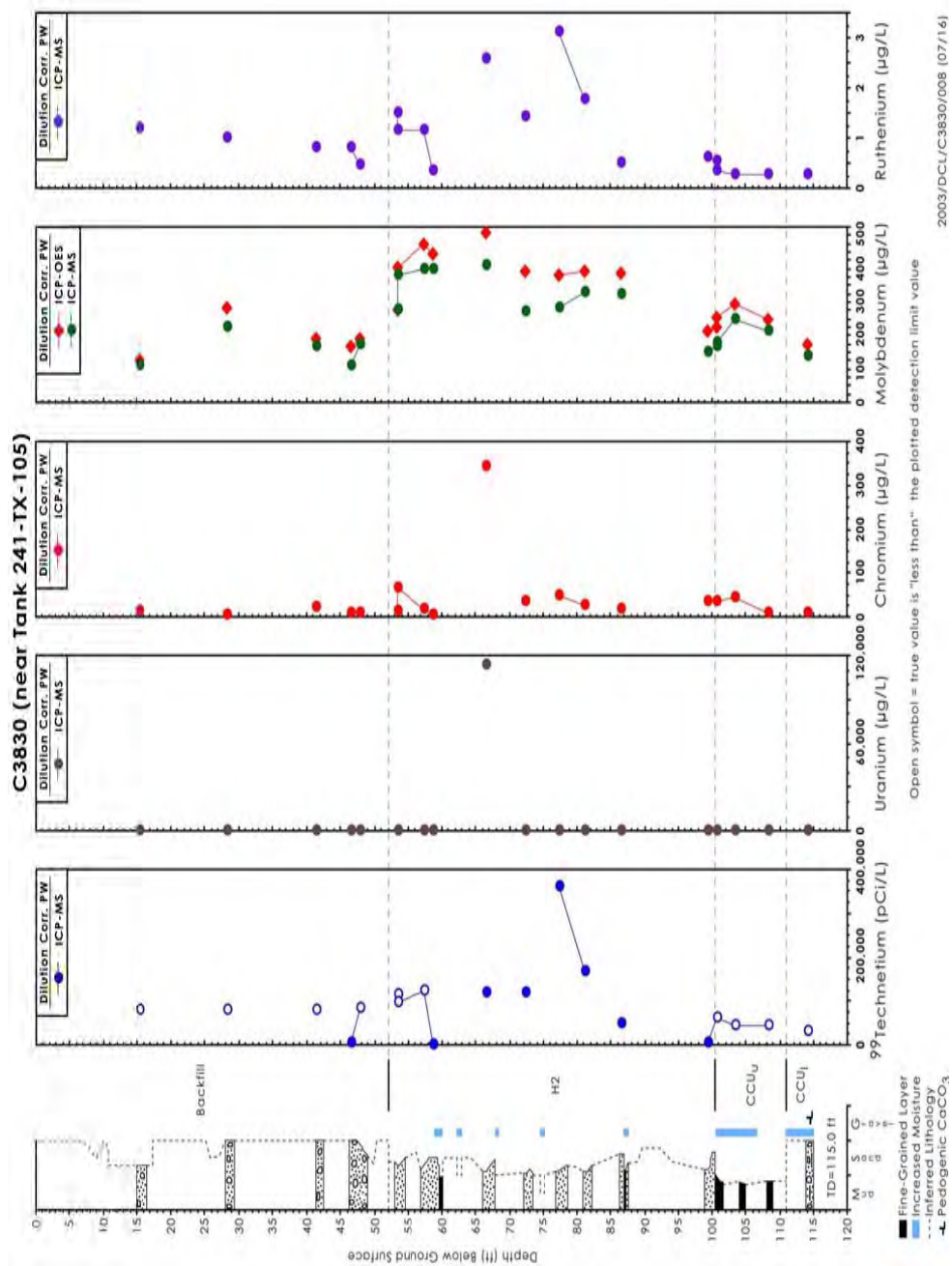
Figure 4.22. Derived Porewater Composition of Mobile Metals in C3830 Vadose Zone Sediments

Table 4.28. Acid-Extractable Cations from C3830 Vadose Zone Sediments (µg/g dry sediment)

Depth (ft bgs)	Stratigraphic Unit	Mg	Ca	Sr	Ba	Na	K
15.98	Bkfl	3.06E+03	3.15E+03	1.99E+01	6.33E+01	- - - - -	1.35E+03
28.92	Bkfl	3.10E+03	4.95E+03	2.06E+01	5.56E+01	- - - - -	7.94E+02
42.10	Bkfl	4.02E+03	6.17E+03	2.27E+01	5.55E+01	- - - - -	8.80E+02
47.18	Bkfl	2.94E+03	5.21E+03	2.15E+01	4.92E+01	- - - - -	8.24E+02
48.63	Bkfl	2.63E+03	4.64E+03	1.79E+01	4.56E+01	- - - - -	6.87E+02
54.02	H2	4.52E+03	7.49E+03	3.21E+01	5.70E+01	- - - - -	1.63E+03
54.02	H2	4.13E+03	6.77E+03	2.62E+01	5.33E+01	- - - - -	1.33E+03
58.03	H2	4.17E+03	6.57E+03	2.67E+01	6.15E+01	- - - - -	1.38E+03
59.35	H2	4.68E+03	7.67E+03	3.16E+01	5.59E+01	- - - - -	1.80E+03
67.11	H2	4.15E+03	6.46E+03	2.68E+01	5.91E+01	- - - - -	1.25E+03
72.63	H2	4.12E+03	6.38E+03	2.65E+01	5.18E+01	- - - - -	1.19E+03
78.01	H2	4.28E+03	6.87E+03	2.78E+01	4.70E+01	- - - - -	1.24E+03
81.89	H2	4.44E+03	6.44E+03	2.83E+01	5.34E+01	- - - - -	1.53E+03
87.09	H2	5.63E+03	9.31E+03	3.90E+01	5.92E+01	- - - - -	2.19E+03
100.02	H2	4.91E+03	9.77E+03	3.39E+01	5.50E+01	- - - - -	1.68E+03
101.37	CCU$_u$	4.33E+03	7.87E+03	2.80E+01	6.81E+01	- - - - -	1.61E+03
101.37	CCU$_u$	5.19E+03	9.61E+03	3.35E+01	7.71E+01	- - - - -	1.93E+03
104.08	CCU$_u$	5.37E+03	1.08E+04	3.15E+01	8.07E+01	- - - - -	1.90E+03
108.87	CCU$_u$	5.97E+03	1.29E+04	4.28E+01	7.00E+01	- - - - -	1.89E+03
114.64	CCU$_l$	1.71E+04	1.14E+05	2.09E+02	7.69E+01	- - - - -	9.68E+02

Table 4.29.   Acid-Extractable Constituents in C3830 Vadose Zone Sediments (µg/g dry sediment)

Depth (ft bgs)	Stratigraphic Unit	Al	Si	Fe	Mn	Zn	P as PO$_4$	S as SO$_4$
15.98	Bkfl	6.06E+03	(1.28E+01)[a]	1.32E+04	2.57E+02	3.70E+01	2.12E+03	4.11E+02
28.92	Bkfl	4.21E+03	(1.06E+01)	1.29E+04	1.97E+02	2.91E+01	2.69E+03	6.43E+02
42.10	Bkfl	4.78E+03	(1.10E+01)	1.40E+04	2.42E+02	3.10E+01	2.48E+03	7.95E+02
47.18	Bkfl	4.61E+03	(1.70E+01)	1.14E+04	1.96E+02	2.86E+01	1.93E+03	6.31E+02
48.63	Bkfl	3.83E+03	(8.65E+00)	1.03E+04	1.55E+02	2.51E+01	1.88E+03	5.67E+02
54.02	H2	6.97E+03	(4.70E+01)	1.24E+04	2.53E+02	3.82E+01	1.33E+03	8.23E+02
54.02	H2	5.81E+03	(8.52E+01)	1.08E+04	2.32E+02	3.31E+01	1.24E+03	6.99E+02
58.03	H2	5.66E+03	(8.62E+01)	1.03E+04	2.50E+02	2.92E+01	1.33E+03	6.75E+02
59.35	H2	7.48E+03	(2.56E+01)	1.24E+04	2.57E+02	3.69E+01	1.98E+03	7.27E+02
67.11	H2	5.84E+03	(8.05E+01)	1.09E+04	2.34E+02	3.50E+01	1.35E+03	7.43E+02
72.63	H2	5.57E+03	(6.19E+01)	1.06E+04	2.25E+02	2.82E+01	1.39E+03	7.11E+02
78.01	H2	5.88E+03	(8.59E+01)	1.09E+04	2.31E+02	3.86E+01	1.42E+03	7.19E+02
81.89	H2	6.55E+03	(8.01E+01)	1.15E+04	2.50E+02	3.22E+01	1.30E+03	6.75E+02
87.09	H2	8.77E+03	(1.31E+01)	1.32E+04	2.98E+02	4.50E+01	2.12E+03	8.91E+02
100.02	H2	7.28E+03	(2.47E+01)	1.36E+04	2.70E+02	4.27E+01	1.63E+03	9.79E+02
101.37	CCU$_u$	6.51E+03	(2.47E+01)	1.07E+04	2.50E+02	3.42E+01	1.40E+03	7.87E+02
101.37	CCU$_u$	8.55E+03	(9.12E+00)	1.36E+04	2.93E+02	5.01E+01	1.68E+03	9.47E+02
104.08	CCU$_u$	8.26E+03	(8.72E+00)	1.22E+04	3.00E+02	3.89E+01	1.69E+03	9.99E+02
108.87	CCU$_u$	8.26E+03	(9.54E+00)	1.34E+04	2.61E+02	4.27E+01	2.43E+03	1.15E+03
114.64	CCU$_l$	5.68E+03	(1.29E+01)	7.24E+03	1.15E+02	1.96E+01	1.04E+03	1.05E+04

(a) Parentheses signify values below level of quantitation but considered valid.

Table 4.30. Acid-Extractable Trace Metals in C3830 Vadose Zone Sediments

Depth (ft bgs)	Stratigraphic Unit	Tc-99[a]	U-238	Cr (ICP-MS)	Cr (ICP)	Mo (ICP-MS)	Mo (ICP)	Ru (ICP-MS)[c]
15.98	Bkfl	(9.48E+00)[b]	3.84E-01	8.10E+00	6.61E+00	1.95E-01	(8.81E-01)	<4.47E-03
28.92	Bkfl	(1.09E+00)	4.37E-01	8.70E+00	6.59E+00	6.64E-01	(1.28E+00)	<5.84E-03
42.10	Bkfl	(2.91E+02)	4.61E-01	9.29E+00	7.17E+00	3.26E-01	(1.46E+00)	<6.93E-03
47.18	Bkfl	(2.48E+02)	3.91E-01	7.63E+00	6.06E+00	1.82E-01	(7.52E-01)	<7.14E-03
48.63	Bkfl	(2.29E+02)	3.89E-01	6.65E+00	5.14E+00	2.65E-01	(9.50E-01)	<7.13E-03
54.02	H2	(2.89E+02)	5.44E-01	1.34E+01	1.21E+01	3.05E-01	1.67E+00	<8.38E-03
54.02	H2	2.52E+02	4.49E-01	1.16E+01	1.00E+01	2.12E-01	1.49E+00	<7.92E-03
58.03	H2	2.70E+02	3.66E-01	1.16E+01	1.06E+01	1.91E-01	(1.29E+00)	<8.65E-03
59.35	H2	(2.71E+02)	5.92E-01	1.55E+01	1.35E+01	3.59E-01	(1.28E+00)	<1.03E-02
67.11	H2	(1.88E+01)	1.65E+01	1.28E+01	1.11E+01	1.79E-01	(1.17E+00)	<6.89E-03
72.63	H2	(8.07E+00)	5.70E-01	1.13E+01	1.11E+01	2.67E-01	(1.28E+00)	<8.15E-03
78.01	H2	(1.97E+01)	5.08E-01	1.28E+01	1.12E+01	2.64E-01	1.51E+00	<7.45E-03
81.89	H2	(9.24E+00)	7.25E-01	1.39E+01	1.19E+01	3.34E-01	1.52E+00	<5.83E-03
87.09	H2	(7.24E+00)	5.63E-01	1.93E+01	1.64E+01	2.58E-01	1.46E+00	<8.84E-03
100.02	H2	(2.42E+02)	6.81E-01	1.48E+01	1.24E+01	2.25E-01	1.57E+00	<8.78E-03
101.37	CCU$_u$	2.39E+02	4.24E-01	1.21E+01	1.05E+01	2.06E-01	1.33E+00	<6.32E-03
101.37	CCU$_u$	(2.83E+02)	6.69E-01	1.67E+01	1.37E+01	2.92E-01	1.69E+00	<6.67E-03
104.08	CCU$_u$	2.50E+02	5.88E-01	1.28E+01	1.17E+01	1.76E-01	1.69E+00	<6.89E-03
108.87	CCU$_u$	(2.71E+02)	6.68E-01	2.15E+01	1.71E+01	3.93E-01	1.71E+00	<9.45E-03
114.64	CCU$_l$	(1.87E+01)	1.62E+00	6.70E+00	6.14E+00	3.20E-01	3.26E+00	1.18E-01

(a) Technetium-99 data are in units of pCi/g while all others are μg/g of dry sediment.
(b) Parentheses signify values below level of quantitation but considered valid.
(c) Values in bold are below detection limit.
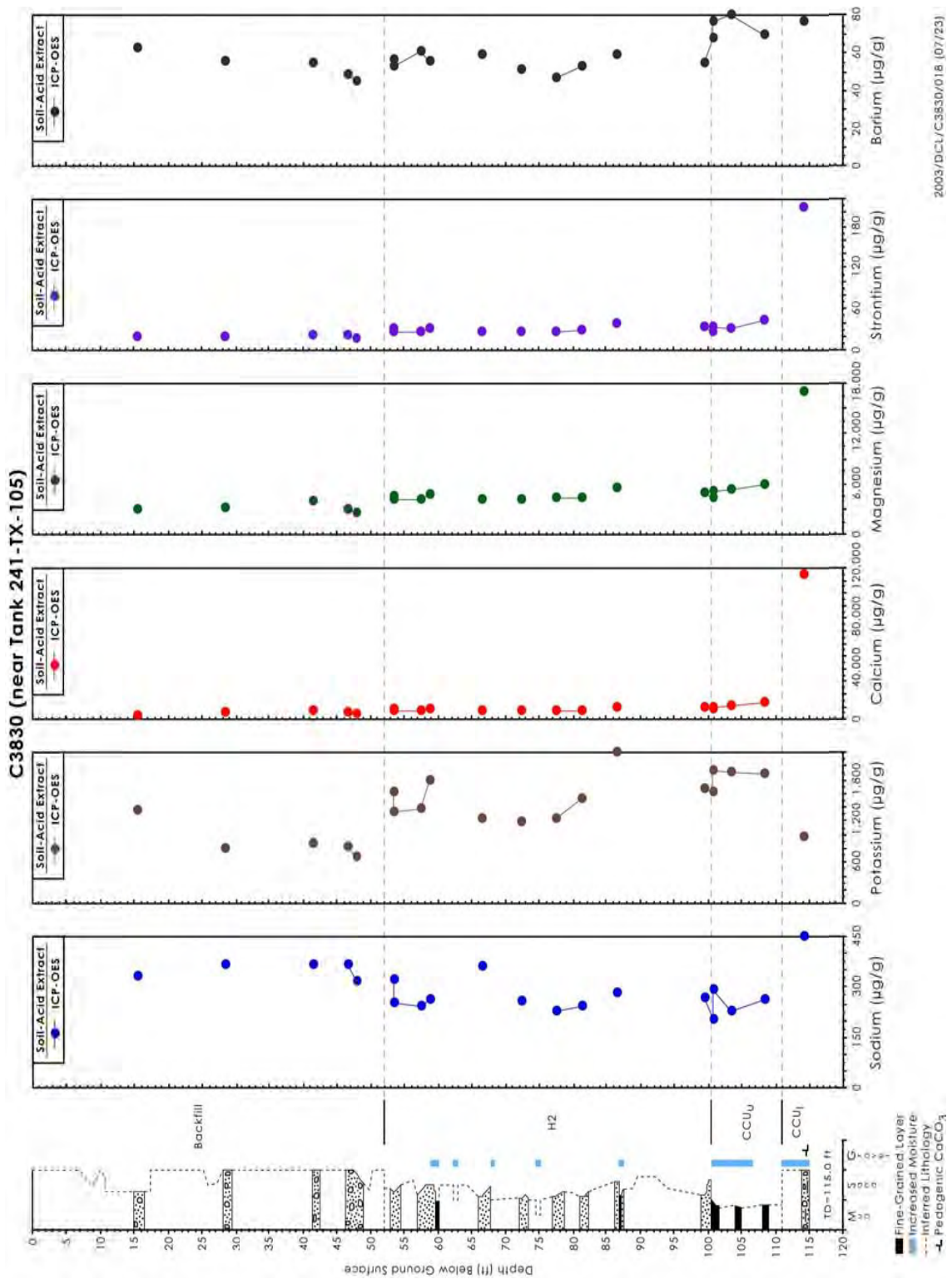
Figure 4.23. Acid-Extractable Cations in C3830 Vadose Zone Sediments (μg/g dry sediment)

2003/DCL/C3830/018 (07/23)

4.68
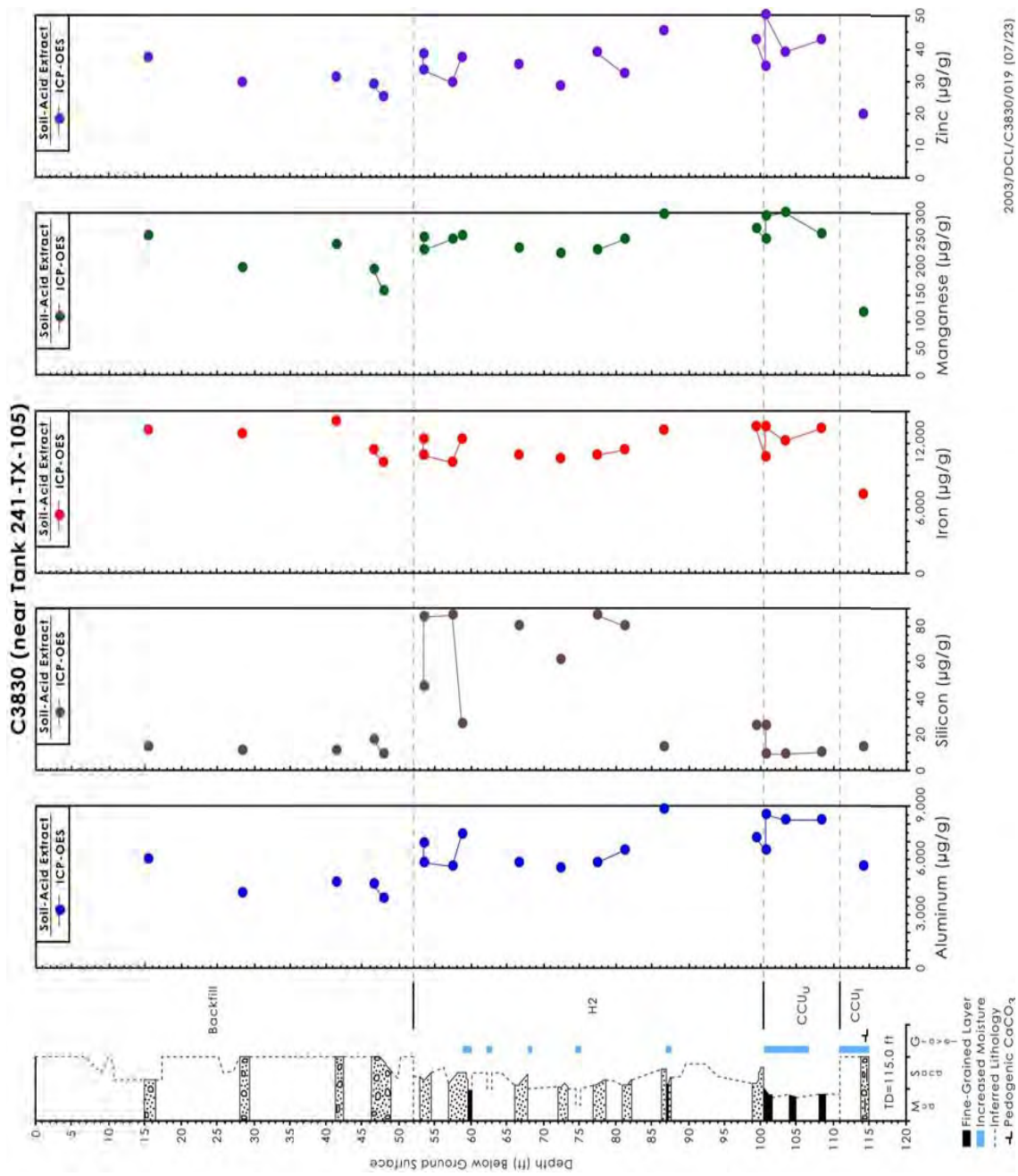
Figure 4.24. Acid-Extractable Metals in C3830 Vadose Zone Sediments (µg/g dry sediment)
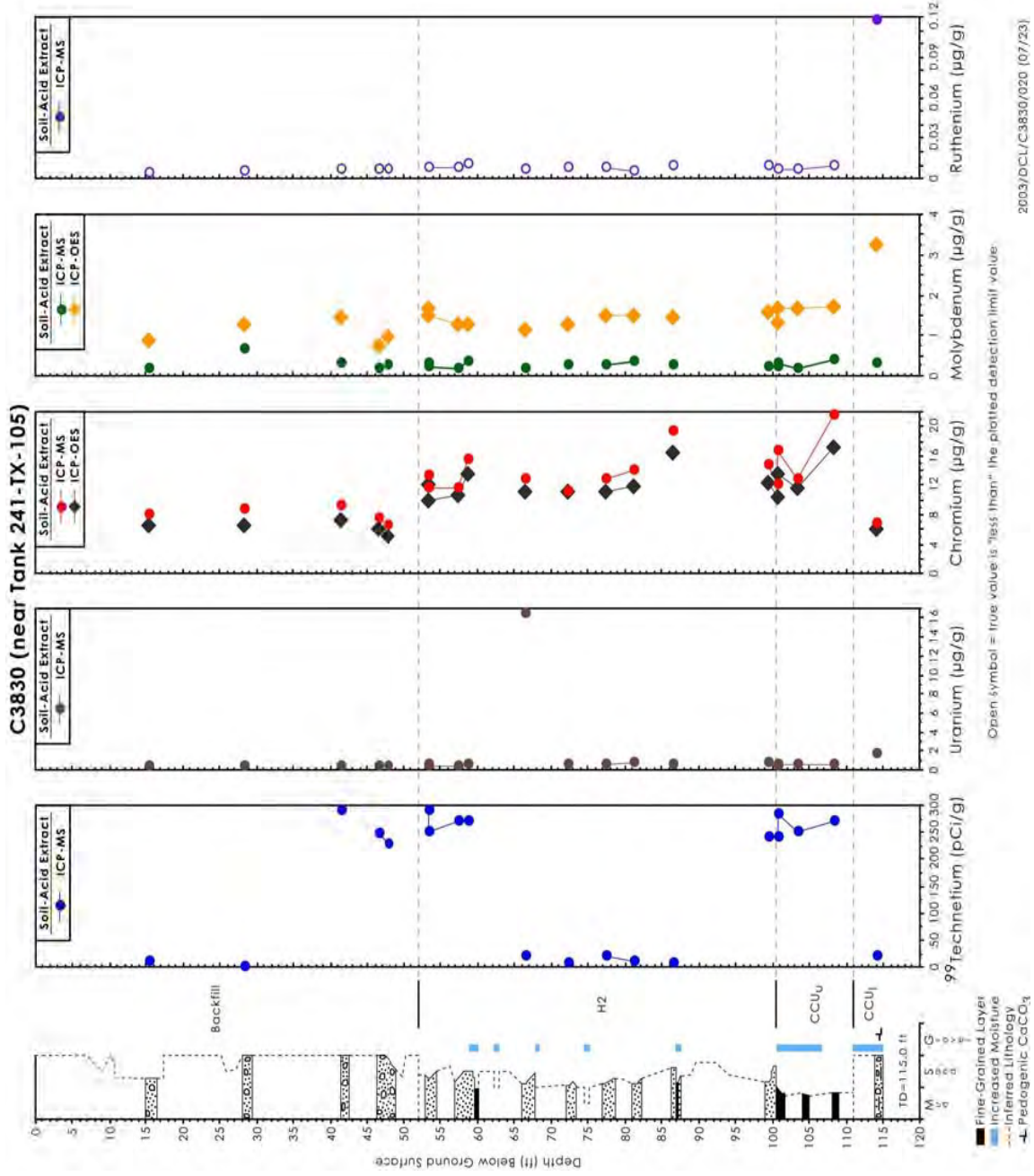
Figure 4.25. Acid-Extractable Trace Metals in C3830 Vadose Zone Sediments (units vary)
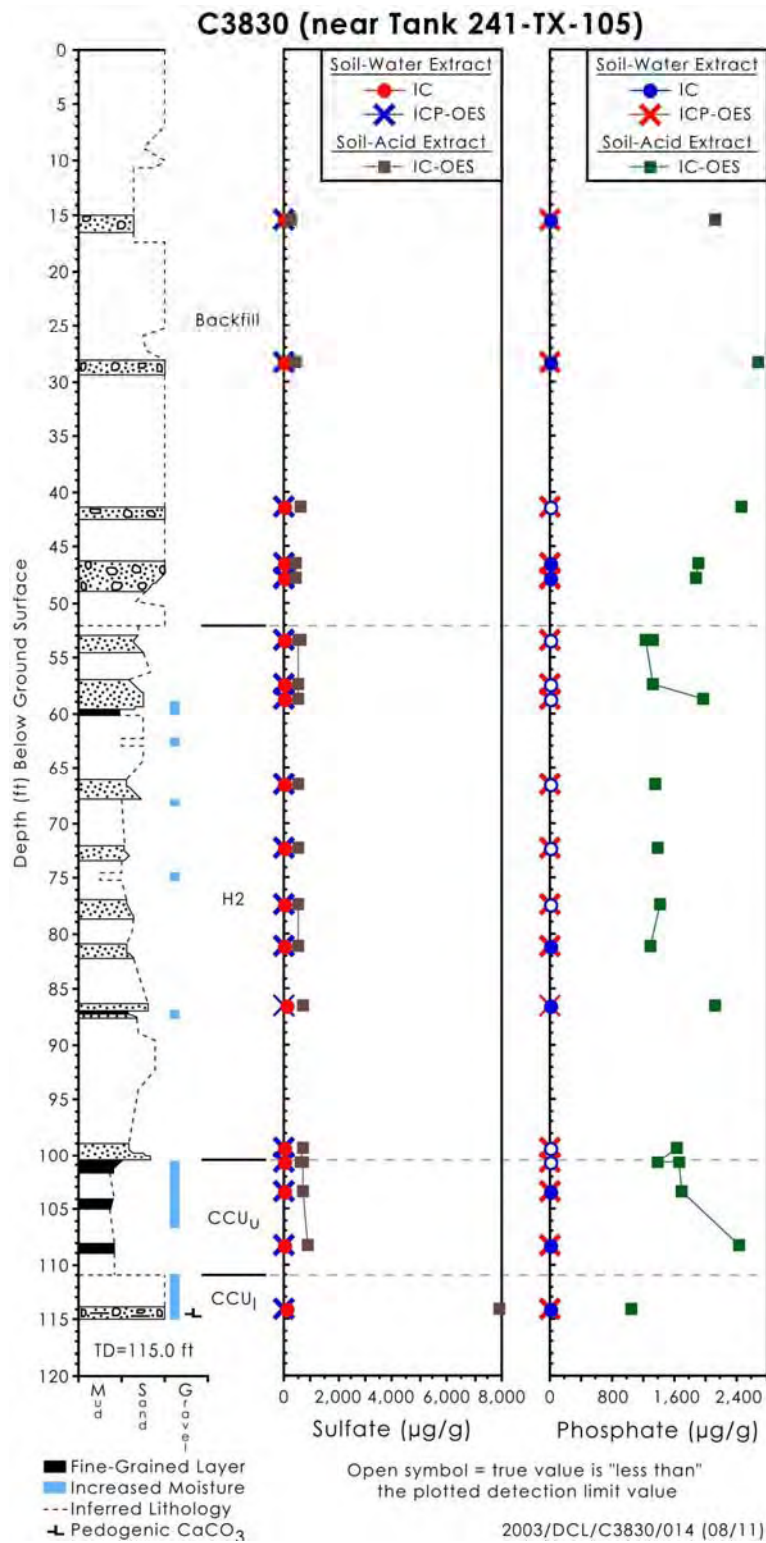
Figure 4.26. Water- versus Acid-Extractable Sulfate and Phosphate in C3830 Vadose Zone Sediments

the TX tanks. This might reflect that tank fluids leaked from shallower positions than the tank bottoms. Alternatively, we may be seeing analytical vagaries in our ability to obtain the same detection limit for technetium-99 from sediment to sediment and month to month. The quantities of technetium-99 that are acid extractable per gram of sediment and the quantities that are water soluble differ. The acid extract data are variable and, as shown in Table 4.30, mostly qualified with parentheses that mean values below our level of quantification. As found in sediments at borehole 299-E33-46 (see Serne et al. 2002f), measuring technetium-99 at low levels by acid extraction yields results that are not as reliable as water extraction data. We thus place more confidence in the technetium-99 data shown in Table 4.23.

The comparison of the water to acid-extractable quantities of each constituent was performed by taking the data in Tables 4.21 to 4.23 and dividing by the data in Tables 4.28 through 4.30. The data are not presented herein but show the same trends as found for the uncontaminated borehole (299-W10-27), wherein less than 0.1% of the acid-extractable quantities of the following elements are water leachable: Al, Ba, Fe, Mn, Cr, and P as phosphate. Less than 0.5% of the acid-extractable quantities of the following elements are water leachable: Ca, K, Mg, Sr, Zn, and U. Less than 20% of the acid-extractable sodium, sulfur, and molybdenum are water extractable excepting the following. The only indication of tank contamination is the high water and acid-extractable uranium value for the sample at 67.11 ft bgs and the presence of technetium-99 in both acid and water extracts. The percentage of the acid-extractable uranium that is also water extractable for the sediment at 67.11 ft bgs is 17% while all other water extracts for samples below the tank are less than 0.5%. The water-extractable sodium percentage is also 17% of the sodium that is acid extractable for this sample. At other tank farms we have found that water extracts of highly contaminated sediments release larger percentages of most constituents than uncontaminated sediments. The water and acid-extractable uranium of the sample at 67.11 ft bgs are 2.8 and 16.5 µg of uranium per g of sediment. These values are small compared to the values in contaminated sediments east of tank BX-102 from borehole 299-E33-45 that contained 300 to 1500 µg of uranium per g of sediment acid-extractable uranium.

The borehole C3830 sediment from the Cold Creek lower subunit (caliche) has elevated acid-extractable levels of uranium, magnesium, calcium, sodium and low levels of acid-extractable potassium in comparison to other samples and the caliche from the uncontaminated 299-W10-27 borehole. The likely cause for these differences is the higher level of evaporites present as indicated by the higher amount of calcium carbonate found in this subunit at C3830 than at 299-W10-27. Caliche contains higher concentrations of acid-extractable uranium, magnesium, calcium, and sodium than other minerals and, when one caliche sample contains more calcium carbonate than another sample, higher amounts of these constituents are acid leachable. The ratio of water- to acid-extractable constituents in the caliche does not indicate significant man-made contamination is present.

Figure 4.25 shows that our acid-extractable molybdenum results from ICP analyses is biased high likely from an unaccounted for spectral interference. The molybdenum results from the ICP-MS are more accurate and detection limits are much lower. Figure 4.26 shows that there is some sulfate present in the sediments that is not readily water extractable and the vast majority of the sediment phosphate content is not water extractable in comparison with the amounts that are acid extractable. The same trend was observed for the uncontaminated sediments from borehole 299-W10-27. Alternatively, some of the acid-extractable phosphorous may be present in a form other than phosphate such that when we convert the acid-extractable phosphorous number to phosphate (essentially multiply by 3), we are inflating the acid-extractable value.

4.2.5 Radionuclide Content in Vadose Zone Sediment from C3830

Aside from the technetium-99 data already presented and the uranium observed near 67 ft bgs, no radionuclides above a few tenths of a pCi/g were found in the core samples obtained from borehole C3830. Further, aside from a small amount of surface cesium-137 contamination, the field logging results of the entire borehole did not find any gamma-emitting contamination. Figures 4.27 and 4.28 show the field logs and results for natural potassium-40 and uranium-238 and for common gamma emitters, respectively. Where field-logging data were above detection limits, the log data are plotted also. The agreement between the field and lab-generated data for gamma emitters is excellent. There are no man-made gamma emitters in the sediment profile above concentrations of a few tenths of a pCi/g, excepting the near surface contamination that has a few pCi/g cesium-137 in shallow backfill sediments.

Gross alpha and beta measurement were made on both the 1:1 sediment:water and sediment:acid extracts. With knowledge of the mass of dry sediment to extraction fluid used, the data were converted to activity of gross beta and alpha leached per gram of dry sediment. None of the water or acid extracts, of the 20 extracts (18 cores from selected depths and two duplicates), showed activities significantly greater than the detection limits for the procedures. For the total beta analyses, our detection limits for the water extracts were 10 to 20 pCi/g dry sediment and 5 to 10 pCi/g dry sediment for the acid extracts. For the total alpha analyses, the detection limit for both extracts was 3 to 5 pCi/g dry sediment. Note that the efficiency of the total beta technique for the low energy techetium-99 is poor such that the total beta analyses can indicate no beta above 10 to 20 pCi/g, yet the ICP-MS measurements for the water and acid extracts show that there may be up to 200 pCi/g of technetium-99 present.

4.2.6 Total Carbon, Calcium Carbonate, and Organic Carbon Content of Vadose Zone Sediment from Borehole C3830

The total, inorganic and organic carbon contents of the C3830 sediments are reported in Table 4.31. The only sample of lower Cold Creek subunit (caliche) obtained, at 114.6 ft bgs, contains significant amounts of calcium-carbonate equivalent material calculated to be 38.25% by weight. We have found samples in 200 West near the SX Tank Farm with almost 50% by weight calcium-carbonate equivalent. The wide range in calcium-carbonate contents reflects the variability in weathering processes and time for paleosol horizon development. The deepest sediment from the upper Cold Creek subunit also contains some elevated calcium-carbonate content. As found in most vadose sediments from the Hanford Reservation there is very little (<0.1% by weight) organic carbon in the vadose zone sediments.
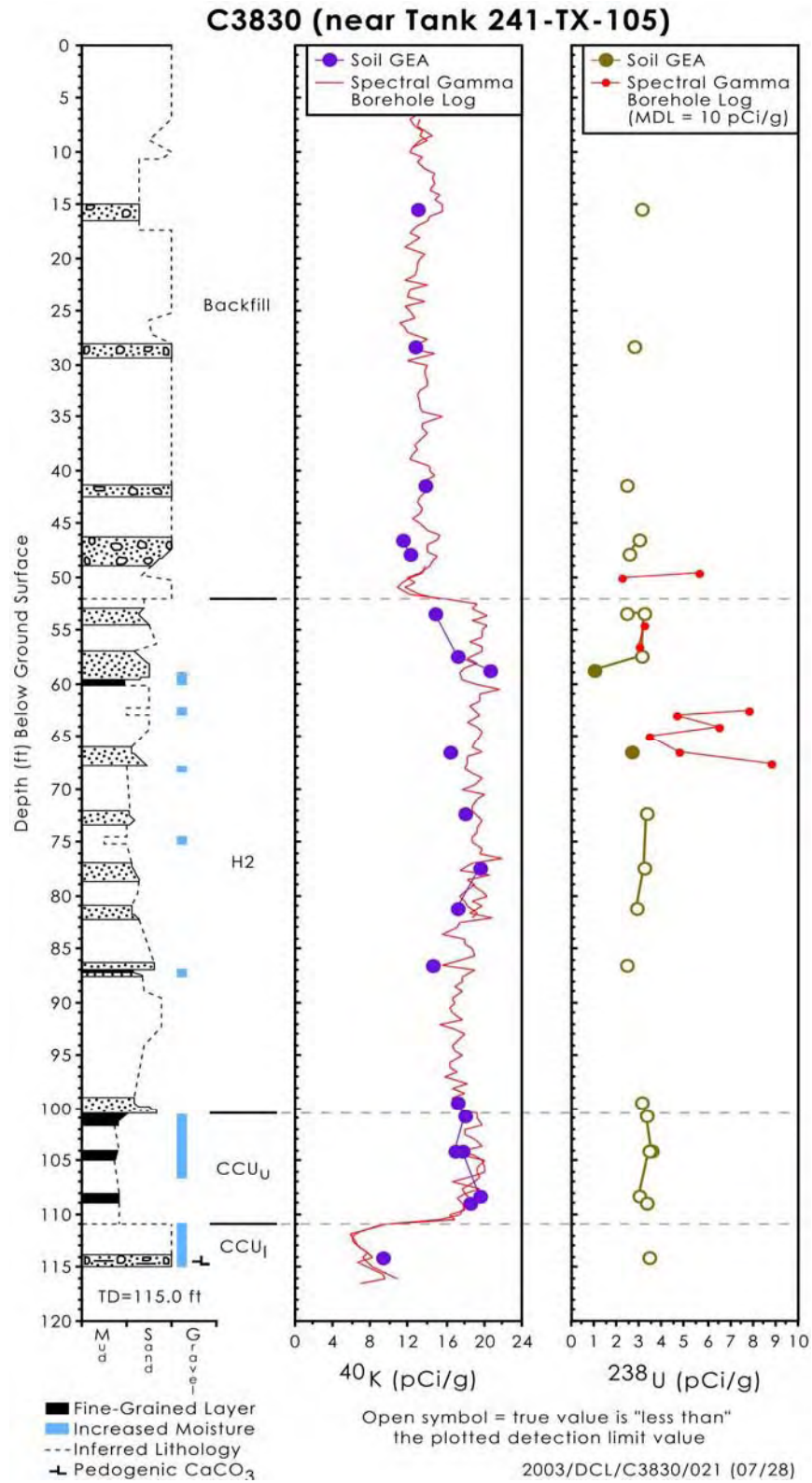
Figure 4.27. Comparison of Lab Gamma Energy Analysis (GEA) and Field Log for Natural Gamma Emitters

4.74
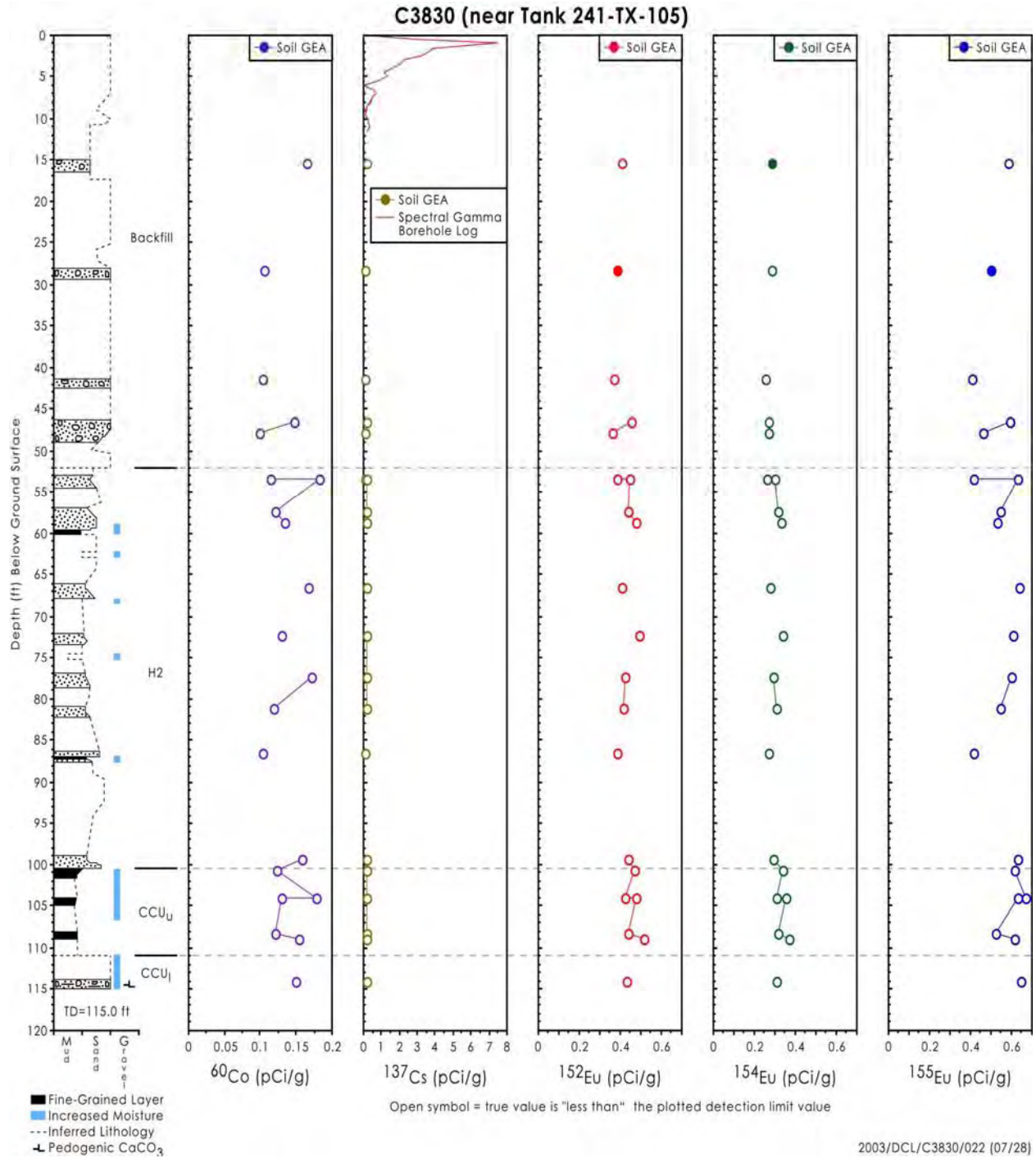
Figure 4.28. Lab and Field Data for Common Gamma Emitters in C3830 Vadose Zone Sediments

Table 4.31.   Carbon Contents of Vadose Zone Sediments in Borehole C3830

Stratigraphic Unit	Depth (ft bgs)	Total Carbon %	Inorganic Carbon %	IC as CaCO$_3$ %	Organic Carbon % (by diff.)
Bkfl	15.98	0.11	0.03	0.25	0.08
Bkfl	28.92	0.13	0.08	0.68	0.05
Bkfl	42.10	0.21	0.14	1.19	0.07
Bkfl	47.18	0.18	0.13	1.12	0.05
Bkfl	48.63	0.25	0.19	1.62	0.06
H2	54.02	0.22	0.19	1.57	0.03
H2	54.02	0.25	0.2	1.69	0.05
H2	58.03	0.24	0.2	1.65	0.04
H2	59.35	0.25	0.21	1.75	0.04
H2	67.11	0.23	0.21	1.71	0.02
H2	72.63	0.28	0.23	1.89	0.05
H2	78.01	0.27	0.23	1.91	0.04
H2	81.89	0.2	0.17	1.42	0.03
H2	87.09	0.31	0.27	2.27	0.04
H2	100.02	0.35	0.32	2.67	0.03
CCU$_u$	101.37	0.34	0.29	2.45	0.05
CCU$_u$	101.37	0.34	0.3	2.49	0.04
CCU$_u$	104.08	0.45	0.4	3.33	0.05
CCU$_u$	108.87	0.61	0.53	4.42	0.08
CCU$_l$	114.64	4.76	4.59	38.25	0.17

4.3   Vadose Zone Sediment from Borehole C3831

Borehole C3831 was pushed into the vadose zone sediment approximately 40 ft southwest of tank TX-107 to evaluate whether there is evidence to support a past decision to designate tank TX-107 as having leaked. The borehole reached a depth of 115.4 ft bgs at which point driving the probe met refusal.

4.3.1   Moisture Content

The moisture content of the 36 cores liners as a function of depth and lithology are shown in Table 4.32 and Figure 2.19. The backfill samples have a mean moisture content of 7.1% by weight with significant variation and a wet zone at the very bottom, at 52 ft bgs. The moisture in the backfill at C3831 is much more variable and on average one percent by weight wetter than the backfill sediments in borehole C3830 near tank TX-105. The Hanford formation H2 unit samples from borehole C3831 have a mean moisture content of 8.7% by weight with variation that tracks variations in particle size (finer-grained samples have slightly higher moisture contents). The Hanford formation H2 sediments in

borehole C3831 are on average 3% by weight wetter than the H2 sediments at borehole C3830. At borehole C3831, the Cold Creek upper subunit has a rather low moisture content for a fine-grained sediment, 5.11% wt. The Cold Creek lower subunit at C3831 has an average moisture content of 11.7% wt, which is very similar to the moisture content observed for the caliche at borehole C3830.

The average moisture content of the H2 unit samples measured in borehole C3831 is about 4% by weight greater than the average for the same stratigraphic unit at the uncontaminated borehole 299-W10-27 (Table 2.5). One could speculate that this wetter Hanford H2 sediment is significant and an indication of the various tank farm operations that encourage higher moisture infiltration.

4.3.2   1:1 Sediment:Water Extracts for Borehole C3831

Twenty A liner and two B liner (run in duplicate) cores were characterized after the geologic descriptions were completed. In total, 24 separate sediment samples were characterized using the 1:1 sediment:water procedure. The following tables and figures present the mass of a given constituent leached per gram of sediment as measured in the water extracts to allow direct comparison to the same data for the background borehole sediments from borehole 299-W10-27 and from the other two boreholes. Other figures show dilution-corrected values that represent concentrations in vadose zone porewater in borehole C3831. As discussed in several other Vadose Zone Characterization Project reports, the dilution-corrected 1:1 sediment:water extracts are a reasonable estimate of the actual vadose zone porewater (see Serne et al. 2002b, 2002c, 2002d, 2002e, 2002f).

Table 4.32.   Moisture Content of Borehole C3831 Cores

Sample No.	Depth (ft bgs)	Stratigraphic Unit	Lithology	Moisture Content % Wt
C3831 15B	15.28	backfill	Silty sandy gravel	5.34%
C3831 15A	15.97			3.05%
C3831 21B	21.18	backfill	Silty sandy gravel	7.30%
C3831 21A	21.93			3.89%
C3831 28B	28.28	backfill	Silty sandy gravel	5.17%
C3831 28A	28.90			4.82%
C3831 45B	45.40	backfill	Silty sand to gravelly sand	10.93%
C3831 45A	46.06			8.33%
C3831 51B	51.35	backfill	Silty gravelly sand to silty sandy gravel to silty sand	5.51%
C3831 51A	52.03			16.54%

Table 4.32. (contd)

Sample No.	Depth (ft bgs)	Stratigraphic Unit	Lithology	Moisture Content % Wt
C3831 52B	52.50	H2	Sand	5.20%
C3831 52A	53.18			6.35%
C3831 59B	59.34	H2	Sand to silty sand	8.43%
C3831 59A	59.94			8.10%
C3831 60B	60.44	H2	Sand, silt and clay (clastic dike) to sand	13.00%
C3831 60A	61.15			4.47%
C3831 67B	67.53	H2	Sand to silty sand	5.93%
C3831 67A	68.21			12.44%
C3831 69B	68.82	H2	Sand to silty sand	11.30%
C3831 69A	69.60			5.49%
C3831 74B	74.36	H2	Sand to silty sand	5.87%
C3831 74A	74.99			18.06%
C3831 77B	77.05	H2	Sand to silty sand	5.98%
C3831 77A	77.67			6.40%
C3831 78B	78.08	H2	Sand to silty sand	10.28%
C3831 78A	78.72			16.22%
C3831 85B	85.37	H2	Sand to silty sand to sandy silt	17.53%
C3831 85A	85.99			14.66%
C3831 88B	88.67	H2	Sand	8.85%
C3831 88A	89.39			5.13%
C3831 93B	93.37	H2	Sand	5.20%
C3831 93A	93.99			5.79%
C3831 97B	97.43	H2	Sand to silty sand and silt	9.56%
C3831 97A	98.07			10.98%
C3831 100B	100.57	H2	Sand to silty sand	10.89%
C3831 100A	101.29			4.95%
C3831 102B	101.97	CCU_u	Silty sand	4.94%
C3831 102A	102.65			5.28%
C3831 114B	114.44	CCU_l	Slightly gravelly muddy sand	10.49%
C3831 114A	115.06			12.94%

4.3.2.1   pH and Electrical Conductivity

The 1:1 sediment:water extract pH and EC data are shown in Table 4.33. Both the measured value and dilution-corrected EC values are shown. Figure 4.29 shows the 1:1 sediment:water extract pH value and dilution-corrected EC as a function of depth and stratigraphy. A comparison of the data in Table 4.33 with the pH and EC of the 299-W10-27 extracts suggests that there is slightly elevated pH in borehole C3831 between 61 and 70 ft bgs that is indicative of alkaline tank fluids interactions. There is also evidence of elevated EC starting at 60 ft bgs all the way to the bottom of the borehole at C3831 when compared to the background sediment from 299-W10-27. Somewhere between the two samples at 53.2 and 59.9 ft bgs, the EC of the 1:1 water extract increases to between 10 and 13 times the background sediment values. Between 67.5 and 78 ft bgs, the EC is about 5 times larger than background sediment extracts. At ~86 ft bgs there is a second peak of high EC at about 11 times the background sediment extract. Below 86 ft bgs to the bottom of the borehole at 115 ft bgs, the EC averages about 3 times higher than that in background sediments. When compared to the EC at borehole C3830 (see Table 4.18), the extract EC values at C3831 are unequivocally higher and indicative of the presence of saline tank-related fluids.

The highest dilution-corrected porewater EC value between 60-61 ft bgs is equivalent to a pore solution of 0.4 M KCl, the salt solution used to calibrate the conductivity cell. As shown in Figure 4.29, the dissolved salts are high in sodium and nitrate. The sodium and nitrate peak values both occur at 61 ft bgs, which is the depth where the borehole intercepted a clastic dike. One plausible cause for the abrupt appearance of high concentrations of sodium and nitrate at 61 ft bgs is that tank fluids moved preferentially along the clastic dike that was ruptured by the borehole drilling. The leaks near the SX-108, SX-109, and BX-102 tanks had peak vadose zone porewater concentrations that were equivalent to much more concentrated waste fluids, 7 to 17 and 0.7 to 1 M KCl solutions, respectively. The maximum dilution-corrected EC at borehole C3831 is 43.3 mS/cm, higher than the dilution-corrected EC at 299-E33-46 (near tank B-110) that contained 15.1 mS/cm and borehole C3830 porewater that contained 12.5 mS/cm.

Table 4.33.   pH and EC Data for Sediment:Water Extracts from Borehole 3831

Sample No.	Depth (ft bgs)	Stratigraphic Unit	pH	Conductivity mS/cm	Conductivity (mS/cm) Dilution-Corrected Porewater
C3831-14.93A	15.97	Bkfl	7.70	0.169	5.578
C3831-20.8A	21.93	Bkfl	7.87	0.212	5.453
C3831-28A	28.90	Bkfl	7.76	0.227	4.720
C3831-45A	46.06	Bkfl	7.82	0.376	4.516
C3831-51A	52.03	Bkfl	7.81	0.175	1.060
C3831-52A	53.18	H2	7.80	0.264	4.159
C3831-59A	59.94	H2	8.15	1.526	18.829
C3831-60A	61.15	H2	8.96	1.932	43.259
C3831-67B	67.53	H2	8.47	0.701	11.843
C3831-67B Dup	67.53	H2	8.80	0.742	12.589
C3831-67A	68.21	H2	8.20	0.502	4.035
C3831-69A	69.60	H2	8.12	0.394	7.315
C3831-74A	74.99	H2	7.91	0.902	4.994
C3831-77A	77.67	H2	7.90	0.348	5.442
C3831-78A	78.72	H2	8.33	0.781	4.814
C3831-85A	85.99	H2	7.81	1.755	11.967
C3831-88A	89.39	H2	7.92	0.349	6.810
C3831-93A	93.99	H2	7.89	0.634	10.964
C3831-97A	98.07	H2	7.87	0.584	5.320
C3831-100A	101.29	H2	7.91	0.407	8.232
C3831-102A	102.65	CCU_u	7.95	0.506	9.660
C3831-114B	114.44	CCU_l	7.80	0.607	5.813
C3831-114B Dup	114.44	CCU_l	7.91	0.496	4.755
C3831-114A	115.06	CCU_l	7.65	0.712	5.501
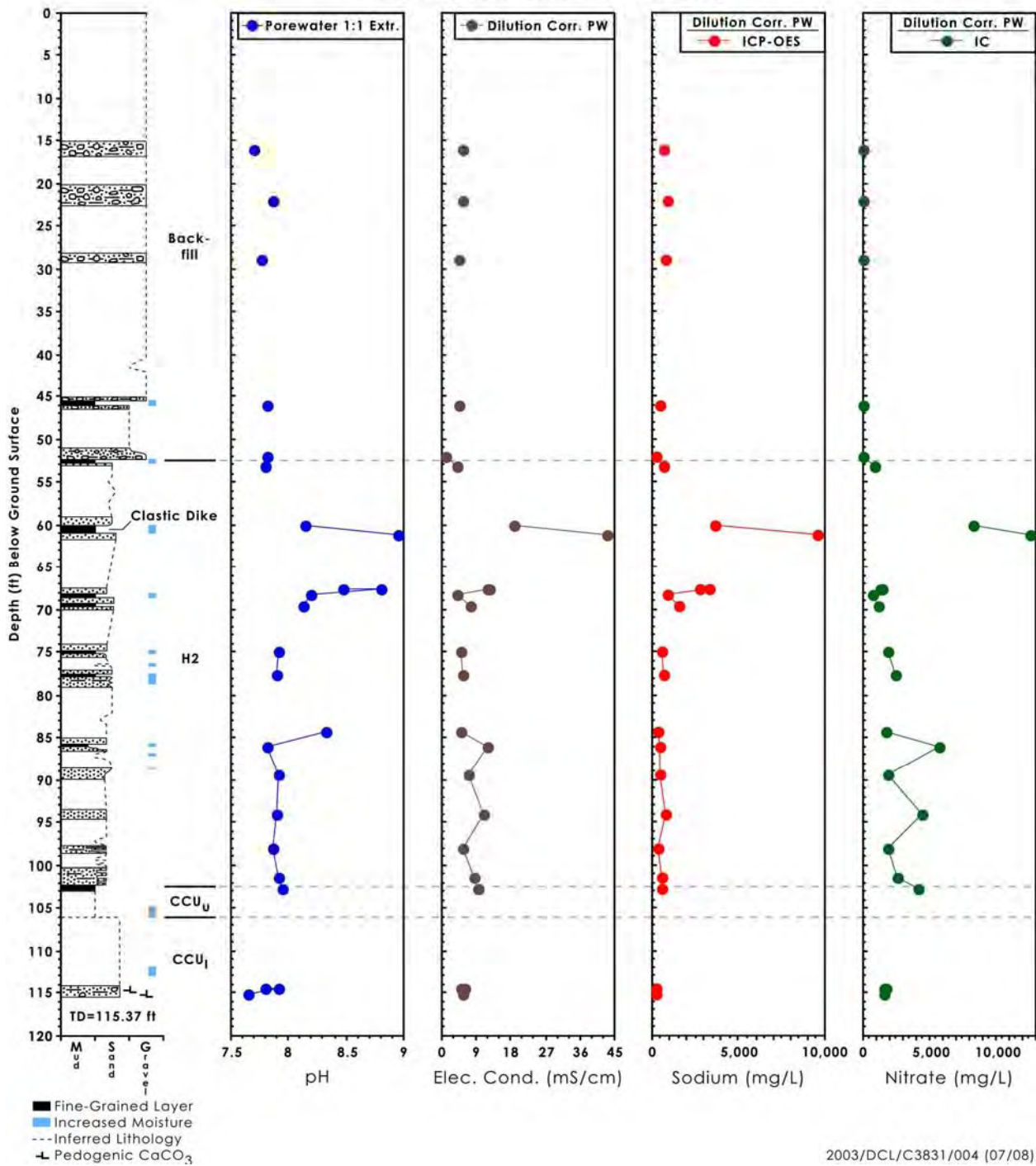
Figure 4.29. Borehole C3831 Sediment-to-Water Extract pH and Calculated Porewater EC, Sodium, and Nitrate

4.3.2.2   Water Extract Composition or the 1:1 Sediment:Water Extract for Borehole C3831

The water extract values for the major cations and anions and several trace constituents are discussed in this section. The anion data are tabulated in Tables 4.34 and 4.35 and Figure 4.30 in units of mass per gram of dry sediment.

The data for the water extracts of borehole C3831 for fluoride and bromide do not differ significantly from the same data for the uncontaminated sediments from borehole 299-W10-27 or borehole C3830. However, there are obvious signs of elevated chloride, nitrate, bicarbonate, sulfate, phosphate, and nitrite in some of the water extracts from borehole C3831 sediments when compared to the uncontaminated sediments and borehole C3830. The chloride values in the C3831 sediments from 46, 60, and 61 ft bgs are 10 to 20 times larger than the background sediment. The water-extractable chloride concentrations in borehole C3831 sediments from 68 ft bgs to the deepest sample obtained at 115 ft bgs are elevated by a factor of ~5 to 10 when compared to water extracts of uncontaminated sediment and by a factor of 2 compared to the water extracts from borehole C3830. The nitrate water extract values for borehole C3831 are elevated compared to the background sediments from 53 ft bgs to the deepest sample obtained. The nitrate water extract values are 20 to 300 times larger than for the background sediments between the depths of 53 and 86 ft bgs. The nitrate concentrations in borehole C3831 are also ~5 to 10 times greater than those at similar depths in borehole C3830. The sulfate water extracts from borehole C3831 are elevated from about 60 ft bgs to the deepest sample obtained and the values exceed the background sediment values by a factor of 3 to 10. The water-extractable sulfate values for sediments from borehole C3831 are in general about twice as high as for borehole C3830. There is one zone of large water-extractable bicarbonate in the H2 unit in the C3831 borehole sediments between 61 to 68 ft bgs. There is also high water-extractable phosphate and nitrite in the C3831 borehole sediments at 61.15 ft bgs and also slightly elevated values 60 to 70 ft bgs for phosphate and 60 to 86 ft bgs for nitrite. The agreement between measuring the water extracts for phosphate and sulfate directly with the ion chromatograph and indirectly by converting the ICP measurements for phosphorous and sulfur are very good (see Figure 4.30). Besides validating the ion chromatography data, we can state that the water-extractable sulfur and phosphorous species exist as primarily sulfate and phosphate.

The water-extractable small organic molecules in the C3831 borehole sediments are shown in Table 4.35. The values are not significantly different than for the uncontaminated sediments from borehole 299-W10-27 or the values at borehole C3830, excepting the sample at 61.15 ft bgs that shows a few ppm of soluble acetate and oxalate. We do not know if these values are indicative of any tank fluid influence such as degradation products of some other man-introduced organics or natural variability.

The water-extractable major cations in the borehole C3831 sediments are tabulated in Table 4.36 and the distribution with depth is shown in Figure 4.31. The distribution of the divalent alkaline earth cations (Mg, Ca, and Sr but not Ba) shows low water-extractable quantities between 61 and 70 ft bgs. High divalent cation water extracts are found in a single sample (86 ft bgs). Conversely, the distribution of water-extractable sodium is very high between the depths of 60 and 75 bgs. The water-extractable sodium values in borehole C3831 sediments are higher than the values in the uncontaminated sediments from borehole 299-W10-27 over the whole borehole profile. These trends suggest that tank fluids that are high in sodium and nitrate did seep into the vadose zone near this borehole, probably along a clastic dike. The sodium in the tank fluids pushed the natural divalent cations and some of the natural potassium off the sediment cation exchange sites in the sediments between 53 and at least 70 ft bgs. We have observed the same cation distribution and ion exchange fronts – where divalent cations, and sometimes potassium

Table 4.34. Water-Extractable Anions in Borehole C3831 Vadose Zone Sediments (µg/g dry sediment)

Depth (ft bgs)	Stratigraphic Unit	Fluoride	Chloride	Nitrate	CO$_3$	Sulfate	Phosphate	Nitrite	Bromide
15.97	Bkfl	1.27	0.55	1.7	87.93	4.55	<0.241	<0.080	<0.138
21.93	Bkfl	0.63	0.81	3.27	99.01	13.63	<0.240	<0.080	<0.137
28.90	Bkfl	1.24	0.84	2.31	104.77	15.82	<0.241	<0.080	<0.137
46.06	Bkfl	0.38	25.67	3.35	104.63	48.83	<0.240	0.23	0.16
52.03	Bkfl	0.78	0.84	1.95	91.37	5.42	<0.240	<0.080	<0.137
53.18	H2	0.4	2.00	55.44	74.17	7.6	<0.240	<0.080	<0.137
59.94	H2	0.4	12.14	**667.32**	120.68	32.77	0.83	0.77	<0.137
61.15	H2	0.65	10.06	**560.84**	**512.57**	32.62	**11.89**	**12.81**	<0.137
67.53	H2	1.21	3.17	72.93	**311.24**	31.99	1.03	0.23	<0.137
67.53	H2	1.49	4.56	87.67	**370.87**	38.02	1.99	0.27	<0.138
68.21	H2	0.69	3.45	91.28	155.86	27.49	1.2	0.09	0.15
69.60	H2	0.75	1.67	60.53	154.86	24.77	1.56	0.42	<0.140
74.99	H2	0.39	7.5	**350.18**	71.29	52.58	<0.240	0.38	<0.137
77.67	H2	0.57	3.63	154.81	77.02	33.82	<0.240	0.42	<0.137
78.72	H2	0.36	6.25	287.03	55.11	49.28	<0.240	**2.01**	<0.137
85.99	H2	0.23	16.52	**846.66**	53.20	66.06	<0.240	**3.27**	<0.137
89.39	H2	0.35	2.52	98	69.40	23.1	<0.240	<0.080	<0.137
93.99	H2	0.29	4.95	252.96	5.71	25	<0.240	<0.080	<0.137
98.07	H2	0.4	4.73	202.78	4.75	37.3	<0.240	0.76	<0.137
101.29	H2	0.34	3.29	127.18	35.18	23.71	<0.240	0.1	<0.137
102.65	CCU$_u$	0.49	5.31	222.42	49.82	34.09	1.76	0.09	<0.138
114.44	CCU$_l$	0.96	5.42	175.96	91.43	77.57	<0.241	<0.080	<0.138
114.44	CCU$_l$	0.97	5.24	169.8	81.22	76.54	<0.241	<0.080	<0.138
115.06	CCU$_l$	0.97	6.41	204.28	82.68	96.7	<0.240	0.12	<0.137

Values in bold type signify highly elevated concentrations of water-extractable constituents.
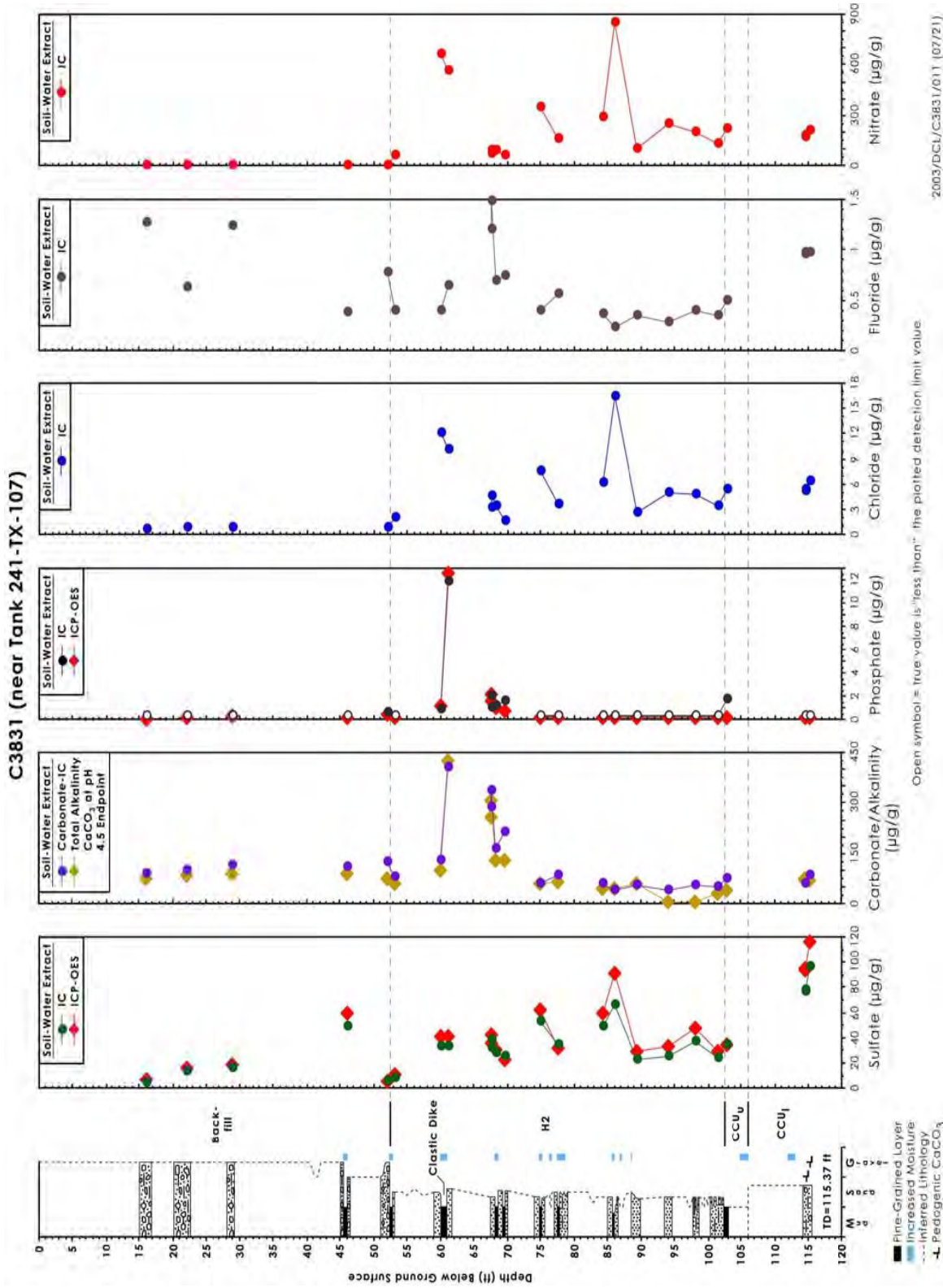
Figure 4.30. C3831 Borehole Water-Extractable Anions (μg/g dry sediment)

4.84

are depleted in the shallow sediments and high levels of water-extractable sodium are present – at both the SX and BX tank farms, where tank fluids have been confirmed as being present (for details, see Serne et al. 2002b, 2002c, 2002d, 2002e, 2002f). Just below the leading edge of the sodium plume one finds elevated levels of divalent cations that were displaced (e.g., 86 ft in C3831). We observe the highest levels of water-extractable divalent cations in a single sample depth (86 ft bgs). At borehole C3831, the water-extractable magnesium, calcium, strontium, barium, potassium, and sodium in the sediments from 75 ft bgs to the bottom of the borehole are greater than for the background sediment in borehole 299-W10-27 by a factor of 3 to 5 and also borehole C3830 sediments by a factor of 2. This likely is an indication of more concentrated leaked tank fluids being present in the C3831 sediments from 75 ft bgs to the bottom of the borehole.

The water-extractable aluminum, silicon, iron, manganese, and zinc in the C3831 borehole sediments are shown in Table 4.37 and Figure 4.32. The water-soluble borehole C3831 aluminum, iron, and manganese data show elevated values between the depths of 60 and 67.5 to 68.2 ft bgs. We speculate that these elevated values indicate some chemical reaction between alkaline tank fluids and native sediments that formed precipitates of aluminum, iron, and manganese that are more water soluble than solid phases present in native sediments. In the zone between 60 and 68.2 ft bgs at borehole C3831 the water-extractable aluminum, iron, and manganese are 2 to 3 times larger than the same zone at borehole C3830.

The phosphorous and sulfur data were converted to water-extractable phosphate and sulfate and plotted with the anion data in Figure 4.30. In general, the agreement between direct measurement of the two anions by ion chromatography and the converted ICP measurements is very good. The water-extractable sulfur values in C3831 do not differ much from those at C3830 but both boreholes show elevated water-soluble sulfate in comparison to sulfur that is water extractable from background sediments. The water-extractable phosphorous at borehole C3831 between the depths of 60 and 69.6 ft bgs is greater than at borehole C3830 and the background sediment by a factor of 2 to 5.

The water-extractable data for potentially mobile metals such as technetium-99, uranium-238, chromium, molybdenum, and ruthenium in borehole C3831 sediments are shown in Table 4.38 and Figure 4.33. In borehole C3831 sediments, technetium-99 and elevated water-soluble ruthenium is present between 53 ft bgs and the bottom of the borehole at 115 ft bgs. There is also elevated water-soluble uranium-238, molybdenum, and chromium in borehole C3831 sediment between 61 and 70 ft bgs. The technetium-99 and ruthenium water extract data suggest that tank fluids may have percolated down through the entire Hanford H2 unit and Cold Creek unit to a depth at least as deep as the bottom of the borehole at 115 ft bgs. However, the abrupt increases in ruthenium, technetium-99, and most other contaminants suggest that tank fluids descended preferentially along the clastic dike that was intercepted at ~60 ft bgs. The maximum technetium-99 concentrations between 59.9 and 61.2 ft bgs are 80 to 140 pCi/g. Between 75 and 94 ft bgs, the technetium-99 varies between 40 and 70 pCi/g. Between 98 and 115 ft bgs at borehole C3831, the technetium-99 concentration is ~35 pCi/g. The technetium-99 values in borehole C3831 are at least 10 times larger than the values at borehole C3830.

The maximum water-soluble uranium concentration is 0.06 µg/g and the maximum water-soluble chromium concentration is 0.07 µg/g. Both occur in the sediment between 61 and 70 ft bgs. Above and below this zone both metals are present at concentrations at least 10 times smaller than in the more elevated but narrow zone between 61 and 70 ft bgs. These water-soluble maxima are small compared to

those at 299-E33-45 (BX-102 uranium overfill [Serne et al. 2002e]) and the SX boreholes where water-soluble chromium from the REDOX process was quite large (Serne et al. 2002b, 2002c, 2002d).

Table 4.35. Water-Extractable Organics in C3831 Vadose Zone Sediments (µg/g)

Depth (ft bgs)	Stratigraphic Unit	Formate	Acetate	Oxalate
15.97	Bkfl	<0.114	0.62	0.44
21.93	Bkfl	0.21	0.82	0.82
28.90	Bkfl	<0.113	<0.160	<0.214
46.06	Bkfl	<0.113	<0.160	<0.214
52.03	Bkfl	<0.113	<0.160	0.41
53.18	H2	0.14	0.78	0.46
59.94	H2	0.16	<0.160	<0.214
61.15	H2	0.43	**3.02**	**2.06**
67.53	H2	<0.113	<0.160	0.4
67.53	H2	0.1	<0.161	0.75
68.21	H2	<0.113	<0.160	0.24
69.60	H2	<0.115	0.21	<0.218
74.99	H2	<0.113	<0.160	<0.214
77.67	H2	<0.113	<0.160	<0.214
78.72	H2	<0.113	<0.160	0.33
85.99	H2	<0.113	<0.160	<0.214
89.39	H2	<0.113	<0.160	<0.214
93.99	H2	<0.113	<0.160	0.23
98.07	H2	<0.113	<0.160	<0.214
101.29	H2	<0.113	<0.160	<0.214
102.65	CCU_u	0.13	0.53	0.29
114.44	CCU_l	<0.113	<0.161	0.5
114.44	CCU_l	0.24	0.5	0.49
115.06	CCU_l	<0.113	0.53	0.54

Bolded values are higher than those in background sediments.

Table 4.36. **Water-Extractable Cations in Borehole C3831 Vadose Zone Sediments**
(µg/g dry sediment)

Depth (ft bgs)	Stratigraphic Unit	Mg	Ca	Sr	Ba	Na	K
15.97	Bkfl	2.40	6.87	3.14E-02	2.23E-02	21.48	5.56
21.93	Bkfl	1.48	6.78	4.34E-02	1.90E-02	32.94	5.88
28.90	Bkfl	1.94	5.81	3.24E-02	3.19E-02	36.71	6.45
46.06	Bkfl	4.64	23.11	1.06E-01	3.54E-02	38.37	12.90
52.03	Bkfl	0.50	2.63	1.30E-02	1.87E-02	32.57	3.84
53.18	H2	1.47	7.00	4.12E-02	3.61E-02	40.94	6.44
59.94	H2	0.87	2.95	2.02E-02	2.34E-02	296.51	12.09
61.15	H2	0.08	1.04	5.87E-03	2.97E-02	430.12	8.43
67.53	H2	0.15	0.98	6.46E-03	2.57E-02	161.29	7.72
67.53	H2	0.13	0.77	5.20E-03	1.55E-02	193.85	8.83
68.21	H2	0.27	1.85	1.02E-02	1.71E-02	104.37	5.48
69.60	H2	0.18	1.25	6.77E-03	2.49E-02	86.93	4.13
74.99	H2	10.81	40.14	2.33E-01	4.71E-02	101.43	19.98
77.67	H2	5.47	19.13	1.18E-01	4.72E-02	42.39	12.31
78.72	H2	13.19	48.45	2.58E-01	4.28E-02	56.80	17.06
85.99	H2	41.37	173.67	8.86E-01	1.16E-01	58.54	29.63
89.39	H2	6.08	24.00	1.33E-01	4.38E-02	24.99	9.83
93.99	H2	10.72	43.16	2.23E-01	6.08E-02	43.13	12.96
98.07	H2	10.19	43.68	2.41E-01	7.50E-02	39.59	13.76
101.29	H2	7.01	31.00	1.70E-01	5.54E-02	25.01	9.62
102.65	CCU$_u$	9.32	38.82	1.99E-01	4.23E-02	29.59	12.12
114.44	CCU$_l$	21.64	48.51	3.68E-01	8.04E-02	29.54	9.50
114.44	CCU$_l$	20.52	48.32	3.69E-01	8.19E-02	29.74	9.07
115.06	CCU$_l$	25.40	55.47	4.27E-01	8.48E-02	31.06	10.18

Table 4.37. Water-Extractable Concentrations of Other Metals in C3831 Vadose Zone Sediments (μg/g dry sediment)

Depth (ft bgs)	Stratigraphic Unit	Al	Si	Fe	Mn	Zn	P as PO$_4$	S as SO$_4$
15.97	Bkfl	3.52E-02	14.73	(2.92E-02)	(1.64E-03)	5.06E-02	3.18E-01	6.27
21.93	Bkfl	6.47E-02	12.30	6.31E-02	3.25E-03	4.53E-02	(1.88E-01)	16.29
28.90	Bkfl	4.39E-02	14.27	(1.12E-02)	(1.58E-03)	5.83E-02	2.64E-01	19.01
46.06	Bkfl	(1.46E-03)	28.01	(6.99E-03)	(1.34E-03)	7.18E-02	(9.12E-02)	58.77
52.03	Bkfl	4.82E-02	13.80	(3.61E-02)	(8.60E-04)	4.72E-02	(4.53E-01)	5.12
53.18	H2	4.95E-02	10.67	(3.56E-02)	(1.36E-03)	9.02E-02	(1.82E-01)	10.31
59.94	H2	1.45E-01	8.83	9.78E-02	2.10E-02	1.03E-01	1.19E+00	40.82
61.15	H2	2.61E-01	13.20	1.01E-01	8.94E-02	1.06E-01	1.26E+01	41.19
67.53	H2	1.96E-01	10.26	2.74E-01	5.45E-02	1.08E-01	1.54E+00	36.01
67.53	H2	2.30E-01	10.18	1.93E-01	3.63E-02	1.22E-01	2.12E+00	41.95
68.21	H2	5.37E-02	9.91	1.91E-01	2.98E-02	8.78E-02	9.74E-01	30.85
69.60	H2	7.32E-02	11.19	(2.82E-02)	4.85E-03	5.81E-02	6.97E-01	22.80
74.99	H2	(1.80E-04)	10.58	(2.11E-02)	6.38E-02	8.05E-02	(1.39E-01)	61.93
77.67	H2	1.13E-01	10.65	(2.74E-02)	5.94E-03	4.73E-02	(1.48E-01)	31.67
78.72	H2	2.50E-02	11.34	(1.80E-02)	5.61E-03	4.27E-02	(1.24E-01)	58.97
85.99	H2	2.50E-02	13.06	(1.57E-02)	3.56E-03	8.51E-02	2.02E-01	90.51
89.39	H2	1.81E-01	12.73	(2.71E-02)	(2.19E-03)	7.05E-02	(1.34E-01)	28.85
93.99	H2	(7.84E-03)	12.57	(1.41E-02)	(1.09E-03)	9.78E-02	(1.22E-01)	33.04
98.07	H2	(8.49E-03)	16.88	(7.68E-03)	(1.25E-02)	8.44E-02	(1.60E-01)	47.85
101.29	H2	(2.30E-02)	12.90	(1.62E-02)	(6.20E-04)	1.01E-01	(1.13E-01)	29.66
102.65	CCU$_u$	(6.72E-03)	14.13	(1.15E-02)	(9.61E-04)	9.07E-02	(1.48E-01)	34.00
114.44	CCU$_l$	2.51E-02	30.88	(8.17E-03)	(1.27E-03)	6.12E-02	(1.23E-01)	94.93
114.44	CCU$_l$	2.51E-02	30.00	(6.88E-03)	(1.02E-03)	6.55E-02	(1.07E-01)	93.93
115.06	CCU$_l$	2.50E-02	31.69	(5.36E-03)	(1.21E-03)	1.29E-01	(1.27E-01)	115.87

(a) Parentheses signify values below level of quantitation but considered valid.

Table 4.38. Water-Extractable Concentrations of Mobile Metals in C3831 Vadose Sediments (µg/g dry sediment)

Depth (ft bgs)	Stratigraphic Unit	Tc-99[a]	U-238	Cr	Mo (ICP-MS)	Mo (ICP)	Ru
15.97	Bktf	(6.82E-02)	2.44E-03	3.32E-04	5.98E-03	8.93E-03	8.55E-05
21.93	Bktf	(2.21E-01)	1.35E-03	4.47E-04	2.25E-02	2.36E-02	1.23E-04
28.90	Bktf	(5.10E-02)	3.84E-03	8.37E-04	2.01E-02	2.35E-02	5.61E-05
46.06	Bktf	(1.70E-01)	4.14E-03	7.08E-03	2.15E-02	2.59E-02	1.70E-05
52.03	Bktf	(5.10E-02)	2.87E-03	5.09E-04	5.01E-03	5.89E-03	1.10E-05
53.18	H2	2.94E+00	9.46E-04	2.80E-03	1.58E-02	1.96E-02	1.53E-04
59.94	H2	7.99E+01	3.05E-03	1.85E-02	7.81E-02	8.31E-02	6.48E-03
61.15	H2	1.37E+02	4.02E-02	7.23E-02	9.29E-02	9.98E-02	2.42E-02
67.53	H2	1.58E+01	3.07E-02	6.50E-02	1.81E-01	1.81E-01	4.16E-03
67.53	H2	1.81E+01	1.62E-02	5.67E-02	1.50E-01	1.63E-01	3.70E-03
68.21	H2	8.39E+00	5.90E-02	6.80E-02	7.95E-01	8.39E-01	1.76E-02
69.60	H2	1.08E+01	2.31E-02	5.37E-02	9.58E-01	1.01E+00	9.21E-03
74.99	H2	5.52E+01	1.71E-03	4.47E-03	3.33E-02	3.49E-02	6.03E-03
77.67	H2	1.98E+01	6.62E-04	1.36E-03	2.24E-02	2.38E-02	1.57E-03
78.72	H2	4.05E+01	1.15E-03	2.20E-03	5.48E-02	6.18E-02	4.41E-03
85.99	H2	6.61E+01	1.93E-03	2.22E-03	3.57E-02	4.85E-02	9.95E-03
89.39	H2	1.68E+01	7.29E-04	9.53E-04	1.08E-02	1.78E-02	1.20E-03
93.99	H2	5.46E+01	8.67E-04	2.49E-03	7.59E-03	1.39E-02	4.92E-03
98.07	H2	2.88E+01	1.23E-03	2.68E-03	2.03E-02	2.84E-02	2.83E-03
101.29	H2	1.76E+01	7.65E-04	1.99E-03	1.10E-02	1.61E-02	1.62E-03
102.65	CCU$_u$	3.23E+01	1.28E-03	2.41E-03	1.67E-02	2.35E-02	2.51E-03
114.44	CCU$_l$	3.49E+01	2.03E-03	1.21E-03	9.56E-03	1.66E-02	2.54E-03
114.44	CCU$_l$	3.30E+01	1.99E-03	1.23E-03	9.52E-03	1.64E-02	2.40E-03
115.06	CCU$_l$	3.81E+01	2.07E-03	1.41E-03	1.45E-02	2.26E-02	3.03E-03

(a) Technetium-99 data are in units of pCi/g while others are µg/g of dry sediment.
(b) Parentheses signify values below level of quantitation but considered valid.
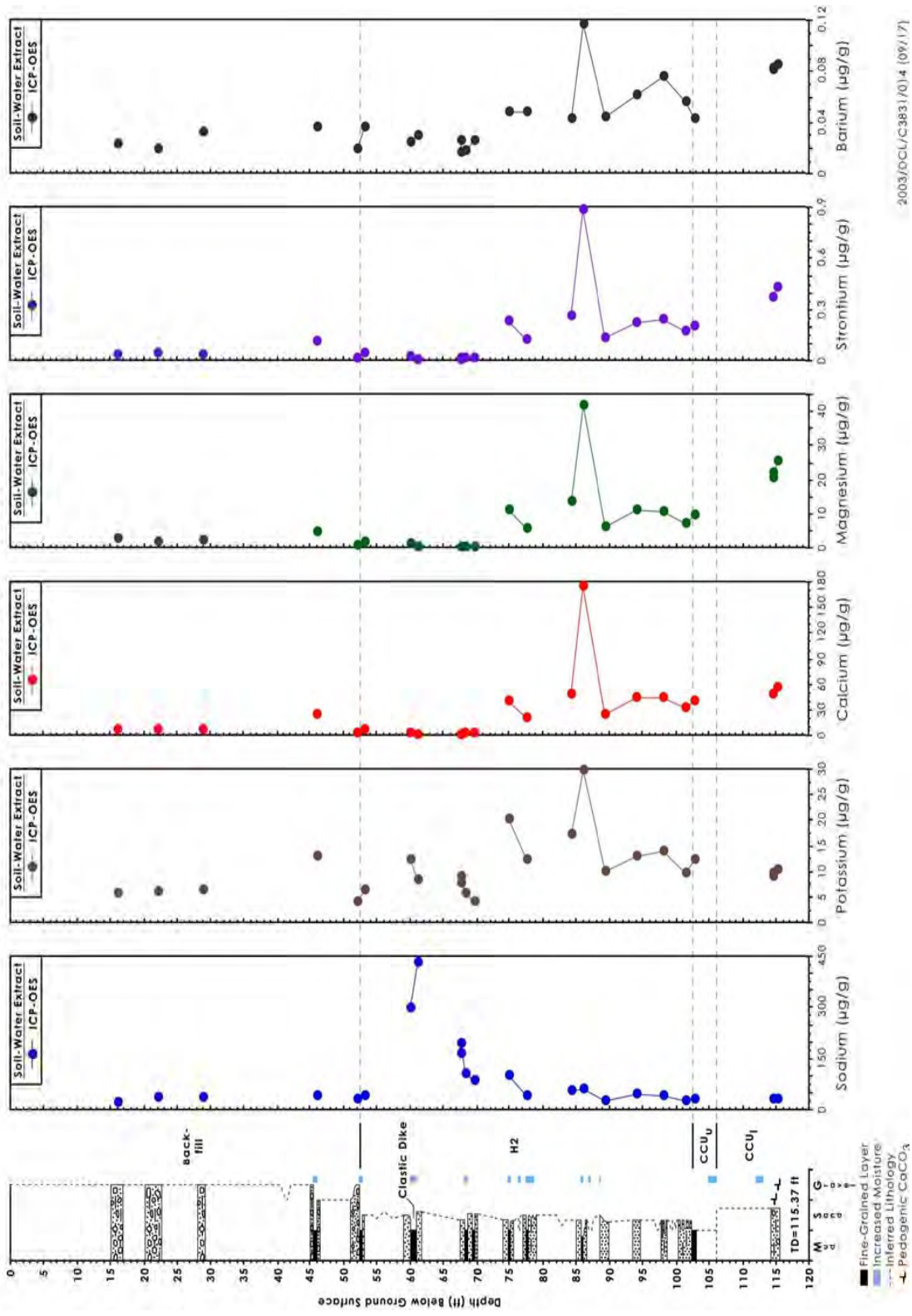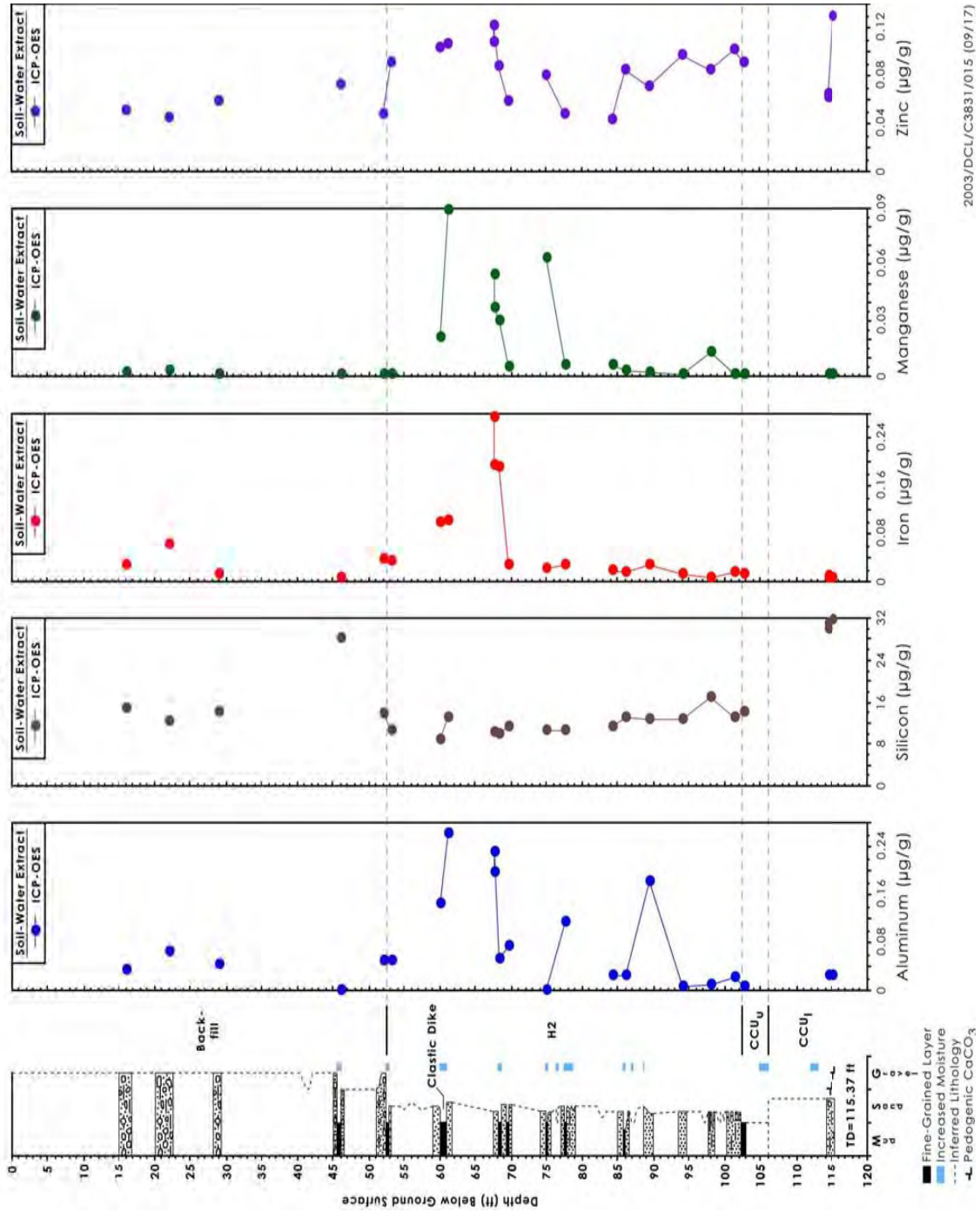
Figure 4.31. Water-Extractable Cations in Borehole C3831 Vadose Zone Sediments (µg/g)

Figure 4.32. Water-Extractable Metals in Borehole C3831 Vadose Sediments (µg/g dry sediment)
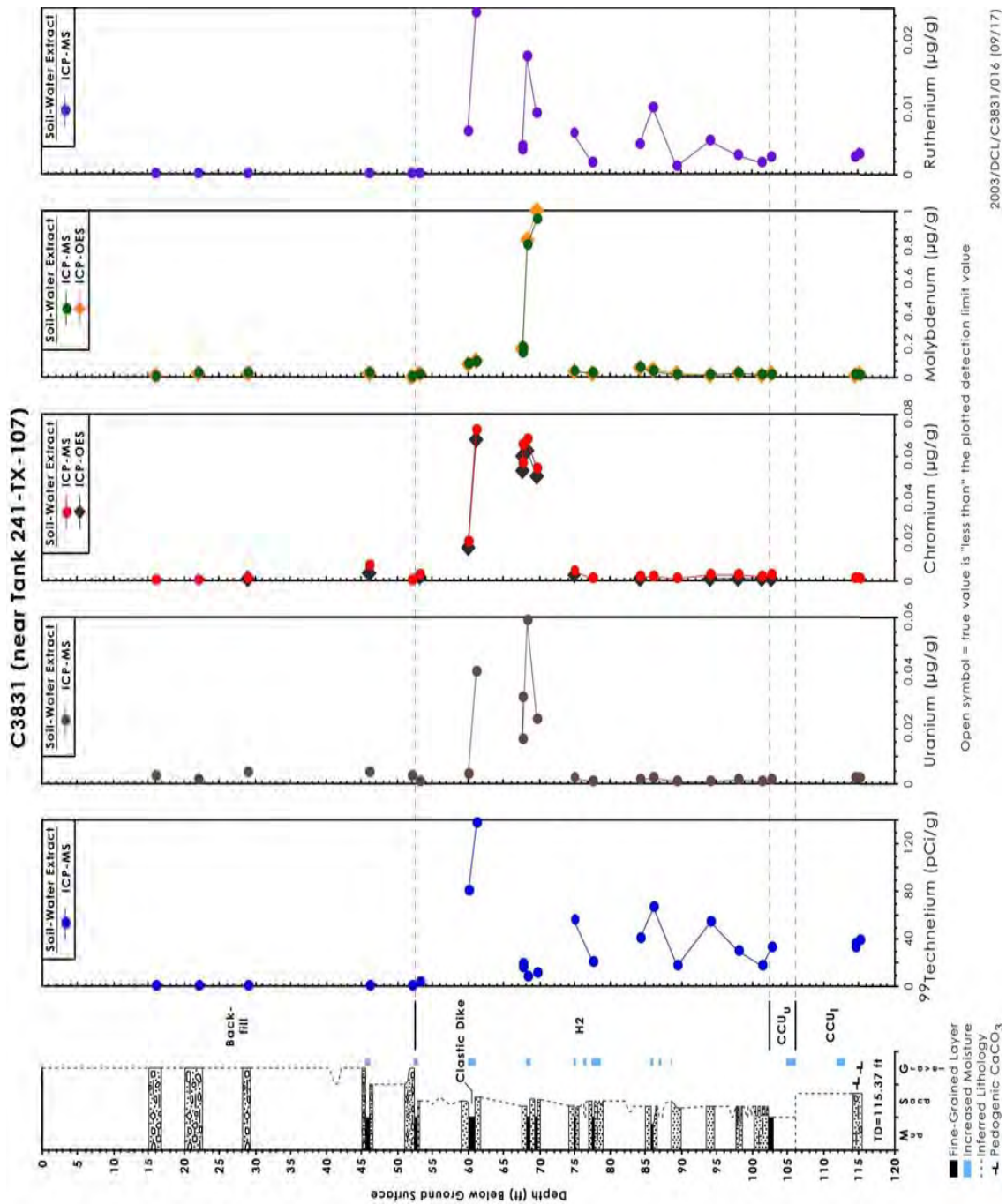
Figure 4.33. Distribution of Mobile Metals in Water Extracts of C3831 Vadose Zone Sediments

4.3.3   Derivation of Vadose Zone Porewater Chemical Composition

The 1:1 water extract data was recalculated to estimate the composition of the vadose zone porewater. From knowledge of the moisture content of the sediment samples taken from the liners of each core we calculated the amount of deionized water that would be needed to make the water extract exactly one part water (total of native porewater and added deionized water) to one part by weight dry sediment. The contaminated or uncontaminated sediments the dilution-corrected water extract data is biased high by a factor of 2 to 7 for many constituents such that the true porewater is less saline.

Tables 4.39 through 4.42 and Figures 4.34 through 4.37 show the calculated porewater composition of key constituents as a function of depth and stratigraphy. The most concentrated porewater is found at a clastic dike at ~ 61 ft bgs and has a total concentration of 424 meq/L cations and anions. The calculated most saline porewater composition consists of 418.5 meq/L Na, 1.2 meq/L Ca, 0.2 meq/L Mg, and 4.7 meq/L K. These cations are neutralized by the following mixture of anions: 202.4 meq/L nitrate, 191.2 meq/L bicarbonate, 15.2 meq/L sulfate and 6.4meq/L chloride, 0.8 meq/L fluoride, and 8.4 meq/L phosphate. This concentration is relatively dilute compared to the vadose zone porewaters found at the SX and BX tank farms (Serne et al. 2002b, 2002c, 2002d, 2002e) where the total ionic strength of the porewaters were as high as 7,000 to 17,000 and 1,000 meq/L, respectively. At the borehole emplaced near tank B-110 the most saline porewater was 150 to 160 meq/L. Thus the porewater maximum at borehole C3831 is ~ 3 and 4 times more concentrated than the vadose zone porewater at 299-E33-46 (Serne et al. 2002f) and at borehole C3830, respectively.

At ~86 ft bgs, where the divalent cations that were stripped from the shallower sediments by sodium reside, there is a second smaller peak in porewater salt content with about 110 meq/L of cations and anions with the following chemical composition: the cation distribution is 17.4 meq/L Na, 59.2 meq/L Ca, 23.2 meq/L Mg, and 5.2 meq/L K; the anion distribution is 93.2 meq/L nitrate, 9.4 meq/L sulfate, 6.0 meq/L bicarbonate, 3.2 meq/L chloride, and 0.08 meq/L fluoride.

The technetium-99 in the porewaters between the depths of 53 to the bottom of the hole at 116 ft bgs ranges from 50,000 to 10^{+6} pCi/L. On a per gram of dry sediment basis, these porewater concentrations are 40 to 140 pCi/g. Because the water content of the H2 unit sediments is so small when equated to porewater concentrations, this small mass of technetium-99 reaches concentrations about 500 to 1000 times larger than the drinking water standard.

The calculated porewater uranium, chromium, molybdenum, and ruthenium concentrations are significantly elevated between 61 and 70 ft bgs and range from 300 to 900, 600 to 1600, 1000 to 17,000 and 60 to 2,000 µg/L, respectively. Below these depths the porewater concentrations are 50 to 100 times lower. The porewaters in borehole C3831 are definitely more contaminated than the porewaters in borehole C3830 sediments.

4.3.4   8 M Nitric Acid-Extractable Amounts of Selected Elements in C3831 Sediments

The same cores that were characterized for water-extractable constituents were also characterized to see how much of various constituents could be leached with hot 8 M nitric acid. A comparison between the quantities that were acid extractable with those that are water extractable often indicates the relative mobility of a given constituent and can sometimes differentiate man-disposed from naturally occurring constituents. Finally, a comparison of the acid-extractable quantities in suspected contaminated

sediments with acid-extractable amounts in uncontaminated sediments can be used to delineate the presence of less mobile contaminants.

The quantities of various constituents in the C3831 vadose zone sediments that were acid extractable are shown in Tables 4.43 to 4.45 and Figures 4.38 through 4.40. Upon comparing the acid extract data for borehole C3831 with similar strata in the uncontaminated borehole 299-W10-27, most of the variation in mass leached per gram of sediment versus depth in found to be lithology-related. That is, for most constituents there are no signs of elevated values of acid-leachable constituents in borehole C3831 sediments excepting acid-extractable sulfur (assumed to represent sulfate), sodium (between the depths of 61 and 67.5 ft bgs), molybdenum (between 67.5 and 70 ft bgs), and ruthenium and technetium-99 throughout most of the depth profile. The acid-extractable sulfate profile in borehole C3831 sediments averages about 4 to 7 times higher than in comparable uncontaminated sediments from borehole 299-W10-27. The acid-extractable sulfur (measured as sulfate) for boreholes C3830 and C3831 are similar. Borehole C3831 shows high acid-leachable technetium-99 and ruthenium throughout the profile and larger acid-extractable sodium and molybdenum in thin zones between 67.5 and 70 and 61 to 67.5 ft bgs, respectively than borehole C3830. The acid-extractable technetium-99 ranges from 50 to 200 pCi/g from 60 ft bgs to the bottom of the borehole. This range is slightly lower than the technetium-99 acid extracts at C3830.

As mentioned, the ratio of water-extractable to acid-extractable quantities of constituents can identify samples that may contain leaked fluids for Hanford waste disposals. The comparison of water to acid extracts suggests that there are unnaturally high percentages of water-leachable uranium, chromium, and molybdenum between the depths of 61 and 70 ft bgs. There are unnaturally high percentages of water-leachable phosphate at the 61 ft bgs depth. The water-extractable percentages versus acid-extractable divalent cations are high between 75 and 98 ft bgs, especially at 86 ft bgs suggesting the impacts of the sodium waste solution ion exchange reaction. The water to acid-extractable sodium percentage is unnaturally high between the depths of 53 and 86 ft bgs, suggesting sodium-enriched fluids reside in the pores of the vadose zone sediments in this zone. The presence of elevated water- and acid-extractable quantities of technetium-99 and ruthenium between 60 ft bgs and the bottom of the borehole at 115 ft bgs suggests the presence of Hanford Site waste fluids in the vadose zone at these depths in borehole C3831.

The borehole C3831 sediment from the Cold Creek lower subunit (caliche) has elevated acid-extractable levels of uranium, magnesium, calcium, strontium, sodium, and potassium and lower acid-extactable silicon, manganese, and zinc in comparison to other samples. The cause for these differences is the higher concentrations of pedogenic calcium carbonate found in this subunit at C3831 than at 299-W10-27. Caliche contains higher concentrations of acid-extractable uranium, magnesium, calcium, and sodium than other minerals and when one caliche sample contains more calcium carbonate than another sample higher amounts of these constituents are acid leachable.

Figure 4.40 shows that our acid-extractable molybdenum results from ICP analyses is biased high likely from an unaccounted for spectral interference. The molybdenum results from the ICP-MS are more accurate and the detection limits are much lower. Figure 4.41 shows that there is some sulfate present in the sediments that is not readily water extractable but the vast majority of the sediment phosphate content is not water extractable in comparison with the amounts that are acid extractable. The same trend was observed for the uncontaminated sediments from borehole 299-W10-27 and samples from borehole C3830. Alternatively, some of the acid-extractable phosphorous may be present in a form other than phosphate such that when we convert the acid-extractable phosphorous number to phosphate (essentially we multiply by 3), we are inflating the acid-extractable value.

Table 4.39.   Calculated Porewater Cation Concentrations in C3831 Vadose Zone Sediments

Depth (ft bgs)	Stratigraphic Unit	mg/L Mg	mg/L Ca	mg/L Sr	µg/L Ba	mg/L Na	mg/L K
15.97	Bkfl	78.82	225.44	1.03	733.04	704.88	182.47
21.93	Bkfl	38.13	174.07	1.11	486.79	845.88	150.88
28.90	Bkfl	40.25	120.57	0.67	661.20	761.68	133.79
46.06	Bkfl	55.71	277.37	1.27	424.33	460.43	154.84
52.03	Bkfl	3.03	15.92	0.08	112.97	196.94	23.24
53.18	H2	23.20	110.14	0.65	568.40	644.53	101.41
59.94	H2	10.69	36.47	0.25	288.41	3659.19	149.25
61.15	H2	1.83	23.35	0.13	665.01	9624.87	188.55
67.53	H2	2.47	16.60	0.11	434.24	2721.01	130.16
67.53	H2	2.19	12.95	0.09	262.10	3270.19	149.01
68.21	H2	2.13	14.85	0.08	137.70	838.95	44.08
69.60	H2	3.26	22.73	0.12	453.96	1584.68	75.30
74.99	H2	59.82	222.22	1.29	260.71	561.46	110.62
77.67	H2	85.49	299.05	1.85	737.48	662.60	192.36
78.72	H2	81.33	298.69	1.59	264.10	350.21	105.19
85.99	H2	282.24	1184.86	6.05	792.93	399.36	202.11
89.39	H2	118.61	468.15	2.59	854.45	487.56	191.79
93.99	H2	185.25	746.01	3.86	1050.94	745.39	223.95
98.07	H2	92.82	397.82	2.20	683.32	360.53	125.33
101.29	H2	141.69	626.77	3.43	1119.95	505.60	194.55
102.65	CCU$_u$	176.55	735.08	3.77	801.21	560.31	229.44
114.44	CCU$_l$	206.37	462.61	3.51	767.11	281.66	90.56
114.44	CCU$_l$	195.70	460.74	3.52	780.64	283.59	86.49
115.06	CCU$_l$	196.22	428.57	3.30	655.03	239.97	78.65

Table 4.40. Calculated Porewater Anion Concentrations in C3831 Vadose Zone Sediments

Depth (ft bgs)	Stratigraphic Unit	mg/L Fluoride	mg/L Chloride	mg/L Nitrate	mg/L Alk as CO$_3$	mg/L Sulfate	mg/L Phosphate
15.97	Bkfl	41.82	18.09	55.73	1443	149.29	<7.921
21.93	Bkfl	16.18	20.92	84.08	1271	349.9	<6.173
28.90	Bkfl	25.68	17.49	47.99	1087	328.17	<4.991
46.06	Bkfl	4.57	308.09	40.24	628	585.92	<2.882
52.03	Bkfl	4.73	5.05	11.82	276	32.75	3.2
53.18	H2	6.35	31.43	872.89	584	119.72	<3.781
59.94	H2	4.92	149.85	8235.31	745	404.45	10.3
61.15	H2	14.55	225.15	12549.92	5735	729.93	266.05
67.53	H2	20.46	53.48	1230.34	2625	539.68	17.35
67.53	H2	25.09	76.99	1478.95	3128	641.37	33.58
68.21	H2	5.52	27.72	733.72	626	220.97	9.63
69.60	H2	13.69	30.36	1103.42	1412	451.53	28.36
74.99	H2	2.15	41.51	1938.52	197	291.06	<1.329
77.67	H2	8.95	56.74	2419.87	237	528.71	<3.753
78.72	H2	2.23	38.54	1769.62	431	303.82	<1.479
85.99	H2	1.58	112.68	5776.26	181	450.68	<1.637
89.39	H2	6.91	49.08	1911.56	677	450.64	<4.683
93.99	H2	5.07	85.58	4372.1	49	432.05	<4.151
98.07	H2	3.64	43.1	1846.59	22	339.66	<2.186
101.29	H2	6.9	66.45	2570.99	356	479.24	<4.854
102.65	CCU$_u$	9.35	100.57	4212.14	472	645.64	33.38
114.44	CCU$_l$	9.15	51.67	1677.87	455	739.65	<2.298
114.44	CCU$_l$	9.26	49.95	1619.18	387	729.84	<2.301
115.06	CCU$_l$	7.46	49.51	1578.17	319	747.02	<1.854

4.96

Table 4.41. Calculated Porewater Concentrations of Selected Constituents in C3831 Vadose Zone Sediments

		µg/L	mg/L	µg/L	µg/L	µg/L	mg/L	mg/L
Depth (ft bgs)	Stratigraphic Unit	Al	Si	Fe	Mn	Zn	PO_4 (ICP)	SO_4 (ICP)
15.97	Bkf	1.15E+03	4.84E+02	(9.58E+02)	(5.39E+01)	1.66E+03	1.04E+01	2.06E+02
21.93	Bkf	1.66E+03	3.16E+02	1.62E+03	8.35E+01	1.16E+03	(4.83E+00)	4.19E+02
28.90	Bkf	9.11E+02	2.96E+02	(2.32E+02)	(3.28E+01)	1.21E+03	5.48E+00	3.95E+02
46.06	Bkf	(1.76E+01)	3.36E+02	(8.38E+01)	(1.60E+01)	8.62E+02	(1.09E+00)	7.06E+02
52.03	Bkf	2.91E+02	8.35E+01	(2.18E+02)	(5.20E+00)	2.85E+02	(2.74E+00)	3.10E+01
53.18	H2	7.79E+02	1.68E+02	(5.61E+02)	(2.13E+01)	1.42E+03	(2.86E+00)	1.63E+02
59.94	H2	1.78E+03	1.09E+02	1.21E+03	2.60E+02	1.27E+03	1.46E+01	5.04E+02
61.15	H2	5.83E+03	2.95E+02	2.27E+03	2.00E+03	2.38E+03	2.81E+02	9.23E+02
67.53	H2	3.30E+03	1.73E+02	4.63E+03	9.19E+02	1.82E+03	2.60E+01	6.08E+02
67.53	H2	3.87E+03	1.72E+02	3.25E+03	6.13E+02	2.05E+03	3.58E+01	7.09E+02
68.21	H2	4.32E+02	7.96E+01	1.53E+03	2.40E+02	7.06E+02	7.82E+00	2.48E+02
69.60	H2	1.33E+03	2.04E+02	(5.15E+02)	8.84E+01	1.06E+03	1.27E+01	4.16E+02
74.99	H2	(9.94E-01)	5.86E+01	(1.17E+02)	3.53E+02	4.46E+02	(7.67E-01)	3.43E+02
77.67	H2	1.77E+03	1.66E+02	(4.29E+02)	9.28E+01	7.39E+02	(2.31E+00)	4.96E+02
78.72	H2	1.54E+02	6.99E+01	(1.11E+02)	3.46E+01	2.63E+02	(7.66E-01)	3.64E+02
85.99	H2	1.70E+02	8.91E+01	(1.07E+02)	2.43E+01	5.80E+02	1.37E+00	6.18E+02
89.39	H2	3.52E+03	2.48E+02	(5.29E+02)	(4.27E+01)	1.38E+03	(2.61E+00)	5.64E+02
93.99	H2	(1.35E+02)	2.17E+02	(2.43E+02)	(1.89E+01)	1.69E+03	(2.11E+00)	5.72E+02
98.07	H2	(7.73E+01)	1.54E+02	(6.99E+01)	(114)	7.69E+02	(1.45E+00)	4.36E+02
101.29	H2	(4.65E+02)	2.61E+02	(3.28E+02)	(1.25E+01)	2.04E+03	(2.27E+00)	6.00E+02
102.65	CCU$_u$	(1.27E+02)	2.68E+02	(2.18E+02)	(1.82E+01)	1.72E+03	(2.81E+00)	6.45E+02
114.44	CCU$_l$	(1.27E+02)	2.94E+02	(7.79E+01)	(1.21E+01)	5.83E+02	(1.17E+00)	9.06E+02
114.44	CCU$_l$	(1.27E+02)	2.86E+02	(6.56E+01)	(9.72E+00)	6.25E+02	(1.02E+00)	8.97E+02
115.06	CCU$_l$	(1.27E+02)	2.45E+02	(4.14E+01)	(9.36E+00)	1.00E+03	(9.77E-01)	8.96E+02

Parentheses signify values below level of quantitation but considered valid.

Table 4.42. Calculated Porewater Concentrations of Potentially Mobile Constituents in C3831 Vadose Sediments

Depth (ft bgs)	Stratigraphic Unit	Tc-99[a] pCi/L	U-238 µg/L	Cr (ICP-MS) µg/L	Mo (ICP) µg/L	Mo (ICP-MS) µg/L	Ru µg/L
15.97	Bkfl	(2.24E+03)[b]	8.01E+01	(1.09E+01)	2.93E+02	1.96E+02	(2.81E+00)
21.93	Bkfl	(5.67E+03)	3.47E+01	(1.15E+01)	6.06E+02	5.79E+02	(3.16E+00)
28.90	Bkfl	(1.06E+03)	7.97E+01	(1.74E+01)	4.87E+02	4.16E+02	(1.16E+00)
46.06	Bkfl	(2.04E+03)	4.97E+01	(8.50E+01)	3.11E+02	2.58E+02	(2.04E-01)
52.03	Bkfl	(3.08E+02)	1.74E+01	(3.08E+00)	3.56E+01	3.03E+01	(6.66E-02)
53.18	H2	4.63E+04	1.49E+01	(4.41E+01)	3.08E+02	2.49E+02	(2.41E+00)
59.94	H2	9.86E+05	3.77E+01	2.28E+02	1.03E+03	9.64E+02	8.00E+01
61.15	H2	3.07E+06	9.00E+02	1.62E+03	2.23E+03	2.08E+03	5.41E+02
67.53	H2	2.67E+05	5.18E+02	1.10E+03	3.06E+03	3.05E+03	7.02E+01
67.53	H2	3.05E+05	2.73E+02	9.57E+02	2.75E+03	2.54E+03	6.23E+01
68.21	H2	6.75E+04	4.75E+02	5.47E+02	6.74E+03	6.39E+03	1.42E+02
69.60	H2	1.97E+05	4.21E+02	9.78E+02	1.84E+04	1.75E+04	1.68E+02
74.99	H2	3.05E+05	9.49E+00	(2.47E+01)	1.93E+02	1.84E+02	3.34E+01
77.67	H2	3.09E+05	1.04E+01	(2.12E+01)	3.73E+02	3.51E+02	2.46E+01
78.72	H2	2.50E+05	7.10E+00	(1.36E+01)	3.81E+02	3.38E+02	2.72E+01
85.99	H2	4.51E+05	1.32E+01	(1.52E+01)	3.31E+02	2.44E+02	6.79E+01
89.39	H2	3.28E+05	1.42E+01	(1.86E+01)	3.47E+02	2.10E+02	2.33E+01
93.99	H2	9.44E+05	1.50E+01	(4.30E+01)	2.40E+02	1.31E+02	8.51E+01
98.07	H2	2.62E+05	1.12E+01	(2.44E+01)	2.59E+02	1.85E+02	2.58E+01
101.29	H2	3.57E+05	1.55E+01	(4.03E+01)	3.25E+02	2.22E+02	3.28E+01
102.65	CCU$_u$	6.12E+05	2.43E+01	(4.56E+01)	4.46E+02	3.16E+02	4.76E+01
114.44	CCU$_l$	3.32E+05	1.93E+01	(1.15E+01)	1.58E+02	9.12E+01	2.42E+01
114.44	CCU$_l$	3.15E+05	1.90E+01	(1.17E+01)	1.57E+02	9.08E+01	2.29E+01
115.06	CCU$_l$	2.94E+05	1.60E+01	(1.09E+01)	1.75E+02	1.12E+02	2.34E+01

(a) Technetium-99 data are in units of pCi/L while all others are µg/L.
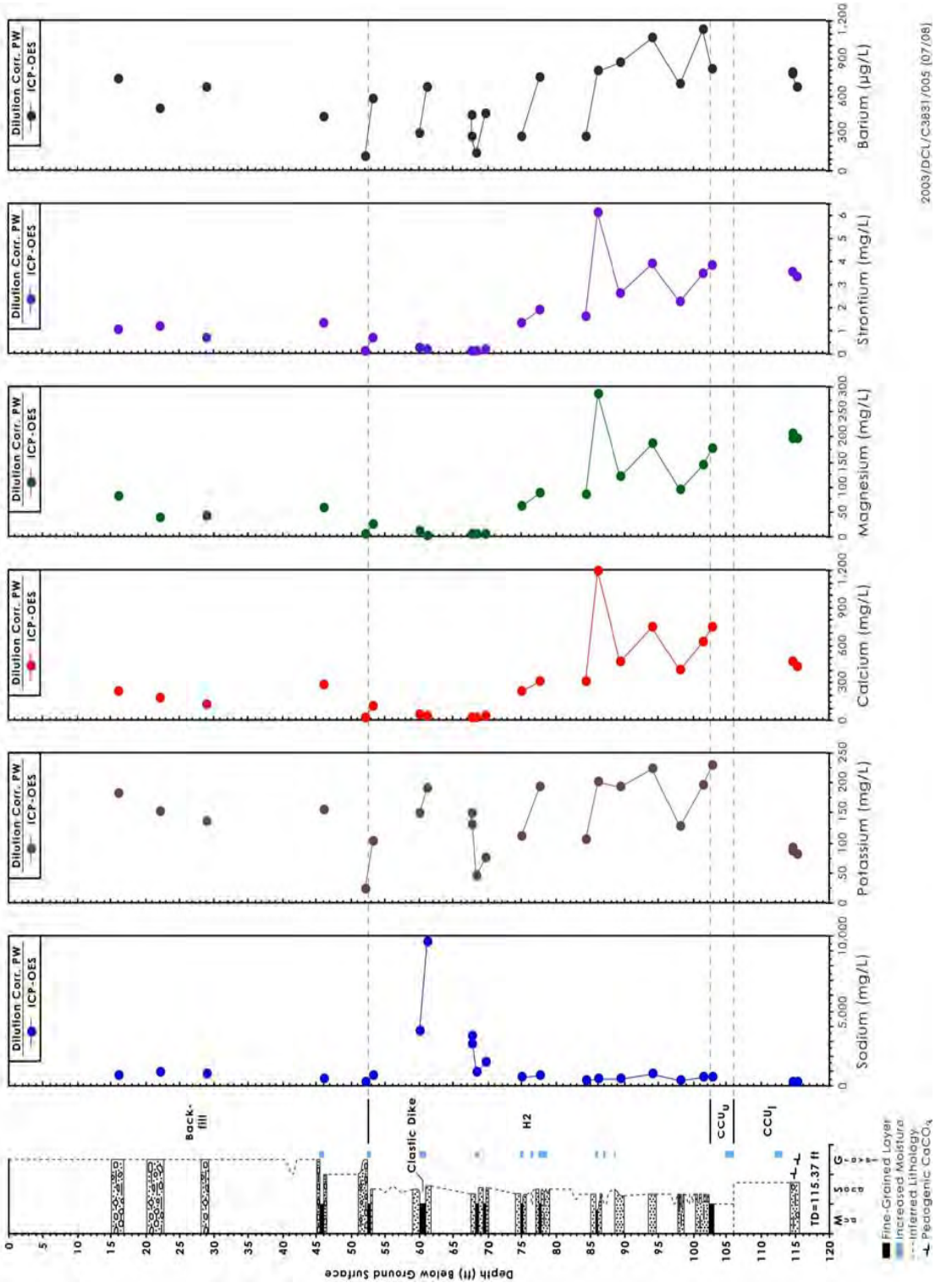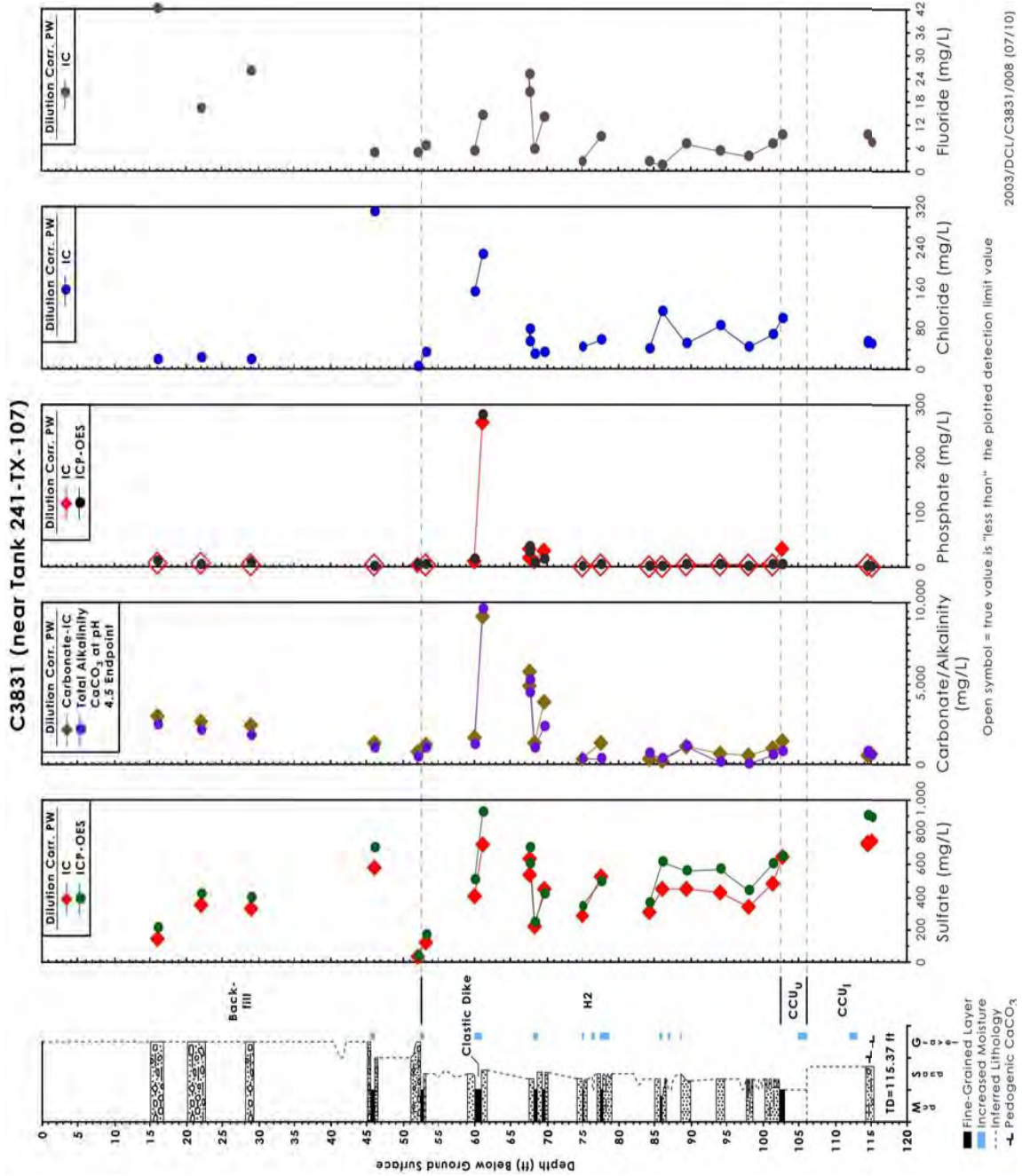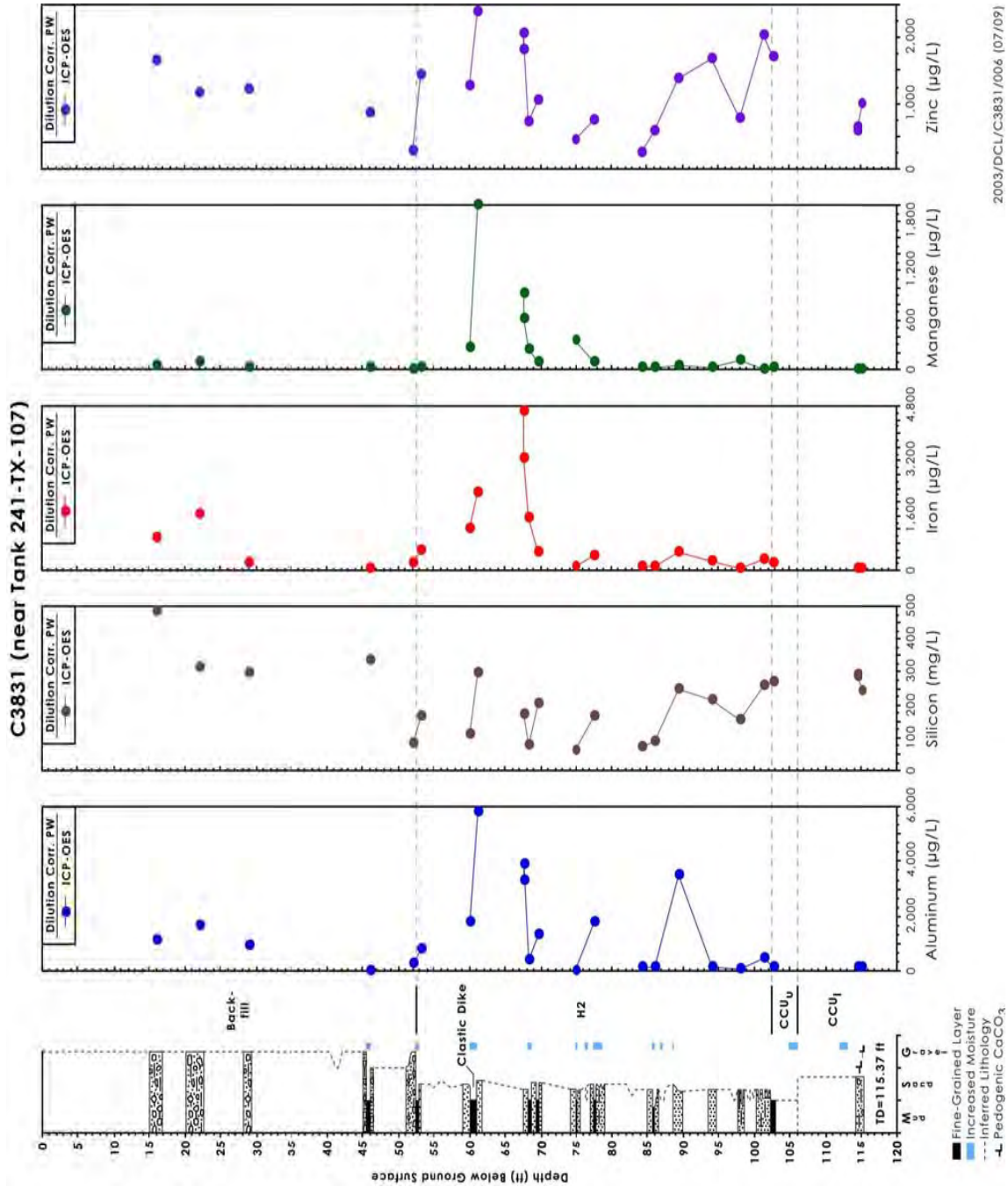(b) Parentheses signify values below level of quantitation but considered valid.

Figure 4.34. Derived Porewater Composition of Major Cations in C3831 Vadose Zone Sediments

Figure 4.35. Derived Porewater Anion Composition in C3831 Vadose Zone Sediments

Figure 4.36. Derived Porewater Composition for Selected Metals in C3831 Vadose Zone Sediments
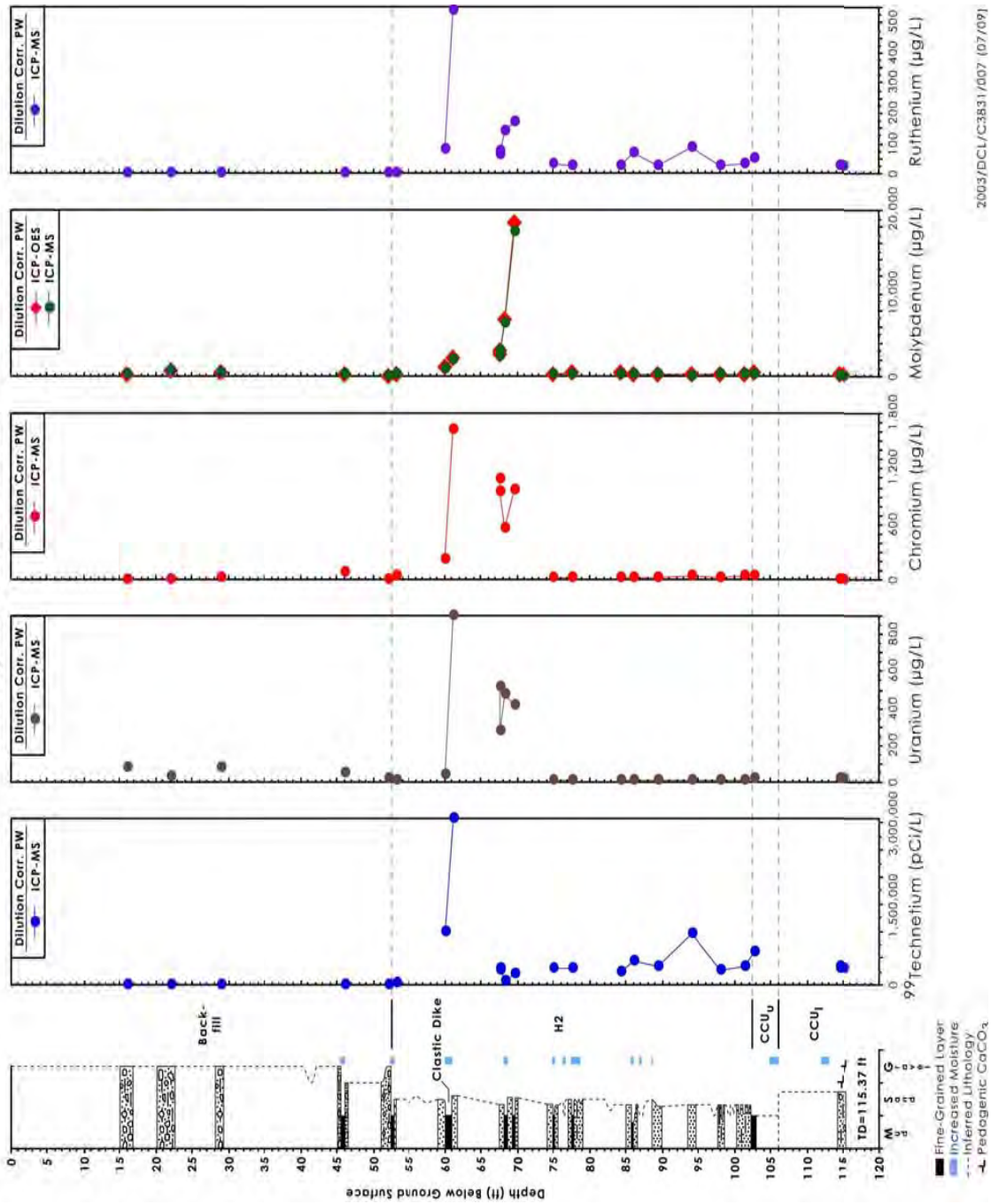
2003/DCL/C3831/006 (07/09)

Figure 4.37. Calculated Porewater Composition of Mobile Metals in C3831 Vadose Zone Sediments

Table 4.43.   Acid-Extractable Cations from C3831 Vadose Zone Sediments (μg/g dry sediment)

Depth (ft bgs)	Lithology	Mg	Ca	Sr	Ba	Na	K
15.97	Bkfl	3.34E+03	5.10E+03	2.18E+01	6.11E+01	- - -	8.59E+02
21.93	Bkfl	3.04E+03	5.26E+03	2.31E+01	5.07E+01	- - -	7.43E+02
28.90	Bkfl	3.10E+03	7.87E+03	2.28E+01	4.75E+01	- - -	7.52E+02
46.06	Bkfl	2.50E+03	1.61E+04	3.67E+01	4.61E+01	- - -	7.07E+02
52.03	Bkfl	5.18E+03	6.95E+03	3.38E+01	7.00E+01	- - -	2.00E+03
53.18	H2	4.52E+03	7.58E+03	3.34E+01	5.75E+01	- - -	1.66E+03
59.94	H2	4.51E+03	6.85E+03	2.89E+01	5.19E+01	- - -	1.56E+03
61.15	H2	4.11E+03	6.67E+03	2.53E+01	5.16E+01	- - -	1.37E+03
67.53	H2	4.17E+03	6.46E+03	2.74E+01	5.03E+01	- - -	1.37E+03
67.53	H2	4.50E+03	7.18E+03	3.28E+01	5.49E+01	- - -	1.62E+03
68.21	H2	4.66E+03	7.46E+03	3.25E+01	4.97E+01	- - -	1.85E+03
69.60	H2	4.74E+03	7.70E+03	3.11E+01	7.42E+01	- - -	1.86E+03
74.99	H2	5.20E+03	7.91E+03	3.55E+01	5.78E+01	- - -	2.24E+03
77.67	H2	5.08E+03	7.37E+03	3.37E+01	9.88E+01	- - -	1.61E+03
78.72	H2	5.22E+03	8.00E+03	3.42E+01	7.19E+01	- - -	2.24E+03
85.99	H2	5.33E+03	9.51E+03	3.56E+01	6.96E+01	- - -	2.62E+03
89.39	H2	4.55E+03	7.14E+03	3.37E+01	5.66E+01	- - -	1.64E+03
93.99	H2	4.67E+03	7.61E+03	3.76E+01	7.43E+01	- - -	1.92E+03
98.07	H2	5.57E+03	1.07E+04	4.66E+01	8.92E+01	- - -	2.74E+03
101.29	H2	4.46E+03	8.77E+03	3.32E+01	6.82E+01	- - -	1.63E+03
102.65	CCU$_u$	4.88E+03	1.18E+04	3.80E+01	5.76E+01	- - -	1.74E+03
114.44	CCU$_l$	7.14E+03	5.38E+04	1.50E+02	6.77E+01	- - -	1.10E+03
114.44	CCU$_l$	7.07E+03	5.75E+04	1.63E+02	6.57E+01	- - -	1.04E+03
115.06	CCU$_l$	1.02E+04	8.38E+04	2.10E+02	1.07E+02	- - -	1.01E+03

Table 4.44. Acid-Extractable Constituents in C3831 Vadose Zone Sediments (µg/g dry sediment)

Depth (ft bgs)	Stratigraphic Unit	Al	Si	Fe	Mn	Zn	P as PO$_4$	S as SO$_4$
15.97	Bkfl	5.37E+03	4.88E+00	1.52E+04	2.18E+02	3.17E+01	2.52E+03	5.31E+02
21.93	Bkfl	5.06E+03	2.68E+00	1.99E+04	2.68E+02	3.17E+01	2.33E+03	5.31E+02
28.90	Bkfl	4.79E+03	7.53E+00	1.34E+04	1.92E+02	2.71E+01	2.31E+03	6.91E+02
46.06	Bkfl	4.40E+03	6.40E+00	1.25E+04	3.22E+02	2.86E+01	2.33E+03	1.75E+03
52.03	Bkfl	9.25E+03	9.97E+00	1.46E+04	2.35E+02	3.73E+01	1.94E+03	5.53E+02
53.18	H2	7.60E+03	2.98E+01	1.32E+04	2.62E+02	3.31E+01	1.29E+03	5.89E+02
59.94	H2	6.82E+03	3.45E+01	1.22E+04	2.48E+02	3.23E+01	1.45E+03	5.91E+02
61.15	H2	6.34E+03	1.95E+01	1.19E+04	2.44E+02	2.98E+01	1.36E+03	5.59E+02
67.53	H2	6.14E+03	1.05E+01	1.17E+04	2.29E+02	3.95E+01	1.33E+03	5.56E+02
67.53	H2	7.51E+03	1.44E+01	1.30E+04	2.41E+02	3.65E+01	1.35E+03	5.95E+02
68.21	H2	8.00E+03	1.95E+01	1.29E+04	2.05E+02	3.57E+01	1.61E+03	5.50E+02
69.60	H2	7.99E+03	1.51E+01	1.39E+04	2.96E+02	4.04E+01	1.39E+03	6.28E+02
74.99	H2	9.27E+03	8.37E+00	1.38E+04	2.71E+02	3.88E+01	1.87E+03	6.07E+02
77.67	H2	7.44E+03	9.38E+00	1.37E+04	2.82E+02	3.88E+01	1.74E+03	6.63E+02
78.72	H2	9.44E+03	6.16E+00	1.48E+04	3.11E+02	4.20E+01	1.52E+03	6.47E+02
85.99	H2	1.05E+04	5.45E+00	1.48E+04	3.10E+02	4.27E+01	1.41E+03	7.01E+02
89.39	H2	7.68E+03	1.83E+01	1.40E+04	2.71E+02	3.36E+01	1.44E+03	5.68E+02
93.99	H2	8.83E+03	3.36E+00	1.43E+04	2.91E+02	3.52E+01	1.38E+03	6.22E+02
98.07	H2	1.13E+04	1.42E+01	1.79E+04	3.78E+02	4.21E+01	1.51E+03	8.27E+02
101.29	H2	7.19E+03	4.64E+01	1.27E+04	2.59E+02	3.84E+01	1.49E+03	6.55E+02
102.65	CCU$_u$	7.78E+03	1.07E+01	1.22E+04	2.59E+02	3.78E+01	1.53E+03	8.53E+02
114.44	CCU$_l$	8.23E+03	7.36E+00	1.12E+04	1.76E+02	2.50E+01	1.47E+03	3.84E+03
114.44	CCU$_l$	7.77E+03	9.09E+00	1.00E+04	1.56E+02	2.15E+01	1.38E+03	4.10E+03
115.06	CCU$_l$	6.66E+03	6.66E+00	8.73E+03	1.33E+02	2.12E+01	1.45E+03	6.00E+03

Table 4.45. Acid-Extractable Trace Metals in C3831 Vadose Zone Sediments

Depth (ft bgs)	Stratigraphic Unit	Tc-99[a][b]	U-238	Cr (ICP-MS)	Cr (ICP)	Mo (ICP-MS)	Mo (ICP)	Ru (ICP-MS)
15.97	Bkfl	(1.35E+01)[b]	5.18E-01	9.47E+00	6.65E+00	4.46E-01	1.83E+00	(9.32E-03)
21.93	Bkfl	(8.76E+00)	4.58E-01	1.05E+02	7.02E+01	1.56E+01	1.29E+01	(7.34E-03)
28.90	Bkfl	(7.61E+00)	5.10E-01	8.37E+00	5.53E+00	4.71E-01	2.43E+00	(1.31E-02)
46.06	Bkfl	(8.52E+00)	5.06E-01	6.51E+00	5.58E+00	5.35E-01	2.64E+00	(8.66E-03)
52.03	Bkfl	(2.77E+01)	6.66E-01	1.63E+01	1.75E+01	3.53E-01	1.88E+00	(6.28E-03)
53.18	H2	(2.43E+01)	5.94E-01	1.11E+01	1.13E+01	2.74E-01	1.29E+00	(6.36E-03)
59.94	H2	1.94E+02	4.58E-01	1.22E+01	1.29E+01	4.77E-01	1.98E+00	(1.86E-02)
61.15	H2	1.94E+02	5.47E-01	1.08E+01	1.23E+01	2.61E-01	1.43E+00	3.08E-02
67.53	H2	(3.68E+01)	6.37E-01	1.24E+01	1.30E+01	9.02E-01	1.89E+00	(1.97E-02)
67.53	H2	(4.15E+01)	6.50E-01	1.74E+01	1.77E+01	2.27E+00	2.83E+00	(2.15E-02)
68.21	H2	(6.23E+01)	8.54E-01	1.36E+01	1.48E+01	1.34E+00	2.58E+00	6.58E-02
69.60	H2	(5.44E+01)	6.76E-01	1.23E+01	1.32E+01	1.16E+00	2.35E+00	5.99E-02
74.99	H2	(7.02E+01)	6.60E-01	1.47E+01	1.58E+01	2.53E-01	1.60E+00	3.93E-02
77.67	H2	(3.98E+01)	6.13E-01	1.56E+01	1.83E+01	2.40E-01	1.65E+00	(1.46E-02)
78.72	H2	(7.76E+01)	6.34E-01	1.18E+01	1.47E+01	2.51E-01	1.59E+00	(1.58E-02)
85.99	H2	1.99E+02	6.03E-01	1.33E+01	1.48E+01	3.06E-01	1.76E+00	(2.68E-02)
89.39	H2	(3.16E+01)	4.90E-01	1.34E+01	1.40E+01	6.22E-01	1.93E+00	(9.99E-03)
93.99	H2	9.03E+01	5.50E-01	1.23E+01	1.31E+01	3.35E-01	1.32E+00	(1.72E-02)
98.07	H2	(6.40E+01)	5.97E-01	1.31E+01	1.46E+01	2.87E-01	1.63E+00	(1.39E-02)
101.29	H2	(2.66E+01)	5.55E-01	1.08E+01	1.16E+01	2.46E-01	1.25E+00	(1.03E-02)
102.65	CCU$_u$	(4.71E+01)	6.28E-01	1.04E+01	1.18E+01	2.63E-01	1.57E+00	(1.43E-02)
114.44	CCU$_l$	(5.66E+01)	1.22E+00	6.33E+00	1.17E+01	3.05E-01	3.98E+00	4.35E-02
114.44	CCU$_l$	(4.59E+01)	8.12E-01	1.08E+01	7.10E+00	1.09E+00	3.05E+00	4.55E-02
115.06	CCU$_l$	(4.76E+01)	8.46E-01	6.88E+00	5.93E+00	3.53E-01	3.30E+00	8.36E-02

(a) Technetium-99 data are in units of pCi/g while all others are µg/g of dry sediment.
(b) Parentheses signify values below level of quantitation but considered valid.
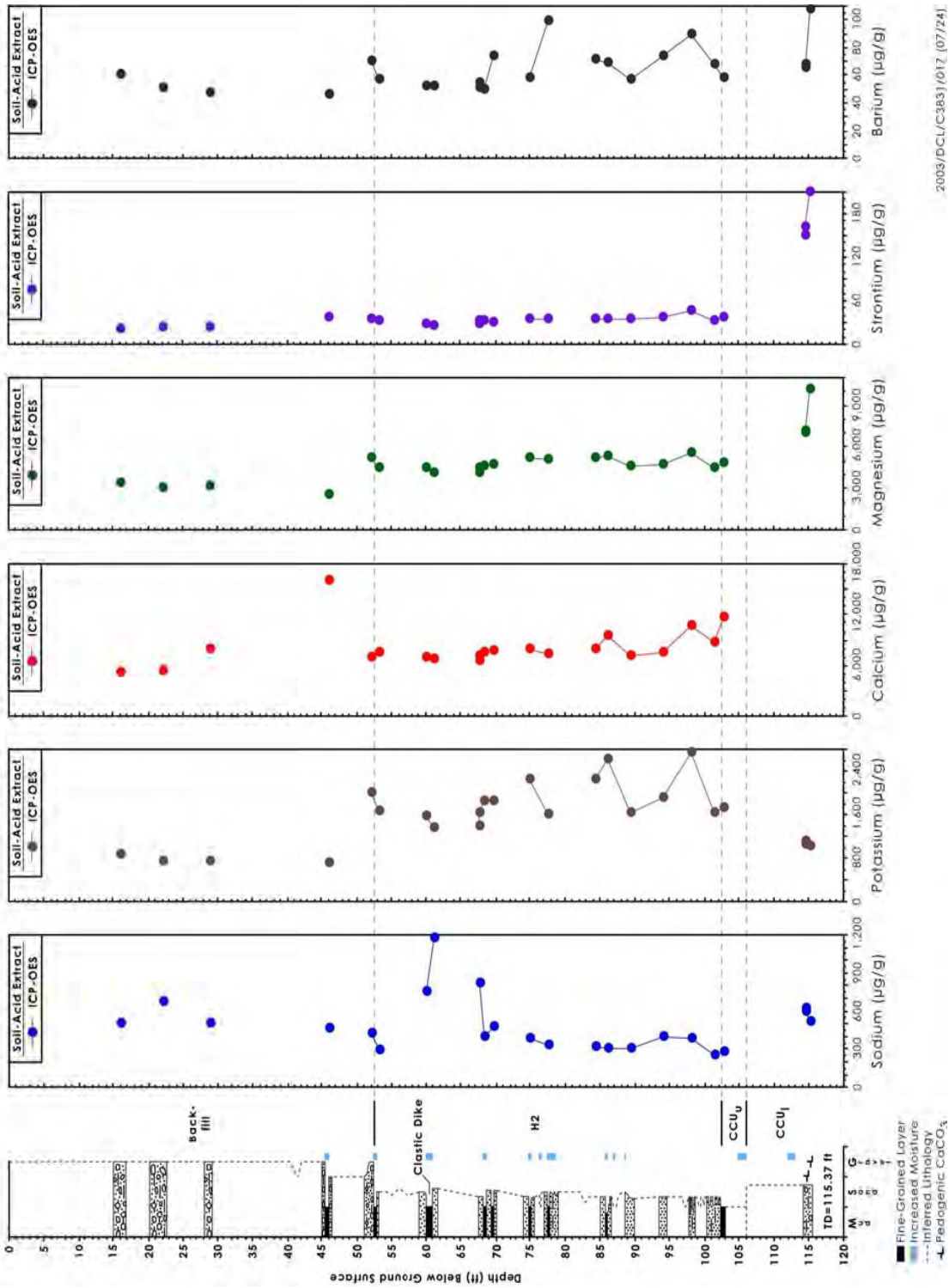
Figure 4.38. Acid-Extractable Cations in C3831 Vadose Zone Sediments (μg/g dry sediment)
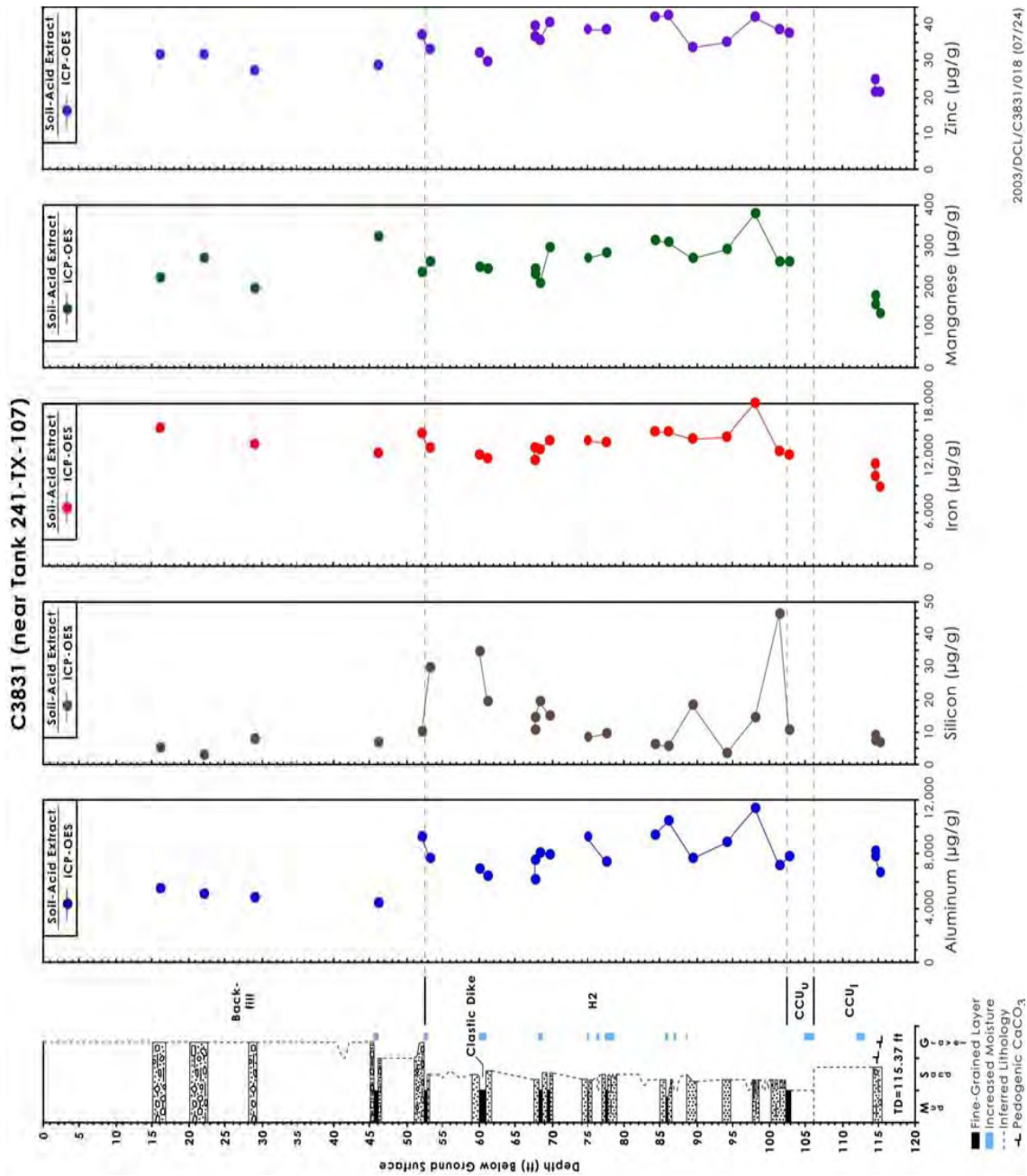
Figure 4.39. Acid-Extractable Metals in C3831 Vadose Zone Sediments (μg/g dry sediment)

4.107
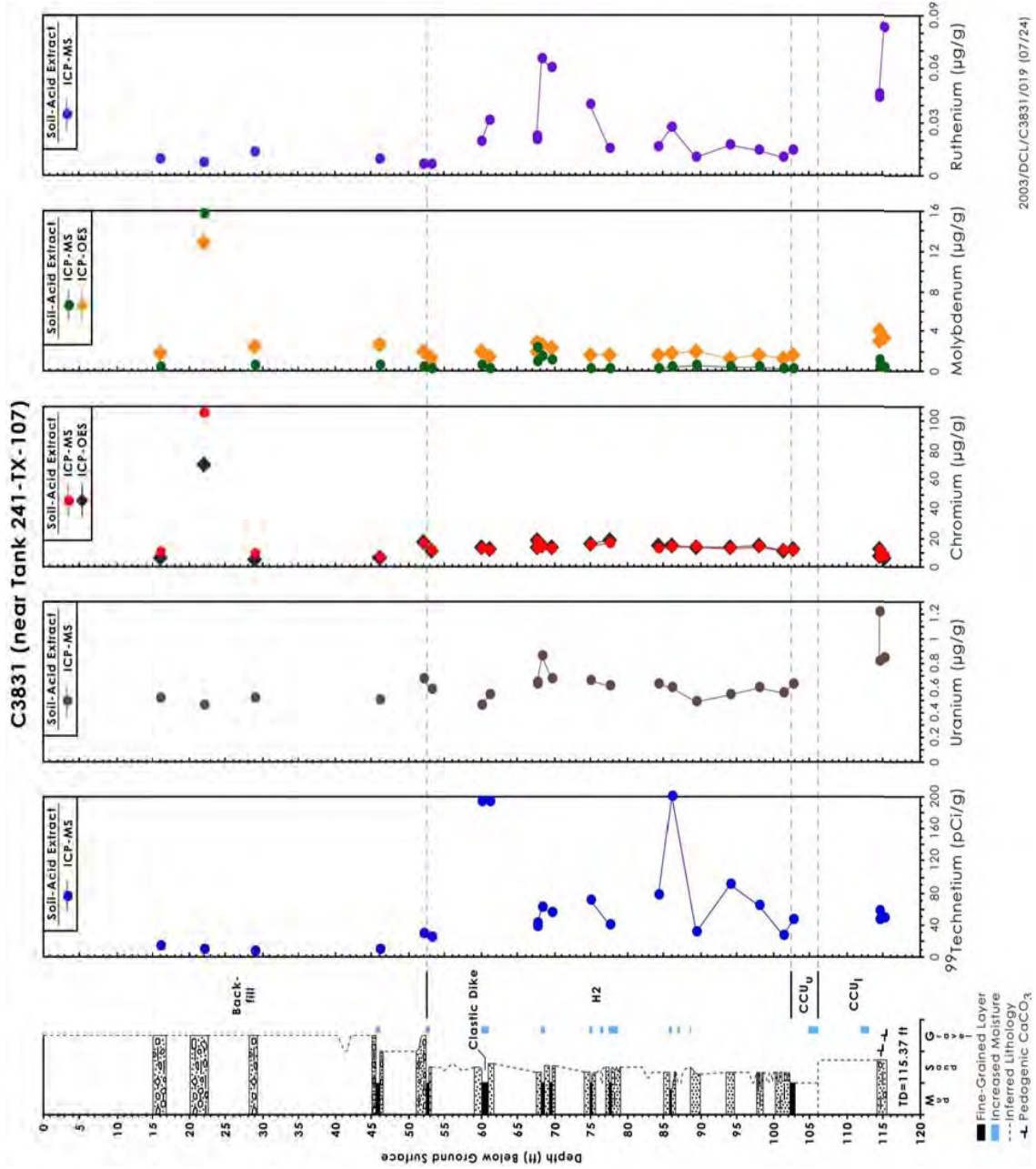
Figure 4.40. Acid-Extractable Trace Metals in C3831 Vadose Zone Sediments (units vary)

2003/DCL/C3831/019 (07/24)

4.3.5   Radionuclide Content in Vadose Zone Sediment from C3831

Aside from the technetium-99 and uranium data already presented, the lab-measured gamma emitters (see Figures 4.42 and 4.43) show natural potassium-40, natural uranium, very sporadic hits of cesium-137 and a small elevated zone of cobalt-60 between the depths of 60 and 85 ft bgs and perhaps down to the bottom of the borehole. The lab measurements of cobalt-60 show activities ranging from approximately one to a few tens of pCi/g while the continuous field log shows values of 40 to 60 pCi/g between 60 and 75 ft bgs. The field log also shows a small amount of surface cesium-137 contamination. The agreement between the field and lab-generated data for gamma emitters is good. Aside from the thin zone of cobalt-60 there are no man-made gamma emitters in the sediment profile above concentrations of a few tenths of a pCi/g excepting the near surface contamination of a few pCi/g cesium-137.

Water and acid extracts of the sediments containing cobalt-60 were performed. The amounts of cobalt-60 that were extractable are compared with the total cobalt-60 measured by direct gamma energy analysis of the sediment in Table 4.46 and Figure 4.44. In almost all cases the acid extract and direct measure of the cobalt-60 in the sediments are similar, as one would expect. The water extract data show in general that some of the cobalt-60 did not extract into the water over the ~16-hour time period allotted. However, as will be discussed in Section 6.5, the in situ desorption K_d values that can be calculated from these data are quite small, <1 mL/g, suggesting that the cobalt-60 in borehole C3831 vadose zone sediments would be fairly mobile.

Gross alpha and beta measurement were made on both the 1:1 sediment:water and sediment:acid extracts following the procedure described in Section 3.3.3.2. With knowledge of the mass of dry sediment to extraction fluid used, the data were converted to activity of gross beta and alpha leached per gram of dry sediment. None of the water or acid extracts of the 24 extracts (22 cores from selected depths and two duplicates) showed any detectable alpha activities above the detection limit of 5 to 8 pCi/g. Both the water and acid extracts contained measurable gross beta between 50 and 100 pCi/g in the sediment profile from 62 ft bgs to the bottom of the borehole. In the thin zone from 59 to 61 ft bgs the gross beta is 300 to 400 pCi/g in both the water or acid extracts. These values likely reflect the presence of both technetium-99 and cobalt-60 contamination. The technetium-99 is equally water or acid extractable. The ICP-MS measurements for both the water and acid extracts show technetium-99 concentrations between 40 and 140 pCi/g, but the water extract ICP-MS data are considered most accurate. Thus we feel that the gross beta values (between 300 and 400 pCi/g) are biased high and that 200 pCi/g is more accurate for a gross beta value in borehole C3831 vadose zone sediments.

4.3.6   Total Carbon, Calcium Carbonate, and Organic Carbon Content of Vadose Zone Sediment from Borehole C3831

The total, inorganic, and organic carbon contents of the C3831 sediments are reported in Table 4.47. The two samples of Cold Creek lower unit contain substantial amounts of caliche between 114.4 and 115.1 ft bgs. The last sample obtained before the probe met refusal has 34 wt% calcium-carbonate equivalent, essentially the same as the bottom sample obtained at borehole C3830. As found in most vadose sediments from the Hanford Reservation, there is very little (<0.1% by weight) organic carbon in the borehole C3831vadose zone sediments. The borehole C3831 backfill sample at 46.1 ft bgs also appears to have elevated inorganic carbon and some (0.4 wt%) organic carbon. Aside from this backfill sample the borehole C3831 carbon values for total, inorganic, and organic are quite similar to those at borehole C3830.
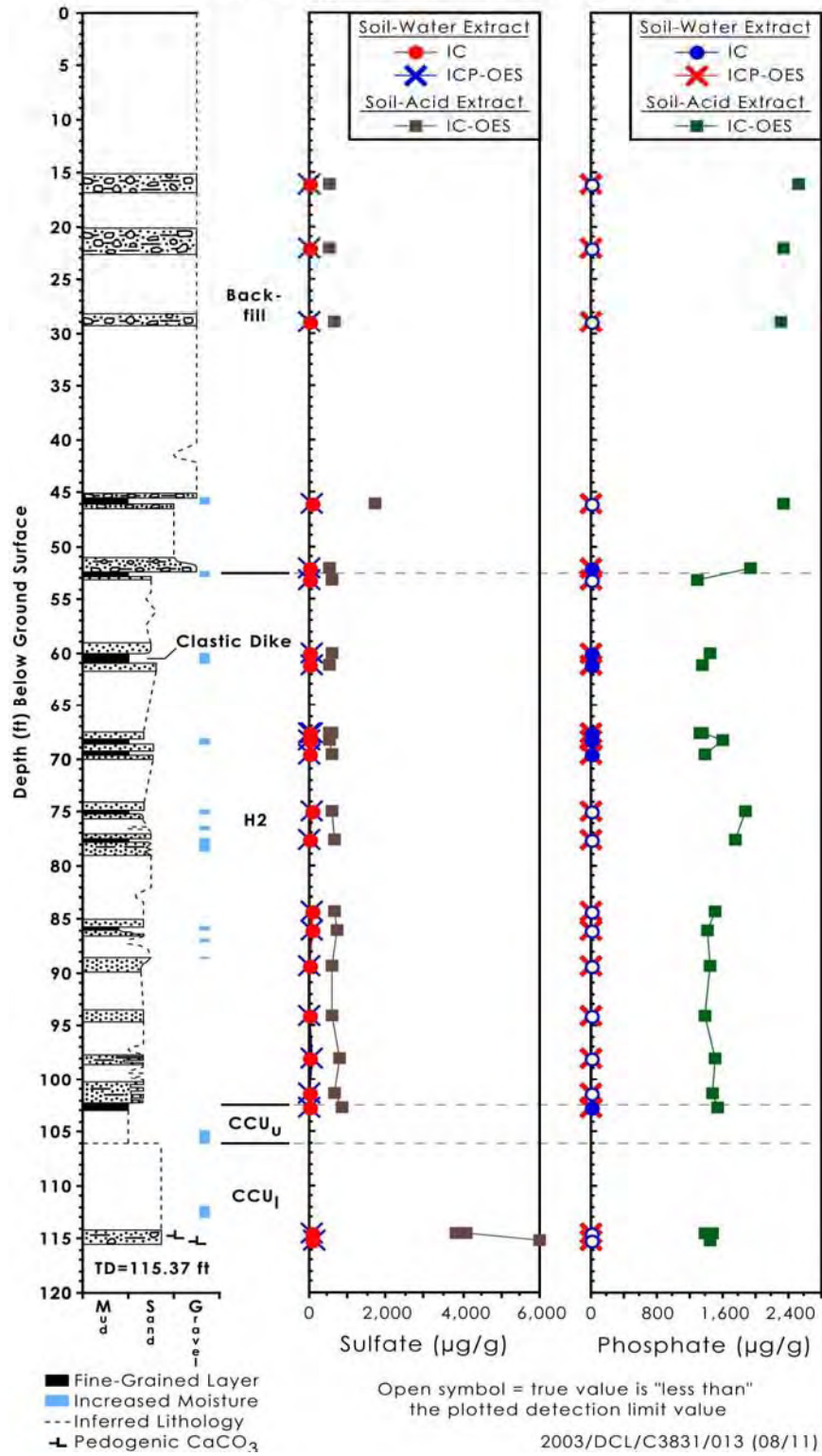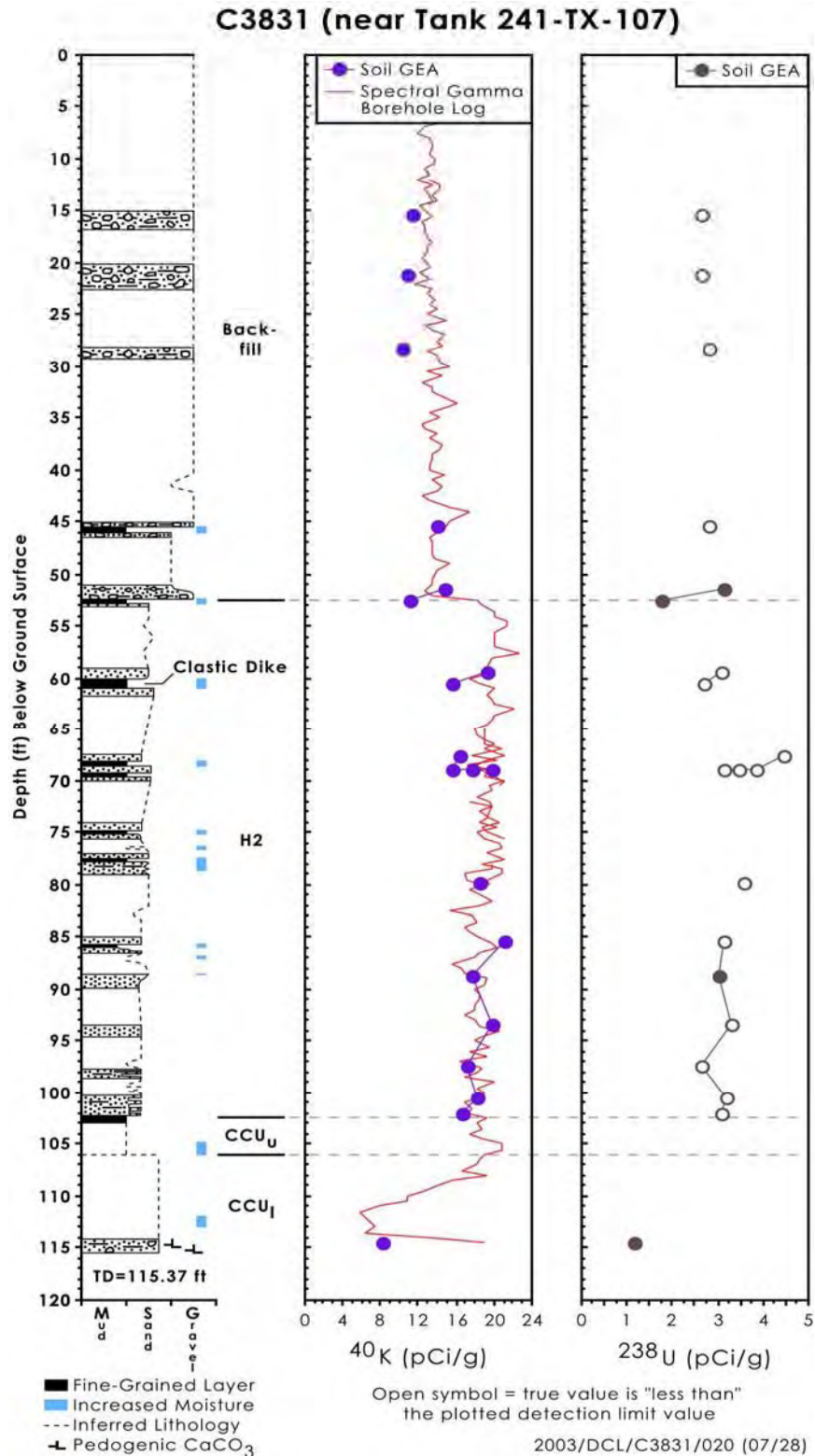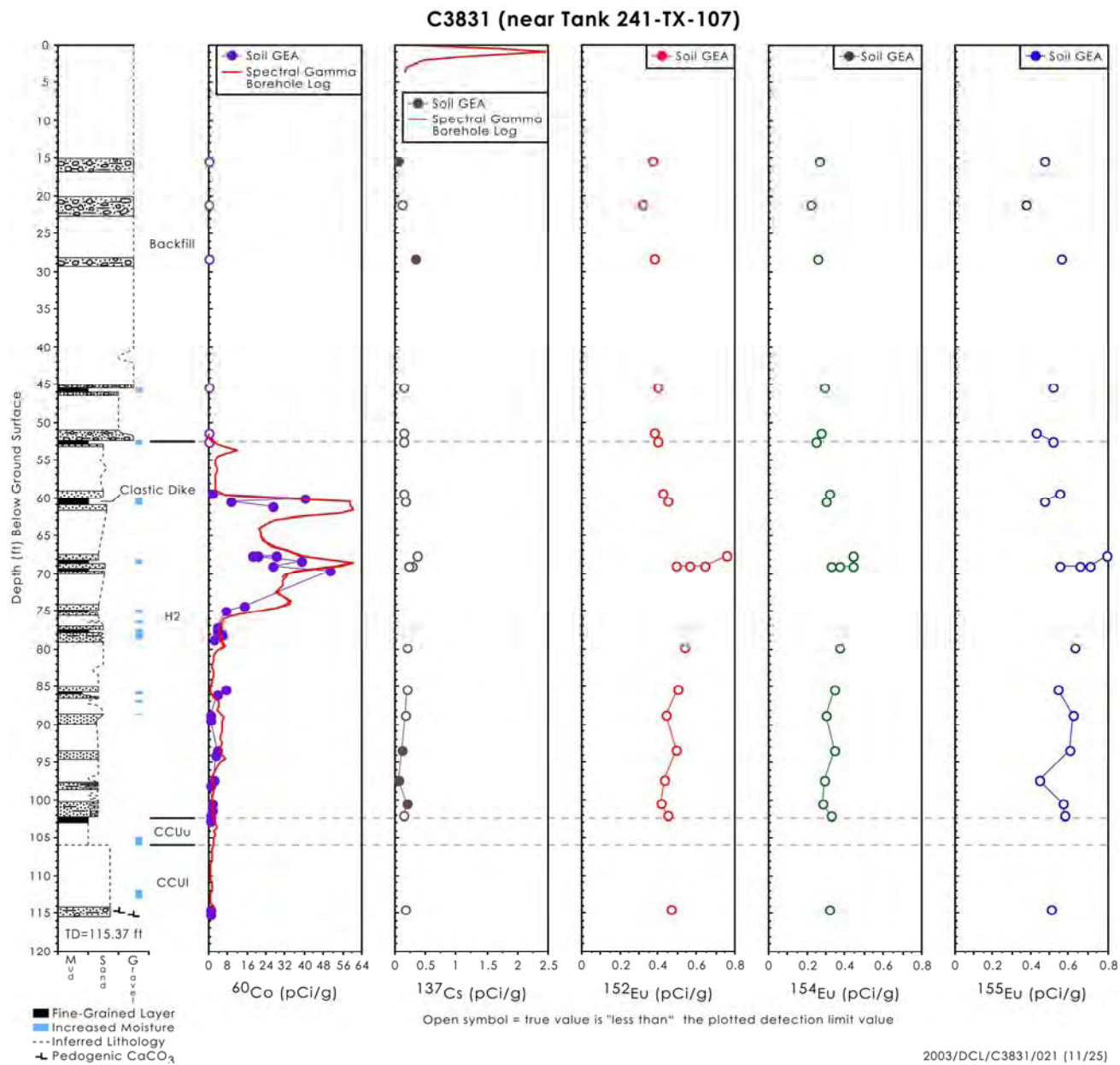
Figure 4.41. Water versus Acid-Extractable Sulfate and Phosphate in C3831 Vadose Zone Sediments

Figure 4.42. Comparison of Lab Gamma Energy Analysis (GEA) and Field Log for Natural Gamma Emitters

4.111

Figure 4.43. Lab and Field Data for Common Gamma Emitters in C3831 Vadose Zone Sediments

Table 4.46. Cobalt-60 Content of Sediment and Extracts for Vadose Zone Sediments in Borehole C3831

Sample No.	Depth (ft bgs)	Co-60 pCi/g dry sediment						
		Direct Gamma Energy Analysis			Acid Extract		Water Extract	
C3831 15B	15.28	<0.107						
C3831 15A	15.97				<3.313			
C3831 21B	21.18	<0.089						
C3831 21A	21.93				<2.185			
C3831 28B	28.28	<0.134						
C3831 28A	28.90				<2.541			
C3831 45B	45.40	<0.105						
C3831 45A	46.06				<3.653			
C3831 51B	51.35	<0.107						
C3831 51A	52.03				<3.324			
C3831 52B	52.50	<0.140						
C3831 52A	53.18				<2.660			
C3831 59B	59.34	1.521						
C3831 59A	59.94	40.120			10.418		11.075	
C3831 60B	60.44	9.356						
C3831 60A	61.15	26.713			31.288		12.115	
C3831 67B	67.53	28.124	20.230	18.618	27.398	24.499	7.690	6.269
C3831 67A	68.21	38.557			48.508		11.090	
C3831 69B	68.82	26.562						
C3831 69A	69.60	50.877			44.751		4.956	
C3831 74B	74.36	15.064						
C3831 74A	74.99	7.337			10.519		3.803	
C3831 77B	77.05	3.569						
C3831 77A	77.67	3.693			<3.431		1.320	
C3831 78B	78.08	5.631						
C3831 78A	78.72	2.068			4.347		1.127	
C3831 85B	85.37	7.165						
C3831 85A	85.99	3.647			<5.210		3.655	
C3831 88B	88.67	0.731						
C3831 88A	89.39	0.452			<2.817		<0.903	
C3831 93B	93.37	3.267						
C3831 93A	93.99	2.708			4.189		1.141	
C3831 97B	97.43	2.363						
C3831 97A	98.07	1.005			<3.663		<1.98	
C3831 100B	100.57	1.152						
C3831 100A	101.29	1.408			<2.785		0.744	
C3831 102B	101.97	0.916						
C3831 102A	102.65	0.582			<3.121		0.540	
C3831 114B	114.44	0.875	0.694	0.579	<4.325	<3.178	<2.16	<0.934
C3831 114A	115.06	0.570			<2.450		<1.550	

C3831 (near Tank 241-TX-107)
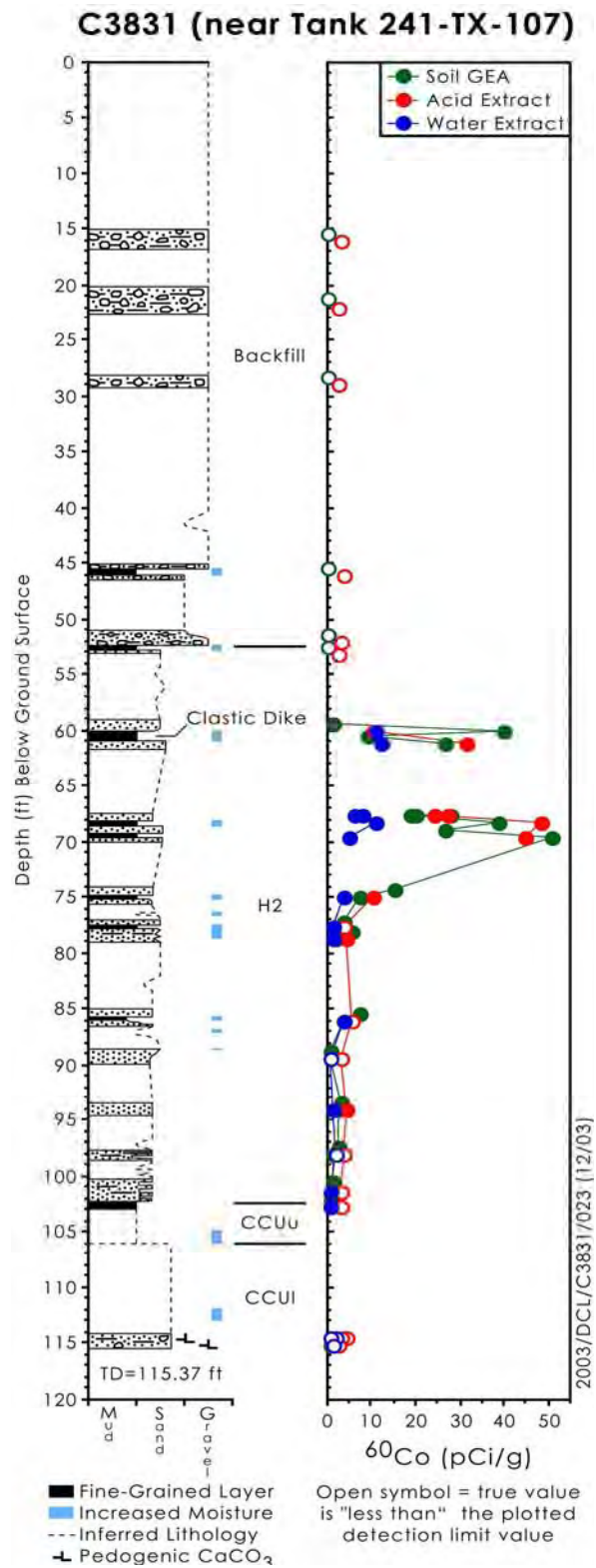
Figure 4.44. Lab Data for Cobalt-60 Extracts of C3831 Vadose Zone Sediments

Table 4.47.   Carbon Contents of Vadose Zone Sediments in Borehole C3831

Depth (ft bgs)	Stratigraphic Unit	Total Carbon %	Inorganic Carbon %	IC as CaCO₃ %	Organic Carbon %
15.97	Bkfl	0.11	0.07	0.59	0.04
21.93	Bkfl	0.13	0.11	0.91	0.02
28.90	Bkfl	0.13	0.14	1.13	0.01
46.06	Bkfl	1.63	1.23	10.26	0.40
52.03	Bkfl	0.23	0.18	1.46	0.05
53.18	H2	0.25	0.19	1.58	0.06
59.94	H2	0.23	0.19	1.58	0.04
61.15	H2	0.22	0.14	1.20	0.08
67.53	H2	0.25	0.20	1.63	0.05
67.53	H2	0.23	0.20	1.65	0.03
68.21	H2	0.25	0.18	1.51	0.07
69.60	H2	0.28	0.24	1.99	0.04
74.99	H2	0.26	0.21	1.71	0.05
77.67	H2	0.22	0.18	1.52	0.04
78.72	H2	0.25	0.21	1.73	0.04
85.99	H2	0.35	0.32	2.71	0.03
89.39	H2	0.24	0.20	1.63	0.04
93.99	H2	0.23	0.20	1.64	0.03
98.07	H2	0.30	0.24	2.00	0.06
101.29	H2	0.26	0.22	1.87	0.04
102.65	CCU$_u$	0.44	0.36	3.01	0.08
114.44*	CCU$_l$	2.14	1.95	**16.26**	0.19
114.44*	CCU$_l$	2.68	2.58	**21.50**	0.10
115.06	CCU$_l$	4.34	4.10	**34.17**	0.23

Bold type represents samples with caliche present.
*   Indicates two subsamples were taken at the same depth and analyzed.

4.4   Vadose Zone Sediment from Borehole C3832

Borehole C3832 was pushed into the vadose zone sediment approximately 20 ft south-southeast of tank TX-104 to evaluate whether there is evidence to support designating tank TX-104 as having leaked in the past. The borehole reached a depth of 115.9 ft bgs at which point driving the probe met refusal.

4.4.1   Moisture Content

The moisture content of the 38 cores liners as a function of depth and lithology are shown in Table 4.48 and Figure 2.26. The backfill samples have a mean moisture content of 7.1% by weight with significant variation and a wet zone at the very bottom at 45 ft bgs. The moisture in the backfill at C3832 is much more variable and, on average, one percent by weight wetter than the backfill sediments in borehole C3830 near tank TX-105, but is the same as the moisture content as borehole C3831 near tank TX-107 (Table 2.5). The Hanford formation H2 samples from borehole C3832 have a mean moisture content of 9.2% by weight with variation that tracks variations in particle size (finer grained samples have slightly higher moisture contents). The Hanford formation H2 sediments in borehole C3832 are on average 3.5% by weight wetter than the H2 sediments at borehole C3830 and 0.5% by weight wetter than the H2 sediments at borehole C3831. At borehole C3832, the Cold Creek upper subunit is ~10% by weight, about typical for a fine-grained sediment in the vadose zone at Hanford. The Cold Creek lower subunit (caliche) at C3832 has an average moisture content of ~11% wt, slightly less than the average for this unit at boreholes C3830 and C3831.

The average moisture content of the H2 unit samples measured in borehole C3832 is about 4.5% by weight greater than the average for the same stratigraphic unit at the uncontaminated borehole 299-W10-27. We speculate that this wetter Hanford H2 sediment is significant and an indication of the various tank farm operations (e.g., gravel cover) that encourage higher moisture infiltration.

4.4.2   1:1 Sediment:Water Extracts for Borehole C3832

The A liners from the 19 and two B liners (run in duplicate) cores were characterized after the geologic descriptions by performing 1:1 water:sediment extracts. In total, 23 separate sediment samples were characterized. The following tables and figures present the mass of a given constituent leached per gram of sediment as measured in the water extracts to allow direct comparison to the same data for the background borehole sediments from borehole 299-W10-27 and the other two boreholes. Other figures show dilution-corrected values that represent concentrations in vadose zone porewater in borehole C3832. As discussed in several other Vadose Zone Characterization Project reports, the dilution-corrected 1:1 water:sediment extracts are a reasonable derivation of the actual vadose zone porewater (see Serne et al. 2002b, 2002c, 2002d, 2002e, 2002f).

Table 4.48. Moisture Content of Borehole C3832 Cores

Sample No.	Depth (ft bgs)	Stratigraphic Unit	Lithology	Moisture Content
15B	16.56	backfill	Silty sandy gravel	4.10%
15A	17.26			5.87%
28B	28.44	backfill	Silty sandy gravel	5.22%
28A	29.14			4.47%
37B	36.44	backfill	Sandy gravel	5.07%
37A	37.14			4.62%
44B	44.49	backfill	Silty sand	15.67%
44A	45.19			10.96%
52B	51.46	H2	Sand	6.77%
52A	52.01			6.57%
53B	53.42	H2	Sand to silty sand	18.40%
53A	54.10			7.39%
61B	60.47	H2	Sand	6.78%
61A	61.17			3.75%
62B	62.16	H2	Silty sand to sand	10.87%
62A	62.96			5.19%
69B	69.34	H2	Sand to silty sand	5.76%
69A	69.99			14.74%
76B	76.34	H2	Sand to silty sand	10.14%
76B Dup	76.34			11.00%
76A	77.04			15.47%
79B	78.80	H2	Sand to silty sand/sandy silt	11.04%
79A	79.81			10.02%
83B	83.33	H2	Sand to silty sand	9.57%
83A	84.01			12.33%
87B	87.35	H2	Sand to silty sand	7.79%
87A	88.06			5.21%
93B	93.35	H2	Sand to silty sand	8.56%
93A	94.05			5.25%
96B	95.99	H2	Sand	11.74%
96A	96.69			7.81%

Table 4.48. (contd)

Sample No.	Depth (ft bgs)	Stratigraphic Unit	Lithology	Moisture Content
104B	104.30	CCU$_u$	Silty sand to silt	9.89%
104A	105.01			9.28%
110B	110.28	CCU$_u$	Silty sand	10.81%
110B Dup	110.28			11.03%
110A	111.02	CCU$_l$	Calcic pebbly muddy sand	13.67%
114B	114.13	CCU$_l$	Pebbly sandy mud	10.74%
114A	114.85			9.21%
121B	114.83	CCU$_l$	Pebbly sandy mud	9.98%
121A	115.54			10.30%

4.4.2.1   pH and Electrical Conductivity (EC)

The 1:1 sediment:water extract pH and EC data are shown in Table 4.49. Both the extract and dilution-corrected EC values are shown. Figure 4.45 shows the 1:1 sediment:water extract pH value and dilution-corrected EC as a function of depth and stratigraphy. A comparison of the data in Table 4.49 with the pH and EC of the 299-W10-27 extracts suggests evidence of slightly elevated EC starting at 63 to 84 ft bgs, and then from 97 ft bgs all the way to the bottom of the borehole at 115.5 ft bgs. In the shallower zone (63 to 83 ft bgs) at C3832, the EC of the 1:1 water extract increases to between 1.6 and 2.6 times the background sediment. Between 67.5 and 78 ft bgs, the EC is about 5 times larger than background sediment extracts. In the Cold Creek unit the EC at borehole C3832 is 2 to 4 times higher than that in background sediments. When compared to the EC at borehole C3830 (see Table 4.18) and borehole C3831 (see Table 4.33), the values at C3832 are lower in the H2 unit and slightly greater than those at C3830 in the Cold Creek units, and unequivocally lower than the EC values at borehole C3831 in both the H2 and CCU$_u$ units. The EC values at borehole C3832 are indicative of the presence of slightly saline tank-related fluids. The borehole C3832 water extract pH values are all below 8, suggesting that the tank fluids were either not strongly alkaline or that the volume of alkaline tank fluids was relatively small and readily neutralized in the sediments.

The highest values of dilution-corrected porewater EC in borehole C3832 occur in two zones, between 61 to 63 ft bgs and 110.3 to the bottom of the hole at 115.5 ft bgs. The dilution-corrected EC values for these two zones are equivalent to a pore solution of 0.042 and 0.051 M KCl, the salt solution used to calibrate the conductivity cell. The leaks near the SX108-109 and BX-102 tanks had peak vadose zone porewater concentrations that were equivalent to much more concentrated waste fluids, 7 to 17 and 0.7 to 1 M KCl solutions, respectively. The maximum dilution-corrected EC at borehole C3832 in the H2 unit is 4.54 mS/cm, lower than the dilution-corrected EC at borehole C3830 (12.5 mS/cm) and 299-E33-46 near tank B-110 that contained 15.1 mS/cm. The highest dilution-corrected EC at borehole C3832 occurs in the CCU$_l$ unit with a value of 6.27 mS/cm.

As shown in Figure 4.45, the dissolved salts are locally high in sodium and nitrate. The sodium peak value occurs at 63 ft bgs at a value of 0.04 M and the nitrate peak value is at the contact (110.4 ft bgs) between the upper Cold Creek mud subunit and the lower Cold Creek (caliche) subunit with a value of 0.015 M.

Table 4.49. pH and EC Data for Sediment-Water Extracts from Borehole 3832

Sample No.	Depth (ft bgs)	Stratigraphic Unit	pH	Conductivity mS/cm	Dilution-Corrected Porewater (mS/cm)
15A	17.26	backfill	7.24	0.150	2.557
28A	29.14	backfill	7.30	0.160	3.577
37A	37.14	backfill	7.36	0.185	4.008
44A	45.19	backfill	7.50	0.217	1.982
52A	52.01	H2	7.42	0.167	2.547
53A	54.10	H2	7.49	0.175	2.409
61A	61.17	H2	7.48	0.161	4.304
62A	62.96	H2	7.70	0.235	4.537
69A	69.99	H2	7.69	0.232	1.576
76B	76.34	H2	7.72	0.391	3.864
76B Dup	76.34	H2	7.92	0.387	3.519
76A	77.04	H2	7.52	0.384	2.484
79A	79.81	H2	7.44	0.245	2.449
83A	84.01	H2	7.37	0.246	1.994
87A	88.06	H2	7.44	0.161	3.097
93A	94.05	H2	7.52	0.173	3.491
96A	96.69	H2	7.51	0.226	2.895
104A	105.01	CCU$_u$	7.46	0.289	3.346
110B	110.28	CCU$_u$	7.55	0.478	4.422
110B Dup	110.28		7.59	0.574	5.213
110A	111.02	CCU$_l$	7.48	0.671	4.920
114A	114.85	CCU$_l$	7.51	0.578	6.273
121A	115.54	CCU$_l$	7.64	0.555	5.389
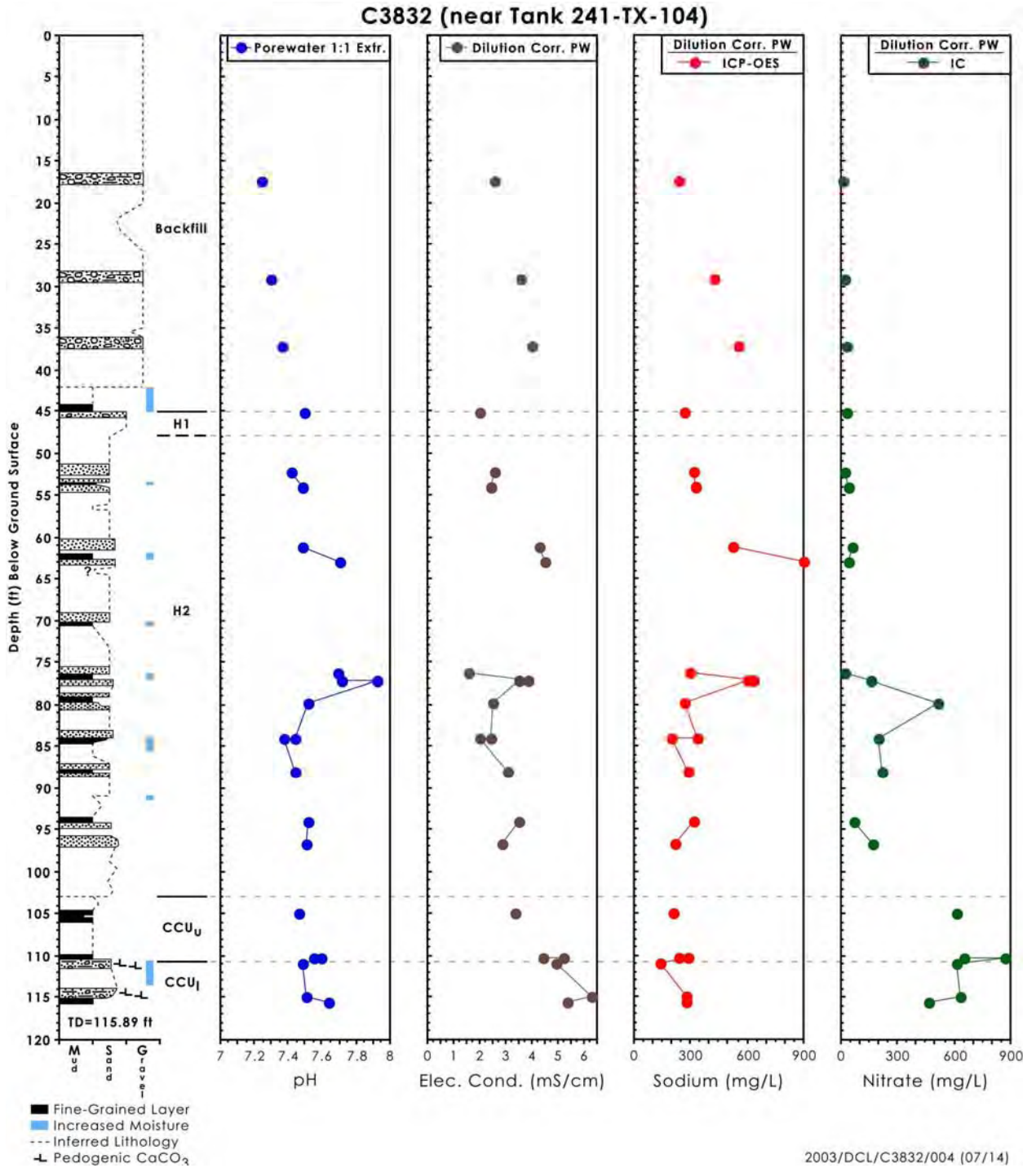
Figure 4.45. Borehole 3832 Sediment-to-Water Extract pH and Calculated Porewater EC, Sodium, and Nitrate

4.4.2.2   Water Extract Composition or the 1:1 Sediment:Water Extract for Borehole C3832

The water extract values for the major cations and anions and several trace constituents are discussed in this section. The anion data are tabulated in Tables 4.50 and 4.51 and Figure 4.46 in units of mass per gram of dry sediment. The data for the water extracts of borehole C3832 for fluoride are elevated slightly in comparison to the background sediment at 299-W10-27 and borehole C3830 but almost a factor of 10 lower than at borehole C3831. The chloride concentrations in the borehole C3832 sediments are elevated in two zones, between 76 to 77 and 105 to 111 ft bgs, by a factor of 10 to 20 times larger than the background sediment. The water-extractable chloride concentrations in C3832 are quite similar to the chloride in borehole C3830 sediments and both are significantly less than the water-extractable chloride in borehole C3831 sediments. The nitrate water extract values for borehole C3832 are elevated compared to the background sediments from 76 ft bgs to the deepest sample obtained except the sample at 94 ft bgs. The nitrate water extract values are 20 to 30 times larger than for the background sediments at 77 ft bgs and between the depths of 105 and 111 ft bgs. The nitrate concentrations in the borehole C3832 are the same as those at borehole C3830 in the H2 sediments down to 97 ft bgs, but higher than the C3830 sediments below 97 ft bgs. Both C3832 and C3830 sediments contain ~5 to 10 times less nitrate than those in borehole C3831. The sulfate water extracts from borehole C3832 are elevated from about 76 ft bgs to the deepest sample obtained and the values exceed the background sediment values by a factor of 3 to 10. The water-extractable sulfate values for sediments from borehole C3832 are similar to those in borehole C3830 in the shallow H2 impacted zone but slightly larger in the sediments below 97 ft bgs than the water-extractable sulfate in borehole C3830. Borehole C3831 water-extractable sulfate values are ~ 2 times larger than those at the other two boreholes.

There is also above background water-extractable phosphate (at one depth 76.34 ft bgs) and nitrite (in two zones (77 to 84 ft bgs and 110.3 to the bottom of the borehole at 115.5 ft bgs) in borehole C3832. The agreement between measuring the water extracts for phosphate and sulfate directly with the ion chromatograph and indirectly by converting the ICP measurements for phosphorous and sulfur are very good (see Figure 4.46). Besides validating the ion chromatography data, we can state that the water-extractable sulfur and phosphorous species exist as sulfate and phosphate.

The water-extractable small organic molecules in the C3832 borehole sediments are shown in Table 4.51. Several samples have values that appear to be slightly elevated over background sediments and for sediments at the other two boreholes, excepting one sample at 61.15 bgs at C3831. The values in C3832 sediments that appear elevated are noted in bold type in Table 4.51. None of the values are above 10 ppm and we do not have enough data on water-extractable formate, acetate, or oxalate from Hanford Area sediments to form conclusions as to whether these values indicate that any organics were present in tank fluid and still persist today in the vadose zone. Note that one of the sample 76 replicates has significantly greater organic concentrations than its mate. Whether this signifies analytical vagaries or true sample heterogeneity is unknown.

The water-extractable major cations in the borehole C3832 sediments are tabulated in Table 4.52 and the distribution with depth is shown in Figure 4.47. The distribution of the divalent alkaline earth cations (Mg, Ca, and Sr but not Ba) shows low water-extractable quantities between 63 and 97 ft bgs excepting the sample at 77 ft bgs. High divalent cation water extracts are found below in the Cold Creek unit. Conversely, the distribution of water-extractable sodium is elevated between the depths of 63 and 77 bgs. The water-extractable sodium values in borehole C3832 sediments are higher than the values in the uncontaminated sediments from borehole 299-W10-27 over the whole borehole profile, even in the

backfill above the tank. These trends suggest that tank fluids that contained sodium did seep into the vadose zone near this borehole. The sodium displaced the natural divalent cations and some of the natural potassium off the sediment cation exchange sites in the sediments between 63 and at least 76 if not all the way to the bottom of the H2 unit at 102 ft bgs. We have observed the same cation distribution and ion exchange fronts where divalent cations and sometimes potassium are depleted and high levels of water-extractable sodium are present in the shallow sediments at both the SX and BX tank farms, where tank fluids have been confirmed as being present (for details, see Serne et al. 2002b, 2002c, 2002d, 2002e, 2002f). Right below the leading edge of the sodium plume one finds elevated levels of divalent cations that were displaced. We observe the highest levels of water-extractable divalent cations in the C3832 samples below the Hanford formation Cold Creek unit contact to the bottom of the borehole. At borehole C3832, the water-extractable magnesium, calcium, strontium, potassium, and sodium in the sediments in both Cold Creek units (from 105 ft bgs to the bottom of the borehole) are larger than for the background sediment in borehole 299-W10-27 and also borehole C3830 sediments by a factor of 2 to 5. This likely is an indication that a larger volume of tank fluids passed through the C3832 sediments from 75 ft bgs to the bottom of the borehole than passed through the vadose zone at borehole 3830. There is no clear indication that tank fluids descended vertically from the tank bottom to 75 ft bgs at borehole C3832. The data for the available samples suggests that tank fluids migrated horizontally at ~ 75 ft into the sediments intercepted by borehole C3832 and then descended vertically.

It is odd that the water-extractable sodium values but not the water-extractable nitrate values are higher in the borehole C3830 and C3832 backfill sediments. Generally, Hanford waste streams are elevated in both constituents. The vadose zone sediment profiles for boreholes C3830 and C3832 may reflect that there were surface spills of waste that had the mobile nitrate pushed deeper by natural recharge. There is evidence of some surface spillage at these two boreholes based on the cesium-137 distribution measured by the field logging activities. The sediment water extract profiles also suggest that there were some tank-related fluids introduced at depths near 55 to 65 ft bgs, somewhat below the depths of the tank bottoms.

Table 4.50. Water-Extractable Anions in Borehole C3832 Vadose Zone Sediments (µg/g dry sediment)

Sample No.	Depth (ft bgs)	Stratigraphic Unit	Fluoride	Chloride	Nitrate	CO_3	Sulfate	Phosphate	Nitrite	Bromide
15A	17.26	backfill	0.65	0.3	0.43	78.47	3.56	<0.240	<0.080	<0.137
28A	29.14	backfill	0.85	0.6	1.02	49.88	4.2	0.25	<0.080	<0.137
37A	37.14	backfill	0.8	0.21	1.63	50.44	7.67	0.46	<0.080	<0.137
44A	45.19	backfill	1.04	0.72	3.2	60.90	6.79	0.45	<0.080	<0.137
52A	52.01	H2	1.22	2.68	1.28	48.55	8.31	<0.240	<0.080	<0.137
53A	54.10	H2	0.96	0.6	3.13	46.38	7.61	0.18	<0.081	<0.139
61A	61.17	H2	0.32	0.95	2.33	39.04	10.22	<0.240	<0.080	<0.137
62A	62.96	H2	0.52	0.78	1.85	58.03	9.03	0.45	<0.080	<0.137
69A	69.99	H2	0.96	0.49	2.62	63.28	8.3	0.45	<0.080	<0.137
76B	76.34	H2	1.05	6.64	14.6	21.40	28.38	0.87	<0.080	<0.137
76B Dup	76.34	H2	1.53	7.94	21.08	73.84	27.51	0.39	<0.080	<0.137
76A	77.04	H2	0.52	4.91	79.04	66.54	40.7	0.24	0.66	<0.137
79A	79.81	H2	0.61	2.3	19.42	2.38	21.53	<0.240	0.12	<0.137
83A	84.01	H2	0.46	3.32	25.12	2.37	21.38	<0.240	0.11	<0.137
87A	88.06	H2	0.36	0.72	11.39	35.21	8.94	<0.240	<0.080	<0.137
93A	94.05	H2	0.55	0.69	3.93	42.33	15.74	<0.254	<0.085	<0.145
96A	96.69	H2	0.47	2.02	13.25	38.96	27.25	<0.240	<0.080	<0.137
104A	105.01	CCU_u	0.33	7.29	57.27	36.26	75.57	<0.258	<0.086	<0.147
110B	110.28	CCU_u	0.35	9.39	72.48	41.42	78.14	<0.240	0.14	<0.137
110B Dup	110.28		0.44	13.59	97.36	45.62	81.17	<0.240	0.1	<0.137
110A	111.02	CCU_l	0.49	12.31	84.18	44.67	170.92	<0.240	0.3	0.14
114A	114.85	CCU_l	0.94	5.4	58.84	32.31	160.83	<0.240	0.26	<0.137
121A	115.54	CCU_l	0.92	8.13	48.09	2.38	130.34	0.31	1.09	0.14
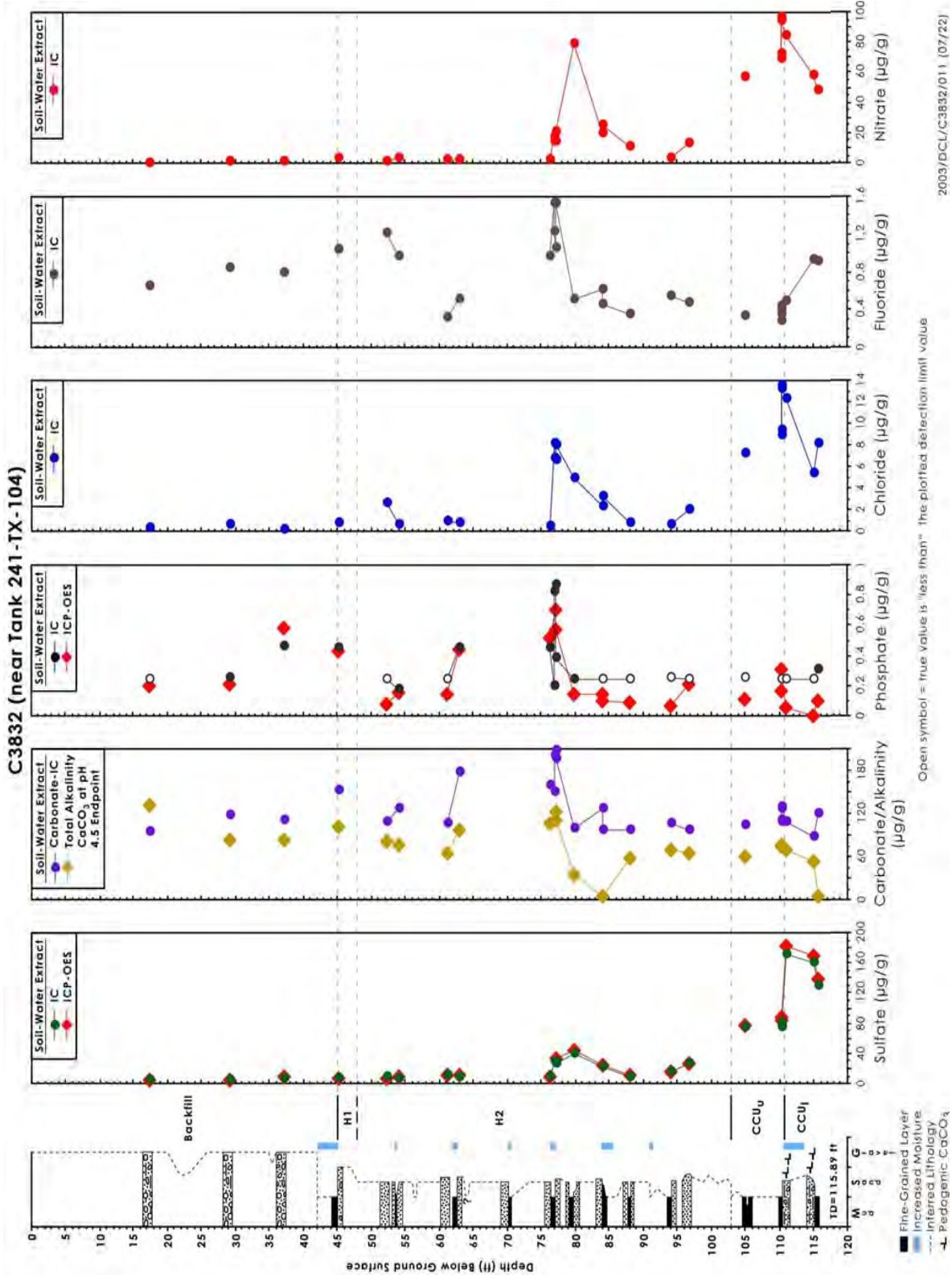
Figure 4.46. C3832 Borehole Water-Extractable Anions (μg/g dry sediment)

The water-extractable aluminum, silicon, iron, manganese, zinc, phosphorous, and sulfur in the C3832 borehole sediments are shown in Table 4.53 and Figure 4.48. The phosphorous and sulfur data were converted to water-extractable phosphate and sulfate and plotted with the anion data in Figure 4.46. In general, the agreement between direct measurement of the two anions by ion chromatography and the converted ICP measurements of water-extractable phosphorous and sulfur are very good. The borehole C3832 water-soluble aluminum data show elevated values between the depths of 63 and 76.3 ft bgs and the water-soluble iron is high at 70 ft bgs. We speculate that these elevated values indicate some chemical reaction between tank fluids and native sediments that formed precipitates of aluminum and iron that are more water soluble than the natural aluminum and iron phases present in the native sediments. In this zone at borehole C3832, the water-extractable aluminum is very similar to the values at borehole C3830 but both are significantly lower than the water-soluble aluminum concentrations at borehole C3831. The water-extractable iron at 70 ft bgs in borehole C3832 is larger than at C3830 and both are lower than at borehole C3831. The water-extractable zinc values at 76.34 ft bgs and from 105 ft bgs to the bottom of borehole C3832 appear to be larger than at borehole C3830 and about the same as at borehole C3831. The water-extractable sulfur values in borehole C3832 in the 76 to 84 ft bgs zone do not differ much from those at borehole C3830 but both boreholes show elevated water-soluble sulfate in comparison to sulfur that is water extractable from background sediments. At borehole C3832 the water-soluble sulfate from 97 ft bgs to the bottom of the borehole is larger than at boreholes C3830 and C3831. This suggests that more sulfate-bearing waste leaked into the Cold Creek units at borehole C3832 than at borehole C3830. The water-extractable phosphorous at borehole C3832 between the depths of 63 and 76.3 ft bgs is greater than at borehole C3830 and the background sediment by a factor of 5 and 10, respectively.

The water-extractable data for potentially mobile metals such as technetium-99, uranium-238, chromium, molybdenum, and ruthenium in borehole C3832 sediments are shown in Table 4.54 and Figure 4.49. In borehole C3832 sediments, technetium-99 is present between 76.34 ft bgs and the bottom of the borehole at 115.54 ft bgs. The concentrations are similar to those found at borehole C3830 and are in the range of 2 to 12 pCi/g. The water-extractable technetium-99 data for borehole C3830 and C3832 sediments below 70 ft bgs are about a factor five lower than for sediments at C3831. In borehole C3831 there is a thin zone along a clastic dike with 140 pCi/g water soluble technetium-99. The technetium-99 water extract data for boreholes C3831 and C3832 may have come from the same source, perhaps a leak from tank TX-107 that becomes diluted as the plume traveled towards borehole C3832. The cobalt-60 content of the sediments at these two boreholes (to be discussed below) also suggests that the vadose zone plume at boreholes C3831 and C3832 may be related.

There is also elevated water-soluble uranium-238 in borehole C3832 sediment between 75 and 110.3 ft bgs, the contact between the Cold Creek mud and caliche units. The water-soluble uranium concentrations are significantly larger in the C3832 sediments than the C3830 and C3831 sediments, excepting the one elevated sample at borehole C3830 at depth 67 ft bgs. The water-extractable uranium concentrations in borehole C3831 and C3832 do not follow the same trends (C3832 data appearing diluted compared to C3831 data) as found for water-extractable technetium-99 and total cobalt-60.

The water-extractable molybdenum values for borehole C3832 below the tank bottom are 2 to 3 times larger than at borehole C3830 but only half the values at borehole C3831. Water-leachable ruthenium values (mostly at the detection limit) are about a factor of 10 larger at borehole C3832 than at the other two boreholes. The reported detection limit, however, is about 10 times less sensitive than the detection limit for data on the other two boreholes so we suspect that the instrument was not operating at its optimal

level. Higher concentrations of water-extractable molybdenum and ruthenium data for borehole C3832 are observed from the shallowest samples in the backfill to the bottom of the borehole. We suspect artifacts in the ICP-MS performance on the day these samples were analyzed compromised the data as opposed to suggesting that surface contamination was pushed throughout the backfill to comingle coincidently with a true tank leak fluids that migrated all the way to the bottom of the borehole.

In summary, the maximum water-soluble technetium-99 concentrations at borehole C3832 occur in the lower Cold Creek subunits between 110 and 115 ft bgs at 10 to 12 pCi/g. Shallower, between 76 and 105 ft bgs, the technetium-99 varies between 2 to 7 pCi/g. The maximum water-soluble uranium concentrations are in the Cold Creek subunit with a concentration of 3 µg/g. The maximum water-soluble chromium concentration is 0.03 µg/g in the sediment between 77 and 84 ft bgs. Above and below this zone, water-soluble chromium is present at concentrations at least 10 times less.

Table 4.51.   Water-Extractable Organics in C3832 Vadose Zone Sediments (µg/g)

Depth (ft bgs)	Stratigraphic Unit	Formate	Acetate	Oxalate
15A	17.26	<0.113	0.32	0.42
28A	29.14	0.16	0.49	0.47
37A	37.14	<0.113	0.34	0.41
44A	45.19	0.13	0.42	0.2
52A	52.01	**8.42**	0.78	0.97
53A	54.10	<0.115	0.45	0.28
61A	61.17	0.09	0.38	0.14
62A	62.96	0.08	**2.3**	0.3
69A	69.99	<0.113	0.82	0.3
76B	76.34	<0.113	<0.160	**2.52**
76B Dup	76.34	**2.1**	**2.25**	**1.56**
76A	77.04	<0.113	0.77	0.44
79A	79.81	<0.113	0.44	<0.214
83A	84.01	<0.113	0.9	<0.214
87A	88.06	<0.113	0.53	<0.214
93A	94.05	0.1	0.36	<0.227
96A	96.69	<0.113	0.32	0.23
104A	105.01	<0.121	<0.172	0.37
110B	110.28	**0.86**	0.56	0.66
110B Dup	110.28	**3.35**	0.65	**1**
110A	111.02	**1.43**	1.15	**0.58**
114A	114.85	**0.37**	1.12	**1.19**
121A	115.54	<0.113	0.32	**1.62**
Values in bold type are high relative to values extracted from background sediments.				

Table 4.52. Water-Extractable Cations in C3832 Borehole Vadose Zone Sediments (μg/g dry sediment)

Sample No.	Depth (ft bgs)	Stratigraphic Unit	Mg	Ca	Sr	Ba	Na	K
15A	17.26	backfill	1.53	7.61	3.66E-02	3.31E-02	14.05	4.89
28A	29.14	backfill	1.37	6.38	3.12E-02	2.35E-02	19.18	5.28
37A	37.14	backfill	1.60	5.41	2.51E-02	2.61E-02	25.85	5.27
44A	45.19	backfill	3.37	5.86	3.60E-02	3.81E-02	29.38	4.80
52A	52.01	H2	1.49	6.29	3.35E-02	3.14E-02	21.05	6.00
53A	54.10	H2	1.59	5.06	3.12E-02	1.78E-02	24.37	5.89
61A	61.17	H2	1.49	5.50	2.98E-02	2.23E-02	19.86	4.04
62A	62.96	H2	0.28	1.13	(4.61E-03)	1.18E-02	46.65	2.84
69A	69.99	H2	0.53	2.23	(1.10E-02)	1.87E-02	44.51	3.82
76B	76.34	H2	2.17	7.19	4.78E-02	3.17E-02	64.32	15.08
76B Dup	76.34	H2	1.55	4.90	3.40E-02	4.68E-02	66.81	15.10
76A	77.04	H2	4.13	17.14	8.98E-02	2.04E-02	42.05	8.73
79A	79.81	H2	1.81	7.24	3.65E-02	2.48E-02	33.64	6.21
83A	84.01	H2	2.45	12.44	6.10E-02	(1.11E-02)	24.19	7.33
87A	88.06	H2	1.82	7.82	3.83E-02	1.49E-02	15.11	4.34
93A	94.05	H2	2.01	8.93	4.36E-02	2.61E-02	16.82	5.39
96A	96.69	H2	2.89	12.70	6.18E-02	2.56E-02	16.96	5.53
104A	105.01	CCU$_u$	8.31	38.01	1.82E-01	3.21E-02	19.40	7.95
110B	110.28	CCU$_u$	9.54	38.98	2.07E-01	4.75E-02	25.74	12.89
110B Dup	110.28		11.55	44.64	2.48E-01	6.37E-02	31.58	21.09
110A	111.02	CCU$_l$	14.93	76.29	3.30E-01	5.27E-02	18.64	8.76
114A	114.85	CCU$_l$	15.22	51.64	3.69E-01	4.43E-02	25.64	9.12
121A	115.54	CCU$_l$	13.92	44.71	2.97E-01	4.88E-02	28.57	18.67

Values in bold type are high and in blue italic type low relative to values extracted from background sediments.

Table 4.53. Water-Extractable Concentrations of Other Metals in C3832 Vadose Zone Sediments (µg/g dry sediment)

Sample No.	Depth (ft bgs)	Stratigraphic Unit	Al	Si	Fe	Mn	Zn	P as PO_4	S as SO_4
15A	17.26	backfill	3.22E-02	12.82	(1.60E-02)[a]	(8.77E-04)	7.24E-02	(1.98E-01)	4.57
28A	29.14	backfill	3.90E-02	12.18	(1.43E-02)	(2.02E-03)	5.88E-02	(2.06E-01)	5.32
37A	37.14	backfill	**2.82E-01**	14.54	**3.97E-01**	(1.14E-02)	6.36E-02	**5.89E-01**	8.82
44A	45.19	backfill	3.17E-02	20.49	(1.79E-02)	(2.48E-03)	6.29E-02	4.33E-01	7.68
52A	52.01	H2	4.66E-02	10.35	(3.36E-02)	(1.91E-03)	6.44E-02	(8.17E-02)	7.20
53A	54.10	H2	5.52E-02	10.72	**9.02E-02**	(1.21E-03)	5.82E-02	(1.57E-01)	8.61
61A	61.17	H2	4.67E-02	9.72	(2.81E-02)	(6.31E-03)	6.53E-02	(1.40E-01)	11.61
62A	62.96	H2	**8.68E-02**	10.57	(2.96E-02)	(6.31E-03)	5.80E-02	**4.38E-01**	10.14
69A	69.99	H2	**6.09E-02**	10.99	**(1.23E-01)**	(6.31E-03)	6.50E-02	**5.18E-01**	9.58
76B	76.34	H2	**9.50E-02**	*8.45*	(2.80E-02)	(6.32E-03)	**2.64E-01**	**6.99E-01**	**32.48**
76B Dup	76.34	H2	**9.26E-02**	*8.56*	(1.99E-02)	(6.39E-03)	**1.69E-01**	**5.70E-01**	**33.01**
76A	77.04	H2	3.34E-02	*9.75*	(2.22E-02)	(3.26E-03)	6.23E-02	(1.39E-01)	**44.75**
79A	79.81	H2	3.68E-02	11.11	(4.44E-02)	(6.31E-03)	6.91E-02	(1.46E-01)	**24.19**
83A	84.01	H2	3.13E-02	10.66	1.45E-01	(2.97E-03)	5.88E-02	(9.95E-02)	**25.49**
87A	88.06	H2	3.52E-02	11.79	(1.50E-02)	(6.31E-03)	6.57E-02	(8.78E-02)	10.20
93A	94.05	H2	3.56E-02	14.12	(1.57E-02)	(6.68E-03)	6.05E-02	(6.35E-02)	16.63
96A	96.69	H2	(1.87E-02)	12.53	(7.54E-03)	(6.30E-03)	6.26E-02	(2.04E-01)	**27.39**
104A	105.01	CCU_u	(3.51E-03)	11.52	(5.22E-03)	(6.77E-03)	**6.12E-02**	(1.13E-01)	**76.22**
110B	110.28	CCU_u	(1.84E-02)	*9.41*	**(2.77E-02)**	**(1.18E-02)**	**6.38E-02**	(1.64E-01)	**83.54**
110B Dup	110.28		(1.74E-02)	*8.40*	(4.48E-03)	(6.31E-03)	**6.47E-02**	(3.05E-01)	**88.87**
110A	111.02	CCU_l	(3.33E-03)	13.02	(5.26E-03)	(9.90E-03)	**6.62E-02**	(5.98E-02)	**182.21**
114A	114.85	CCU_l	(2.85E-03)	26.82	(1.45E-03)	(6.30E-03)	**6.15E-02**	(2.81E-03)	**169.58**
121A	115.54	CCU_l	(1.16E-02)	18.13	(2.24E-03)	(7.55E-03)	**5.91E-02**	(1.04E-01)	**137.65**

(a) Parentheses signify values below level of quantitation but considered valid.
Values in bold type are high and in blue italic type are low relative to values extracted from background sediments.

Table 4.54. Water-Extractable Concentrations of Mobile Metals in C3832 Vadose Sediments (µg/g dry sediment)

Sample No.	Depth (ft bgs)	Stratigraphic Unit	Tc-99[a]	U-238	Cr	Mo (ICP-MS)	Mo (ICP)	Ru
15A	17.26	backfill	(0.00E+00)[b]	1.70E-03	(1.29E-04)	1.15E-02[c]	(9.63E-03)	<5.00E-04
28A	29.14	backfill	<8.48E-01	9.88E-04	(1.45E-04)	1.45E-02	(1.20E-02)	<5.00E-04
37A	37.14	backfill	<8.49E-01	2.24E-03	5.15E-04	1.26E-02	(9.47E-03)	<5.01E-04
44A	45.19	backfill	<8.49E-01	4.81E-03	(4.98E-04)	2.44E-02	(2.12E-02)	<5.01E-04
52A	52.01	H2	<8.49E-01	8.77E-04	(3.58E-04)	1.68E-02	(1.39E-02)	<5.01E-04
53A	54.10	H2	<8.62E-01	4.44E-03	(4.27E-04)	2.58E-02	(2.24E-02)	<5.08E-04
61A	61.17	H2	<8.50E-01	1.72E-02	(4.93E-04)	1.43E-02	(1.16E-02)	<5.01E-04
62A	62.96	H2	(0.00E+00)	1.46E-01	5.48E-04	2.09E-02	(1.67E-02)	<5.01E-04
69A	69.99	H2	(1.87E-01)	1.81E+00	1.36E-03	9.40E-02	8.31E-02	<5.01E-04
76B	76.34	H2	2.35E+00	2.82E-01	1.21E-03	5.65E-02	5.12E-02	(2.91E-05)
76B Dup	76.34	H2	2.29E+00	1.32E-01	7.49E-04	6.08E-02	5.46E-02	<5.00E-04
76A	77.04	H2	7.16E+00	1.26E+00	9.66E-03	6.19E-02	5.61E-02	8.40E-04
79A	79.81	H2	2.34E+00	1.26E+00	1.79E-02	3.70E-02	(3.58E-02)	(2.66E-04)
83A	84.01	H2	1.76E+00	5.57E-01	2.85E-02	2.84E-02	(2.55E-02)	(1.33E-04)
87A	88.06	H2	1.80E+00	4.71E-01	1.50E-03	7.36E-03	(4.44E-03)	(7.91E-05)
93A	94.05	H2	(5.22E-01)	5.90E-01	3.95E-03	6.28E-03	(2.99E-03)	(9.65E-05)
96A	96.69	H2	1.46E+00	1.06E+00	2.81E-03	2.14E-02	(1.60E-02)	(1.34E-04)
104A	105.01	CCU$_u$	6.51E+00	2.65E+00	1.90E-03	2.46E-02	(1.99E-02)	(3.87E-04)
110B	110.28	CCU$_u$	1.08E+01	2.60E+00	9.10E-04	1.85E-02	(1.53E-02)	(4.50E-04)
110B Dup	110.28	CCU$_u$	1.18E+01	2.61E+00	1.03E-03	3.44E-02	(3.17E-02)	(4.45E-04)
110A	111.02	CCU$_l$	5.11E+00	4.82E-03	9.28E-04	2.13E-02	(2.24E-02)	(4.75E-04)
114A	114.85	CCU$_l$	1.07E+01	3.15E-03	1.92E-03	2.10E-02	(1.90E-02)	(4.82E-04)
121A	115.54	CCU$_l$	2.50E+00	1.18E-01	9.11E-04	3.36E-01	3.04E-01	(2.29E-04)

(a) Technetium-99 data are in units of pCi/g while others are µg/g of dry sediment.
(b) Parentheses signify values below level of quantitation but considered valid.
(c) Values in bold type are high relative to values extracted from background sediments.

4.129
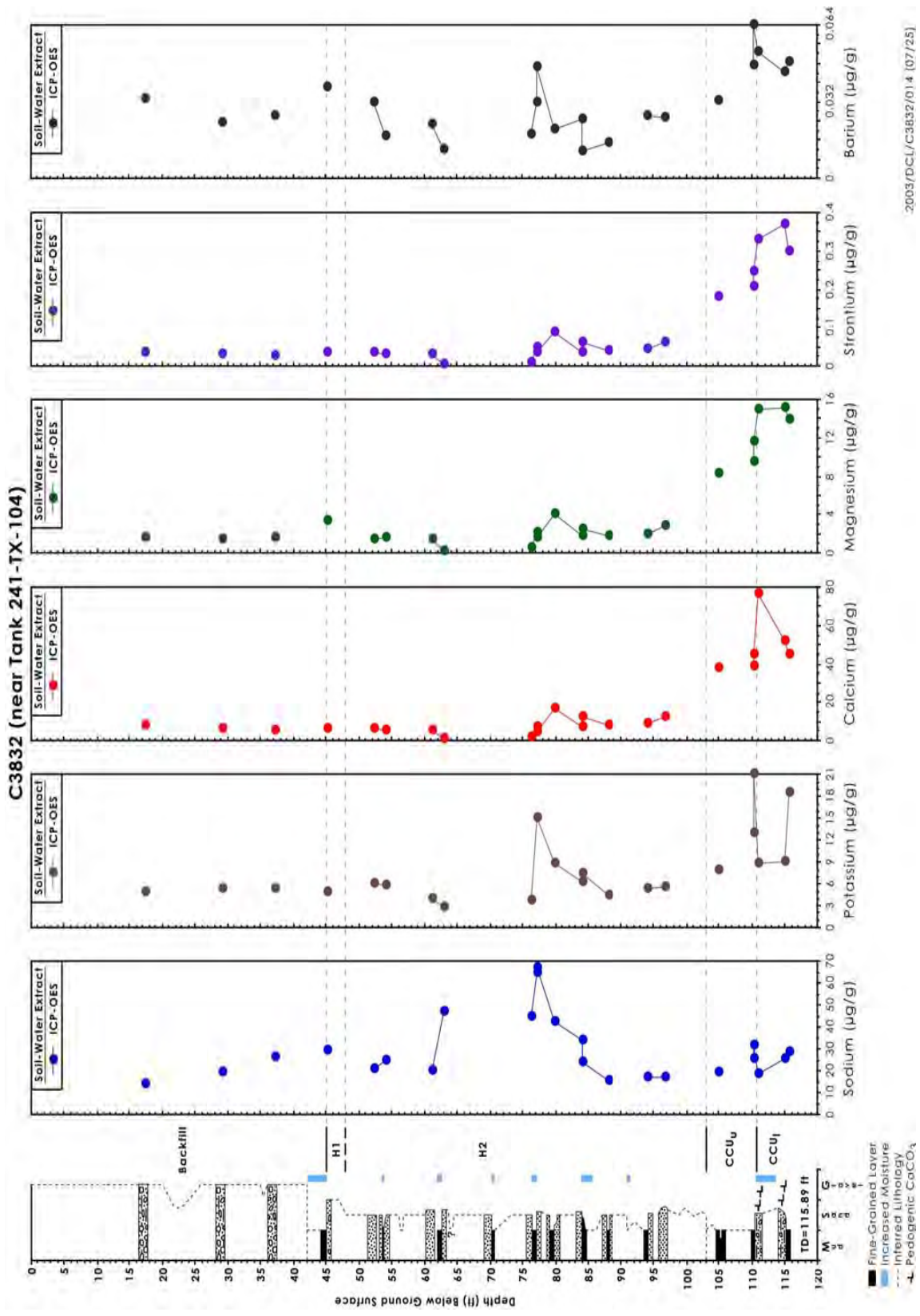
Figure 4.47. Water-Extractable Cations in Borehole C3832 Vadose Zone Sediments (µg/g)
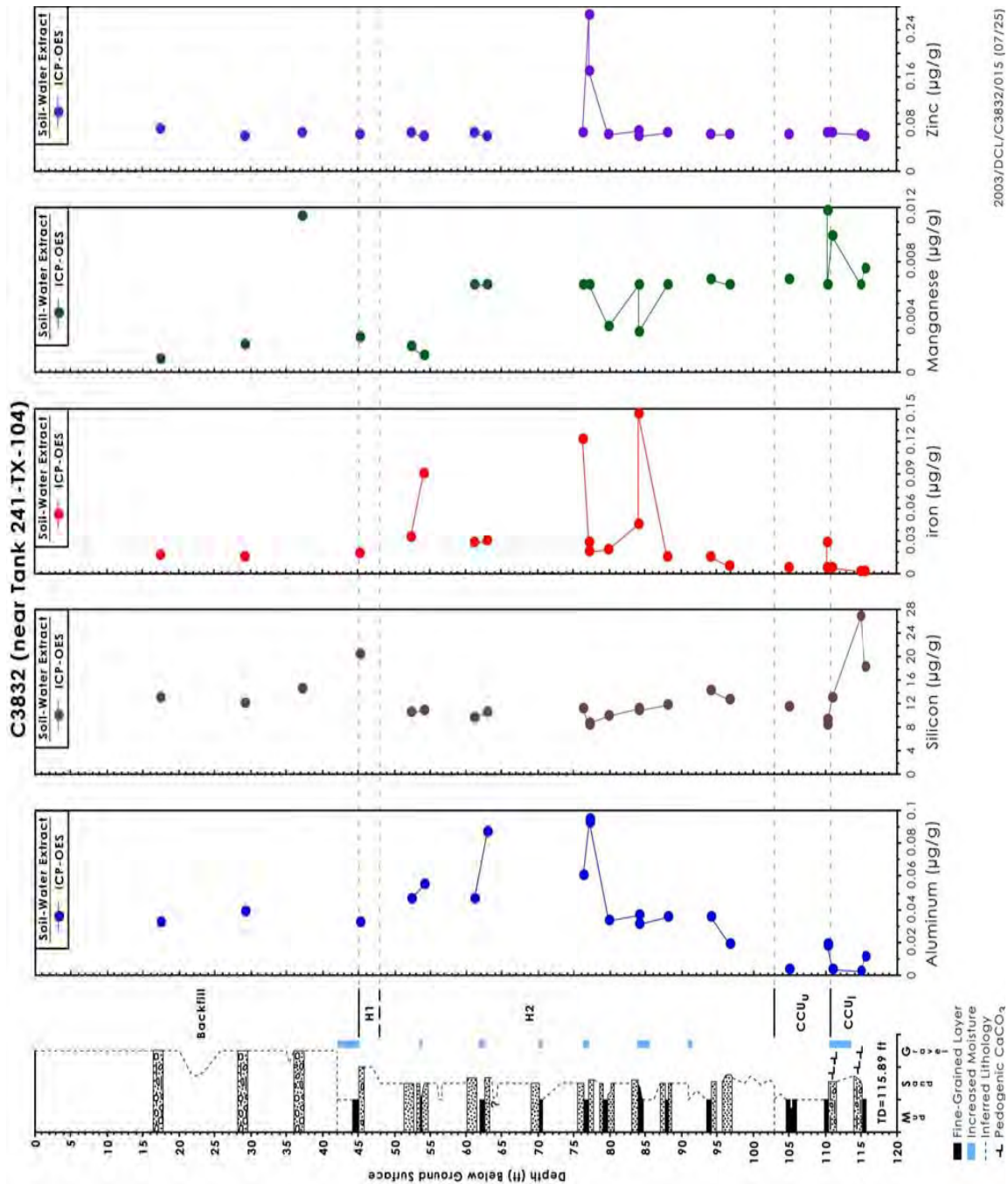
Figure 4.48. Water-Extractable Metals in C3832 Borehole Vadose Sediments (μg/g dry sediment)

2003/DCL/C3832/015 (07/25)

4.131
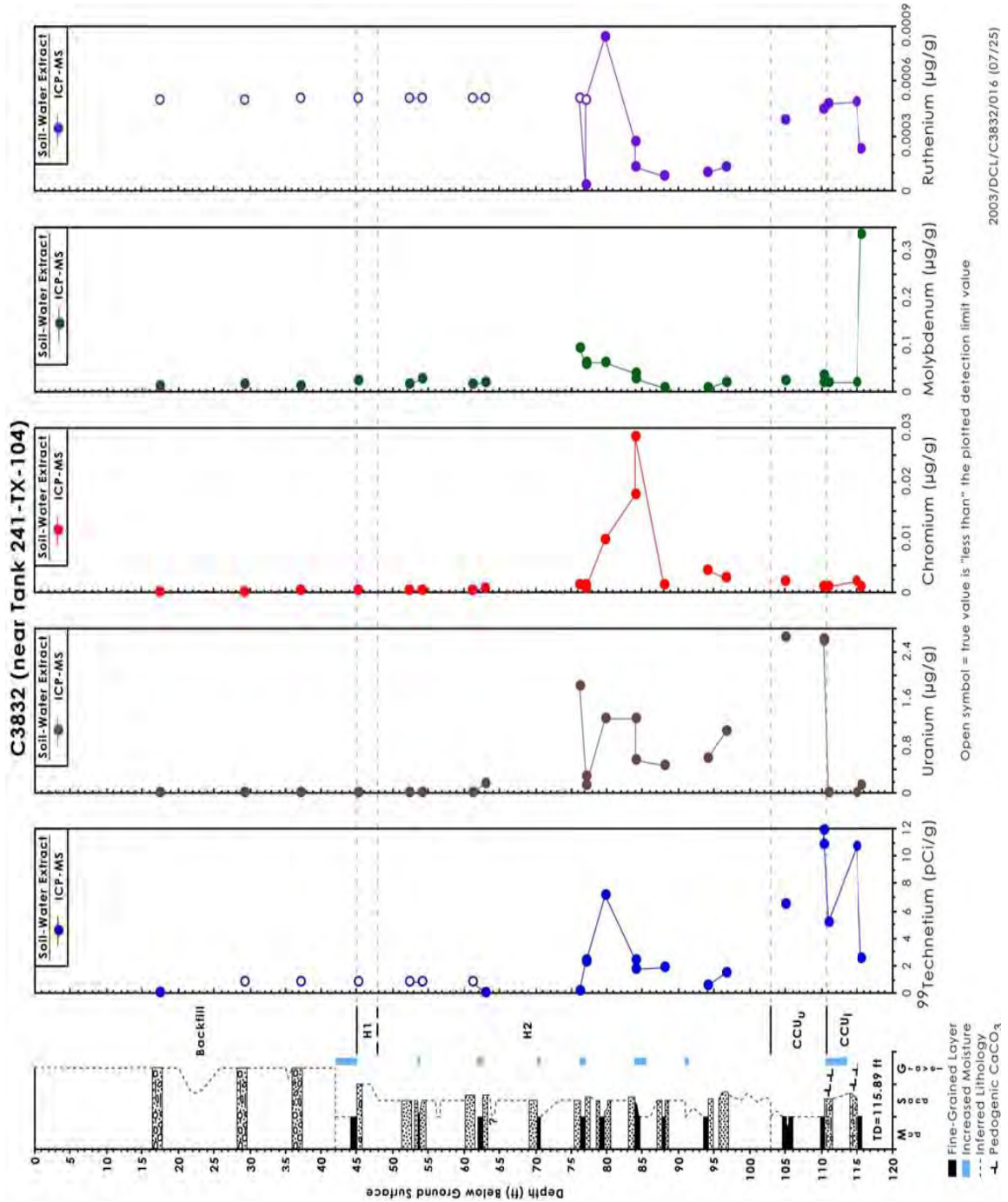
Figure 4.49. Distribution of Mobile Metals in Water Extracts of C3832 Vadose Zone Sediments

2003/DCL/C3832/016 (07/25)

4.4.3 Derivation of Vadose Zone Porewater Chemical Composition

The 1:1 water extract data was recalculated to derive an estimate of the porewater composition of the vadose zone porewater. From knowledge of the moisture content of the sediment samples taken from the A liners of each core, we calculated the amount of deionized water that would be needed to make the water extract exactly one part water (total of native porewater and added deionized water) to one part by weight dry sediment. The contaminated or uncontaminated sediment dilution-corrected water extract data is biased high by a factor of 2 to 7 for many constituents such that the true porewater is less saline.

Tables 4.55 through 4.58 and Figures 4.50 through 4.53 show the derived porewater composition of key constituents as a function of depth and stratigraphy. There are two concentrated porewaters, one shallow at 63 ft bgs and one deep at ~115 ft bgs. The shallow porewater has a total concentration of ~ 42 meq/L of cations and anions consisting of 0.44 meq/L Mg, 1.1 meq/L Ca, 39.1 meq/L Na, 1.4 meq/L K, 0.5 meq/L F, 0.4 meq/L Cl, 37.3 meq/L bicarbonate, 0.6 meq/L nitrate, and 0.3 meq/L phosphate. The deeper saline porewater contains ~58 meq/L cations and anions consisting of 13.6 meq/L Mg, 30 meq/L Ca, 12.1 meq/L Na, 2.5 meq/L K, 0.5 meq/L F, 1.6 meq/L Cl, 11 meq/L bicarbonate, 10 meq/L nitrate, and 36 meq/L sulfate.

These two calculated porewater concentrations are very dilute compared to the vadose zone porewaters found at the SX and BX tank farms where the total ionic strength of the porewaters were as high as 7,000 to 17,000 and1,000 meq/L, respectively (Serne et al. 2002c, 2002d, 2002e). At the borehole emplaced near tank B-110 the most saline porewater was 150 to 160 meq/L. Thus the porewater maximum at borehole C3831 is ~ 3 and 4 times more concentrated than the vadose zone porewater at 299-E33-46 and at borehole C3830, respectively. The porewater concentration ~10 ft below the tank bottom at borehole C3832 has about one-half the concentration as that at borehole C3830 and is ~ 10 times more dilute than at borehole C3831. Deeper in the C3832 borehole in the Cold Creek upper unit the porewater is more saline than at borehole C3830, suggesting that at borehole C3832 tank fluids migrated to deeper depths than at borehole C3830 and may have come from a more distant source than Tank TX-104.

Technetium-99 in the C3832 porewaters between the depths of 76.3 and the bottom of the borehole at 115.5 ft bgs contains about 20,000 to 40,000 pCi/L in the H2 unit and 50,000 to 110,000 pCi/L in the Cold Creek units. On a per gram of dry sediment basis, these porewater concentrations are 10 to 12 pCi/g. Because the water content of the vadose sediments is so small when equated to porewater concentrations, this small mass of technetium-99 reaches concentrations about 50 to 100 times larger than the drinking water standard. The derived porewater uranium concentration for the H2 unit between 80 and 97 ft bgs is ~12,000 µg/L and increases to 25,000 µg/L in the upper Cold Creek subunit (mud). The chromium porewater concentrations between 77 and 84 ft bgs are 200 to 300 µg/L.

Table 4.55. Derived Porewater Cation Concentrations in C3832 Vadose Zone Sediments

Sample No.	Depth (ft bgs)	Units Stratigraphic Unit	mg/L Mg	mg/L Ca	mg/L Sr	µg/L Ba	mg/L Na	mg/L K
15A	17.26	backfill	26.04	129.61	0.62	563.91	239.28	83.28
28A	29.14	backfill	30.63	142.73	0.70	525.71	428.88	118.16
37A	37.14	backfill	34.56	117.04	0.54	564.04	559.33	114.06
44A	45.19	backfill	30.77	53.49	0.33	347.33	268.02	43.80
52A	52.01	H2	22.66	95.78	0.51	477.94	320.39	91.29
53A	54.10	H2	21.49	68.45	0.42	240.69	329.98	79.72
61A	61.17	H2	39.77	146.65	0.80	593.65	529.87	107.73
62A	62.96	H2	5.32	21.72	(8.89E-02)	227.93	899.65	54.79
69A	69.99	H2	3.63	15.13	(7.48E-02)	126.57	301.97	25.94
76B	76.34	H2	21.39	70.83	0.47	312.35	634.06	148.60
76B Dup	76.34	H2	14.07	44.54	0.31	425.55	607.37	137.27
76A	77.04	H2	26.67	110.78	0.58	131.89	271.75	56.41
79A	79.81	H2	18.06	72.31	0.36	247.47	335.79	62.02
83A	84.01	H2	19.86	100.92	0.50	(9.04E+01)	196.20	59.42
87A	88.06	H2	34.89	150.23	0.73	286.81	290.37	83.38
93A	94.05	H2	38.16	169.93	0.83	496.84	320.03	102.57
96A	96.69	H2	37.06	162.76	0.79	327.53	217.30	70.83
104A	105.01	CCU$_u$	89.57	409.52	1.96	345.53	209.01	85.62
110B	110.28	CCU$_u$	88.26	360.54	1.92	438.99	238.14	119.27
110B Dup	110.28		104.73	404.87	2.25	578.13	286.42	191.30
110A	111.02	CCU$_l$	109.29	558.29	2.42	385.56	136.38	64.13
114A	114.85	CCU$_l$	165.22	560.46	4.01	480.87	278.24	98.96
121A	115.54	CCU$_l$	135.10	433.92	2.89	474.01	277.28	181.15

Parentheses signify values below level of quantitation but considered valid.

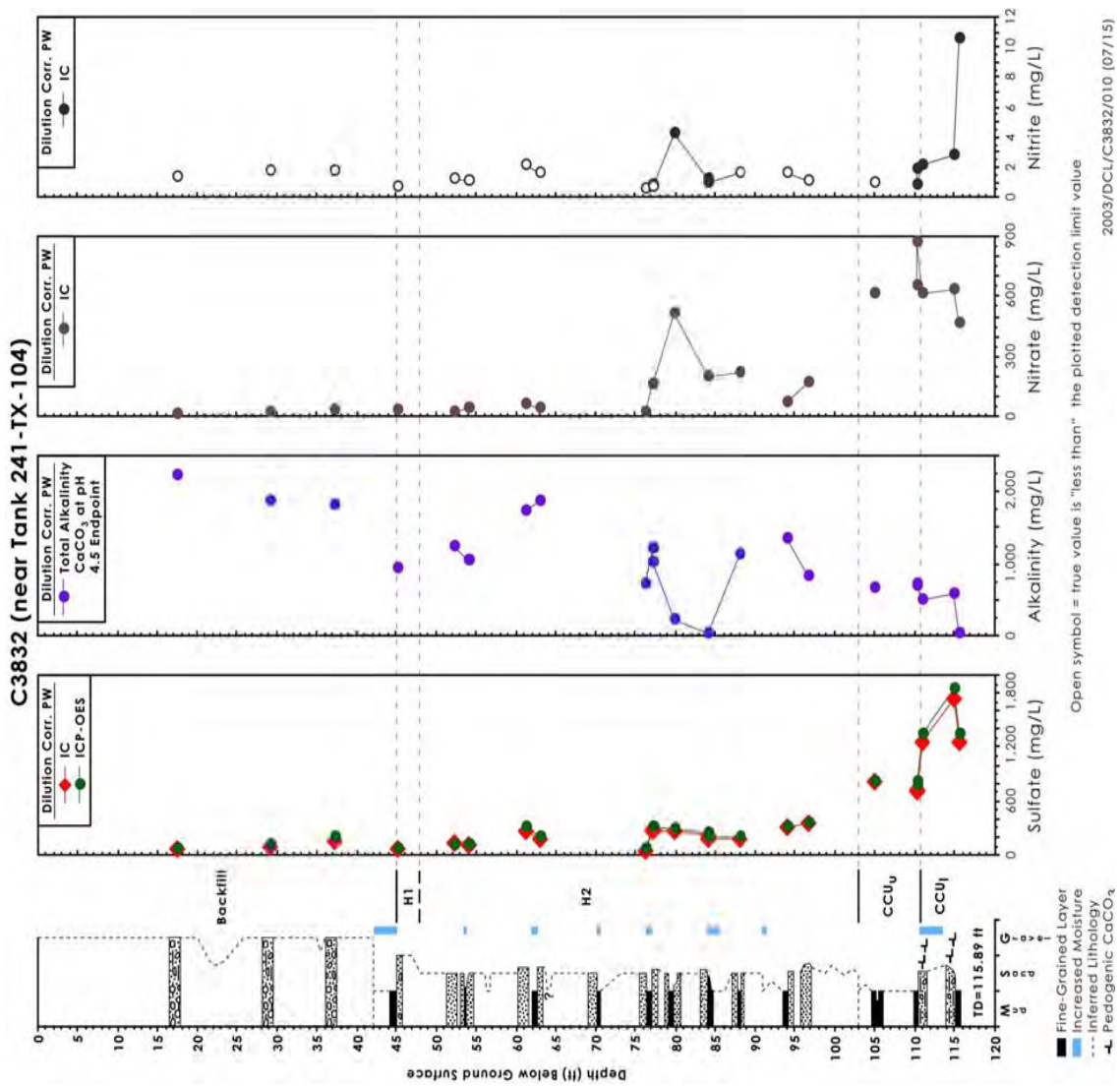**Table 4.56. Calculated Porewater Anion Concentrations in C3832 Vadose Zone Sediments**

Sample No.	Depth (ft bgs)	Stratigraphic Unit	Fluoride (mg/L)	Chloride (mg/L)	Nitrate (mg/L)	Alk as CO$_3$ (mg/L)	Sulfate (mg/L)	Phosphate (mg/L)
15A	17.26	backfill	11.12	5.10	7.40	1336.8	60.60	**<4.09**[a]
28A	29.14	backfill	19.04	13.44	22.85	1115.4	93.88	5.64
37A	37.14	backfill	17.23	4.51	35.35	1091.2	165.90	9.98
44A	45.19	backfill	9.50	6.53	29.19	555.5	61.95	4.10
52A	52.01	H2	18.61	40.74	19.42	739.1	126.46	**<3.66**
53A	54.10	H2	13.01	8.09	42.37	627.9	103.03	2.48
61A	61.17	H2	8.64	25.34	62.28	1041.6	272.73	**<6.42**
62A	62.96	H2	9.96	14.96	35.70	1119.2	174.06	8.62
69A	69.99	H2	6.49	3.33	17.76	429.3	56.29	3.05
76B	76.34	H2	12.68	72.91	160.80	727.9	280.30	5.25
76B Dup	76.34	H2	12.59	66.59	161.79	604.9	255.79	5.54
76A	77.04	H2	3.36	31.71	510.78	138.3	263.03	**<1.55**
79A	79.81	H2	6.05	22.93	193.87	23.7	214.92	**<2.40**
83A	84.01	H2	3.76	26.93	203.70	19.3	173.43	**<1.94**
87A	88.06	H2	7.00	13.91	218.85	676.4	171.76	**<4.62**
93A	94.05	H2	10.39	13.07	74.76	805.5	299.45	**<4.84**
96A	96.69	H2	6.08	25.83	169.74	499.2	349.15	**<3.07**
104A	105.01	CCU$_u$	3.53	78.57	617.01	390.6	814.18	**<2.78**
110B	110.28	CCU$_u$	2.97	85.03	657.35	422.0	707.43	**<2.22**
110B Dup	110.28	CCU$_u$	3.82	121.39	869.48	405.7	722.59	**<2.18**
110A	111.02	CCU$_l$	3.59	90.10	615.98	303.1	1250.77	**<1.76**
114A	114.85	CCU$_l$	10.19	58.58	638.59	350.7	1745.46	**<2.60**
121A	115.54	CCU$_l$	8.93	78.93	466.68	23.1	1264.89	2.98

(a) Values in bold are below the instrument detection limit.

Table 4.57. Derived Porewater Concentrations of Selected Constituents in C3832 Vadose Zone Sediments

Sample No.	Depth (ft bgs)	Stratigraphic Unit	Al µg/L	Si mg/L	Fe µg/L	Mn µg/L	Zn µg/L	PO$_4$ (ICP) mg/L	SO$_4$ (ICP) mg/L
15A	17.26	backfill	548	218.5	(2.73E+02)[a]	(1.49E+01)	1234	(3.37)	78
28A	29.14	backfill	871	272.3	(3.20E+02)	(4.51E+01)	1316	(4.61)	119
37A	37.14	backfill	6102	314.6	8.58E+03	(2.47E+02)	1375	12.74	191
44A	45.19	backfill	289	186.9	(1.63E+02)	(2.26E+01)	574	3.95	70
52A	52.01	H2	709	157.6	(5.12E+02)	(2.91E+01)	981	(1.24)	110
53A	54.10	H2	747	145.2	(1.22E+03)	(1.64E+01)	789	(2.13)	117
61A	61.17	H2	1246	259.3	(7.51E+02)	(1.68E+02)	1743	(3.72)	310
62A	62.96	H2	1675	203.9	(5.71E+02)	(1.22E+02)	1119	8.44	196
69A	69.99	H2	413	74.6	(8.32E+02)	(4.28E+01)	441	3.51	65
76B	76.34	H2	936	83.3	(2.76E+02)	(6.23E+01)	2603	6.89	320
76B Dup	76.34	H2	842	77.8	(1.81E+02)	(5.81E+01)	1540	5.18	300
76A	77.04	H2	216	63.0	(1.44E+02)	(2.10E+01)	403	(0.90)	289
79A	79.81	H2	367	110.9	(4.43E+02)	(6.30E+01)	689	(1.46)	241
83A	84.01	H2	254	86.5	1.17E+03	(2.41E+01)	477	(0.81)	207
87A	88.06	H2	676	226.6	(2.88E+02)	(1.21E+02)	1263	(1.69)	196
93A	94.05	H2	678	268.7	(2.99E+02)	(1.27E+02)	1152	(1.21)	317
96A	96.69	H2	(2.40E+02)	160.5	(9.66E+01)	(8.07E+01)	802	(2.62)	351
104A	105.01	CCU$_u$	(3.78E+01)	124.1	(5.62E+01)	(7.29E+01)	660	(1.22)	821
110B	110.28	CCU$_u$	(1.70E+02)	87.0	(2.56E+02)	(1.09E+02)	590	(1.51)	773
110B Dup	110.28	CCU$_l$	(1.58E+02)	76.2	(4.06E+01)	(5.72E+01)	587	(2.76)	806
110A	111.02	CCU$_l$	(2.43E+01)	95.3	(3.85E+01)	(7.24E+01)	485	(0.44)	1333
114A	114.85	CCU$_l$	(3.09E+01)	291.0	(1.57E+01)	(6.84E+01)	668	(0.03)	1840
121A	115.54	CCU$_l$	(1.12E+02)	176.0	(2.18E+01)	(7.33E+01)	574	(1.01)	1336

(a) Parentheses signify values below level of quantitation but considered valid.

Table 4.58.   Calculated Porewater Concentrations of Potentially Mobile Constituents in C3832 Vadose Sediments

Sample No.	Depth (ft bgs)	Units Stratigraphic Unit	pCi/L Tc-99[a],[c]	µg/L U-238	µg/L Cr (ICP-MS)	µg/L Mo	µg/L Mo (ICP-MS)	µg/L Ru
15A	17.26	Backfill	(0.00E+00)[c]	2.90E+01	(2.20E+00)	(1.64E+02)	1.95E+02	**<8.52E+00**[b]
28A	29.14	Backfill	<1.90E+04	2.21E+01	(3.24E+00)	(2.69E+02)	3.24E+02	**<1.12E+01**
37A	37.14	Backfill	<1.84E+04	4.85E+01	1.12E+01	(2.05E+02)	2.74E+02	**<1.08E+01**
44A	45.19	Backfill	<7.74E+03	4.39E+01	(4.54E+00)	(1.93E+02)	2.23E+02	**<4.57E+00**
52A	52.01	H2	<1.29E+04	1.34E+01	(5.44E+00)	(2.12E+02)	2.56E+02	**<7.62E+00**
53A	54.10	H2	<1.17E+04	6.01E+01	(5.78E+00)	(3.03E+02)	3.49E+02	**<6.88E+00**
61A	61.17	H2	<2.27E+04	4.60E+02	(1.31E+01)	(3.09E+02)	3.81E+02	**<1.34E+01**
62A	62.96	H2	(0.00E+00)	2.82E+03	1.06E+01	(3.22E+02)	4.03E+02	**<9.65E+00**
69A	69.99	H2	(1.27E+03)	1.23E+04	9.22E+00	5.64E+02	6.38E+02	**<3.40E+00**
76B	76.34	H2	2.31E+04	2.78E+03	1.19E+01	5.05E+02	5.57E+02	(2.87E-01)
76B Dup	76.34	H2	2.08E+04	1.20E+03	6.81E+00	4.97E+02	5.53E+02	**<4.55E+00**
76A	77.04	H2	4.63E+04	8.14E+03	6.24E+01	3.63E+02	4.00E+02	5.43E+00
79A	79.81	H2	2.34E+04	1.26E+04	1.79E+02	(3.57E+02)	3.69E+02	(2.66E+00)
83A	84.01	H2	1.43E+04	4.52E+03	2.31E+02	(2.06E+02)	2.31E+02	(1.08E+00)
87A	88.06	H2	3.46E+04	9.04E+03	2.89E+01	(8.53E+01)	1.41E+02	(1.52E+00)
93A	94.05	H2	(9.92E+03)	1.12E+04	7.52E+01	(5.68E+01)	1.19E+02	(1.84E+00)
96A	96.69	H2	1.87E+04	1.36E+04	3.59E+01	(2.06E+02)	2.74E+02	(1.72E+00)
104A	105.01	CCU_u	7.01E+04	2.85E+04	2.05E+01	(2.15E+02)	2.65E+02	(4.17E+00)
110B	110.28	CCU_u	9.99E+04	2.41E+04	8.42E+00	(1.42E+02)	1.71E+02	(4.16E+00)
110B Dup	110.28		1.07E+05	2.36E+04	9.33E+00	(2.87E+02)	3.12E+02	(4.03E+00)
110A	111.02	CCU_l	3.74E+04	3.52E+01	6.79E+00	(1.64E+02)	1.56E+02	(3.48E+00)
114A	114.85	CCU_l	1.16E+05	3.42E+01	2.09E+01	(2.06E+02)	2.28E+02	(5.23E+00)
121A	115.54	CCU_l	2.43E+04	1.14E+03	8.85E+00	2.95E+03	3.27E+03	(2.22E+00)

(a) Technetium-99 data are in units of pCi/g while all others are µg/g of dry sediment.
(b) Values in bold are below detection limit.
(c) Parentheses signify values below level of quantitation but considered valid.
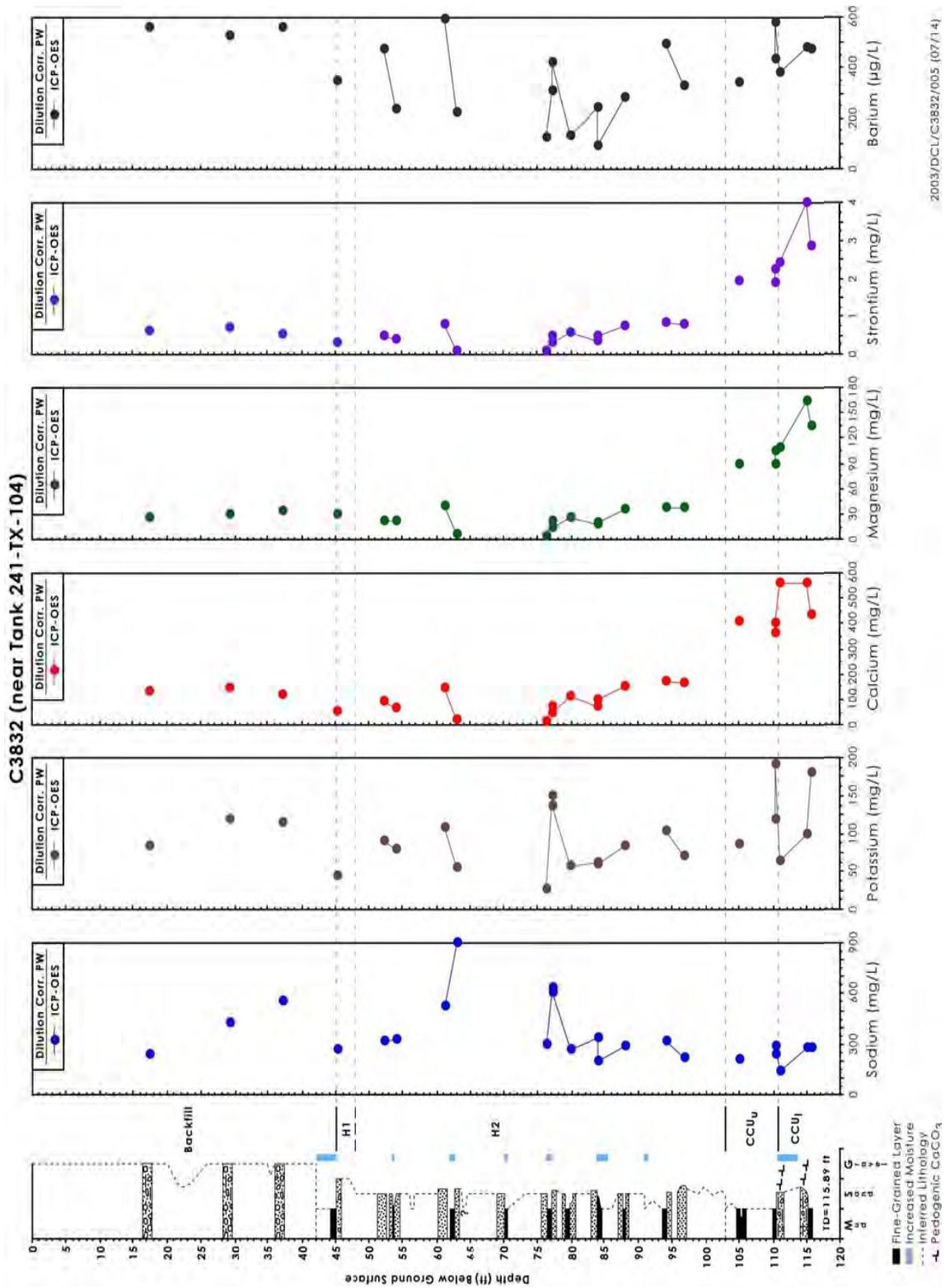
Figure 4.50. Calculated Porewater Composition of Major Cations in C3832 Vadose Zone Sediments

Figure 4.51. Calculated Porewater Anion Composition in C3832 Vadose Zone Sediments
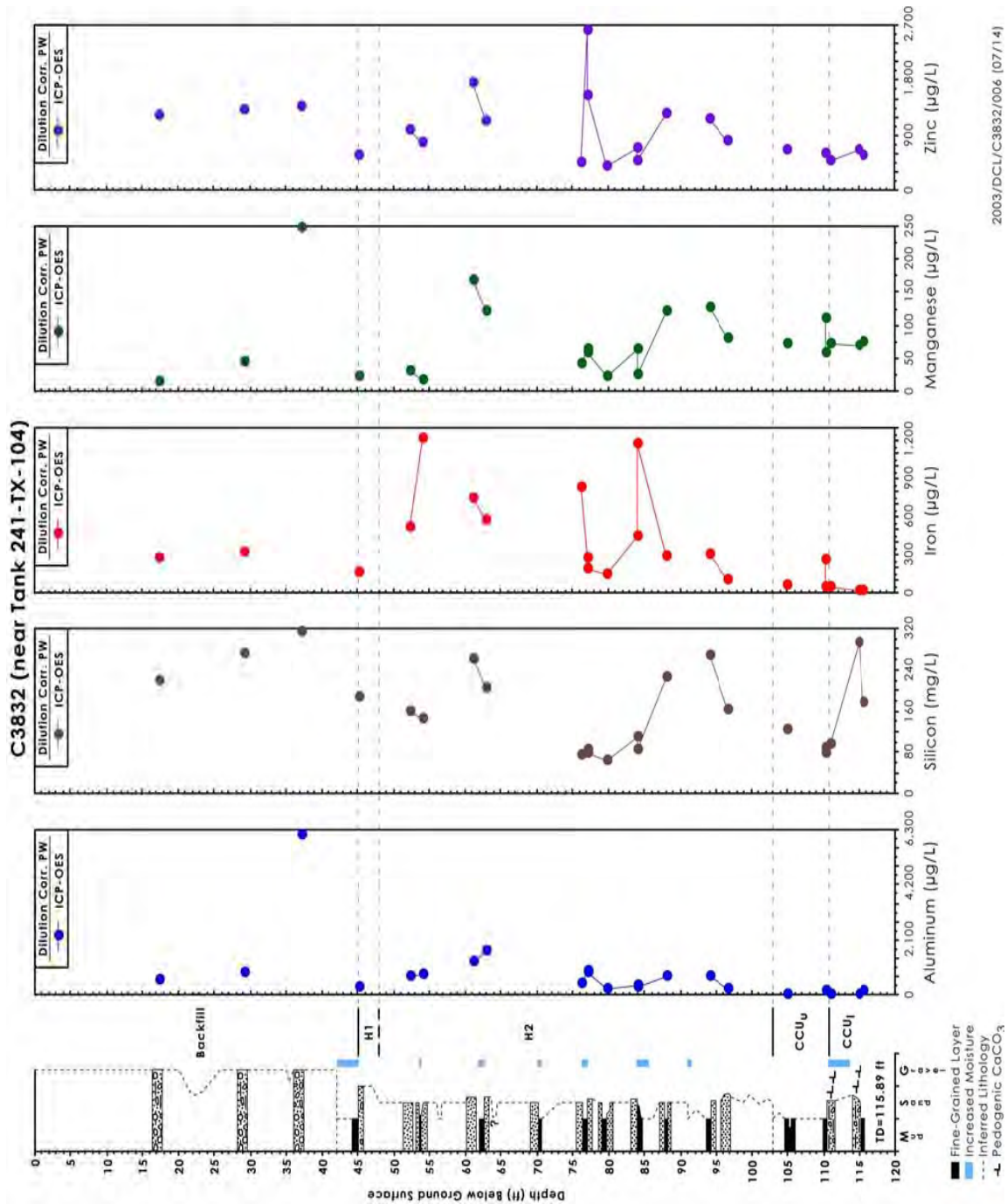
Figure 4.52. Calculated Porewater Composition for Selected Metals in C3832 Vadose Zone Sediments
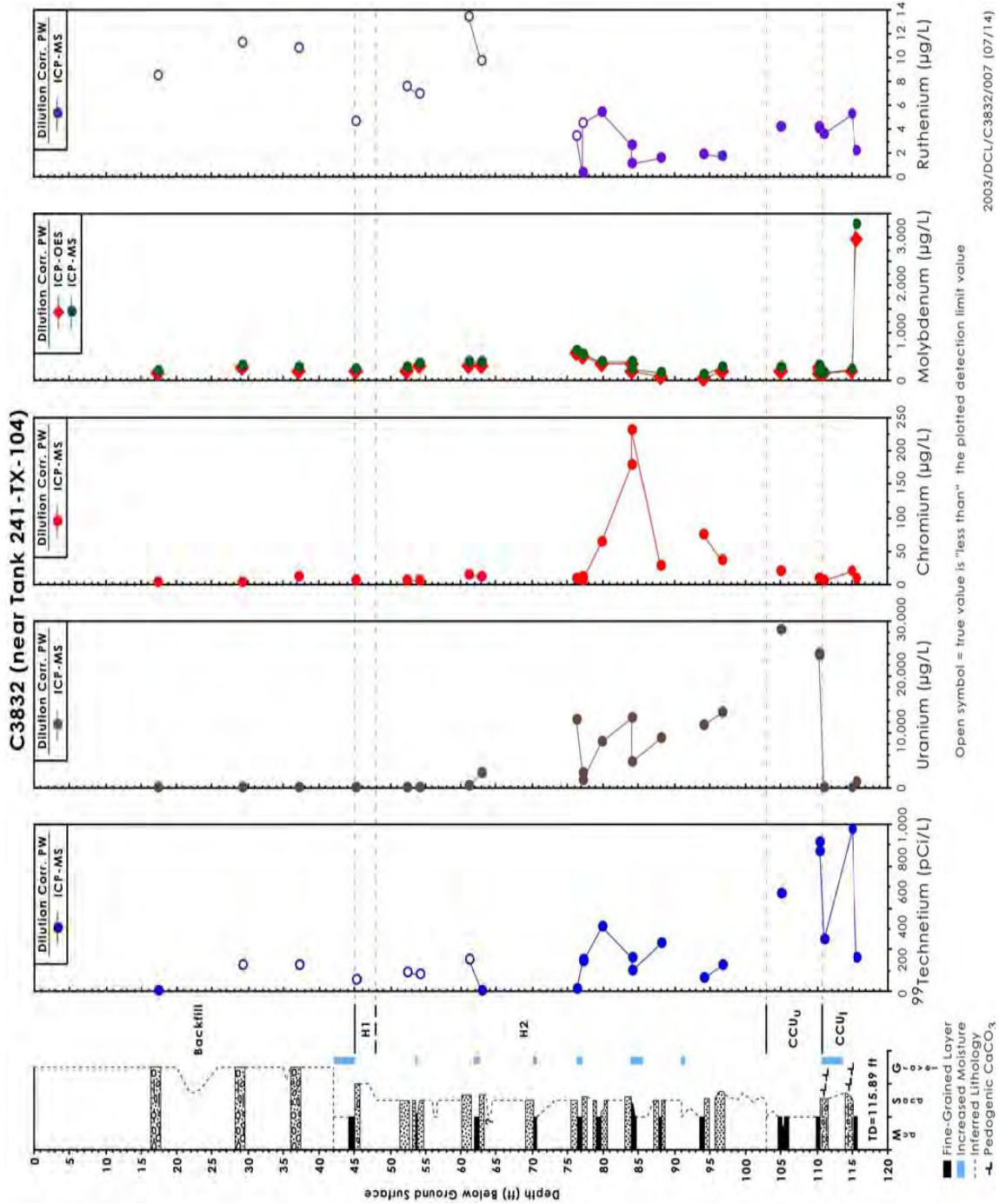
Figure 4.53. Calculated Porewater Composition of Mobile Metals in C3832 Vadose Zone Sediments

4.141

4.4.4 8 M Nitric Acid-Extractable Amounts of Selected Elements in C3832 Sediments

The same cores that were characterized for water-extractable constituents were also characterized to see how much of various constituents could be leached with hot 8 M nitric acid. A comparison between the quantities that were acid extractable with those that are water extractable often indicates the relative mobility of a given constituent and can sometimes differentiate man-disposed from naturally occurring constituents. Finally, a comparison of the acid-extractable quantities in suspected contaminated sediments with acid-extractable amounts in uncontaminated sediments can be used to delineate the presence of less mobile contaminants.

The quantities of various constituents in the C3832 vadose zone sediments that were acid extractable are shown in Tables 4.59 to 4.61 and Figures 4.54 through 4.56. Upon comparing the acid extract data for borehole C3832 with similar lithologies in the uncontaminated borehole 299-W10-27, most of the variation in mass leached per gram of sediment versus depth in found to be lithology related. That is, for most constituents there are no signs of elevated values of acid-leachable constituents in borehole C3832 sediments excepting acid-extractable sodium in the backfill, and often in the H2 unit below the tank bottom. At C3832, we did not observe any elevated acid-extractable sulfur (assumed to represent sulfate) as was found in borehole C3831 sediments. Acid-extractable technetium-99 in borehole C3832 appears to be slightly above the background sediments but the same as in borehole C3831 and somewhat lower than acid-extractable technetium-99 in borehole C3830. There are greater acid-extractable concentrations of uranium at borehole C3832 from 70 ft bgs all the way to the bottom of the borehole than at either of the other two boreholes. Acid-extractable uranium concentrations vary from 1 to 30 µg/g over this interval. There also appears to be a zone elevated acid-extractable chromium in borehole C3832 between 70 and 76 ft bgs with a concentration of 25 µg/g. Values of acid-extractable chromium at the other two boreholes never exceed 15 µg/g. The acid-extractable molybdenum at borehole C3832 is larger than at C3830 but similar to acid-extractable molybdenum at borehole C3831. As mentioned below for alkaline earth cations, some of the differences in acid extract concentrations may reflect differences in the efficiency of the acid digestion.

The acid-extractable silicon at depths 61 to 63 ft bgs at borehole C3832 is elevated in comparison to background sediment and the other two boreholes suggesting some more soluble silicate phase may exist at this depth as a result of tank fluid (likely caustic) interaction with native sediments. The acid-extractable phosphate in the backfill between 17 and 45 ft bgs appears elevated compared to the background sediment and other two boreholes. This suggests that some phosphate-bearing waste fluid may have been spilled near the surface and percolated into the backfill; however, phosphate is generally not very mobile/soluble in Hanford sediments and porewaters. Thus the elevated phosphate may be an analytical artifact or natural variability in the native sediments.

The acid-extractable magnesium, calcium, strontium, and barium at borehole C3832 is higher than at either of the other two boreholes but not the background sediment, suggesting that we may have some variation in efficiency of extraction by the technique. (Perhaps efficiency is dependent on temperature and time of extraction.) The acid-extractable sodium concentration profile at borehole C3832 is larger than at borehole C3830 but only one-half that at borehole C3831. This indicates that C3831 waste was more concentrated than the fluids that leaked near borehole C3830 and C3832, as corroborated by the pore water compositions. The clastic dike intercepted at borehole C3831 may have allowed tank fluids to "short-circuit" many of the sediment interactions, including dilution with native porewaters that would occur in more "homogeneously layered" porous media.

Figure 4.57 shows that the vast majority of the sediment phosphate content is not water extractable in comparison with the amounts that are acid extractable. The same trend was observed for the uncontaminated sediments from borehole 299-W10-27 and other two boreholes. Alternatively, some of the acid-extractable phosphorous may be present in a form other than phosphate such that when we convert the acid-extractable phosphorous number to phosphate (essentially multiply by 3) we are inflating the acid-extractable value

As mentioned, the ratio of water-extractable to acid-extractable quantities of constituents can identify samples that may contain leaked fluids from Hanford waste disposals. The comparison of water to acid extracts for borehole C3832 sediments suggests that there are unnaturally high percentages of water-leachable technetium-99 and uranium-238 between 76 and 115 and 61 to 110.3 ft bgs, respectively. There is also slightly high water-extractable sodium between 63 and 77 ft bgs. The total mass of tank fluids that are present in C3832 borehole sediments and the percentages that are water leachable versus the concentrations that are acid leachable are lower than at borehole C3831. The two data sets suggest that the tank-related fluids in borehole C3832 may in fact be the leading edge of fluids that leaked from tank TX-107 that were intercepted by borehole C3831. It also appears that the vadose zone plume dips to the southwest between the two boreholes as does the stratigraphy (see discussion in Section 2).

Table 4.59. Acid-Extractable Cations from C3832 Vadose Zone Sediments (µg/g dry sediment)

Sample No.	Depth (ft bgs)	Stratigraphic Unit	Mg	Ca	Sr	Ba	Na	K
15A	17.26	Backfill	4.50E+03	6.60E+03	2.87E+01	1.13E+02	- - -	8.58E+02
28A	29.14	Backfill	4.40E+03	7.28E+03	3.46E+01	9.44E+01	- - -	9.59E+02
37A	37.14	Backfill	4.27E+03	5.88E+03	2.46E+01	6.18E+01	- - -	8.71E+02
44A	45.19	Backfill	5.51E+03	1.37E+04	3.92E+01	9.10E+01	- - -	1.39E+03
52A	52.01	H2	5.46E+03	9.73E+03	4.18E+01	8.62E+01	- - -	1.66E+03
53A	54.10	H2	5.44E+03	9.77E+03	3.77E+01	5.83E+01	- - -	1.57E+03
61A	61.17	H2	5.38E+03	7.93E+03	3.57E+01	7.59E+01	- - -	1.54E+03
62A	62.96	H2	5.57E+03	8.93E+03	3.52E+01	6.30E+01	- - -	1.40E+03
69A	69.99	H2	6.24E+03	9.86E+03	4.47E+01	6.62E+01	- - -	1.97E+03
76B	76.34	H2	5.92E+03	9.37E+03	4.44E+01	8.71E+01	- - -	1.88E+03
76B Dup	76.34	H2	5.80E+03	9.76E+03	4.24E+01	8.70E+01	- - -	1.63E+03
76A	77.04	H2	6.51E+03	9.88E+03	4.37E+01	8.73E+01	- - -	2.08E+03
79A	79.81	H2	5.61E+03	8.45E+03	4.08E+01	8.49E+01	- - -	1.62E+03
83A	84.01	H2	6.28E+03	1.10E+04	3.48E+01	8.49E+01	- - -	2.06E+03
87A	88.06	H2	4.91E+03	7.60E+03	3.66E+01	7.13E+01	- - -	1.10E+03
93A	94.05	H2	5.75E+03	1.04E+04	4.75E+01	9.20E+01	- - -	1.82E+03
96A	96.69	H2	5.88E+03	1.39E+04	5.46E+01	1.12E+02	- - -	1.75E+03
104A	105.01	CCU$_u$	7.29E+03	1.48E+04	4.53E+01	1.07E+02	- - -	2.18E+03
110B	110.28	CCU$_u$	7.45E+03	2.52E+04	5.51E+01	8.22E+01	- - -	1.41E+03
110B Dup	110.28		8.12E+03	2.22E+04	5.79E+01	9.16E+01	- - -	1.75E+03
110A	111.02	CCU$_l$	4.81E+03	1.50E+05	1.70E+02	9.21E+01	- - -	7.13E+02
114A	114.85	CCU$_l$	8.16E+03	1.65E+05	1.99E+02	1.02E+02	- - -	7.58E+02
121A	115.54	CCU$_l$	1.17E+04	1.77E+05	3.18E+02	1.44E+02	- - -	1.55E+03

Table 4.60.   Acid-Extractable Constituents in C3832 Vadose Zone Sediments (µg/g dry sediment)

Sample No.	Depth (ft bgs)	Stratigraphic Unit	Al	Si	Fe	Mn	Zn	P as PO_4	S as SO_4
15A	17.26	Backfill	6.62E+03	(1.65E+01)[a]	2.17E+04	3.26E+02	3.89E+01	3.43E+03	NA[b]
28A	29.14	Backfill	7.23E+03	(1.81E+01)	2.17E+04	3.38E+02	3.86E+01	3.31E+03	NA
37A	37.14	Backfill	6.09E+03	(2.13E+01)	1.90E+04	2.92E+02	3.39E+01	3.32E+03	NA
44A	45.19	Backfill	8.70E+03	(2.48E+01)	2.11E+04	3.84E+02	4.40E+01	2.93E+03	NA
52A	52.01	H2	9.13E+03	(1.38E+01)	1.63E+04	3.59E+02	3.83E+01	1.56E+03	NA
53A	54.10	H2	8.28E+03	(4.70E+01)	1.64E+04	3.45E+02	3.74E+01	1.65E+03	NA
61A	61.17	H2	7.98E+03	(1.58E+02)	1.50E+04	3.16E+02	3.69E+01	1.46E+03	NA
62A	62.96	H2	8.18E+03	(1.36E+02)	1.59E+04	3.18E+02	3.78E+01	1.53E+03	NA
69A	69.99	H2	1.13E+04	(1.99E+01)	1.75E+04	2.84E+02	4.54E+01	2.19E+03	NA
76B	76.34	H2	1.03E+04	(1.59E+01)	2.08E+04	3.56E+02	4.22E+01	1.84E+03	NA
76B Dup	76.34	H2	9.49E+03	(2.02E+01)	1.80E+04	3.40E+02	3.86E+01	1.94E+03	NA
76A	77.04	H2	1.13E+04	(1.23E+01)	1.90E+04	3.31E+02	4.64E+01	2.32E+03	NA
79A	79.81	H2	9.38E+03	(3.34E+01)	1.85E+04	3.64E+02	4.06E+01	1.76E+03	NA
83A	84.01	H2	9.97E+03	(2.04E+01)	1.69E+04	3.44E+02	4.63E+01	1.69E+03	NA
87A	88.06	H2	7.76E+03	(5.20E+01)	1.65E+04	3.02E+02	3.55E+01	1.96E+03	NA
93A	94.05	H2	1.06E+04	(2.89E+01)	2.02E+04	3.80E+02	4.37E+01	1.87E+03	NA
96A	96.69	H2	1.11E+04	(3.12E+01)	2.22E+04	3.95E+02	4.68E+01	2.26E+03	NA
104A	105.01	CCU_u	1.22E+04	(9.93E+00)	1.95E+04	4.07E+02	5.10E+01	1.91E+03	NA
110B	110.28	CCU_u	9.17E+03	(9.70E+00)	1.68E+04	3.10E+02	3.63E+01	2.01E+03	NA
110B Dup	110.28		1.00E+04	(1.06E+01)	1.77E+04	3.21E+02	3.86E+01	2.34E+03	NA
110A	111.02	CCU_l	6.89E+03	(9.55E+00)	1.08E+04	1.84E+02	2.02E+01	1.77E+03	NA
114A	114.85	CCU_l	6.43E+03	(1.26E+01)	9.39E+03	1.66E+02	1.71E+01	1.38E+03	NA
121A	115.54	CCU_l	1.04E+04	(8.10E+00)	1.61E+04	2.68E+02	4.84E+01	1.98E+03	NA

(a) Parentheses signify values below level of quantitation but considered valid.
(b) NA = Not Analyzed.

Table 4.61. Acid-Extractable Trace Metals in C3832 Vadose Zone Sediments

Sample No.	Depth (ft bgs)	Stratigraphic Unit	Tc-99[a]	U-238	Cr (ICP-MS)	Cr (ICP)	Mo (ICP-MS)	Mo (ICP)[c]	Ru (ICP-MS)
15A	17.26	backfill	(3.83E+01)[b]	3.97E-01	1.69E+01	1.63E+01	2.36E+00	NA[c]	1.10E-02
28A	29.14	backfill	(3.33E+01)	4.20E-01	1.30E+01	1.04E+01	1.60E+00	NA	1.74E-02
37A	37.14	backfill	(1.98E+01)	3.84E-01	1.15E+01	1.05E+01	1.04E+00	NA	1.25E-02
44A	45.19	backfill	(1.31E+01)	4.72E-01	1.11E+01	9.78E+00	2.80E-01	NA	2.09E-02
52A	52.01	H2	(1.85E+01)	5.54E-01	1.51E+01	1.33E+01	5.80E-01	NA	2.27E-02
53A	54.10	H2	(1.47E+01)	7.05E-01	1.67E+01	1.37E+01	9.57E-01	NA	2.22E-02
61A	61.17	H2	(1.21E+01)	1.02E+00	1.51E+01	1.28E+01	2.91E-01	NA	2.09E-02
62A	62.96	H2	(1.47E+01)	2.85E+00	1.31E+01	1.25E+01	2.32E-01	NA	1.83E-02
69A	69.99	H2	(1.28E+01)	1.46E+01	2.22E+01	1.82E+01	5.14E-01	NA	2.72E-02
76B	76.34	H2	(3.11E+01)	5.82E+00	3.10E+01	2.68E+01	6.28E+00	NA	2.71E-02
76B Dup	76.34	H2	(2.19E+01)	8.55E+00	2.00E+01	1.61E+01	1.21E+00	NA	2.45E-02
76A	77.04	H2	(3.34E+01)	1.22E+01	1.39E+01	1.89E+01	2.70E-01	NA	1.88E-02
79A	79.81	H2	(1.94E+01)	6.94E+00	1.32E+01	1.44E+01	3.55E-01	NA	1.83E-02
83A	84.01	H2	(2.04E+01)	1.09E+01	1.81E+01	1.35E+01	3.92E-01	NA	2.50E-02
87A	88.06	H2	(1.21E+01)	4.29E+00	1.57E+01	1.23E+01	4.90E-01	NA	2.29E-02
93A	94.05	H2	(1.03E+01)	2.39E+00	1.64E+01	1.38E+01	4.40E-01	NA	2.48E-02
96A	96.69	H2	(1.32E+01)	6.02E+00	1.69E+01	1.27E+01	7.65E-01	NA	3.04E-02
104A	105.01	CCU$_u$	(1.63E+01)	2.73E+01	2.35E+01	1.87E+01	1.90E+00	NA	3.34E-02
110B	110.28	CCU$_u$	(2.57E+01)	3.07E+01	2.06E+01	1.87E+01	2.82E+00	NA	3.77E-02
110B Dup	110.28		(3.25E+01)	3.05E+01	3.18E+01	2.71E+01	6.78E+00	NA	3.79E-02
110A	111.02	CCU$_l$	(2.92E+01)	1.40E+01	1.09E+01	7.60E+00	6.67E-01	NA	1.47E-01
114A	114.85	CCU$_l$	(3.39E+01)	1.40E+01	8.82E+00	6.05E+00	2.52E-01	NA	1.68E-01
121A	115.54	CCU$_l$	(4.27E+01)	1.90E+01	3.18E+01	2.13E+01	3.88E+00	NA	3.01E-01

(a) Technetium-99 data are in units of pCi/g while all others are μg/g of dry sediment.
(b) Parentheses signify values below level of quantitation but considered valid.
(c) NA = Not analyzed.
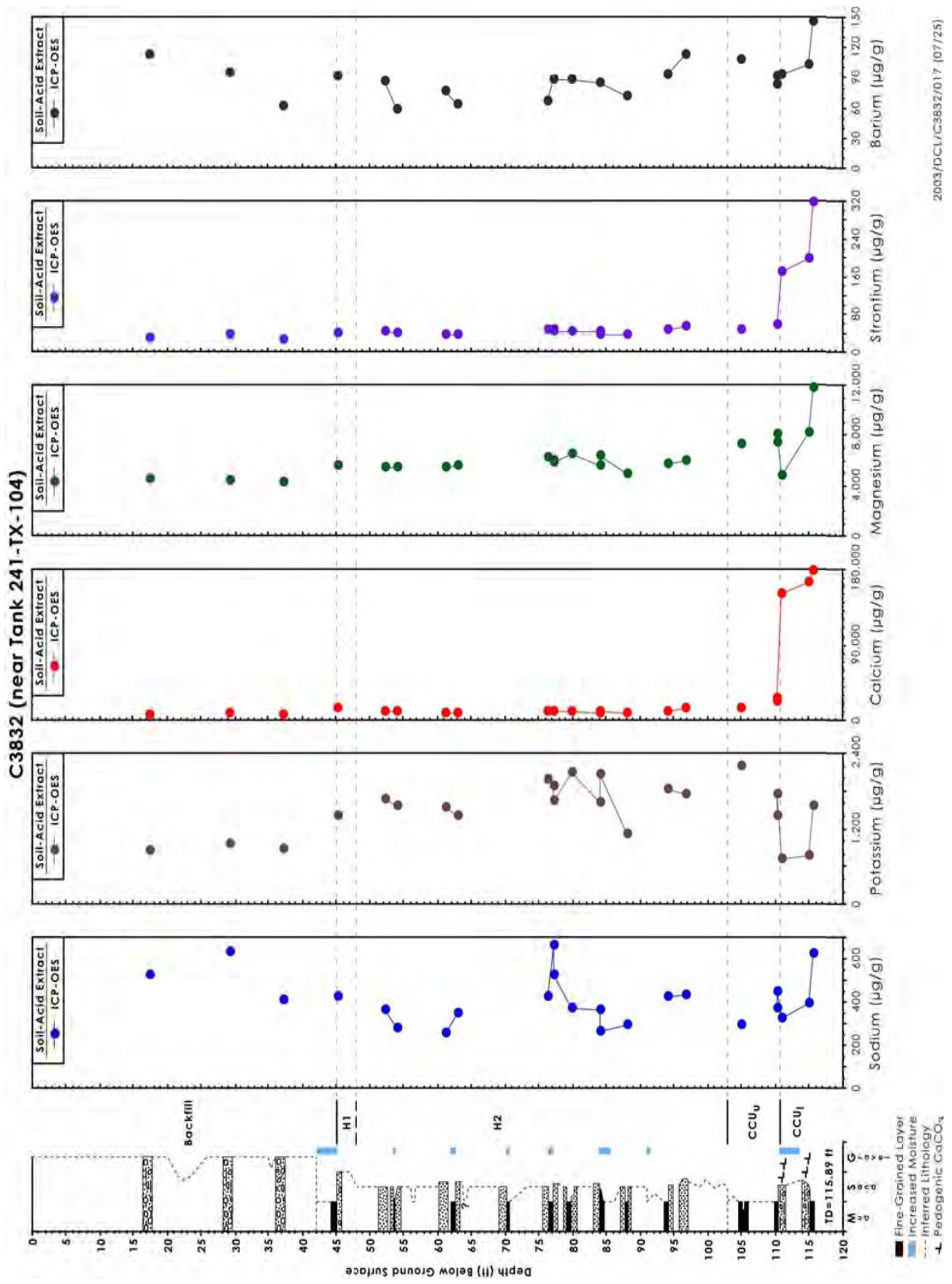
Figure 4.54. Acid-Extractable Cations in C3832 Vadose Zone Sediments (μg/g dry sediment)

4.147
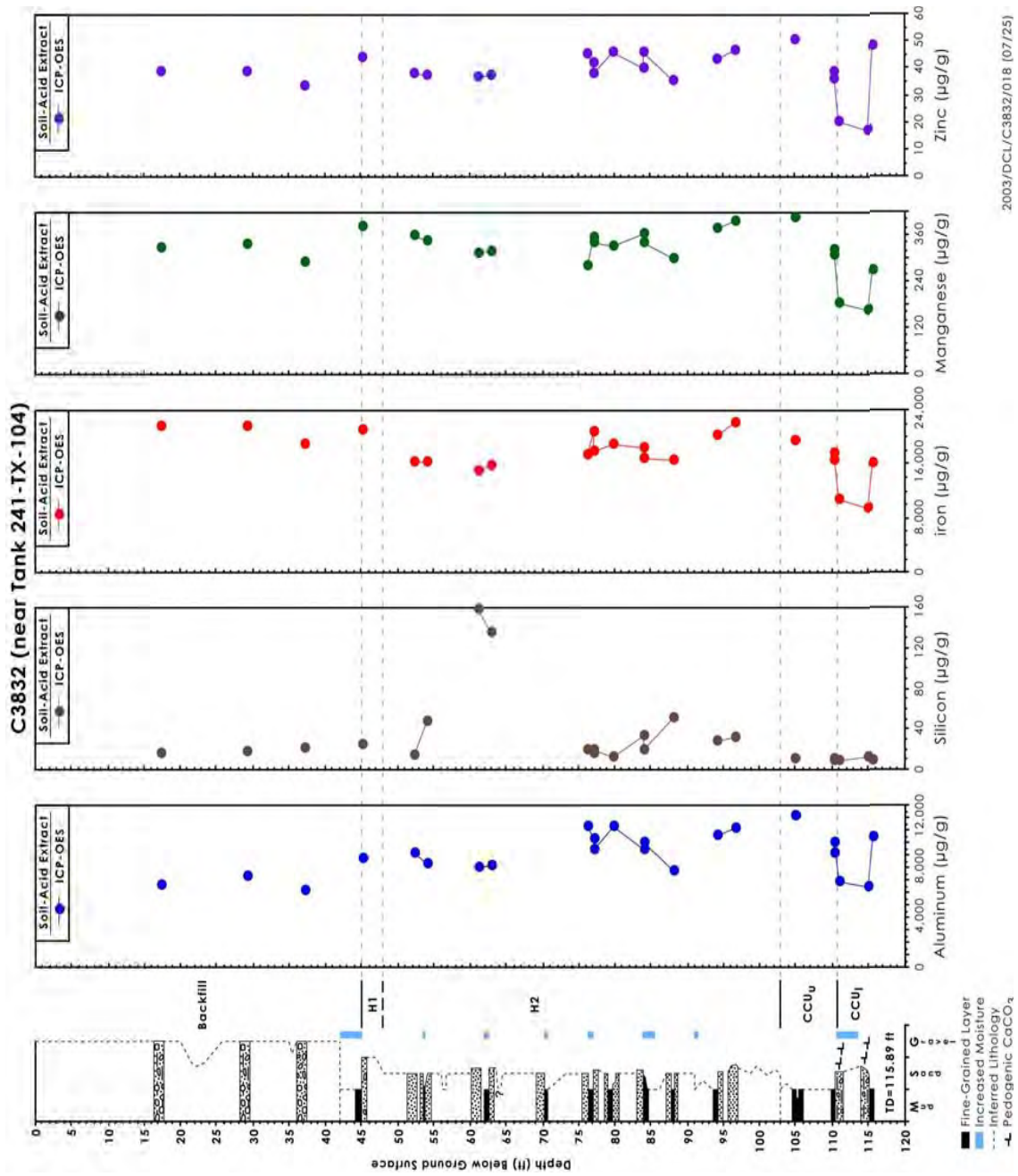
Figure 4.55. Acid-Extractable Metals in C3832 Vadose Zone Sediments (μg/g dry sediment)

4.148
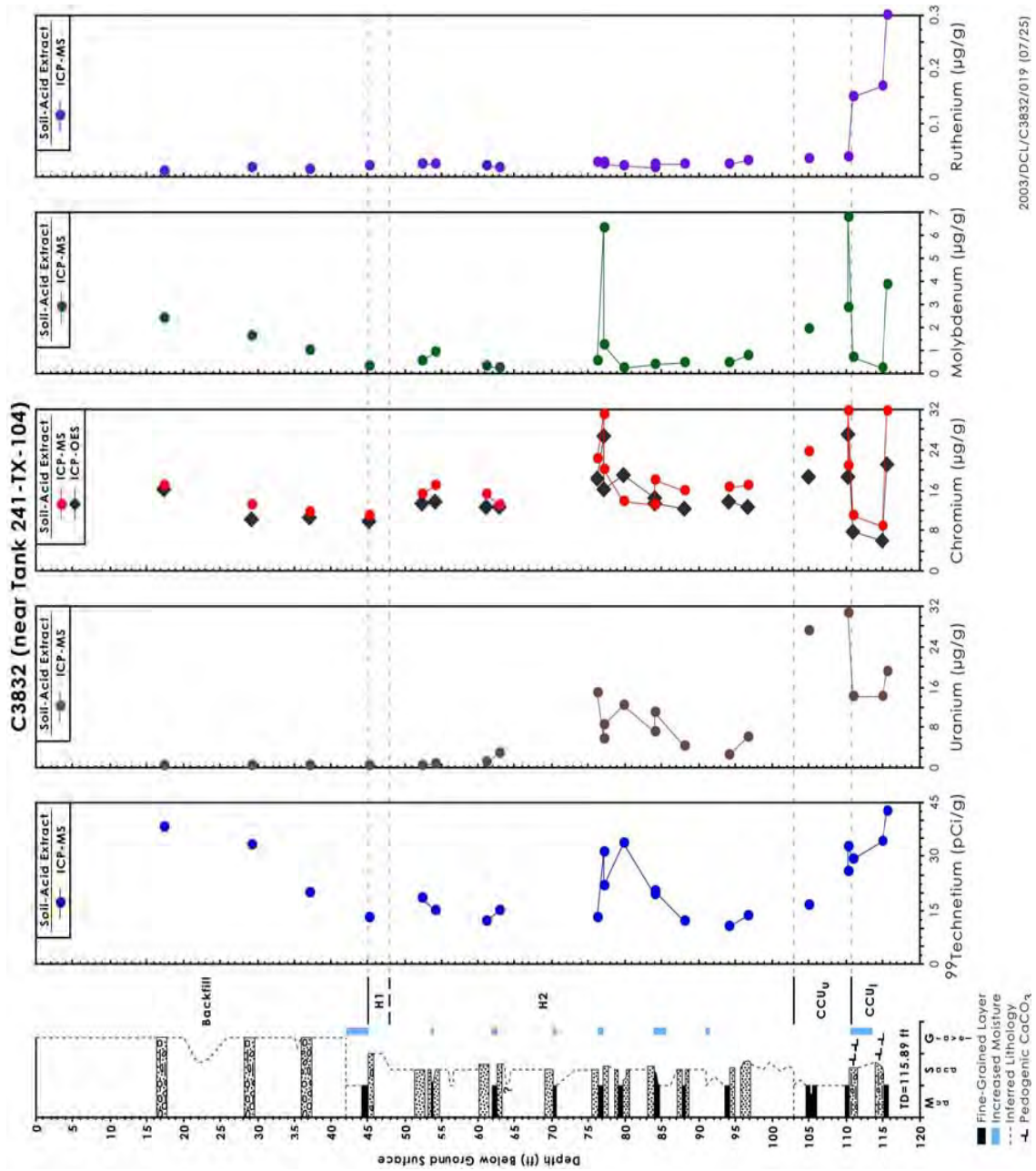
Figure 4.56. Acid-Extractable Trace Metals in C3832 Vadose Zone Sediments (units vary)

4.149
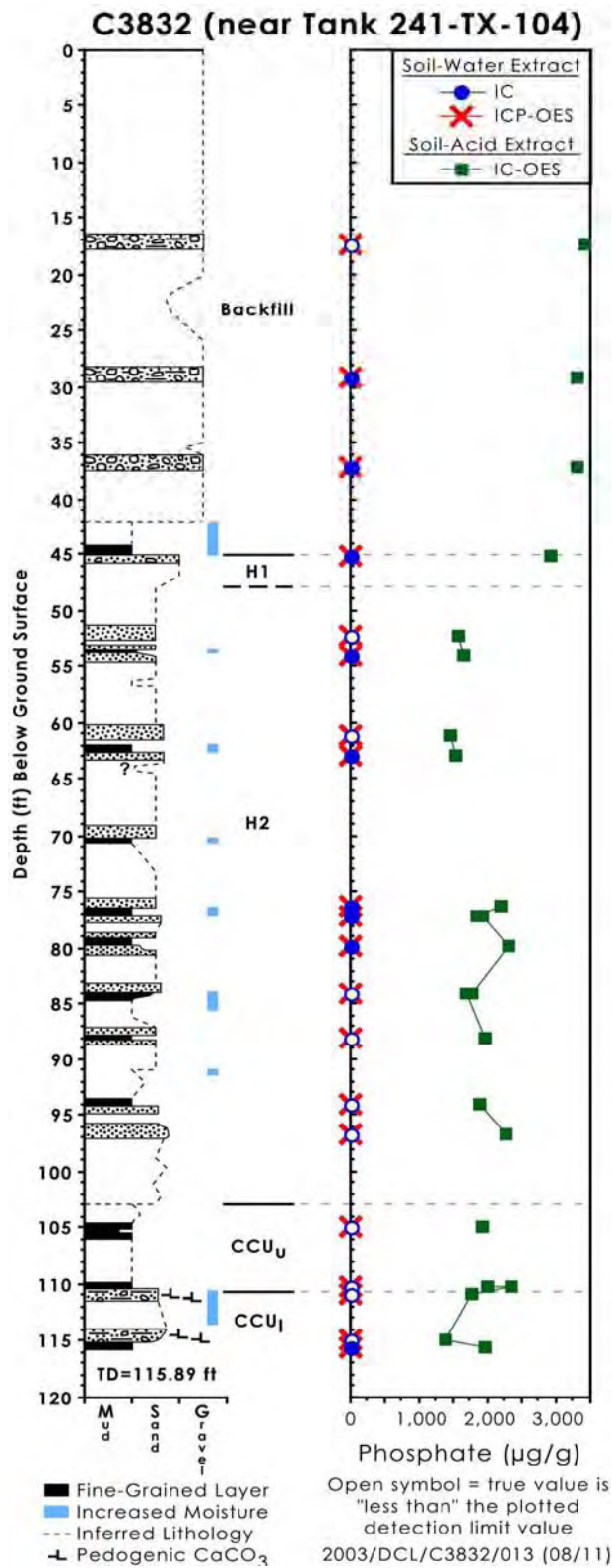
Figure 4.57.   Water- versus Acid-Extractable Phosphate in C3832 Vadose Zone Sediments

4.4.5   Radionuclide Content in Vadose Zone Sediment from C3832

Aside from the technetium-99 and uranium-238 data already presented, our gamma energy analyses of sediment from the B core liners found low concentrations of cobalt-60 and cesium-137 in the borehole C3832 sediments between the depths of 60 and 115 ft bgs (see Table 4.62). Aside from a small amount of surface cesium-137 contamination, the field logging results of the entire borehole casing did not find any other gamma emitting fission product contamination. Figures 4.58 and 4.59 show the laboratory results for natural potassium-40 and uranium-238 and the lab results for common gamma emitters, respectively. Where field-logging data was above detection limits, the log data are plotted also. The agreement between the field and lab generated data for gamma emitters is excellent. There are no man-made gamma emitters in the sediment profile above concentrations of a few tenths of a pCi/g excepting the uranium that is several pCi/g. It is possible that the low concentrations of cobalt-60 (between 0.5 and 1.2 pCi/g) found in the borehole C3832 sediments between 77 and 115 ft bgs are an extension of the tens of pCi/g values found in borehole C3831 sediments between the depths of 60 and 80 ft bgs. As shown in Figure 2.6, the bottom of the H2 strata does dip towards the southwest, which is the position of borehole C3832 in juxtaposition with borehole C3831. The uranium-238 concentrations in the sediment at borehole C3832 are greater than at borehole C3831, which suggests the plume at borehole C3832 is not an extension of the plume intercepted by borehole C3831.

Gross alpha and beta measurement were made on both the 1:1 sediment:water and sediment:acid extracts. With knowledge of the mass of dry sediment to extraction fluid used the data were converted to activity of gross beta and alpha leached per gram of dry sediment. None of the water or acid extracts of the 23 extracts (21 cores from selected depths and two duplicates) showed activities significantly greater than the detection limits for the procedures. For total beta analyses our detection limits for the water extracts were 10 to 20 pCi/g dry sediment and 5 to 10 pCi/g gram dry sediment for the acid extracts. For the total alpha analyses the detection limit for both extracts was 3 to 5 pCi/g dry sediment. Note that the efficiency of the total beta technique for the low energy technetium-99 is poor such that the total beta analyses can indicate no beta above 10 to 20 pCi/g, yet the ICP-MS measurements for the water and acid extracts for technetium-99 show that there may be 5 to 10 and 10 to 50 pCi/g of technetium-99, respectively, in the borehole C3832 sediments. We have more confidence in the accuracy of the water extract technetium-99 data.

4.4.6   Total Carbon, Calcium Carbonate, and Organic Carbon Content of Vadose Zone Sediment from Borehole C3832

The total, inorganic and organic carbon contents of the C3832 sediments are reported in Table 4.63. The lower Cold Creek subunit (caliche) samples obtained between 111 and 115.54 ft bgs contain significant amounts of calcium-carbonate equivalent material with 38 to 46% by weight. The deepest sediment from the upper Cold Creek subunit at 105 ft bgs and a Hanford H2 sample at 84 ft bgs also contains about 3% by weight calcium-carbonate content. As found in most vadose sediments from the Hanford Reservation, there is very little (<0.1% by weight) organic carbon in the vadose zone sediments.

The caliche at borehole C3832 has the most calcium-carbonate equivalent solid of all three boreholes and the uncontaminated background sediment from 299-W10-27 based on available samples. The calcium-carbonate content ranges from 20 to 34% at borehole C3830, 22% at 299-W10-27, 38% at borehole C3831, and 38 to 46% at borehole C3832. Such variability is considered "normal" for paleosols at the Hanford Site.

Table 4.62. Gamma Emitter Concentrations in Vadose Zone Sediments in Borehole C3832 (pCi/g)

Sample No.	Depth (ft bgs)	Stratigraphic Unit	Co-60	Cs-137	U-238
15B	16.56	backfill	<0.042	<0.047	1.12
28B	28.44	backfill	<0.034	0.081	<0.915
37B	36.44	backfill	<0.033	<0.040	3.71
44B	44.49	backfill	<0.052	0.099	3.28
52B	51.46	H2	<0.037	0.061	1.65
53B	53.42	H2	<0.059	<0.067	3.16
61B	60.47	H2	<0.038	0.091	<1.30
62B	62.16	H2	0.037	<0.050	8.67
69B	69.34	H2	<0.049	<0.054	6.12
76B	76.34	H2	0.15	0.052	5.55
79B	78.80	H2	0.32	<0.017	2.90
83B	83.33	H2	0.78	<0.060	6.08
87B	87.35	H2	0.14	0.037	5.57
93B	93.35	H2	0.26	0.078	7.67
96B	95.99	H2	0.31	0.043	9.35
104B	104.30	CCU_u	0.18	0.019	<1.33
110B	110.28	CCU_u	0.22	<0.050	18.29
114B	114.13	CCU_l	0.25	0.058	3.14
121B	114.83	CCU_l	0.22	0.044	4.83
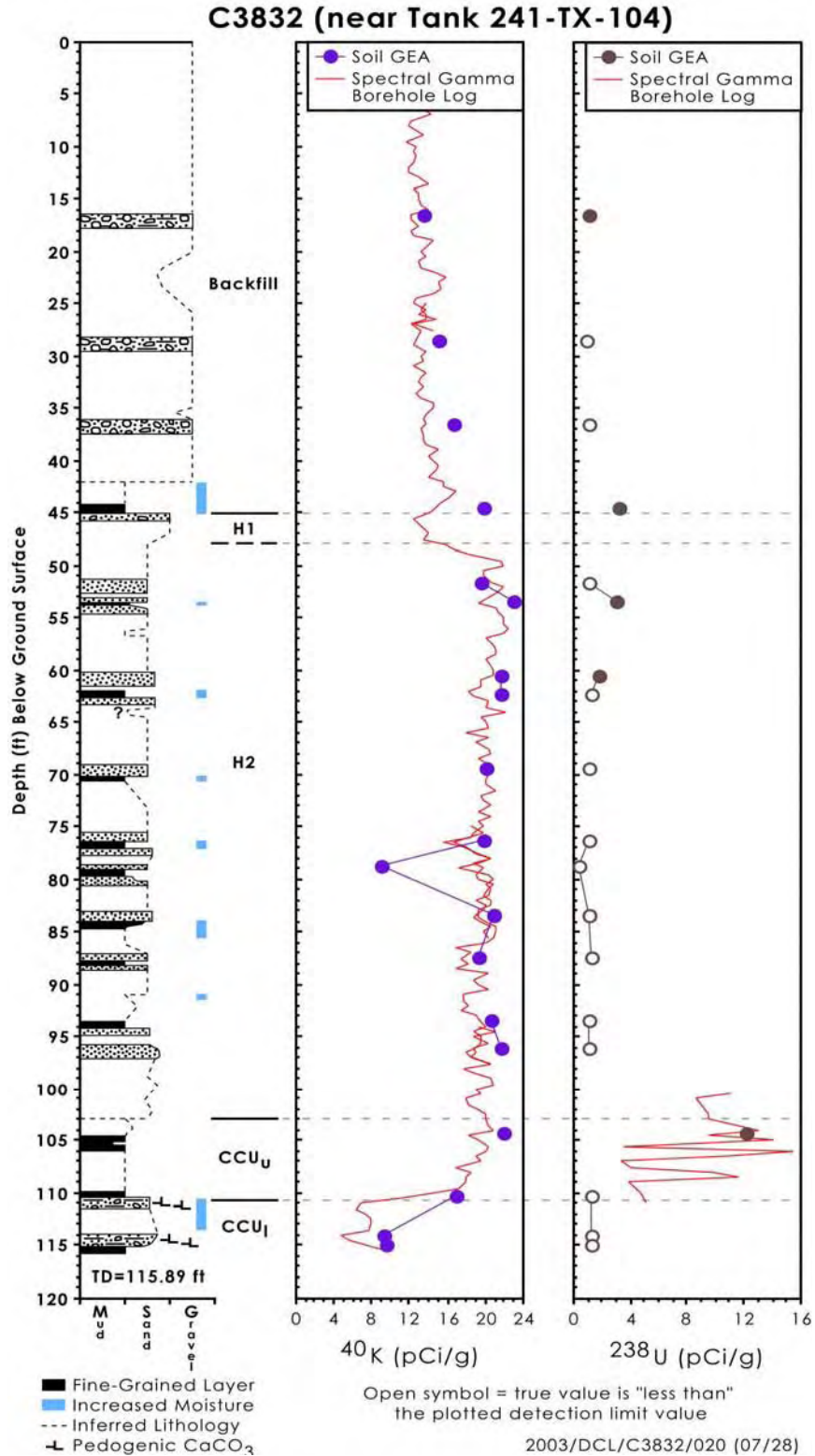
Figure 4.58. Comparison of Lab Gamma Energy Analysis (GEA) and Field Log for Natural Gamma Emitters

4.153
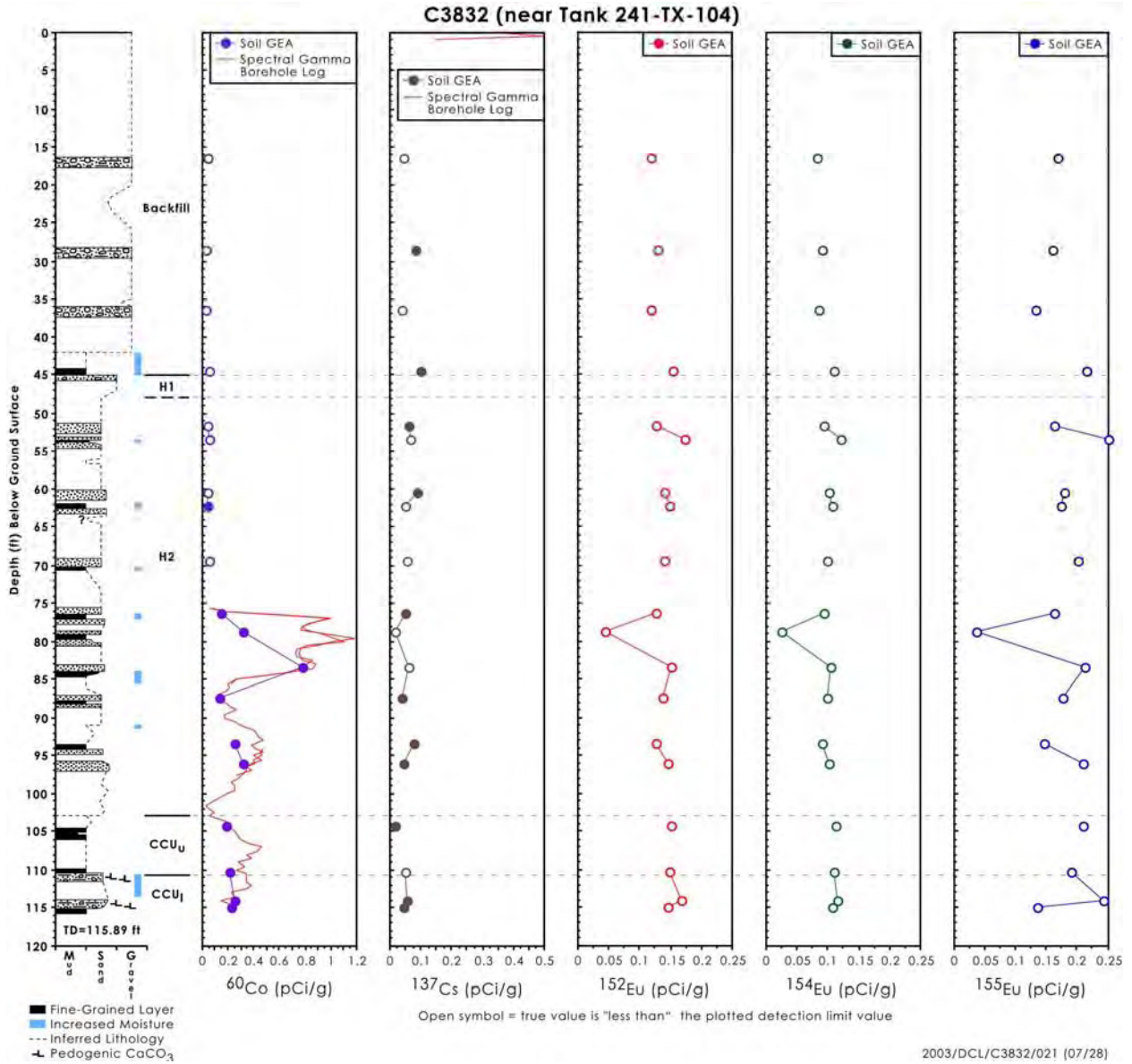
Figure 4.59. Lab and Field Data for Common Gamma Emitters in C3832 Vadose Zone Sediments

Table 4.63. **Carbon Contents of Vadose Zone Sediments in Borehole C3832**

Sample No.	Depth (ft bgs)	Stratigraphic Unit	Total Carbon %	Inorganic Carbon (IC) %	IC as CaCO$_3$ %	Organic Carbon % (by diff.)
15A	17.26	Backfill	0.17	0.06	0.51	0.11
28A	29.14	Backfill	0.17	0.07	0.56	0.11
37A	37.14	Backfill	0.15	0.06	0.54	0.08
44A	45.19	Backfill	0.34	0.24	2.00	0.10
52A	52.01	H2	0.26	0.21	1.71	0.05
53A	54.10	H2	0.23	0.18	1.52	0.05
61A	61.17	H2	0.21	0.16	1.33	0.05
62A	62.96	H2	0.24	0.19	1.59	0.05
69A	69.99	H2	0.25	0.21	1.78	0.03
76A	77.04	H2	0.24	0.17	1.45	0.07
79A	79.81	H2	0.28	0.22	1.87	0.05
83A	84.01	H2	0.36	0.32	2.65	0.05
87A	88.06	H2	0.16	0.13	1.07	0.03
93A	94.05	H2	0.20	0.17	1.41	0.04
96A	96.69	H2	0.29	0.24	1.98	0.05
104A	105.01	CCUu	0.44	0.39	3.23	0.05
110A	111.02	CCUl	4.95	4.69	**39.10**	0.26
114A	114.85	CCUl	5.74	5.48	**45.64**	0.26
121A	115.54	CCUl	4.63	4.52	**37.66**	0.11

Bold type represents samples with caliche present.

5.0   Groundwater Status Below the TX Tank Farm

This section summarizes historical as well as recent groundwater data from the uppermost, unconfined aquifer in the vicinity of WMA TX-TY. The data then are used to describe the nature and extent of contamination in the area. The primary focus of this effort is to relate ambient groundwater contamination to releases from waste storage and disposal facilities within or near the Waste Management Area (WMA). Accordingly, historical water levels and flow directions, and contaminant histories in key wells near the WMA are reviewed as background information to better understand the current groundwater contaminant distribution patterns and their relationship to possible waste management area sources.

Selected ratios of mobile contaminants in 1) the vadose zone sediments sampled by the three boreholes, C3830, C3831, and C3832 (see Section 4), 2) the groundwater, and 3) specific single-shell tanks, cribs and trenches at the time of suspected leaks and disposal campaigns, respectively, are used to assess whether there are indications that the groundwater contamination is related to current vadose zone contamination below a specific facility or to chemistry in the tanks at the time of suspected leaks. Figure 5.1 shows the location of all wells discussed in this section.

5.1   Aquifer Properties

This section provides information on the properties of the uppermost, unconfined aquifer in the immediate region of WMA TX-TY. Aquifer properties were determined from stratigraphic interpretations, current water level elevations, and aquifer testing.

Beneath the 200 West Area, the suprabasalt aquifer system contains the uppermost, unconfined aquifer and the underlying Ringold confined aquifer. Deeper confined and semi-confined aquifer systems also exist beneath these sedimentary aquifers in the basalt flow tops, flow bottom zones, and sedimentary interbeds (DOE 1988). Groundwater flow, both vertically and horizontally, in the suprabasalt aquifers is less constrained than in the deeper basalt aquifers.

The suprabasalt aquifers below the Hanford Reservation have been impacted by past practice, liquid waste disposal operations, and unplanned releases, in some instances from single-shell tank leaks. In the area of WMA TX-TY, large volumes of waste water disposed to the ground between the 1940s and 1997 created large artificial groundwater mounds, particularly beneath the 216-T pond system, north of WMA TX-TY, and beneath the 216-U pond, southwest of WMA TX-TY. The disposed liquids contained many of the contaminants that now move through the upper unconfined aquifer. Water mounding has declined significantly since the 1997 cessation of non-permitted liquid waste disposal.

The following discussion focuses on the uppermost, suprabasalt aquifer system within the Ringold and Hanford formations. The suprabasalt aquifers are the uppermost regionally extensive aquifers beneath the WMA TX-TY. Groundwater within this aquifer system is contained within the fluvial-lacustrine sediments of the Ringold Formation.

Only one well, 299-W11-13, near WMA TX-TY extends to the top of basalt and has recent water level data. (Well 299-W11-13 is located about 275 m east of the 241-TY tank farm.) Based on the March 2003 water table elevation, the suprabasalt aquifer system is approximately 73-m thick at this well.
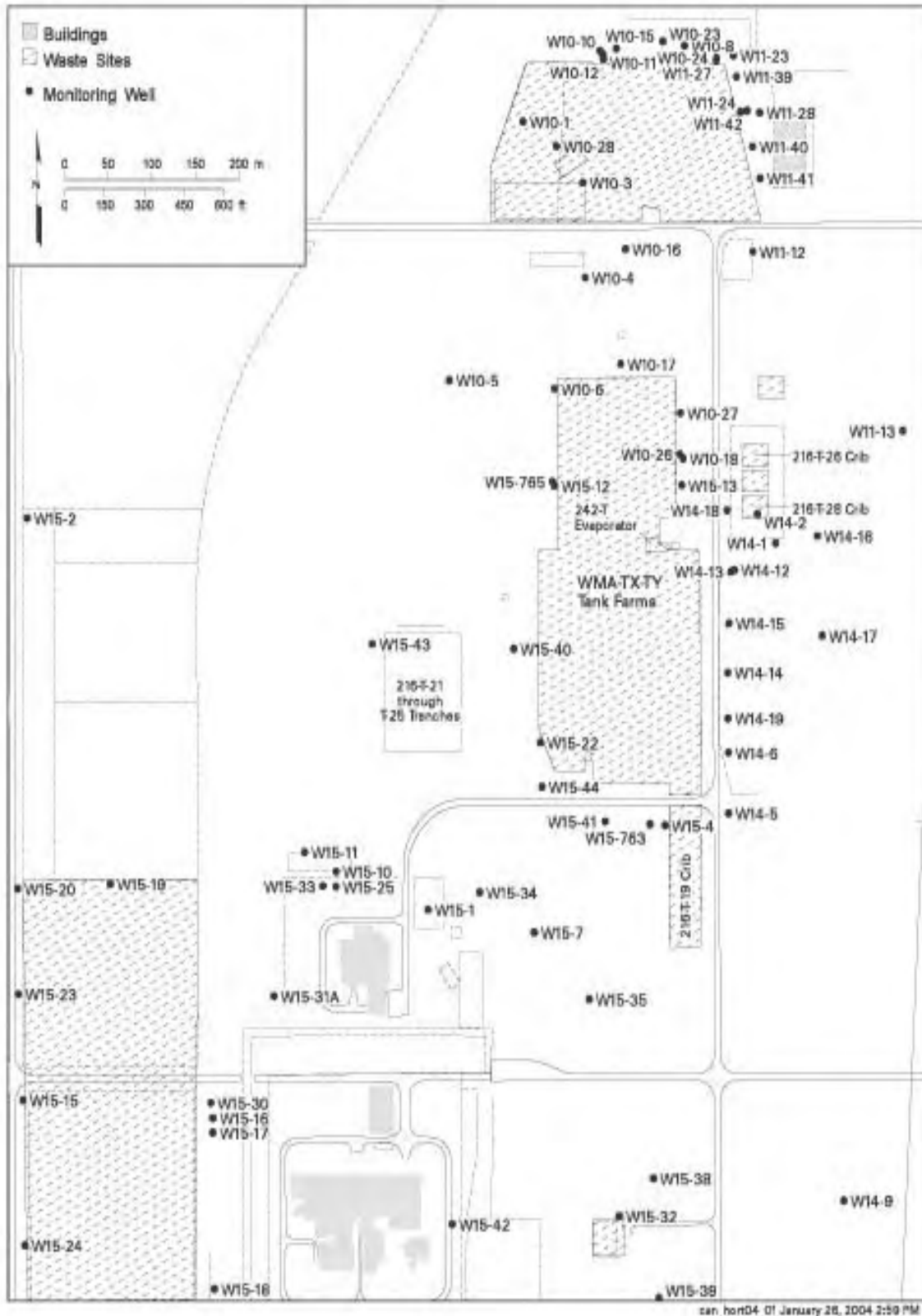
Figure 5.1. Well Location Map for WMA TX-TY

The base of the uppermost, unconfined aquifer generally is regarded as the basalt surface and, where this is the case, the entire suprabasalt aquifer is unconfined. However, beneath WMA TX-TY (and beneath the entire 200 West Area), the silt and clay deposits of the Ringold Formation lower mud unit (hydrogeologic unit 8 of Williams et al. [2002]) form a confining layer that separates the suprabasalt aquifer into the uppermost, unconfined aquifer and the underlying, Ringold confined aquifer (Williams et al. 2002). Thus, the uppermost, unconfined aquifer in the area of interest extends from the water table down to the top of the lower mud unit. The unconfined aquifer is about 55-m thick at well 299-W14-14, east of WMA TX-TY, based on the August 2003 water level. The unconfined aquifer consists of sandy gravels and gravelly sands of the Ringold Formation member of Wooded Island unit E (hydrogeologic unit 5 of Williams et al. 2002). The Ringold confined aquifer is 18-m thick based on the 2003 data. All wells in the WMA TX-TY monitoring networks are screened in hydrogeologic unit 5. Currently, the water table at WMA TX-TY is 136 to 137 m above sea level.

Water levels in the uppermost, unconfined aquifer raised as much as 13.5 m (above the pre-Hanford natural water table) beneath WMA T and TX-TY because of artificial recharge from liquid waste disposal operations active since the mid-1940s. The largest volumes of discharge were to the 216-T pond system and the 216-U-10 pond. Figure 5.2 shows the liquid discharge history for the two ponds. The 216-T pond system is estimated to have received approximately 424 billion liters of effluent (Alexander et al. 1995) and the 216-U pond to have received about 158 billion liters of effluent (Last 1994). The large-volume disposals to the ponds (and lesser volumes to cribs and ditches) artificially recharged the uppermost unconfined aquifer, creating large water-table mounds. The increase in water-table elevation was most rapid from 1949 to 1956, and was somewhat stabilized between the late 1960s and the late 1980s. Water levels began to decline in the late 1980s beneath WMA T and TX-TY when wastewater discharges in the 200 West Area were reduced. The decline in water levels may have implications for the groundwater monitoring network at WMA TX-TY, as discussed later.
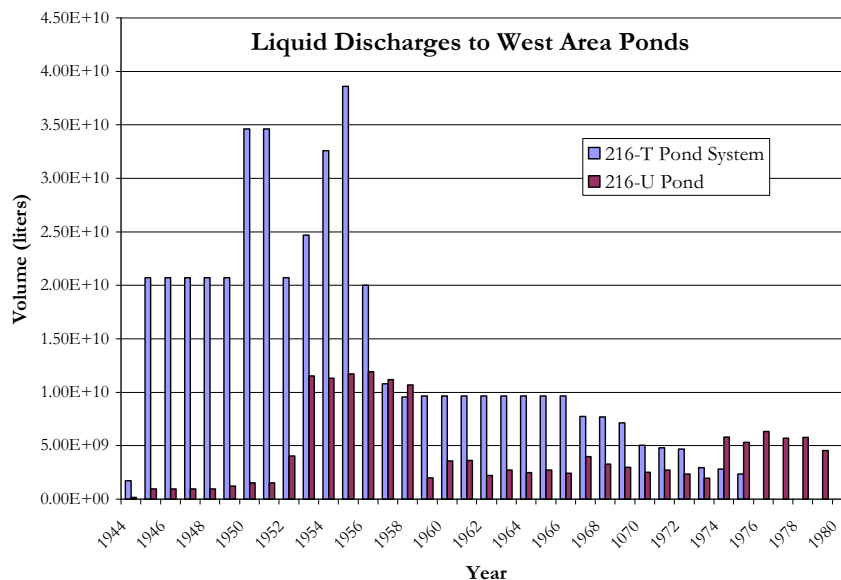
Figure 5.2. **Discharge History for the 216-T Pond and the 216-U Pond. Data for the 216-T Pond are from Alexander et. al 1995 and Data for the 216-U Pond are from Last 1994**

5.3

Accompanying the changes in water level were changes in groundwater flow direction. Pre-Hanford Site groundwater flow direction was toward the east (Kipp and Mudd 1974). Figure 5.3 contains hydrographs that show that groundwater flow had changed toward the south in the area in the late 1940s and early 1950s. This shift resulted from disposal of large volumes of liquid to the 216-T pond system. In 1956, groundwater flow direction changed again and started flowing towards the north due to the increasing influence of the groundwater mound under 216-U pond and a decreasing influence of the mound under 216-T pond. Discharges to 216-T pond ended in 1976 but continued at 216-U pond until 1984. Consequently, the flow direction changed again in about 1996 when all non-permitted discharges to the ground ceased and the influence of the 216-U pond mound on the groundwater beneath the TX and TY tank farms diminished. Around 1996, the groundwater flow direction began to return toward the east or southeast.

Hydrographs
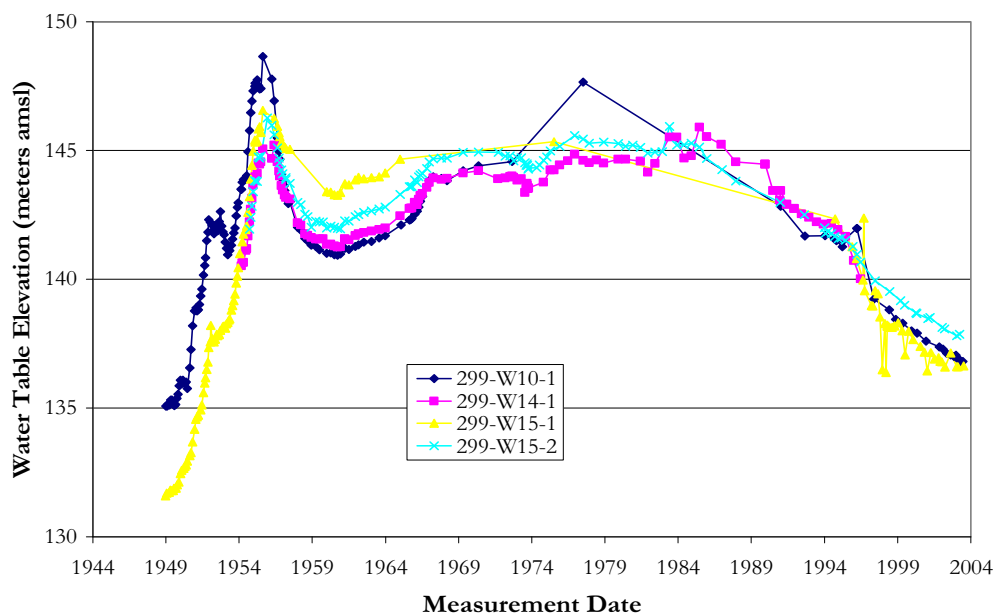
Figure 5.3. **Hydrographs of Selected Wells in North 200 West Area.**
See Figure 5.1 for Locations of Wells

These large shifts in groundwater flow direction have large implications for contaminant distribution in the uppermost aquifer beneath WMA TX-TY. In the late 1940s and early 1950s, contamination was spread south in the aquifer. Then, in the late 1950s and until the mid-1990s, that same contamination returned to the north along with any new contamination that entered the aquifer after the 1950s. Today, groundwater contamination beneath the WMA and the surrounding area is generally migrating east.

Figure 5.4 and 5.5 show hydrographs for monitoring wells around the TX and TY tank farms. These hydrographs and the regional water table map (Figure 5.6) show that the groundwater flow direction beneath the TY tank farm and the northern and central parts of the TX tank farm is currently toward the southeast. Groundwater flow beneath the southern part of the TX tank farm, which is strongly influenced by the 200-ZP-1 pump-and-treat system, is toward the south, or possibly the south-southwest. (The nearest 200-ZP-1 extraction wells to the TX tank farm are shown as open triangles on the water table map in Figure 5.6.)
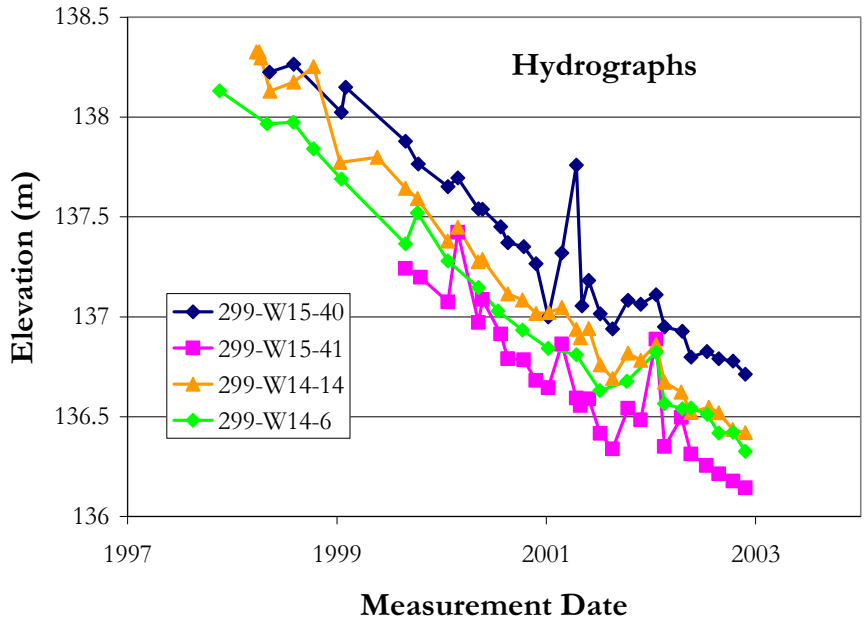
Figure 5.4. **Water Levels in Selected Wells Around the TX Tank Farm. See Figure 5.1 for Well Locations**
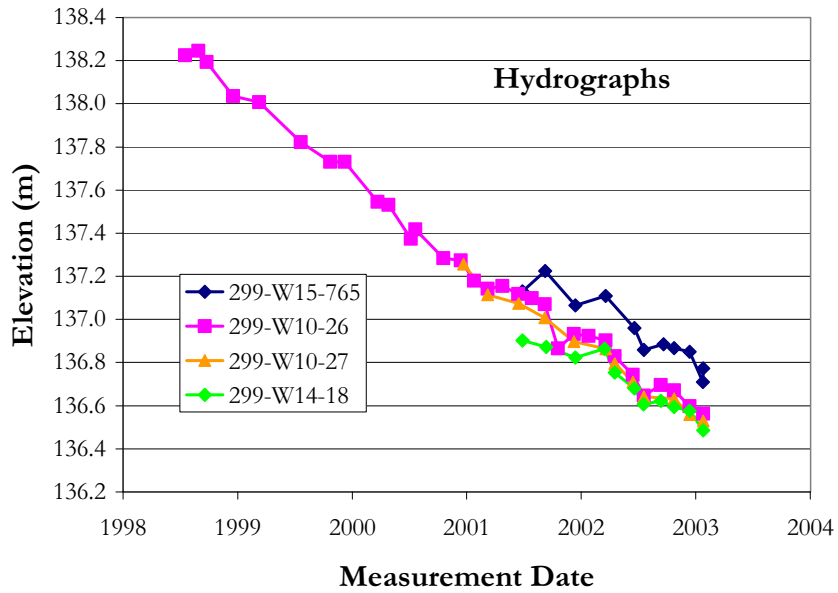
Figure 5.5. **Water Levels in Selected Wells Around the TY Tank Farm. See Figure 5.1 for Well Locations**
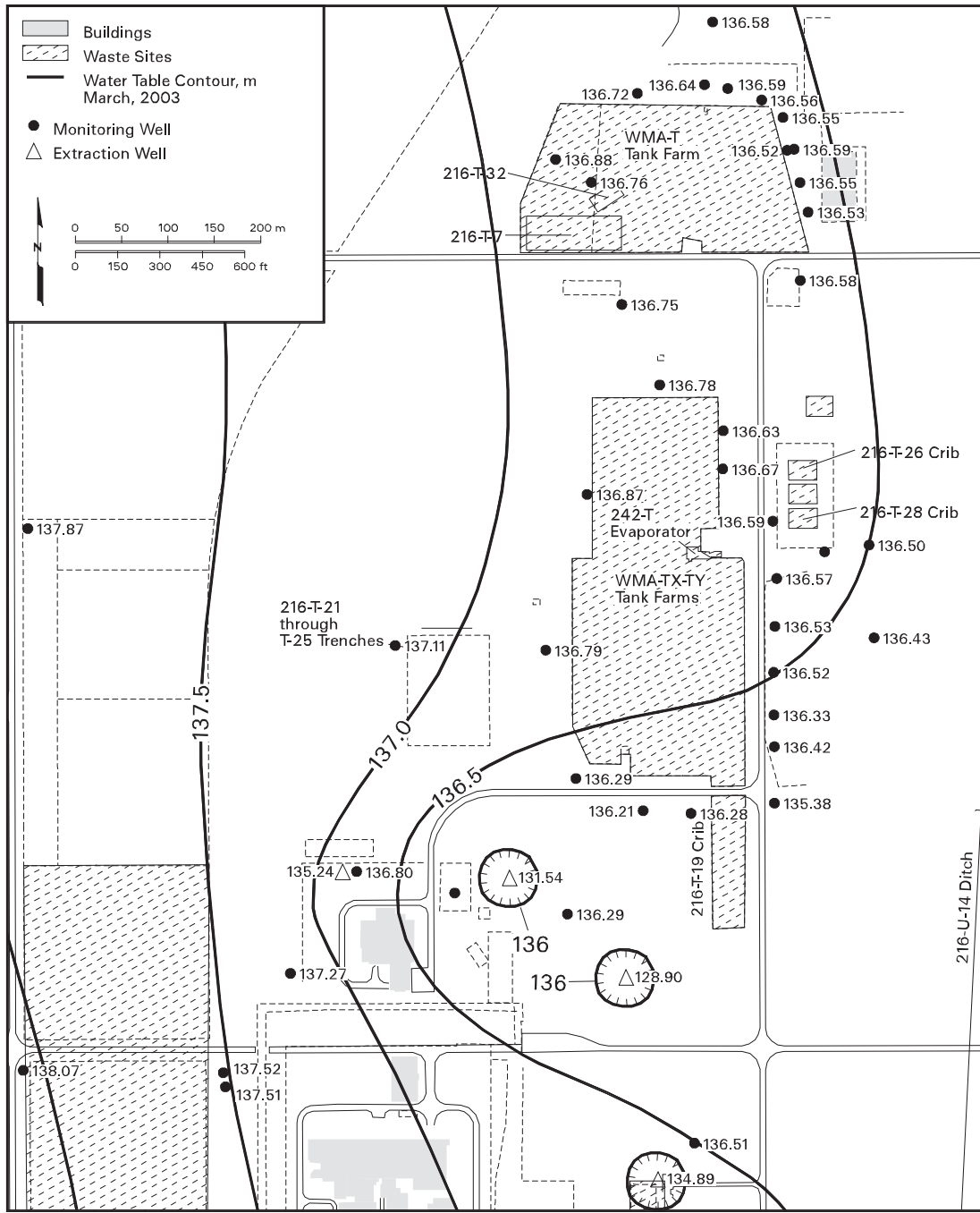
Figure 5.6.   March 2003 Water Table Map for the WMA TX-TY Area

Four trend-surface analyses of the water table have been done at WMA TX-TY in recent years (Table 5.1). One trend-surface analysis of the water table was done at well 299-W10-26 east of the TY tank farm area using May 1999 water levels. The analysis yielded a flow direction 72 degrees east of south (S 72° E) and a gradient of 0.00073 (Spane et al. 2001a). The calculated flow direction is somewhat more southerly than the flow direction indicated by the latest water table map (Figure 5.6).

The most northern analysis at the TX tank farm was done at well 29-W14-13 and gave the same flow direction (S 72° E) and hydraulic gradient (0.00073) as obtained for the analysis of well 299-W10-26 at TY tank farm. (This is because the same data set, except for the subject well, was used in both analyses.) A flow direction of S 72° E at this well is in good agreement with the water table map.

Further south, along the downgradient side of the TX tank farm, groundwater flow direction changes from S 72° E at well 299-W14-13, to S 64° E to S 59° E at well 299-W-14-15 (Spane et al. 2001a, 2002). Still further south, at well 299-W14-14, a trend analysis indicates a flow direction of S 47° E (Spane et al. 2003). The flow directions from the trend surface analyses are in general agreement with the current water table map (Figure 5.6). These data show that the groundwater flow direction becomes increasingly more southerly toward the south. Groundwater beneath this part of the WMA is obviously influenced by the extraction wells of the 200-ZP-1 pump-and-treat system. Figure 5.6 shows the location of the nearest extraction wells for this pump-and-treat to WMA TX-TY.

Table 5.1. **Groundwater Flow Characterization Results Based on Trend Surface Analyses.** **(Data are from Spane et al. 2001a, 2002, and 2003)**

Well	Measurement Date	Groundwater Flow Direction	Hydraulic Gradient	Wells Used in Analysis
TX Tank Farm				
299-W14-13	5/3/99	S 72° E	0.00073	299-W10-17 299-W10-18 299-W14-12 299-W15-12 299-W15-22
299-W14-14	7/12/02	S 47° E	0.00114	299-W14-13 299-W14-15
	7/22/02	S 47° E	0.00109	299-W14-16 299-W14-17
299-W14-15	7/30/01	S 59° E	0.00135	299-W14-13 299-W14-14
	8/2/01	S 64 ° E	0.00140	299-W14-16 299-W14-17
TY Tank Farm				
299-W10-26	5/3/99	S 72° E	0.00073	299-W10-17 299-W10-18 299-W14-12 299-W15-12 299-W15-22

Borehole tracer dilution and tracer pumpback tests were conducted in one new RCRA monitoring well at TY tank farm (299-W10-26) and two new RCRA wells (299-W14-13 and 299-W14-14) at TX tank farm between fiscal years 1999 and 2002. These tests permitted some inferences about flow rate as well as aquifer homogeneity. The tests allowed direct observation of the effect of lateral groundwater

flow through the screened interval of the wells, and, thus, provided an indication of the variability of flow through the screened intervals. Details of the test methods, computations, and the results are included in Spane et al. 2001a, 2001b, 2002, and 2003.

A significant finding of the tracer dilution test results is evidence for downward, vertical hydraulic gradients within the upper portion of the aquifer in wells 299-W10-26, 299-W14-13, and 299-W14-14. Vertical flow within these wells was first indicated by tracer-dilution studies in 1999 and later confirmed, also in 1999 (for two of the wells), by vertical tracer tests specifically designed to detect vertical flow within a borehole (Spane et al. 2001a, 2003). Downward vertical flow in these two wells was subsequently confirmed by electromagnetic flow-meter surveys in 2000 (Waldrop and Pearson 2000). The electromagnetic flow-meter surveys found that the depth of maximum downward flow was at 4.9 m below the water table in well 299-W10-26 and at 5.6 m below the water table in well 299-W14-13. Hydrogeologic data from all three tests are shown in Table 5.2.

Table 5.2. **In-Well, Downward Vertical, Flow-Velocity Summary for Wells 299-W10-26 and 299-W-14-13 at WMA TX-TY (Spane et al. 2001a; Spane et al. 2003)**

Test Well	Tracer-Dilution Profile		Vertical Tracer Test[a]		Electromagnetic Flow-Meter Survey	
	Range (m/min)	Average (m/min)	Range (m/min)	Average (m/min)	Range (m/min)	Average (m/min)
TY Tank Farm						
299-W10-26	0.002 – 0.004	0.003	0.004 – 0.008	0.005	0.003 – 0.006	0.004
TX Tank Farm						
299-W14-13	0.008 – 0.015	0.011	0.013 – 0.014	0.012	0.012 – 0.013	0.012
299-W14-14	0.0054 – 0.0058	0.0056	ND	ND	ND	ND
(a) In-well, vertical, flow-velocity range calculated using tracer peak arrival method for selected sensor depth, while the average was determined using the center-of-mass technique.						
ND = Not Determined						

All three wells that show in-well, vertical flow have fairly homogeneous lithology throughout the screened interval and the well development drawdown data do not indicate substantial variations in hydraulic conductivity. The existence of vertical flow in a well does not necessarily reflect actual groundwater flow conditions within the surrounding aquifer, but its presence implies a vertical flow gradient and has implications pertaining to the representativeness of groundwater samples collected from the wells. The vertical gradient detected in some wells along the eastern edge of the TX and TY tank farms may have an impact on contaminant distribution patterns in the area. (See Section 5.2.1.4 for discussion of possible causes of vertical flow within these wells.)

A second finding of the hydrologic test data is the suggestion of higher hydraulic conductivity at certain depths within the screened interval of some wells relative to other depths. Aquifer tests in well 299-W15-41, located just south of the TX tank farm, indicate that the middle and lower parts of the screened interval have higher permeability than the upper part (Spane et al. 2001b). However, development pumping data (which is not as definitive as aquifer testing) indicate that the upper part of the

screened interval in nearby well 299-W15-763 has higher permeability than the lower parts (Horton 2002). Thus, apparent differences in hydraulic conductivity do not appear to correlate from well to well.

For the WMA TX-TY groundwater assessment, new hydraulic conductivity data were obtained from slug tests and drawdown tests conducted in 11 new wells drilled since 1999. Effective porosities were determined from tracer drift and tracer pumpback tests. Hydraulic properties are discussed in detail by Spane et al. 2001a, 2001b, Spane 2002, and Spane et al. 2003 and are presented in Tables 5.3 and 5.4.

Table 5.3 shows horizontal groundwater flow velocities determined from tracer pumpback tests. These velocities are about an order of magnitude greater than the calculated velocities in Table 5.4 for wells 299-W10-26, 299-W14-13, and 299-W14-14, all of which have downward vertical flow in the well. The vertical flow in these wells probably resulted in overestimation of measured flow velocities. Both the measured and calculated velocities are about the same for well 299-W15-41, which has no vertical flow. The relatively high Darcy velocity in well 299-W15-41 is probably due to the relatively high gradient caused by the 200-ZP-1 pump-and-treat extraction wells.

The horizontal velocity in well 299-W14-15 is substantially greater than the velocity calculated for any other wells. Very rapid recovery during slug testing was noted, which suggests a fairly permeable formation (Spane et al. 2002). Pumping tests at well 299-W14-15 did not cause significant drawdown when the well was pumped at 73.2 liters per minute for 285 minutes, which also indicates a relatively permeable formation (Spane et al. 2002). However, there is nothing in the geologist's log to suggest that the formation in the screened interval of well 299-W14-15 is significantly different than the formation at nearby wells. Conversely, slug tests in well 299-W10-27 resulted in extremely long response recoveries indicating low permeability and, thus, a slow groundwater flow velocity. Overall, the calculated Darcy velocities from tests in new wells show approximately one order of magnitude variation in the data.

Taken as a whole, the geologist's logs, geophysical logs, development pumping data, and the hydrologic testing data all indicate heterogeneity in aquifer properties within the screened intervals of several individual wells and among wells at WMA TX-TY. No widespread trends have been identified.

The hydrographs in Figure 5.7 show that water levels have declined by about 6 m since 1991 beneath the TX and TY tank farms. This decline, resulting from decreasing effluent discharge in the 200 West Area, became much steeper in 1995 with the effective cessation of discharge to all non-permitted facilities in this area. Between 1998 and 2003 the average rate of water table decline was between about 0.3 and 0.4 m per year in all monitoring wells at WMA TX-TY. The rapid decrease in water levels after 1995 has resulted in monitoring wells going dry more than previously predicted and has necessitated the drilling of 14 new monitoring wells since 2000.

The pre-Manhattan Project water table was postulated to be at approximately 123 m above sea level by Kipp and Mudd (1974). More recently, Bergeron and Wurstner (2000) modeled the elevation of the water table beneath the Hanford Site for the Immobilized Low-Activity Waste Performance Assessment. Their results predict a water table elevation between about 130 and 132 m above sea level in the TX and TY tank farm area for post-Hanford Site influence.

Table 5.3. Results from Tracer-Dilution and Tracer-Pumpback Tests in Wells at WMA TX-TY (Spane et al. 2001a, 2001b, Spane et al. 2002; Spane et al. 2003)

Well	Effective Porosity[a]	Groundwater[a] Flow Velocity (m/d)	Average In-Well Flow Velocity[b]
TY Tank Farm			
299-W10-26[c]	0.010	0.124	0.086
TX Tank Farm			
299-W14-13[d]	0.009	0.191	ND[e]
299-W14-14[c]	0.020	0.122	0.041
299-W14-15	0.002	1.1	0.119
299-W15-41	0.068	0.374	0.311
(a) Data from tracer pumpback tests.			
(b) Data from tracer dilution tests.			
(c) Slight downward vertical flow, data uncertain.			
(d) Strong downward vertical flow, data highly uncertain.			
(e) ND = Not Determined.			

Table 5.4. Hydraulic Properties from Slug and Constant Rate Pumping Tests and Calculated Darcy Velocities at New Wells at WMA TX-TY

Well	Hydraulic[a,b] Conductivity (m/d)	Hydraulic[a,c] Conductivity (m/d)	Transmissivity[a,c] (m²/d)	Specific[a,c] Yield	Calculated Flow Velocity (m/d)
TY Tank Farm					
299-W10-26	1.39 – 1.95	1.49	82	0.14	0.014[d]
299-W10-27	0.05 – 0.07	ND	ND	ND	0.0007[e]
TX Tank Farm					
299-W14-13	1.66 – 2.43	2.45	135	0.12	0.020[d,]
299-W14-14	2.31 – 3.22	2.21	121	0.12	0.027[d]
299-W14-15	3.52 – 4.92	4.09	225	0.01	2.46[f]
299-W14-16	3.90 – 5.08	ND	ND	ND	0.051[e]
299-W14-17	3.71 – 4.89	ND	ND	ND	0.489[e]
299-W14-18	0.39 – 0.54	ND	ND	ND	0.005[e]
299-W15-40	0.88 – 1.22	ND	ND	ND	0.012[e]
299-W15-41	14.2 – 19.9	19.6	1130	0.12	0.29[f]
299-W15-763	0.71 – 0.93	ND	ND	ND	0.009[e]

(a) Data from Spane et al. 2001a,b, Spane et al. 2002, and Spane et al. 2003)

(b) Slug test data.

(c) Constant rate pumping test data.

(d) Estimated using maximum hydraulic conductivity value, a gradient of 0.001, and specific yield from this Table. Specific yield was used because downward flow in the well resulted in uncertain effective porosity.

(e) Estimated using maximum hydraulic conductivity value, a gradient of 0.001 and effective porosity values of 0.1.

(f) Estimated using maximum hydraulic conductivity value, a gradient of 0.001, and effective porosity value from Table 5.3.

(g) Indicates average hydraulic conductivity obtained from high-permeability, non-linear type-curve analysis method.

ND = Not Determined.
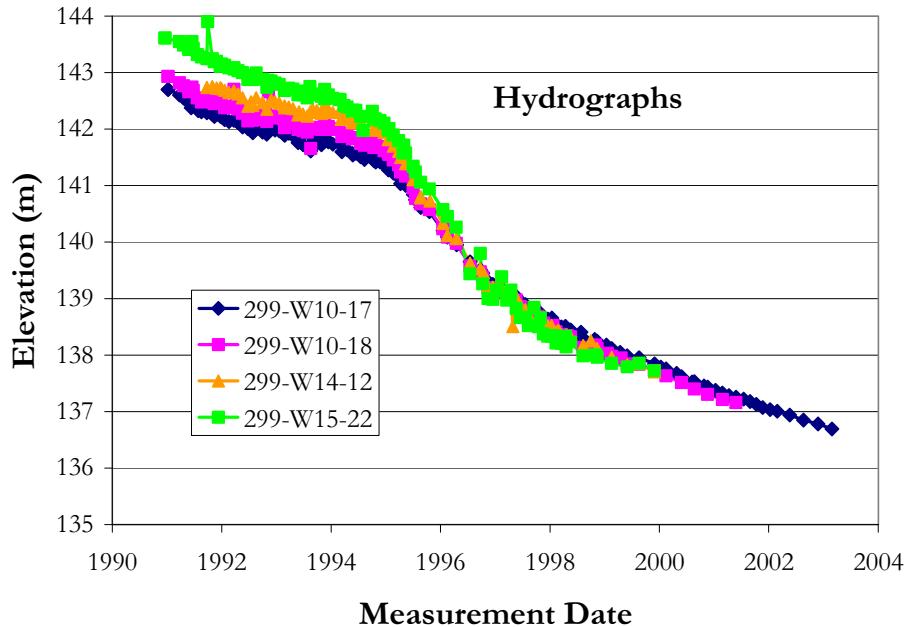
Figure 5.7. **Historical Water Level Data from Wells at WMA TX-TY. All Wells Used in the Figure Are Now Dry**

5.2 Existing Groundwater Contamination

This section discusses the current and historical groundwater contamination at WMA TX-TY. The evaluation of contamination includes descriptions of the types and concentrations of contaminants in the groundwater, the depth distribution of contaminants in the aquifer, and the areal extent of contamination in the area.

Monitoring results from new and existing wells, results of depth sampling during and after installation of new monitoring wells, and comparison of groundwater chemistry in old wells and their adjacent replacement wells, provide new insights into the occurrence and nature of groundwater contamination in the TX and TY tank farm area. The information given in this section is taken largely from Horton (2002) and is updated with more current groundwater data.

Groundwater at the TX and TY tank farms contains elevated concentrations of carbon tetrachloride (CCl_4), chromium (Cr), iodine-129 (I-129), nitrate (NO_3^-), technetium-99 (Tc-99), and tritium (^3H). This contamination is a result of mixing of wastes from a number of past waste-disposal activities, including the disposal of tank waste process water, and steam condensate at nearby cribs and trenches, disposal of plutonium processing waste at cribs and trenches associated with the Plutonium Finishing Plant, and leaks from single-shell tanks and transfer lines within the TX and TY tank farms.

5.2.1 Extent of Contamination – Depth Distribution

Determining the vertical extent of contaminants within the uppermost aquifer is part of the RCRA groundwater quality assessment currently underway at WMA TX-TY. A variety of data including discrete depth sampling during drilling, comparison of adjacent wells that sample different parts of the aquifer, depth discrete sampling using dialysis sampling techniques, and detailed specific conductance profiling provide important information about the depth distribution of contaminants.

5.2.1.1 Specific Conductance Profiling

In September 2002, specific conductance measurements were taken at 0.5- to 1-m intervals throughout the screened intervals of three groundwater monitoring wells around the TX and TY tank farms. Significant differences in specific conductance with depth were found in one of these wells (299-W14-13). The remaining two wells (299-W15-41, and 299-W15-763) showed no variation of specific conductance with depth.

Specific conductance versus depth measured in the screened interval of well 299-W14-13, a downgradient well at WMA TX-TY, is shown in Figure 5.8. Specific conductance in this well decreases significantly with depth between 1 and 4 m below the water table and then stabilizes at deeper depths. There also appears to be a maximum value of ~1635 µS/cm between 0.5 and 2 m above which specific conductance decreases with decreasing depth. Very near the surface, at 0.04 m below the water table, the specific conductance falls to about 1480 µS/cm. (The sample from 0.04-m depth was measured in the field with a conductivity meter from a bailed sample approximately six months after the conductivity profile was measured.)

Also shown on Figure 5.8 are four specific conductance values measured during routine quarterly sampling that occurred during fiscal year 2002 and prior to performing the depth profile measurements. All of the pumped specific conductance values range between 1203 and 1250 µS/cm and are less than the ambient values of the depth profile. This indicates that, after purging the well, the pumped samples are not representative of ambient conditions. During purging, the specific conductivity in well 299-W14-13 decreases with increasing purge time. Table 5.5 shows the initial and final specific conductance values after purging and sampling the quarterly samples in 2002. The initial specific conductance values are closer to, but still lower than, the profile values. Evidently, purging the well causes dilution of the samples.

Interpreting the contaminant distribution in well 299-W14-13 is very difficult because groundwater at the well contains high concentrations of several contaminants that show different vertical concentration profiles and probably come from several sources in the area. These variations are discussed later in Section 5.2.1.4. For now, the specific conductance indicates that there are concentration gradients in the screened interval of well 299-W14-13 and that the highest conductance, which probably reflects the highest nitrate concentration, occurs between 0.5 and 2 m beneath the water table.
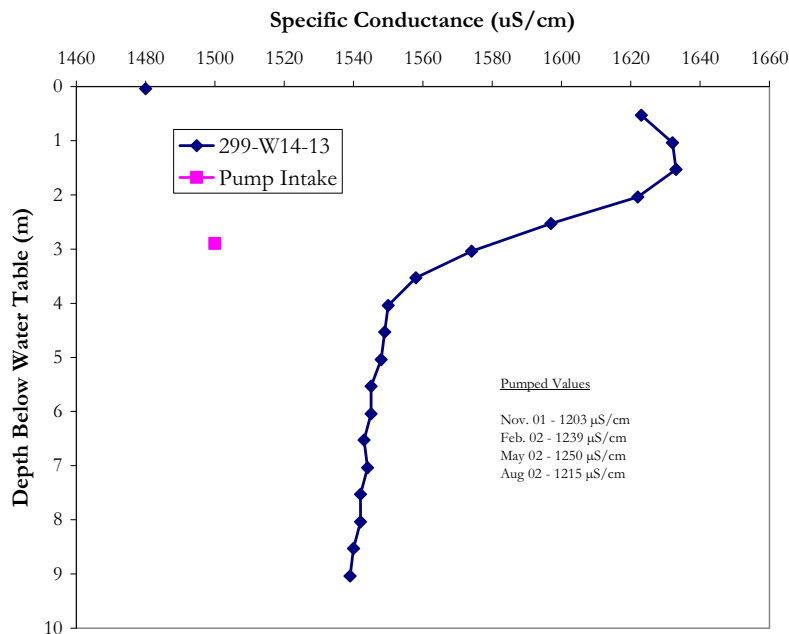
Figure 5.8. **Specific Conductance versus Depth in Well 299-W14-13. The Red Box is at the Depth of the Sample Pump Intake. See text for discussion.**

Table 5.5. **Initial and Final Specific Conductance Values from Four Routine Quarterly Sampling Events During Calendar Year 2002 at 299-W14-13**

Sample Date	Initial Specific Conductance (μS/cm)	Final Specific Conductance (μS/cm)
November 2001	1395	1203
February 2002	1354	1239
May 2002	1443	1250
August 2002	1476	1215

5.2.1.2 Comparison of Chemical Data from New and Replaced Wells

Replacement wells, when located immediately adjacent to older wells, offer an opportunity to look for vertical variation within the upper part of the aquifer. Data from three well pairs at the TX and TY tank farms suggest vertical stratification of contaminants in the upper part of the aquifer. In each case, the old well and its replacement well are separated by only a few meters. In addition, in each case, the older well was last sampled when there was a fraction of a meter of water within the screened interval and the replacement well was sampled with a pump placed at least 3 m below the water table within a 10.7-m screened interval. Thus, the last samples from the old well represent the top of the aquifer and the samples from the replacement well represent a composite of water pumped from the length of the screened interval that includes both the water from near the water table and water from deeper parts of the aquifer.

Well 299-W14-13 is at the northeast corner of the TX tank farm on the downgradient side of WMA TX-TY (Figure 5.1). This well currently has the highest concentration of technetium-99, tritium, iodine-129, fluoride (F), nitrate, and chromium of any well in TX and TY tank farm monitoring network. Well 299-W14-13 is the replacement well for well 299-W14-12 that went dry in early 1999. The two wells are located ~ 3 m apart. The last sampling of well 299-W14-12 took place in January 1999 and sampling of replacement well 299-W14-13 started in December 1998, allowing a sampling overlap between the two adjacent wells. The last samples collected from well 299-W14-12 represent the top of the aquifer. The samples collected from well 299-W14-13 represent water throughout the screened interval, which extends from the water table to 10 m below the water table. The pump intake is at 4.8 m below the water table.

Trend plots for several key constituents are shown in the series of Figures 5.9 to 5.12. The results for technetium-99 are particularly interesting (Figure 5.9). The concentration of technetium-99 in the last sample from well 299-W14-12 was ~ 6,000 pCi/L. This represented the concentration of technetium-99 at the top of the aquifer in January 1999. The sample from replacement well 299-W14-13, taken about the same time, contained ~ 2,500 pCi/L technetium-99. That sample represented the technetium-99 concentration throughout much of the upper 10 m of the aquifer. The conclusion is that technetium-99 existed at the top of the aquifer at about 6,000 pCi/L and the concentration decreased deeper in the aquifer. The 2,500 pCi/L technetium-99 value from well 299-W14-13 is a mixture of the relatively concentrated technetium-99 near the water table with more dilute groundwater from deeper in the aquifer.

Technetium-99 in the area of well 299-W14-12 began decreasing from a maximum of ~ 13,500 pCi/L in 1993 and continued to decrease until about January 1997. At that time, technetium-99 began to increase and reached 6,000 pCi/L in January 1999 when the well went dry. The increasing technetium-99 trend was continued in the replacement well (although offset to lower concentrations) until early 2000 when technetium-99 concentrations climbed to ~ 8,000 pCi/L. In early 2000, technetium-99 began to decrease and dropped to about 3,300 pCi/L in early 2001 at which time the concentration began to increase again. The latest increase continued until February 2003 and reached 8,740 pCi/L.

The results for nitrate in wells 299-W14-12 and 299-W14-13 (Figure 5.10) show a trend similar to that seen for technetium-99. The concentration of nitrate in the last sample from well 299-W14-12 was about 600,000 µg/L, and this represented the concentration of nitrate at the top of the aquifer. The sample from well 299-W14-13, taken at about the same time, contained only about 315,000 µg/L of nitrate. Just as for technetium-99, the conclusion is that nitrate existed at the water table at about 600,000 µg/L in January 1999, and the concentration decreased with depth in the aquifer. The 315,000 µg/L nitrate value from well 299-W14-13 is a mixture of the high nitrate-bearing water at the top of the aquifer with lower nitrate-bearing water deeper in the aquifer.

The nitrate concentration trends through time are the similar to those seen for technetium-99 (compare Figures 5.9 and 5.10). Nitrate began to decrease from a maximum or about 540,000 µg/L in 1993 to about 200,000 µg/L in early 1997. Nitrate then began to increase, reaching 580,000 µg/L in January 1999. The increasing nitrate trend was continued in the replacement well until early 2000 when concentrations reached ~ 440,000 µg/L. Nitrate began to decrease a second time until early 2001, at which time it began a second increasing trend that lasted through the beginning of 2003. Since that time nitrate concentration has decreased somewhat.

The analytical results for tritium in wells 299-W14-12 and 299-W14-13 (Figure 5.11) show a different trend than that seen for technetium-99 and nitrate. The concentration of tritium in the last sample from well 299-W14-12 was 1,170,000 pCi/L. The sample from well 299-W14-13, obtained about one month later, contained 1,160,000 pCi/L tritium. Following the same logic as used for technetium-99 and nitrate, the sample from well 299-W14-12 represents the tritium concentration at the top of the aquifer, whereas the sample from well 299-W14-13 represents the upper 10 m of the aquifer. Both results are the same, indicating little, if any, vertical concentration differences for tritium. Thus, unlike nitrate and technetium-99, the upper part of the aquifer at this location appears to be fairly homogeneous with respect to tritium concentration.

However, tritium concentrations in the groundwater show the same trends with time as shown by nitrate and technetium-99. Tritium began to decrease in concentration in 1993 and began to increase in early 1997 to a maximum of 2,940,000 pCi/L in early 2000. At that time, tritium began to decrease until early 2001 when tritium concentrations began to increase again. The latest increase reached 2,170,000 pCi/L in February 2003 and concentrations have declined since that time.

The concentrations of chromium in filtered samples from wells 299-W14-12 and 299-W14-13 are shown in Figure 5.12. The data suggest a different distribution of chromium in the upper part of the aquifer than the distributions of nitrate, technetium-99, and tritium. The data from the well pair indicate that the concentration of chromium is low at the top of the aquifer and increases at some depth below the water table. Chromium concentrations in the upgradient well pair, 299-W15-12 and 299-W15-765, seem to support this distribution of chromium in the aquifer (Figure 5.13), although the concentration in both upgradient wells is much lower than at the 299-W14-12 and 299-W14-13 pair. As will be discussed later, detailed depth-discrete sampling in well 299-W14-13 suggests that the chromium concentration at the water table is slightly greater than the concentration throughout the rest of the screened interval. This is contrary to the conclusion drawn from comparing the chromium concentrations in well 299-W14-12 and 299-W14-13. In addition, the concentrations of technetium-99 and chromium in well 299-W14-13 track each other through time and the ratio of the two is fairly constant (Figure 5.14). This suggests that the two contaminants are from the same source and, if this is the case, they should not be fractionated differently in the aquifer versus depth or time. Thus, there is some discrepancy among the data as to the interpretation of the distribution of chromium in this well pair and its relation to technetium-99.

Two other well pairs were examined at the TY tank farm. No concentration differences versus water depth were noted for technetium-99, tritium, chromium or nitrate in well pair 299-W10-18 and 299-W10-26, located downgradient (east) of TY tank farm. Data from well pair 299-W15-12 and 299-W15-765, located upgradient of the TY tank farm and not in a high contamination area, suggest that technetium-99 concentrations are somewhat greater at the water table than at depth in the screened interval.
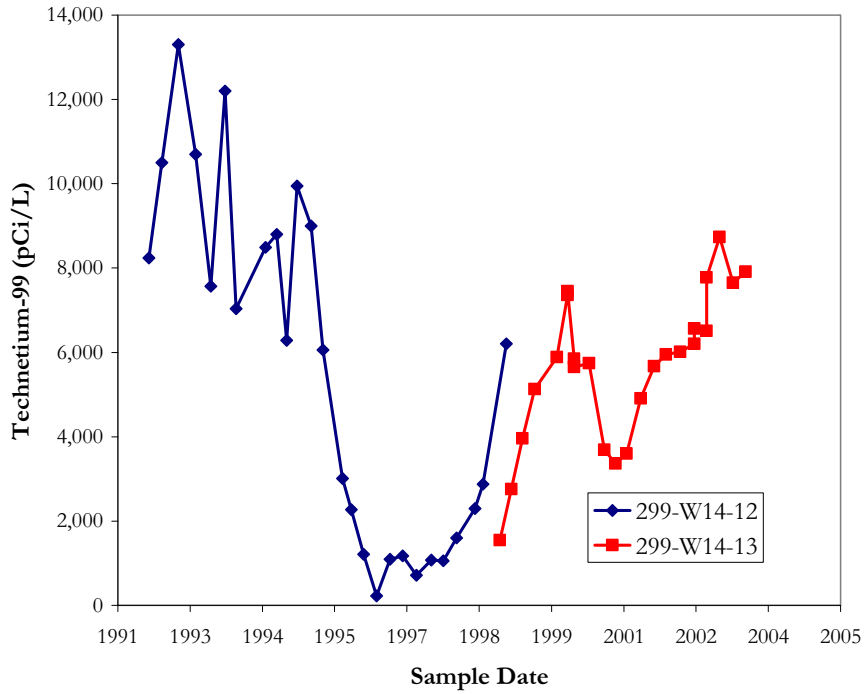
Figure 5.9.   Technetium-99 Concentration in Wells 299-W14-12 and 299-W14-13 in WMA TX-TY
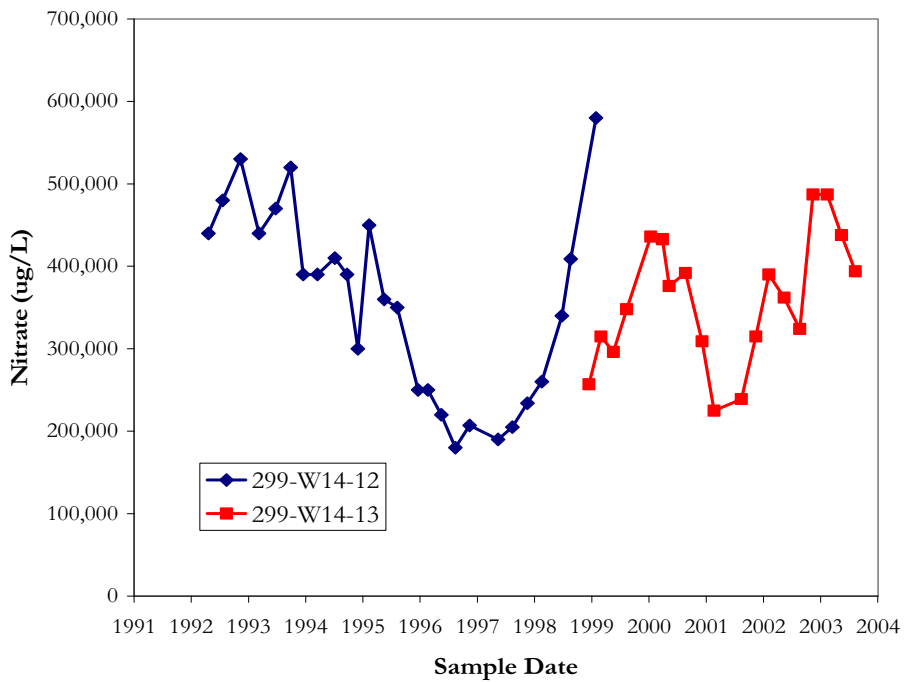
Figure 5.10.   Nitrate Concentrations in Wells 299-W14-12 and 299-W14-13 at WMA TX-TY
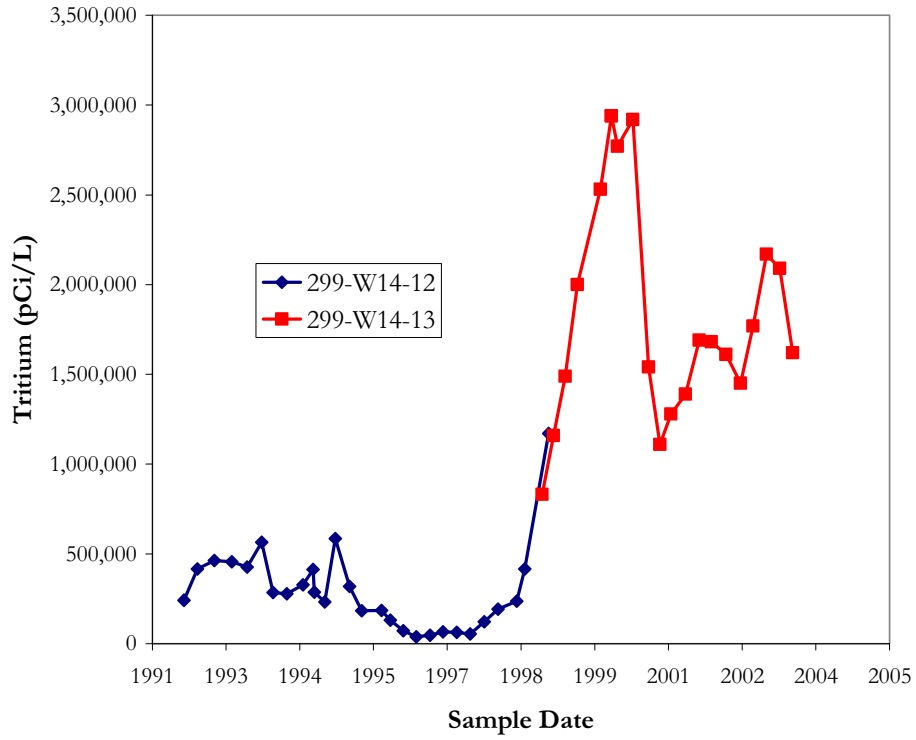
Figure 5.11. Tritium Concentrations in Wells 299-W14-12 and 299-W14-13 at WMA TX-TY
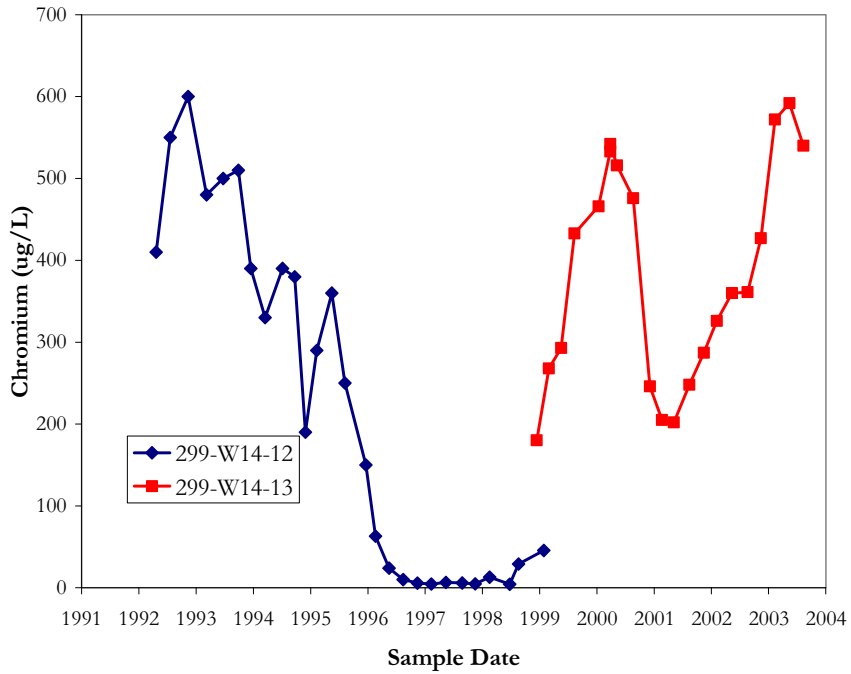
Figure 5.12. Chromium Concentrations in Wells 299-W14-12 and 299-W14-13 at WMA TX-TY
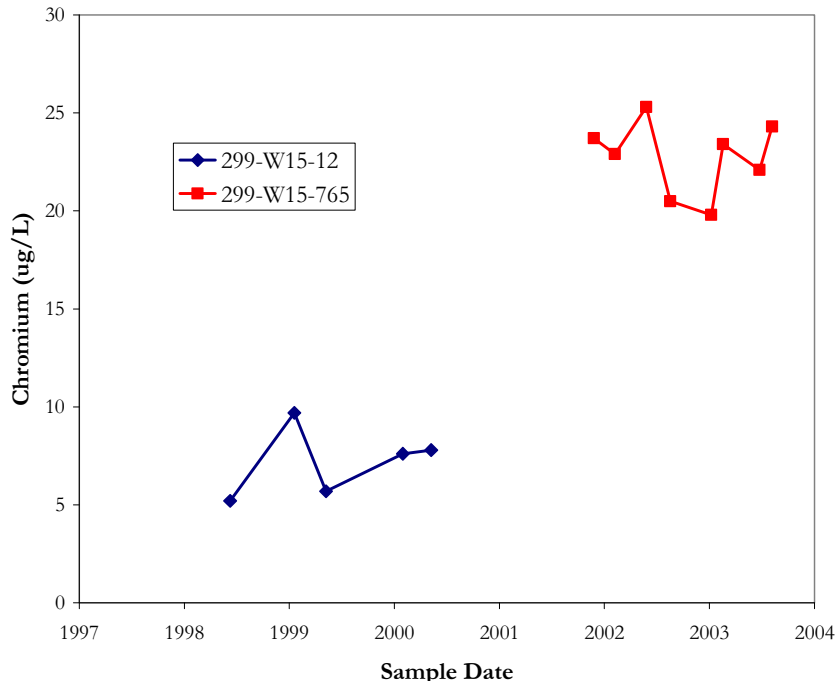
Figure 5.13. Chromium concentrations in well pair 299-W15-12 and 299-W15-765. Well 299 W15-765 is the newer replacement well; well 299-W15-12 is now dry.
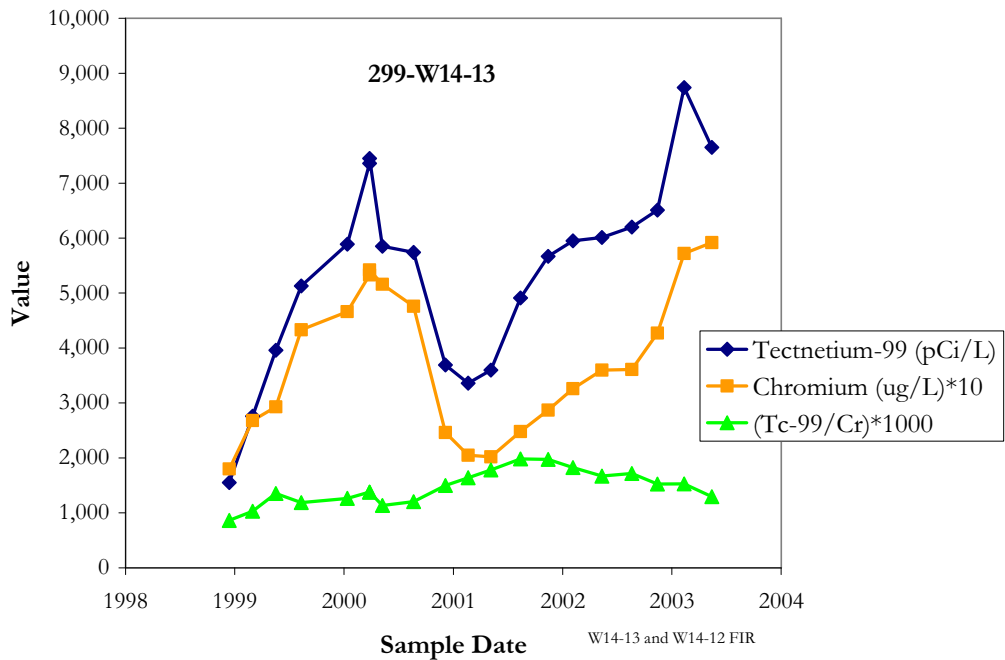
Figure 5.14. Tc-99 and Cr (*10) Concentrations, and Tc-99/Cr (*1000) Ratios in Well 299-W14-13

5.18

5.2.1.3 Sampling During Drilling

Groundwater and saturated sediments brought to the surface during drilling can give an indication of vertical chemical variations within the aquifer. Seven new wells have been sampled during drilling since 2000.

Groundwater samples were collected by pumping during drilling of well 299-W14-14 east of TX tank farm. Each sample interval was isolated by packers before sampling. Figure 5.15 shows the results of analysis of those samples for technetium-99, nitrate, tritium, and carbon tetrachloride. The uppermost sample on Figure 5.15 was collected by pumping from the screened interval after the well was completed.

The depth distribution of tritium and carbon tetrachloride showed maximums at about 40 m below the water table. The Ringold Formation lower mud unit (hydrogeologic unit 8) occurs between 56 and 67 m below the water table in well 299-W14-14. The largest concentrations of carbon tetrachloride (920 µg/L) and tritium (9,010 pCi/L) occur above this unit at 46 m below the water table. Concentrations of both constituents decrease near the top of, but within, the lower mud unit at 58 m depth and increase again near the bottom contact of the lower mud unit with the underlying Ringold Formation unit A (hydrogeologic unit 9). Concentrations of both constituents show increases in the deepest sample indicating that the deepest occurrence of these constituents was not encountered in the well and that significant concentrations exist in the confined Ringold Formation aquifer.

The maximum concentrations of technetium-99 (556 pCi/L) and nitrate (226,000 µg/L) occurred at 15.4 m below the water table. Concentrations decreased immediately below 15.4 m and remained constant throughout the remainder of the drilled depth. No concentration changes were noted across the lower mud unit. The maximum concentrations of technetium-99 and nitrate occur about 10 m below the current pump intake in well 299-W14-14.

Air lifted samples of groundwater and sediment cuttings were collected from wells 299-W14-19 and 299-W15-44 during drilling at TX tank farm. The samples were collected at 6-m intervals down to 36 m below the water table and analyzed for metals, anions, tritium, and technetium-99 (Horton 2003). No high levels of contamination were encountered. Several metals and anions, however, showed concentration variations with depth in the aquifer. The results from well 299-W14-19 are similar to those from well 299-W15-44.

Additional groundwater samples were collected from drilling slurries at well 299-W15-44 for analysis of nitrate in the field. The nitrate data from well 299-W15-44 are shown in Figure 5.16. Figure 5.16 shows that nitrate in well 299-W15-44 is relatively high at the water table and decreases with depth down to about 20 m below the water table. This is followed by an increase in concentration at about 60 m below the water table, below which the nitrate concentration remains constant to the bottom of the borehole. In all TX-TY wells that have been sampled during drilling, nitrate has been found to vary in concentration with depth in the aquifer (Table 5.6). In most wells with sufficient samples to define a trend, nitrate concentration is shown to increase with increasing depth.

The high nitrate concentrations near the water table in well 299-W15-44 are interpreted to be from a nearby source such that either the nitrate has not traveled far enough in the aquifer to become more highly dispersed, or has not resided long enough in the aquifer to descend deeper due, perhaps, to higher density in the contaminant plume. The nearby source for the nitrate is probably the TX tank farm. The deeper,

relatively high nitrate concentrations in well 299-W15-44, and in other wells at WMA TX-TY, have been interpreted elsewhere to represent past-practice discharges, probably from the Plutonium Finishing Plant, that were disposed to U pond (Hodges and Chou 2001; Johnson and Chou 2001). The large groundwater mound from the pond probably drove contaminated pond water deep into the aquifer before it moved northward beneath WMA TX-TY. Thus, the deeper nitrate concentrations represent a widespread, regional plume.

5.2.1.4   Multi-Level Dialysis Sampling In Well 299-W14-13

Well 299-W14-13 is located on the east (downgradient) side of WMA TX-TY in an area of high chromium, nitrate, technetium-99, iodine-129, and tritium groundwater contamination. Previous interpretations of chromium and technetium-99 distributions in the well suggested that the two contaminants existed at different depths within the aquifer, implying two different sources for the technetium-99 and chromium. The concentrations of chromium and technetium-99 show the same increasing and decreasing trends through time, however, suggesting either a single source for both contaminants or dilution of the entire upper aquifer. Multi-level, depth-discrete sampling was done in the well to help determine the source or sources of chromium and technetium-99 and to refine the chromium distribution in the upper part of the aquifer.
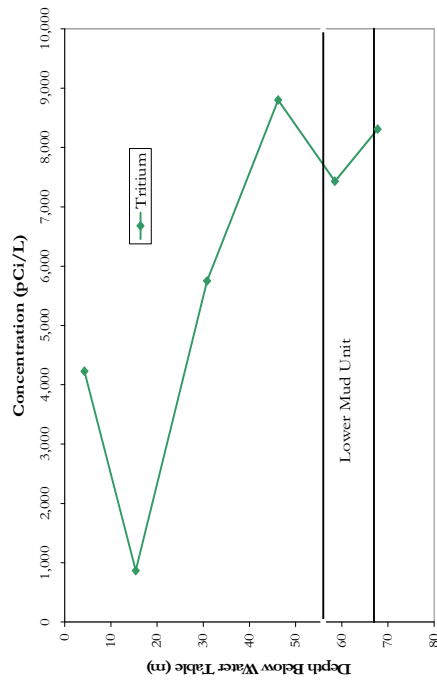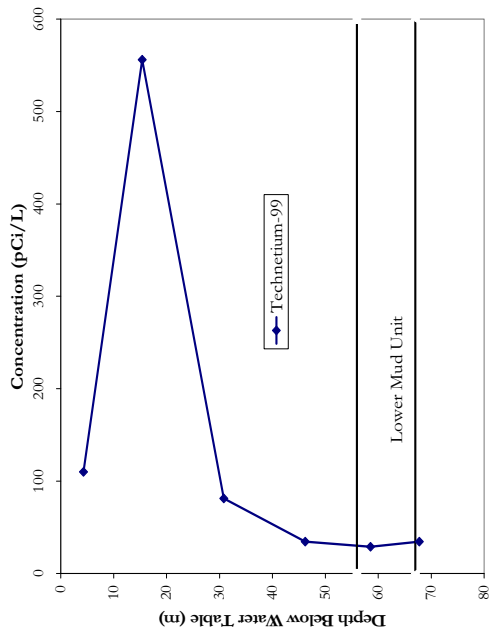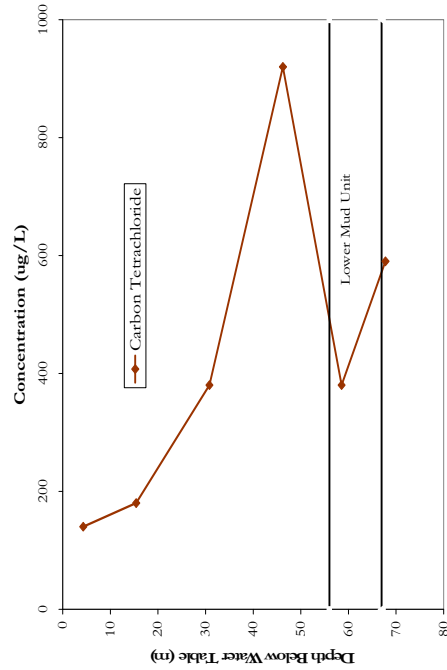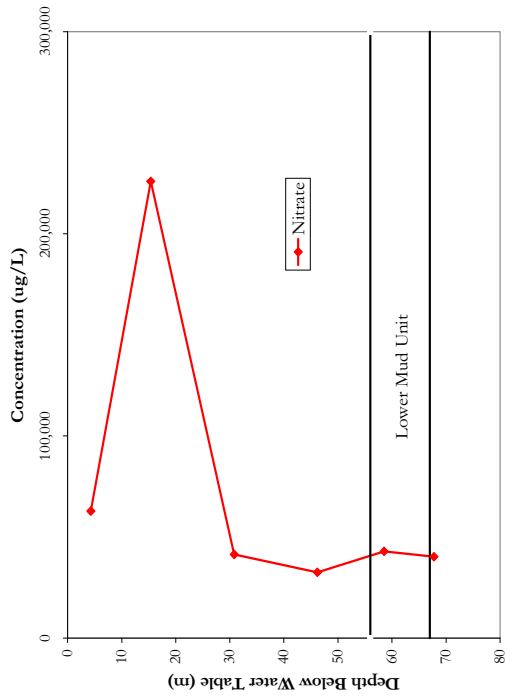
Figure 5.15. Contaminant Distributions in Samples Collected During Drilling of Well 299-W14-14
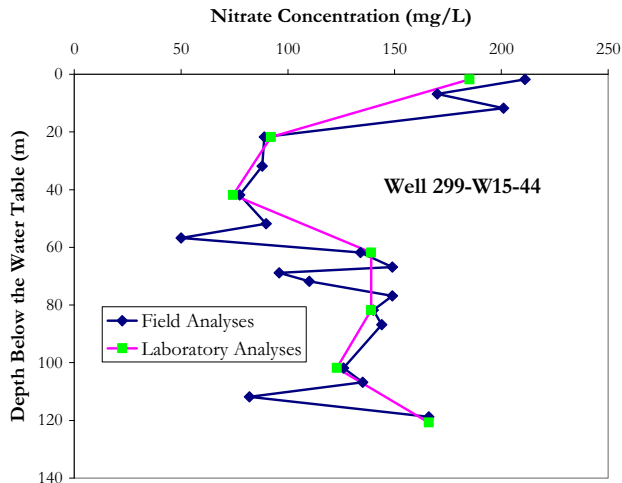
Figure 5.16. Nitrate Concentration in Groundwater versus Depth in Well 299-W15-44 During Drilling

Table 5.6. Nitrate Concentration in Groundwater Collected During Drilling of New RCRA Wells

Depth Below the Water Table (m)	Nitrate Concentration (μg/L)	Depth Below the Water Table (m)	Nitrate Concentration (μg/L)
299-W14-15[1]		**299-W14-16[1]**	
3.4	66,000	3.1	30,000
5.1	94,000	6.1	46,000
9.6	111,000	9.1	80,000
299-W15-765[2]		13.1	149,000
5.5	24,270	**299-W14-18[2]**	
13.8	52,111	At the water table	56,850
-	-	12.6	3,260
(1) Field Analysis			
(2) Laboratory Analysis			

A multi-level, dialysis sampling device was deployed in well 299-W14-13 in September 2002. The sampling device was left in the well for about one month to allow equilibration of the water in the dialysis tubes with the groundwater. Samples were obtained every 1.5 m from about 1 m below the top of the aquifer to the bottom of the well screen at about 9 m below the water table. Samples were analyzed for major cations, anions, tritium, chromium, and technetium-99.

In addition, one sample was collected from about 4 cm below the water table using a mini-bailer. The bailed sample was analyzed for chromium and nitrate in the field and chromium and technetium-99 in the laboratory.

The analytical results from both the multi-level dialysis and the bailed samples are shown in Figure 5.17. The results show that, except for a zone at about 2.5 m below the water table, the concentrations of most cations and anions are fairly constant throughout the screened interval of the aquifer. Neither the geology, the geophysical logs, nor aquifer testing results show any evidence of changes in the formation at 2.5 m below the water table, so the reason for the increased concentrations at this depth is unknown.

In contrast, nitrate and technetium-99 show increased concentrations with depth from the shallowest dialysis sample at 1 m below the water table to about 4 to 5 m below the water table. For nitrate, there is an extremely large increase in concentration between the shallowest dialysis sample and the bailed sample near the water table. For technetium-99, the mini-bailed sample has lower technetium-99 concentration than any the dialysis samples.

Contaminant concentrations in the upper meter of the aquifer at well 299-W14-13 are difficult to interpret. The dialysis and mini-bailer data indicate a large increase in nitrate concentration at the water table relative to deeper in the screened interval, a small increase in chromium concentration, and a decrease in technetium-99 concentration relative to concentrations deeper in the screened interval. (Technetium-99 concentration does increase with decreasing depth between about 4 and 1 m, however.) Comparisons of samples from wells 299-W14-12 and 299-W14-13 support higher concentrations of nitrate at the water table but suggest lower chromium and higher technetium-99 concentrations than supported by the dialysis sampling. Also, the specific conductance profile from well 299-W14-13 indicates fairly large changes in salinity within the upper meter of the aquifer.

The solid squares on Figure 5.17 represent the concentrations of the various constituents in routine quarterly, pumped samples collected the quarter before and the quarter after the dialysis samples were collected. The data show that for some cations and anions, the concentrations in the pumped samples are similar to the dialysis concentrations throughout the screened interval. Exceptions are calcium, chromium, nitrate, and technetium-99. The pumped concentrations of calcium, chromium, and technetium-99 are substantially less than the ambient concentrations measured from the dialysis samples. For nitrate the opposite is true.

Considering all available data, there are inconsistencies in the current understanding of contaminant distribution within the upper meter or so of the aquifer at well 299-W14-13. More detailed sampling within the upper 1 m of the aquifer may help resolve these inconsistencies.
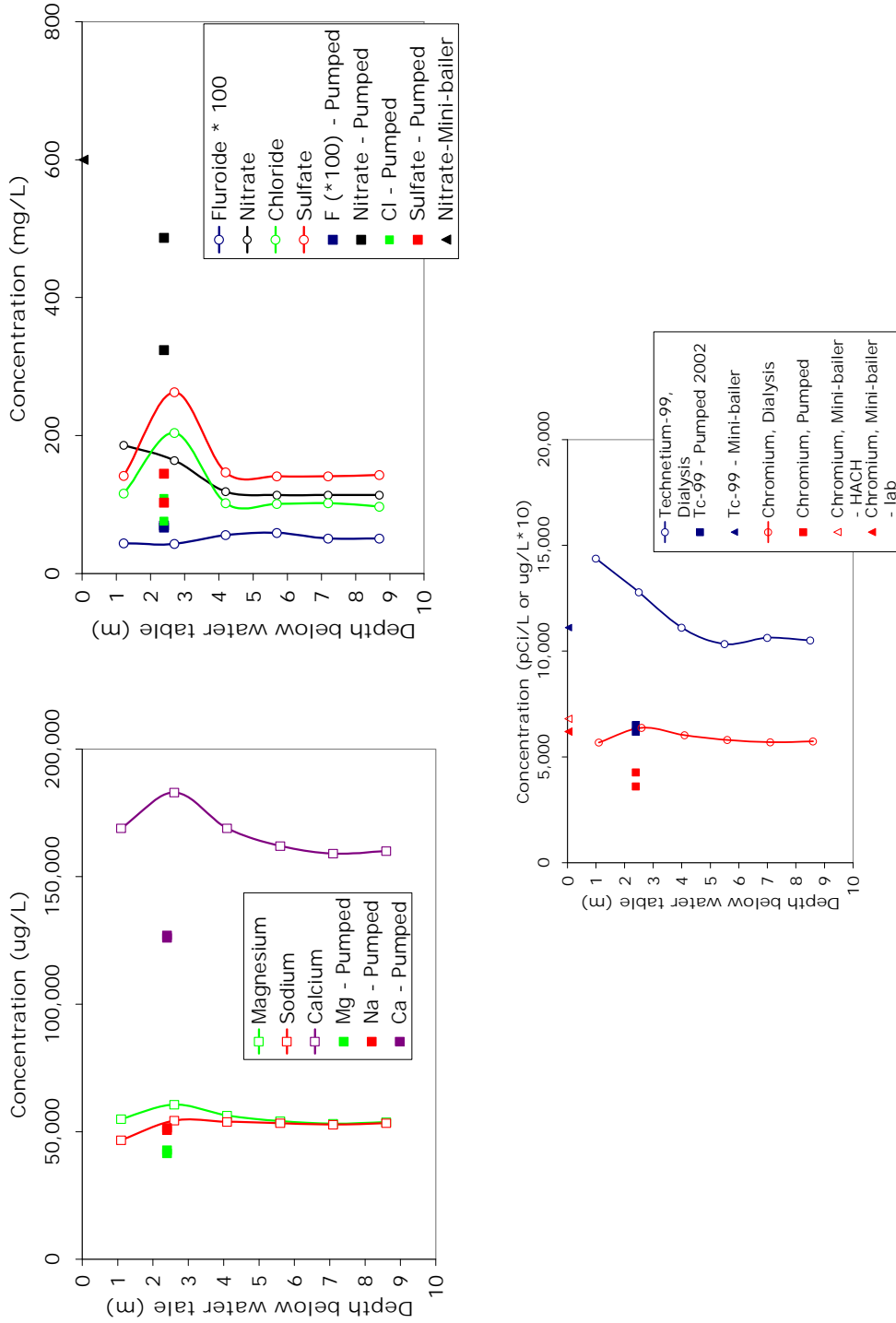
Figure 5.17. Results of Multi-Depth Sampling of Well 299-W14-13

Despite a rigorous QA/QC program in the contract analytical laboratory and well-established sample collection and preservation protocols, it may be that sampling and analytical vagaries are the cause of some of these inconsistent trends in the results from samples collected at different depths and different times using different techniques. However, there are feasible explanations for the data variabilities.

Aquifer testing showed that well 299-W14-13 has a downward flow gradient within the well bore (see Section 5.1). This implies potential zones of different permeability in the screened interval. Alternatively, downward flow may, in part, be driven by differences in density. If the major cations and anion concentrations at 1-m depth are increased proportionally to the nitrate concentration at 4-cm depth, the resulting salinity of the water at 4 cm is 2.3‰. This is in contrast to the estimated salinity from the deepest dialysis sample which is 0.63‰. The salinity difference between the top and bottom of the screened interval may be sufficient to cause a downward, density-driven flow within the well bore.

Regardless of the mechanism responsible for the downward flow, contaminants existing near the top of the aquifer will be transported downward in the well. If the contaminant concentrations are relatively high near the top of the aquifer, the highly contaminated water will be transported downward and diluted with less contaminated water at depth. This is important because the well itself is helping to spread contamination.

When well 299-W14-13 is purged, all the ambient water is removed. The resulting pumped samples consist of a mixture of the relatively high concentrations of contaminants from near the water table diluted with less contaminated water from deeper in the well. This could yield pumped samples with the concentrations shown on Figure 5.17. Although difficult to interpret, the data from well 299-W14-13 indicate that concentrations measured from pumped samples may not represent actual concentrations in the aquifer.

5.2.2   Geographical Distribution of Contaminants

This section summarizes the areal distribution of contaminants in groundwater at WMA TX-TY. Spatial variation in contaminant concentrations may provide some clues about source areas. Because concentrations change over time, a time period must be chosen to examine spatial distribution patterns. For this purpose, the most recent data (average of five sampling events) was chosen. Data were first grouped by geographic location and tabulated as shown in Table 5.7. Data were then plotted and inspected for distribution patterns or groupings. Contour maps of contaminant concentrations were drawn to identify spatial patterns that might be indicative of source areas. The maps are shown in the series of Figures 5.18 through 5.22.

Contamination in two areas near the TX and TY tank farms warrants consideration: east and downgradient of 241-TX and 241-TY tank farms, and south of 241-TX tank farm. The contaminants of interest east of WMA TX-TY are technetium-99, iodine-129, nitrate, tritium, and chromium. The contaminant of interest south of TX tank farm is technetium-99.

Carbon tetrachloride is a contaminant both east and south of the TX tank farm. The maximum carbon tetrachloride found in the area in 2002 was 5,800 µg/L (average of fiscal year 2002 samples) in well 299-W15-1, south of the TX tank farm (Hartman et al. 2003). The carbon tetrachloride is believed to be from pre-1973 waste from the Plutonium Finishing Plant. The major identified sources are the 216-Z-9 trench, the 216-Z-1A tile field, and the 216-Z-18 crib.

The part of the carbon tetrachloride plume exceeding 2,000 µg/L extends west of WMA TX-TY. This part of the plume is intercepted by well 299-W15-40 which averaged 2,400 µg/L carbon tetrachloride in 2003. Extraction wells for the 200-ZP-1 pump-and-treat in the area may be responsible for the increased carbon tetrachloride in the well and are probably responsible for increased technetium-99 in nearby well 299-W15-41.

Table 5.7. **Average Concentration of Mobile Contaminants in Groundwater in the Vicinity of the TX-TY WMA for the Time Period August 2002 to August 2003**

WELLS	NO$_3$ (µg/L)	F (µg/L)	Cr[2] (µg/L)	CCl$_4$ (µg/L)	Tc-99 (pCi/g)	^{3}H (pCi/g)	I-129 (pCi/g)
West (Upgradient) Side of WMA TX-TY							
299-W15-40	94,940[1] (5)	330 (5)	14.7 (5)	2,400 (3)	72.7 (5)	4,224 (5)	NA[3]
299-W15-765	146,600 (5)	332 (5)	22.0 (5)	3,200 (2)	83.7 (5)	4,722 (5)	ND[4]
East (Downgradient) Side of WMA TX-TY							
W10-26	103,433 (6)	1,533 (6)	8.6 (6)	NA	99.8 (6)	8,200 (6)	ND
W10-27	103,050 (4)	972 (4)	5.2 (2)	NA	117.9 (4)	12,850 (4)	NA
W14-5	94,640 (5)	1,260 (5)	5.2 (1)	NA	247 (5)	1,113 (5)	NA
W14-6	98,940 (5)	1,060 (5)	ND	NA	282 (5)	603 (5)	NA
W14-13	426,000 (5)	768 (5)	498.4 (5)	NA	7,474 (5)	1,820,000 (5)	33 (3)
W14-14	93,620 (5)	1,010 (5)	ND	360 (1)	250 (5)	2,724 (5)	ND
W14-15	79,500 (5)	1,200 (5)	62.4 (5)	NA	509 (5)	27,800 (5)	2.3 (1)
W14-16	77,200 (5)	572 (5)	ND	NA	216 .6 (5)	2,190 (5)	ND
W14-17	158,000 (5)	582 (5)	ND	NA	474 (5)	636 (5)	ND
W14-18	121,333 (6)	273 (6)	4.3 (1)	NA	409.8 (6)	8,301 (6)	ND
W14-19	100,100 (3)	1,067 (3)	ND	NA	265 (3)	2,807 (3)	ND
South of WMA TX-TY							
299-W15-41	68,060 (5)	579 (5)	6.2 (4)	1.300 (1)	611.8 (5)	5,942 (5)	ND
299-W15-44	95,300 (3)	433 (3)	11.3 (3)	2,900 (1)	107.4 (3)	4,610 (3)	ND
299-W15-763	37,400 (6)	607 (6)	4.9 (4)	NA	86.2 (6)	2,033 (6)	NA

(1) Numbers in parenthesis are the number of detects.
(2) Filtered samples.
(3) Not Analyzed.
(4) Not Detected.

5.2.2.1   Contamination East of WMA TX-TY

Figure 5.18 shows a plume map for chromium at the end August 2003. The figure shows that chromium was detected in one downgradient well (299-W14-13) above the drinking water standard of 100 μg/L. The concentration of chromium in the well in August 2003 was 540 μg/L. Given the current direction of groundwater flow, one potential source for the chromium is the 241-TY tank farm. However, about 1,060 kilograms of chromium were disposed to the TY cribs located about 65 m northeast of the well (Simpson et al. 2001). Since the general dip of the strata in the area is toward the west or southwest, it is possible that contamination from the cribs migrated through the vadose zone toward well 299-W14-13. In the past, water from a tanker truck filling station, located about 140 m up dip of the TY cribs, was seen leaking onto the ground from the fill spout. Water was seen to pool on the ground and run about 100 m down slope (toward the TX and TY tank farms) in a ditch along the side of the gravel road. Infiltration of this water could have mobilized contamination in the vadose zone beneath the TY cribs and moved the contamination down dip toward well 299-W14-13.

Also, Fecht et al. (1977) state that gross gamma logs obtained prior to 1977 showed contamination at the 216-T-28 crib extended from near the surface to the water table and that breakthrough to groundwater could have occurred at the site. They also state that waste from the crib was noted in a well 299-W14-1, located 38 m south of the crib so that considerable lateral spreading had occurred in the vadose zone beneath the TY cribs. Therefore, we cannot currently assign an origin for the elevated chromium in well 299-W14-13 to a particular facility.

Figure 5.19 shows a plume map for technetium-99 at the end of August 2003. Technetium-99 was detected in one downgradient well (299-W14-13) above the drinking water standard of 900 pCi/L. Given the current direction of groundwater flow, one potential source for the technetium-99 is single-shell tanks in WMA TX-TY. However, three other sources also may have contributed some technetium-99 to the groundwater east of WMA TX-TY. As mentioned above, Fecht et al. (1977) state that considerable lateral spreading of discharged water and contaminants occurred south of the 216-T-28 crib and that breakthrough to the groundwater could have occurred at that site. The 216-T-28 crib received about 10.9 curies of technetium-99 (Kincaid et al. 1998). Thus, some of the technetium in the groundwater east of TX-TY today may be from the 216-T-28 crib.

The 216-T-19 tile field is also a potential source for some of the technetium-99 east of WMA TX-TY. The tile field received 455 million liters of primarily steam condensate from the 242-T evaporator (DOE 1992), which contained 9.89 curies of technetium-99. Groundwater flow was toward the northeast from the tile field (thus towards) the location of well 299-W14-13 during the last approximately 25 years that the tile field was used.

Finally, a fourth potential source for some of the technetium-99 east of the WMA is leaks from the 242-T evaporator building. The evaporator is approximately 70 m upgradient of well 299-W14-13. Given a groundwater flow rate of 0.19 m/d (from aquifer tests, Table 5.3) in well 299-W14-13, a pre-1997 (when flow direction changed toward the east) leak from the evaporator would just recently be intercepted by the well. However, if the slower, Darcy velocities from Table 5.4 are used, an evaporator leak would not yet have reached the well. This indicates that leaks from the 242 Evaporator might be contributing to contamination at well 299-W14-13 today but would not have contributed to the plume encountered by well 299-W14-12 in the early 1990s.

The plume maps for chromium and technetium-99 (see Figure 5.18 and 19) show that the contaminant plumes are relatively small and centered near well 299-W14-13. Concentrations of both contaminants drop sharply both to the north in well 299-W14-18 and to the south in well 299-W14-15, although concentrations of technetium-99 have been increasing slightly in both wells over the past two years. Technetium-99 concentrations increased from 189 to 468 pCi/L in well 299-W14-18 since the end of 2001 and from 380 to 472 pCi/L in well 299-W14-15 since the end of 2000. These wells may be on the edge of the plume apparently centered at well 299-W14-13.

Well 299-W14-17 is about 125 m downgradient (south east) of well 299-W14-13. Given a flow rate of 0.19 m per day, the technetium-99 seen at well 299-W14-13 is expected to have traveled about 70 m toward well 299-W14-17 since the 1997 change in flow direction. Technetium-99 concentrations have decreased in well 299-W14-17, from 576 pCi/L to 456 pCi/L, during the last two years. Thus, the technetium-99 plume at well 299-W14-13 does not appear to have spread to the downgradient well, 299-W14-17, at this time.

Figure 5.20 shows a plume map for nitrate at the end of August 2003. Almost all wells in the groundwater monitoring network at WMA TX-TY, including the upgradient wells, have had nitrate concentrations greater than the MCL of 45,000 μg/L throughout most of their sampling life. The highest nitrate concentrations have been at well 299-W14-13. This well has had nitrate concentrations greater than those in the regional plume since it was drilled in late 1998. Before that time, nitrate in well 299-W14-12 (now dry, but adjacent to well 299-W14-13) was between 450,000 and 550,000 μg/L since it was drilled in 1992. Subsequently, nitrate in well 299-W14-12 decreased to about 200,000 μg/L in 1997 before increasing to about 580,000 μg/L when it went dry in late 1998 (see Figure 5.10).

Nitrate in the area of wells 299-W14-12 and 299-W14-13 is probably from several sources including a regional nitrate plume from Plutonium Finishing Plant disposal sites. Other potential sources are those mentioned above as potential sources for chromium and technetium-99.

An area of relatively low nitrate concentration, north of well 299-W14-13, has existed since at least the mid-1990s (Figure 5.20). The cause for the low nitrate in the area is not known. Dilution by liquids disposed to the 216-T-26 through 216-T-28 cribs does not appear to be probable because 1,000,000 kilograms of nitrate were in the waste stream sent to the 216-T-26 crib (DOE 1992).

Figure 5.21 shows a plume map for tritium at the end of August 2003. Tritium was detected in one downgradient well (299-W14-13) above the drinking water standard of 20,000 pCi/L. Like nitrate, tritium most likely has several sources that include WMA TX-TY and several cribs and trenches in the area. Hodges (1998) used tritium/technetium-99 ratios to show that contamination in the area of the now dry well 299-W14-12 was probably a mixture of regional contamination and tank waste.

Two other contaminants, cobalt-60 and iodine-129, have been found at WMA TX-TY. Cobalt-60 was found in four wells prior to 1982. Cobalt-60 was highly variable in well 299-W14-2, located at the 216-T-28 crib; between 1971 and 1976, it reached a maximum of 75 pCi/L in 1971. Since that time, cobalt-60 decreased to between 10 and 25 pCi/L (between 1976 and 1981) and has been undetectable since 1982.

Well 299-W14-5, located east of the TX tank farm, showed highly variable cobalt-60 concentrations between in 1975 and 1976 with the highest concentration reaching 52 pCi/L. Cobalt-60 concentrations

decreased to less than detectable in the well after 1977. Cobalt-60 concentrations were also high in well 299-W14-6, south of well 299-W14-5, in 1975 (68 pCi/L). Subsequently, the well was not sampled for 10 years and cobalt-60 has been undetected in the well since 1988.

Well 299-W15-4, located south of the TX tank farm, also showed high concentrations of cobalt-60 between 1971 and 1976 with the maximum reaching 42 pCi/L. Like well 299-W14-6, well 299-W15-4 was not sampled between 1976 and 1987 after which cobalt-60 was essentially undetected in groundwater samples.

Cobalt-60 was found in well 299-W14-12 during the entire life of the well, between 1992 and 1999. The cobalt-60 concentration was 28 pCi/L in late 1992 and decreased to about 4 pCi/L in early 1996. Cobalt-60 increased to 16 pCi/L in 1999 when the well was last sampled before it went dry. Cobalt-60 has not been found in replacement well 299-W14-13.

Apparently, there was an early 1970s cobalt-60 plume in the area east and south of the TX tank farm. That plume either dissipated or passed through the area in the late 1970s. A second plume, isolated to well 299-W14-12, was noted during the 1990s but has not been found in any other wells at the WMA.

Iodine-129 was found in well 299-W14-2 at the 218-T-28 crib between 1996 and December 2000 when the well was went dry. Concentrations were quite variable during this time and the last concentration measured in the well was 64 pCi/L. This was the highest iodine-129 concentration seen in the well.

Iodine-129 has also been found in well 299-W14-12 and its replacement well 299-W14-13. Iodine-129 reached about 28 pCi/L in well 299-W14-12 in 1992 before decreasing to undetectable levels in 1996. Iodine-129 began to increase in the well in the last two samples obtained before the well went dry. The last concentration was 16.4 pCi/L iodine-129. Iodine-129 concentrations have varied between 16 and 50 pCi/L in replacement well 299-W14-13.

The source of the iodine-129 east of the TX tank farm is not known for certain. One possible source is the 216-T-26 through 216-T-28 cribs which received up to 0.0725 Ci of iodine-129 during their operation (Kincaid et al. 1998). It is also possible that the SSTs in the WMA could be the source of the iodine-129.
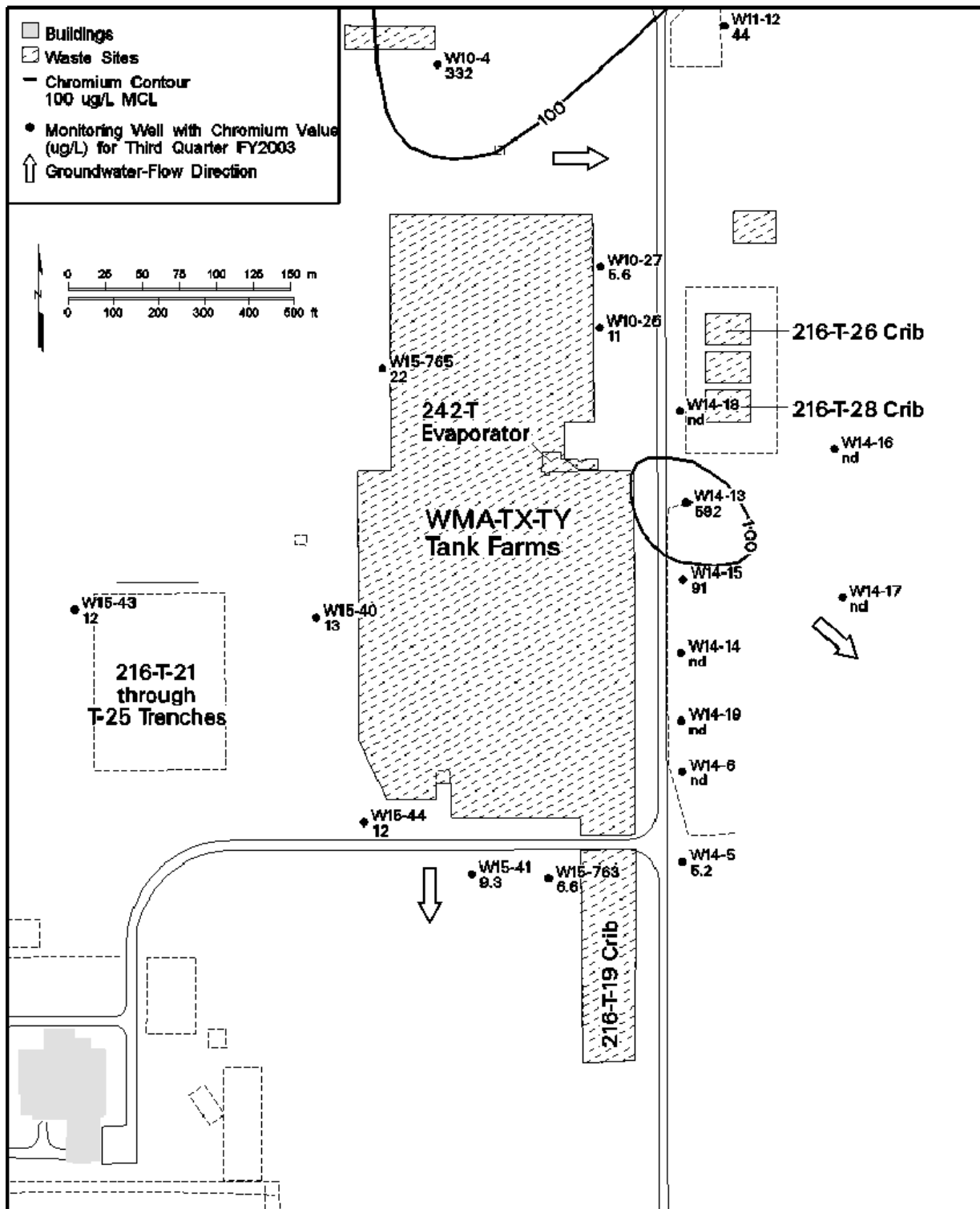
Figure 5.18. Chromium Plume Map at WMA TX-TY for the Fourth Quarter of Calendar Year 2002
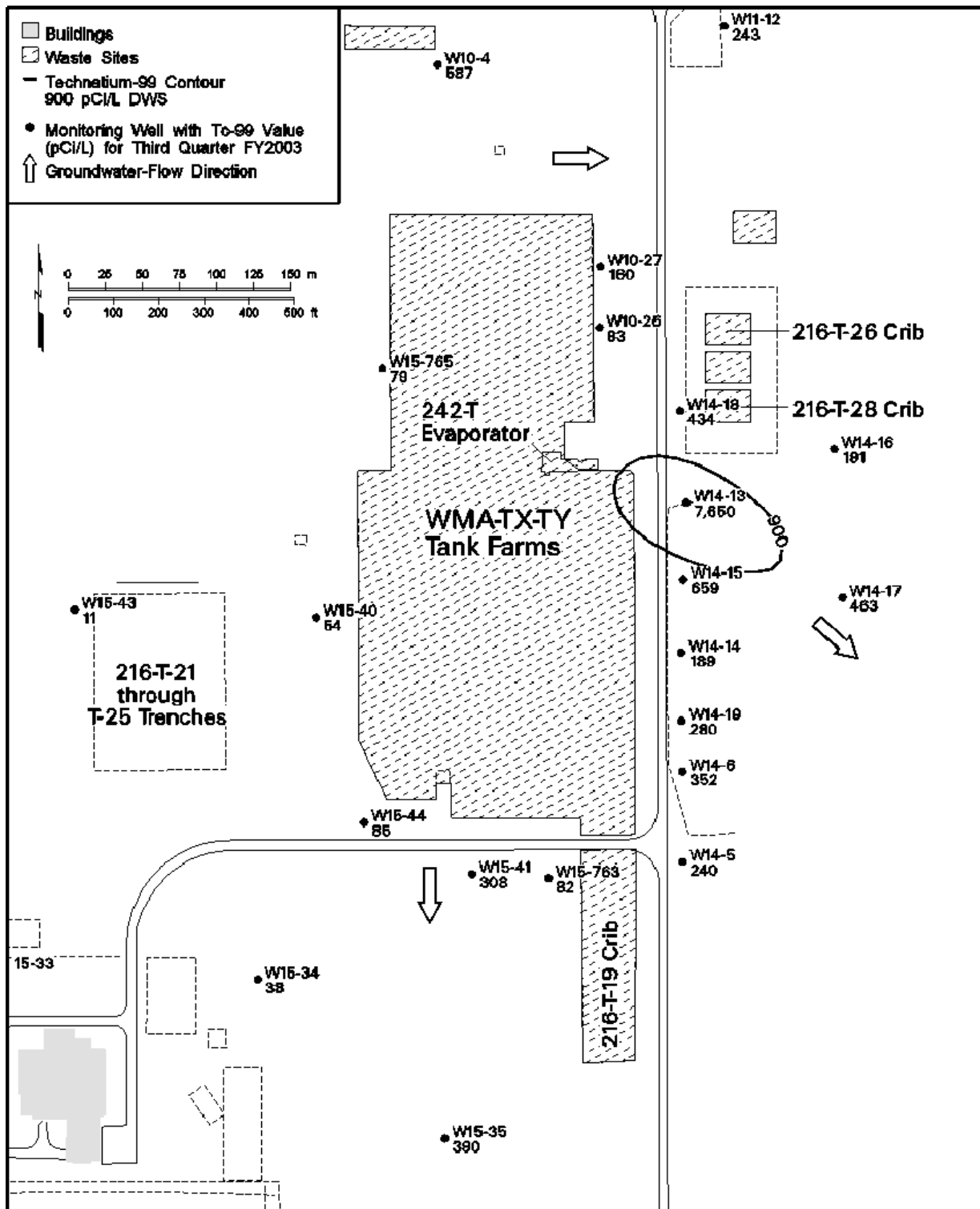
Figure 5.19. Technetium-99 Plume Map at WMA TX-TY for the Fourth Quarter of Calendar Year 2002
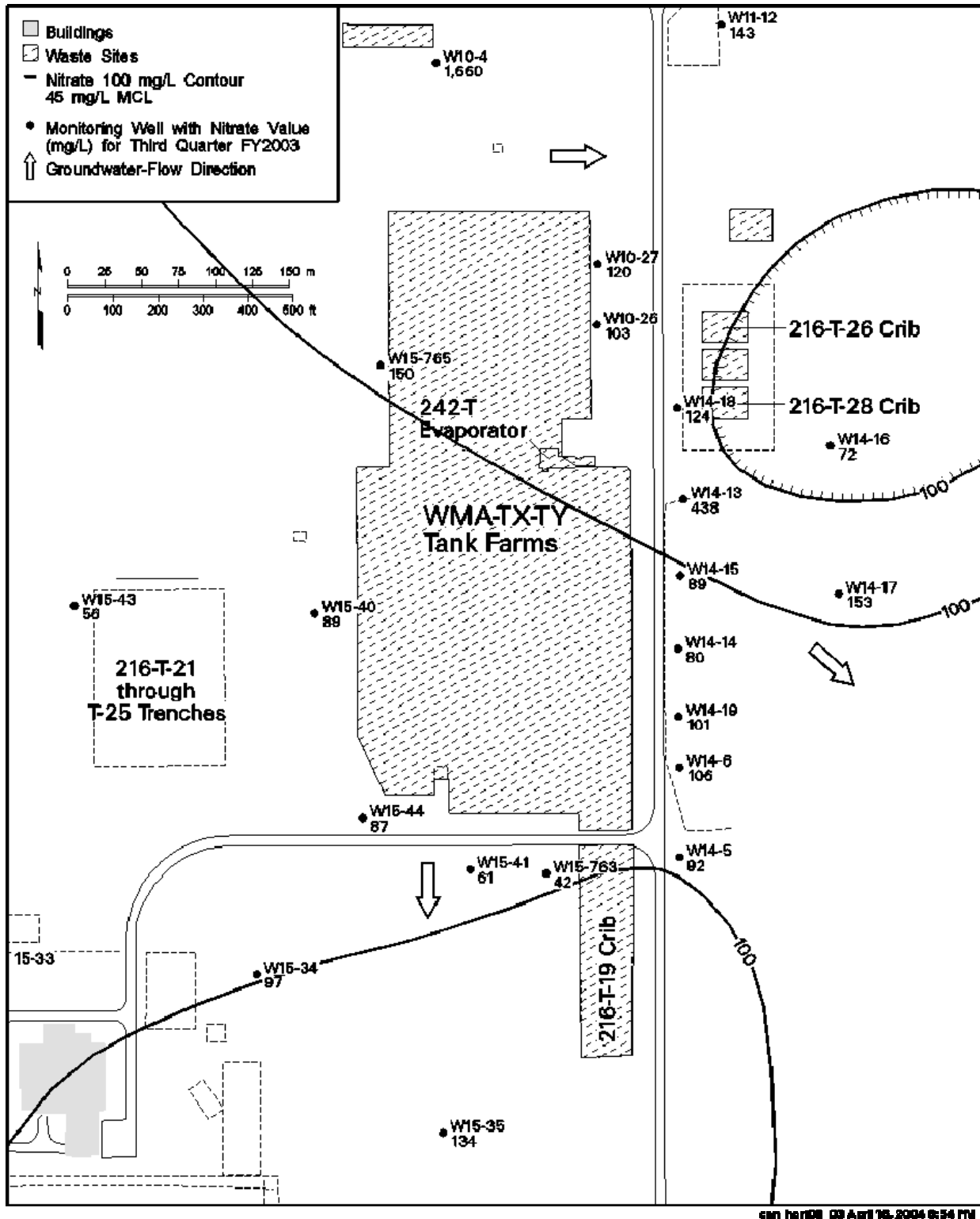
Figure 5.20.   Nitrate Plume Map at WMA TX-TY for the Fourth Quarter of Calendar Year 2002

5.2.2.2   Southern Boundary of Waste Management Area TX-TY

The 200-ZP-1 pump-and-treat operation began in 1994 with one extraction well. The operation was expanded to three wells in 1996 and, finally, to six extraction wells in August 1997. The first distinct effects of the pump-and-treat operation on groundwater flow direction beneath WMA TX-TY was observed on the June 1998 water-table map (Hartman 1999). Well 299-W15-22, located at the southwest corner of the WMA, and originally drilled as an upgradient well, was the closest to the 200-ZP-1 pump-and-treat extraction wells before it went dry in 1998. Technetium-99 began to increase in this well in May 1997, exceeded the maximum contaminant level in August 1997, and reached a high of 3,680 pCi/L in May 1998. The well was last sampled in August 1998.

Well 299-W15-4 is an older pre-RCRA well originally drilled to monitor the 216-T-19 crib at the southeast corner of the WMA. Prior to May 1998, the well was sampled only on an annual basis; however, available data indicate that technetium-99 started to increase in this well in mid-1997 and reached a peak value of 980 pCi/L in July 1999. The last sampling in October 1999 yielded a value of 640 pCi/L technetium-99. Chromium began to increase in well 299-W15-4 in 1999, but the peak concentration of chromium (20 µg/L) was below the maximum contaminant level in the last samples from the well before it went dry.

Well 299-W15-763 was completed as a replacement well for 299-W15-4 in 2001. The first routine sample from this well, taken in May 2001, indicated a technetium-99 level of 57 pCi/L. The most recent sample taken from this well contained 123 pCi/L technetium-99. Technetium-99 concentrations in this well are anomalously low when compared to other wells in the area. The geologist's log noted cemented zones in the screened interval of this well. Thus, changes in lithology may account for the difference between technetium-99 concentrations in this and adjacent wells.

Well 299-W15-41 was completed in January 2000 and was first sampled in March 2000. The initial sampling yielded a technetium-99 concentration of 1,980 pCi/L. Concentrations of technetium-99 have subsequently decreased to about 328 pCi/L since August 2002. No significant concentrations of chromium have been found in samples from this well.

Technetium-99 in wells along the southern boundary of WMA TX-TY started to increase approximately one year after Phase II of the 200-ZP-1 pump-and-treat operation began. (Phase II, consisting of three extraction wells, began the use of the closest extraction wells to the WMA, wells 299-W15-34 and 299-W15-35.) Given the southerly groundwater flow direction imposed on the southern portion of the WMA by the pump-and-treat operation, the most reasonable explanation for the increasing technetium-99 is that groundwater contaminated with technetium-99 is being drawn from beneath the WMA into the pump-and-treat system. Alternatively, technetium-99 may be originating from the 216-T-19 crib and tile field (DOE 2002b). Given the changing groundwater flow direction along the southern boundary of the WMA, the few available monitoring wells, and the lack in continuity of monitoring data due to dry wells and new wells, it is currently impossible to fully evaluate this problem.

5.3   Comparison of Groundwater Vadose Zone Porewater Compositions at the TX Tank Farm

As mentioned previously, borehole C3830 was drilled to investigate a possible leak from tank TX-105, borehole C3831 was drilled to investigate possible leaks from TX-107 (used for many

intra-tank farm transfers), and borehole C3832 was drilled to investigate a possible leak from tank TX-104. All potential leaks were estimated to have occurred in the 1975 to 1977 time frame. The leak from tank TX-107 is presumed to be the largest leak and was probably at least 30,200 liters (8,000 gallons) (Crumpler 2002).

The travel time of the leaked fluids through the vadose zone to the unconfined aquifer is difficult to estimate because it depends on several variables including density of the leaked fluid, leak volume and leak rate, recharge rate since the leaks, details of stratigraphy, contaminant distribution coefficients, and presence (or not) of preferential pathway to groundwater. Several estimated travel times through the vadose zone have been made (e.g., Ward et al. 1997, WHC 1990), but none are specific to the TX tank farm or the leaks from tank TX-107.

As a first approximation, a travel time through the vadose zone is estimated here following the method of one dimensional analysis used in Appendix B of WHC (1990). The approximation assumes:

1. the entire tank leak of 30,200 liters occurred within one month,

2. the leak occurred over an area of 410 square meters (this estimate is the cross section area of a single-shell tank bottom in TX tank farm and is probably much larger than the actual area of the leak. A smaller leak area would result in a faster flux and shorter travel time),

3. a stratigraphy similar to borehole 299-W15-7 (from Wood et al. 2001),

4. saturated moisture contents of 0.5 for gravel and coarse sand and 0.4 for silt and caliche (from WHC 1990, Appendix B),

5. saturated hydraulic conductivities of 0.005 cm/sec for gravel, 0.001 cm/sec for coarse sand, 0.0004 cm/sec for silt, and 0.00005 cm/sec for caliche (from WHC 1990, Appendix B),

6. unsaturated moisture contents of 0.06 m^3/m^3 for gravel, 0.09 m^3/m^3 for coarse sand, 0.18 m^3/m^3 for silt, and 0.23 m^3/m^3 for caliche, and

7. a retardation factor of 1 (i.e., a contaminant with no adsorption or reaction with the sediment surface adsorption sites).

Using the above assumptions, a travel time through the vadose zone to the water table is estimated to be five to six years. This is probably much too quick because there is no allowance for lateral spreading and generalized moisture curves for the Hanford Site were used. This estimate is used here, however.

Given 1) a leak from tank TX-107 in 1977, 2) a travel time from tank TX-107 to the vadose zone of five years, 3) a groundwater flow direction of north to north-northeast in the late 1970s (i.e., from tank TX-107 toward wells 299-W14-1, 299-W14-2, and 299-W14-12), and 4) a groundwater flow rate of 0.05 m/d (a reasonable estimate from the data in Table 5.4 although flow rates may have been faster in the late 1970s because of a steeper U pond groundwater mound), a highly mobile contaminant should have reached well 299-W14-2 after 17 years, or about 1994 (five years in the vadose zone and 12 years in the groundwater).
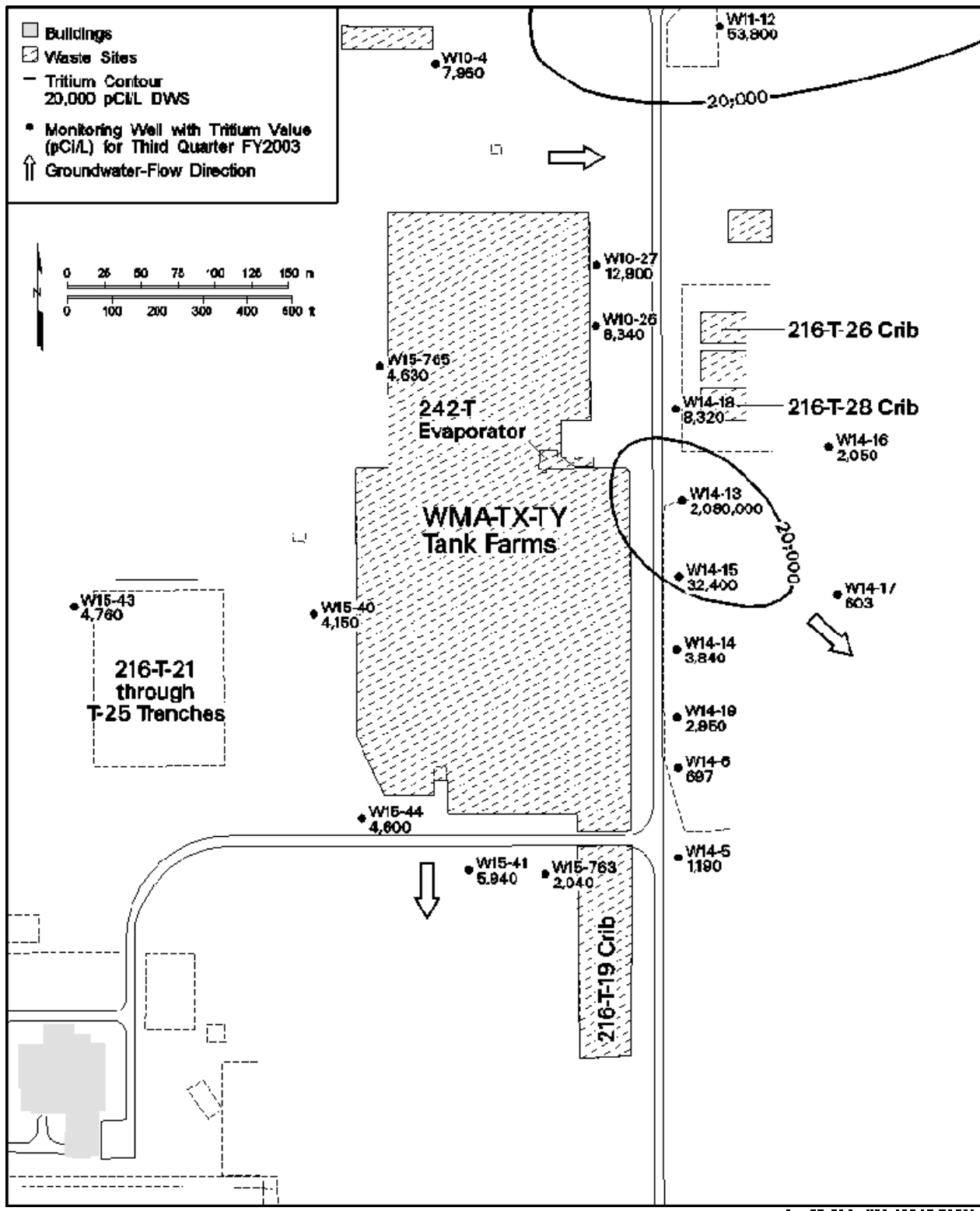
Figure 5.21. **Tritium Plume Map at WMA TX-TY for the Fourth Quarter of Calendar Year 2002**

The data in Section 4 and in situ desorption K_ds calculated in Section 6.5 show that the more mobile contaminants in the porewater from boreholes C3830 through C3832 are cobalt-60, technetium-99, nitrate, sulfate (SO_4^{2-}) and uranium (U), which is less mobile than the others. Therefore, it is these constituents that would be expected in the groundwater if tank fluids have entered the groundwater.

A plume of cobalt-60, strontium-90, and nitrate passed well 299-W14-2 between 1971 and about 1980 (see Figure 5.22). A cobalt-60, nitrate, and tritium plume also passed through the area of wells 299-W14-5 and 299-W15-4 during the early to mid-1970s. These latter two wells are to the east and south, respectively, of the TX tank farm and not downgradient of the TX-107 tank during the 1970s and 1980s. This early cobalt-60, nitrate, tritium (and strontium-90) plume appears to have begun passing through the area a few years before the reported tank T-107 leak.

A cobalt-60, chromium, nitrate, technetium-99, and tritium plume passed well 299-W14-12 in the early- to mid- 1990s (Figures 5.9 through 5.12 and Figure 5.23). This is approximately the time estimated for the fluids from tank TX-107 to reach the well. To test whether this plume (and the earlier 1970s plume) may have been from tank TX-107, several ratios of contaminant concentration in groundwater from well 299-W14-12 were compared to the same concentration ratios in the vadose zone porewater from borehole C3831.
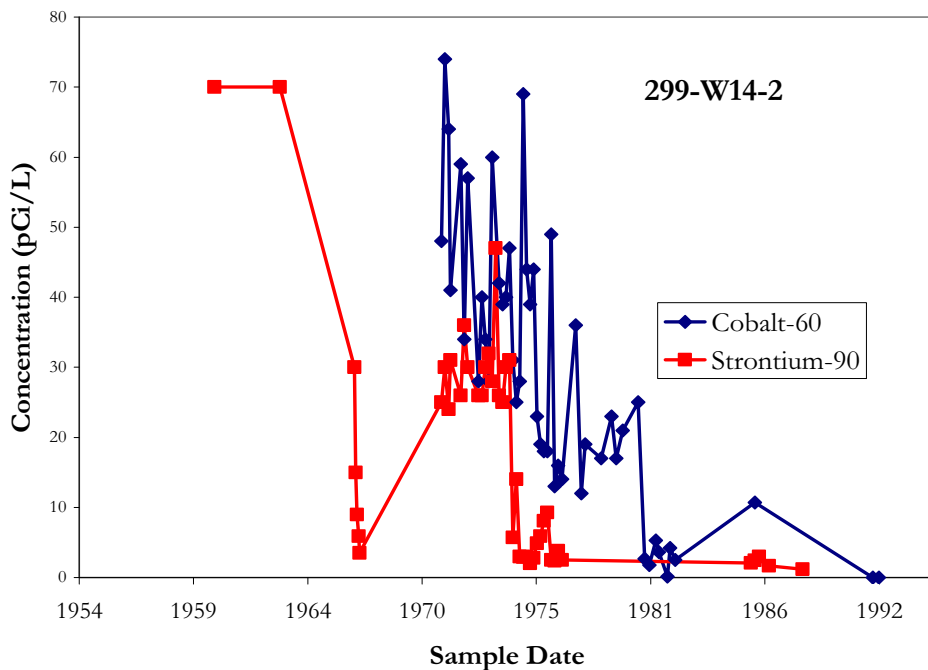
Figure 5.22. Cobalt-60 and Strontium-90 Concentrations in Well 299-W14-2
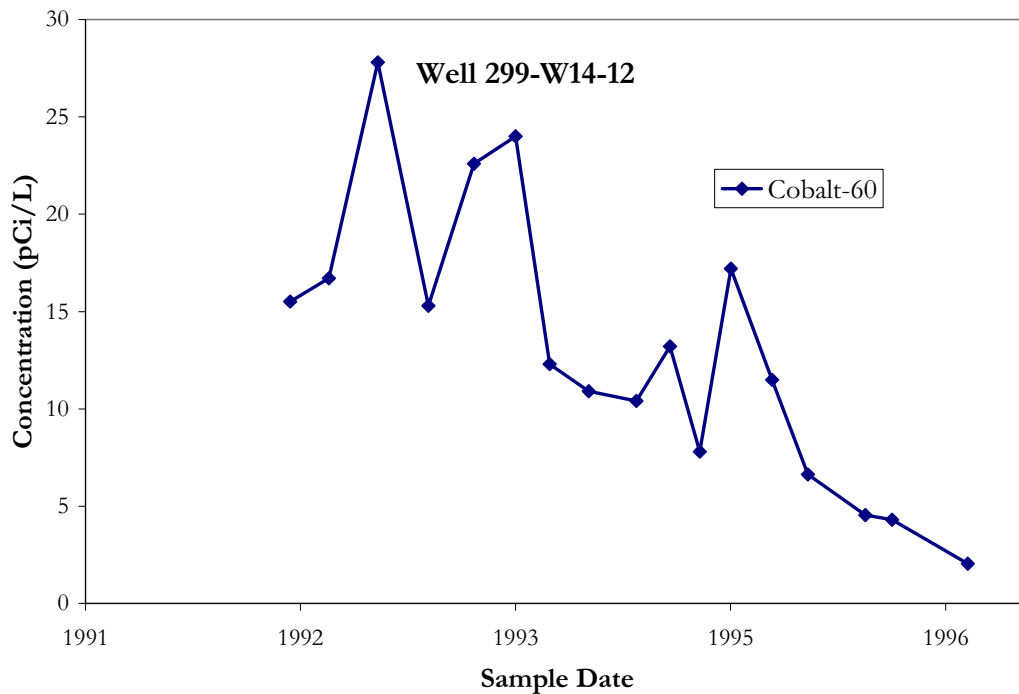
Figure 5.23. Cobalt-60 Concentrations in Well 299-W14-12

Several geochemical parameters were used to compare the porewater composition to groundwater composition. The first attempts to relate the groundwater and porewater compositions used the ratio of the concentration of various geochemical components (technetium-99, calcium, fluoride, chromium, sulfate, and sodium [Na]) to the concentration of nitrate. The ratios for porewater are given in Table 5.8; contaminant ratios for groundwater, using all available data with no laboratory qualifiers since about 1960, are shown in Table 5.9.

The agreement between the two data sets is not good. Some ratios for groundwater are larger than those for the vadose zone porewater (Cr/NO_3^-, F/NO_3^-) and others are smaller than the vadose zone porewater ($Tc-99/NO_3^-$, Na/NO_3^-). The lack of agreement between the groundwater ratios and the contaminated borehole sediment porewater rations suggests that the groundwater contamination has been influenced by fluids from nearby cribs and trenches. The ratios of most mobile species in the vadose zone porewaters should remain stable as tank fluids percolate through the sediment because the only reaction between the tank waste and the vadose zone sediment should be dilution as dispersion and mixing occurs with native porewater. That is, the concentrations of mobile constituents will change proportionately to each other and their ratios will remain constant as the fluids descend towards the water table. The ratio for $Tc-99/NO_3^-$, shown in Table 5.8 as a function of depth, shows a fairly constant value (0.16 ± 0.04 pCi/µg) between the depths of 69.6 and 115.1 ft bgs in borehole C3831 and 0.12 ± 0.03 pCi/µg between depths of 70.0 and 110.0 ft bgs in borehole C3832 (not shown in Table 5.80). Based on chemical composition data presented in Simpson et al. (2001), the $Tc-99/NO_3^-$ ratio for liquids that leaked from TX-107 was 6.07E-01 pCi/µg, whereas the $Tc-99/NO_3^-$ ratio of the liquids disposed to the nearby 216-T-19 tile field and 216-T-28 crib were 6.89E-04 and 8.45E-04 pCi/mg, respectively. Based on the large difference in $Tc-99/NO_3^-$ ratio of the liquids that leaked from the tank and the low values for nearby cribs and tile fields and the proximity of the boreholes to TX tanks, it is likely that the

boreholes intercepted only tank leak fluids. But because the boreholes met refusal in the Cold Creek lower subunit and the groundwater Tc-99/NO_3^- ratios are much lower, it is difficult to determine whether fluids that leaked from TX tanks, especially TX104, TX105 and TX107 that were investigated with the three boreholes (C3832, C3830, and C3831, respectively), has reached the groundwater below the TX-TY WMA.

A second attempt was made to compare groundwater and the contaminated borehole sediment porewater compositions by eliminating nitrate (an anion common to both tank waste and liquid disposed to nearby cribs and trenches) from the ratios. These results are shown in Tables 5.10 and 5.11 for porewater and groundwater, respectively. Comparison of the data in the two tables shows that the groundwater and porewater compositions are very different. If the porewater composition represents the composition of tank waste, then the contamination in the groundwater either is not tank waste or is a mixture of tank waste and other contaminant sources such that the nature of the tank waste is no longer recognizable.

In summary, there is no current similarity between the present or past groundwater contamination and current porewater compositions from the contaminated borehole sediments. Therefore, we cannot link the contaminants in the groundwater, currently or during the era of contaminant introduction into the vadose zone, to the porewaters currently in the borehole sediments, which are known to be derived from liquids that leaked from tank TX-107.

Table 5.8. Contaminant Concentration Ratios for Vadose Zone Porewater from Borehole C3831 as a Function of Depth and From Tank TX-107 Fluids

Depth	Tc-99/NO_3^- (pCi/µg)	Cr/NO_3^- (µg/µg)	F/NO_3^- (mg/mg)	Na/NO_3^- (mg/mg)	Ca/NO_3^- (mg/mg)	SO_4^{2-}/NO_3^- (mg/mg)
15.97	0.040	0.000195	0.750404	12.65	4.045	2.68
21.93	0.067	0.000136	0.192436	10.06	2.070	4.16
28.90	0.022	0.000362	0.535111	15.87	2.512	6.84
46.06	0.051	0.002111	0.113569	11.44	6.893	14.56
52.03	0.026	0.000260	0.400169	16.66	1.347	2.77
53.18	0.053	0.000051	0.007275	0.74	0.126	0.14
59.94	0.120	0.000028	0.000597	0.44	0.004	0.05
61.15	0.245	0.000129	0.001159	0.77	0.002	0.06
67.53	0.217	0.000891	0.016630	2.21	0.013	0.44
67.53	0.206	0.000647	0.016965	2.21	0.009	0.43
68.21	0.092	0.000745	0.007523	1.14	0.020	0.30
69.60	0.179	0.000886	0.012407	1.44	0.021	0.41
74.99	0.158	0.000013	0.001109	0.29	0.115	0.15
77.67	0.128	0.000009	0.003699	0.27	0.124	0.22
78.72	0.141	0.000008	0.001260	0.20	0.169	0.17
85.99	0.078	0.000003	0.000274	0.07	0.205	0.08
89.39	0.172	0.000010	0.003615	0.26	0.245	0.24
93.99	0.216	0.000010	0.001160	0.17	0.171	0.10
98.07	0.142	0.000013	0.001971	0.20	0.215	0.18
101.29	0.139	0.000016	0.002684	0.20	0.244	0.19
102.65	0.145	0.000011	0.002220	0.13	0.175	0.15
114.44	0.198	0.000007	0.005453	0.17	0.276	0.44
114.44	0.194	0.000007	0.005719	0.18	0.285	0.45
115.06	0.187	0.000007	0.004727	0.15	0.272	0.47
Tank TX-107						
from Simpson et al. 2001	0.60686	0.01728	0.00619	0.931	0.00450	0.0781

Table 5.9. Contaminant Concentration Ratios for Groundwater Samples from Well 299-W14-12

Sample Date	Tc-99/NO$_3^-$ (pCi/µg)	Cr/NO$_3^-$ (µg/µg)	F/NO$_3^-$ (mg/mg)	Na/NO$_3^-$ (mg/mg)	SO$_4^{2-}$/NO$_3^-$ (mg/mg)
4/21/1992	0.0187	0.0932	0.227273	0.054545	0.170455
7/20/1992	0.0219	0.1146	0.104167	0.052083	0.175
11/11/1992	0.0251	0.1132	0.188679	0.04717	0.177358
3/9/1993	0.0243	0.1091	0.181818	0.054545	0.190909
6/23/1993	0.0161	0.1064	0.191489	0.051064	0.204255
9/28/1993	0.0235	0.0981	1.019231	0.046154	0.184615
12/16/1993	0.0181	0.1000	0.230769	0.064103	0.192308
3/17/1994	0.0009	0.0846	0.25641	0.064103	0.194872
7/6/1994	0.0207	0.0951	0.268293	0.060976	0.185366
9/22/1994	0.0226	0.0974	0.282051	0.066667	0.189744
11/30/1994	0.0210	0.0633	0.333333	0.09	0.216667
2/10/1995	0.0221	0.0644	0.222222	0.064444	0.186667
5/17/1995	0.0250	0.1000	1	0.086111	0.202778
8/8/1995	0.0173	0.0714	0.285714	0.085714	0.16
12/20/1995	0.0121	0.0600	0.44	0.112	0.212
2/20/1996	0.0091	0.0252	0.34	0.104	0.168
5/16/1996	0.0055	0.0109	0.395455	0.109091	0.172727
8/14/1996	0.0013	0.0056	0.666667	0.15	0.2
11/13/1996	0.0053	0.0028	0.309179	0.13913	0.199517
2/10/1997	0.0494	0.0192	1.757322	0.155263	0.197368
5/14/1997	0.0037	0.0034	0.345263	0.123932	0.181951
11/17/1997	0.0045	0.0021	0.275122	0.117308	0.163248
2/17/1998	0.0062	0.0050	0.228205	0.102059	0.153077
6/25/1998	0.0068	0.0012	0.215	0.084597	0.130294
8/20/1998	0.0070	0.0071	0.158235	0.068448	0.140831
1/28/1999	0.0107	0.0079	0.156235	0.054545	0.131034

Table 5.10. Contaminant Concentration Ratios for Vadose Zone Porewater from Borehole C3831 as a Function of Depth and From Tank TX-107 Fluids

Depth (ft bgs)	Tc-99/Na (pCi/mg)	Tc-99/Cr (pCi/µg)	Tc-99/F (pCi/mg)
15.97	NA	205.58	0.0535
21.93	NA	494.35	0.3505
28.90	NA	60.93	0.0412
46.06	NA	23.97	0.4457
52.03	NA	100.16	0.0651
53.18	71.82	1049.40	7.2894
59.94	269.51	4324.19	200.4449
61.15	319.25	1900.35	211.1818
67.53	98.04	243.45	13.0383
67.53	93.27	318.84	12.1571
68.21	80.43	123.43	12.2241
69.60	124.58	201.83	14.4209
74.99	543.95	12343.34	142.0491
77.67	466.31	14549.63	34.5223
78.72	713.76	18447.11	112.0922
85.99	1129.53	29744.82	285.4978
89.39	673.34	17654.06	47.5097
93.99	1267.05	21941.02	186.2815
98.07	727.64	10753.58	72.0698
101.29	705.57	8859.07	51.7009
102.65	1092.68	13424.60	65.4806
114.44	1180.43	28930.93	36.3368
114.44	1109.97	26803.72	33.9935
115.06	1226.87	27104.64	39.4654
Tank T-107 Leak			
from Simpson et al. 2001	0.0007	35.1145	0.09810
NA = Not Available - data not measured.			

Table 5.11. Contaminant Concentration Ratios for Groundwater Samples from Well 299-W14-12

Date	Tc-99/Na (pCi/mg)	Tc-99/Cr (pCi/µg)	Tc-99/F (pCi/mg)
4/21/1992	0.3433	NA	8.2400
7/20/1992	0.4200	19.0909	21.0000
11/11/1992	0.5320	22.1667	13.3000
3/9/1993	0.4458	22.2917	13.3750
6/23/1993	0.3154	15.1400	8.4111
9/28/1993	0.5083	23.9216	2.3019
12/16/1993	0.2816	18.0513	7.8222
3/17/1994	0.0148	1.1182	0.3690
7/6/1994	0.3396	21.7692	7.7182
9/22/1994	0.3385	23.1579	8.0000
11/30/1994	0.2330	33.1053	6.2900
2/10/1995	0.3431	34.3103	9.9500
5/17/1995	0.2903	25.0000	2.5000
8/8/1995	0.2020	24.2400	6.0600
12/20/1995	0.1077	20.0993	2.7408
2/20/1996	0.0873	36.0397	2.6712
5/16/1996	0.0503	50.3333	1.3885
8/14/1996	0.0084	22.7040	0.1892
11/13/1996	0.0378	191.2281	1.7031
2/10/1997	0.0442	256.5217	2.8095
5/14/1997	0.0241	109.2308	1.0823
8/12/1997	NA	NA	0.0000
8/26/1997	0.0376	180.0000	
11/17/1997	0.0366	220.8333	1.9850
2/17/1998	0.0525	123.0769	2.8623
6/25/1998	0.0663	547.6190	4.2751
8/20/1998	0.0832	98.9691	4.5070
1/28/1999	0.1562	135.9649	15.9794
NA = Not Available - data not measured			

6.0   Summary and Conclusions

In this section, we present summary information about our interpretation of the TX borehole sediment characterization data. Conclusions are included to aid in making decisions on what interim actions and future studies are needed to make sound waste-management decisions at TX tank farm.

6.1   Drilling and Sampling Summary at the TX Tank Farm

Three boreholes were placed inside the TX Tank Farm area for the specific purpose of collecting core samples for physical and chemical characterization. Boreholes C3830, C3831, and C3832 were drilled via the closed-end probe method within the TX Tank Farm. Core samples, 1.25-ft-long by 2.5-in.-diameter, were collected at predetermined intervals within these boreholes. Each core contained two, 0.5-ft-long stainless-steel liners that contained sediment. An uncontaminated borehole (299-W10-27) was drilled outside the northeast corner of TY Tank Farm using a different sampling procedure. Two, 4-in.-diameter, 1-ft-long lexan-lined core samples were recovered from each 2.5-ft-long splitspoon in 299-W10-27. Sampling above 50 ft was limited to core-barrel grab samples every 5 ft, between 50 and 132 ft bgs near continuous core was collected while below 132 ft bgs grab samples were collected every 5 ft from the hard-tool drill cuttings. An additional three splitspoon cores were collected between hard-tooled intervals from the saturated zone within Ringold Formation member of Wooded Island (formerly called Unit E) gravels.

Borehole C3830 was located approximately 40 ft (12.2 m) southwest of single-shell tank 241-TX-105 to a total depth of 116.75 ft (35.6 m) bgs; the hole was terminated when refusal was encountered near the top of the lower Cold Creek unit (caliche). During drilling, a total of 18 splitspoon core samples were collected intermittently between August 20, 2002 and early September 2002. In all, about 25 ft of core was obtained from C3830, or about 22% of the total length of the hole. No samples or drill cuttings were collected between the 18 core runs because the hole was advanced in a closed configuration using a solid, removable tip.

Borehole C3831 was drilled and sampled using the driven-probe technique between July 1 and August 7, 2002. The borehole was located approximately 40 ft (12 m) southwest of single-shell tank 241-TX-107. During drilling, a total of 20 splitspoon core samples were collected intermittently starting at a depth of 15 ft bgs. The hole was terminated when refusal was encountered at 115.4 ft bgs in the caliche within the lower Cold Creek unit. In all, 26.74 ft of core was obtained from C3831, which accounts for about 23% of the total length of the hole. No samples or drill cuttings were collected between the 20 core runs because the hole was advanced in a closed configuration using a solid, removable tip.

Borehole C3832 was drilled and sampled using the driven-probe technique between May 2 and June 3, 2002. The borehole is located about 20 ft (6 m) south-southeast of single-shell tank 241-TX-104. During drilling, a total of 19 splitspoon core samples were collected intermittently starting at a depth of about 16 ft bgs. In all, 27.09 ft of core was collected, which accounts for about 23% of the total length of the hole. The hole was terminated when refusal was encountered at 115.9 ft bgs in the caliche within the lower Cold Creek unit. No samples or drill cuttings were collected between the 19 core runs because the hole was advanced in a closed configuration using a solid, removable tip.

Each of the 6-in. long liners from all three boreholes were opened in the chemistry lab and geologically described during the subsampling process to obtain aliquots used in the various characterization activities. The geology between core samples was inferred and interpreted based on the geophysical log and blow-count data.

6.2   Conceptual Model for TX Tank Farm Geology

Three primary stratigraphic units were encountered in each of the three boreholes: 1) backfill material, 2) the Hanford formation, and 3) the Cold Creek unit. The deeper Ringold Formation was only penetrated in the "clean" borehole 299-W10-27. Table 6.1 summarizes the contacts between the various stratigraphic units in the three boreholes and "clean" borehole.

For all three boreholes, the backfill consists of predominantly grayish-brown, very poorly to moderately sorted, massive, gravelly sand to slightly gravelly sand, which is unconsolidated and weakly to strongly calcareous. This unit appears to be rather homogeneous and lacks lithologic variation suggested by relatively uniform geophysical logs and blow-count data. Near the bottom of the backfill at C3831 near 46 ft bgs, a finer-grained 1-ft thick layer of laminated silty sand occurred. In the backfill at C3832, several feet or more of wet to moist, cohesive, well-sorted, strongly calcareous, dark grayish-brown, silty-fine sand was present at the base of the backfill sequence. Free water was reported in this material during core sampling. Fine-grained sand and silt was occasionally placed at and toward the base of the backfill within the TX Tank Farm, apparently to improve traction for construction vehicles (DOE-GJO 1997). This observation may explain the fine-grained and wetter nature of the backfill sediments at boreholes C3831 and C3832.

Below the backfill in all three boreholes lies the Hanford formation, which is divided into three informal units (H1, H2, and H3). However, at two of the boreholes the H1 unit was completely removed during excavation and then later used as backfill. We infer that a thin remnant of the H1 unit exists between 45 and 47 ft bgs at borehole C3832. Further, at the three boreholes there is no indication that H3 unit materials are present above the contact with Cold Creek units. Therefore below the TX tanks, the stratigraphy is dominated by the Hanford formation H2 unit. The Hanford formation H2 unit consists of predominantly fine-to-coarse-grained sand with an overall gray to brownish-gray color. This sand has the appearance of "salt and pepper", with the "pepper" fraction consisting of basaltic rock fragments, and the "salt" fraction consisting of mostly quartz and feldspar grains (as discussed in Section 2.1.3). The H2 sands are sometimes capped or interbedded with thin beds of silty-fine sand to silt. The fine- to coarse-sand beds are loose, massive to laminated, moderately to well-sorted, and weakly to moderately calcareous. Finer-grained beds are generally well sorted, cohesive, massive to laminated, yellowish to olive-brown, and moderately to strongly calcareous.

Table 6.1.   Stratigraphic Units and Contacts (ft bgs)

Hole	299-W10-27	C3830 (TX-105)	C3831 (TX-107)	C3832 (TX-104)
Recent Eolian	0 to 4.5	—	—	—
Backfill	—	0 to 52	0 to 52.3	0 to 45
H1	4.5 to 41.5	gone	gone	45 to 47
H2	41.5 to 89.4	52 to 100.4	52.3 to 102.2	47 to 103
CCU$_u$	89.4 to 98	100.4 to 111	102.2 to 106	103 to 110.4
CCU$_l$	98 to 112	111 to bottom	106 to bottom	110.4 to bottom
R$_{tf}$	112 to 124	Hole stopped	Hole stopped	Hole stopped
R$_{wi}$	124 to hole bottom	Hole stopped	Hole stopped	Hole stopped
H1 = Hanford formation Unit 1 – gravel dominated cataclysmic flood deposits. H2 = Hanford formation Unit 2 – sand dominated cataclysmic flood deposits. CCU$_u$ = Cold Creek Unit upper subunit – well-sorted silt and/or fine sand of eolian and/or fluvial origin. CCU$_l$ = Cold Creek Unit lower subunit – calic paleosol sequences. R$_{tf}$ = Ringold Formation member of Taylor Flat – generally fluvial sands and silts. R$_{wi}$ = Ringold Formation member of Wooded Island – fluvial sand and gravel.				

At borehole C3830, based on cores and the field moisture, spectral gamma, and blow-count logs, we infer there are four, thin fine-grained layers in the H2 unit. At borehole C3831 we infer that there are at least eight fine-grained layers in the H2 unit. At C3831, a clastic dike was observed within the Hanford formation H2 unit at about 60 ft bgs. The clastic dike is characterized by compact and cohesive, sub-vertically laminated, grayish-brown sand to dark gray silt and clay. A few small pebbles are also present within the dike, which is moderately calcareous. The clastic dike shows higher moisture content compared to adjacent strata, probably as a result of the presence of more fine grained material, which tends to retain more moisture. The contamination profile at C3831 suggests that fluids may have been captured by this clastic dike and preferentially transported along the dike. That is, at C3831 there are no signs of tank fluids above the depth where the borehole intercepted the clastic dike and the contamination is present from the intercept depth to near the bottom of the hole. There are at least eight, thin fine-grained interbeds in the H2 unit at borehole C3832. These thin fine-grained lenses found at all three boreholes within the H2 sands may impact the flow of leaked fluids and effected irregular and horizontal flow.

The upper Cold Creek unit, CCU$_u$, at borehole C3830 is 10.6-ft thick. Six samples of the upper CCU were collected for physical and chemical characterization at three different depths within the upper CCU. Sediments from this unit are compact and well-sorted silt to silty-fine sand, which range from laminated to massive, and are moderately to strongly calcareous. This unit has an average gravimetric moisture content of 11.0 %. At borehole C3831, the CCU$_u$ is compact and well-sorted silt to silty-fine sands, which range from laminated to massive, and are moderately to strongly calcareous. The upper CCU in C3831 is relatively thin (only 3.8-ft thick). The upper CCU in C3832 is 7.4-ft thick and consists of compacted and well-sorted, mottled to laminated, moderately to strongly calcareous, yellowish-brown to olive-brown, silt to silty-fine sand. The top of the upper CCU, especially at C3832, is defined by a dramatic decrease in grain size and an increase in the total gamma activity.

We define the top of the lower CCU as the top of the first pedogenically altered, carbonate-rich, cemented zone, that is accompanied by a sudden drop in natural-gamma activity. The lower Cold Creek unit, CCU_l, was sparsely sampled in boreholes C3830 and C3831 but five samples were obtained out of borehole C3832. Sediments from this unit are slightly moist (gravimetric moisture content 11 to 13%), mottled and cemented, pinkish-gray, very poorly sorted sand, silt, and olive-colored clay, some with a few small pebbles of angular basalt and others with pedogenic calcium carbonate stringers and nodules. All the samples are very strongly calcareous. The lower CCU represents a highly weathered paleosurface that developed unconformably on top of the Ringold Formation (Brown 1959, 1960) following a period of downcutting and degradation within the central Pasco Basin. The overall thickness of the lower CCU beneath the TX Tank Farm is generally 10-20 ft and dips to the southwest about one degree (Wood et al. 2001). In the vicinity of the TX Tank Farm, multiple, calcic-rich zones in the CCU_l subunit may be separated by relatively non-calcareous, un-cemented material, indicating some rapid accumulations occurred periodically between periods of soil development.

Deeper sediments were only sampled in the "clean" borehole, 299-W10-27, but based on other boreholes studied in the past, we offer the following geologic description. Generally, only fluvial gravel and sand facies are represented in the Ringold Formation vadose zone beneath the TX Tank Farm. The Ringold Formation member of Taylor Flat (R_{tf}) within the T-TX-TY WMA (also referred to as the upper Ringold unit) consists of interstratified, well-bedded fine to coarse sand to silt belonging to a mixture of fluvial-sand and overbank facies associations. Post-Ringold Formation erosion has locally stripped away this member, including all the area beneath TX Tank Farm. Below the Ringold Formation Taylor Flat Member is the Ringold Formation Wooded Island Member ([R_{wi}], also referred to as the Ringold Unit E) that consists predominantly of the fluvial-gravel facies association with occasional thin beds of the fluvial sand and/or the overbank facies associations. R_{wi} within the TX Tank Farm averages about 85-m (275 ft) thick and the top of the unit dips very gently to the southwest. The water table lies within R_{wi} gravels at about 220-ft (67 m) depth, about halfway between basalt bedrock and the ground surface.

6.3 Stratigraphy and Moisture Content

In general, heterogeneities including fine-grained thin lenses in the Hanford formation and the relatively thick Cold Creek unit likely cause anisotropy in water flow. Increased moisture was found to correlate with each of the fine-grained thin lenses intercepted by the coring and other fine-grained lenses are inferred to be present in the Hanford formation H2 unit based on the field neutron logging profiles. Recall that only about 25% of the profiles in the boreholes were cored. Several findings and hypotheses on the relationship between moisture content and water and contaminant flow that are gleaned from the characterization efforts reported herein include:

- Relatively high moisture contents occur in the Cold Creek unit in all three boreholes, especially for the lower CCU (i.e., caliche).

- Average moisture content for the Hanford formation H2 unit in "clean" borehole, 299-W10-27, is significantly less than in the three boreholes. This may be attributed to either:
  1. greater artificial recharge to the vadose zone associated with the boreholes (i.e., tank leaks, tank dome water diversion/shedding),

2. sample bias. Moisture samples from the H2 unit at 299-W10-27 were collected at regular 1-ft intervals, whereas the borehole intervals were pre-selected based on suspected contamination (i.e., high moisture), or

3. higher natural recharge beneath the tank farms due to the removal of surface vegetation and placement of gravel, which significantly reduces or eliminates near-surface transpiration of moisture back to the atmosphere.

6.4   Vertical Extent of Contamination

The following paragraphs describe measurements of various parameters that help us determine the extent of vertical migration of tank or ancillary equipment leaks. We used several parameters including moisture content, pH, electrical conductivity, nitrate, technetium-99, sodium, and uranium concentrations in water and acid extract as indicators to determine the leading edge of the plume. The concentrations of water-extractable (for mobile constituents) and acid-extractable or directly measured constituents in the sediment (for sorbing constituents) were used to delineate the total inventory of constituents within the plume. For technetium-99, the water-extractable data were judged to be a more accurate indication of past tank leaks than acid-extractable concentrations. In this section, we discuss all of the parameters measured except uranium and sodium.

Based on evaluating all these measurements, we conclude that the borehole data do not establish the vertical extent of tank contamination, especially in boreholes C3831 and C3832, because contamination was found at the bottom of these boreholes.

The first parameter, moisture content, is a direct measure of the mass of water in the vadose zone sediment. One would logically assume that wetter than normal conditions would represent the existence of leaked tank liquor but, as found at most of the boreholes studied to date, the moisture content in the three boreholes is indicative mainly of grain size.

The second parameter measured was the pH of water extracts of the vadose zone sediment. Based on the assumption that tank fluids are generally caustic and often very caustic (>1 M free hydroxide), elevated pH profiles should be indicative of the zones impacted by leaked fluids. The pH profiles for sediments from the three boreholes show slightly elevated pH in borehole C3831, at 61 ft bgs, that is indicative of alkaline tank fluid interactions. But the pH data at all other depths in borehole C3831 and at all depths in boreholes C3830 and C3832 show no indication of elevated pH values. Based on observations at other tank farms (SX and BX) where it is certain that caustic wastes are in the vadose zone, yet water extract pH values never exceed 10, we have concluded that pH is not a very sensitive parameter to use for evaluating the extent of plume migration in the vadose zone. A paper that provides a technically based conceptualization of the evolution of pH in sediments in contact with caustic fluids is in publication (see Wan et al. 2004).

The third parameter that was assessed to estimate the vertical extent of the leaked plume was dilution-corrected water extract electrical conductivity (EC). The EC depth profiles for the three boreholes do show elevated EC in comparison to the background sediments from borehole 299-W10-27. There is slightly elevated EC in the C3830 borehole sediments from 59.4 ft bgs to the bottom of the borehole samples. The highest dilution-corrected porewater EC is equivalent to a pore solution of 0.12 M KCl, the salt solution used to calibrate the conductivity probe.

There is also evidence of elevated EC starting at 60 ft bgs all the way to the bottom of the borehole at C3831. Somewhere between the two C3831 samples at 53.2 and 59.9 ft bgs, the EC of the 1:1 water extract increases to between 10 and 13 times the background sediment. At ~ 86 ft bgs in C3831 there is a second peak of high EC at about 11 times the background sediment water extract. Below 86 ft bgs to the bottom of the C3831 borehole at 115 ft bgs, the EC averages about 3 times higher than that in background sediments. When compared to the EC at borehole C3830 and C3832, the values at C3831 are unequivocally higher and indicative of the presence of saline tank-related fluids. The highest dilution-corrected porewater EC value for borehole C3831, between 60-61 ft bgs, is equivalent to a pore solution of 0.4 M KCl.

The EC values at C3832 are lower in the H2 unit and slightly larger than those at C3830 in the Cold Creek units and unequivocally lower than the EC values at borehole C3831 in both the H2 and CCU_u units. The highest values of dilution-corrected porewater EC in borehole C3832 occur in two zones, between 61 to 63 ft bgs and 110.3 to the bottom of the hole at 115.5 ft bgs. The C3832 dilution-corrected EC values for these two zones are equivalent to a pore solution of 0.042 and 0.051 M KCl. The maximum dilution-corrected EC at borehole C3832 in the H2 unit is 4.54 mS/cm, lower than the dilution-corrected EC at borehole C3830 (12.5 mS/cm). The highest dilution-corrected EC at borehole C3832 occurs in the CCU_l unit with a value of 6.27 mS/cm.

Because the three boreholes could not be pushed through the CCU_l unit to deeper depths, it is difficult to judge whether the vadose zone plumes of saline fluids stopped at the caliche layer as was found at the SX tank farm (see Serne et al. 2002b, 2002d). It does seem that the more elevated portions of the EC profile at borehole C3830 currently resides at the bottom of a fine-grained thin lens in the H2 unit at 87 ft bgs. At C3831, we lack good sample coverage in the fine-grained CCU_u mud unit and the caliche unit to ascertain whether the salt plume has significantly descended into the Cold Creek sediments. There is strong indication at borehole C3832 that the saline plume has descended into the Cold Creek unit at least to the bottom of the borehole.

Despite the evidence that elevated EC values may be present in all three boreholes to their depth of refusal, the concentrations are not large. For example, the maximum dilution-corrected EC at borehole C3832 is 6.27 mS/cm; at borehole C3830, the maximum is 12.5 mS/cm; at borehole C3831, the maximum is 43.3 mS/cm. The leaks near the SX108-109 and BX-102 tanks had peak vadose zone porewater concentrations that were equivalent to much more concentrated waste fluids, 524 to 1774 and 77 mS/cm, respectively. At 299-E33-46 near tank B-110 the dilution-corrected EC was 15.1 mS/cm, and at 299-W23-19 near tank SX-115, which contained dilute waste, the dilution-corrected EC was 33 mS/cm.

The fourth parameter evaluated to define the vertical extent of contamination was nitrate. The nitrate water extract values for borehole C3830 are elevated from 67 ft bgs to the deepest sample obtained. The nitrate water extract values are 10 to 50 times larger than for the background sediments in similar uncontaminated lithologies in borehole 299-W10-27. The nitrate water extract values for borehole C3831 are elevated compared to the background sediments from 53 ft bgs to the deepest sample obtained. The nitrate water extract values in C3831 borehole sediments are 20 to 300 times larger than for the background sediments between the depths of 53 and 86 ft bgs. The nitrate concentrations in the borehole C3831 are also ~ 5 to 10 times larger than those at similar depths in borehole C3830. The nitrate water extract values for borehole C3832 are elevated compared to the background sediments from 76 ft bgs to the deepest sample obtained. The nitrate concentrations in the borehole C3832 are the same as those at

borehole C3830 in the H2 sediments down to 97 ft bgs, but higher than the C3830 sediments below 97 ft bgs. Both C3832 and C3830 sediments contain ~ 5 to 10 times less nitrate than the sediments in borehole C3831. Thus, as found for the EC data, it is difficult to judge whether the vadose zone nitrate plumes were successfully stopped at the caliche layer as was found at the SX tank farm. It does appear that the nitrate plume in borehole C3832 may be a diluted and a deeper extension of the plume at C3831.

The fifth indicator species often used to define the vertical extent of contamination is technetium-99 in water extract samples. For the boreholes at the TX tank farm, the technetium-99 concentrations are not high enough to get a good indication on the vertical extent of tank related waste. The technetium-99 concentration levels are discussed in Section 6.6.

In summary, the moisture content, pH, electrical conductivity, nitrate, and technetium-99 profiles versus depth do not clearly identify the leading edge of the plume. The profiles do collectively suggest that tank-related fluids in borehole C3832 have traveled deeper than at the other two boreholes and that the C3832 plume's most saline concentrations have reached the caliche in the Cold Creek lower subunit to a depth of at least 116 ft bgs.

6.5   Detailed Characterization to Elucidate Controlling Geochemical Processes

The more detailed characterization activities of the cores from 299-W10-27 and the three boreholes added some insight on the processes that control the observed vertical distribution of contaminants and on the migration potential of key contaminants in the future. The porewaters, calculated by dilution correction of the 1:1 water extracts, in the sediment from the boreholes in the Hanford formation unit (H2) were dominated by sodium, nitrate, and bicarbonate for sediments with obvious signs of tank fluids. The most concentrated porewaters in the H2 and Cold Creek units for the three boreholes are shown in Table 6.2 in units of meq/L. Also included in the table for comparison are the maximum porewater concentrations found in other characterization work previously reported for the BX, B, and SX Tank Farms.

For borehole C3830, the most saline calculated porewater resides in the H2 unit and has a chemical composition of sodium (0.032 N), calcium (0.042 N), magnesium (0.018 N), potassium (0.005 N), nitrate (0.040 N), bicarbonate (0.034 N), sulfate (0.020 N), and chloride (0.008 N). The most saline calculated porewater in borehole C3831 is also present in the H2 sediments and is significantly more saline than the porewaters in C3830 and C3832. The maximum calculated porewater concentration in borehole C3831 has sodium (0.418 N), potassium (0.005 N), calcium (0.001 N), magnesium (0.0002 N), nitrate (0.202 N), bicarbonate (0.191 N), sulfate (0.015 N), phosphate (0.008 N), and chloride (0.006 N). A much more dilute, yet still tank-influenced porewater that consists of a more alkaline earth dominated system, is found in the borehole C3831 Cold Creek unit's sediments. The calculated porewater ionic strength in borehole C3832 sediments is more dilute than either of the other two boreholes but has more salinity in the Cold Creek sediments than in the H2 sediments. This suggests that the source of the fluids may be more distant from this borehole. That is, a plume descending within dipping strata with several fine-grained lens migrates in a "stair-step fashion" that would yield a pattern in vertical boreholes where contamination would be found deeper in the downgradient borehole. This stair-step pattern is observed when comparing boreholes C3831 and C3832 where some of the constituents' distributions in borehole C3831 suggest that the plume that is observed in both C3831 and C3832 could be from tank TX-107.

However, as discussed below not all constituents have distributions between the two boreholes that fit this hypothesis (see water-extractable uranium discussion). Further, the vertical distribution of contaminants at borehole C3831 may be controlled by the clastic dike that was intercepted at 60 ft bgs.

As shown in Table 6.2, the calculated porewaters in the TX boreholes are much less concentrated than porewaters found in the vadose zone sediments from either the BX and SX WMAs.

The water-extractable major cations' distributions in the three borehole sediments suggest that an ion-exchange process dominates the porewater/sediment interactions where tank fluid passed by or currently exists. The depth profiles for the divalent alkaline earth cations (calcium, magnesium, and strontium) versus sodium show remarkable similarities in all three boreholes. All show depleted divalent (alkaline earth) cation concentrations in the shallow Hanford formation H2 sediments below the tank bottoms. Conversely, the water-extractable sodium concentrations in this zone are elevated. At borehole C3830, the distribution of the divalent alkaline earth cations (magnesium, calcium, and strontium but not barium) and the monovalent cation potassium show low water-extractable quantities between 54 to 58 and 67 to 72 ft bgs with the lowest values of all at 67 ft bgs. Conversely, the distribution of water-extractable sodium is higher than the mass that is water leachable from uncontaminated sediments in the whole profile excepting at the 59.35 ft depth. The water-extractable sodium peak value occurs at 65 ft bgs and the peak nitrate and EC value occur at ~ 77 ft bgs. These trends suggest that tank fluids that are high in sodium (and nitrate based on the anion data) did seep into the vadose zone near this borehole. The water-extractable masses of all cations in the 59.35 ft bgs sample are very similar to uncontaminated background sediments. There is a fine-grained lens near this depth that may have forced the tank fluids to flow laterally around this zone.

At borehole C3831, the distribution of the divalent alkaline earth cations (magnesium, calcium, and strontium but not barium) shows low water-extractable quantities between 61 and 70 ft bgs. High divalent cation water extracts are found below in a narrow zone between 78.7 and 86 ft bgs. Conversely, the distribution of water-extractable sodium is very high between the depths of 60 and 75 bgs. The water-extractable sodium values in borehole C3831 sediments are higher than the values in the uncontaminated sediments from borehole 299-W10-27 over the whole borehole profile. These trends suggest that tank fluids that are high in sodium and nitrate did seep into the vadose zone near this borehole. The sodium pushed the natural divalent cations and some of the natural potassium off the sediment cation exchange sites in the sediments between 61 and at least 70 ft bgs. Right below the leading edge of the sodium plume one finds elevated levels of divalent cations that were displaced. We observe the highest levels of water-extractable divalent cations in the samples between 78.7 and 86 ft bgs. At borehole C3831, the water-extractable magnesium, calcium, strontium, barium, potassium, and sodium in the sediments from 75 ft bgs to the bottom of the borehole are larger than the background sediment in borehole 299-W10-27 by a factor of 3 to 5 and borehole C3830 sediments by a factor of 2. This probably is an indication that either more volume of fluid and/or higher concentration tank fluids are present in the C3831 sediments from 75 ft bgs to the bottom of the borehole than are present in the sediments obtained from borehole C3830.

Table 6.2. Maximum Pore Water Concentrations in Sediments from Hanford Formation and Cold Creek Units

Tank	TX-105	TX-107		TX-104		BX-102	B-110	SX-115	SX-109	SX-108
Borehole/Strata	C3830-H2	C3831-H2	C3831-CC	C3832-H2	C3832-CC	E33-45	E33-46	W23-19	41-09-39	Slant
					meq/L					
Na	32	418.5	24.4	39.1	12.1	525	150	35.6	6066	16900
Ca	42	1.2	37.0	1.1	30	114	4	280.9	619	90
Mg	18	0.2	17.1	0.44	13.6	62	2.5	94.6	24	10
K	10	4.7	5.9	1.4	2.5	13	0.5	3.6	42	92
Sr	0	0	0.1	0	0	0	0	1.5	4.4	1
UO2	0	0	0	0	0	2	0	0	0	0
Total Cats	102	424	84.4	42	58	716	157	416.2	6755.4	17093
NO3	40	202.4	55.4	0.6	10	100	3	420	6710	15677
NO2	0	0	0.0	0	0	0	0	0	28	32
SO4	20	15.2	12.6	5.8	36	570	14	3.3	95	500
CrO4	0	0	0.0	0	0	0	0	100	0	0
PO4	0	8.4	0.9	0.3	0	0	0	0	0	0
Cl	8	6.4	2.3	0.4	1.6	5	0	6	119	147
F	0	0.8	0.4	0.5	0.5	1	10	0	0	0
HCO3	34	191.2	12.8	37.3	11	40	130	7	0	666
Total Anions	102	424	84.4	42	58	716	157	536.3	6952	17022
dil-corrected EC (mS/cm)	12.5	43.26	9.66	4.54	6.27	76.8	15.1	33.1	524	1772

Yellow shaded cells signifies some round off to give electrical charge balance between the cations and anions.

6.9

At borehole C3832, the distribution of the divalent alkaline earth cations (magnesium, calcium, and strontium, but not barium) shows low water-extractable quantities between 63 and 97 ft bgs excepting the sample at 77 ft bgs. High divalent cation water extracts are found below in the Cold Creek unit. Conversely, the distribution of water-extractable sodium is elevated between the depths of 63 and 77 bgs. The water-extractable sodium values in borehole C3832 sediments are higher than the values in the uncontaminated sediments from borehole 299-W10-27 over the whole borehole profile including the backfill above the tank. These trends suggest that tank fluids that contained sodium did seep into the vadose zone near this borehole. The sodium pushed the natural divalent cations and some of the natural potassium off the sediment cation exchange sites between 63 to at least 76 ft bgs, if not all the way to the bottom of the H2 unit at 102 ft bgs. Right below the leading edge of the sodium plume there are elevated levels of divalent cations that were displaced. We observe the highest levels of water-extractable divalent cations in the C3832 samples below the Hanford formation H2 contact with the Cold Creek upper subunit to the bottom of the borehole. At borehole C3832, the water-extractable magnesium, calcium, strontium, potassium, and sodium concentrations in the sediments in both Cold Creek units (from 105 ft bgs to the bottom of the borehole) are greater than for the background sediment in borehole 299-W10-27 and also borehole C3830 sediments by a factor of 2 to 5. This likely is an indication that a larger volume of tank fluids passed through the C3832 sediments to the bottom of the borehole than passed through the vadose zone at borehole 3830. The water-extractable sodium concentrations at borehole C3831 are larger than at C3832 and it is possible that the plume from a leak at tank TX-107 could have been intercepted by both C3831 and C3832 boreholes. The sodium concentrations in borehole C3832 in almost all instances are more dilute down to the bottom of the H2 unit but are larger in the Cold Creek sediments that lay below. This distribution is compatible with a scenario where the source of the fluid is closer to borehole C3831 and descends with some dilution with existing vadose zone porewater towards borehole C3832. There is such a southwesterly dip to the Cold Creek units and older strata below the TX Tank Farm.

6.6 Estimates of Contaminant Inventory and Sorption-Desorption Values

In this section, we discuss our measurements and data synthesis used to quantify the inventory of key risk contaminants and our estimates of their adsorption-desorption tendencies. We did not perform any site-specific sorption or desorption studies per se because none of the contaminants were present at large enough concentrations to make testing practical. Further, because contaminant levels at TX are much lower than concentrations needed at other tank farms to cause predicted future risk concerns, detailed desorption testing did not appear to be necessary. However, by combining the data from the dilution-corrected 1:1 water extracts, which represent the porewater, with the concentrations measured on the sediment, we can estimate the desorption K_d values for contaminants of interest. For a contaminant that has very little water-soluble mass such as cesium-137, the in situ desorption K_d can be approximated as the mass in the total sample per gram of dry sediment divided by the mass in the porewater per milliliter. For a contaminant that is quite soluble in the water extract (this is approximately equivalent to stating that the contaminant resides mainly in the porewater within the sediment), one needs to subtract the amount that was present in the porewater from the total amount present in the moist sediment sample to obtain a value for the amount that would remain on the solid at equilibrium with the pore fluid.

We will first describe our inventory estimates and then address the mobility status of contaminants presently found in the TX vadose zone sediments. Tables 6.3 through 6.5 provide our best estimate of the inventory of potentially mobile contaminants found in each of the three boreholes. Potential contaminants of concern that have been selected for discussion include technetium-99, uranium, cobalt-60, chromium(VI), and nitrate.

The concentrations of technetium-99 found in the sediment are very close to our detection limit, but the others are present at high enough concentrations that we are comfortable that precise and accurate data were obtained. For the technetium-99 inventory we suggest that the water extract data is most accurate and should be used to estimate technetium-99 inventory versus depth. However, we do present the technetium-99 acid extract data as the worst-case maximum inventory estimate. We assume that all technetium is water soluble in the sediments, as found during our characterization studies at BX and the SX WMAs (Serne et al. 2002b, 2002c, 2002d, and 2002e), and that the acid-extract data are biased high and are generally of suspect quality.

For uranium and chromium, we have found that one must separate the natural background concentrations from Hanford added material in discussing risk potential. The natural uranium and chromium are almost entirely resistant to water leaching and to becoming mobile, whereas the material added by Hanford activities is somewhat mobile. We thus recommend using the water-extractable uranium and chromium data as representative of the concentrations that could enter the water table for future risk calculations. However, we present the acid-extractable chromium and uranium inventories to allow very conservative risk calculations to be performed that assume all acid-extractable masses could ultimately become released to percolating recharge waters. For the cobalt-60, we present the total activity present in the sediments.

For nitrate, as for technetium-99, we assume that the water extract concentrations represent the total inventory. We have no other method to measure nitrate besides the water extract method. We use 8 M nitric acid as our technique to measure the total amount of a constituent that is acid leachable. Thus, the nitric acid leachant overwhelms any nitrate present in the sediment. We have also designated in the

tables, using yellow shading, samples that may contain Hanford-related wastes as opposed to samples that are likely uncontaminated natural sediments.

Semi-quantitative estimates of desorption K_d values for the potential contaminants identified in Tables 6.3 through 6.5 can be calculated using the inventory estimates (mass or activity per gram of sediment) divided by the estimated porewater concentration of the constituent. These values are found in Tables 4.30, 4.45, 4.60 (acid extract) and 4.27, 4.42, and 4.57 (porewaters), respectively. Table 6.6 shows the estimated desorption K_d values for the sediment cores obtained from each of the three boreholes. In Table 6.6, the depths where the bulk of the contamination is present are highlighted in red (bold) type and the desorption K_d values that suggest contamination being present at even very low concentrations are highlighted in yellow (darker) shading. The faint blue (lighter) shading in Table 6.6 designates data that are more dominated by natural constituents or impacted by low precision analytical values. From the table one can see two trends. First where there are significant concentrations of contaminants in the sediments (between 67 to 87, 61 to 70, and 61 to 110 ft bgs, at C3830, 3831, 3832, respectively), the K_d values for uranium, chromium, and technetium-99 are smaller than their values at shallower and deeper depths. This is caused both by there being more saline porewaters (competing ions) and higher contributions of waste species for chromium and uranium being present, which are generally more water leachable than naturally present species. The changes in K_d values for technetium-99 outside the zone of significant contamination are likely more a function of imprecision in the acid versus water extract analytical results. The other trend is that the desorption K_d values for technetium-99 in the main portion of the vadose zone plumes is very close to 0 mL/g, while the desorption K_d value for uranium and chromium in the main portion of the plumes vary between 0 to 2 mL/g, and 7 to 70 mL/g.

Table 6.3. Inventory Estimates for Potential Contaminants of Concern in Borehole C3830 Sediments

Depth (ft bgs)	Strat. Unit	Extract Water Nitrate	Tc-99	U-238	Cr	Acid Tc-99	U-238	Cr
Units		µg/g	pCi/g	µg/g	µg/g	pCi/g	µg/g	µg/g
15.98	Bkfl	4.91		8.05E-04	6.79E-04	(9.48E+00)	3.84E-01	8.10E+00
28.92	Bkfl	1.58		1.72E-03	(2.94E-04)	(1.09E+00)	4.37E-01	8.70E+00
42.10	Bkfl	1.18		7.44E-03	1.16E-03	(2.91E+02)	4.61E-01	9.29E+00
47.18	Bkfl	1.57	(3.48E-01)	2.09E-03	(3.91E-04)	(2.48E+02)	3.91E-01	7.63E+00
48.63	Bkfl	0.80		1.58E-03	(4.34E-04)	(2.29E+02)	3.89E-01	6.65E+00
54.02	H2	0.59		1.83E-03	5.06E-04	(2.89E+02)	5.44E-01	1.34E+01
54.02	H2	1.91		1.12E-03	2.98E-03	2.52E+02	4.49E-01	1.16E+01
58.03	H2	2.94		4.61E-04	5.48E-04	2.70E+02	3.66E-01	1.16E+01
59.35	H2	1.46	(1.70E-01)	1.07E-03	(4.37E-04)	(2.71E+02)	5.92E-01	1.55E+01
67.11	H2	28.24	(2.88E+00)	2.79E+00	8.39E-03	(1.88E+01)	1.65E+01	1.28E+01
72.63	H2	41.87	(4.08E+00)	8.21E-04	1.27E-03	(8.07E+00)	5.70E-01	1.13E+01
78.01	H2	84.13	1.14E+01	2.09E-04	1.55E-03	(1.97E+01)	5.08E-01	1.28E+01
81.89	H2	62.17	6.19E+00	1.49E-03	1.05E-03	(9.24E+00)	7.25E-01	1.39E+01
87.09	H2	69.28	5.60E+00	5.77E-04	2.02E-03	(7.24E+00)	5.63E-01	1.93E+01
100.02	H2	27.97	(3.39E-01)	5.67E-04	1.86E-03	(2.42E+02)	6.81E-01	1.48E+01
101.37	CCUu	22.84		3.12E-04	2.45E-03	2.39E+02	4.24E-01	1.21E+01
101.37	CCUu	24.21		3.52E-04	2.62E-03	(2.83E+02)	6.69E-01	1.67E+01
104.08	CCUu	37.25		6.26E-04	5.49E-03	2.50E+02	5.88E-01	1.28E+01
108.87	CCUu	20.21		1.35E-03	8.52E-04	(2.71E+02)	6.68E-01	2.15E+01
114.64	CCUl	31.75		2.89E-03	1.28E-03	(1.87E+01)	1.62E+00	6.70E+00

( ) = Data below quantification values but deemed qualitatively useful.
Yellow shading represents samples that do or may indicate some Hanford waste fluids are present.

Table 6.4. Inventory Estimates for Potential Contaminants of Concern in Borehole C3831 Sediments

Depth (ft bgs)	Strat. Unit	Nitrate	Tc-99	U-238	Cr	Tc-99	U-238	Cr	Co-60
Extract		Water				Acid			Direct
Units		µg/g	pCi/g	µg/g	µg/g	pCi/g	µg/g	µg/g	pCi/g
15.97	Bkfl	1.7		2.44E-03	3.32E-04		5.18E-01	9.47E+00	<0.107
21.93	Bkfl	3.27		1.35E-03	4.47E-04		4.58E-01	1.05E+02	<0.089
28.90	Bkfl	2.31		3.84E-03	8.37E-04		5.10E-01	8.37E+00	<0.134
46.06	Bkfl	3.35		4.14E-03	7.08E-03		5.06E-01	6.51E+00	<0.105
52.03	Bkfl	1.95		2.87E-03	5.09E-04		6.66E-01	1.63E+01	<0.107
53.18	H2	55.44	2.94E+00	9.46E-04	2.80E-03	(2.43E+01)	5.94E-01	1.11E+01	1.521
59.94	H2	667.32	7.99E+01	3.05E-03	1.85E-02	1.94E+02	4.58E-01	1.22E+01	40.120
61.15	H2	560.84	1.37E+02	4.02E-02	7.23E-02	1.94E+02	5.47E-01	1.08E+01	26.713
67.53	H2	72.93	1.58E+01	3.07E-02	6.50E-02	(3.68E+01)	6.37E-01	1.24E+01	28.124
67.53	H2	87.67	1.81E+01	1.62E-02	5.67E-02	(4.15E+01)	6.50E-01	1.74E+01	20.230
68.21	H2	91.28	8.39E+00	5.90E-02	6.80E-02	(6.23E+01)	8.54E-01	1.36E+01	38.557
69.60	H2	60.53	1.08E+01	2.31E-02	5.37E-02	(5.44E+01)	6.76E-01	1.23E+01	50.877
74.99	H2	350.18	5.52E+01	1.71E-03	4.47E-03	(7.02E+01)	6.60E-01	1.47E+01	7.337
77.67	H2	154.81	1.98E+01	6.62E-04	1.36E-03	(3.98E+01)	6.13E-01	1.56E+01	3.693
78.72	H2	287.03	4.05E+01	1.15E-03	2.20E-03	(7.76E+01)	6.34E-01	1.18E+01	2.068
85.99	H2	846.66	6.61E+01	1.93E-03	2.22E-03	1.99E+02	6.03E-01	1.33E+01	3.647
89.39	H2	98	1.68E+01	7.29E-04	9.53E-04	(3.16E+01)	4.90E-01	1.34E+01	0.452
93.99	H2	252.96	5.46E+01	8.67E-04	2.49E-03	9.03E+01	5.50E-01	1.23E+01	2.708
98.07	H2	202.78	2.88E+01	1.23E-03	2.68E-03	(6.40E+01)	5.97E-01	1.31E+01	1.005
101.29	H2	127.18	1.76E+01	7.65E-04	1.99E-03	(2.66E+01)	5.55E-01	1.08E+01	1.408
102.65	CCU$_u$	222.42	3.23E+01	1.28E-03	2.41E-03	(4.71E+01)	6.28E-01	1.04E+01	0.582
114.44	CCU$_l$	175.96	3.49E+01	2.03E-03	1.21E-03	(5.66E+01)	1.22E+00	6.33E+00	0.694
114.44	CCU$_l$	169.8	3.30E+01	1.99E-03	1.23E-03	(4.59E+01)	8.12E-01	1.08E+01	0.579
115.06	CCU$_l$	204.28	3.81E+01	2.07E-03	1.41E-03	(4.76E+01)	8.46E-01	6.88E+00	0.570

(   ) = Data below quantification values but deemed qualitatively useful.
Yellow shading represents samples that do have or may indicate some Hanford waste fluids present.

Table 6.5. Inventory Estimates for Potential Contaminants of Concern in Borehole C3832 Sediments

Depth (ft bgs)	Strat. Unit	Nitrate	Tc-99	U-238	Cr	Tc-99	U-238	Cr
Extract		**Water**				**Acid**		
Units		µg/g	pCi/g	µg/g	µg/g	pCi/g	µg/g	µg/g
17.26	backfill	0.43		1.70E-03	(1.29E-04)	(3.83E+01)	3.97E-01	1.69E+01
29.14	backfill	1.02		9.88E-04	(1.45E-04)	(3.33E+01)	4.20E-01	1.30E+01
37.14	backfill	1.63		2.24E-03	5.15E-04	(1.98E+01)	3.84E-01	1.15E+01
45.19	backfill	3.2		4.81E-03	(4.98E-04)	(1.31E+01)	4.72E-01	1.11E+01
52.01	H2	1.28		8.77E-04	(3.58E-04)	(1.85E+01)	5.54E-01	1.51E+01
54.10	H2	3.13		4.44E-03	(4.27E-04)	(1.47E+01)	7.05E-01	1.67E+01
61.17	H2	2.33		1.72E-02	(4.93E-04)	(1.21E+01)	1.02E+00	1.51E+01
62.96	H2	1.85		1.46E-01	5.48E-04	(1.47E+01)	2.85E+00	1.31E+01
69.99	H2	2.62	(1.87E-01)	1.81E+00	1.36E-03	(1.28E+01)	1.46E+01	2.22E+01
76.34	H2	14.6	2.35E+00	2.82E-01	1.21E-03	(3.11E+01)	5.82E+00	3.10E+01
76.34	H2	21.08	2.29E+00	1.32E-01	7.49E-04	(2.19E+01)	8.55E+00	2.00E+01
77.04	H2	79.04	7.16E+00	1.26E+00	9.66E-03	(3.34E+01)	1.22E+01	1.39E+01
79.81	H2	19.42	2.34E+00	1.26E+00	1.79E-02	(1.94E+01)	6.94E+00	1.32E+01
84.01	H2	25.12	1.76E+00	5.57E-01	2.85E-02	(2.04E+01)	1.09E+01	1.81E+01
88.06	H2	11.39	1.80E+00	4.71E-01	1.50E-03	(1.21E+01)	4.29E+00	1.57E+01
94.05	H2	3.93	(5.22E-01)	5.90E-01	3.95E-03	(1.03E+01)	2.39E+00	1.64E+01
96.69	H2	13.25	1.46E+00	1.06E+00	2.81E-03	(1.32E+01)	6.02E+00	1.69E+01
105.01	CCUu	57.27	6.51E+00	2.65E+00	1.90E-03	(1.63E+01)	2.73E+01	2.35E+01
110.28	CCU$_u$	72.48	1.08E+01	2.60E+00	9.10E-04	(2.57E+01)	3.07E+01	2.06E+01
110.28		97.36	1.18E+01	2.61E+00	1.03E-03	(3.25E+01)	3.05E+01	3.18E+01
111.02	CCU$_l$	84.18	5.11E+00	4.82E-03	9.28E-04	(2.92E+01)	1.40E+01	1.09E+01
114.85	CCU$_l$	58.84	1.07E+01	3.15E-03	1.92E-03	(3.39E+01)	1.40E+01	8.82E+00
115.54	CCU$_l$	48.09	2.50E+00	1.18E-01	9.11E-04	(4.27E+01)	1.90E+01	3.18E+01

(   ) = Data below quantification values but deemed qualitatively useful.
Yellow shading represents samples that do or may indicate some Hanford waste fluids are present.

Table 6.6. Desorption K_d Values (mL/g) for Potential Contaminants of Concern

| C3830 | | | | | C3831 | | | | | | C3832 | | | | |
Depth (ft bgs)	Strat. Unit	Tc-99	U	Cr	Depth (ft bgs)	Strat. Unit	Tc-99	U	Cr	Co-60	Depth (ft bgs)	Strat. Unit	Tc-99	U	Cr
		mL/g	mL/g	mL/g			mL/g	mL/g	mL/g	mL/g			mL/g	mL/g	mL/g
15.98	Bkfl	0.07	26	640	15.97	Bkfl	-0.03	6	869	NA	17.26	Bkfl	0.00	14	7674
28.92	Bkfl	-0.04	14	1589	21.93	Bkfl	-0.04	13	9134	NA	29.14	Bkfl	1.70	19	4020
42.10	Bkfl	3.66	3	442	28.90	Bkfl	-0.05	6	482	NA	37.14	Bkfl	1.02	8	1031
47.18	Bkfl	36.76	10	1008	46.06	Bkfl	-0.08	10	77	NA	45.19	Bkfl	1.63	11	2443
48.63	Bkfl	2.63	12	761	52.03	Bkfl	-0.17	38	5300	NA	52.01	H2	1.37	41	2765
54.02	H2	2.48	11	980	53.18	H2	0.46	40	252	NA	54.10	H2	1.20	12	2897
54.02	H2	2.55	17	169	59.94	H2	0.12	12	54	0.264	61.17	H2	0.47	2	1152
58.03	H2	2.13	27	723	61.15	H2	0.02	1	7	0.048	62.96	H2	0.00	1	1244
59.35	H2	198.07	69	4405	67.53	H2	0.08	1	11	0.069	69.99	H2	10.05	1	2412
67.11	H2	0.14	0	37	67.53	H2	0.08	2	18	0.071	76.34	H2	1.29	2	2602
72.63	H2	0.03	24	307	68.21	H2	0.80	2	25	0.163	76.34	H2	0.99	7	2932
78.01	H2	0.02	76	259	69.60	H2	0.22	2	13	0.398	77.04	H2	0.66	1	222
81.89	H2	0.02	18	488	74.99	H2	0.05	69	595	0.115	79.81	H2	0.77	0	74
87.09	H2	0.03	109	1066	77.67	H2	0.06	59	733	0.206	84.01	H2	1.37	2	78
100.02	H2	35.21	59	394	78.72	H2	0.15	89	870	0.070	88.06	H2	0.29	0	544
101.37	CCU$_u$	3.79	93	338	85.99	H2	0.30	46	874	0.000	94.05	H2	0.97	0	219
101.37	CCU$_u$	4.65	134	450	89.39	H2	0.04	34	722	-0.019	96.69	H2	0.65	0	470

Table 6.6   (cont)

C3830					C3831						C3832				
Depth (ft bgs)	Strat. Unit	Tc-99 mL/g	U mL/g	Cr mL/g	Depth (ft bgs)	Strat. Unit	Tc-99 mL/g	U mL/g	Cr mL/g	Co-60 mL/g	Depth (ft bgs)	Strat. Unit	Tc-99 mL/g	U mL/g	Cr mL/g
104.08	CCU$_u$	5.47	118	294	93.99	H2	0.04	37	287	0.047	**105.01**	CCU$_u$	0.17	1	1149
108.87	CCU$_u$	6.16	48	2473	98.07	H2	0.13	53	538	-0.039	**110.28**	CCU$_u$	0.20	1	2453
114.64	CCU$_l$	0.47	78	726	101.29	H2	0.03	36	268	0.070	**110.28**		0.24	1	3409
					102.65	CCU$_u$	0.02	26	229	0.003	111.02	CCU$_l$	0.72	398	1600
					114.44	CCU$_l$	0.07	63	551	-0.062	114.85	CCU$_l$	0.23	410	422
					114.44	CCU$_l$	0.04	43	921	-0.025	115.54	CCU$_l$	1.70	17	3589
					115.06	CCU$_l$	0.03	53	633	-0.049					

NA = No detectable Co-60 in the sediment or the water extracts; thus can not calculate a K$_d$.
Red (bold) type signifies depths where sediments show obvious signs of some tank related fluids.
Yellow (dark) shading signifies K$_d$ values that are dominated by tank fluids as opposed to a mix of natural and Hanford constituents. Faint blue (light) shading data are likely more dominated by natural constituents (uranium and chromium) or imprecise analytical data (technetium-99 and cobalt-60).

6.17

In borehole C3831 where cobalt-60 was present, the desorption K_d values, as determined by direct gamma energy analysis from the direct counting of the moist sediment and water extracts, are fairly low (0.00 to 0.4 mL/g). Thus, cobalt-60 in these vadose zone sediments would be considered quite mobile. The in situ desorption K_d results suggest that of the potential contaminants, technetium-99 is the most mobile, with cobalt-60 slightly less mobile or of equal mobility to technetium-99. Uranium is considerably less mobile, and chromium the least mobile.

For conservative modeling purposes we recommend using K_d values of 0 mL/g for nitrate and technetium-99, a value of 0.05 mL/g for cobalt-60, a value of 1 mL/g for uranium, and 10 mL/g for chromium to represent the entire vadose zone profile from the bottoms of the tanks to the water table. The technetium in situ desorption K_d value of zero is consistent with a wealth of literature that finds essentially no technetium adsorption onto Hanford Site sediment (Kaplan and Serne 1995; Kaplan and Serne 2000). The cobalt-60 results suggest that some complex that perhaps has a net negative charge is altering the cobalt's inherent cationic nature. Cobalt-60 has been found in the Hanford groundwater at several places, especially in the 1950s, and can still be measured in a few locations, most notably in the northern 200 East Area.

6.7   Other Geochemical Characterization Observations

The comparison of the percentage of a constituent that is water extractable versus acid extractable from the contaminated sediment and the total mass that is acid leachable can be used to infer contamination for Hanford tank constituents such as sodium, sulfate, uranium, chromium, and other trace metals that occur naturally in the environment.

For borehole C3830, the acid extract data suggest that variations in mass leached per gram of sediment versus depth are lithology-related more so than an indication of tank fluid contamination. That is, for most constituents there are no signs of elevated values of acid-leachable constituents in borehole C3830 sediments, excepting acid-extractable sulfur (assumed to represent sulfate) and technetium-99. The acid-extractable sulfate profile in borehole C3830 sediments averages about 4 to 7 times higher than in comparable uncontaminated sediments from borehole 299-W10-27. The acid-extractable technetium-99 profile in the C3830 borehole sediments is elevated from 42 ft bgs to 109 ft bgs by a factor of 4 over the distribution of acid-extractable technetium-99 in the background sediment, which was a measure of our detection limit. The deepest sample obtained in borehole C3830 within the Cold Creek caliche does not have this slightly elevated acid-extractable technetium-99, suggesting that the bulk of the technetium-99 vadose zone plume has not migrated to the bottom of the borehole.

The only other indication of tank contamination at borehole C3830 is the high water- and acid-extractable uranium value for the sample at 67.11 ft bgs. As mentioned in Sections 4.2.4, 4.3.4, and 4.4.4, contaminated sediments generally exhibit high ratios for water- to acid-extractable constituents when compared to uncontaminated sediment ratios. The percentage of the acid-extractable uranium that is also water extractable for the sample at 67.11 ft bgs is 17% while all other uranium water extracts for sediments below the tank, leached less than 0.5% of the acid-extractable uranium. The water-extractable sodium percentage for the sample at 67.11 ft bgs is also 17% of the sodium that is acid extractable, which also is slightly higher than for uncontaminated sediments.

Comparing the acid extract data for borehole C3831 with similar lithologies in the uncontaminated borehole, 299-W10-27, suggest most of the variation in mass leached per gram of sediment versus depth

is lithology related. Again, for most constituents there are no signs of elevated values of acid-leachable constituents in borehole C3831 sediments excepting acid-extractable sulfur (assumed to represent sulfate), sodium (between the depths of 61 and 67.5 ft bgs), molybdenum (between 67.5 and 70 ft bgs), and ruthenium and technetium-99 throughout most of the profile. The acid-extractable sulfate profile in borehole C3831 sediments averages about 4 to 7 times higher than in comparable uncontaminated sediments from borehole 299-W10-27. The acid-extractable sulfur (measured as sulfate) for boreholes C3830 and C3831 are similar. Borehole C3831 shows high acid-leachable technetium-99 and ruthenium throughout the profile and larger acid-extractable sodium and molybdenum in thin zones between 67.5 and 70 and 61 to 67.5 ft bgs, respectively, than borehole C3830. The comparison of water to acid extracts for borehole C3831 sediments suggests that there are unnaturally high percentages of water-leachable uranium, chromium, and molybdenum between the depths of 61 and 70 ft bgs. The water- to acid-extractable sodium percentage is unnaturally high between the depths of 53 and 86 ft bgs, suggesting sodium-enriched fluids or readily acid-soluble solids reside in the pores of the vadose zone sediments in this zone. The presence of elevated water and acid-extractable quantities of technetium-99 and ruthenium between 60 ft bgs and the bottom of the borehole at 115 ft bgs suggests the presence of Hanford waste fluids in the vadose zone at these depths in borehole C3831. Thus the leading edge of contamination extends beyond the bottom of the borehole.

Acid-extractable technetium-99 in borehole C3832 also appears to be slightly above the background sediments but is the same as in borehole C3831 and somewhat lower than acid-extractable technetium-99 in borehole C3830. The comparison of water to acid extracts for borehole C3832 sediments suggests that there are unnaturally high percentages of water-leachable technetium-99 and uranium-238 between 76 and 115, and 61 to 110.3 ft bgs, respectively. There is also slightly high water-extractable sodium between 63 and 77 ft bgs. The total mass of tank fluids that are present in borehole C3832 sediments and the percentages that are water leachable versus the concentrations that are acid leachable are lower for most constituents than at borehole C3831.

The two data sets suggest that the tank-related fluids in borehole C3832 may, in fact, be the leading edge of fluids that leaked from tank TX-107, which were first intercepted by borehole C3831. If so, then it also appears that the vadose zone plume dips to the southwest between boreholes C3831 and 3832, which is supported by discussions in Section 2.0. However, the uranium water and acid extract data for sediments at boreholes C3831and C3832 do not fit our hypothesis that a plume of saline fluids has leaked from tank TX-107 and migrated and descended to deeper depths to the southwest. Unlike many other constituents, the uranium data for borehole C3831 sediments (closer to TX-107) show significantly lower water- and acid-leachable uranium than the sediments from C3832 (farther from TX-107 and down dip). Unless a mechanism can be hypothesized that allows uranium to leak from tank TX-107, without showing significant interactions with the sediments until migrating to the southwest where it is captured by the C3832 borehole, the uranium data suggest separate sources of contamination with different leak events. There are greater acid-extractable concentrations of uranium at borehole C3832 from 61.2 ft bgs all the way to the bottom of the borehole than at either of the other two boreholes, C3830 and C3831. Acid-extractable uranium concentrations vary from 1 to 30 ug/g over this interval and are significantly greater than values in borehole C3831.

As part of our characterization strategy for contaminated sediments, other parameters that can control contaminant migration were measured. For the TX tank farm characterization only calcium carbonate content was measured. Particle size measurements were performed only on uncontaminated sediment from selected samples from borehole 299-W10-27; however, photographs in Appendix A and the field

moisture log, blow counts, and laboratory moisture contents identify that several fine-grained thin lenses are present within the Hanford formation H2 unit that can promote lateral spreading of leaked fluids. The upper and lower portions of the Cold Creek unit also contain a high percentage of fines that can lead to perching conditions and/or lateral spreading of percolating fluids.

There are highly calcareous zones associated with the lower Cold Creek subunit in each of the three boreholes and the background borehole at depths that range from 98 to 112, 111 to the bottom of the borehole, 106 to the bottom of the borehole, and 110.4 to the bottom of the borings at 299-W10-27, C3830, C3831, and C3832, respectively. The caliche at borehole C3832 has the most calcium-carbonate equivalent solid of the three boreholes and the uncontaminated background sediment from 299-W10-27, based on available samples. The calcium-carbonate content in the Cold Creek lower subunit ranges from 20 to 34% at borehole C3830, 22% at 299-W10-27, and 38% at borehole C3831, to 38 to 46% at borehole C3832. As found in most vadose sediments from the Hanford Reservation, there is very little (<0.1% by weight) organic carbon in the vadose zone sediments. The borehole C3831 backfill sample at 46.1 ft bgs appears to have elevated inorganic carbon (10.3 wt% as calcium carbonate) and some (0.4 wt%) organic carbon. Aside from this backfill sample, carbon values for total, inorganic, and organic carbon are low and quite similar in the backfill and Hanford formation sediments from C3830, C3831, and C3832.

The matric potential data from a portion of the vadose zone profile at 299-W10-27 (zone where cores were collected were entirely within the Hanford formation H2 unit) show water potentials are generally much less than the gravity potential. The last sample taken at 123.5 ft bgs appears to have a matric potential larger than the theoretical line, which represents the profile for matric potential in a sediment profile that is neither draining nor drier than (actively evapotranspiring) equilibrium. Matric potential values less than the gravity unit gradient suggest a draining profile. The water potential data from 299-W10-27's H2 unit, the unit where most of the contaminants reside in the TX boreholes, are consistent with a draining profile.

6.8   Description of TX-TY Upper Unconfined Aquifer

The suprabasalt aquifer is separated into the uppermost unconfined aquifer and the underlying Ringold Formation confined aquifer beneath WMA TX-TY by the silt and clay deposits of the Ringold Formation lower mud unit. Currently, the unconfined aquifer is about 55 m thick at well 299-W14-14, east of WMA TX-TY. The unconfined aquifer consists of sandy gravels and gravelly sands of the Ringold Formation member of Wooded Island unit E. Water levels beneath WMA TX-TY were raised as much as 13.5 m above the pre-Hanford natural water table because of artificial recharge from liquid waste disposal operations active since the mid-1940s. The largest volumes of discharge were to the 216-T pond system and the 216-U-10 pond. The increase in water-table elevation was most rapid from 1949 to 1956 and was somewhat stabilized between the late 1960s and the late 1980s. Water levels began to decline in the late 1980s.

Accompanying the changes in water level were changes in groundwater flow direction. Pre-Hanford Site groundwater flow direction was toward the east; it changed toward the south in the late 1940s and early 1950s. This shift resulted from disposal of large volumes of liquid to the 216-T pond. Around 1956, groundwater flow direction changed again and started flowing towards the north due to the increasing influence of the groundwater mound under 216-U pond. Discharges to 216-T pond ended in 1976 but continued at 216-U pond until 1984. Consequently, the flow direction changed again around 1996 when all discharges to the ground ceased and the influence of the 216-U pond mound on the

groundwater beneath the TX and TY tank farms diminished. Around 1996, the groundwater flow direction began to return toward the east or southeast. Today, groundwater contamination beneath the WMA and surrounding area is generally migrating easterly. Hydrologic data show that the groundwater flow direction becomes increasingly more southerly toward the south of WMA TX-TY. Groundwater beneath this part of the WMA is influenced by the extraction wells of the 200-ZP-1 pump-and-treat system. Extraction wells W15-33, W15-34, and W15-35 for the 200-ZP-1 pump-and-treat operation are 300 m southwest of WMA TX tank farm fenceline.

Results of the tracer dilution test show downward, vertical hydraulic gradients within the upper portion of the aquifer in wells 299-W10-26, 299-W14-13, and 299-W14-14. These three wells have fairly homogeneous lithology throughout the screened interval and comprehensive drawdown data do not indicate substantial variations in hydraulic conductivity. The existence of vertical flow in a well does not necessarily reflect actual groundwater flow conditions within the surrounding aquifer, but its presence implies a vertical flow gradient within the well screens and has implications pertaining to the representativeness of groundwater samples collected from the wells. The vertical gradient detected in these wells along the eastern edge of the TX and TY tank farms may have an impact on contaminant distribution patterns in the area.

A second finding of the hydrologic test data is the suggestion of higher hydraulic conductivities at certain depths within the screened interval of some wells relative to other depths. Aquifer tests in well 299-W15-41, located just south of the TX tank farm, indicate that the middle and lower parts of the screened interval have higher permeability than the upper part. However, development pumping data (which is not as definitive as aquifer testing) indicates that the upper part of the screened interval in nearby well 299-W15-763 has higher permeability than the lower parts. Thus, apparent differences in hydraulic conductivity do not appear to correlate from well to well. Taken as a whole, the geologist's logs, geophysical logs, development pumping data, and the hydrologic testing data all indicate heterogeneity in aquifer properties within the screened intervals of several individual wells and among wells at WMA TX-TY.

6.9   Existing Groundwater Contamination

Groundwater at the TX and TY tank farms contains elevated concentrations of carbon tetrachloride, chromium, iodine-129, nitrate, technetium-99, and tritium. This contamination appears to result from the mixing of wastes from a number of past waste-disposal activities, including the disposal of waste process water, and steam condensate at nearby cribs and trenches, disposal of plutonium processing waste at cribs and trenches associated with the Plutonium Finishing Plant, and leaks from single-shell tanks and transfer lines within the TX and TY tank farms.

Contamination in two areas near the TX and TY tank farms warrants consideration: east and downgradient of 241-TX and 241-TY tank farms, and south of 241- TX tank farm. The contaminants of interest east of WMA TX-TY are technetium-99, iodine-129, nitrate, tritium, chromium, and carbon tetrachloride. The contaminants of interest south of TX tank farm are technetium-99 and carbon tetrachloride.

The maximum carbon tetrachloride found in the area of WMA TX-TY in 2002 was 5,800 µg/L in well 299-W15-1, south of the TX tank farm. The carbon tetrachloride is believed to be from pre-1973 waste from the Plutonium Finishing Plant. The major identified sources are the 216-Z-9 trench, the 216-Z-1A tile field, and the 216-Z-18 crib.

East of WMA TX-TY, chromium occurs in one downgradient well (299-W14-13) above the drinking water standard. In August 2003, the concentration was 540 µg/L. Given the current direction of groundwater flow, one potential source for the chromium is the 241-TY tank farm. However, about 1,060 kilograms of chromium were disposed to the TY cribs located about 65 m northeast of the well. Since the general dip of the strata in the area is toward the west or southwest, it is possible that contamination from the cribs migrated through the vadose zone toward well 299-W14-13. Further, a tanker truck filling station, located about 140 m up dip of the TY cribs, was seen leaking onto the ground from the fill spout in the 1990s. Water was seen to pool on the ground and run about 100 m down slope (toward the TX and TY tank farms) in a ditch along the side of the gravel road. Infiltration of this water could have mobilized contamination in the vadose zone beneath the TY cribs and moved the contamination down dip toward well 299-W14-13. Furthermore, in the 1970s, contamination at the 216-T-28 crib extended from near the surface to the water table and thus breakthrough to groundwater could have occurred at the 216-T-28 crib site. Therefore, we can not currently assign an origin for the elevated chromium in well 299-W14-13 to a particular facility.

Technetium-99 was detected in this downgradient well (299-W14-13) above the drinking water standard. Given the current direction of groundwater flow, one potential source for the technetium-99 is single shell tanks in WMA TX-TY. However, three other sources, 216-T-28 crib, 216-T-19 tile field, and the 242-T evaporator building, also may have contributed some technetium-99 to the groundwater east of WMA TX-TY. Current groundwater plume maps for chromium and technetium-99 show that the contaminant plumes are relatively small and centered near well 299-W14-13. Concentrations of both contaminants drop sharply to the north in well 299-W14-18 and to the south in well 299-W14-15.

Almost all wells in the groundwater monitoring network at WMA TX-TY, including the upgradient wells, have had nitrate concentrations greater than the MCL of 45 mg/L throughout most of their sampling life. The highest nitrate concentrations (580 mg/L) have been at well 299-W14-13. This well has had nitrate concentrations greater than those in the regional plume since it was drilled in late 1998. Besides the regional source of nitrate from the Plutonium Finishing Plant and disposal to U Pond, other potential contaminant sources are those mentioned above as potential sources for chromium and technetium-99. Tritium has also been above the drinking water standard in well 299-W14-13. Like nitrate, tritium most likely has several sources that include WMA TX-TY and several cribs and trenches in the area.

South of the TX-TY WMA the key contaminants are technetium-99 and carbon tetrachloride. The groundwater in this area is currently impacted (since June 1998) by the 200-ZP-1 pump-and-treat operation. Technetium-99 concentrations in wells along the southern boundary of WMA TX-TY started to increase about 1 year after Phase II of the 200-ZP-1 pump-and-treat operation began. (Phase II, consisting of three extraction wells, began the use of the closest extraction wells to the WMA, wells 299-W15-34 and 299-W15-35.) Given the southerly groundwater flow direction imposed on the southern portion of the WMA by the pump-and-treat operation, the most reasonable explanation for the increasing technetium-99 is that groundwater contaminated with technetium-99 is being drawn from beneath the WMA into the pump-and-treat system. Alternatively, technetium-99 may be originating from the

216-T-19 crib and tile field. Given the changing groundwater flow direction along the southern boundary of the WMA, the few available monitoring wells, and the lack in continuity of monitoring data due to dry wells and new wells, it is currently impossible to fully evaluate this problem.

6.10 Complexities in Groundwater Data (Vertical and Temporal Variations)

The groundwater data are complicated by signs that vertical stratification in contaminant and common solutes is present in many wells. Significant differences in specific conductance, technetium-99, chromium, nitrate, and tritium with depth were found in some monitoring wells. After purging some TX-TY wells, the pumped samples do not appear to be representative of ambient water because purging the well causes mixing of strata with different contaminant concentrations. Thus, interpreting the contaminant distribution in wells such as the most contaminated well in the WMA (299-W14-13) is very difficult because groundwater at the well contains high concentrations of several contaminants that show different vertical concentration profiles and probably come from several sources in the area.

Well pair 299-W14-12 and 299-W14-13 is at the northeast corner of the TX tank farm on the downgradient side of WMA TX-TY and currently has the highest concentration of technetium-99, tritium, iodine-129, fluoride, nitrate, and chromium of any well in the TX and TY tank farm monitoring network. This and other wells also show a time-varying contaminant distribution over the last 50 years. Technetium-99 in the area of the well pair 299-W14-12/13 began decreasing from a maximum of ~ 13,500 pCi/L in 1993 and continued to decrease until about January 1997. At that time, technetium-99 began to increase until early 2000 when technetium-99 concentrations climbed to ~ 8,000 pCi/L. In early 2000, technetium-99 began to decrease and dropped to about 3,300 pCi/L in early 2001, at which time the concentration began to increase again. The latest increase continued until February 2003 and reached 8,740 pCi/L. The results for nitrate in well pair 299-W14-12/13 show a trend similar to that seen for technetium-99. Nitrate began to decrease from a maximum of about 540,000 µg/L in 1993 to about 200,000 µg/L in early 1997. Nitrate then began to increase until early 2000 when concentrations reached ~ 440,000 µg/L. Nitrate began to decrease a second time until early 2001, at which time it began a second increasing trend that lasted through the beginning of 2003. Since that time, the nitrate concentration has decreased somewhat. Analytical results for tritium in well pair 299-W14-12/13 show a different trend in vertical distribution than that seen for technetium-99 and nitrate, but show the same trends with time. The chromium data suggest a different vertical distribution of chromium in the aquifer than the distributions of nitrate, technetium-99, and tritium. The data from the well pair indicate that the concentration of chromium is low at the top of the aquifer and increases at some depth below the water table but, again, the chromium distribution with time tracks the same as technetium, nitrate, and tritium. The similar trends with time suggest that these contaminants are from the same source. If so, they should not be fractionated differently in the aquifer versus depth. Thus, there is some discrepancy among the data as to the interpretation of the vertical distribution data.

Samples collected from several wells during drilling indicate an increase in nitrate concentration with increasing depth in the aquifer. A few wells show a second zone of high nitrate concentration near the water table. The shallow zone of high nitrate is interpreted to be from nearby local sources whereas the deeper, and more widespread, zone of high nitrate represents a regional plume from past practice discharges, probably from the Plutonium Finishing Plant that were disposed of to U pond. Depth distributions of tritium and carbon tetrachloride in well 299-W14-14 showed maximums at about 40 m

below the water table, suggesting that significant concentrations of these contaminants may exist in the confined Ringold Formation aquifer.

6.11 Vadose Zone Porewater and Groundwater Chemical Ratio Comparisons

Selected concentration ratios of mobile contaminants in a) the vadose zone sediments sampled by the three boreholes, b) the TX-TY groundwater contaminant plumes and c) specific single-shell tanks, cribs and trenches at the time of suspected leaks and disposal campaigns, respectively, were used to assess whether there are indications that the groundwater contamination is related to current vadose zone contamination and can be associated with a specific facility or a specific tank leak.

Our initial attempts to relate the groundwater and porewater compositions used the ratios of the concentrations of technetium-99, calcium, fluoride, chromium, sulfate, and sodium to the concentration of nitrate. The agreement between the vadose zone porewater and contaminated groundwater data sets is not good. Some ratios for groundwater are larger than those for the vadose zone porewater (Cr/NO_3^-, F/NO_3^-) and other groundwater ratios are smaller than the vadose zone porewater ratios (Tc-$99/NO_3^-$, Na/NO_3^-). The lack of agreement between the groundwater ratios and the contaminated borehole sediment porewater ratios suggests that the groundwater contamination has been influenced by fluids from nearby cribs and trenches. The ratios of most mobile species in the vadose zone porewaters should remain stable as tank fluids percolate through the sediment because the only reaction between the tank waste and the vadose zone sediment mobile constituents should be dilution, as dispersion and mixing occurs with native porewater.

Based on the large difference in Tc-$99/NO_3^-$ ratio of the liquids that leaked from the TX tanks, the low values for nearby cribs and tile fields, and the proximity of the three boreholes to TX tanks, it is likely that the three boreholes intercepted only tank leak fluids. However, because the three boreholes did not sample below the upper Cold Creek subunit, we do not know whether tank fluids leaked from TX tanks, especially TX104, TX105 and TX107, have reached the groundwater below the TX-TY WMA. Comparison of the mobile constituent ratios for these two fluids shows that the groundwater and porewater compositions are very different. If the contaminated vadose zone sediment porewater composition represents the composition of tank waste, then the contamination in the groundwater either is not tank waste or it is a mixture of tank waste and other contaminant sources such that the nature of the tank waste is no longer recognizable.

In summary, there is no current similarity between the present or past groundwater contamination and current porewater compositions from the contaminated borehole sediments. Therefore, we cannot link the contaminants in the groundwater, currently or during the era of contamination introduction in the vadose zone, to the porewaters currently in the borehole sediments, which are known to be derived from the liquids that leaked from tanks in the TX tank farm, especially tank TX-107.

7.0   References

Alexander DJ, SD Evelo, VG Johnson, and MD Sweeney. 1995. *Groundwater Impact Assessment Report for the 216-T-4-2 Ditch*. WHC-EP-0815, Westinghouse Hanford Company, Richland, Washington.

American Society of Agronomy (ASA). 1986a. "Hydrometer Method." Chapter 15-5 in *Methods of Soil Analysis-Part 1*, *2nd edition of Physical and Mineralogical Methods*, SSSA Book Series No. 5, ed. A Klute, pp. 404-408. Soil Science Society of America, Madison, Wisconsin.

American Society of Agronomy (ASA). 1986b. "Pynchnometer Method." Chapter 14-3 in *Methods of Soil Analysis-Part 1, 2nd edition of Physical and Mineralogical Methods*, SSSA Book Series No. 5, ed. A Klute, pp. 378-379. Soil Science Society of America, Madison, Wisconsin.

American Society of Agronomy (ASA). 1996a. *Methods of Soil Analysis-Part 3, Chemical Methods*, SSSA Book Series 5, ed. DL Sparks, Soil Science Society of America, Madison, Wisconsin.

American Society of Agronomy (ASA). 1996b. "Elemental Analysis by XRF Spectroscopy." Chapter 7 in *Methods of Soil Analysis-Part 3, Chemical Methods*, SSSA Book Series 5, ed. DL Sparks, pp. 161-223. Soil Science Society of America, Madison, Wisconsin.

American Society for Testing and Materials (ASTM) D4129-88. 1988. *Standard Test Method for Total and Organic Carbon in Water by High Temperature Oxidation and by Coulometric Detection.* American Society for Testing and Materials, West Conshohocken, Pennsylvania.

American Society for Testing and Materials (ASTM) D2488-93. 1993. *Standard Practice for Description and Identification of Soils (Visual-Manual Procedure).* American Society for Testing and Materials, West Conshohocken, Pennsylvania.

American Society for Testing and Materials (ASTM) D2216-98. 1998. *Test Method for Laboratory Determination of Water (Moisture) Content of Soil and Rock by Mass*. American Society for Testing and Materials, West Conshohocken, Pennsylvania.

American Society for Testing and Materials (ASTM) D5298-94. 2002. *Test Method for Measurement of Soil Potential (Suction) Using Filter Paper*. American Society for Testing and Materials, West Conshohocken, Pennsylvania.

Baker VR, BN Bjornstad, AJ Busacca, KR Fecht, EP Kiver, UL Moody, JG Rigby, DF Stradling, and AM Tallman. 1991. "Quaternary Geology of the Columbia Plateau." In *Quaternary Nonglacial Geology: Conterminous U.S. Geology of North America*, ed. RB Morisson, K-2:215-250. Geological Society of America, Boulder, Colorado.

Baker VR and RC Bunker. 1985, "Cataclysmic Late-Pleistocene Flooding from Glacial Lake Missoula: A Review." *Quaternary Science Reviews*, 4:1-41.

Bergeron MP and SK Wurstner. 2000. *Groundwater Flow and Transport Calculations Supporting the Immobilized Low-Activity Waste Disposal Facility Performance Assessment*. PNNL-13400, Pacific Northwest National Laboratory, Richland, Washington.

Bjornstad BN. 1984. *Suprabasalt Stratigraphy Within and Adjacent to the Reference Repository Location*. SD-BWI-DP-039, Rockwell Hanford Operations, Richland, Washington.

Bjornstad BN. 1990. *Geohydrology of the 218-W-5 Burial Ground*. PNL-7336, Pacific Northwest Laboratory, Richland, Washington.

Bjornstad BN, KR Fecht, and CJ Pluhar. 2001. "Long History of Pre-Wisconsin, Ice-Age, Cataclysmic Floods: Evidence from Southeastern Washington State." *Journal of Geology,* 109:695-713.

Bjornstad BN, GV Last, SP Reidel, DG Horton, KR Fecht, GA Smith, and KA Lindsey. 2002. "Characterization and Proposed Formalization (Hanford formation) for Ice Age Flood Deposits Within the Pacific Northwest." In *Geological Society of America, Abstracts with Programs*, p. A-24, Geological Society of America, Boulder, Colorado.

Bjornstad BN, GV Last, and DG Horton. 2003. *Hydrogeology of the Hanford Site Vadose Zone*, 4th Symposium on the Hydrogeology of Washington State, Program Abstracts, Olympia, Washington.

Black RF. 1979. *Clastic Dikes of the Pasco Basin, Southeastern Washington*. RHO-BWI-C-64, Rockwell Hanford Operations, Richland, Washington.

Brown DJ. 1959. *Subsurface Geology of the Hanford Separation Areas*. HW-61780, General Electric Company, Richland, Washington.

Brown DJ. 1960. *An Eolian Deposit Beneath the 200 West Area*. HW-67549, General Electric Company, Richland, Washington.

Brown RE. 1970. *Interrelationships of Geologic Formations and Processes Affecting Ecology as Exposed at Rattlesnake Springs*. BNWL-B-29, Battelle Northwest Laboratory, Richland, Washington.

Caggiano JA and SM Goodwin. 1991. *Interim Status Groundwater Monitoring Plan for the Single-Shell Tanks*. WHC-SD-EN-AP-012, Westinghouse Hanford Company, Richland, Washington.

Connelly MP, BH Ford, and JV Borghese. 1992a. *Hydrogeologic Model for the 200 West Groundwater Aggregate Area*. WHC-SD-EN-TI-014, Westinghouse Hanford Company, Richland, Washington.

Connelly MP, JV Borghese, CD Delaney, BH Ford, JW Lindberg, and SJ Trent. 1992b. *Hydrogeologic Model for the 200 East Groundwater Aggregate Area*. WHC-SD-EN-TI-019, Westinghouse Hanford Company, Richland, Washington.

Crumpler JD. 2002. *Site Specific SST Phase 1 RFI/CMS Work Plan Addendum for WMAs T and TX-TY*. RPP-7578, Rev. 2, CH2M HILL Hanford Group, Inc., Richland, Washington.

Deka RN M Wairiu, PW Mtakwa, CE Mullins, EM Veenendaal, and J Towend. 1995. "Use and Accuracy of the Filter Paper Method for Measuring Soil Matric Potential." *European J. of Soil Sci.* 46:233-238.

Delaney CD, KA Lindsey, and SP Reidel. 1991. *Geology and Hydrology of the Hanford Site: A Standardized Text for Use in Westinghouse Hanford Company Documents and Reports.* WHC-SC-ER-TI-003, Westinghouse Hanford Company, Richland, Washington.

DOE (U.S. Department of Energy). 1984. *Draft Environmental Assessment, Reference Repository Location, Hanford Site, Washington*, DOE/RW-0017, U.S. Department of Energy, Washington, D.C.

DOE (U.S. Department of Energy). 1988. *Consultation Draft Site Characterization Plan, Reference Repository Location, Hanford Site, Washington.* DOE/RW-0164, U. S. Department of Energy, Office of Civilian Radioactive Waste Management, Washington, D. C.

DOE (U.S. Department of Energy). 1992. *T Plant Source Aggregate Area Management Report.* DOE/RL 91-61, U. S. Department of Energy, Richland Operations Office, Richland, Washington.

DOE (U.S. Department of Energy). 1999. *Phase 1 RCRA Facility Investigation/Corrective Measures Study Work Plan for the SST Waste Management Areas.* DOE/RL-99-36, Rev. 0, U.S. Department of Energy, Richland Operations Office, Richland, Washington.

DOE (U.S. Department of Energy). 2002a. *Standardized Stratigraphic Nomenclature for Post-Ringold-Formation Sediments Within the Pasco Basin.* DOE/RL-2002-39, U.S. Department of Energy, Richland Operations Office, Richland Washington.

DOE (U.S. Department of Energy). 2002b. *Fiscal Year 2001 Annual Summary Report for the 200-UP-1 and 200-ZP-1 Operable Unit Pump-and-Treat Operations.* DOE/RL-2001-53, U. S. Department of Energy, Richland Operations Office, Richland, Washington.

DOE-GJO (U.S. Department of Energy–Grand Junction Office). 1997. *Hanford Tank Farms Vadose Zone, TX Tank Farm Report.* GJO-HAN-11, prepared by U.S. Department of Energy–Grand Junction Office for U.S. Department of Energy, Richland Operations Office, Richland Washington.

EPA (U.S. Environmental Protection Agency). 1986. *Test Methods for Evaluating Solid Waste: Physical/Chemical Methods, SW-846*, 3rd ed. U.S. Environmental Protection Agency, Office of Solid Waste and Emergency Response, Washington, D.C., [Online manual]. Available URL: http://www.epa.gov/epaoswer/hazwaste/test/sw846.htm

EPA Method 300.0A. 1984. *Test Method for the Determination of Inorganic Anions in Water by Ion Chromatography.* EPA-600/4-84-017, U.S. Environmental Protection Agency, Washington, D.C.

EPA Method 3050B. 2000a. "Acid Digestion of Sediments, Sludges, and Soils." *Test Methods for Evaluating Solid Waste, Physical/Chemical Methods.* EPA Publication SW-846, [Online manual]. Available URL: http://www.epa.gov/epaoswer/hazwaste/test/sw846.htm

EPA Method 6010B. 2000b. "Inductively Coupled Plasma-Atomic Emission Spectrometry." *Test Methods for Evaluating Solid Waste, Physical/Chemical Methods*. EPA Publication SW-846, [Online manual]. Available URL: http://www.epa.gov/epaoswer/hazwaste/test/sw846.htm

EPA Method 6020. 2000c. "Inductively Coupled Plasma-Mass Spectrometry." *Test Methods for Evaluating Solid Waste, Physical/Chemical Methods*. EPA Publication SW-846, [Online manual]. Available URL: http://www.epa.gov/epaoswer/hazwaste/test/sw846.htm

Fecht KR and DC Weekes. 1996. *Geologic Field Inspection of the Sedimentary Sequence at the Environmental Restoration Disposal Facility*. BHI-00230, Bechtel Hanford, Inc., Richland, Washington.

Fecht KR, BN Bjornstad, DG Horton, GV Last, SP Reidel, and KA Lindsey. 1999. *Clastic Injection Dikes of the Pasco Basin and Vicinity: Geologic Atlas Series*. BHI-01103, Rev. 0, Bechtel Hanford Company, Richland, Washington.

Fecht KR, GV Last, and KR Price, 1977. *Evaluation of Scintillation Probe Profiles from 200 Area Crib Monitoring Wells, Volume III*. ARH-ST-156, Atlantic Richfield Hanford Company, Richland, Washington.

Flint RF. 1938. "Origin of the Cheney-Palouse Scabland Tract." *Geological Society of America Bulletin*, 49:461-524.

Folk RL. 1968. *Petrology of Sedimentary Rocks*. Hemphill, Austin, Texas.

Gardner MG, KD Reynolds, and DE Skoglie. 2002a. *Completion Report for Probe Hole C3831 (TX-107) TX Tank Farm 200 West Area*. RPP-12293, Rev. 0, Prepared for the Office of River Protection, CH2M HILL Hanford Group, Inc., Richland, Washington.

Gardner MG, KD Reynolds, and DE Skoglie. 2002b. *Completion Report for Probe Hole C3832 (TX-104) TX Tank Farm 200 West Area*. RPP-12017, Rev. 0-A, Prepared for the Office of River Protection, CH2M HILL Hanford Group, Inc., Richland, Washington.

Gee GW. 1987. *Recharge at the Hanford Site. Status Report*. PNL-6403, Pacific Northwest Laboratory, Richland, Washington.

Gee GW, MJ Fayer, ML Rockhold, and MD Campbell. 1992. "Variations in Recharge at the Hanford Site," *NW Sci*. 66:237-250.

Hartman MJ, ed. 1999. *Hanford Site Groundwater Monitoring for Fiscal Year 1998*. PNNL-12086, Pacific Northwest National Laboratory, Richland, Washington.

Hartman MJ, LF Morasch, and WD Webber, eds. 2003. *Hanford Site Groundwater Monitoring for Fiscal Year 2002*. PNNL-14187, Pacific Northwest National Laboratory, Richland, Washington.

Hodges FN, 1998. *Results of Phase 1 Groundwater Quality Assessment for Single-Shell Tank Waste Management Areas T and TX-TY at the Hanford Site*. PNNL-11809, Pacific Northwest National Laboratory, Richland, Washington.

Hodges FN and CJ Chou, 2001. *RCRA Assessment Plan for Single-Shell Tank Waste Management Area TX-TY at the Hanford Site*. PNNL-12072, Pacific Northwest National Laboratory, Richland, Washington.

Horton DG. 2002. *Groundwater Conditions at Single-Shell Tank Waste Management Area TX-TY (January 1998 through December 2001)*. PNNL-14099, Pacific Northwest National Laboratory, Richland, Washington.

Horton DG. 2003. *Data Package for Calendar Year 2002 RCRA Groundwater Monitoring Wells at Single-Shell Tank Waste Management Area TX-TY*. PNNL-14249, Pacific Northwest National Laboratory, Richland, Washington.

Johnson VG and CJ Chou, 2001. *RCRA Groundwater Quality Assessment Report for Waste Management Area S-SX (November 1997 through April 2000)*. PNNL-13441, Pacific Northwest National Laboratory, Richland, Washington.

Johnson VG, TE Jones, SP Reidel, and MI Wood. 1999. *Subsurface Physical Conditions of the S-SX Waste Management Area*. HNF-4936, Lockheed Martin Hanford Corporation, Richland, Washington.

Kaplan DI and RJ Serne. 1995. *Distribution Coefficient Values Describing Iodine, Neptunium, Selenium, Technetium, and Uranium Sorption to Hanford Sediment*. PNL-10379, Supplement 1, Pacific Northwest Laboratory, Richland, Washington.

Kaplan DI and RJ Serne. 2000. *Geochemical Data Package for the Hanford Immobilized Low-Activity Tank Waste Performance Assessment (ILAW-PA)*. PNNL-13037, Rev.1, Pacific Northwest National Laboratory, Richland, Washington.

Kincaid CT, MP Bergeron, CR Cole, MD Freshley, VG Johnson, DI Kaplan, RJ Serne, GP Streile, DL Strenge, PD Thorne, LW Vail, GA Whyatt, and SK Wurstner. 1998. *Composite Analysis for Low-Level Waste Disposal in the 200 Area Plateau of the Hanford Site*. PNNL-11800, Pacific Northwest National Laboratory, Richland, Washington.

Kipp RL and RD Mudd, 1974. *Selected Water Table Contour Maps and Well Hydrographs for the Hanford Reservation, 1944-1973*. BNWL-B-360, Pacific Northwest Laboratories, Richland, Washington.

Last GV, ed. 1994. *216-U-10 Pond and 216-Z-19 Ditch Characterization Studies*. WHC-EP-0707 (formerly RHO-ST-45), Westinghouse Hanford Company, Richland, Washington.

Last GV, BN Bjornstad, MP Bergeron, DW Wallace, DR Newcomer, JA Schramke, MA Chamness, CS Cline, SP Airhart, and JS Wilbur. 1989. *Hydrogeology of the 200 Areas Low-Level Burial Grounds - An Interim Report*. PNL-6820, 2 volumes, Pacific Northwest Laboratory, Richland, Washington.

Lindenmeier CW, RJ Serne, BN Bjornstad, GW Gee, HT Schaef , DC Lanigan, MJ Lindberg, RE Clayton, VL LeGore, IV Kutnyakov, SR Baum, KN Geiszler, KMM Valenta, TS Vickerman, and LJ Royack. 2002. *Characterization of Vadose Zone Sediment: RCRA Borehole 299-E33-338 Located Near the B-BX-BY Waste Management Area*, PNNL-14121, Pacific Northwest National Laboratory, Richland, Washington.

Lindsey KA. 1995. *Miocene-to Pliocene-Aged Suprabasalt Sediments of the Hanford Site, South-Central Washington*, BHI-00184, Bechtel Hanford Inc., Richland, Washington.

Lindsey KA. 1996. *Miocene-Pliocene Ringold Formation and Associated Deposits of the Ancestral Columbia River System, South-Central Washington and North-Central Oregon, Washington.* Department of Natural Resources, Division of Geology and Earth Resources Open-File Report 96-8, Olympia, Washington, 45 p.

Lindsey KA, BN Bjornstad, JW Lindberg, and KM Hoffman. 1992a. *Geologic Setting of the 200 East Area: An Update*. WHC-SD-EN-TI-012, Westinghouse Hanford Company, Richland, Washington.

Lindsey KA, MP Connelly, and BN Bjornstad. 1992b. *Geologic Setting of the 200 West Area – An Update*. WHC-SD-EN-TI-008, Westinghouse Hanford Company, Richland, Washington.

Lindsey KA, SE Kos, and KD Reynolds. 2000. *Vadose Zone Geology of the Boreholes 299-W22-50 and 299-W23-19 S-SX Waste Management Area, Hanford Site, South-Central Washington*. RPP-6149, Rev. 0, prepared for the Office of River Protection, CH2M HILL Group, Inc., Richland, Washington.

Lindsey KA, SE Kos, and KD Reynolds. 2001. *Vadose Zone Geology of Boreholes 299-W10-27 and 299-W11-39 T-TX-TY Waste Management Area, Hanford Site, South-Central Washington*. RPP-8531, Rev. 0, prepared for the Office of River Protection, CH2M HILL Group, Inc., Richland, Washington.

Lindsey KA, SP Reidel, KR Fecht, JL Slate, AG Law, and AM Tallman. 1994a. "Geohydrologic Setting of the Hanford Site, South-Central Washington." In *Geologic Field Trips in the Pacific Northwest,* eds. DA Swanson and RA Hagerud, pp. 1C-1 to 1C-16. Geological Society of America Meeting, Geological Society of America, Boulder, Colorado.

Lindsey KA, JL Slate, GK Jaeger, KJ Swett, and RB Mercer. 1994b. *Geologic Setting of the Low-Level Burial Grounds*. WHC-SD-EN-TI-290, Rev. 0, Westinghouse Hanford Company, Richland, Washington.

Maxfield HL. 1979. *Handbook 200 Areas Waste Sites, Volume II*. RHO-CD-673, Rockwell Hanford Operations, Richland, Washington.

Moody UL. 1987. *Late Quaternary Stratigraphy of the Channeled Scabland and Adjacent Areas*, Ph.D. Thesis, University of Idaho, Moscow, Idaho.

Myers CW and SM Price, eds. 1979. *Geologic Studies of the Columbia Plateau – A Status Report*. RHO-BWI-ST-4, Rockwell Hanford Operations, Richland, Washington.

O'Connor JE. 1993. *Hydrology, Hydraulics, and Geomorphology of the Bonneville Flood*. Special Paper #274, Geological Society of America, Boulder, Colorado, 83 p.

Or D and JM Wraith. 2002. "Soil Water Content and Water Potential Relationships." In *Soil Physics Companion*, ed. AW Warrick, pp. 49-84, CRC Press, Boca Raton, Florida.

Pacific Northwest Laboratory (PNL). 1990a. *Procedures for Groundwater Investigations*. PNL-MA-567-DO-1, Pacific Northwest Laboratory, Richland, Washington.

Pacific Northwest Laboratory (PNL). 1990b. *Procedures for Groundwater Investigations*. PNL-MA-567-SFA-2, Pacific Northwest Laboratory, Richland, Washington.

Pacific Northwest National Laboratory (PNNL). 1997. *Gamma Energy Analysis Operation and Instrument Verification Using the Genie2000™ Support Software*. PNNL-RRL-01, Pacific Northwest National Laboratory, Richland, Washington.

Pacific Northwest National Laboratory (PNNL). 1998. *Inductively Coupled Plasma Mass Spectrometric (ICP-MS) Analysis*. PNNL-AGG-415, Pacific Northwest National Laboratory, Richland, Washington.

Pacific Northwest National Laboratory (PNNL). 1999. *Visual Description and Classification of Potentially Contaminated Borehole Samples*. PNL Procedure D9T81-99-GVL-1, Pacific Northwest National Laboratory, Richland, Washington, 6 p.

Pacific Northwest National Laboratory (PNNL). 2000. *Liquid Scintillation Counting and Instrument Verification Using the 1400 DSM™ Support Software*. PNNL-AGG-002, Pacific Northwest National Laboratory, Richland, Washington.

Pacific Northwest National Laboratory (PNNL). 2004. [Online listing of borehole geophysical logs for Well 299W10-27; as accessed March 8, 2004.] Available URL: http://boreholelogs.pnl.gov/200WEST/W10027

Price WH and KR Fecht. 1976. *Geology of the 241-TX Tank Farm*. ARH-LD-136, Atlantic Richfield Hanford Company, Richland, Washington.

Reidel SP and KR Fecht. 1994. *Geologic Map of the Priest Rapids 1:100,000 Quadrangle*, Washington. Washington Division of Geology and Earth Resources Open-File Report 94-13, 22 p.

Reidel SP, KA Lindsey, and KR Fecht. 1992. *Field Trip Guide to the Hanford Site*. WHC-MR-0391, Westinghouse Hanford Company, Richland, Washington.

Reineck HE and IB Singh. 1975. *Depositional Sedimentary Environments*. 439p. Springer-Verlag, New York.

Reynolds KD. 2003. *Completion Report for Probe Hole C3830 (TX-105) TX Tank Farm 200 West Area*. RPP-13741, Prepared for the Office of River Protection, CH2M HILL Hanford Group, Inc., Richland, Washington.

Rhoades JD. 1996. "Salinity: Electrical Conductivity and Total Dissolved Solids." In *Methods of Soil Analysis Part 3,* ed. JM Bigham, pp. 417-435. American Society of Agronomy, Madison, Wisconsin.

Salvador A, ed. 1994. *International Stratigraphic Guide*. 2nd ed. International Union of Geological Sciences and the Geological Society of America, Boulder, Colorado.

Serne RJ, HT Schaef, BN Bjornstad, BA Williams, DC Lanigan, DG Horton, RE Clayton, VL LeGore, MJ O'Hara, CF Brown, KE Parker, IV Kutnyakov, JN Serne, AV Mitroshkov, GV Last, SC Smith, CW Lindenmeier, JM Zachara, and DS Burke. 2002a. *Characterization of Vadose Zone Sediment: Uncontaminated RCRA Borehole Core Samples and Composite Samples*. PNNL-13757-1, Pacific Northwest National Laboratory, Richland, Washington.

Serne RJ, HT Schaef, BN Bjornstad, DC Lanigan, GW Gee, CW Lindenmeier, RE Clayton, VL LeGore, MJ O'Hara, CF Brown, RD Orr, G.V Last, IV Kutnyakov, DS Burke, TC Wilson, and BA Williams. 2002b. *Characterization of Vadose Zone Sediment: Borehole 299-W23-19 [SX-115] in the S-SX Waste Management Area*. PNNL-13757-2, Pacific Northwest National Laboratory, Richland, Washington.

Serne RJ, GV Last, HT Schaef, DC Lanigan, CW Lindenmeier, CC Ainsworth, RE Clayton, VL LeGore, MJ O'Hara, CF Brown, RD Orr, IV Kutnyakov, TC Wilson, KB Wagnon, BA Williams, and DB Burke. 2002c. *Characterization of Vadose Zone Sediment, Part 4: Slant Borehole SX-108 in the S-SX Waste Management Area*. PNNL-13757-4, Pacific Northwest National Laboratory, Richland, Washington.

Serne RJ, GV Last, GW Gee, HT Schaef, DC Lanigan, CW Lindenmeier, RE Clayton, VL LeGore, RD Orr, MJ O'Hara, CF Brown, DS Burke, AT Owen, IV Kutnyakov, and TC Wilson. 2002d. *Characterization of Vadose Zone Sediment: Borehole 41-09-39 in the S-SX Waste Management Area*. PNNL-13757-3, Pacific Northwest National Laboratory, Richland, Washington.

Serne RJ, GV Last, GW Gee, HT Schaef, DC Lanigan, CW Lindenmeier, MJ Lindberg, RE Clayton, VL LeGore, RD Orr, IV Kutnyakov, SR Baum, KN Geiszler, CF Brown, MM Valenta, and TS Vickerman. 2002e. *Characterization of Vadose Zone Sediment: Borehole 299-E33-45 Near BX-102 in the B-BX-BY Waste Management Area*, PNNL-14083, Pacific Northwest National Laboratory, Richland, Washington.

Serne RJ, BN Bjornstad, GW Gee, HT Schaef, DC Lanigan, CW Lindenmeier, RD Orr, VL LeGore, RE Clayton, MJ Lindberg, IV Kutnyakov, SR Baum, KN Geiszler, MM Valenta, TS Vickerman, and LJ Royack. 2002f. *Characterization of Vadose Zone Sediment: Borehole 299-E33-46 Near B-110 in the B-BX-BY Waste Management Area*, PNNL-14119, Pacific Northwest National Laboratory, Richland, Washington.

Shaw J, M Munro-Stasuik, B Sawyer, C Beaney, JE Lesemann, A Musacchio, B Rains, and RR Young. 1999. "The Channeled Scabland: Back to Bretz," *Geology*, 27:605-608.

Simpson BC, RA Corbin, and SF Agnew, 2001. *Hanford Soil Inventory Model*. BHI-01496 Rev. 0, Bechtel Hanford, Inc., Richland, Washington.

Slate JL. 1996. "Buried Carbonate Paleosols Developed in Pliocene-Pleistocene Deposits of the Pasco Basin, South-Central Washington." *USA: Quaternary International*, 34-36:191-196.

Slate JL. 2000. *Nature and Variability of the Plio-Pleistocene Unit in the 200 West Area of the Hanford Site*. BHI-01203, Rev. 0, Bechtel Hanford, Inc., Richland, Washington.

Smith GA. 1993. "Missoula Flood Dynamics and Magnitudes Inferred from Sedimentology of Slack-Water Deposits on the Columbia Plateau." *Geological Society of America Bulletin*, 195:77-100.

Spane FA, Jr., PD Thorne, and DR Newcomer. 2001a. *Results of Detailed Hydrologic Characterization Tests – Fiscal Year 1999*. PNNL-13378, Pacific Northwest National Laboratory, Richland, Washington.

Spane FA, Jr., PD Thorne, and DR Newcomer. 2001b. *Results of Detailed Hydrologic Characterization Tests – Fiscal Year 2000*. PNNL-13514, Pacific Northwest National Laboratory, Richland, Washington.

Spane FA, Jr., PD Thorne, and DR Newcomer. 2002. *Results of Detailed Hydrologic Characterization Tests – Fiscal Year 2001*. PNNL-14113, Pacific Northwest National Laboratory, Richland, Washington.

Spane FA, Jr., PD Thorne, and DR Newcomer. 2003. *Results of Detailed Hydrologic Characterization Tests – Fiscal Year 2002*. PNNL-14186, Pacific Northwest National Laboratory, Richland, Washington.

Tallman AM, KR Fecht, MC Marratt, and GV Last. 1979. *Geology of the Separations Areas, Hanford Site, South-Central Washington*. RHO-ST-23, Rockwell Hanford Operations, Richland, Washington.

Tallman AM, JT Lillie, and KR Fecht. 1981. "Suprabasalt Sediment of the Cold Creek Syncline Area," In *Subsurface Geology of the Cold Creek Syncline*, eds. CW Myers and SM Price, RHO-BWI-ST-14, Rockwell Hanford Operations, Richland, Washington.

USGS (United States Geological Survey). 2001. "Alkalinity and Acid Neutralizing Capacity." *National Field Manual for the Collection of Water-Quality Data,* 2nd ed., eds. SA Rounds and FD Wilde. March 23, 2004 Available URL: http://water.usgs.gov/owq/FieldManual/Chapter6/section6.6/html/section6.6.htm

Waldrop WR and HS Pearson. 2000. *Results of Field Tests with the Electromagnetic Borehole Flowmeter at the Pacific Northwest National Laboratory, Richland, WA*. QEC-T-132, Quantum Engineering Corporation, London, Tennessee.

Wan J, JT Larsen, TK Tokunaga, and Z Zheng. 2004. "pH Neutralization and Zonation in Alkaline-Saline Tank Waste Plumes." *Environ. Sci. Technol*. 38:1321-1329.

Ward AL, GW Gee, and MD White. 1997. *A Comprehensive Analysis of Contaminant Transport in the Vadose Zone Beneath Tank SX-109*. PNNL-11463, Pacific Northwest National Laboratory, Richland, Washington.

Webster GD and JW Crosby. 1982. *Stratigraphic Investigation of the Skagit/Hanford Nuclear Project, Volume 4,* Puget Sound Power and Light Company, Bellevue, Washington.

Wentworth CK. 1922. "A grade scale and class terms for clastic sediments." *Journal of Geology*, 30:377-392.

WHC 1990. 1990. *Liquid Effluent Study Final Project Report*. WHC-EP-0367, Westinghouse Hanford Company, Richland, Washington.

Williams BA, BN Bjornstad, R Schalla, and WD Webber. 2002. *Revised Hydrogeology for the Suprabasalt Aquifer System, 200-West Area and Vicinity*, Hanford Site, Washington. PNNL-13858, Pacific Northwest National Laboratory, Richland, Washington.

Wood MI, R Schalla, BN Bjornstad, and FN Hodges. 2001. *Subsurface Conditions Description of the T and TX-TY Waste Management Areas*. RPP-7123, Rev. 0, CH2M HILL Hanford Group, Inc., Richland, Washington.

Wood MI, TE Jones, R Schalla, BN Bjornstad, and FN Hodges. 2001. *Subsurface Conditions Description of the T and TX-TY Waste Management Areas*. RPP-7123, Rev. 0. CH2M HILL Hanford Group, Inc., Richland, Washington.

APPENDIX A. CORE PHOTOGRAPHS

A.1   C3125 (299-W10-27)

A.2   C3830

A.3   C3831

A.4   C3832

APPENDIX A.1

C3125 (299-W10-27)

SPLITSPOON CORE

SAMPLE PHOTOGRAPHS

Contents

Figures

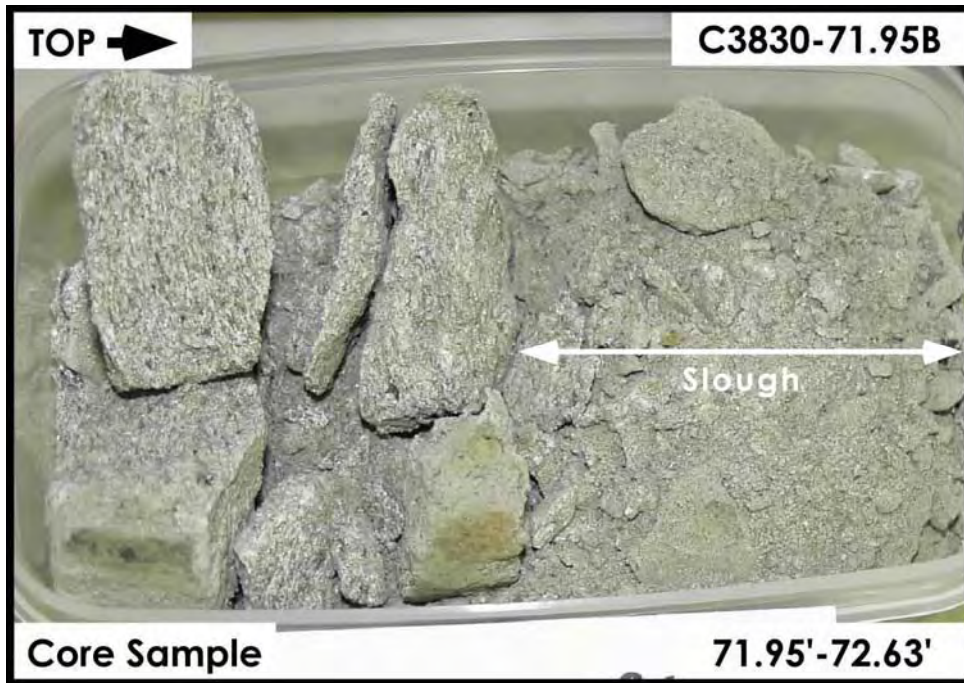**Figure A-1.1.   Hanford Formation (H2 unit) 50 ft – 51 ft**

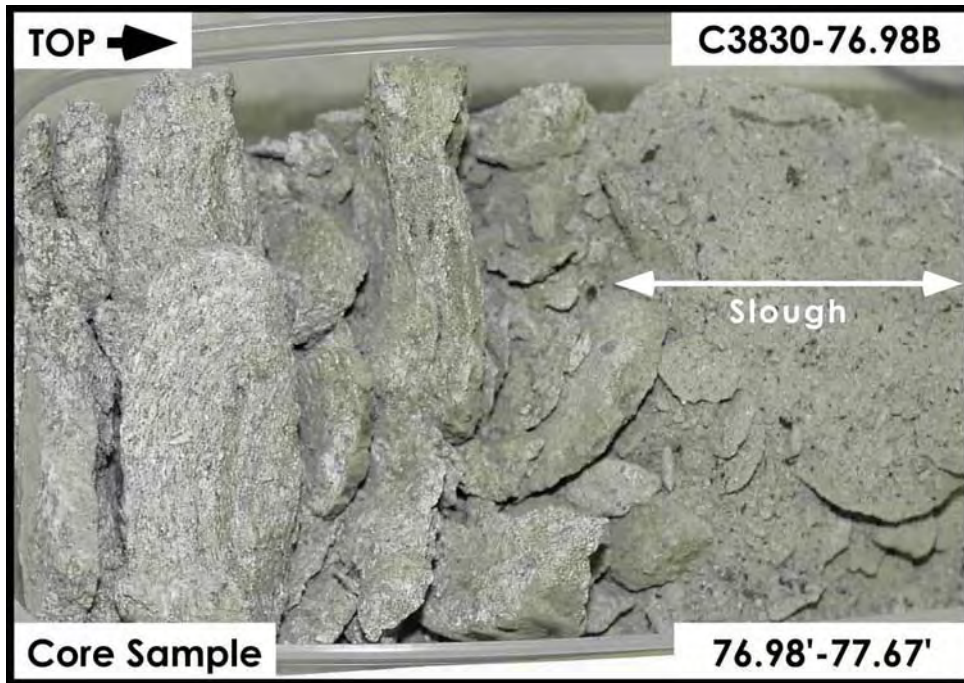**Figure A-1.2.   Hanford Formation (H2 unit) 51 ft – 52 ft**

Figure A-1.3.   Hanford Formation (H2 unit) 52.5 ft – 53.5 ft
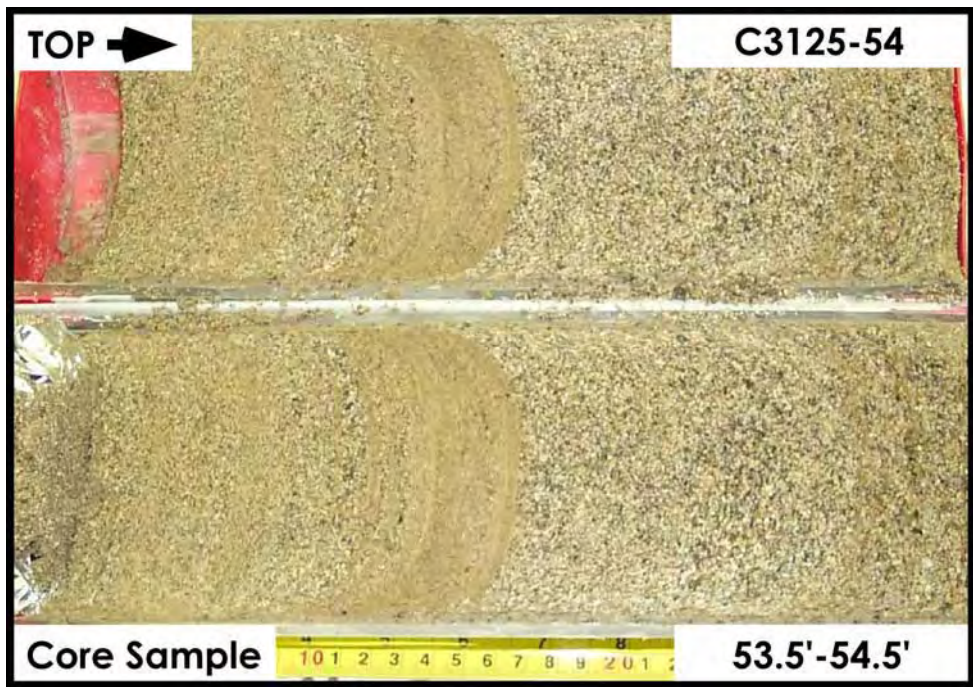
Figure A-1.4.   Hanford Formation (H2 unit) 53.5 ft – 54.5 ft
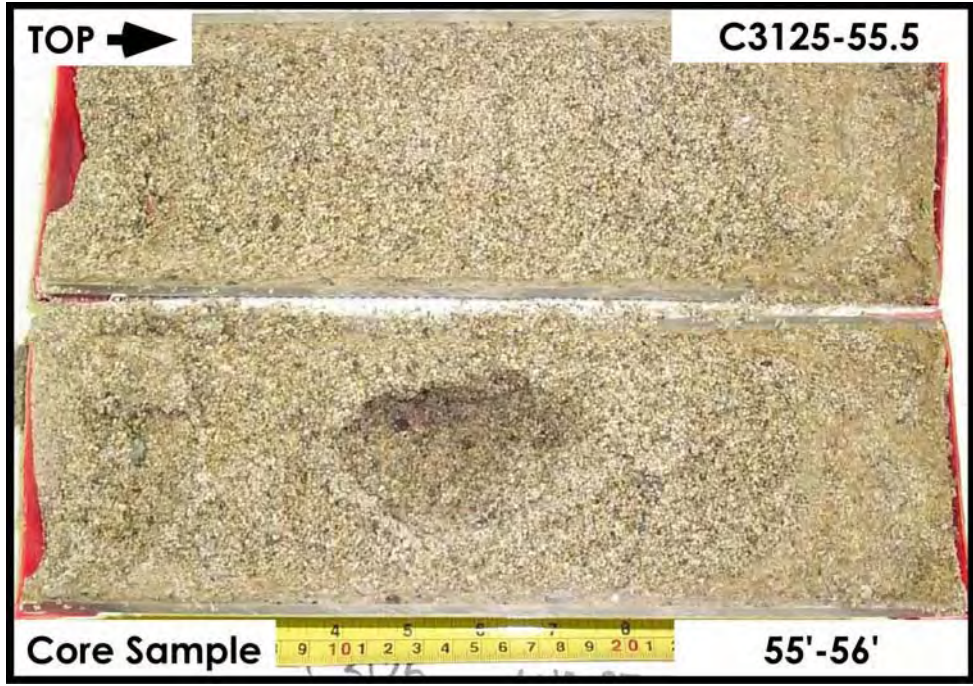
Figure A-1.5.   Hanford Formation (H2 unit) 55 ft – 56 ft
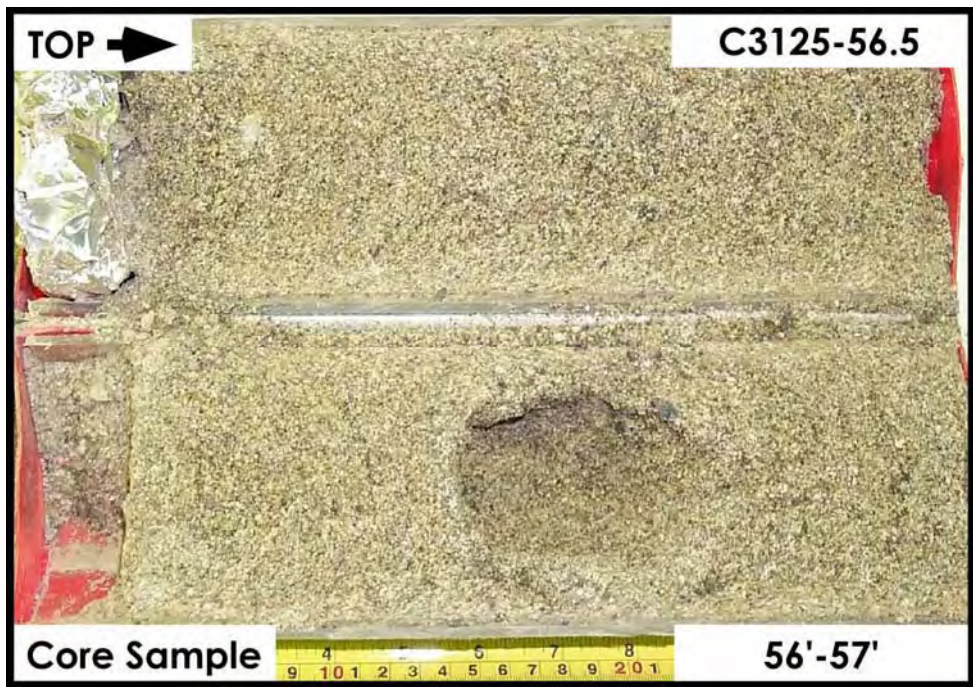
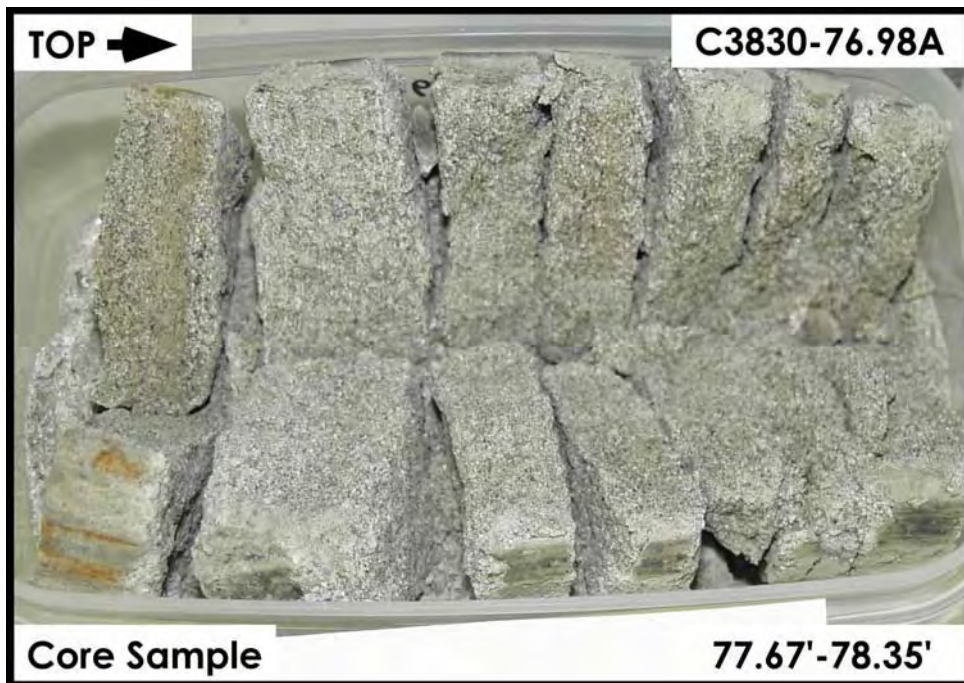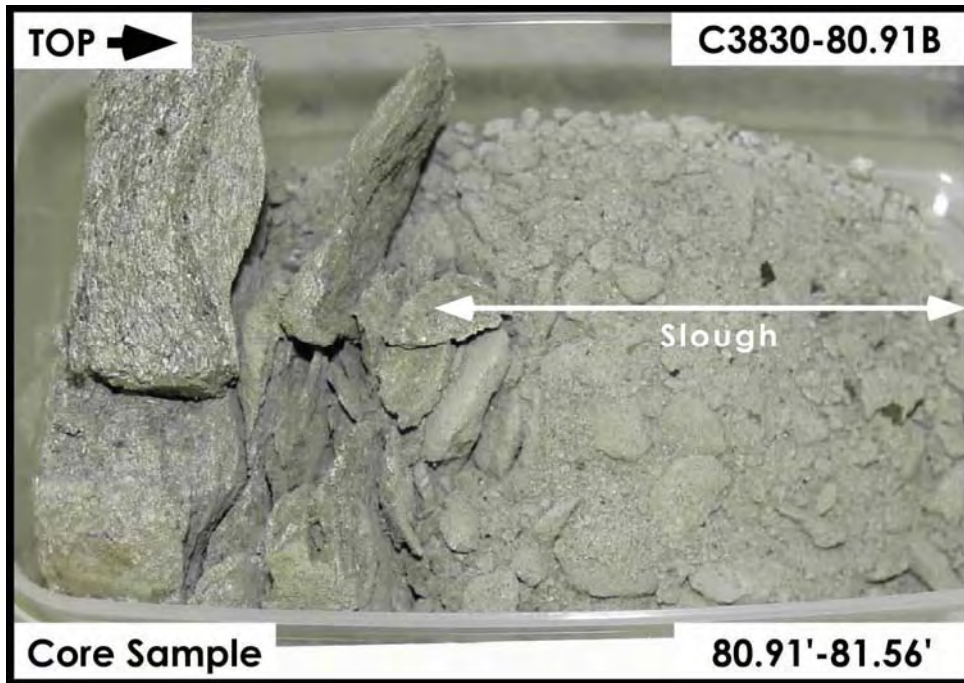**Figure A-1.6.   Hanford Formation (H2 unit) 56 ft – 57 ft**
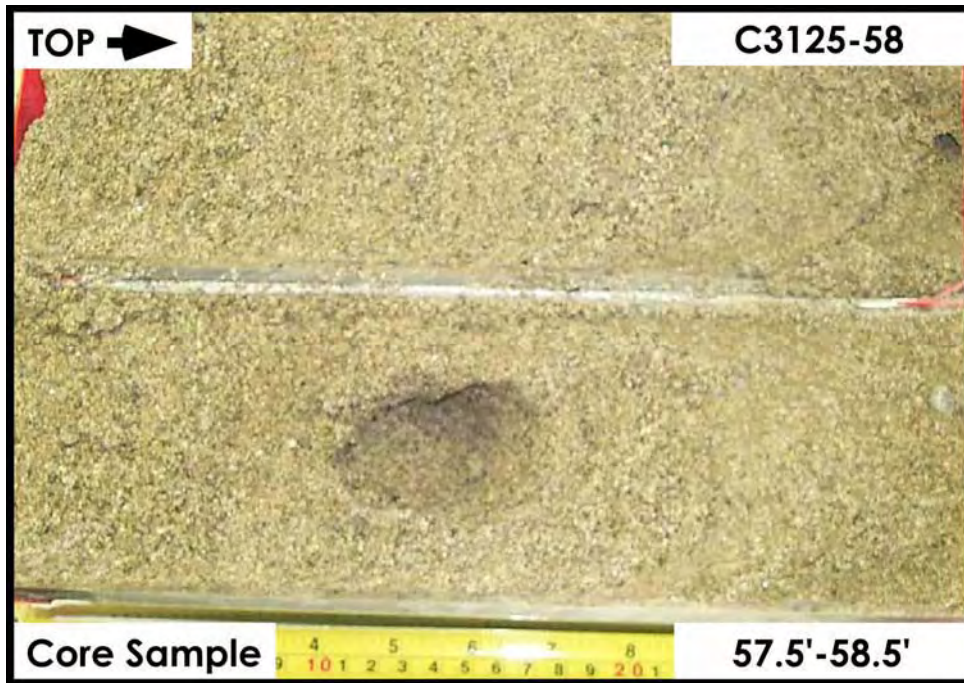
Figure A-1.7.   Hanford Formation (H2 unit) 57.5 ft – 58.5 ft
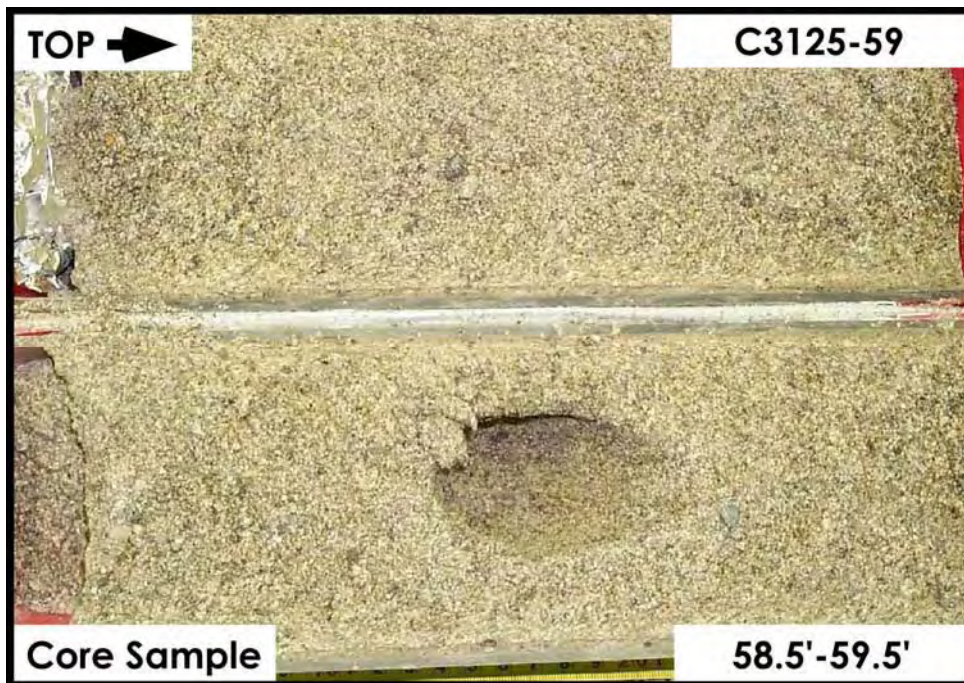
Figure A-1.8.   Hanford Formation (H2 unit) 58.5 ft – 59.5 ft
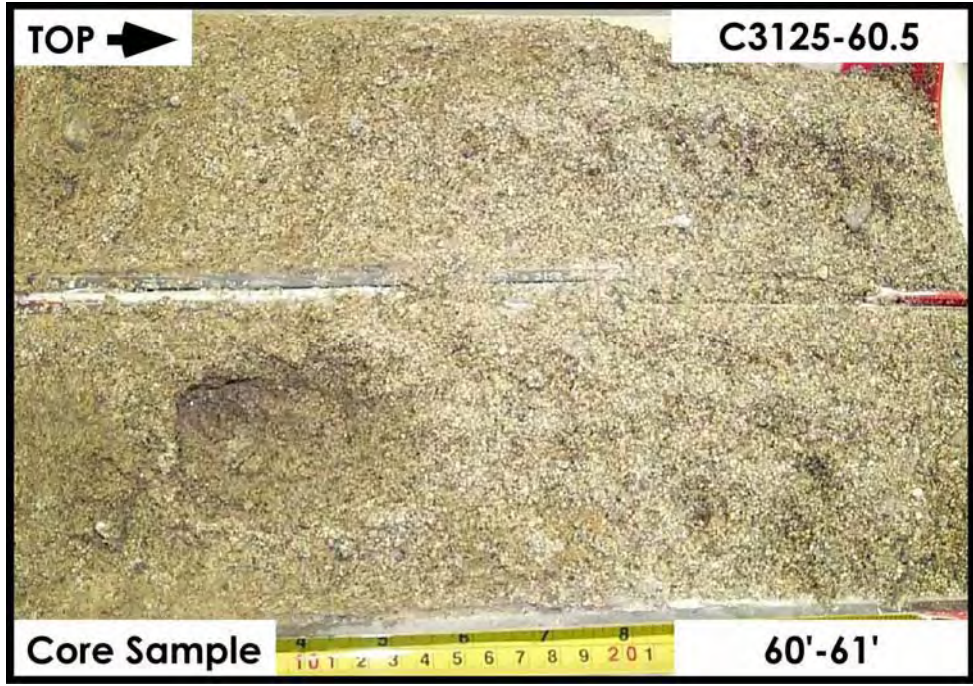
Figure A-1.9.   Hanford Formation (H2 unit) 60 ft – 61 ft
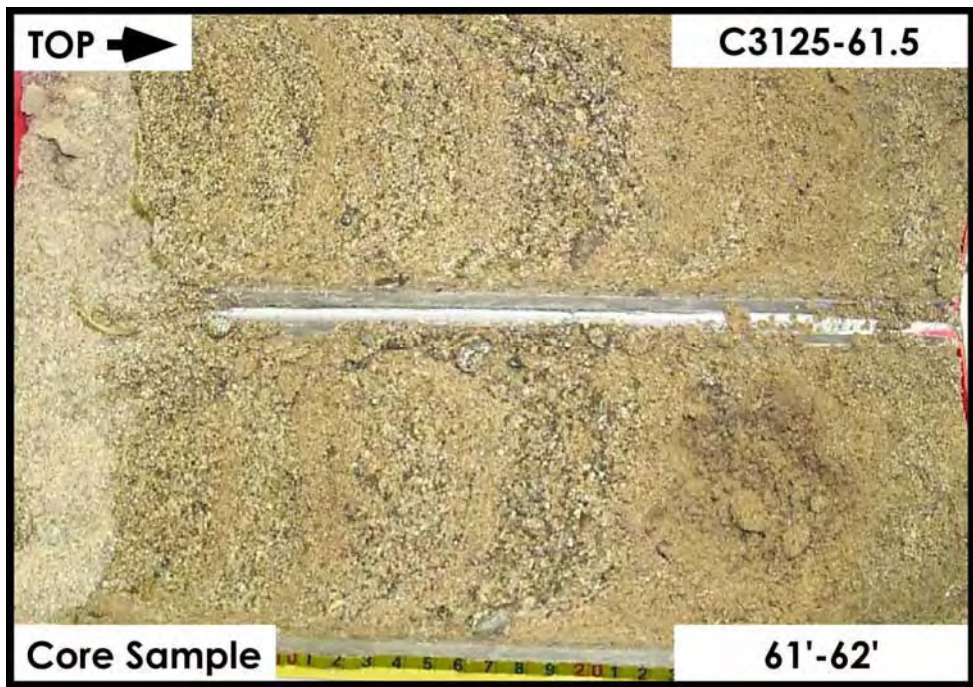
Figure A-1.10. Hanford Formation (H2 unit) 61 ft – 62 ft
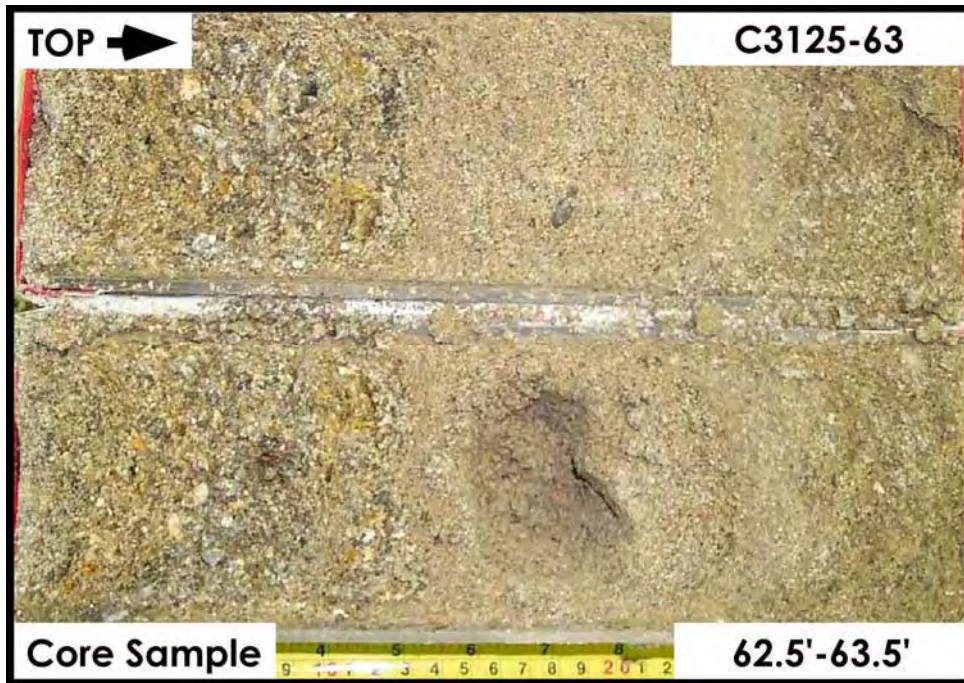
Figure A-1.11. Hanford Formation (H2 unit) 62.5 ft – 63.5 ft
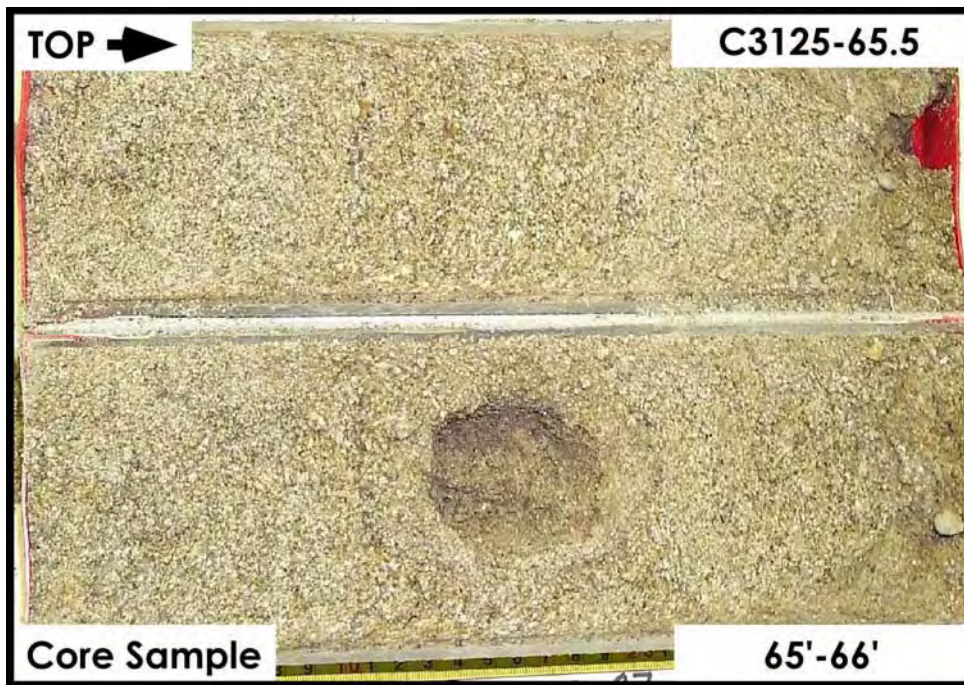
Figure A-1.12. Hanford Formation (H2 unit) 65 ft – 66 ft
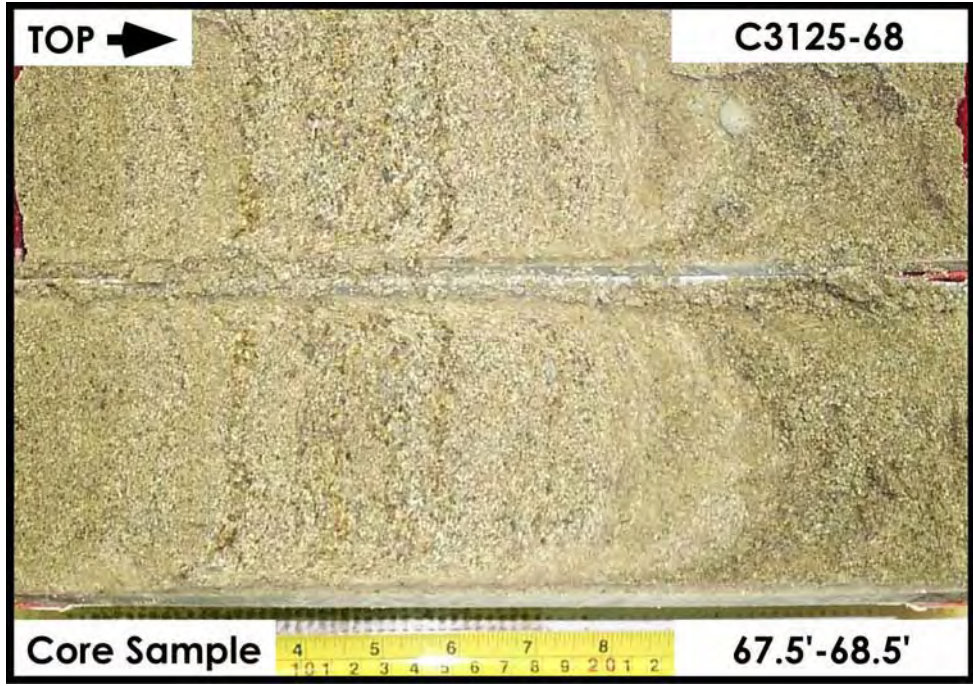
Figure A-1.13. Hanford Formation (H2 unit) 67.5 ft – 68.5 ft
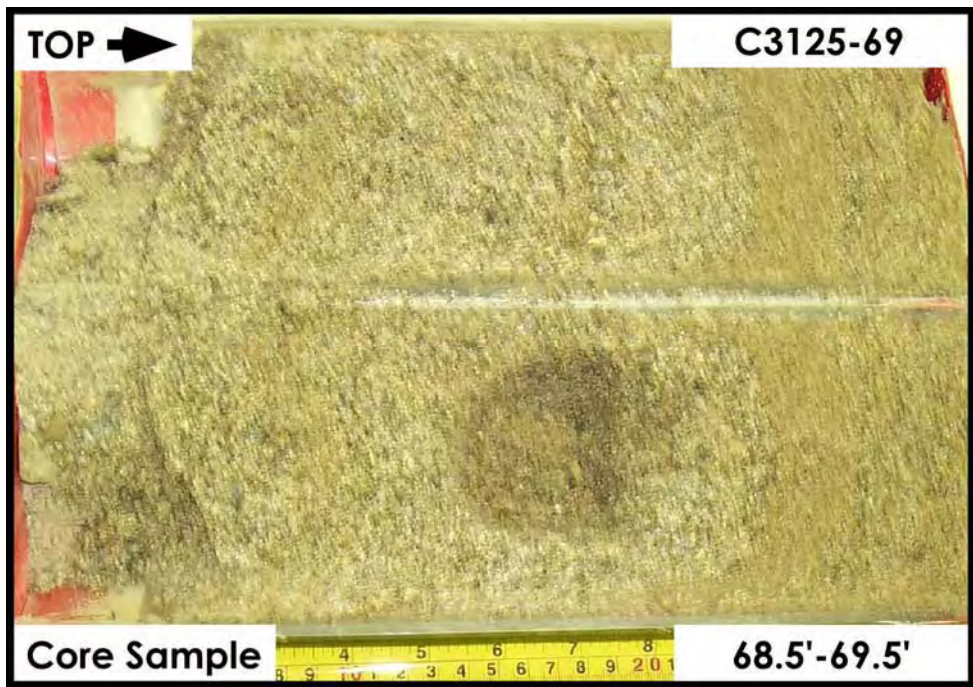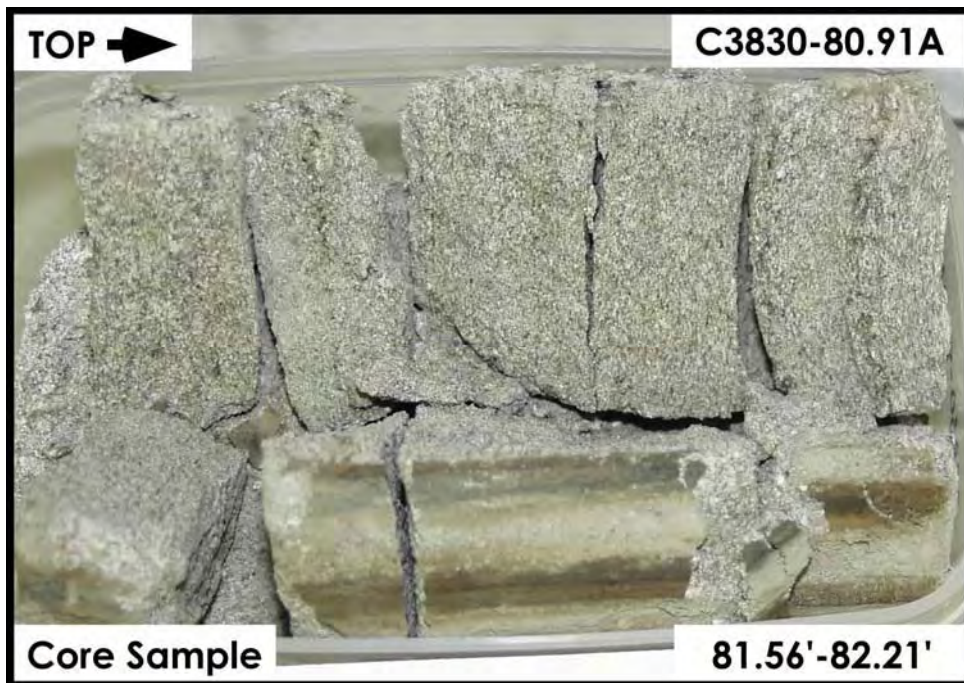

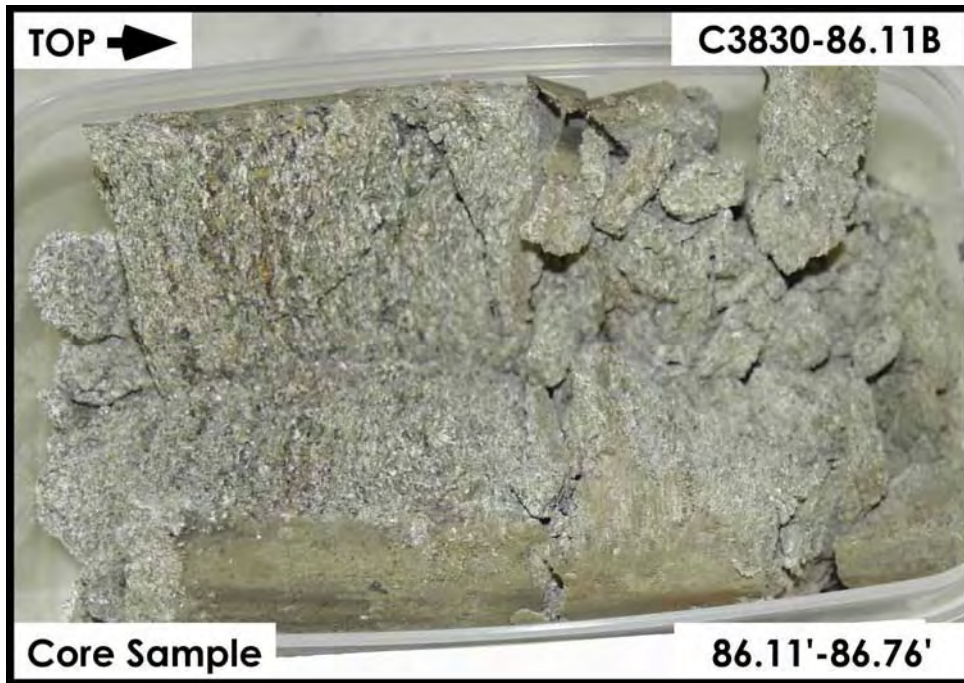**Figure A-1.14. Hanford Formation (H2 unit) 68.5 ft – 69.5 ft**
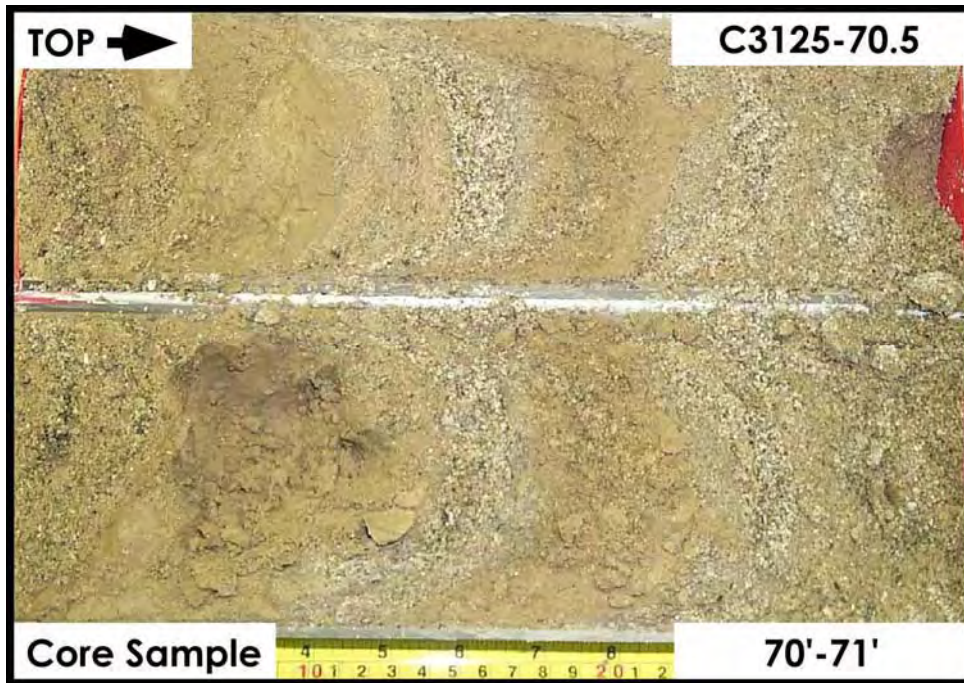
Figure A-1.15. Hanford Formation (H2 unit) 70 ft – 71 ft
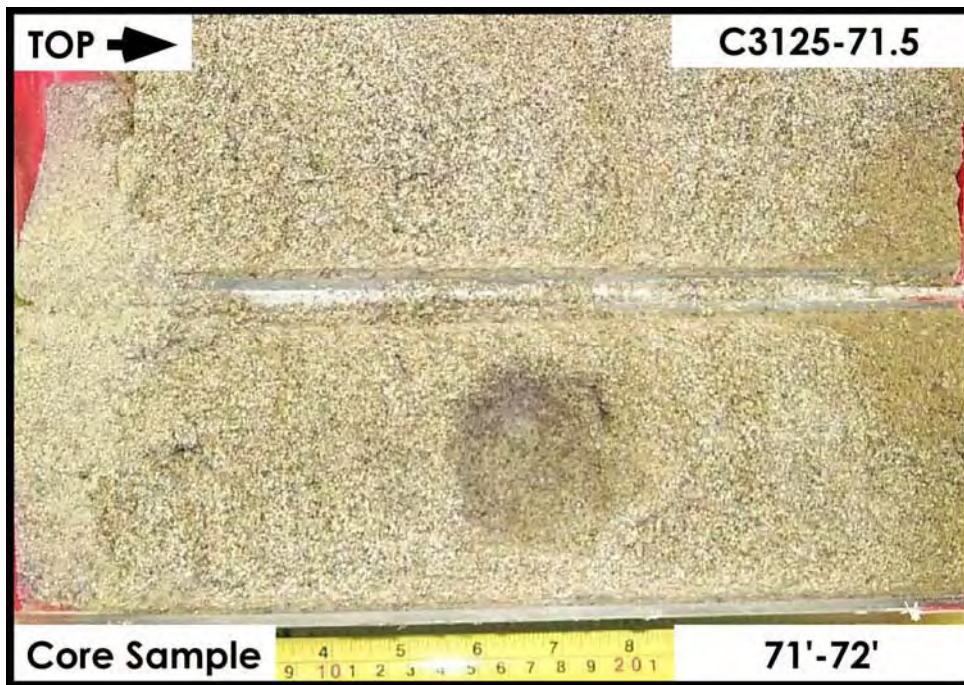
Figure A-1.16. Hanford Formation (H2 unit) 71 ft – 72 ft
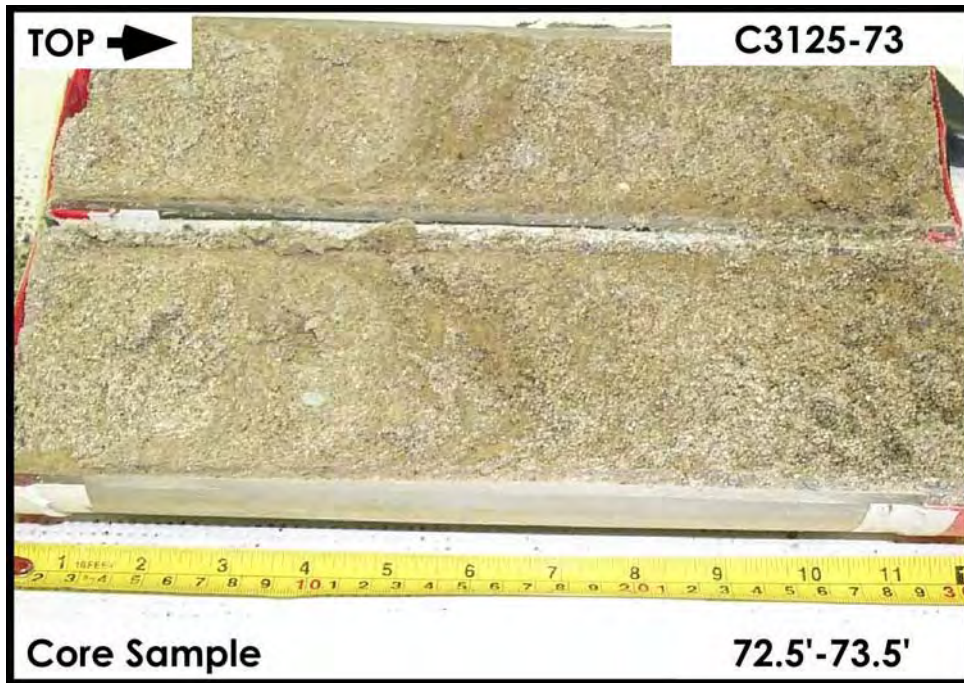
Figure A-1.17. Hanford Formation (H2 unit) 72.5 ft – 73.5 ft
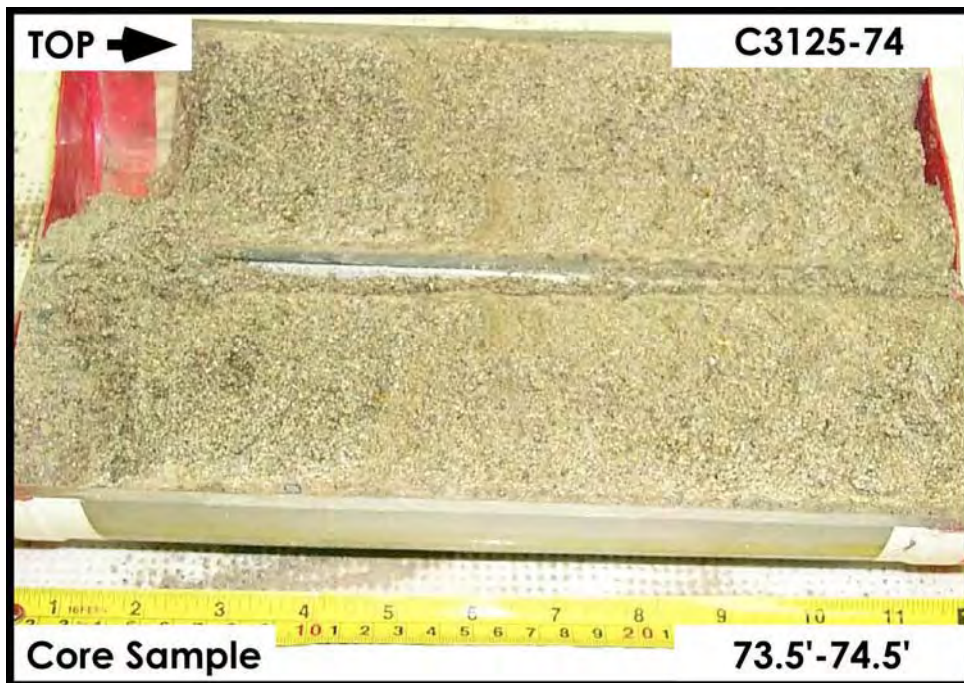
Figure A-1.18. Hanford Formation (H2 unit) 73.5 ft – 74.5 ft
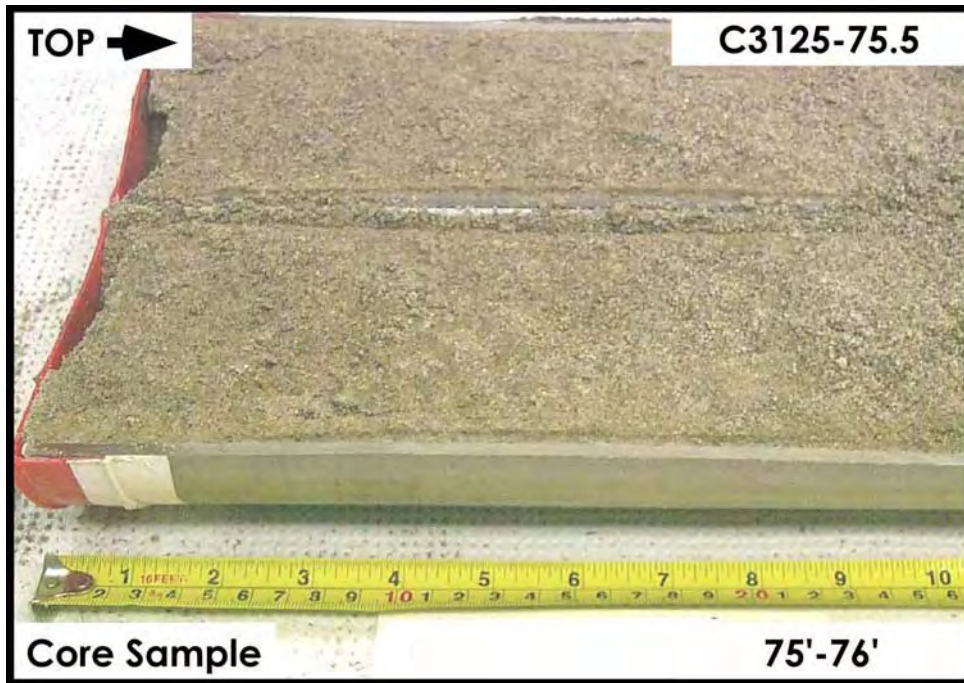
Figure A-1.19. Hanford Formation (H2 unit) 75 ft – 76 ft
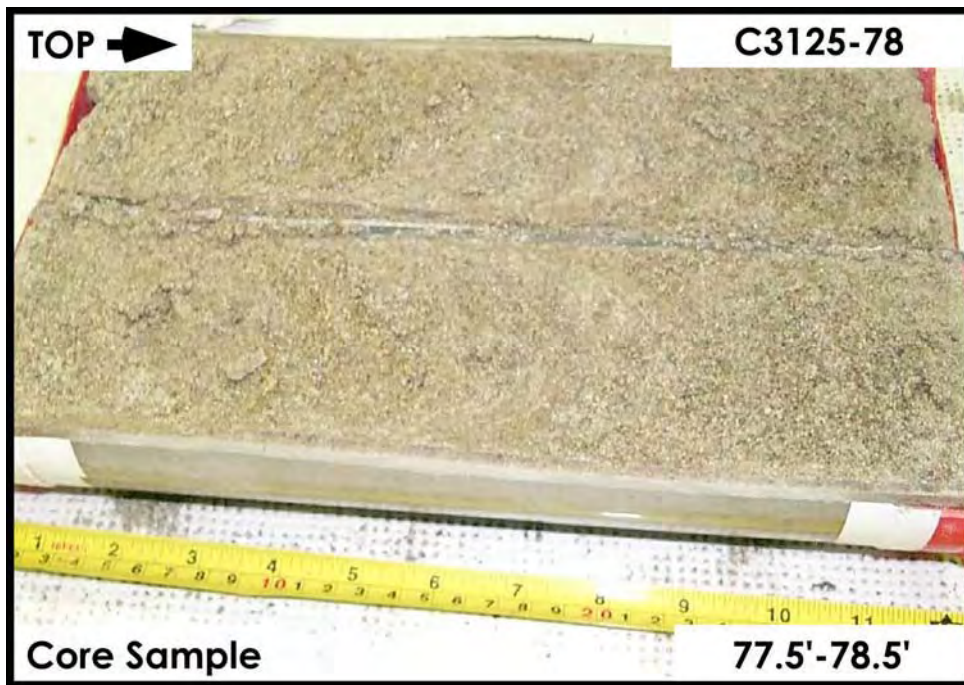
Figure A-1.20. Hanford Formation (H2 unit) 77.5 ft – 78.5 ft
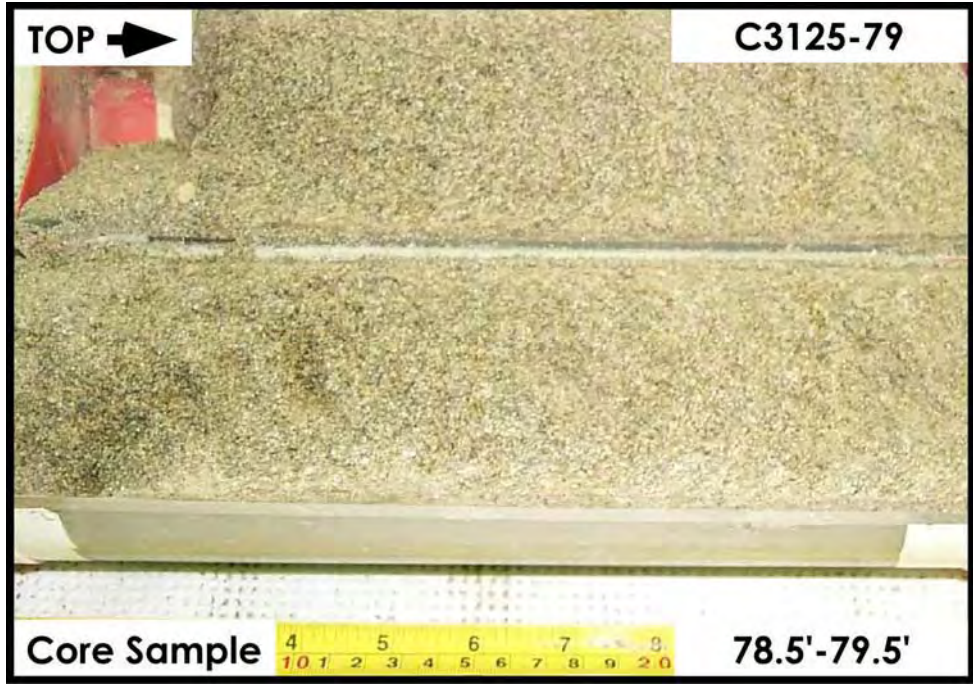
Figure A-1.21. Hanford Formation (H2 unit) 78.5 ft – 79.5 ft
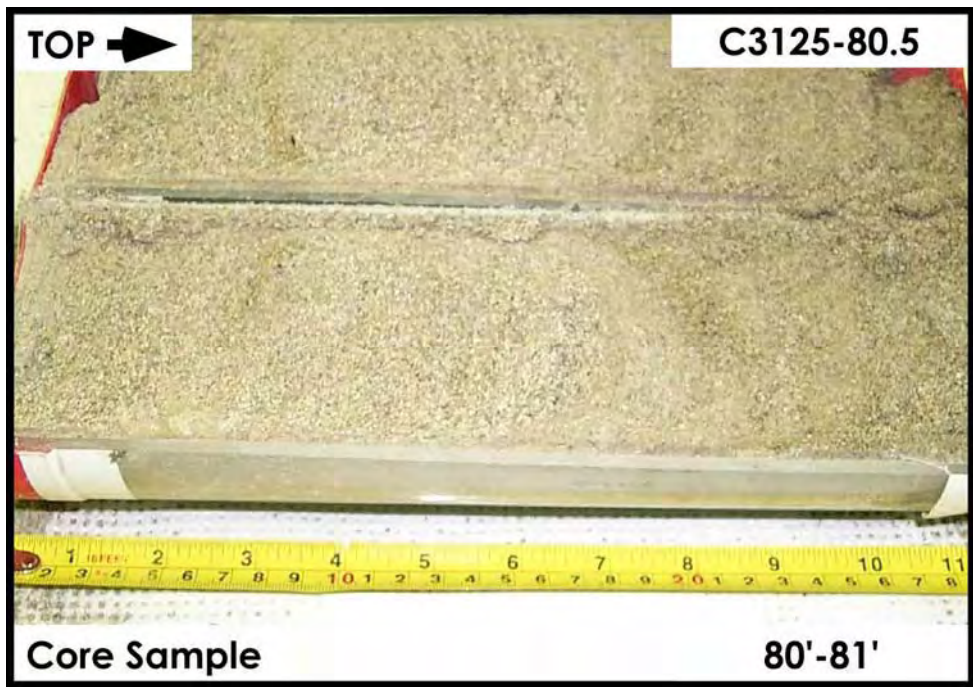
Figure A-1.22. Hanford Formation (H2 unit) 80 ft – 81 ft

Figure A-1.23. Hanford Formation (H2 unit) 81 ft – 82 ft
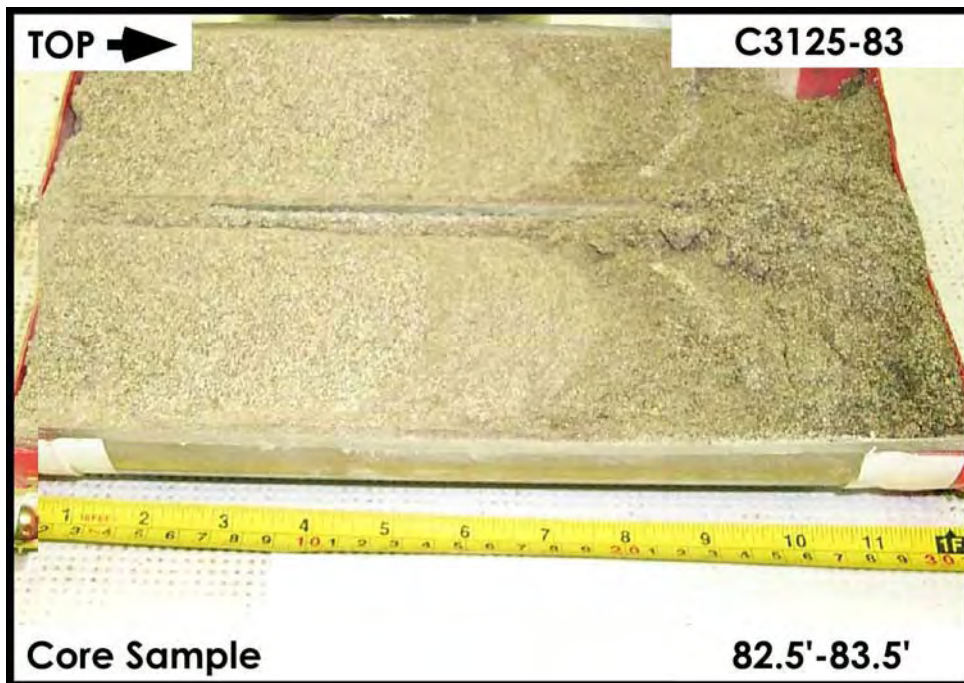
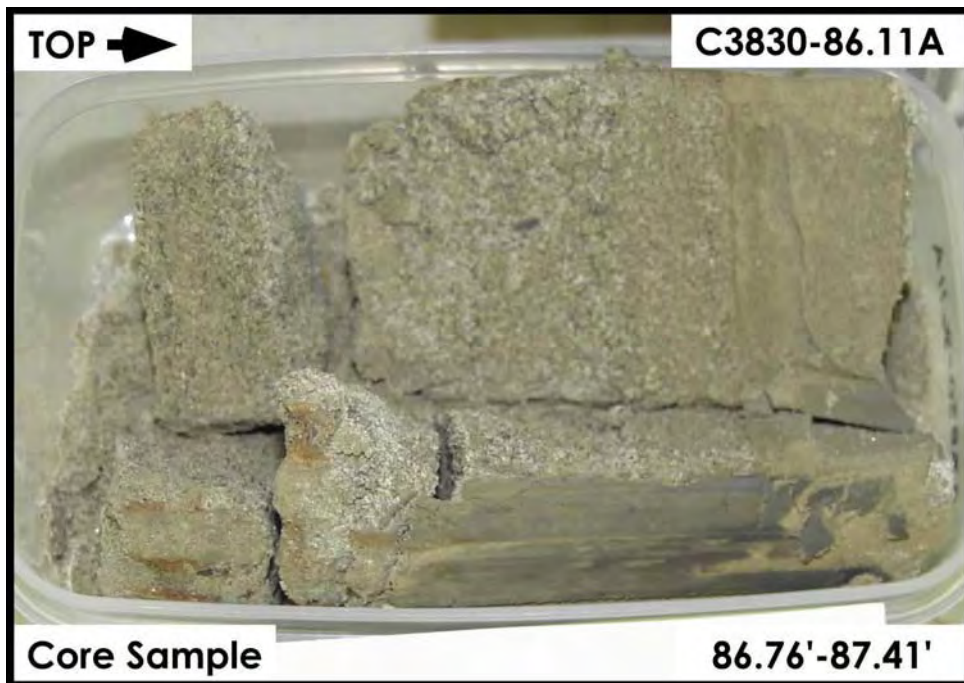**Figure A-1.24. Hanford Formation (H2 unit) 82.5 ft – 83.5 ft**
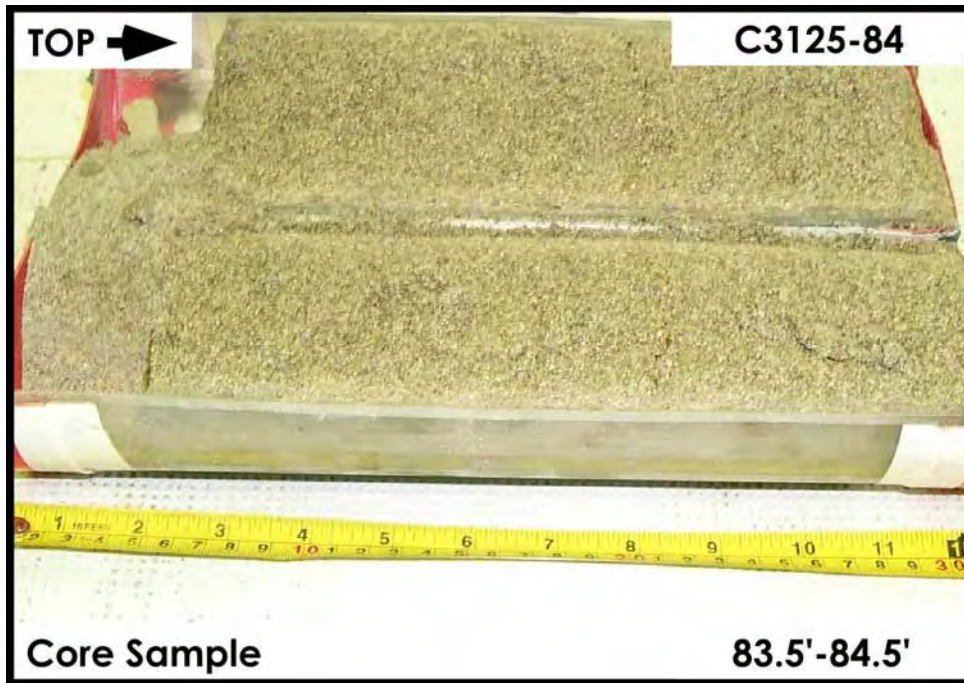
Figure A-1.25. Hanford Formation (H2 unit) 83.5 ft – 84.5 ft
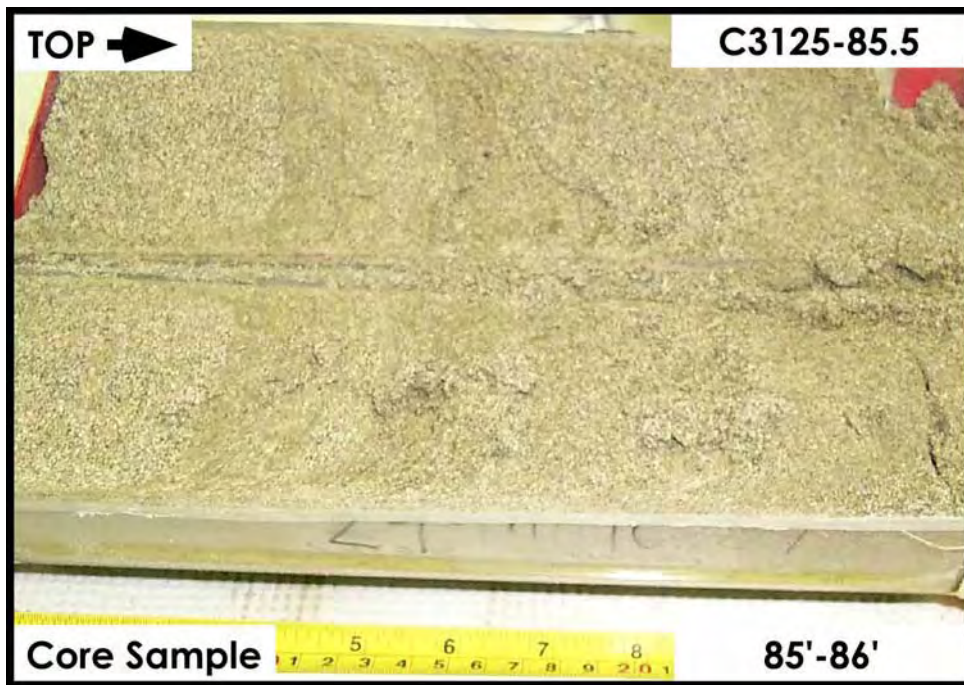
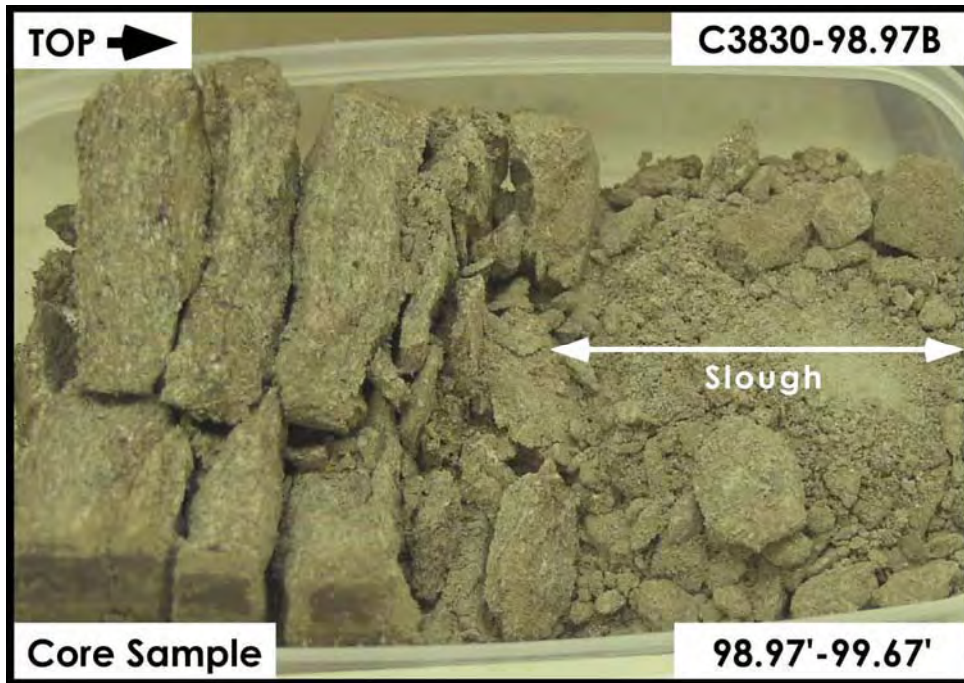**Figure A-1.26. Hanford Formation (H2 unit) 85 ft – 86 ft**
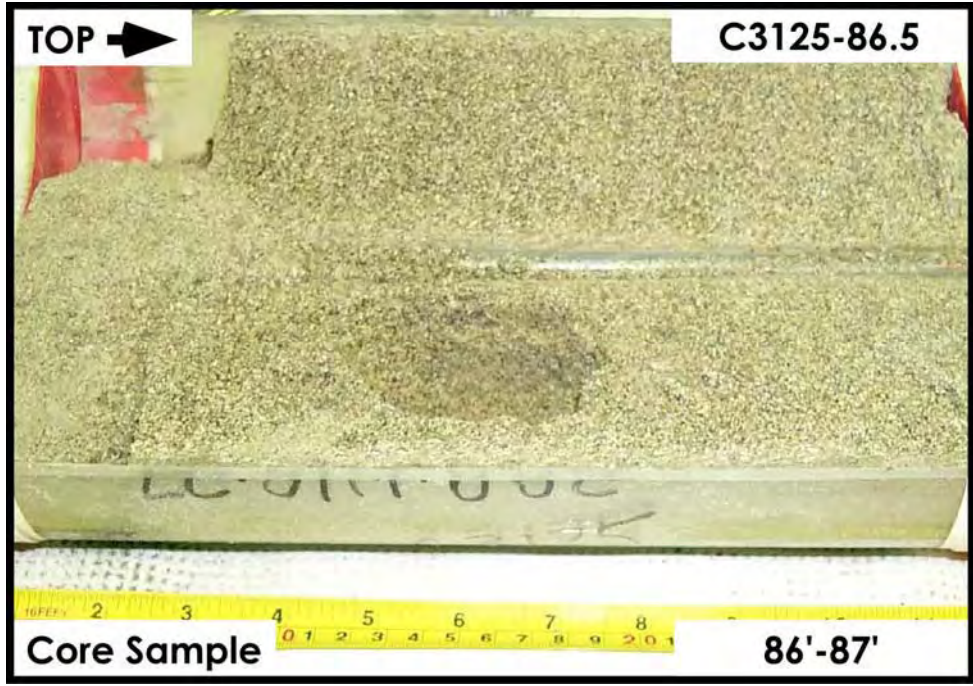
Figure A-1.27. Hanford Formation (H2 unit) 86 ft – 87 ft
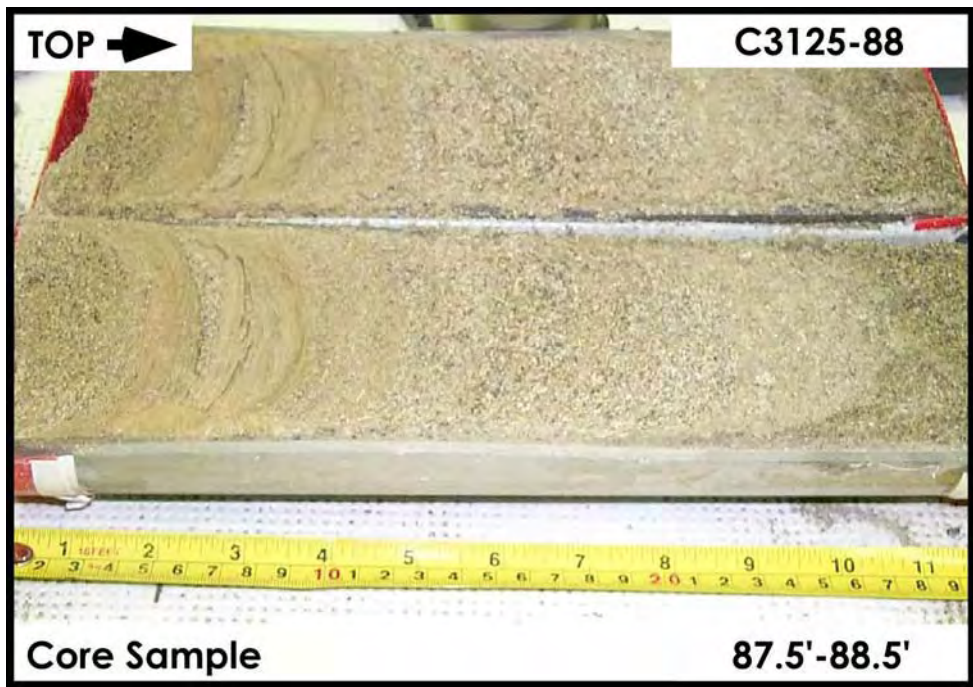
Figure A-1.28. Hanford Formation (H2 unit) 87.5 ft – 88.5 ft
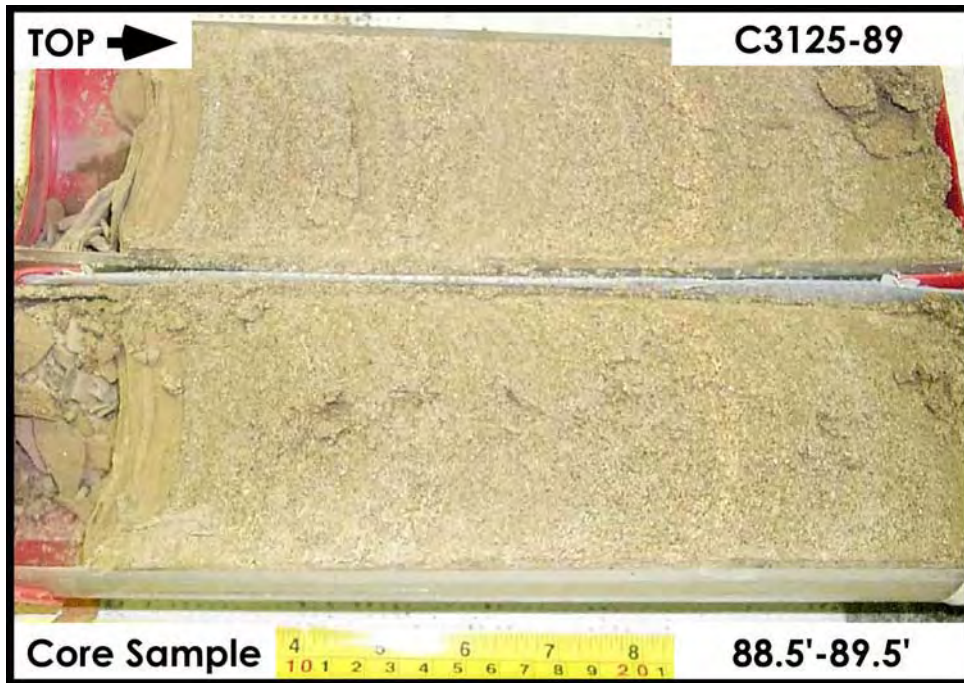
Figure A-1.29. Hanford Formation (H2 unit) 88.5 ft – 89.5 ft
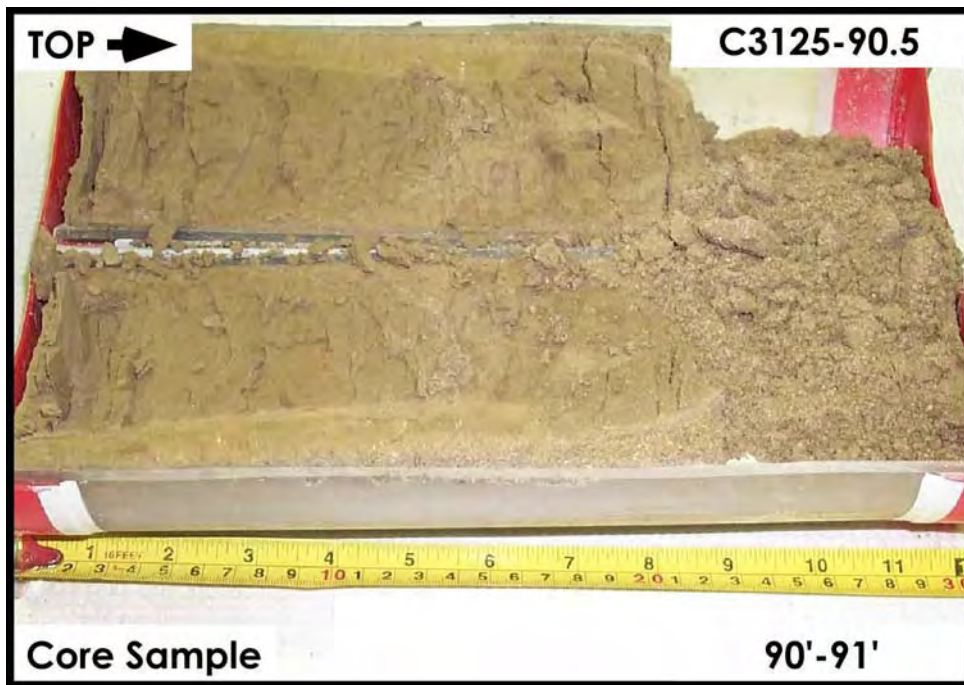
Figure A-1.30. Cold Creek Unit – Upper (CCU$_u$) 90 ft – 91 ft
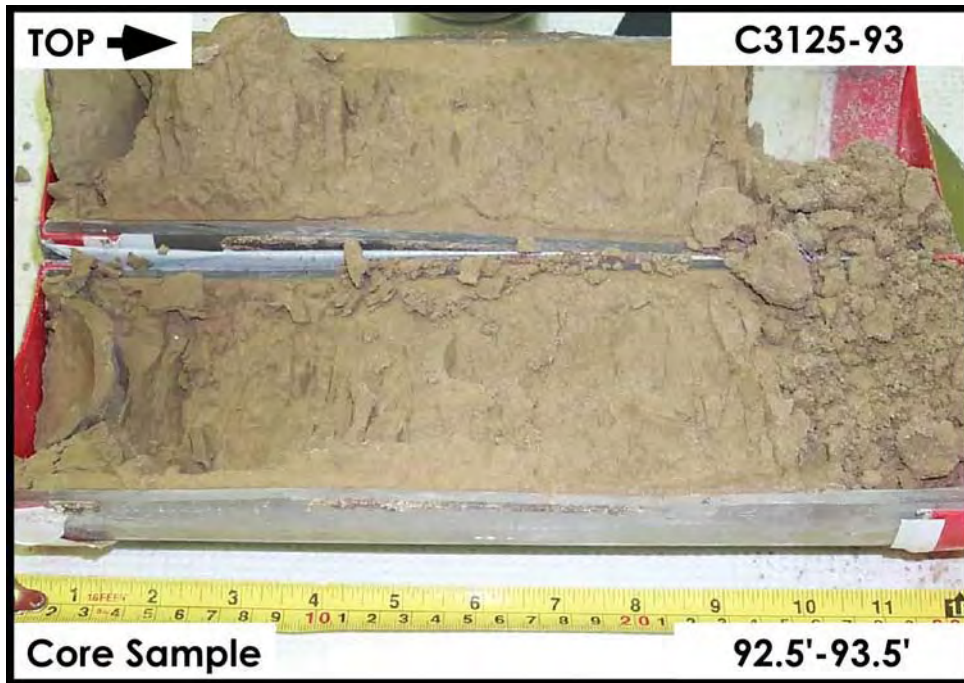
Figure A-1.31. Cold Creek Unit – Upper (CCU$_u$) 92.5 ft – 93.5 ft
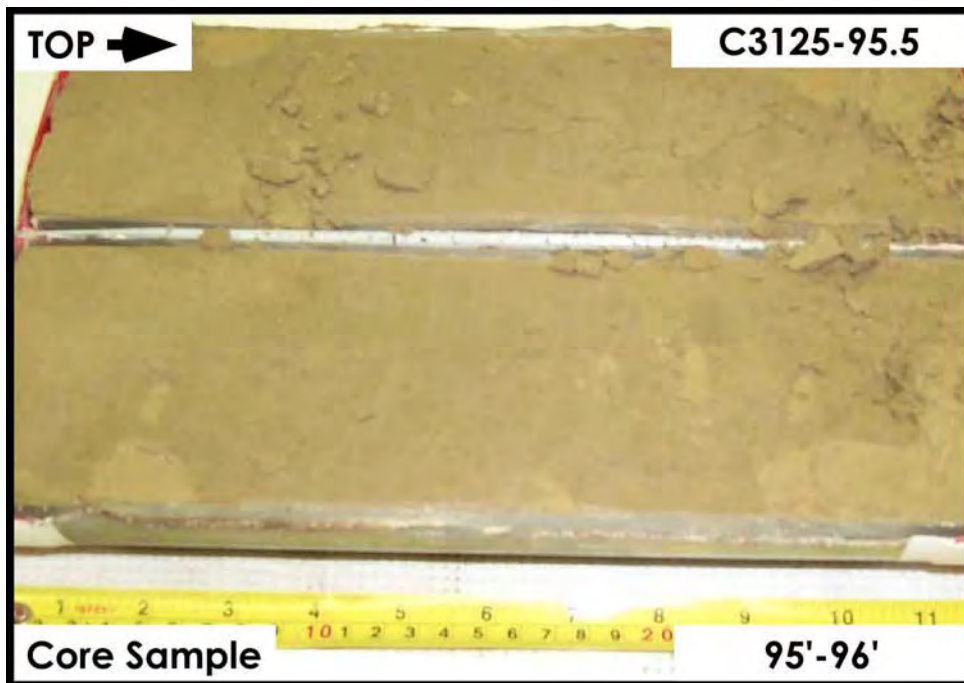
Figure A-1.32. Cold Creek Unit – Upper (CCU$_u$) 95 ft – 96 ft
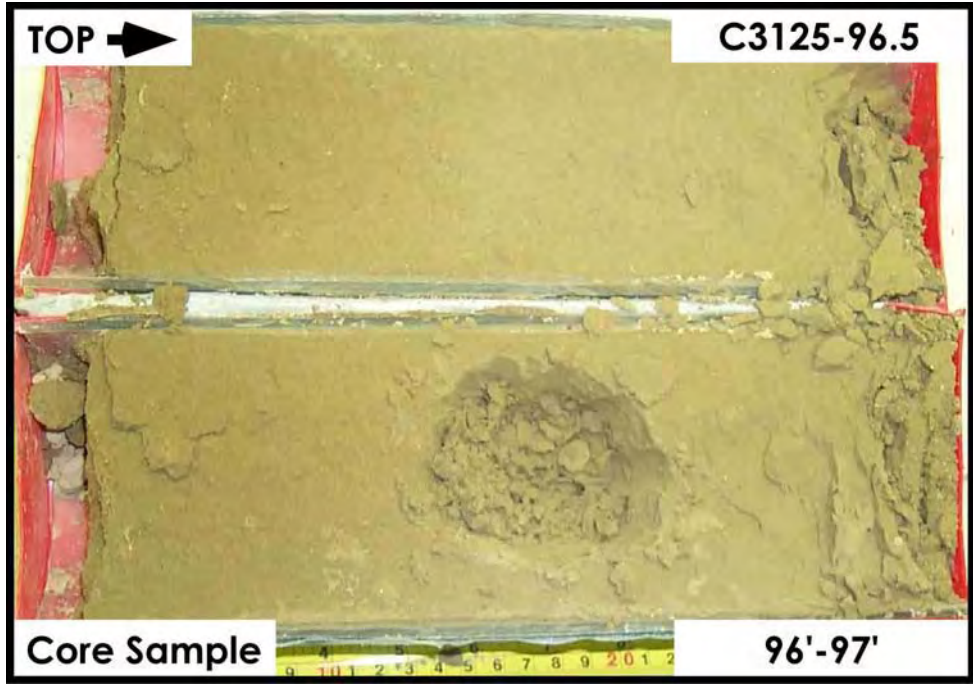
Figure A-1.33. Cold Creek Unit – Upper (CCU$_u$) 96 ft – 97 ft
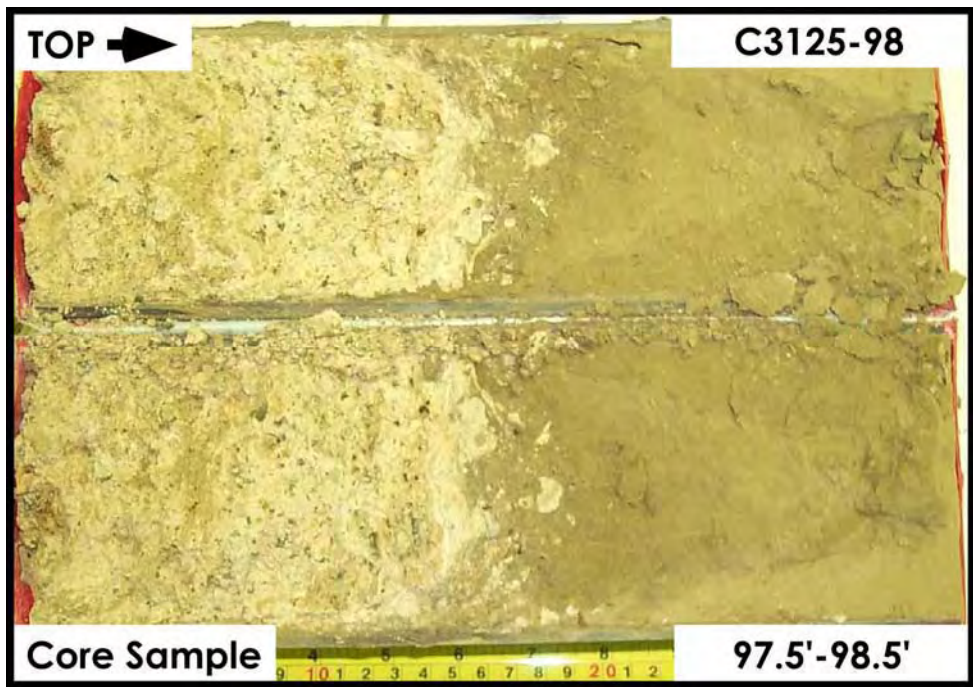
Figure A-1.34. Cold Creek Unit – Upper (CCU$_u$) 97.5 ft – 98.5 ft
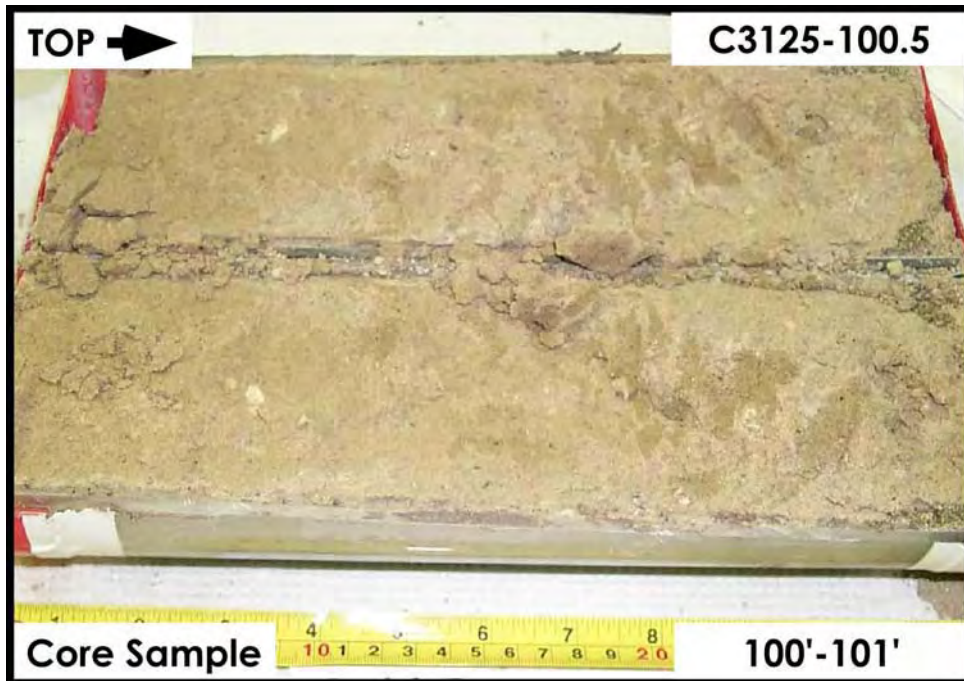
Figure A-1.35. Cold Creek Unit – Lower (CCU_l) 100 ft – 101 ft
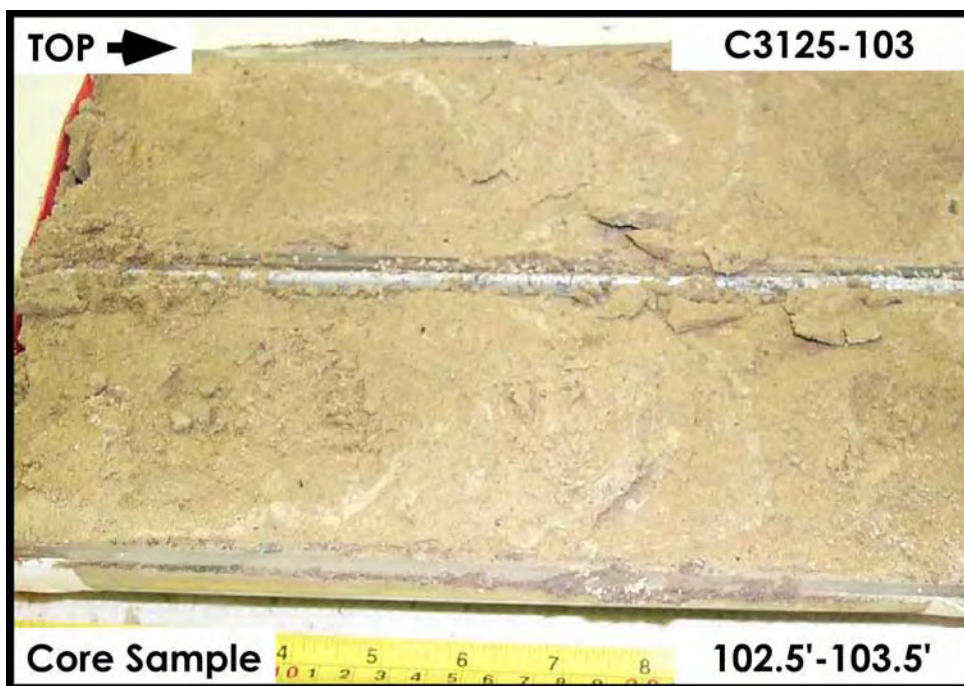
Figure A-1.36. Cold Creek Unit – Lower (CCU_l) 102.5 ft – 103.5 ft
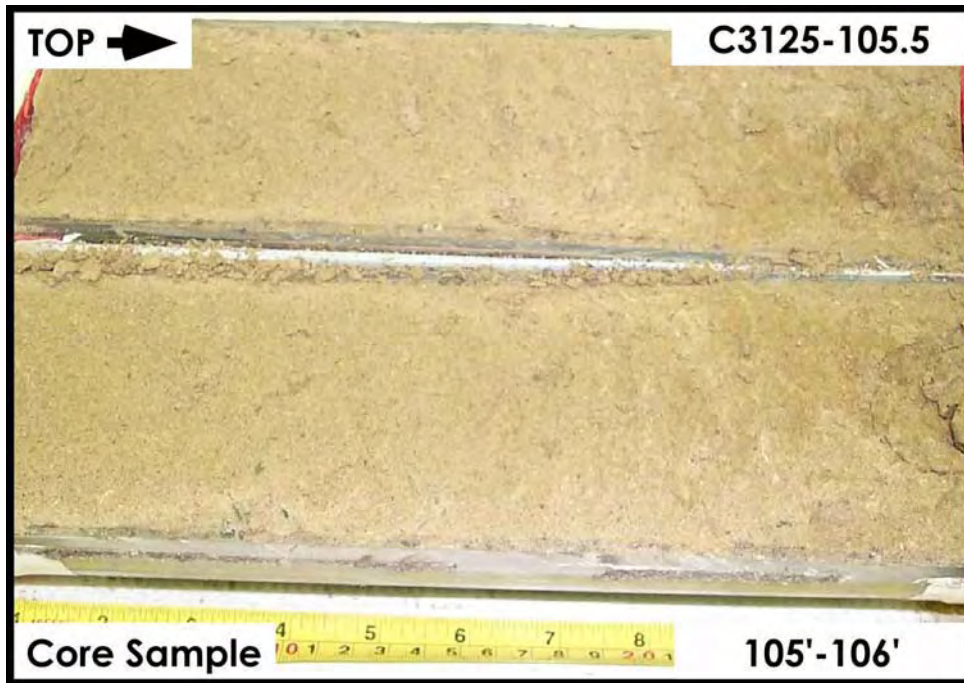
Figure A-1.37. Cold Creek Unit – Lower (CCU$_l$) 105 ft – 106 ft
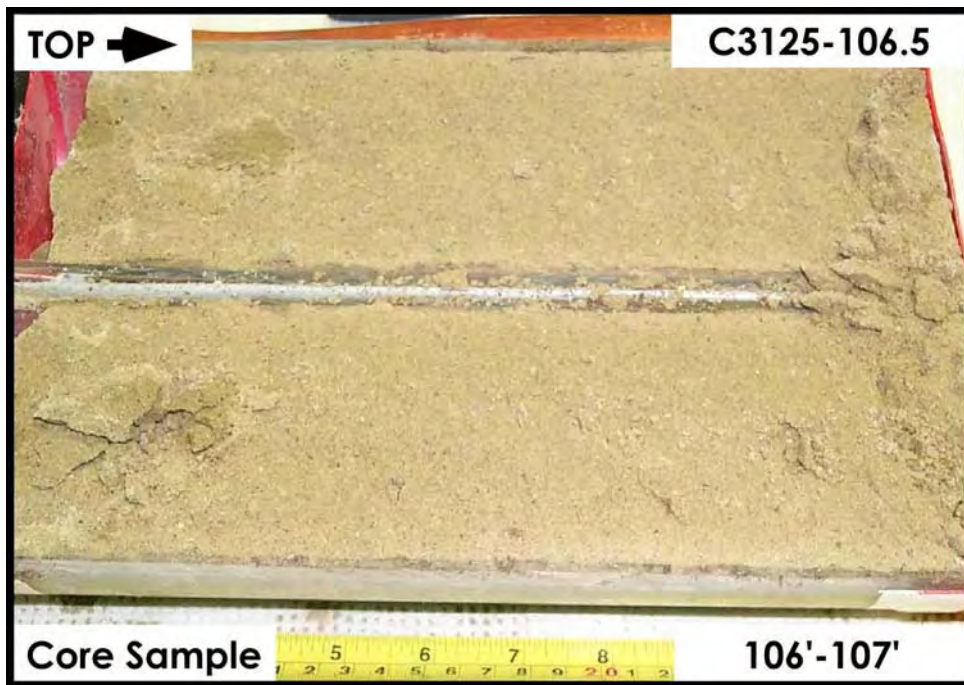
Figure A-1.38. Cold Creek Unit – Lower (CCU$_l$) 106 ft – 107 ft

Figure A-1.39. Cold Creek Unit – Lower (CCU$_l$) 107.5 ft – 108.5 ft
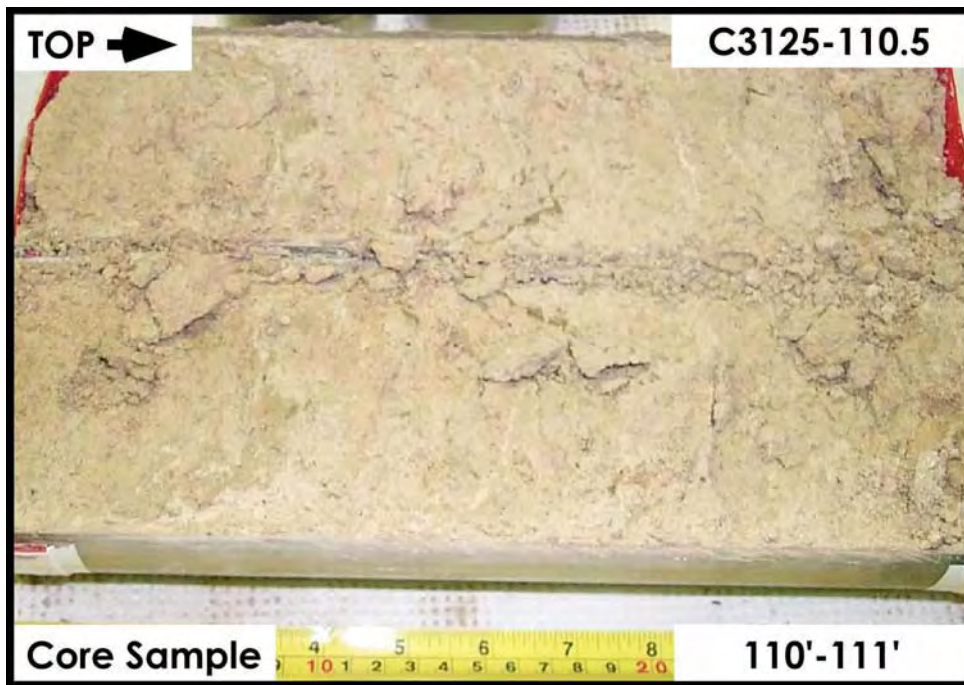
Figure A-1.40. Cold Creek Unit – Lower (CCU$_l$) 110 ft – 111 ft
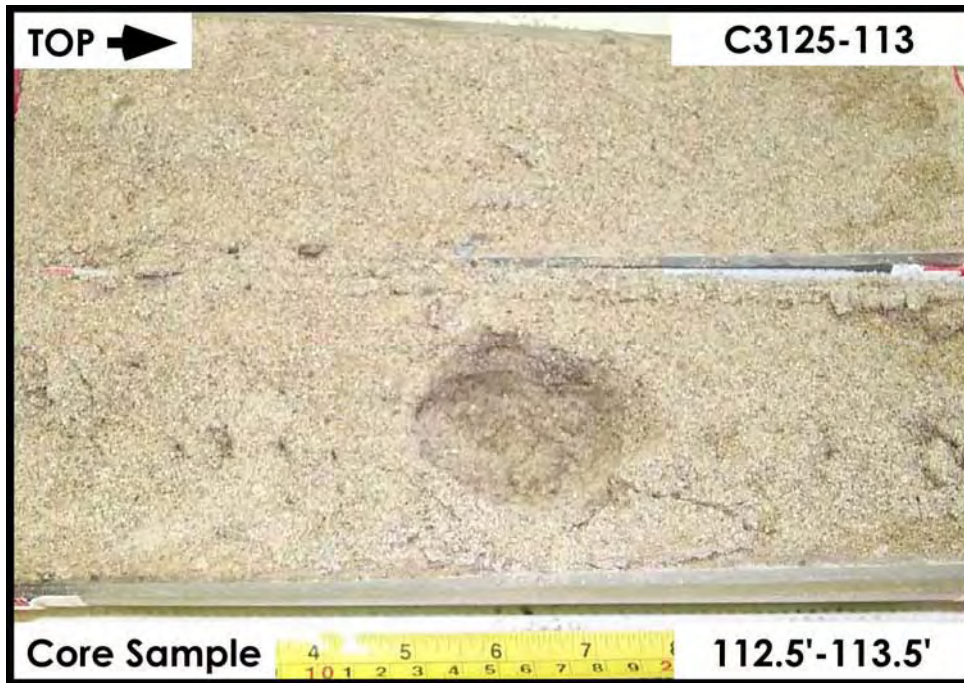
Figure A-1.41. Ringold Formation – Member of Taylor Flat (R$_{tf}$) 112.5 ft – 113.5 ft

Figure A-1.42. Ringold Formation – Member of Taylor Flat (R$_{tf}$) 113.5 ft – 114.5 ft
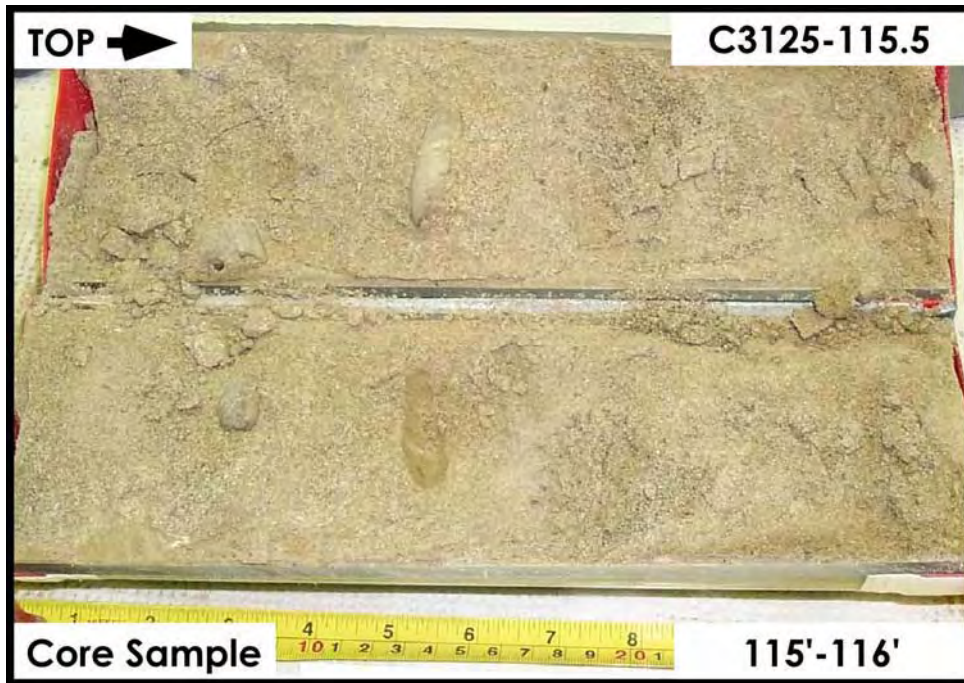
Figure A-1.43. Ringold Formation – Member of Taylor Flat (R_{tf}) 115 ft – 116 ft

Figure A-1.44. Ringold Formation – Member of Taylor Flat (R_{tf}) 116 ft – 117 ft
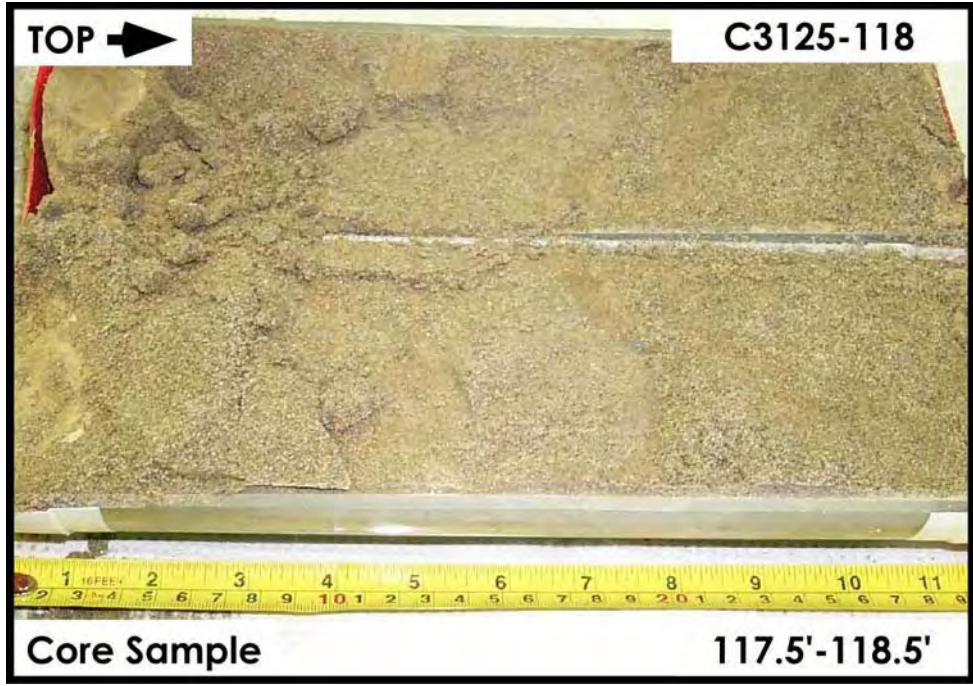
Figure A-1.45. Ringold Formation – Member of Taylor Flat (R_{tf}) 117.5 ft – 118.5 ft
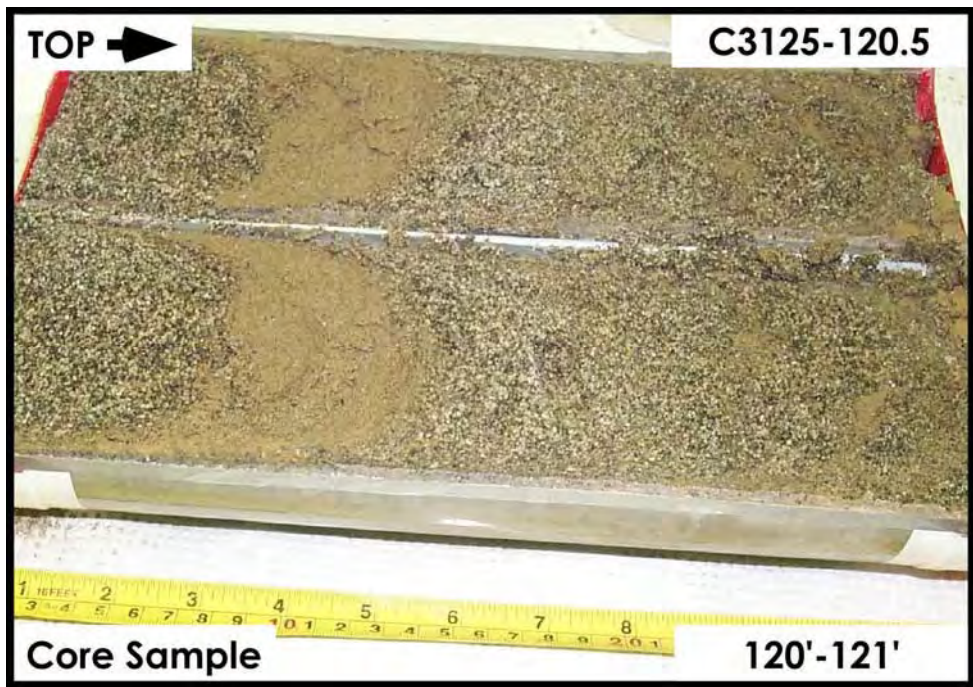
Figure A-1.46. Ringold Formation – Member of Taylor Flat (R_{tf}) 120 ft – 121 ft
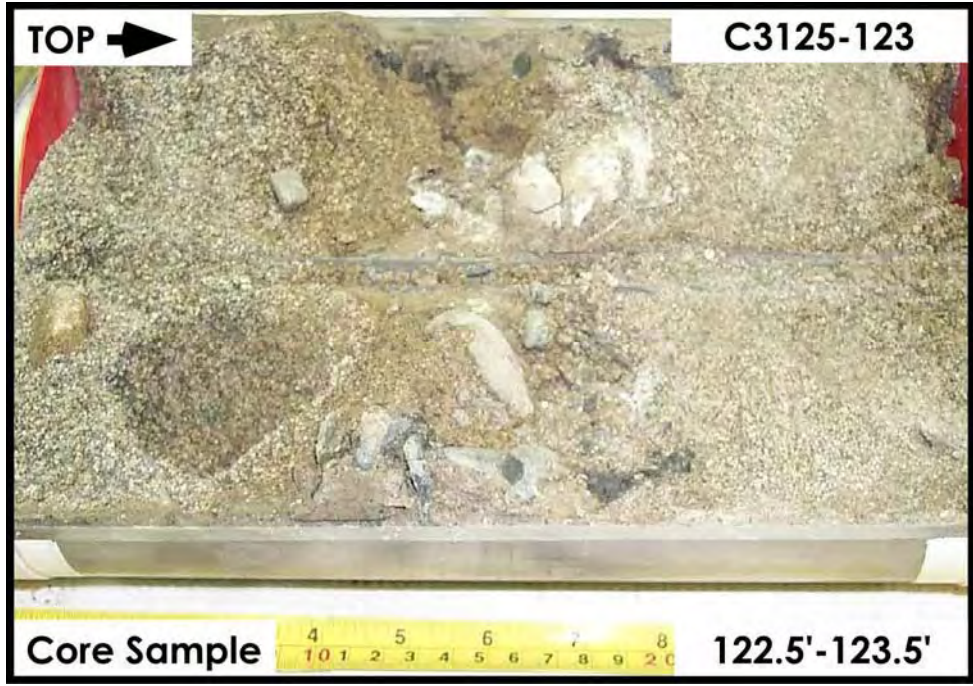
Figure A-1.47. Ringold Formation – Member of Wooded Island (R_{wi}) 122.5 ft – 123.5 ft
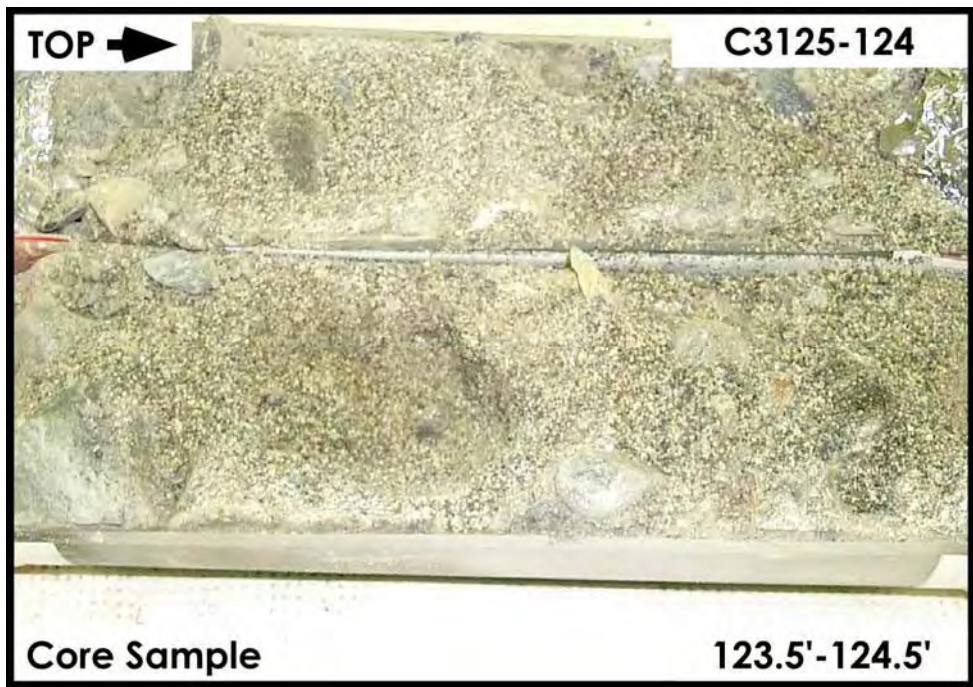
Figure A-1.48. Ringold Formation – Member of Wooded Island (R_{wi}) 123.5 ft – 124.5 ft
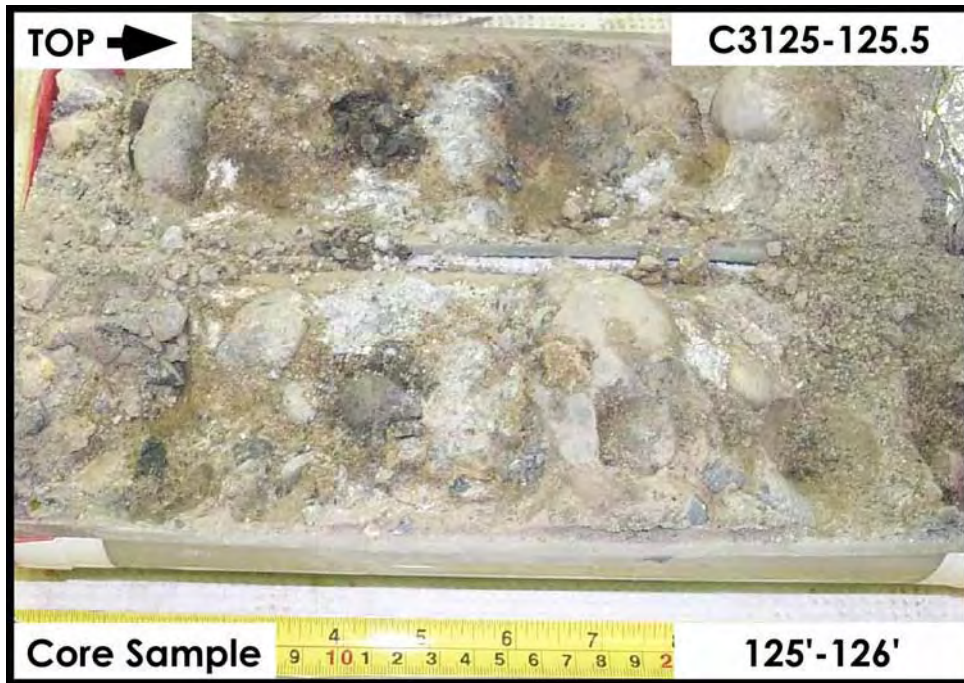
Figure A-1.49. Ringold Formation – Member of Wooded Island (R$_{wi}$) 125 ft – 126 ft
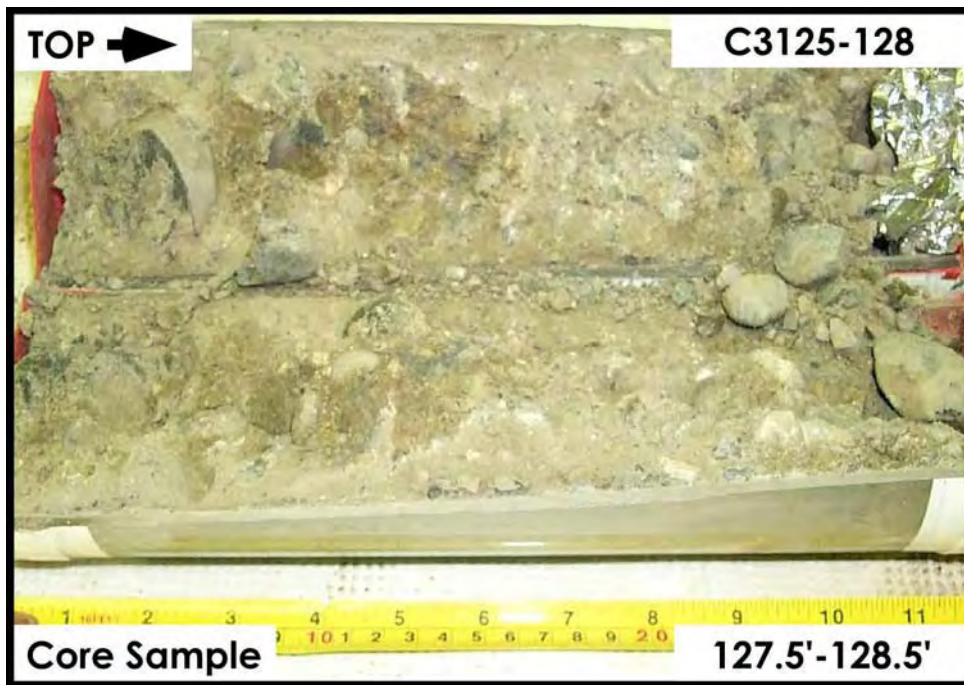
Figure A-1.50. Ringold Formation – Member of Wooded Island (R$_{wi}$) 127.5 ft – 128.5 ft
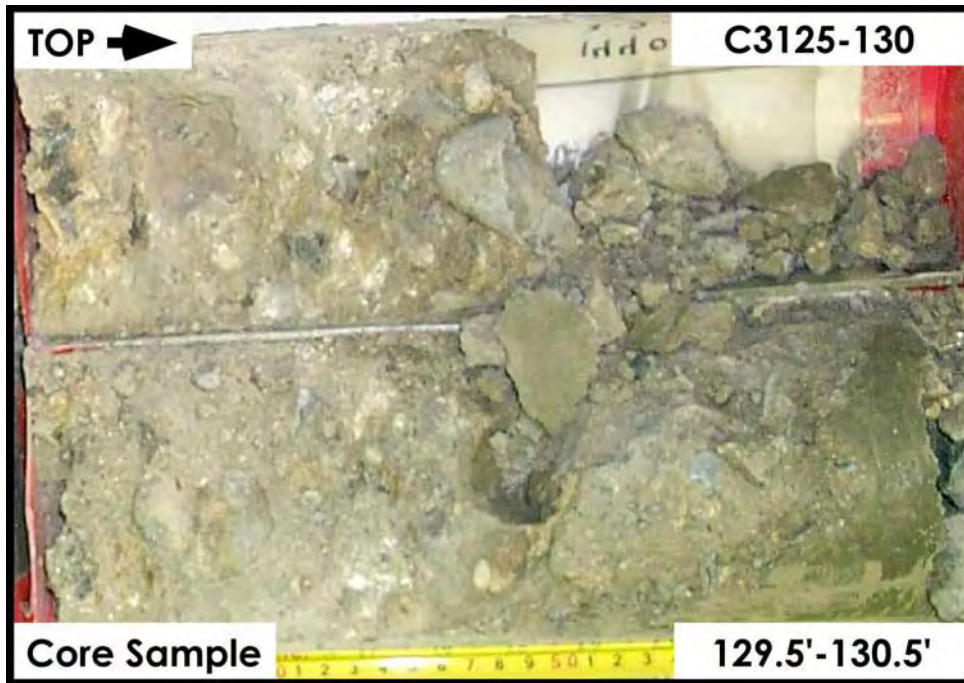
Figure A-1.51. Ringold Formation – Member of Wooded Island (R$_{wi}$) 129.5 ft – 130.5 ft
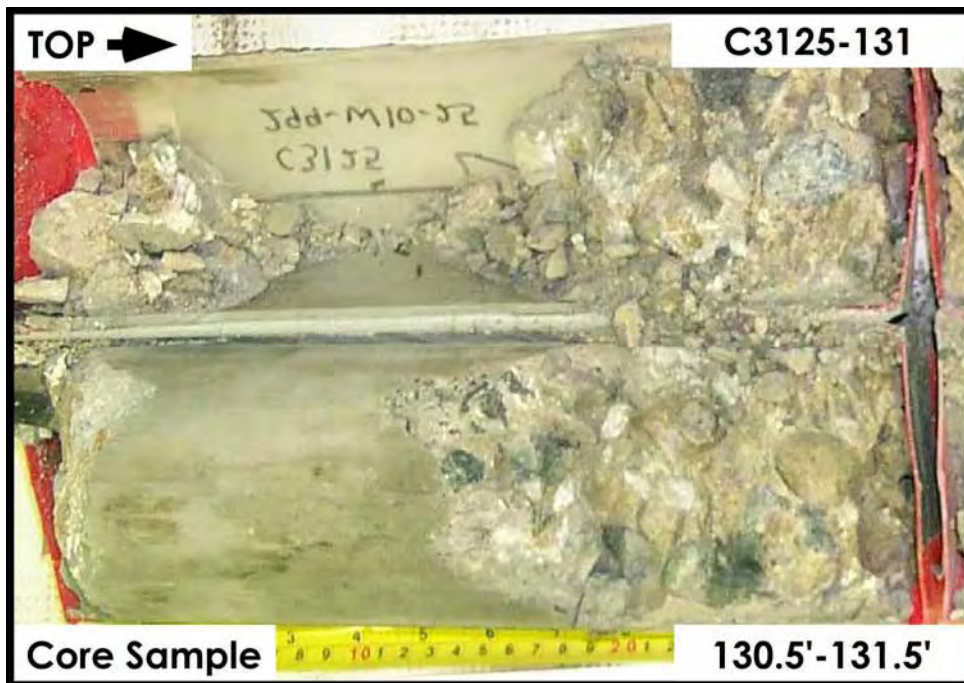
Figure A-1.52. Ringold Formation – Member of Wooded Island (R$_{wi}$) 130.5 ft – 131.5 ft

APPENDIX A.2

C3830 (TX-105)

SPLITSPOON CORE

SAMPLE PHOTOGRAPHS

Contents

Figures

Figure A-2.1.   Backfill 14.96 ft – 15.64 ft

Figure A-2.2.   Backfill 15.64 ft – 16.31 ft

Figure A-2.3.   Backfill 27.19 ft – 28.58 ft

Figure A-2.4.   Backfill 28.58 ft – 29.25ft
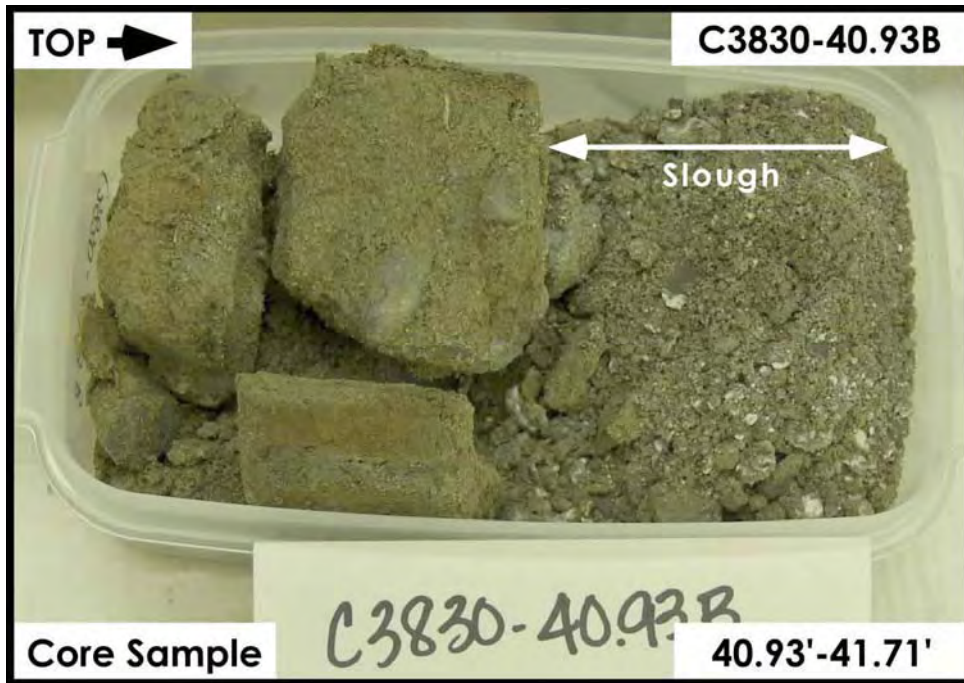
Figure A-2.5.   Backfill 40.93 ft – 41.71 ft
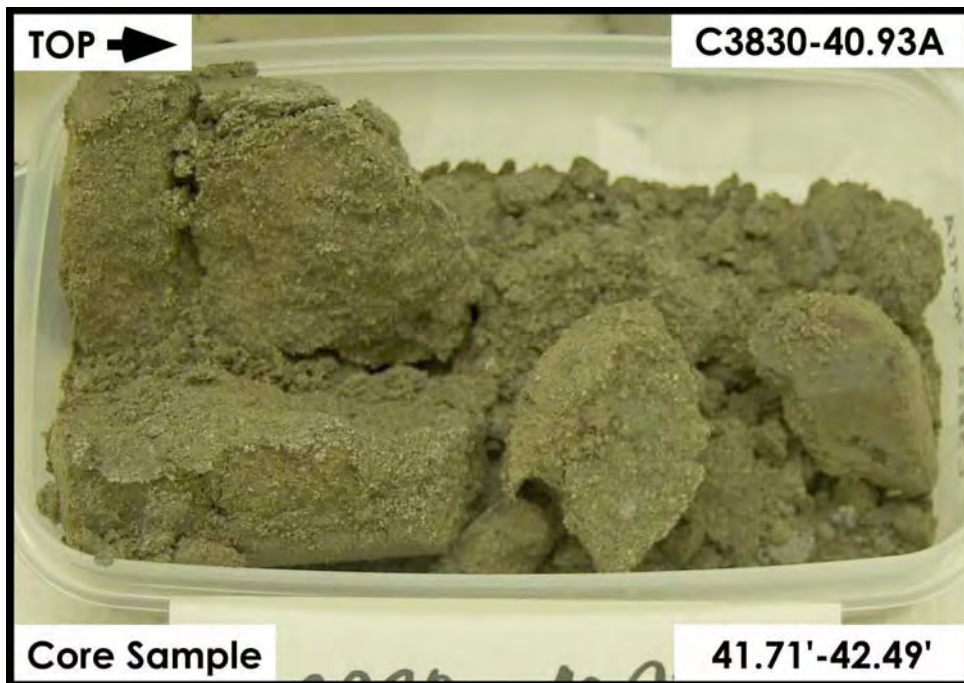
Figure A-2.6.   Backfill 41.71 ft – 42.49 ft
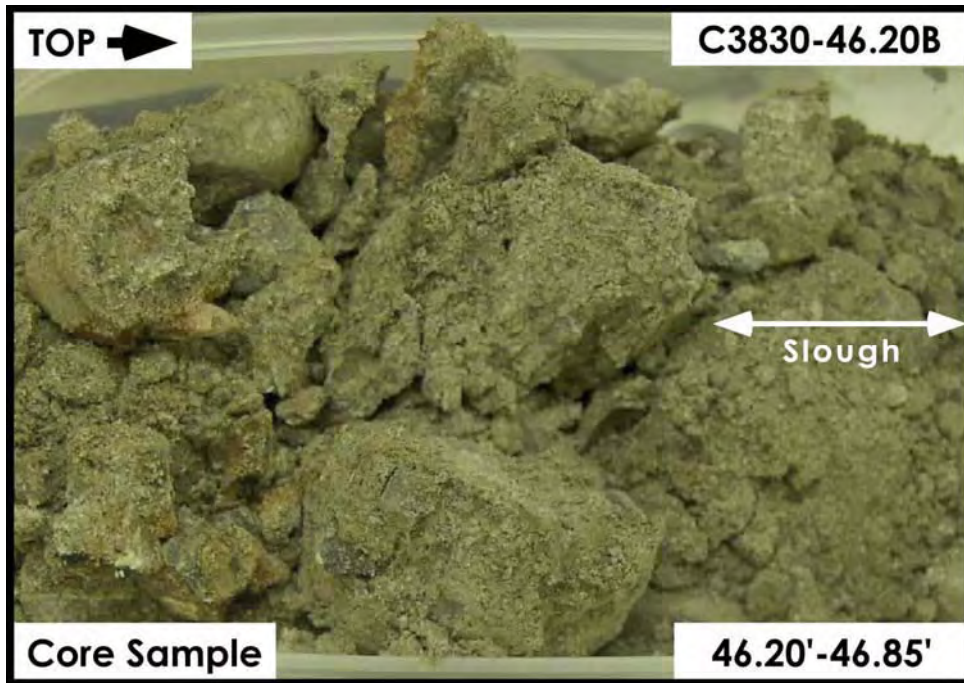
Figure A-2.7.   Backfill 46.20 ft – 46.85 ft
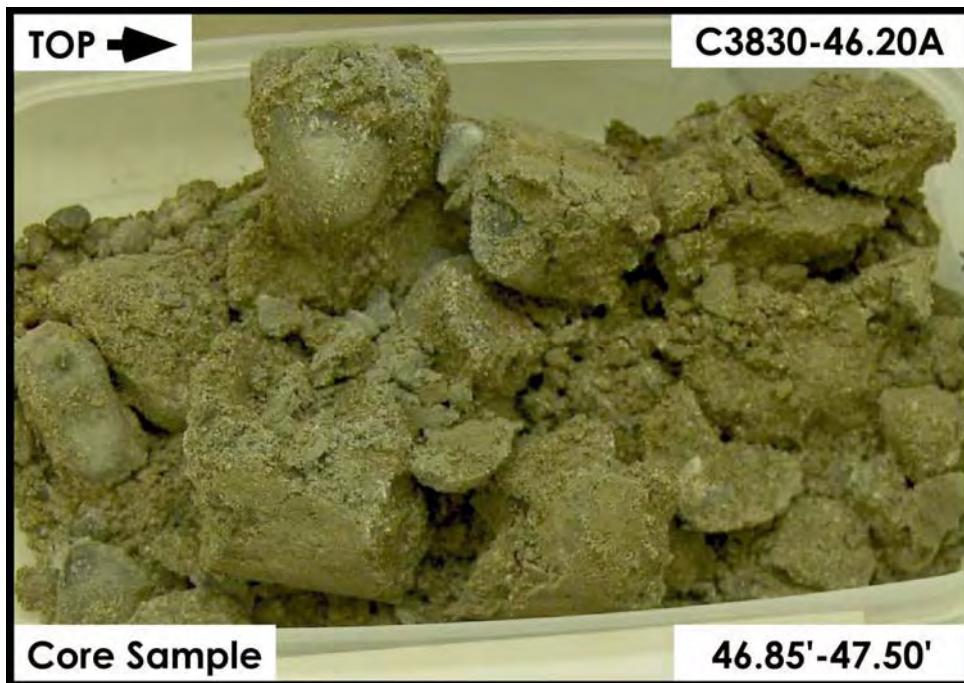
Figure A-2.8.   Backfill 46.85 ft – 47.50 ft
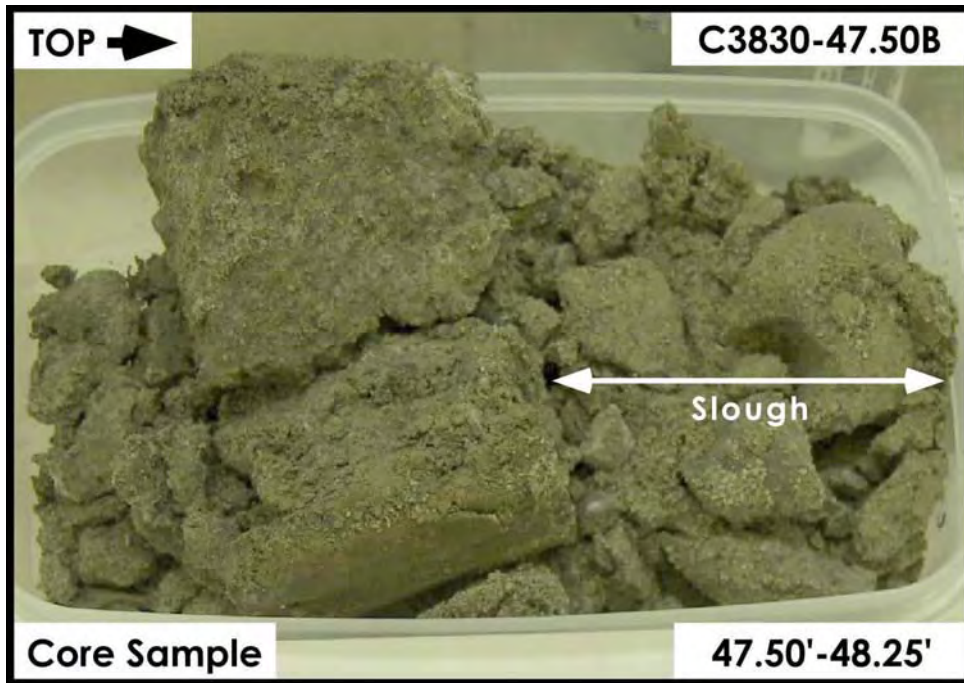
Figure A-2.9. Backfill 47.50 ft – 48.25 ft
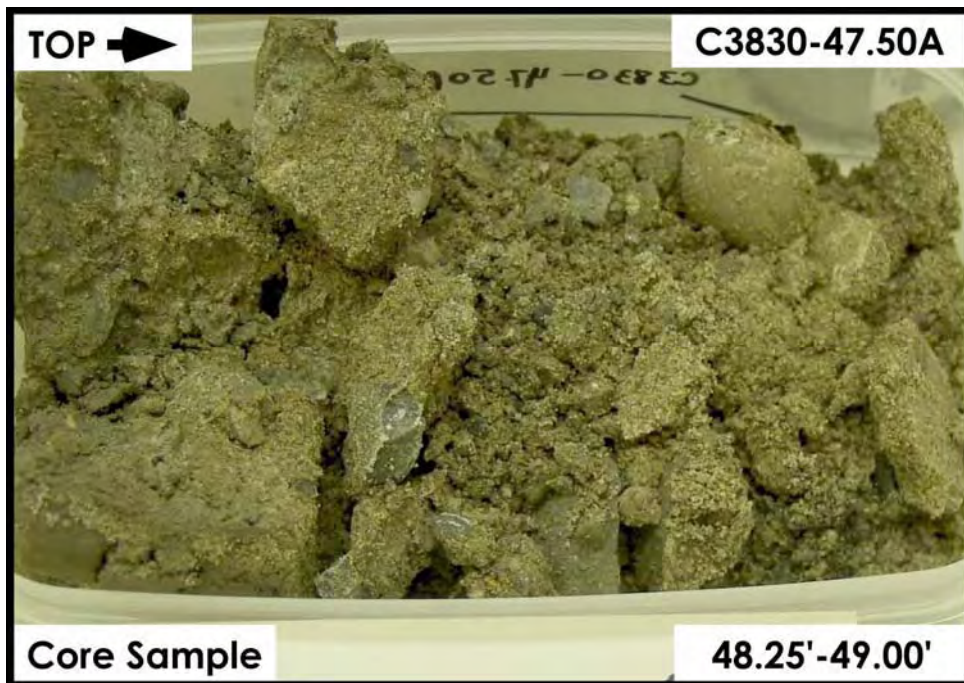
Figure A-2.10. Backfill 48.25 ft – 49.00 ft
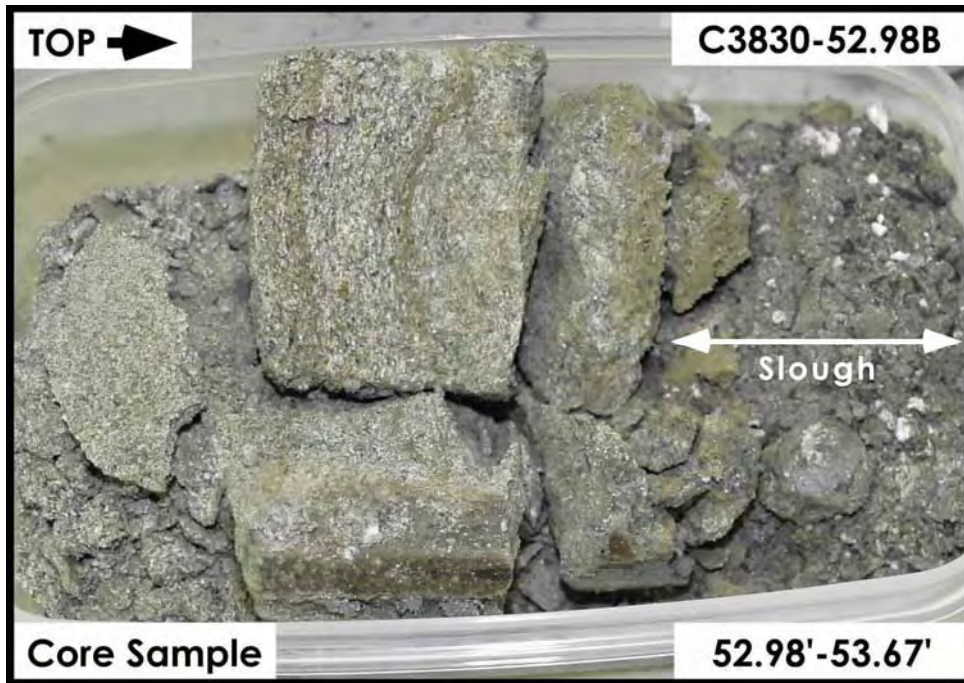
Figure A-2.11. Hanford Formation (H2 unit) 52.98 ft – 53.67 ft
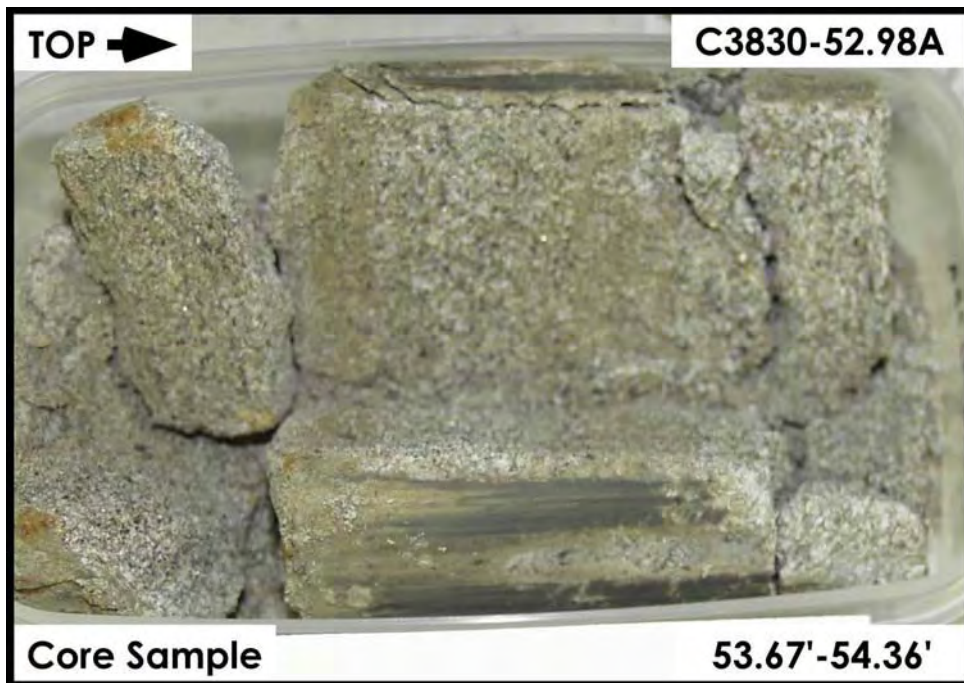
Figure A-2.12. Hanford Formation (H2 unit) 53.67 ft – 54.36 ft
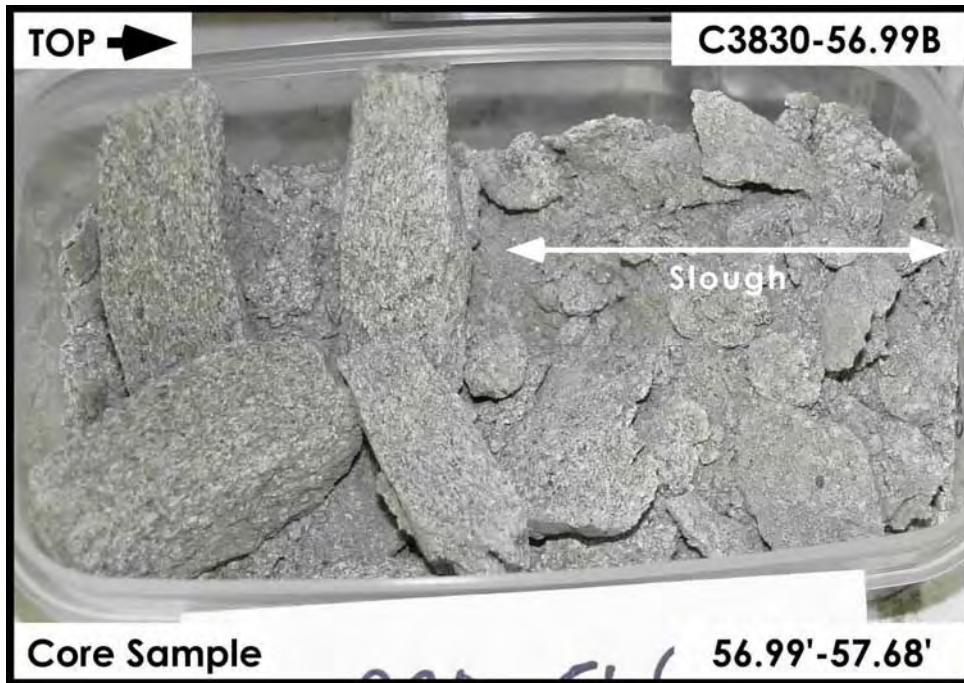
Figure A-2.13. Hanford Formation (H2 unit) 56.99 ft – 57.68 ft
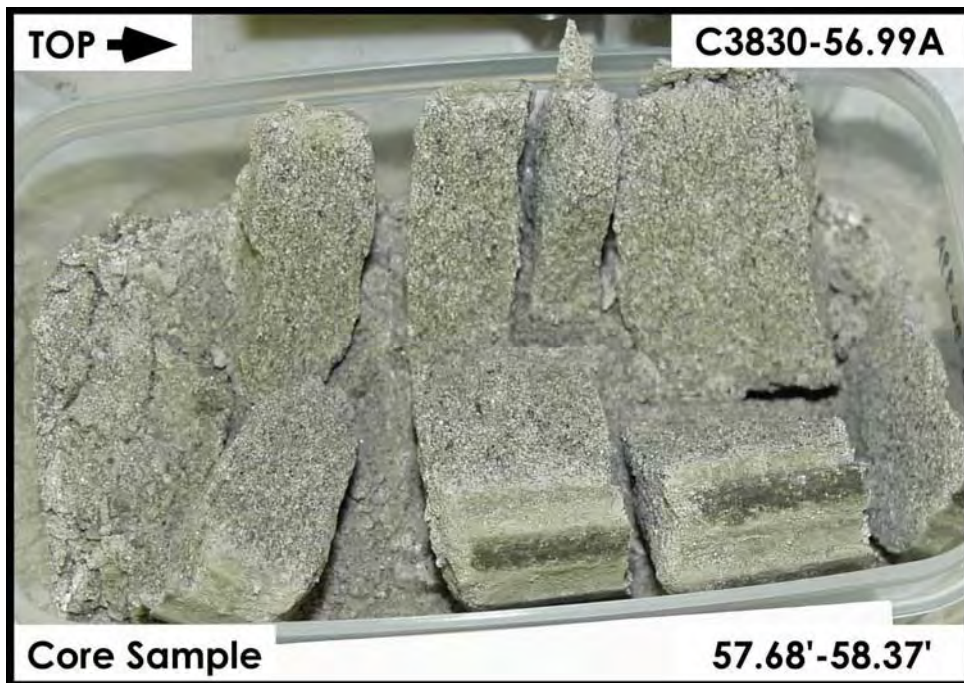
Figure A-2.14. Hanford Formation (H2 unit) 57.68 ft – 58.37 ft
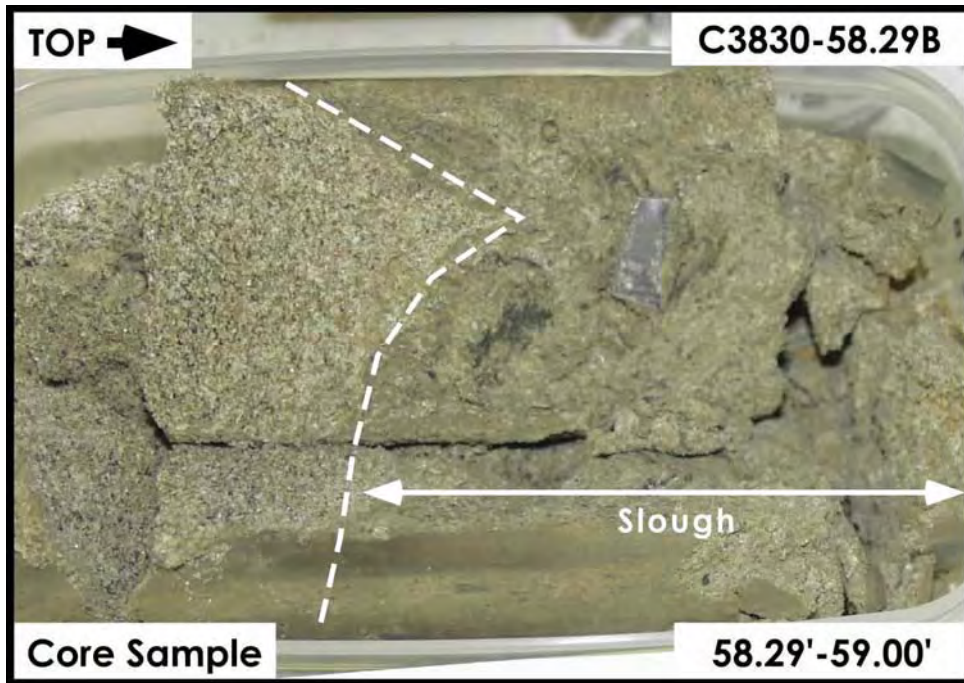
Figure A-2.15. Hanford Formation (H2 unit) 58.29 ft – 59.00 ft
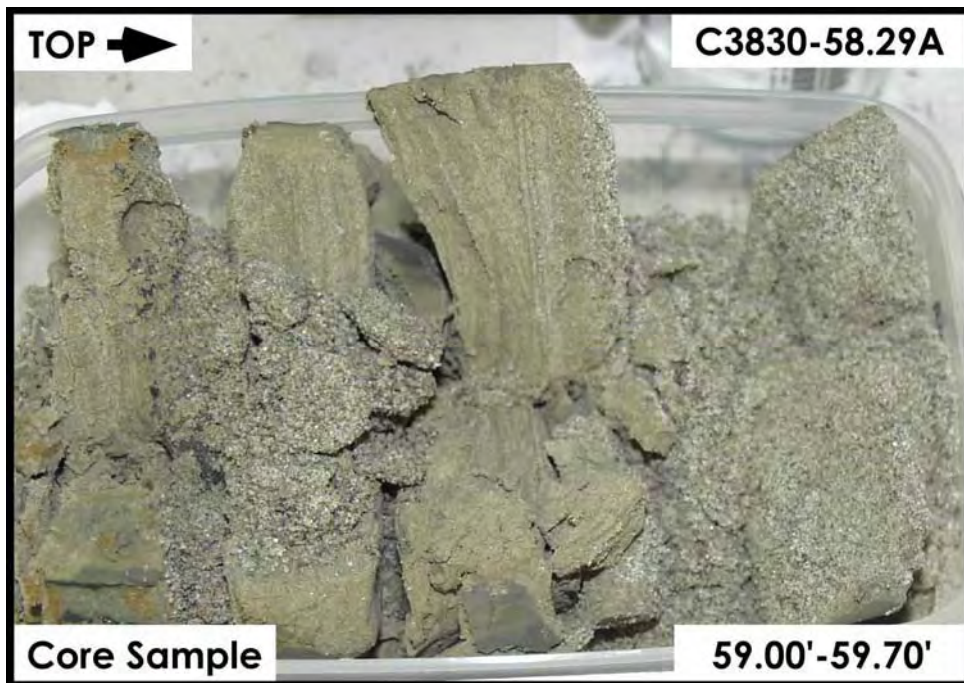
Figure A-2.16. Hanford Formation (H2 unit) 59.00 ft – 59.70 ft
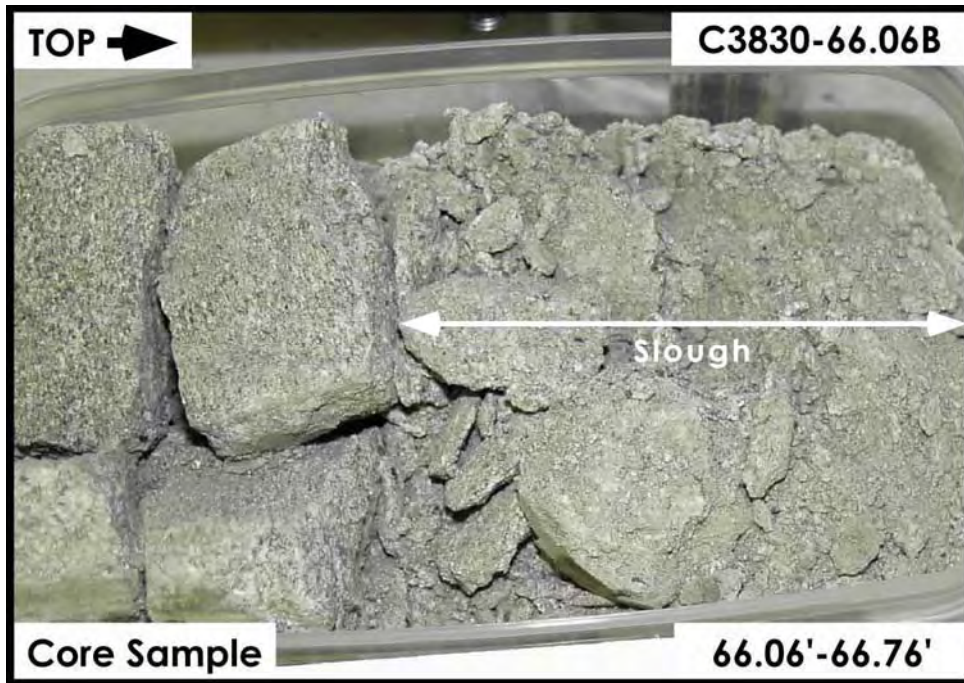
Figure A-2.17. Hanford Formation (H2 unit) 66.06 ft – 66.76 ft
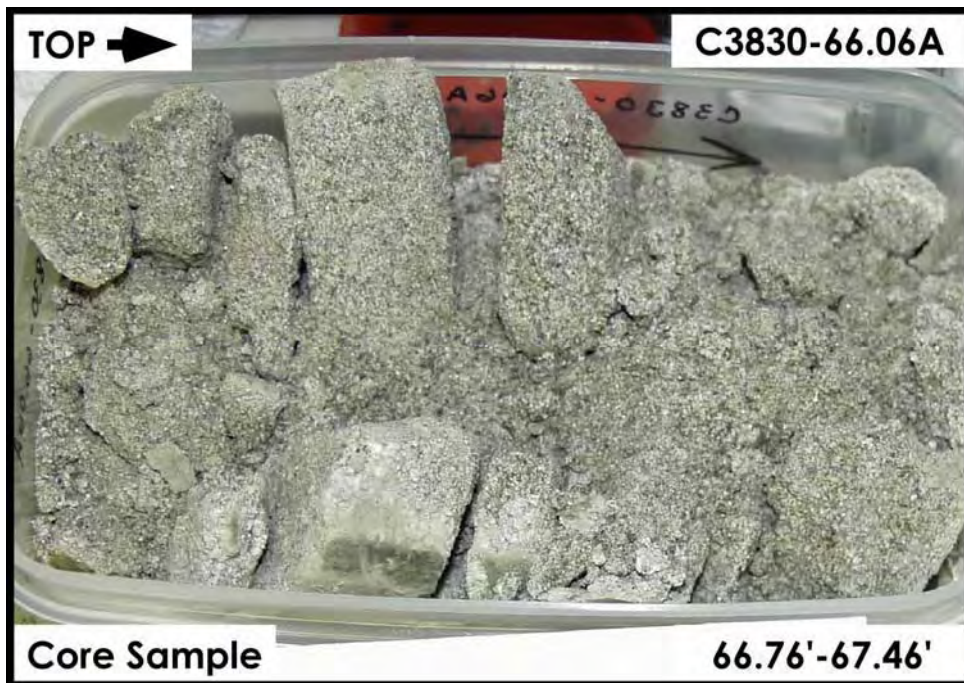
Figure A-2.18. Hanford Formation (H2 unit) 66.76 ft – 67.46 ft

Figure A-2.19. Hanford Formation (H2 unit) 71.95 ft – 72.63 ft
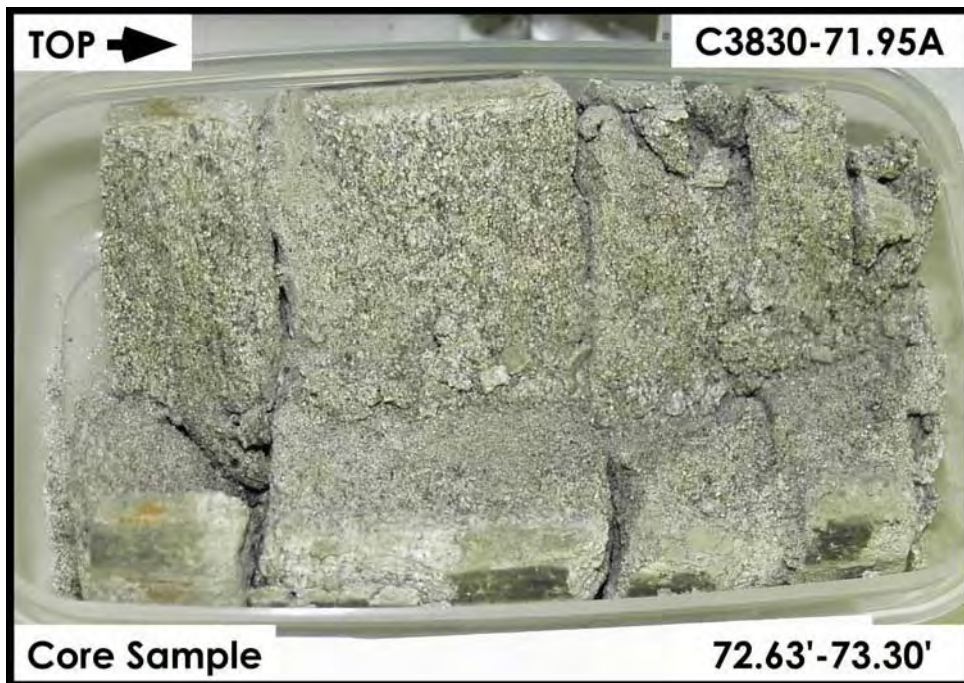
Figure A-2.20. Hanford Formation (H2 unit) 72.63 ft – 73.30 ft

Figure A-2.21. Hanford Formation (H2 unit) 76.98 ft – 77.67 ft

Figure A-2.22. Hanford Formation (H2 unit) 77.67 ft – 78.35 ft

Figure A-2.23. Hanford Formation (H2 unit) 80.91 ft – 81.56 ft

Figure A-2.24. Hanford Formation (H2 unit) 81.56 ft – 82.21 ft

Figure A-2.25. Hanford Formation (H2 unit) 86.11 ft – 86.76 ft

Figure A-2.26. Hanford Formation (H2 unit) 86.76 ft – 87.41 ft

Figure A-2.27. Hanford Formation (H2 unit) 98.97 ft – 99.67 ft

Figure A-2.28. Hanford Formation (H2 unit) 99.67 ft – 100.36 ft
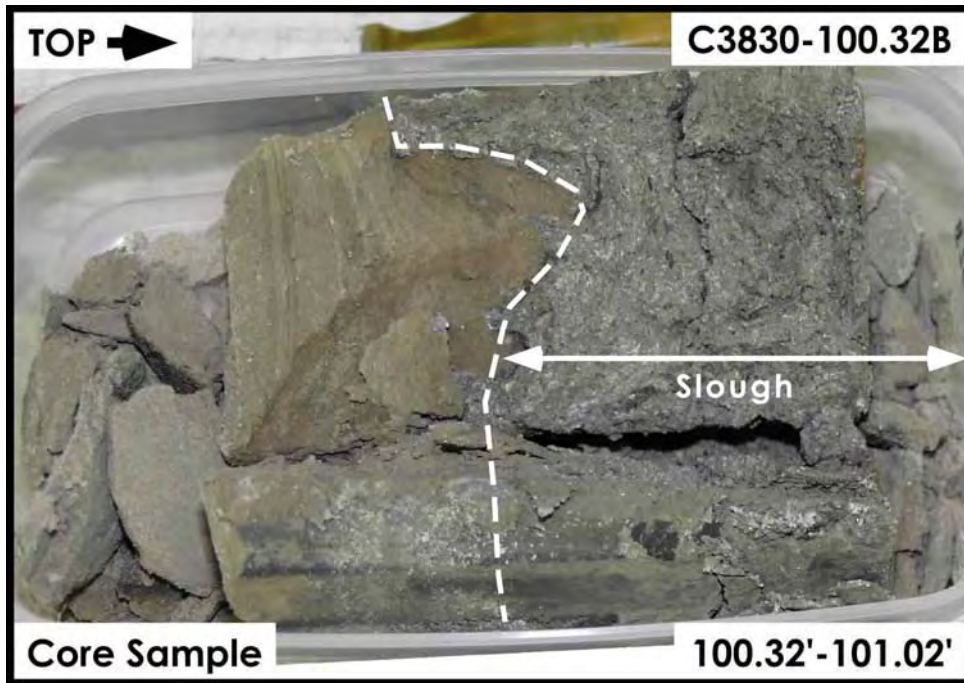
Figure A-2.29. Cold Creek Unit – Upper (CCU$_u$) 100.32 ft – 101.02 ft
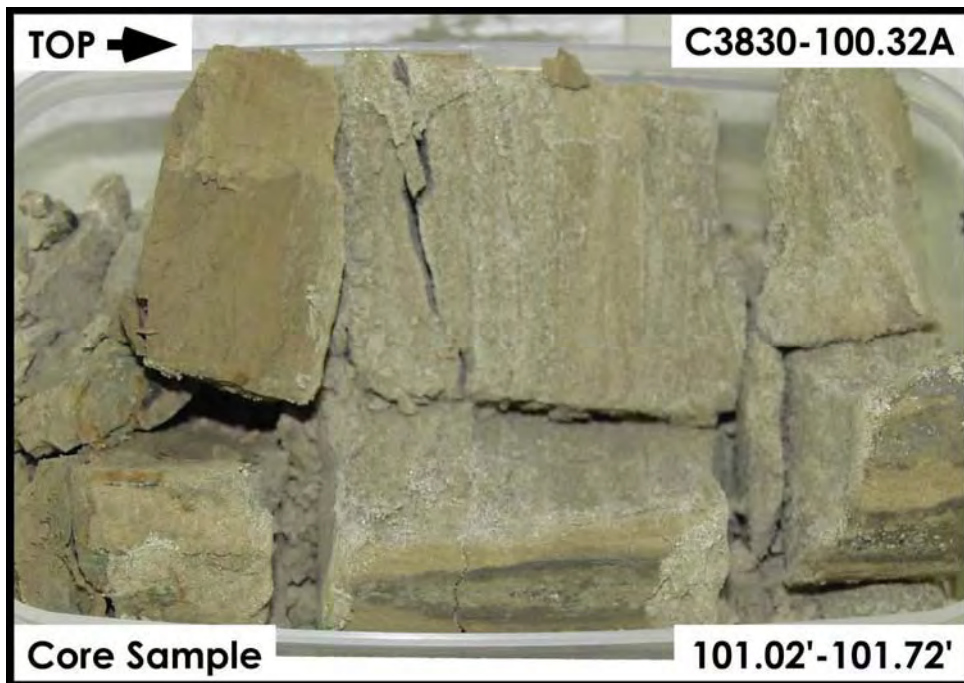
Figure A-2.30. Cold Creek Unit – Upper (CCU$_u$) 101.02 ft – 101.72 ft
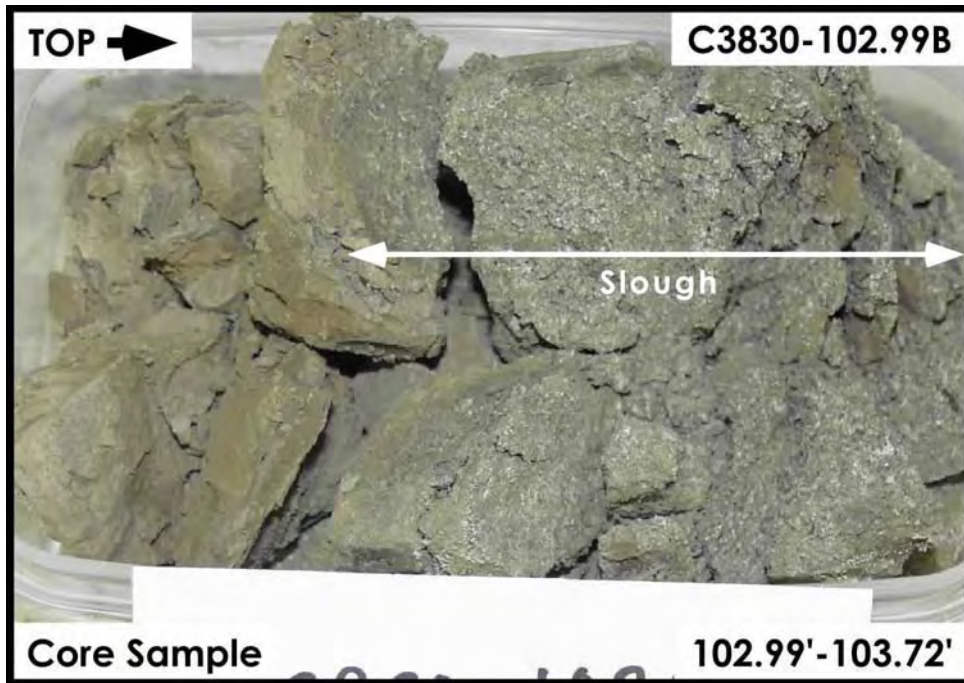
Figure A-2.31. Cold Creek Unit – Upper (CCU$_u$) 102.99 ft – 103.72 ft
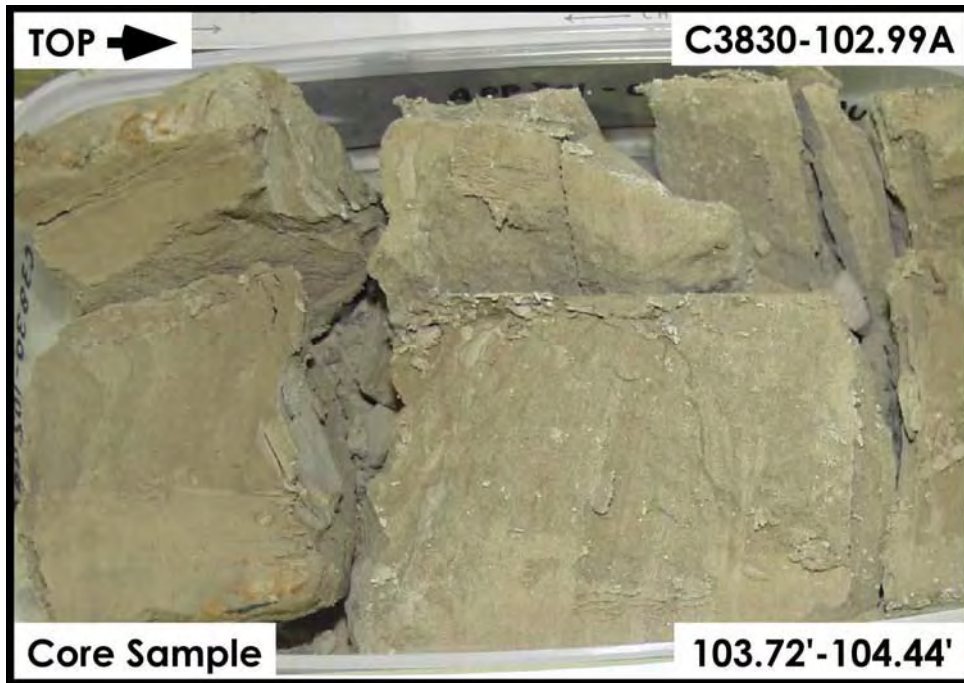
Figure A-2.32. Cold Creek Unit – Upper (CCU$_u$) 103.72 ft – 104.44 ft
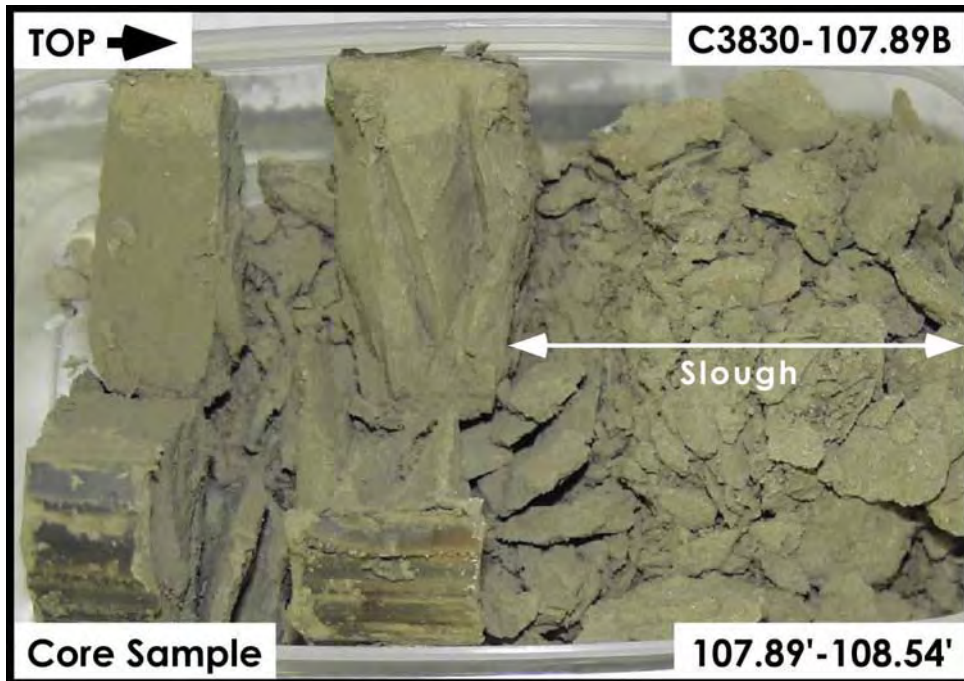
Figure A-2.33. Cold Creek Unit – Upper (CCU$_u$) 107.89 ft – 108.54 ft
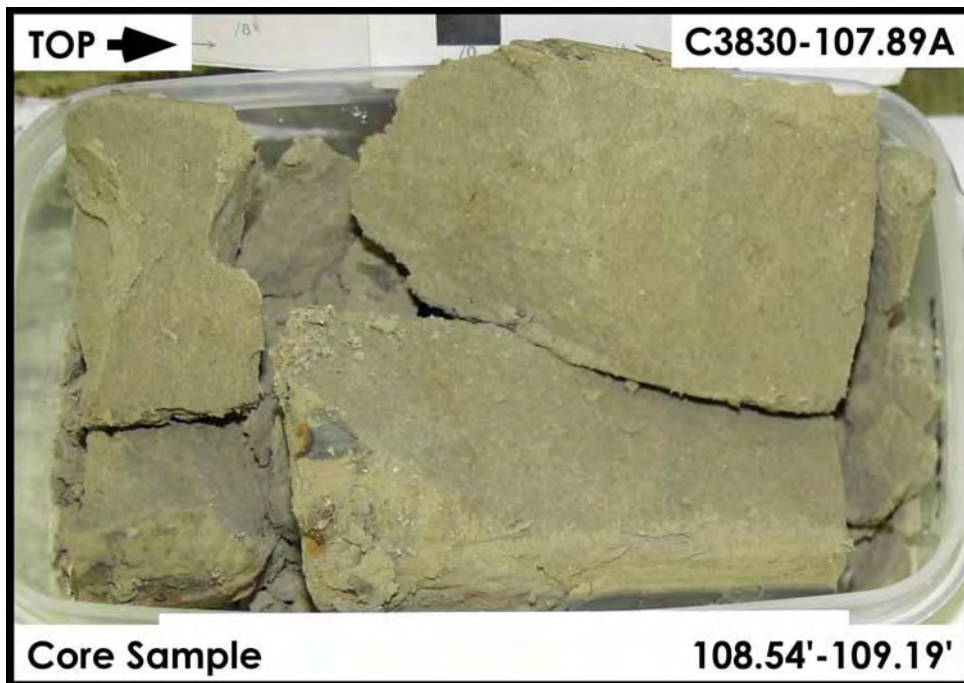
Figure A-2.34. Cold Creek Unit – Upper (CCU$_u$) 108.54 ft – 109.19 ft
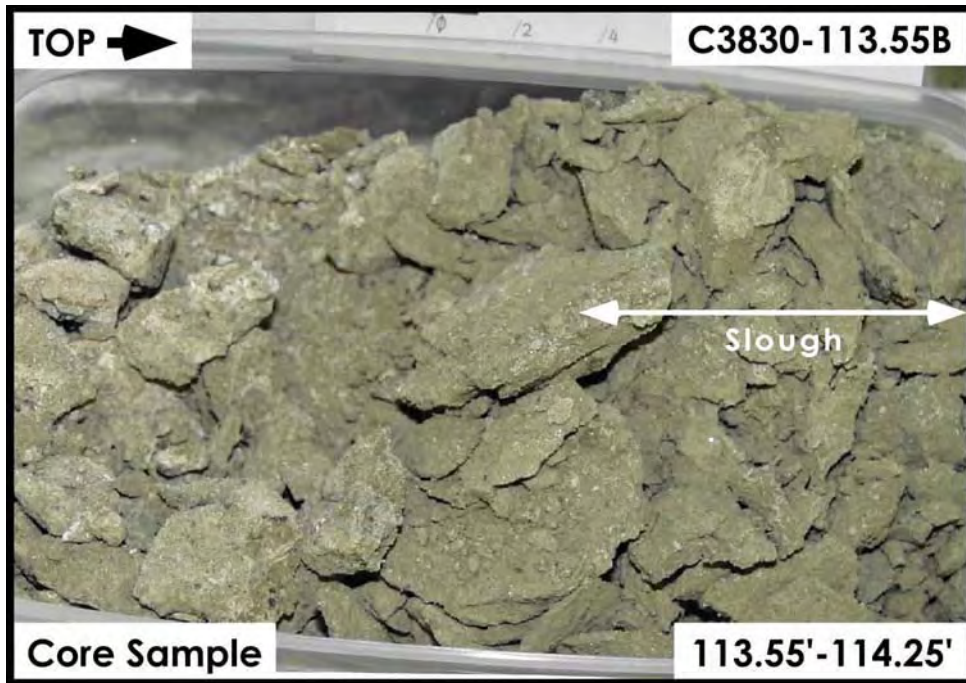
Figure A-2.35. Cold Creek Unit – Lower (CCU$_l$) 113.55 ft – 114.25 ft
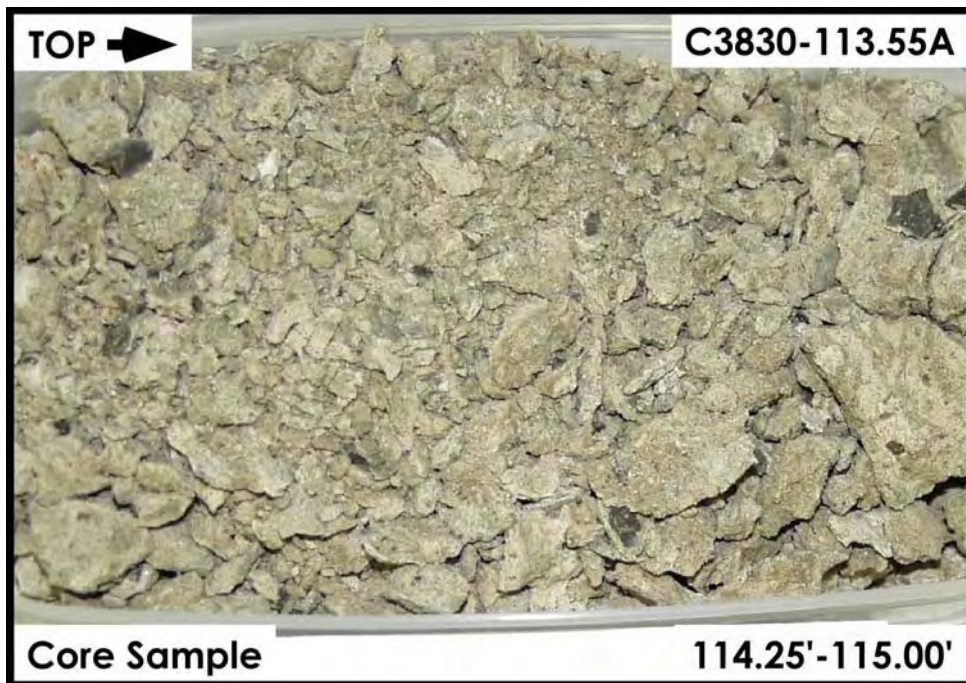
Figure A-2.36. Cold Creek Unit – Lower (CCU$_l$) 114.25 ft – 115.00 ft

APPENDIX A.3

C3831 (TX-107)

SPLITSPOON CORE

SAMPLE PHOTOGRAPHS
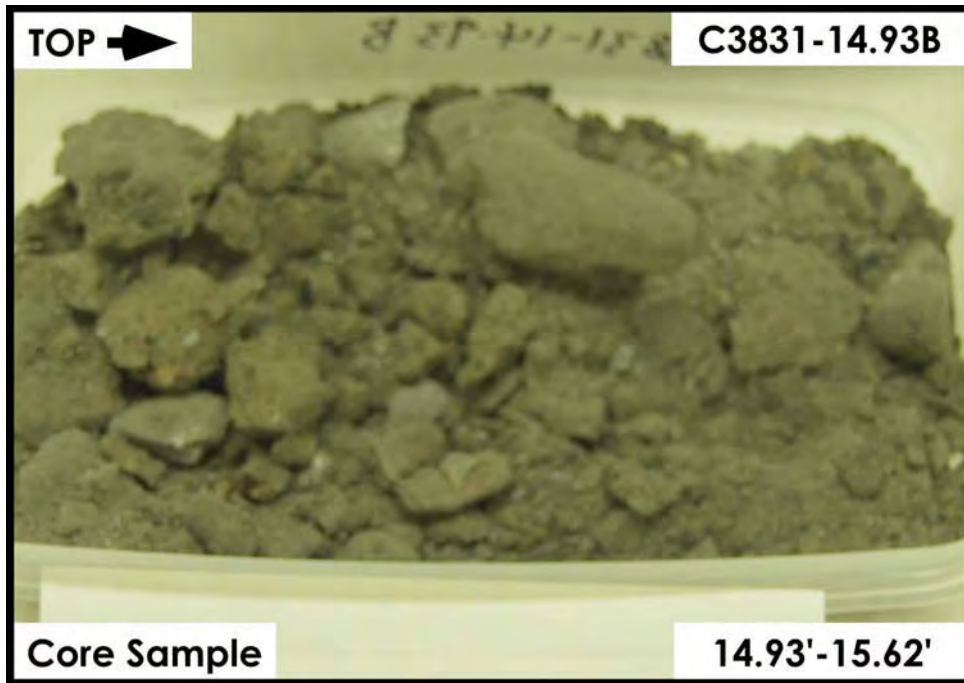
Contents

Figures

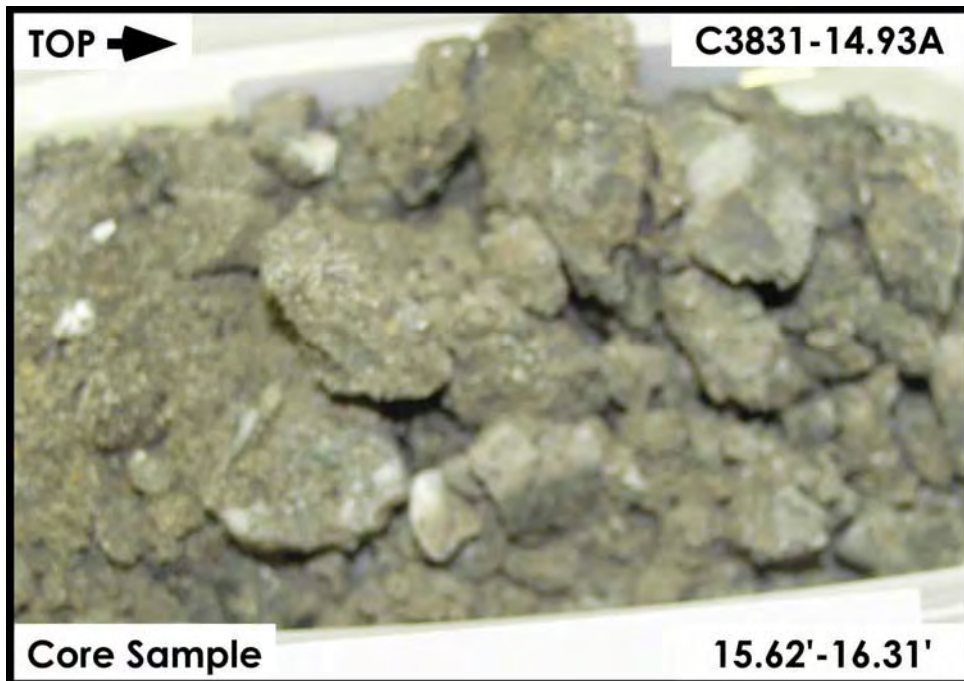**Figure A-3.1.   Backfill 14.93 ft – 15.62 ft**

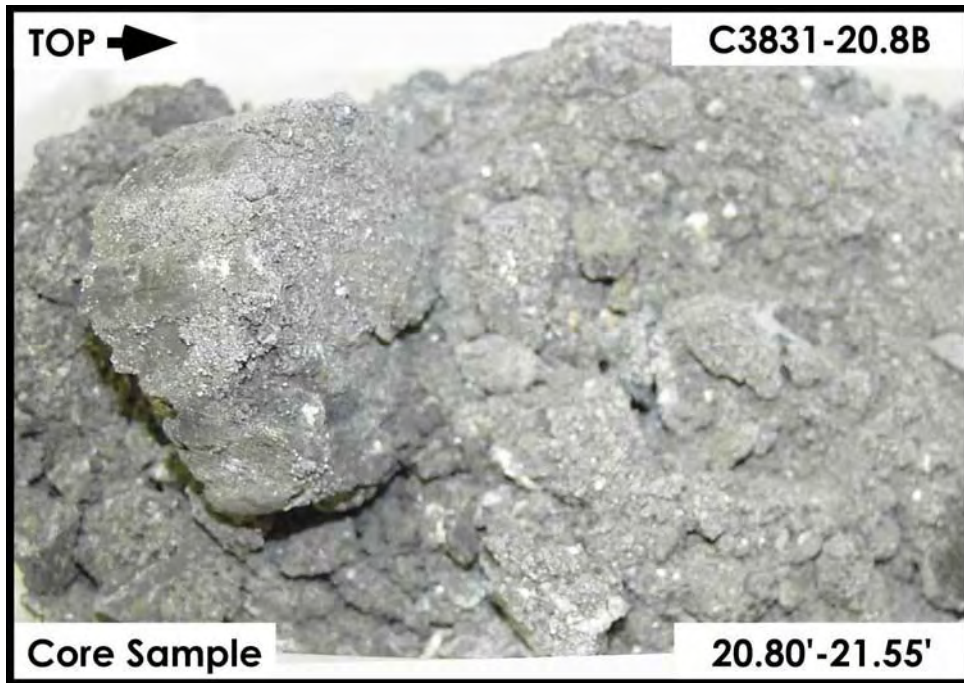**Figure A-3.2.   Backfill 15.62 ft – 16.31 ft**

Figure A-3.3. Backfill 20.80 ft – 21.55 ft

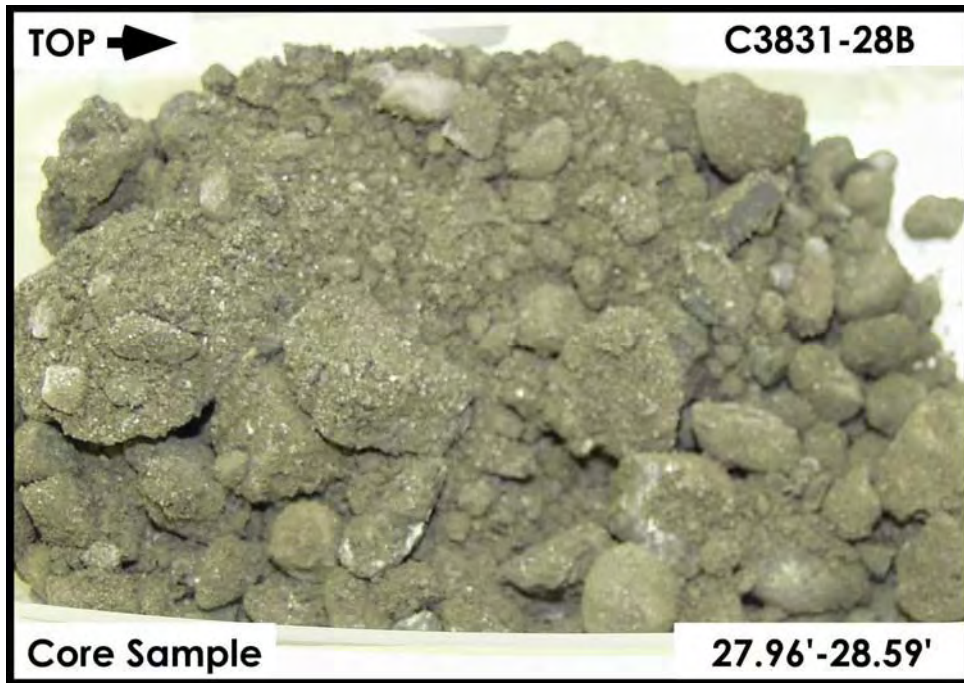**Figure A-3.4. Backfill 21.55 ft – 22.30 ft**

Figure A-3.5. Backfill 27.96 ft – 28.59 ft
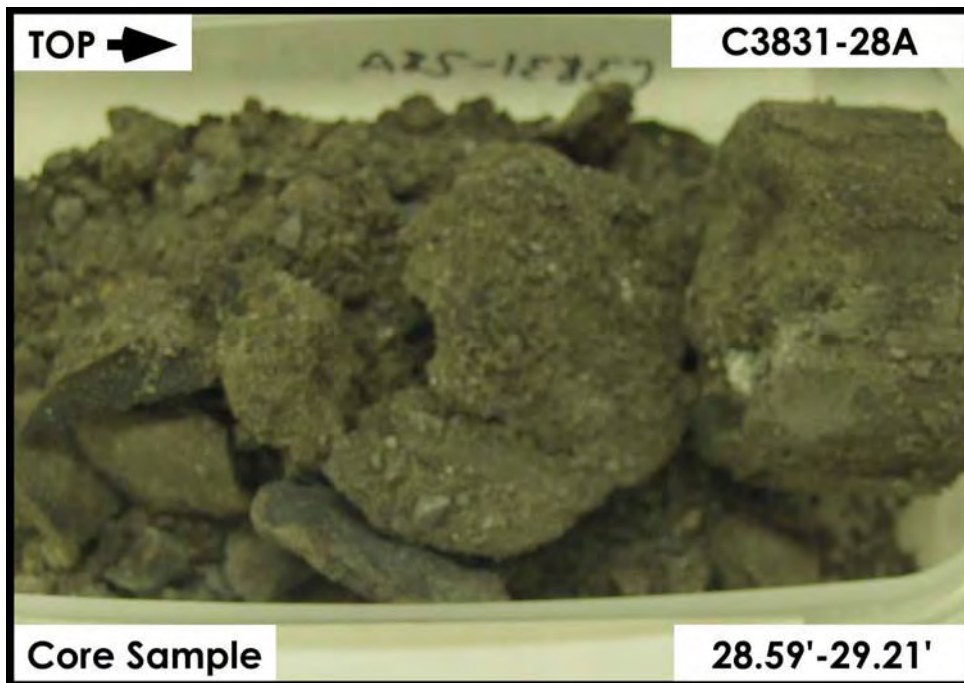

Figure A-3.6. Backfill 28.59 ft – 29.21 ft
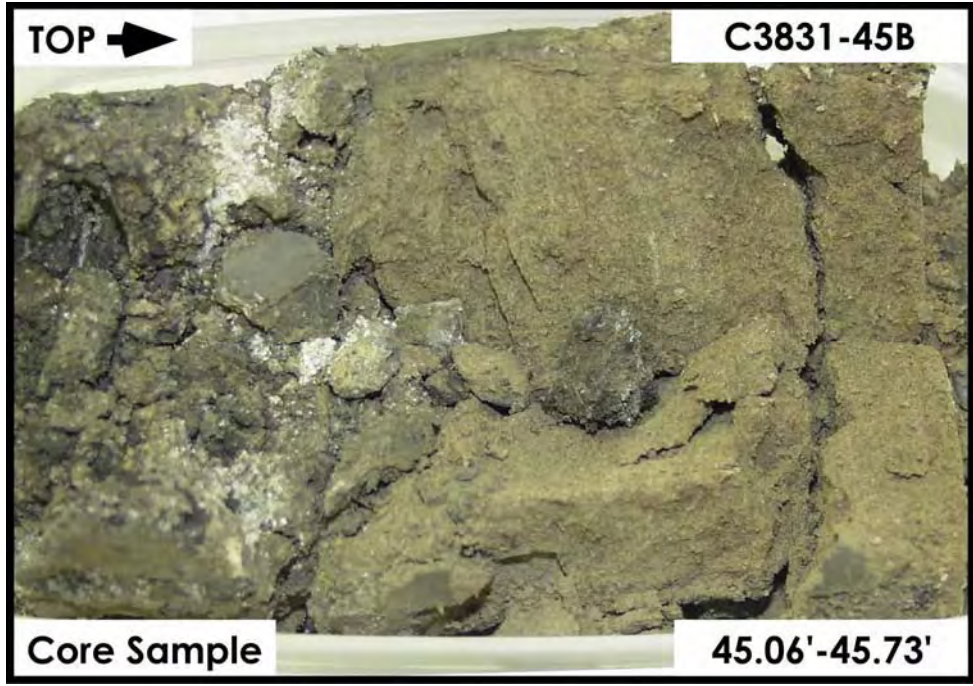
Figure A-3.7.   Backfill 45.06 ft – 45.73 ft
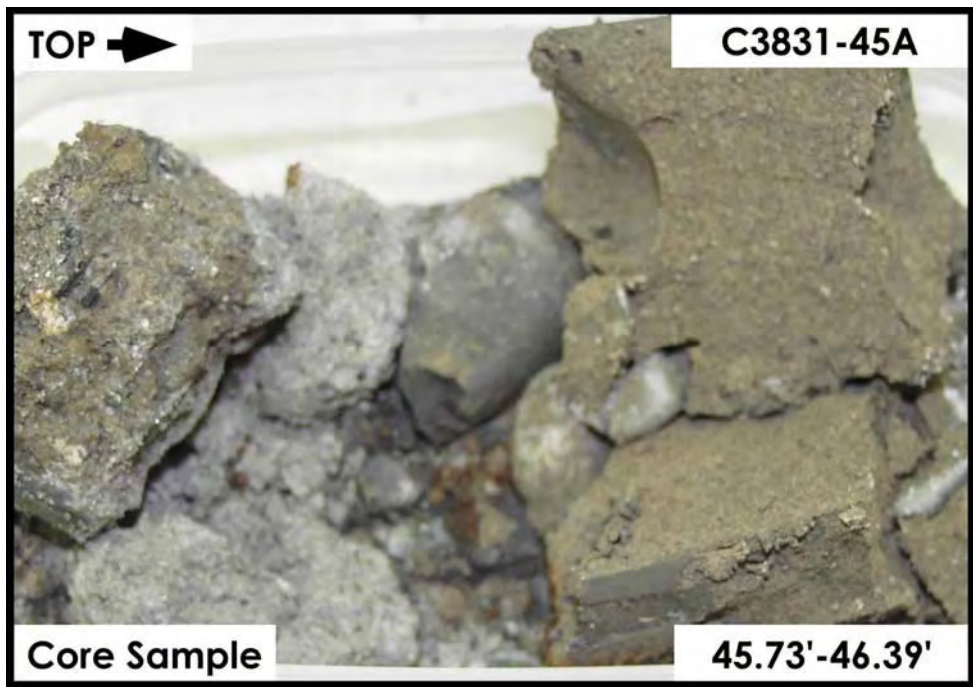
Figure A-3.8.   Backfill 45.73 ft – 46.39 ft
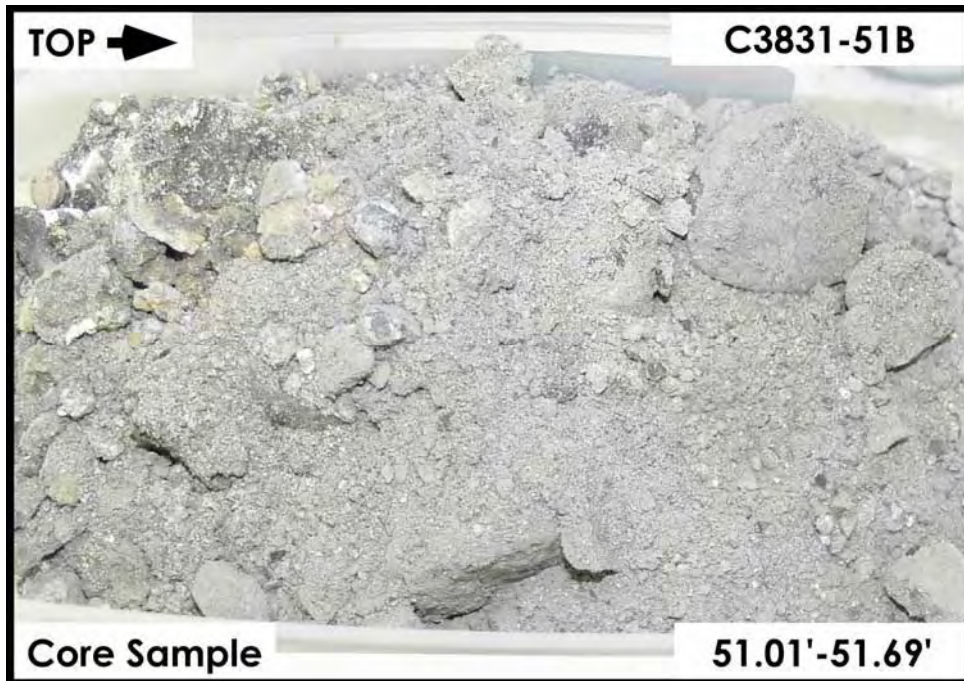
Figure A-3.9.   Backfill 51.01 ft – 51.69 ft
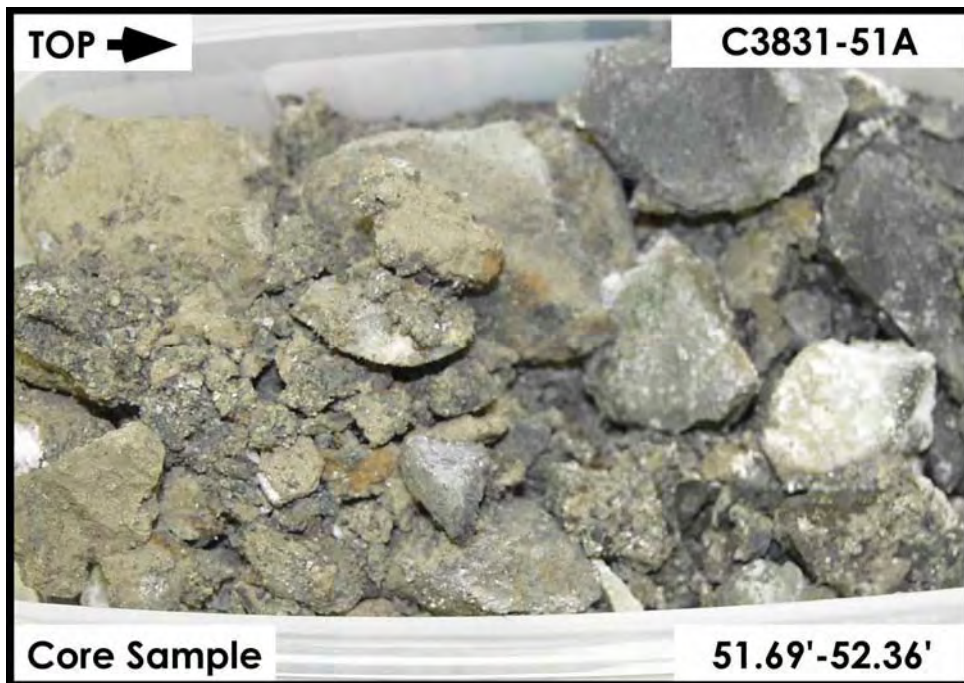
Figure A-3.10. Backfill/Hanford Formation (H2 unit) 51.69 ft – 52.36 ft
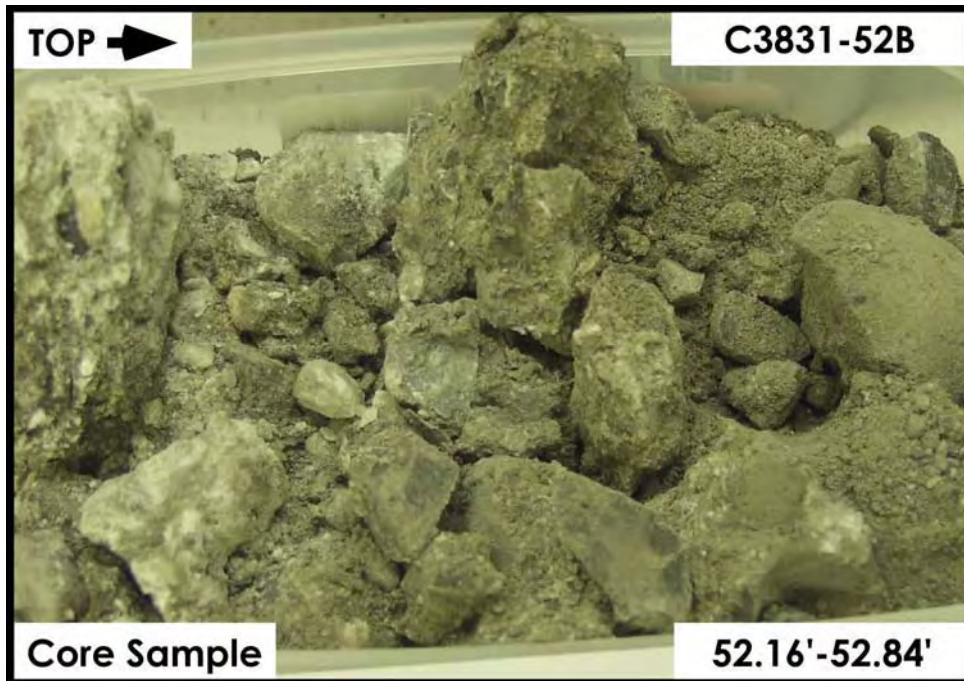
Figure A-3.11. Hanford Formation (H2 unit) 52.16 ft – 52.84 ft
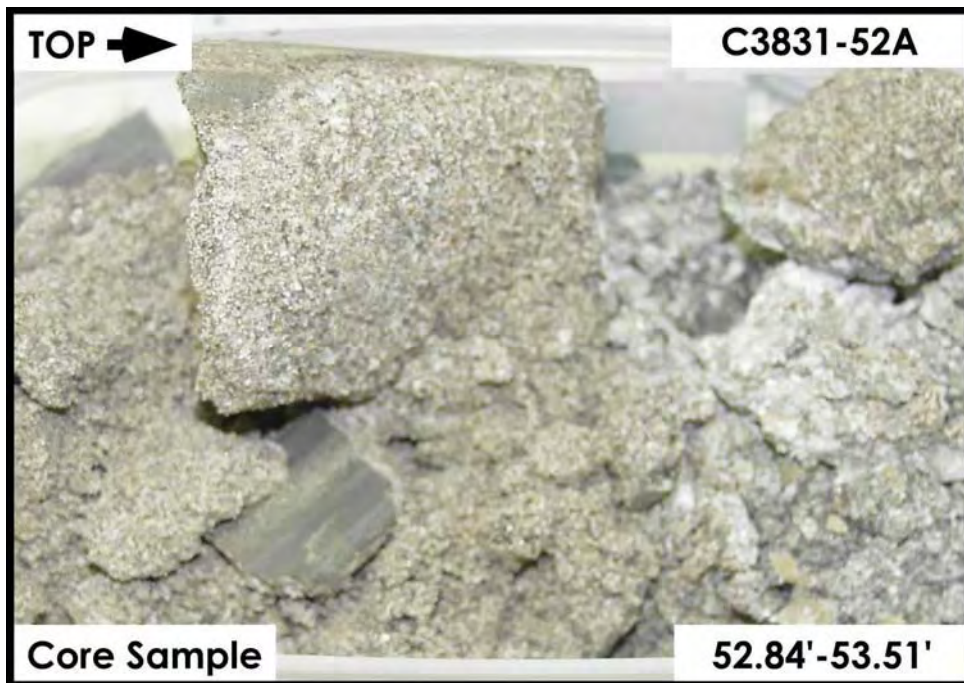
Figure A-3.12. Hanford Formation (H2 unit) 52.84 ft – 53.51 ft
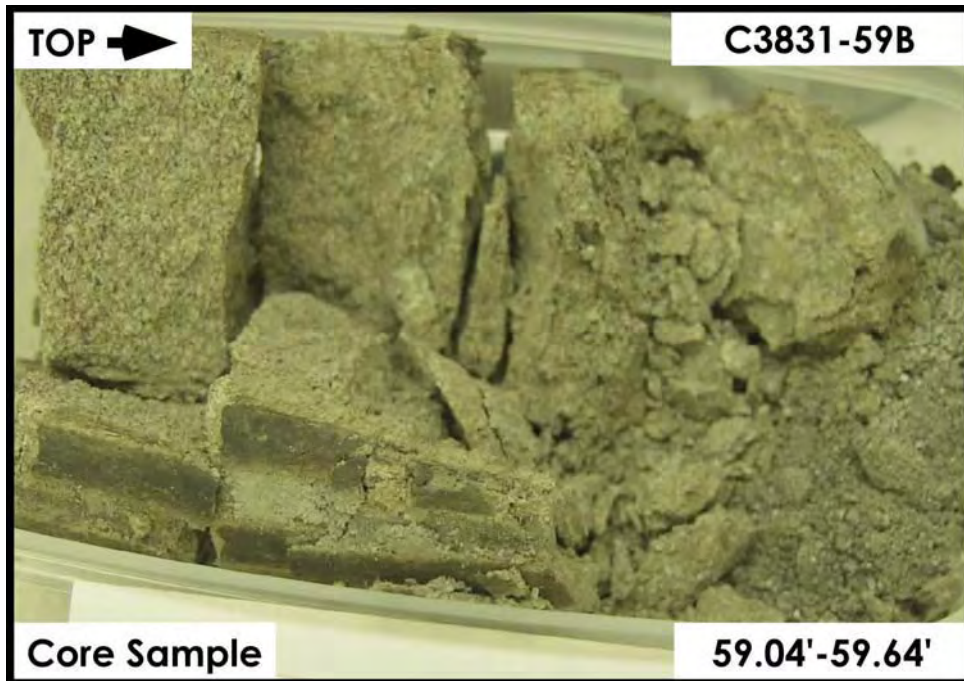
Figure A-3.13. Hanford Formation (H2 unit) 59.04 ft – 59.64 ft
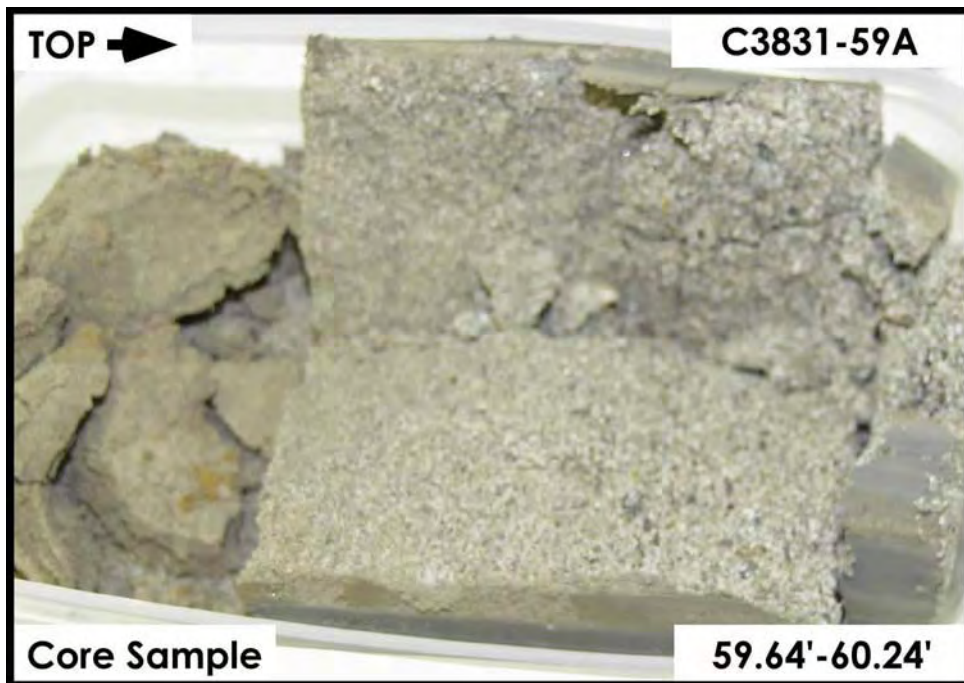
Figure A-3.14. Hanford Formation (H2 unit) 59.64 ft – 60.24 ft
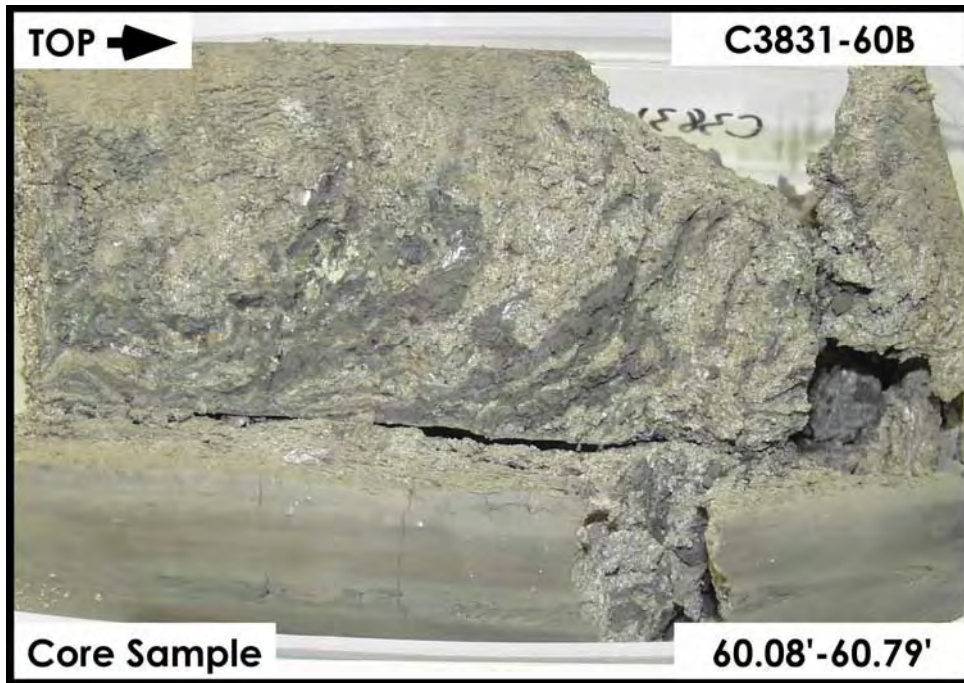
Figure A-3.15. Hanford Formation (H2 unit) 60.08 ft – 60.79 ft
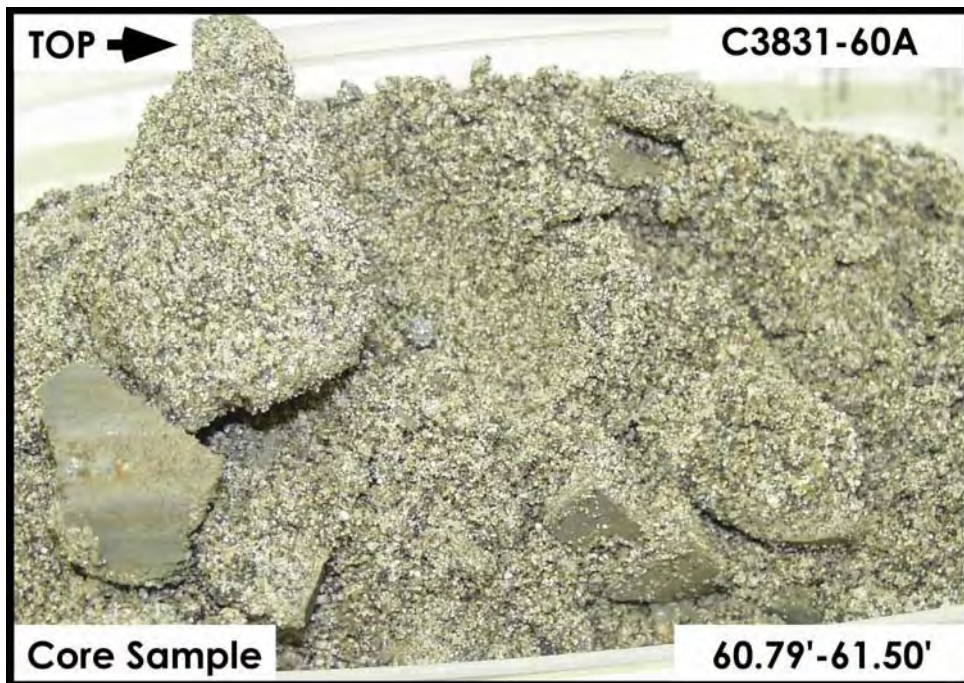
Figure A-3.16. Hanford Formation (H2 unit) 60.79 ft – 61.50 ft
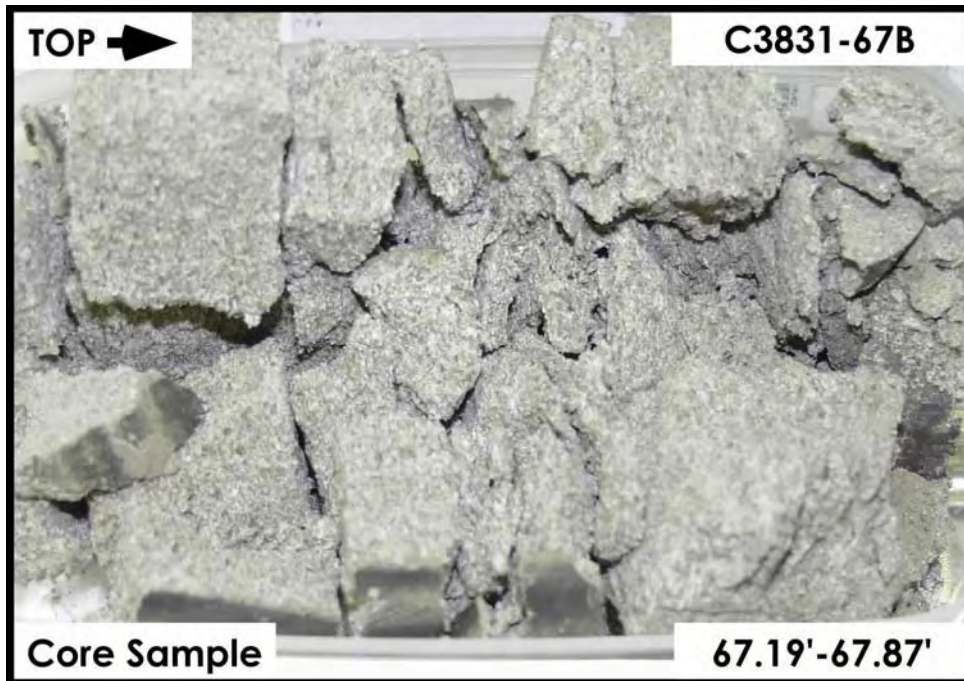
Figure A-3.17. Hanford Formation (H2 unit) 67.19 ft – 67.87 ft

Figure A-3.18. Hanford Formation (H2 unit) 67.87 ft – 68.54 ft
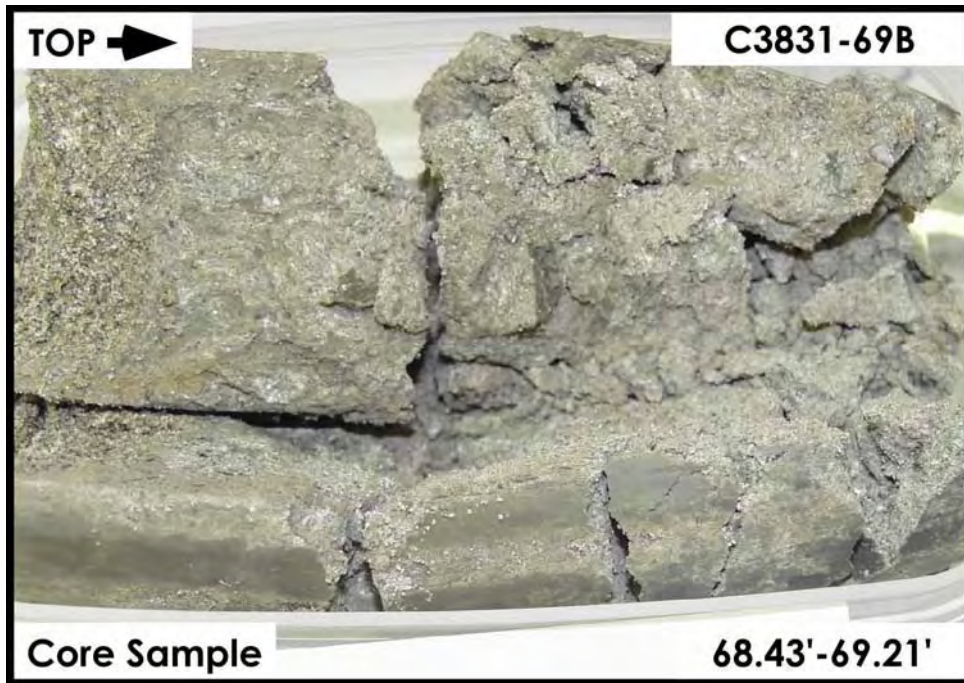
Figure A-3.19. Hanford Formation (H2 unit) 68.43 ft – 69.21 ft
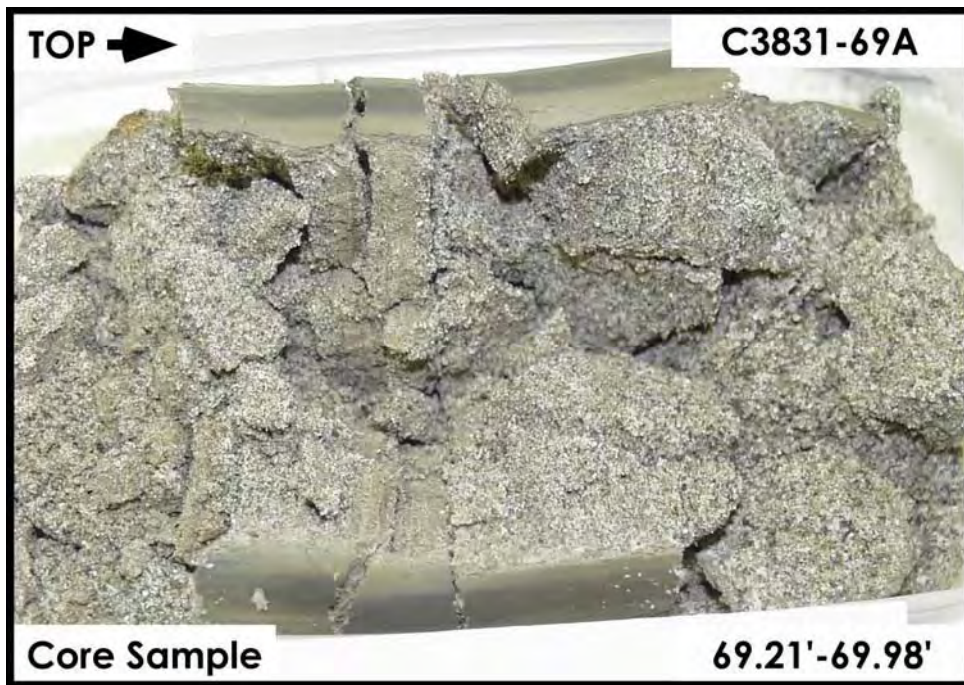
Figure A-3.20. Hanford Formation (H2 unit) 69.21 ft – 69.98 ft
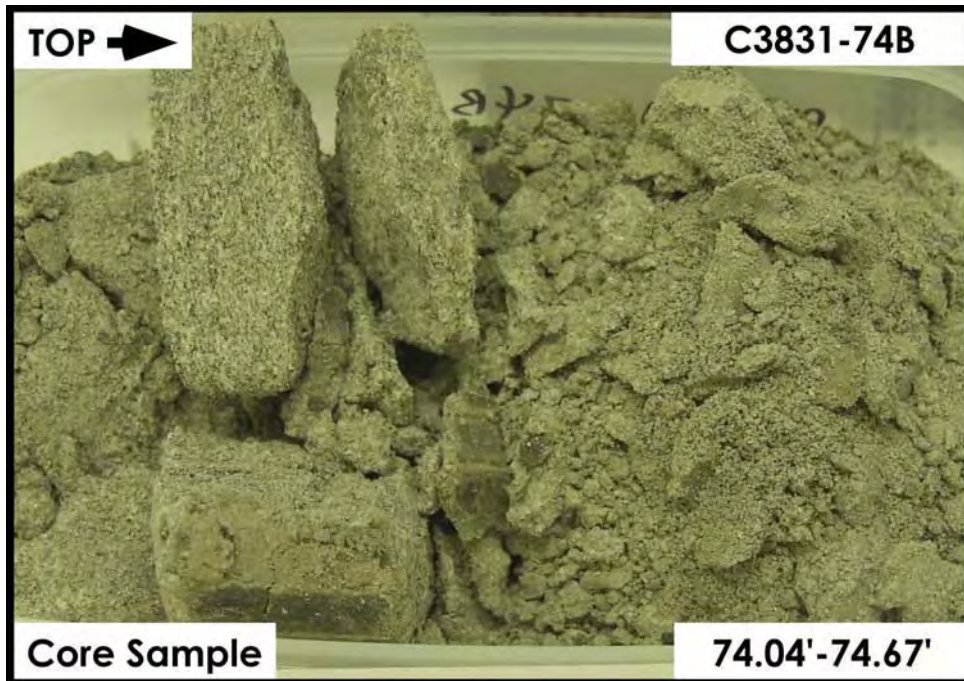
Figure A-3.21. Hanford Formation (H2 unit) 74.04 ft – 74.67 ft
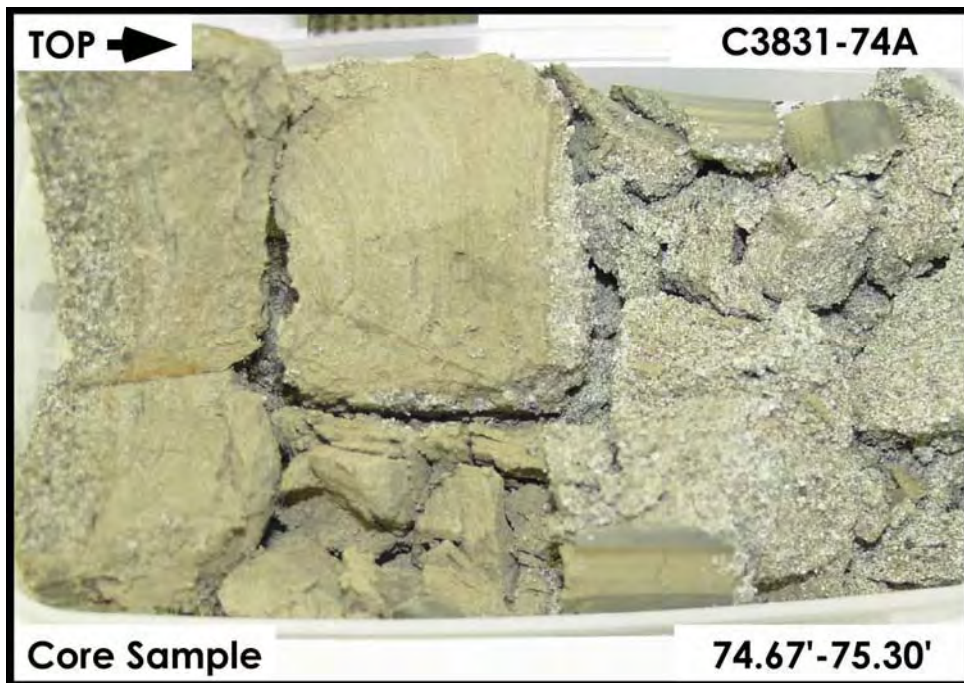
Figure A-3.22. Hanford Formation (H2 unit) 74.67 ft – 75.30 ft
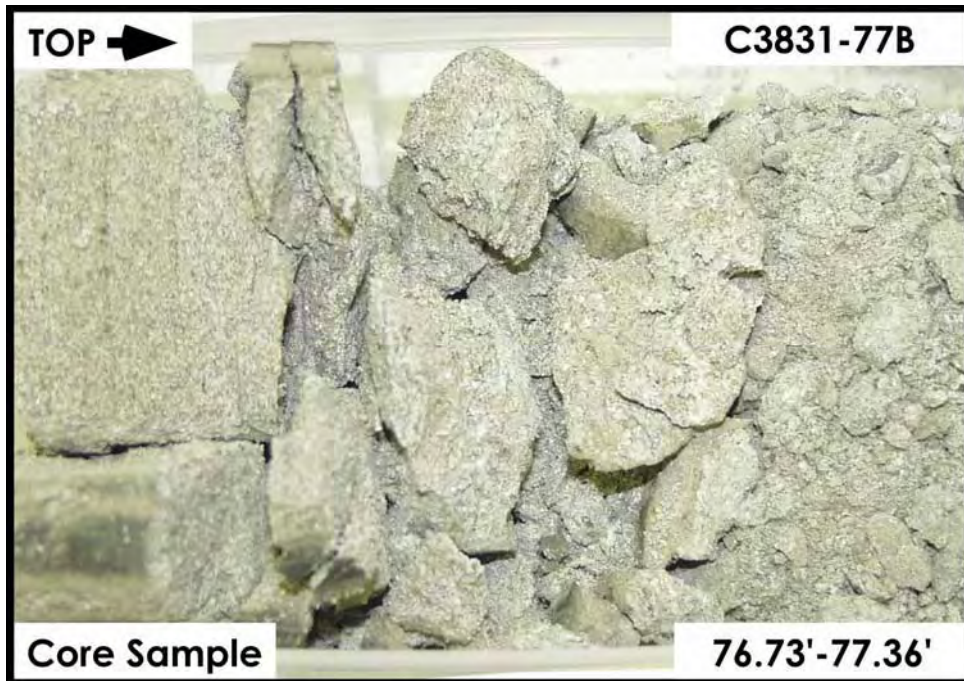
Figure A-3.23. Hanford Formation (H2 unit) 76.73 ft – 77.36 ft

Figure A-3.24. Hanford Formation (H2 unit) 77.36 ft – 77.98 ft
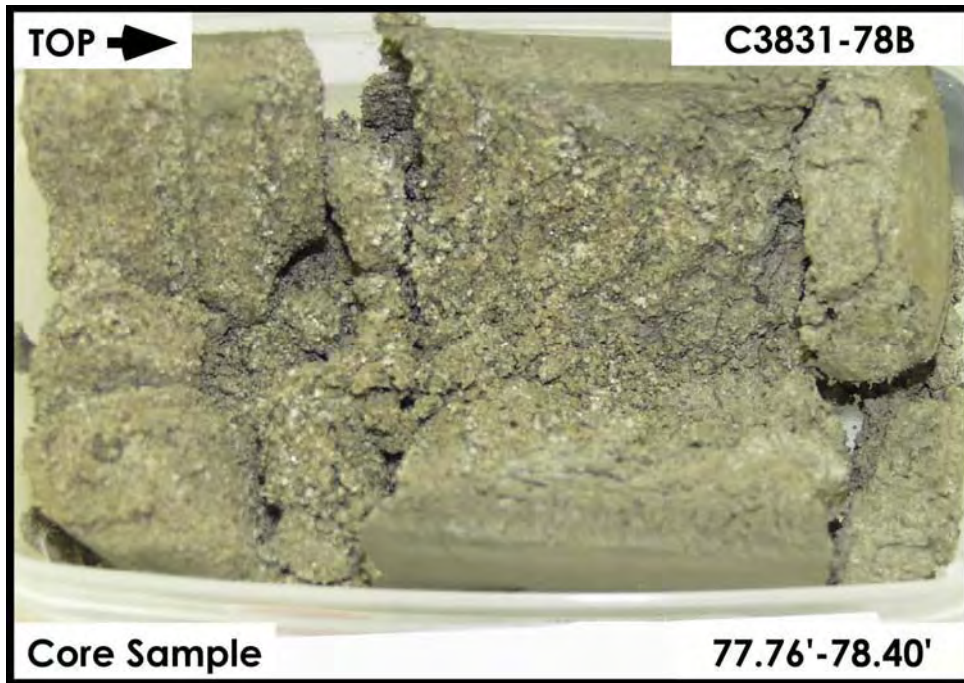
Figure A-3.25. Hanford Formation (H2 unit) 77.76 ft – 78.40 ft
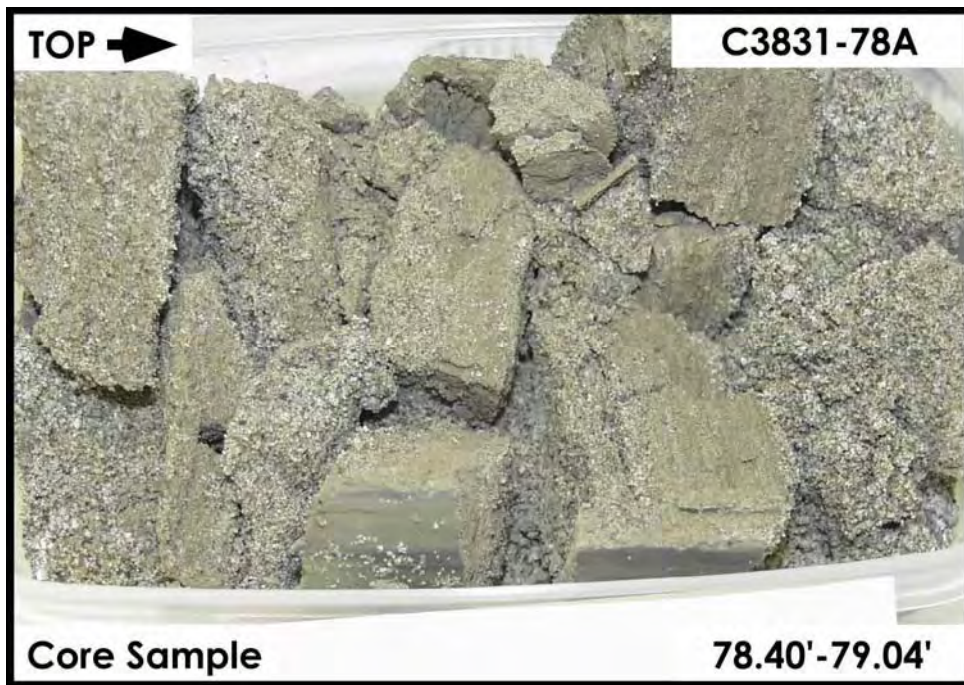
Figure A-3.26. Hanford Formation (H2 unit) 78.40 ft – 79.04 ft
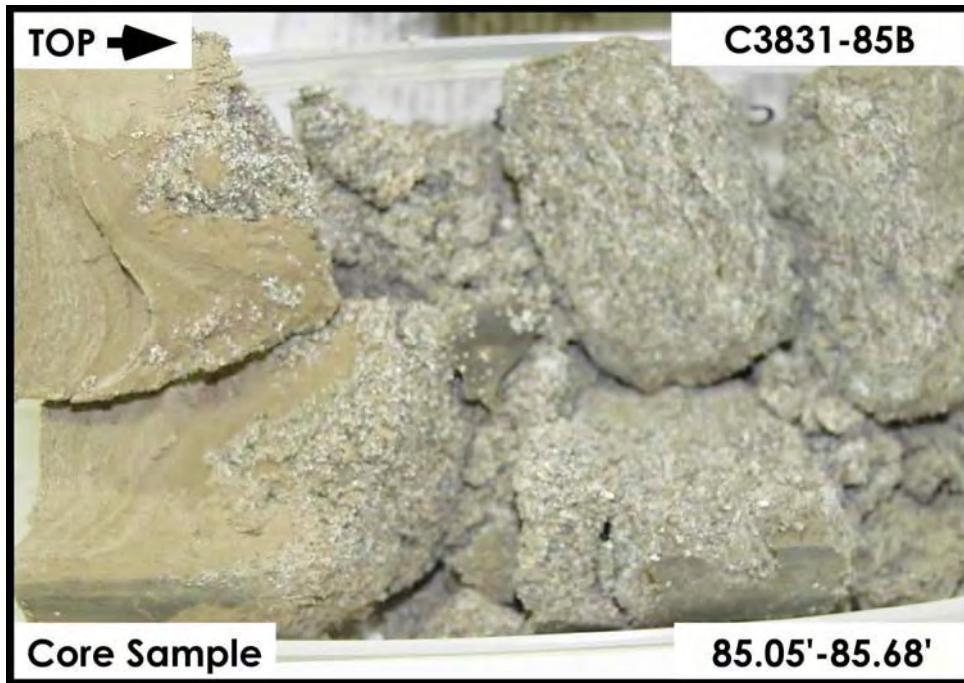
Figure A-3.27. Hanford Formation (H2 unit) 85.05 ft – 85.68 ft

Figure A-3.28. Hanford Formation (H2 unit) 85.68 ft – 86.30 ft
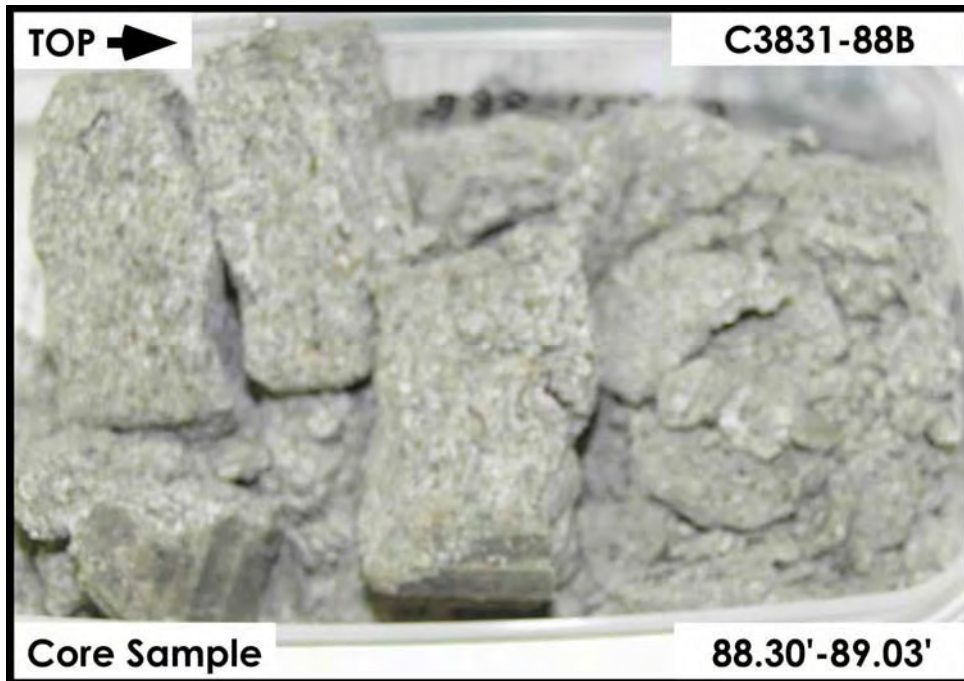
Figure A-3.29. Hanford Formation (H2 unit) 88.30 ft – 89.03 ft
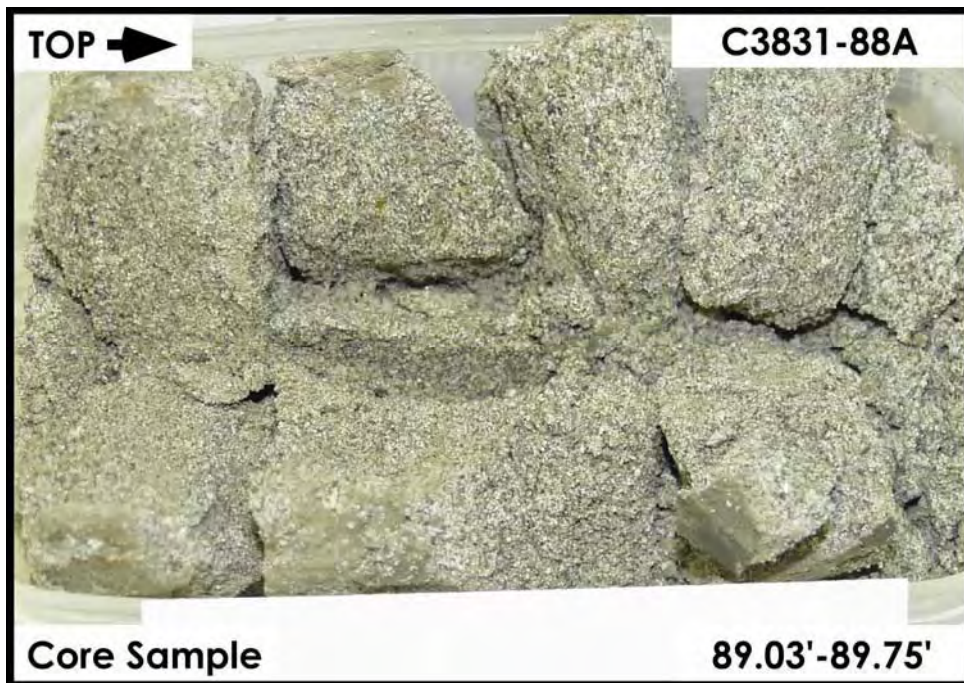
Figure A-3.30. Hanford Formation (H2 unit) 89.03 ft – 89.75 ft
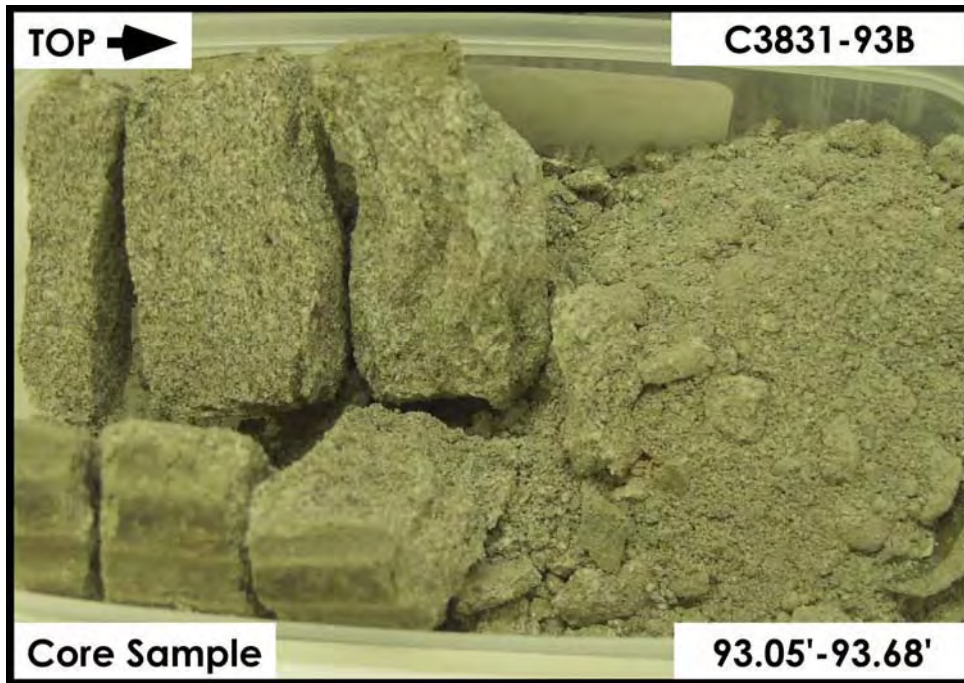
Figure A-3.31. Hanford Formation (H2 unit) 93.05 ft – 93.68 ft

Figure A-3.32. Hanford Formation (H2 unit) 93.68 ft – 94.30 ft
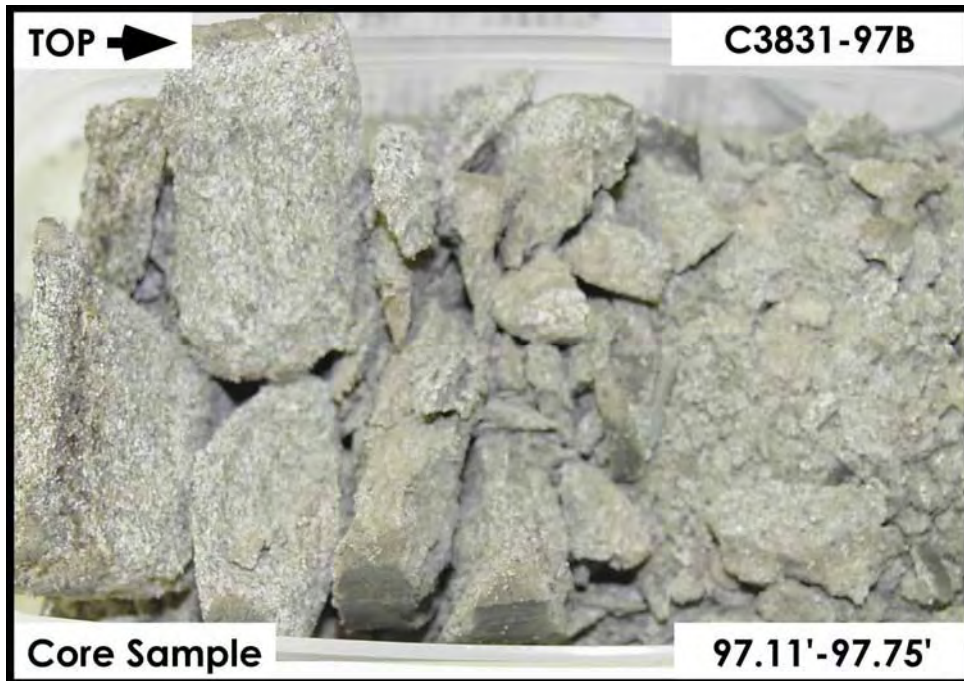
Figure A-3.33. Hanford Formation (H2 unit) 97.11 ft – 97.75 ft
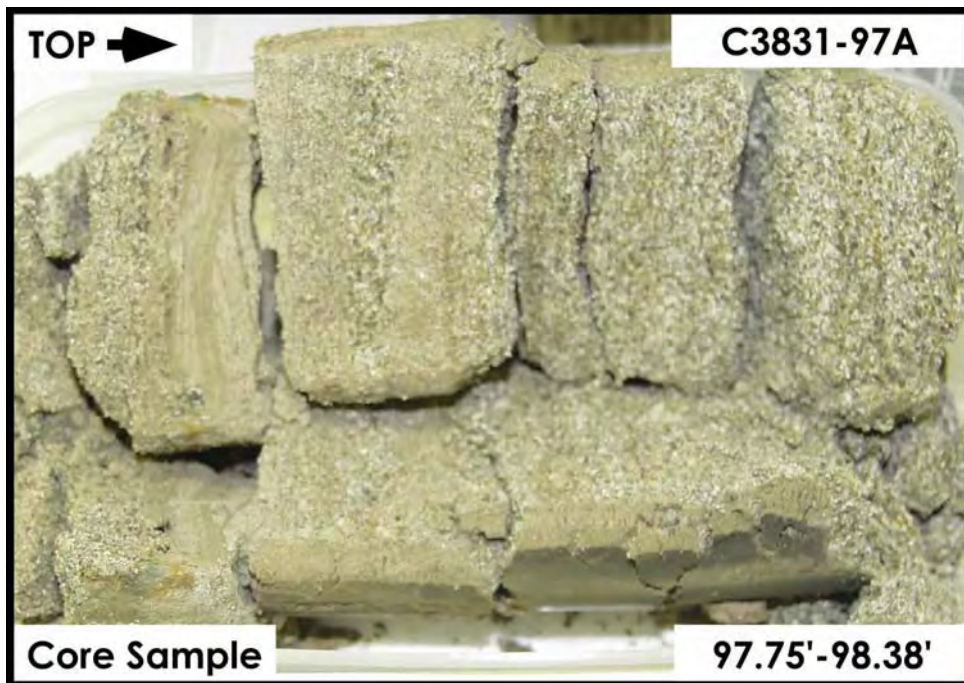
Figure A-3.34. Hanford Formation (H2 unit) 97.75 ft – 98.38 ft
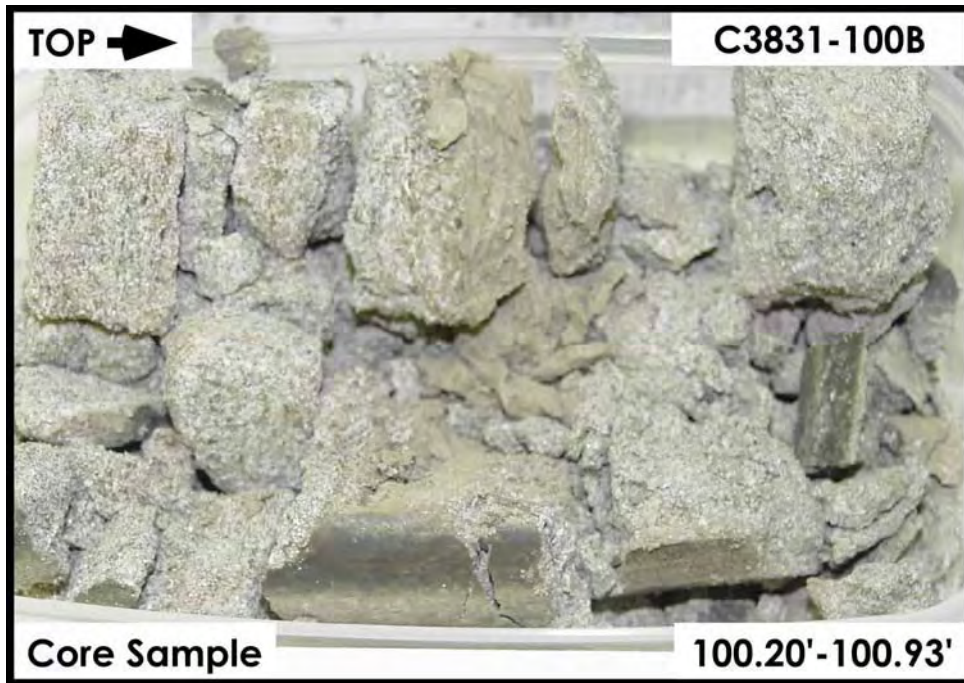
Figure A-3.35. Hanford Formation (H2 unit) 100.20 ft – 100.93 ft
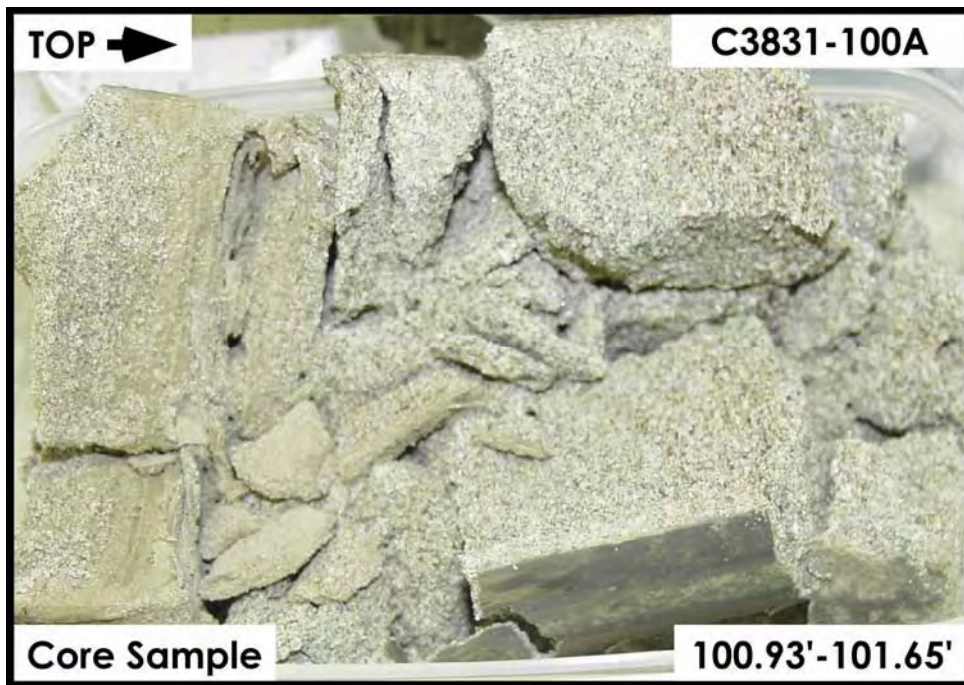
Figure A-3.36. Hanford Formation (H2 unit) 100.93 ft – 101.65 ft
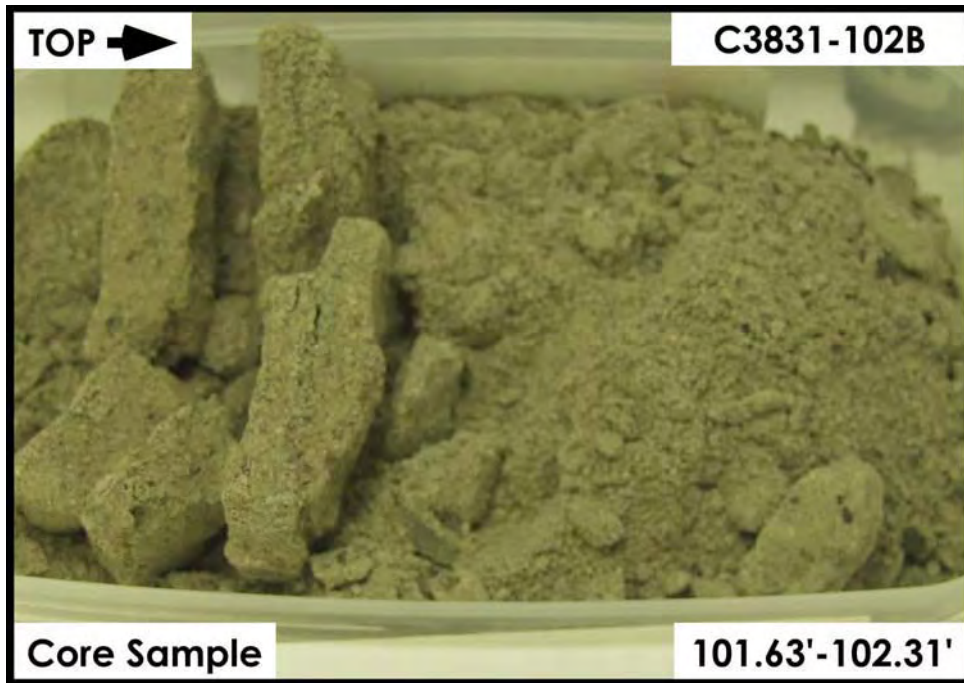
Figure A-3.37. Cold Creek Unit – Upper (CCU$_u$) 101.63 ft – 102.31 ft
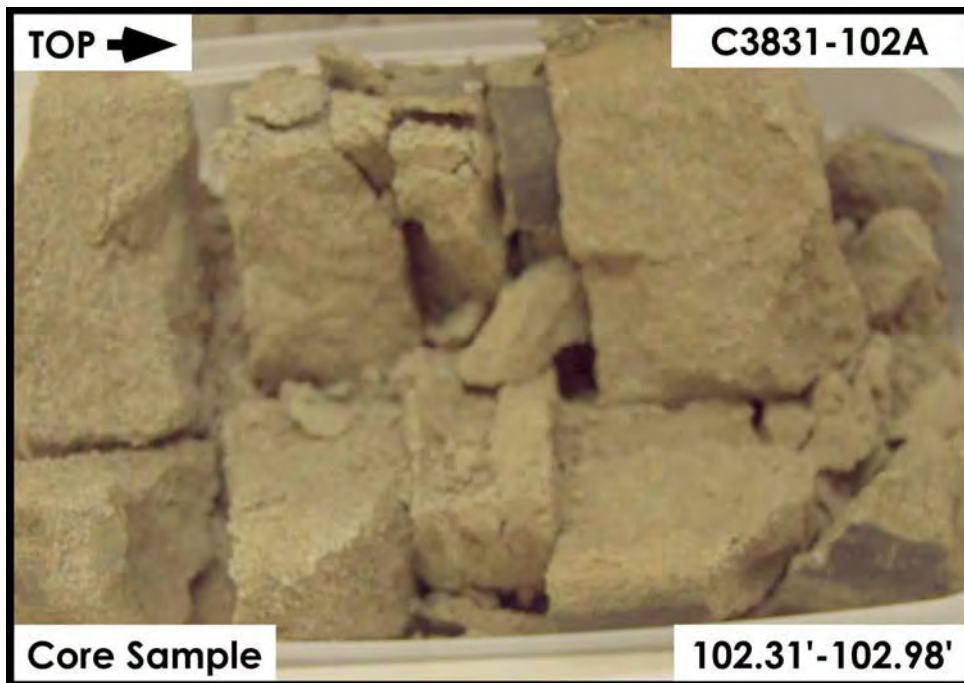
Figure A-3.38. Cold Creek Unit – Upper (CCU$_u$) 102.31 ft – 102.98 ft
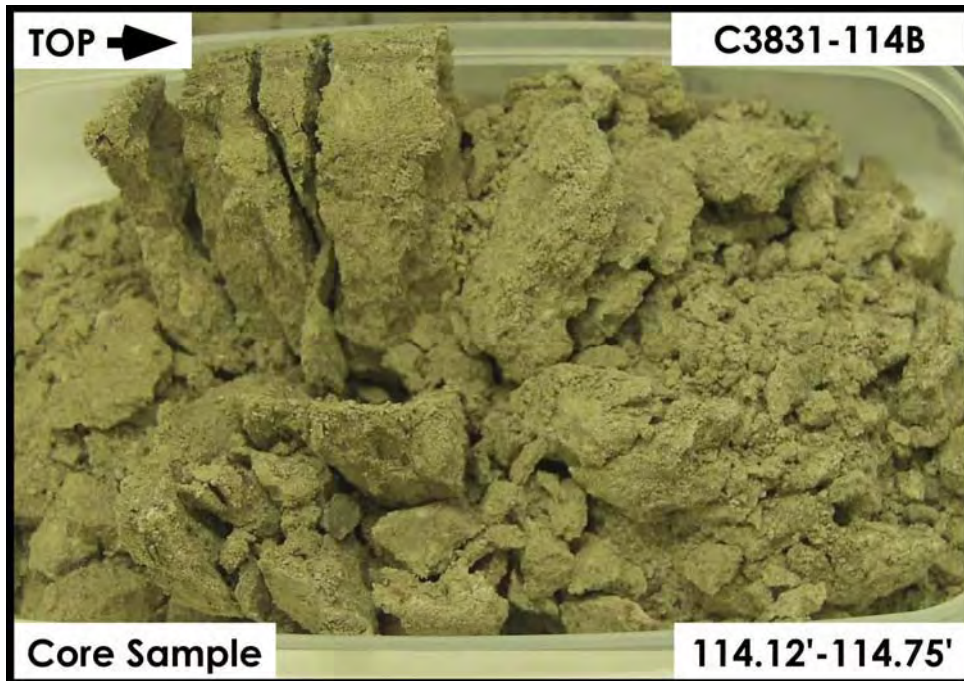
Figure A-3.39. Cold Creek Unit – Lower (CCU$_l$) 114.12 ft – 114.75 ft
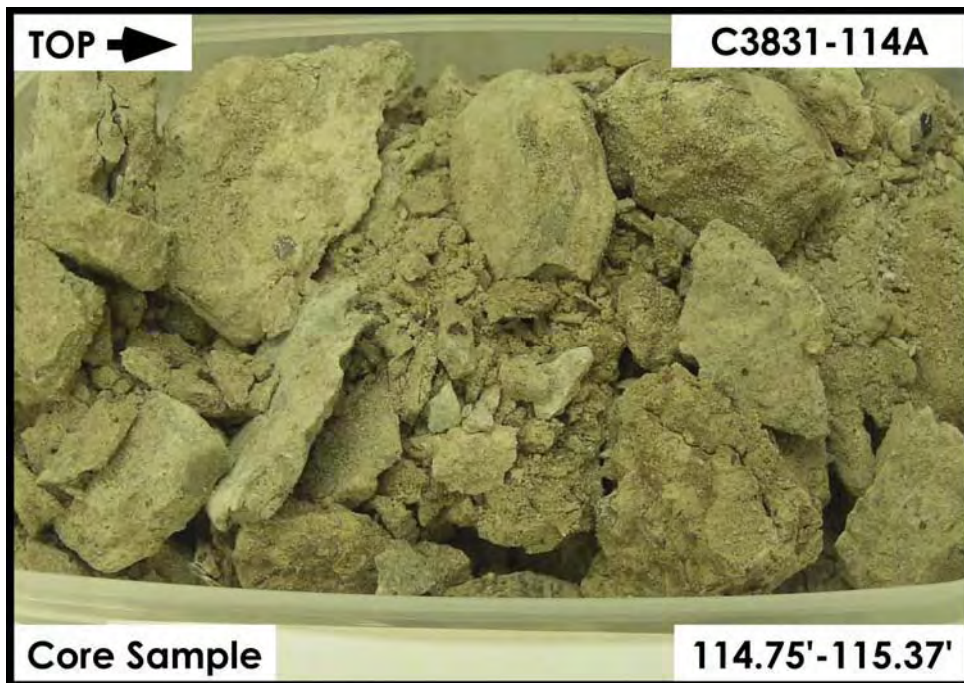
Figure A-3.40. Cold Creek Unit – Lower (CCU$_l$) 114.75 ft – 115.37 ft

Appendix A.4

C3832 (TX-104)

SPLITSPOON CORE

SAMPLE PHOTOGRAPHS

Contents

Figures

Figure A-4.1.   Backfill 16.21 ft – 16.91 ft

Figure A-4.2.   Backfill 16.91 ft – 17.61 ft

Figure A-4.3.   Backfill 28.09 ft – 28.79 ft

Figure A-4.4.   Backfill 28.79 ft – 29.49 ft
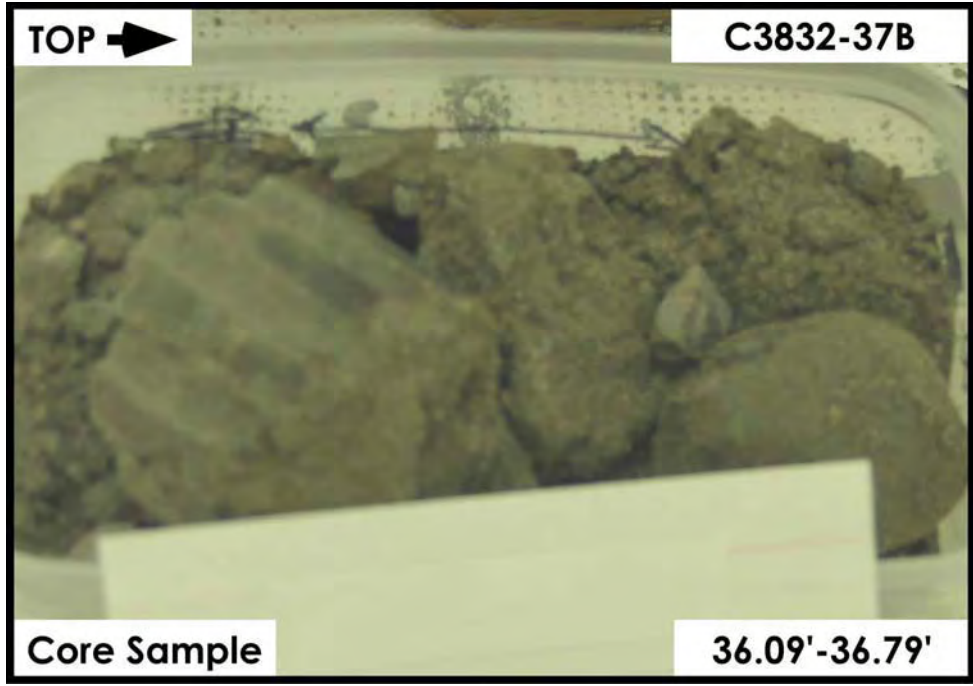
Figure A-4.5.   Backfill 36.09 ft – 36.79 ft
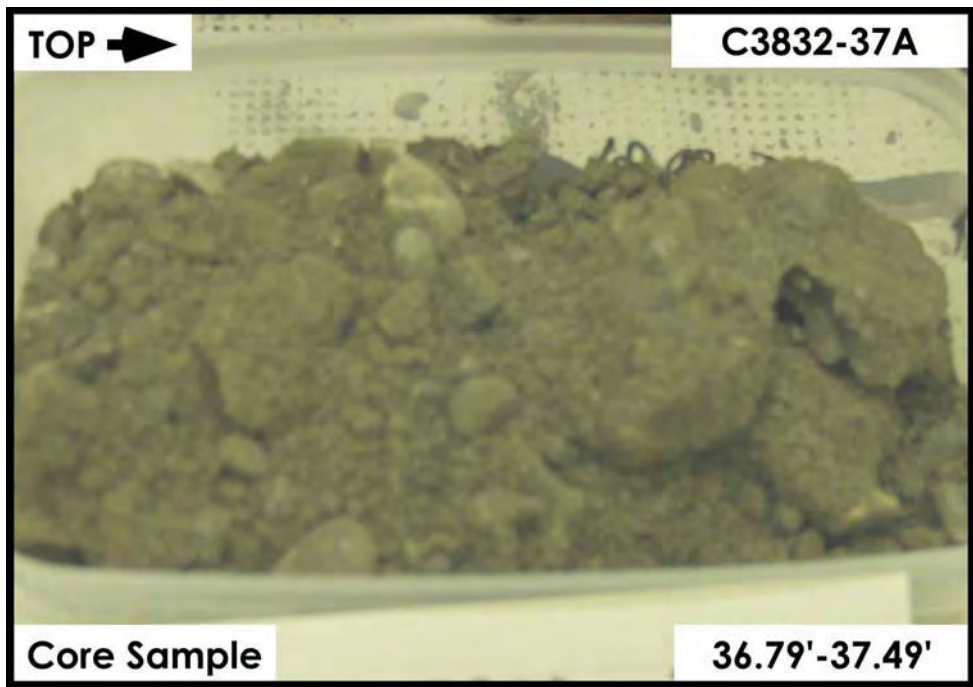
Figure A-4.6.   Backfill 36.79 ft – 37.49 ft
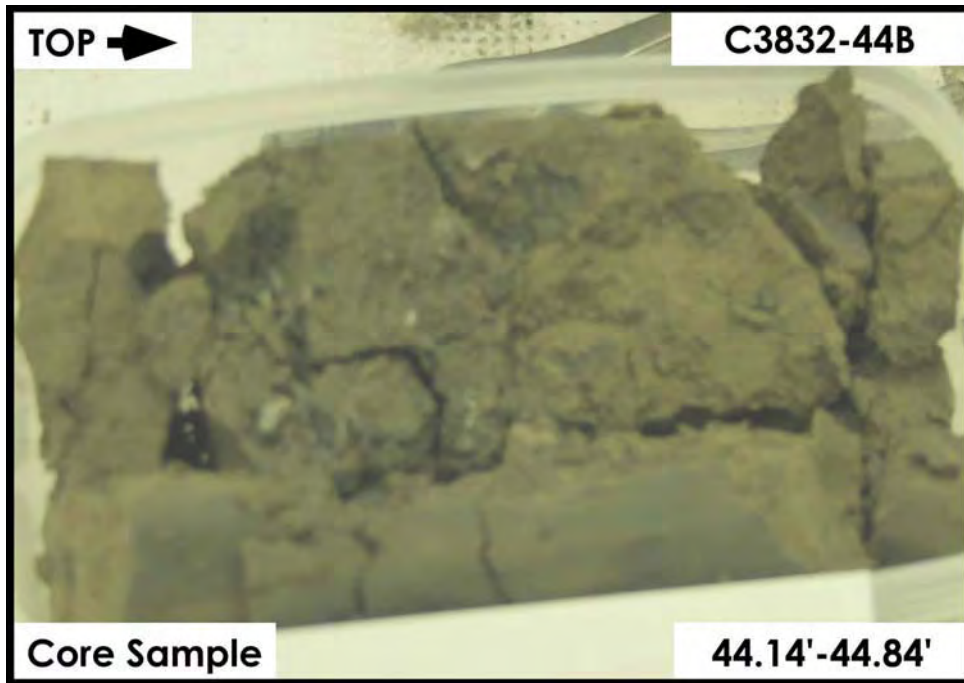
Figure A-4.7.   Backfill 44.14 ft – 44.84 ft
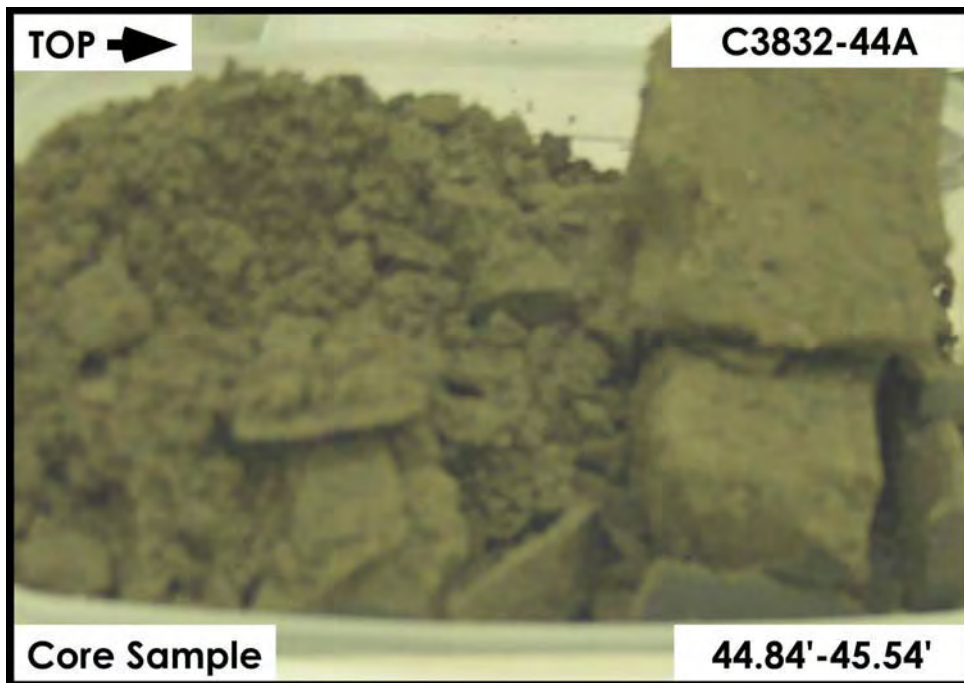
Figure A-4.8.   Backfill 44.84 ft – 45.54 ft
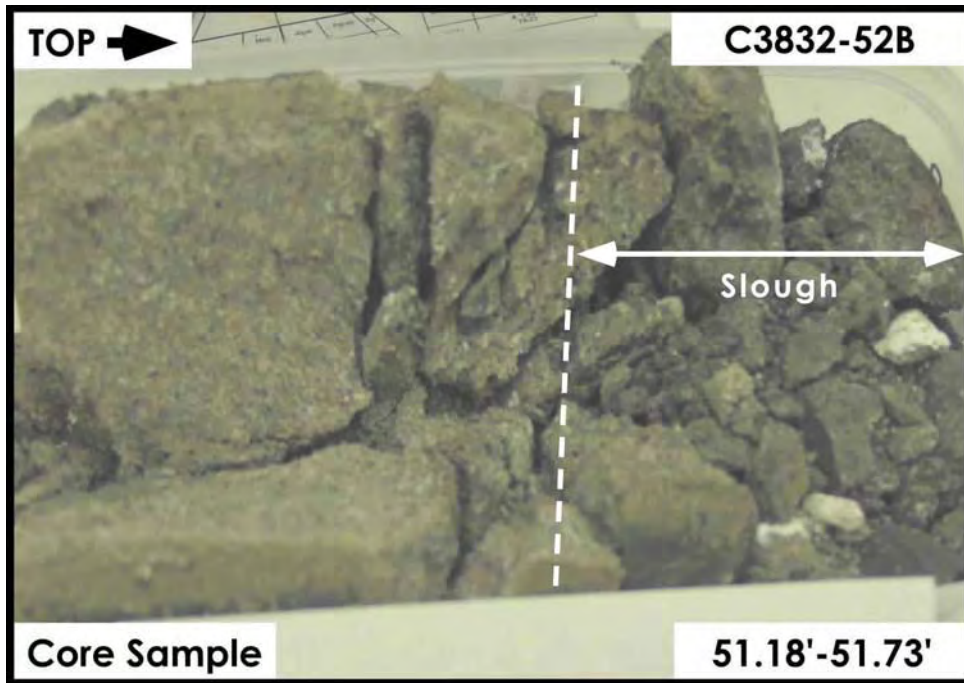
Figure A-4.9.   Hanford Formation (H2 unit) 51.18 ft – 51.73 ft
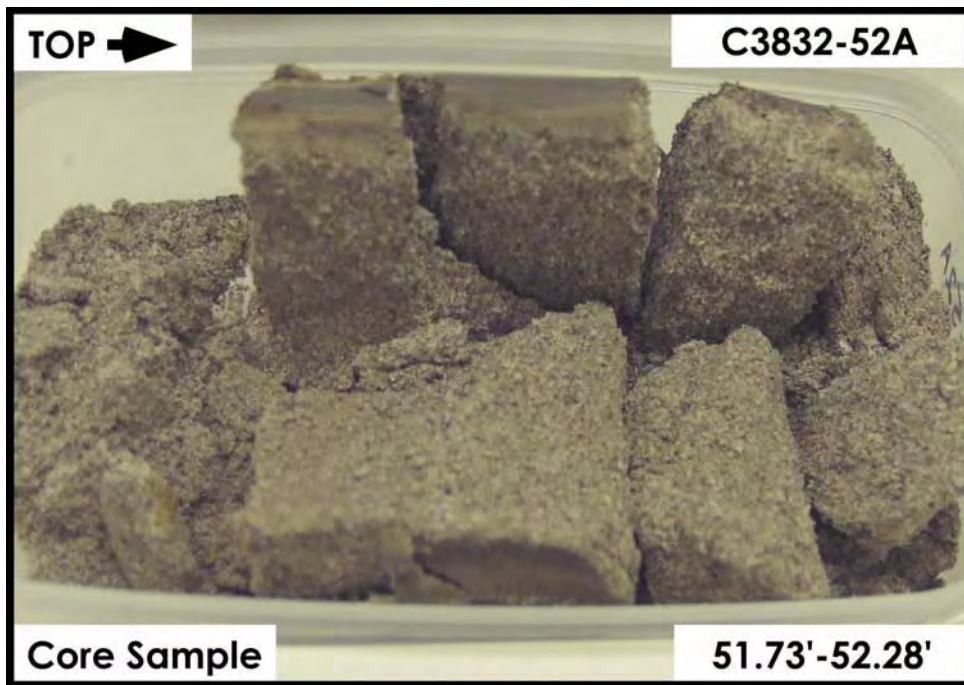
Figure A-4.10. Hanford Formation (H2 unit) 51.73 ft – 52.28 ft
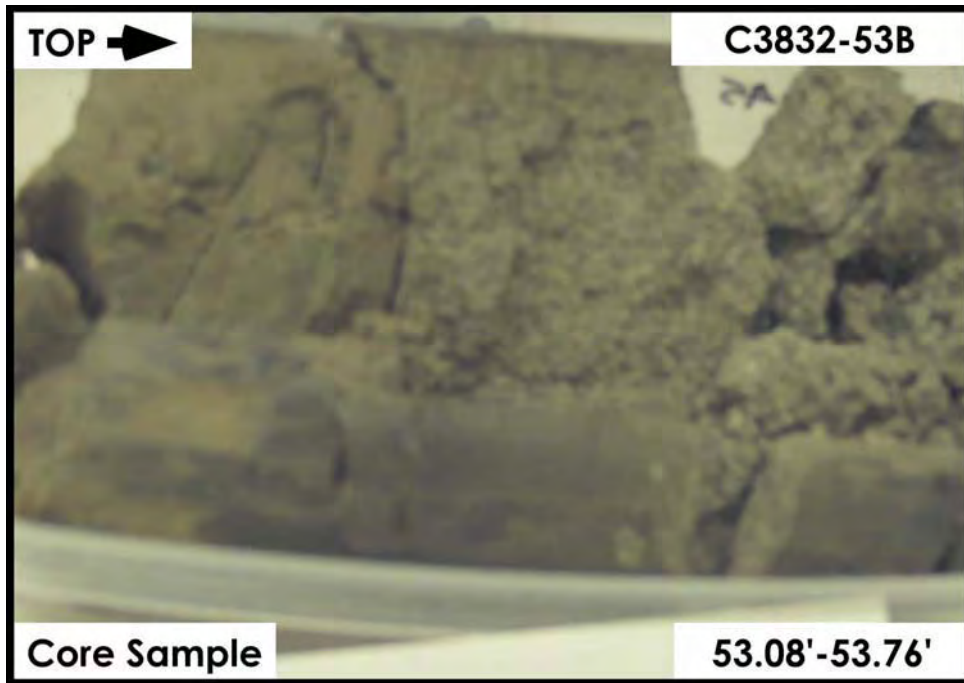
Figure A-4.11. Hanford Formation (H2 unit) 53.08 ft – 53.76 ft
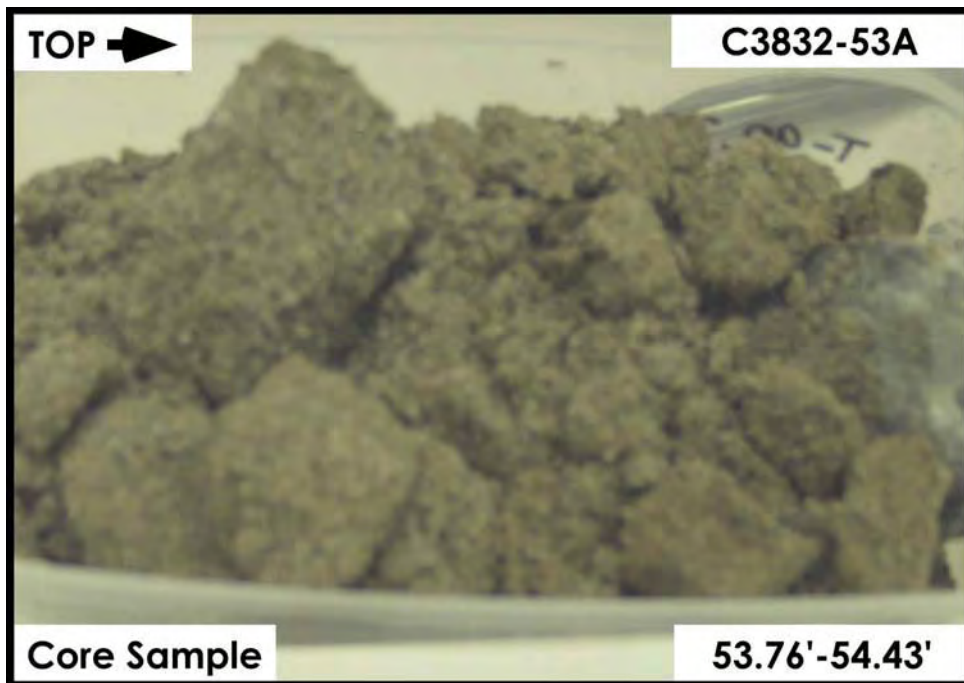
Figure A-4.12. Hanford Formation (H2 unit) 53.76 ft – 54.43 ft
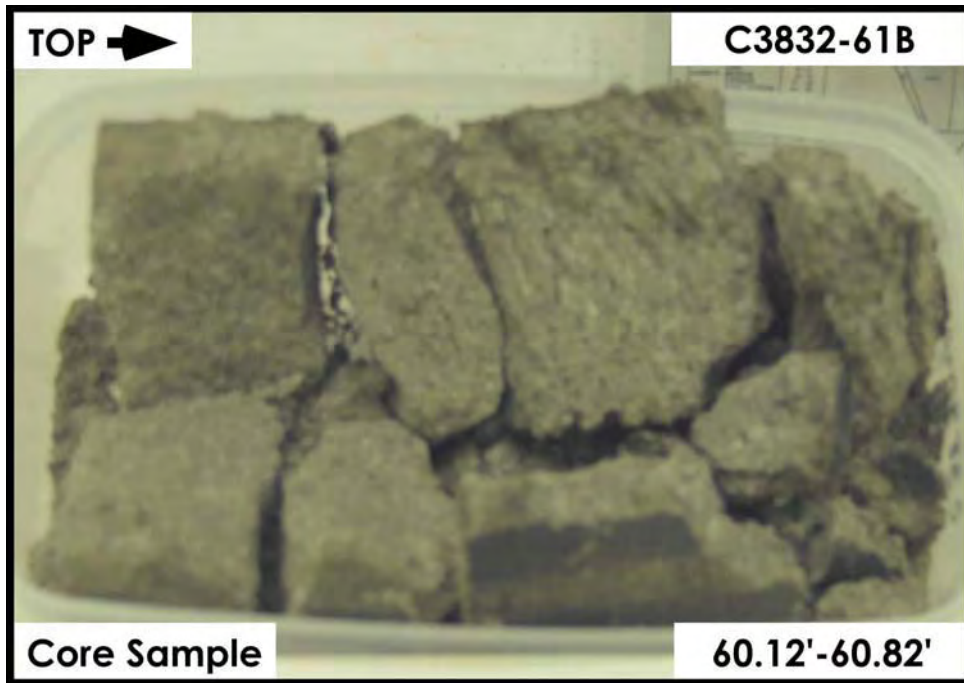
Figure A-4.13. Hanford Formation (H2 unit) 60.12 ft – 60.82 ft
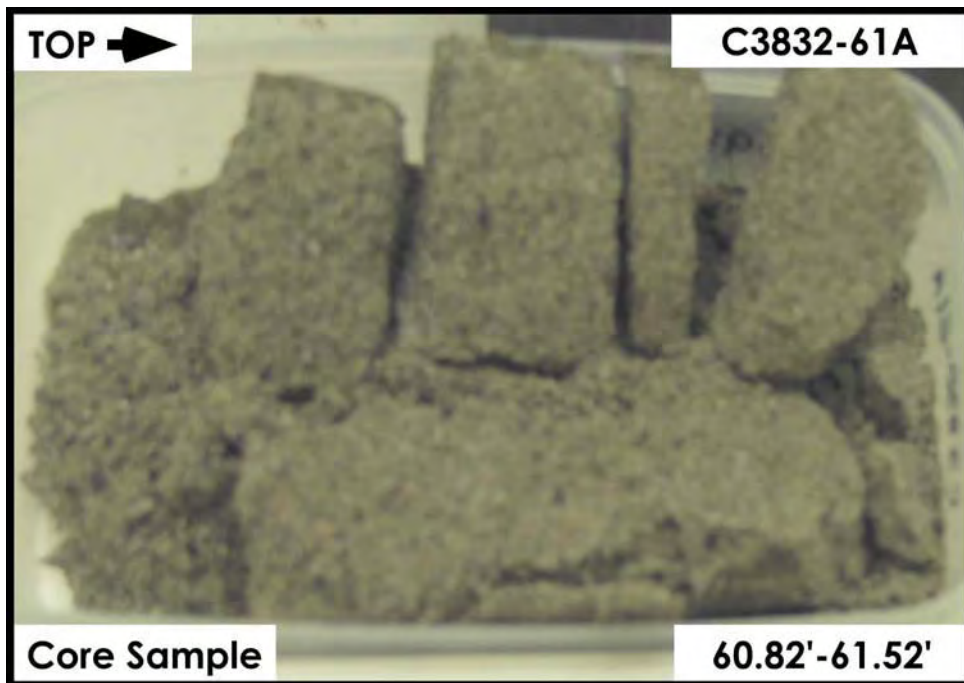
Figure A-4.14. Hanford Formation (H2 unit) 60.82 ft – 61.52 ft
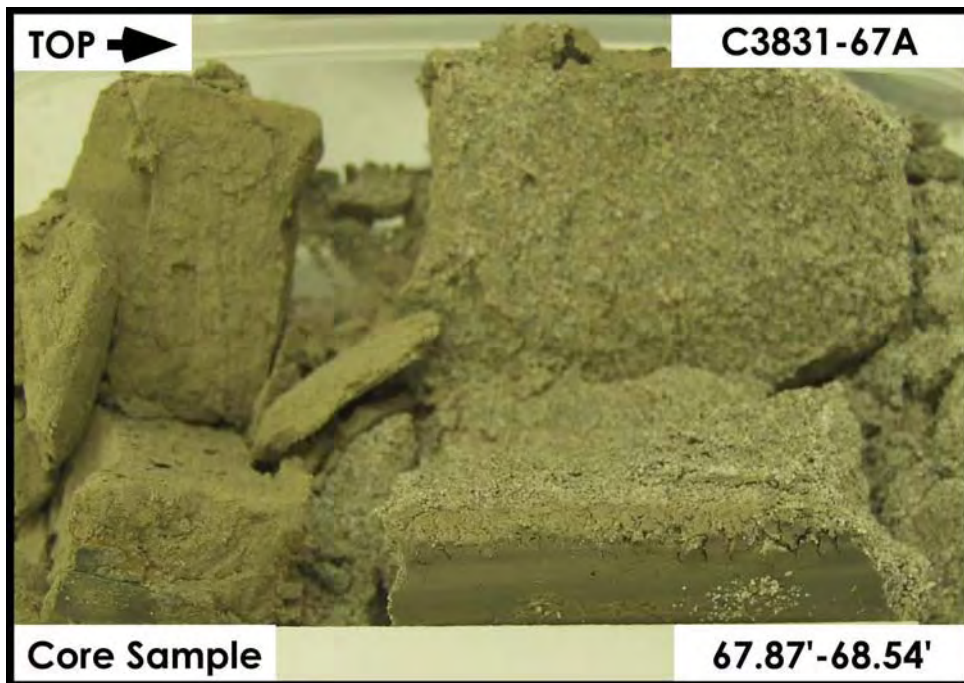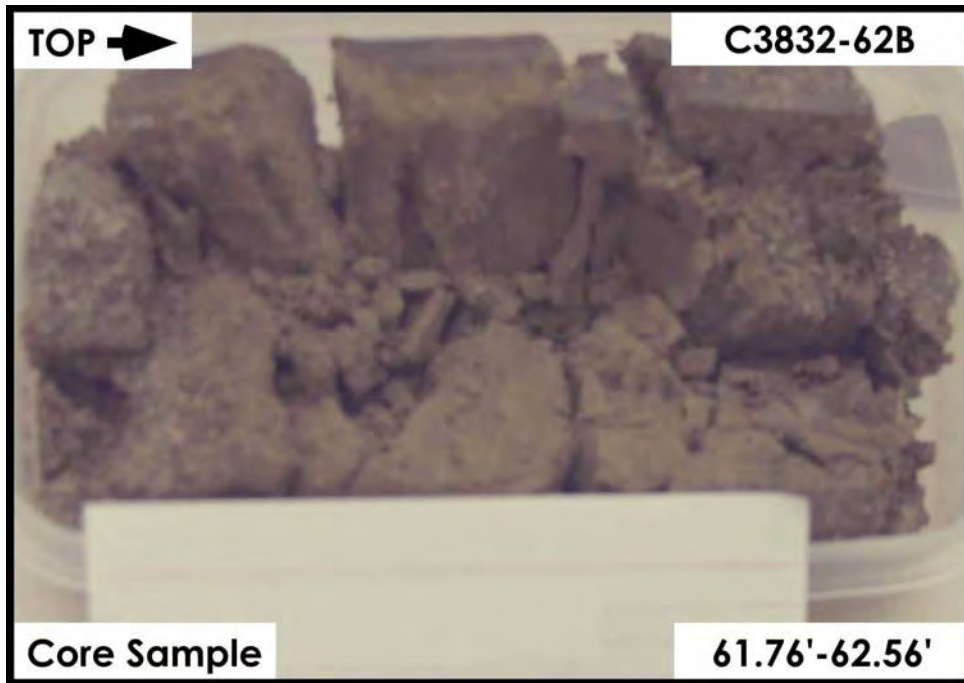
Figure A-4.15. Hanford Formation (H2 unit) 61.76 ft – 62.56 ft
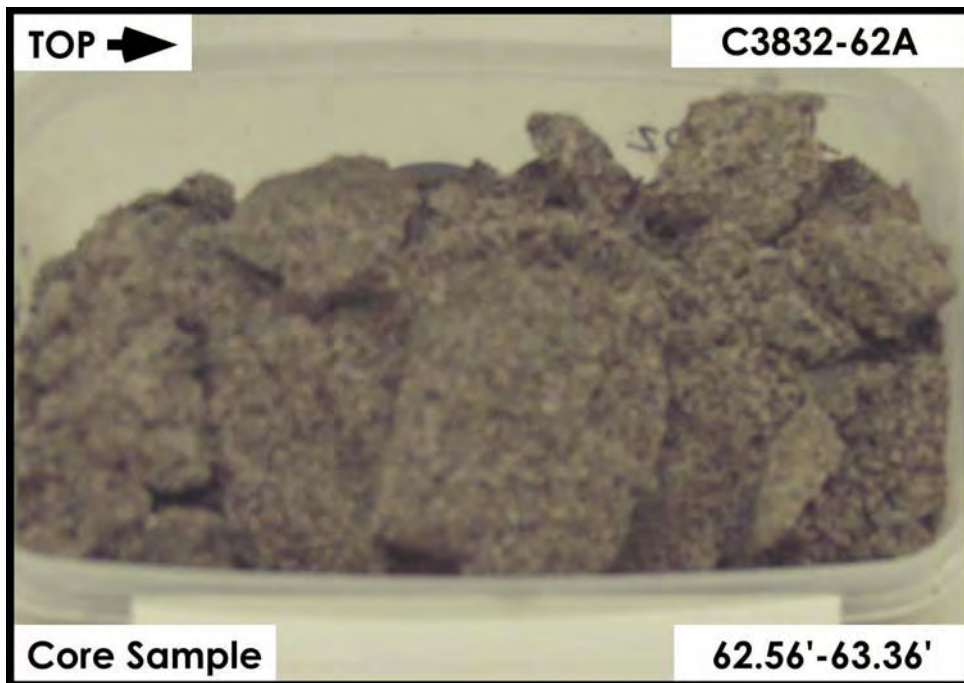
Figure A-4.16. Hanford Formation (H2 unit) 62.56 ft – 63.36 ft
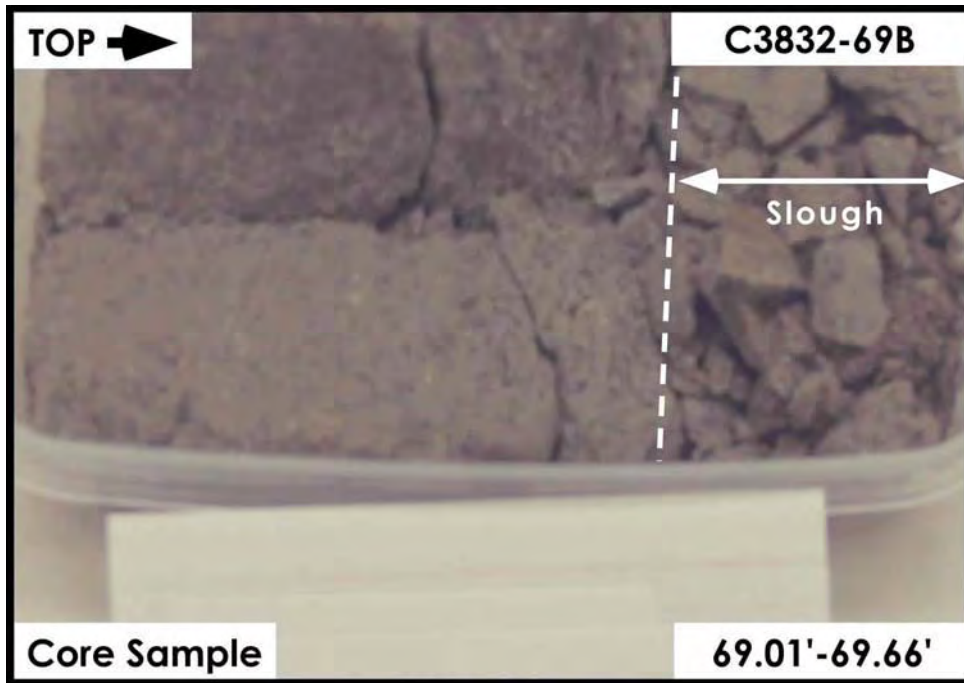
Figure A-4.17. Hanford Formation (H2 unit) 69.01 ft – 69.66 ft
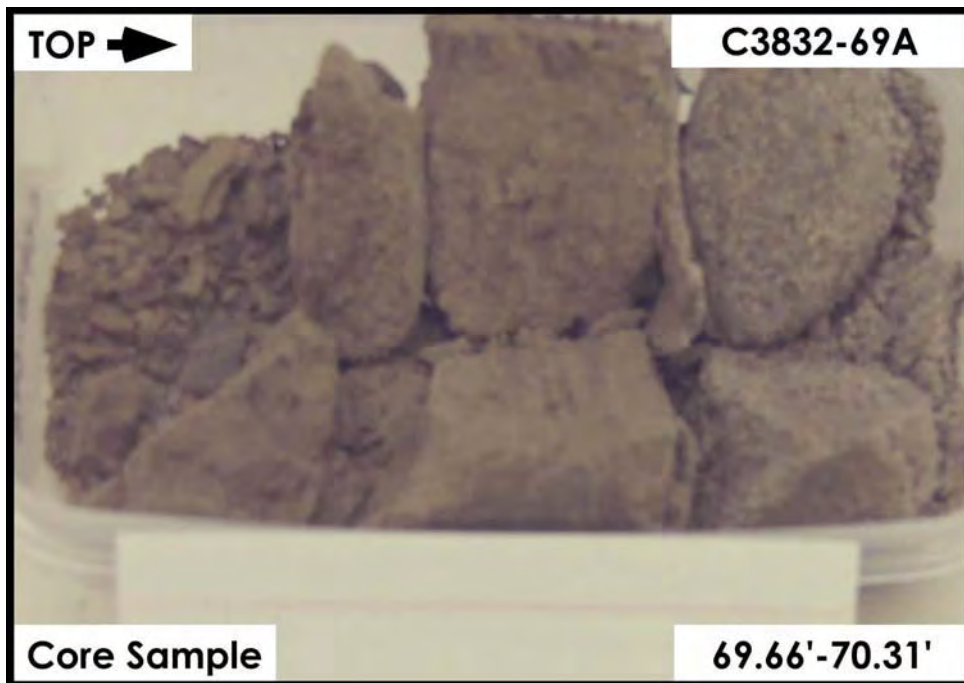
Figure A-4.18. Hanford Formation (H2 unit) 69.66 ft – 70.31 ft
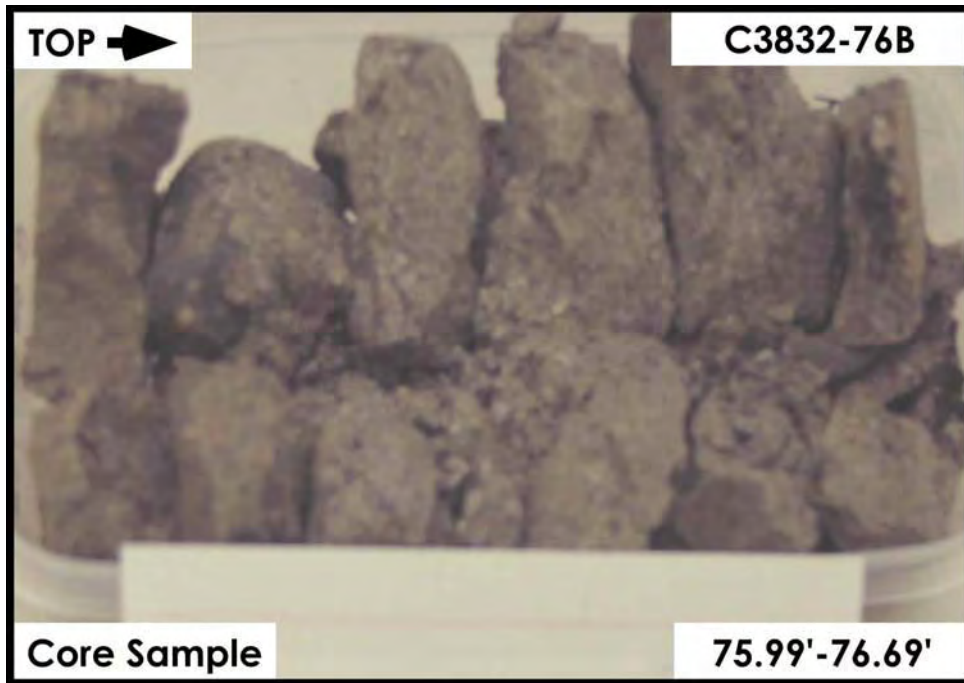
Figure A-4.19. Hanford Formation (H2 unit) 75.99 ft – 76.69 ft
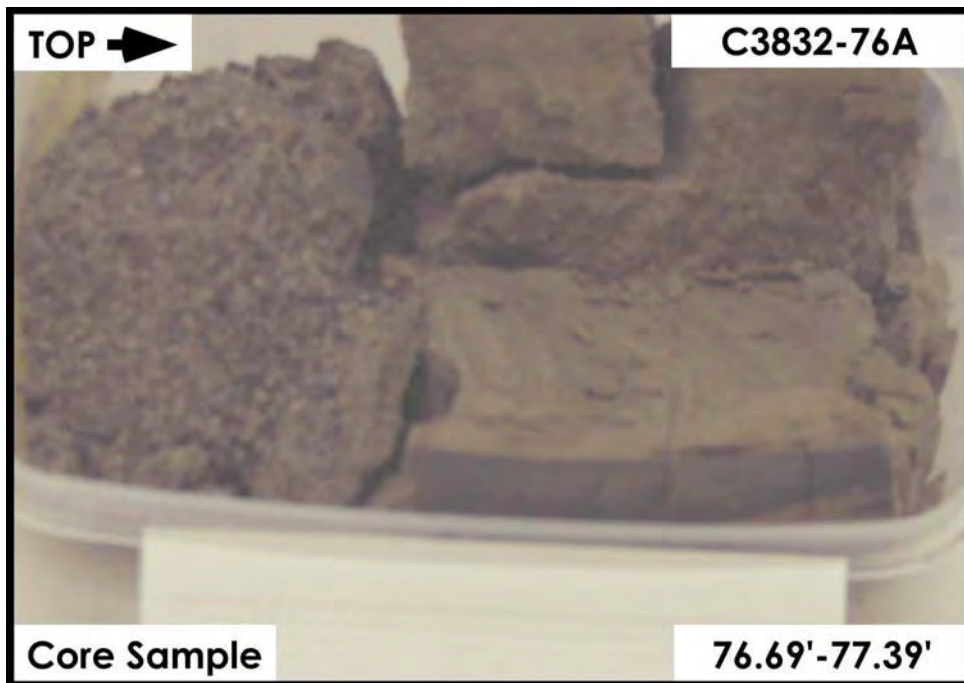
Figure A-4.20. Hanford Formation (H2 unit) 76.69 ft – 77.39 ft
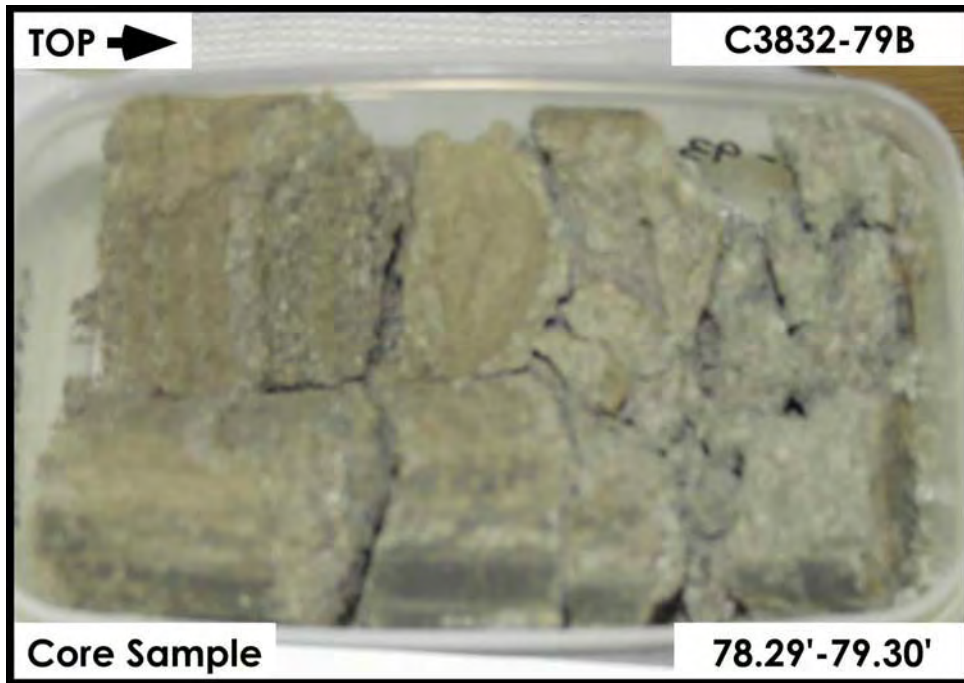
Figure A-4.21. Hanford Formation (H2 unit) 78.29 ft – 79.30 ft
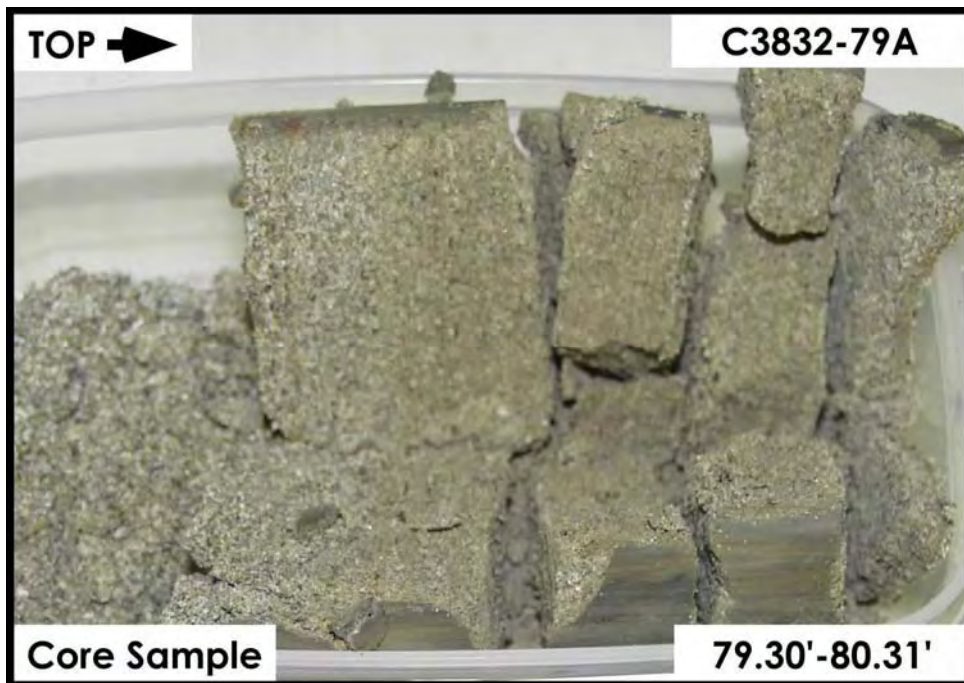
Figure A-4.22. Hanford Formation (H2 unit) 79.30 ft – 80.31 ft
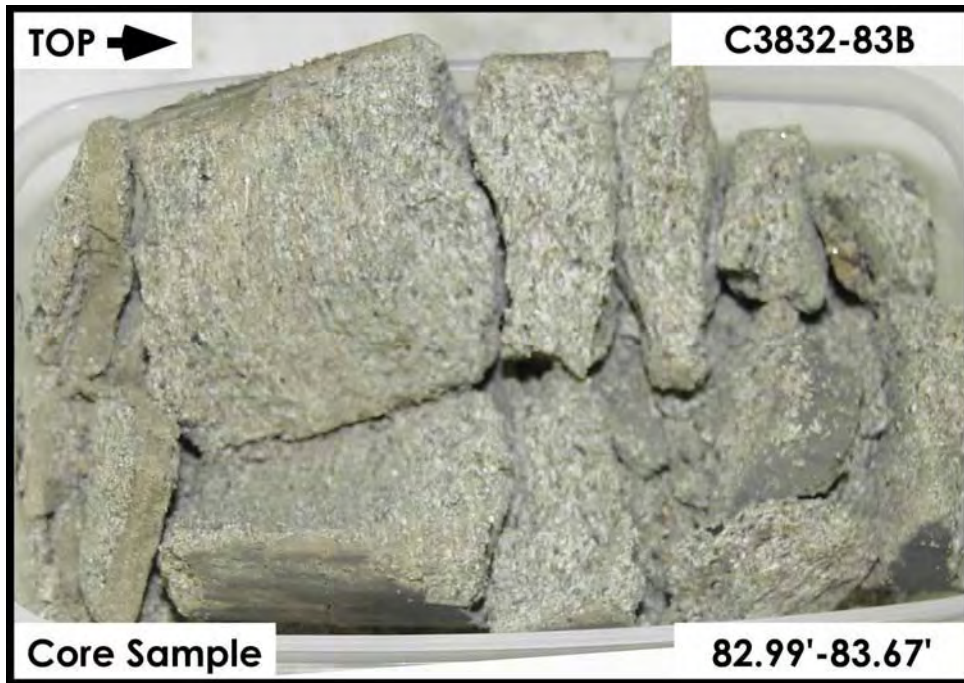
Figure A-4.23. Hanford Formation (H2 unit) 82.99 ft – 83.67 ft
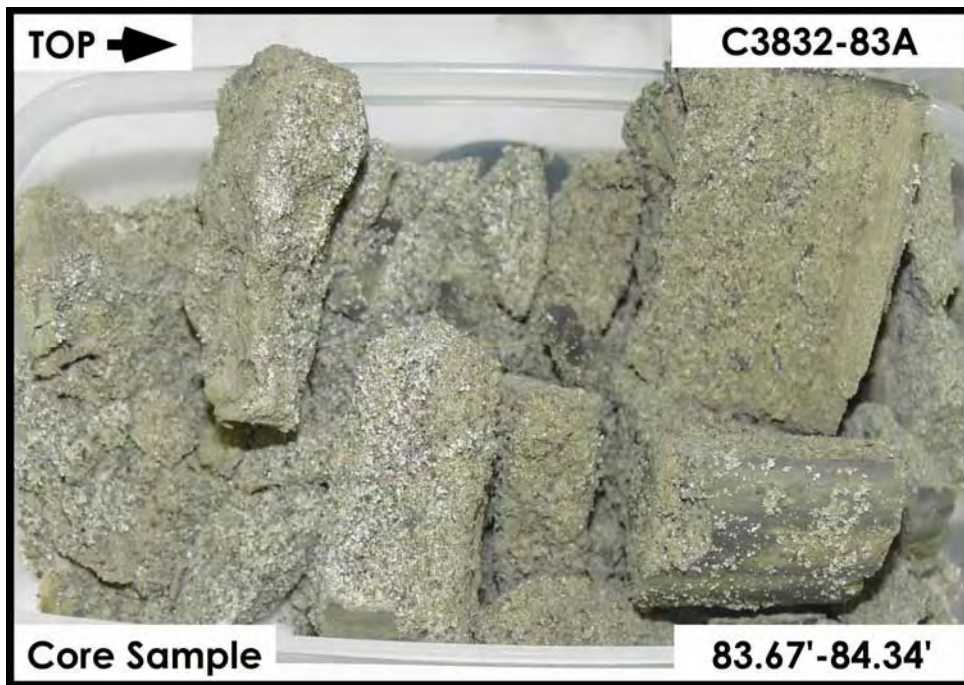
Figure A-4.24. Hanford Formation (H2 unit) 83.67 ft – 84.34 ft
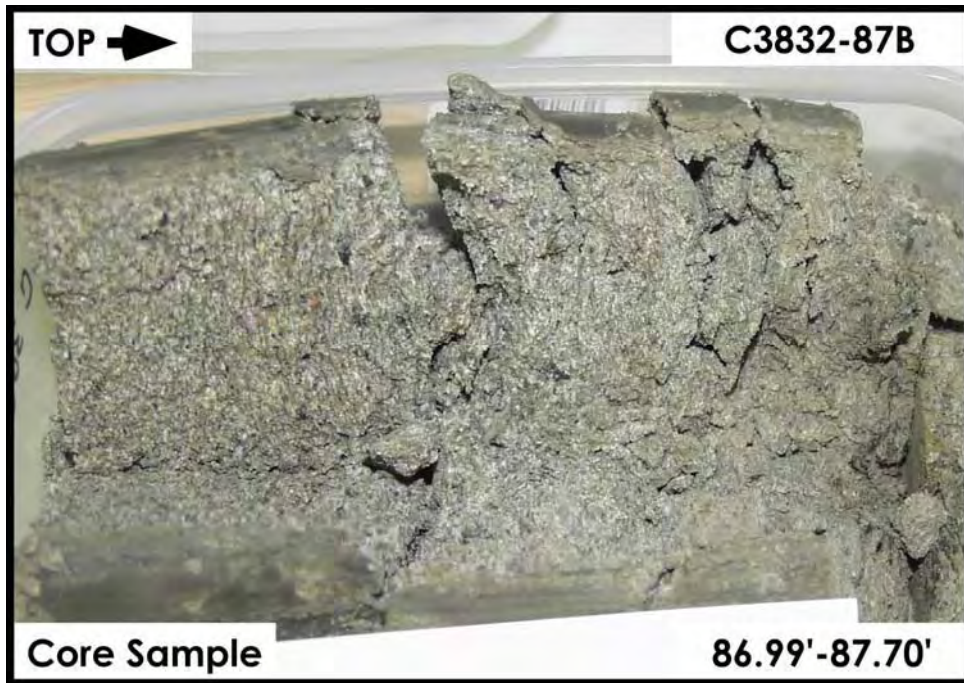
Figure A-4.25. Hanford Formation (H2 unit) 86.99 ft – 87.70 ft
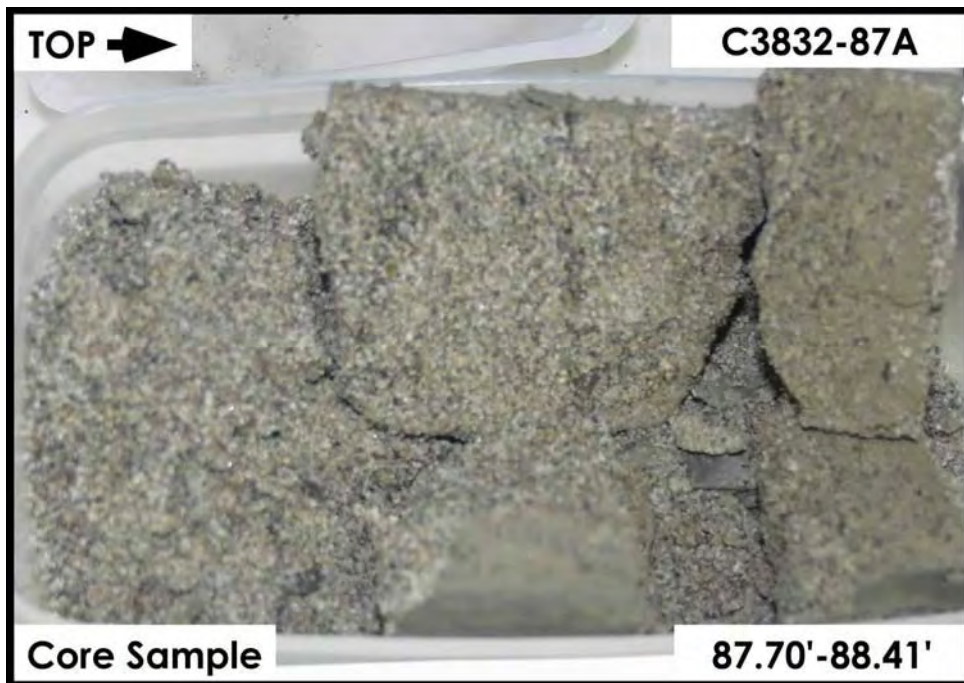
Figure A-4.26. Hanford Formation (H2 unit) 87.70 ft – 88.41 ft
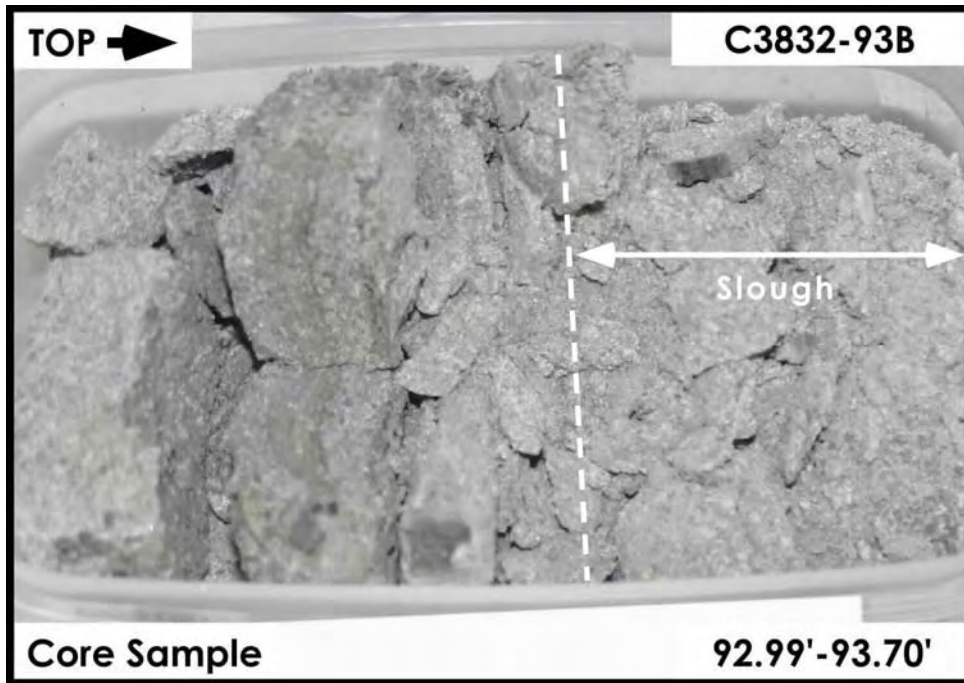
Figure A-4.27. Hanford Formation (H2 unit) 92.99 ft – 93.70 ft
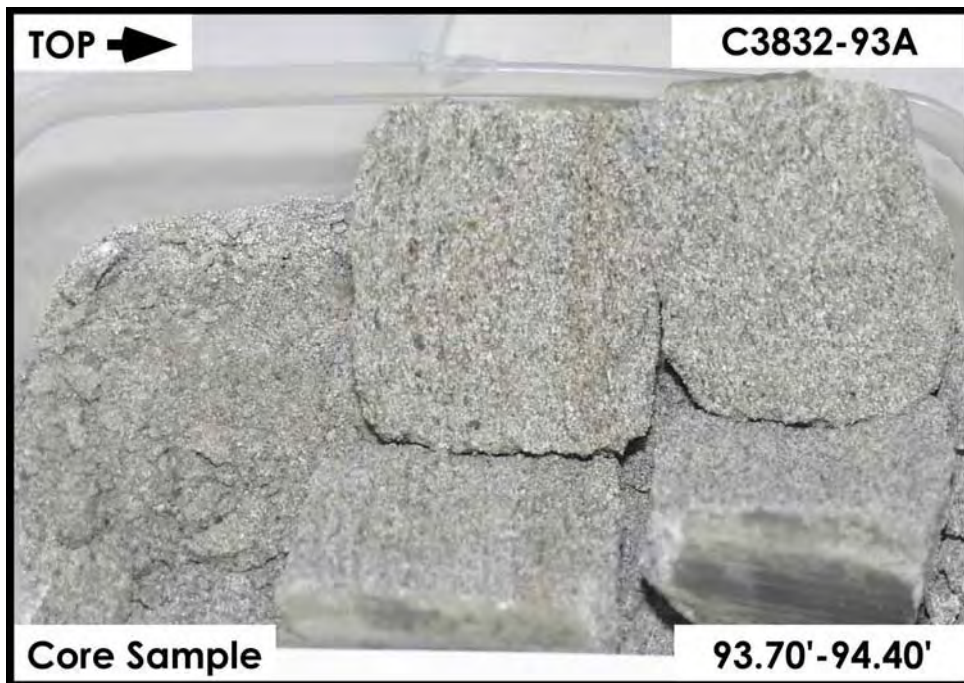
Figure A-4.28. Hanford Formation (H2 unit) 93.70 ft – 94.40 ft
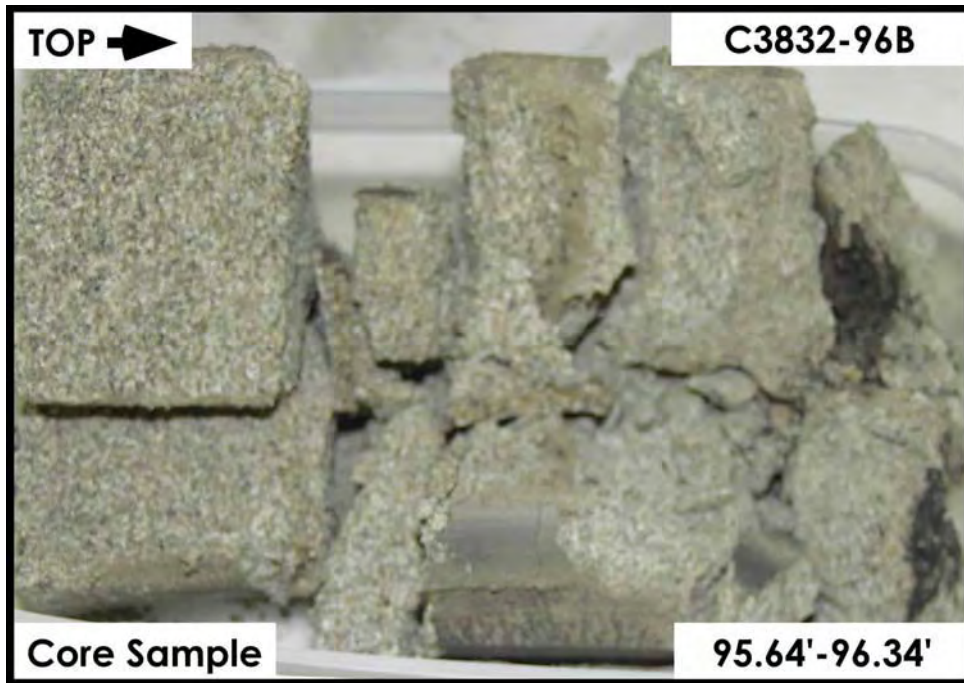
Figure A-4.29. Hanford Formation (H2 unit) 95.64 ft – 96.34 ft
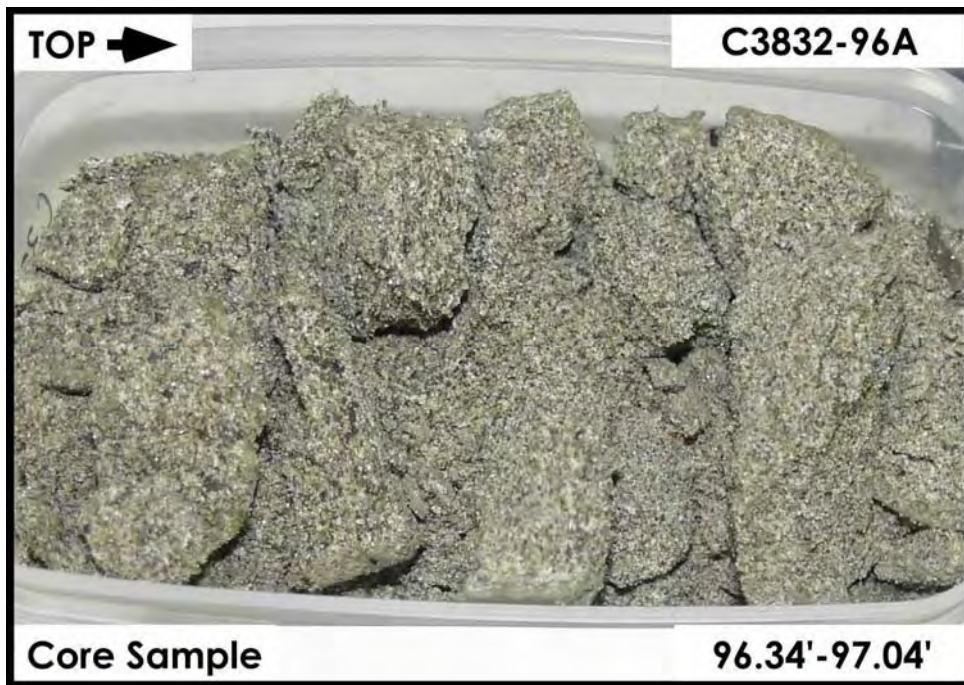
Figure A-4.30. Hanford Formation (H2 unit) 96.34 ft – 97.04 ft
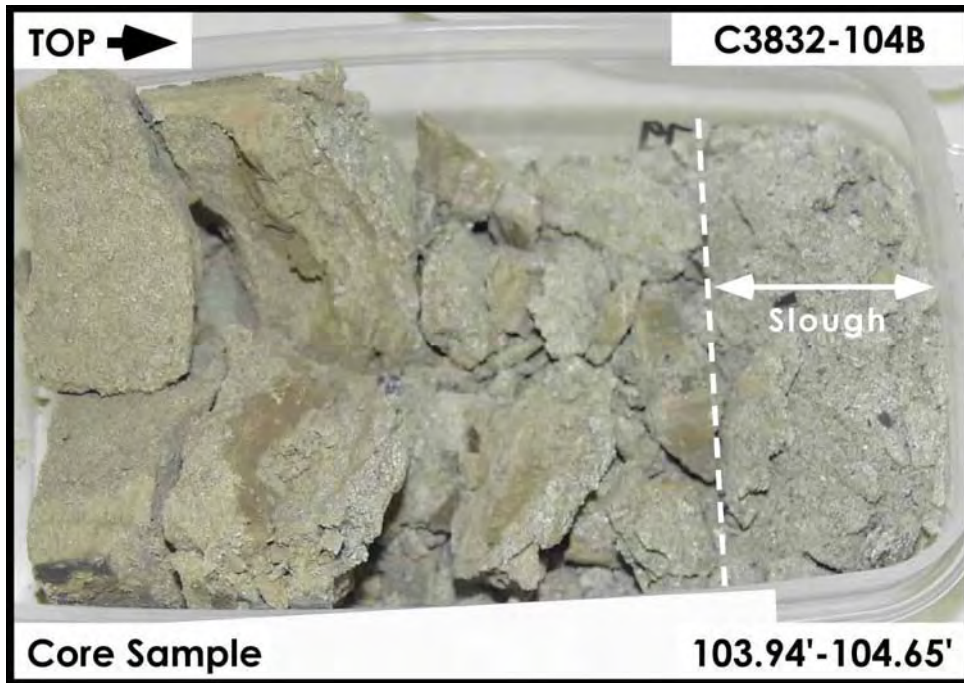
Figure A-4.31. Cold Creek Unit – Upper (CCU$_u$) 103.94 ft – 104.65 ft
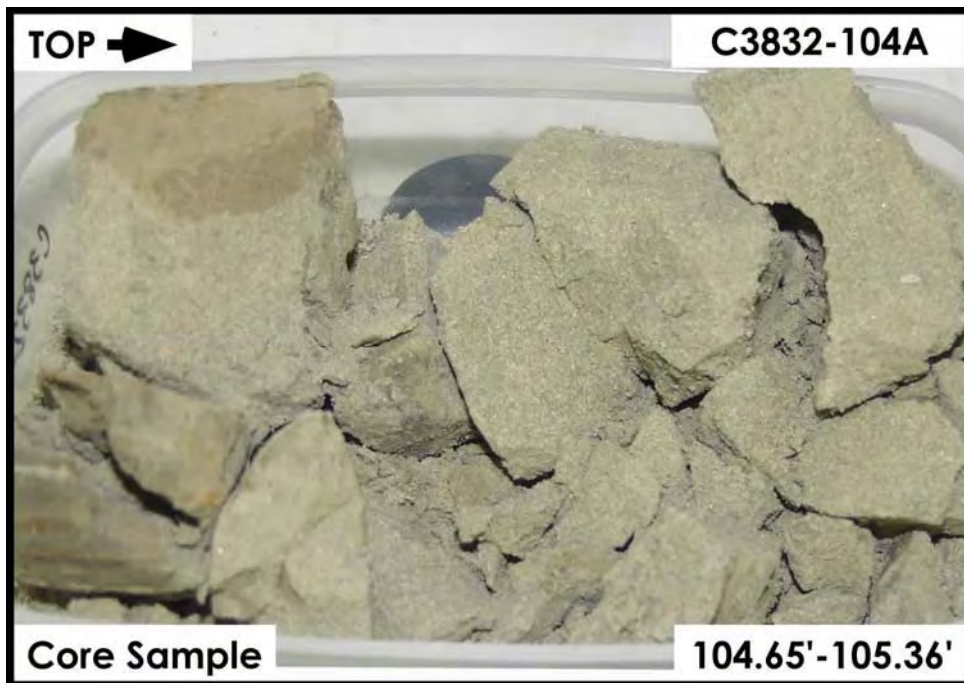
Figure A-4.32. Cold Creek Unit – Upper (CCU$_u$) 104.65 ft – 105.36 ft
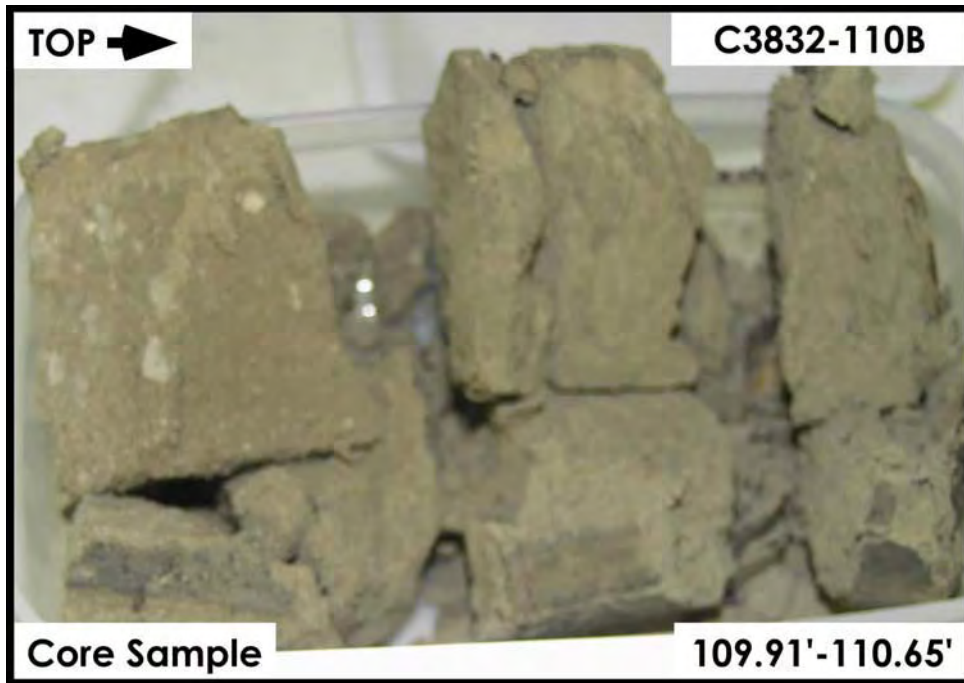
Figure A-4.33. Cold Creek Unit – Upper (CCU$_u$) 109.91 ft – 110.65 ft
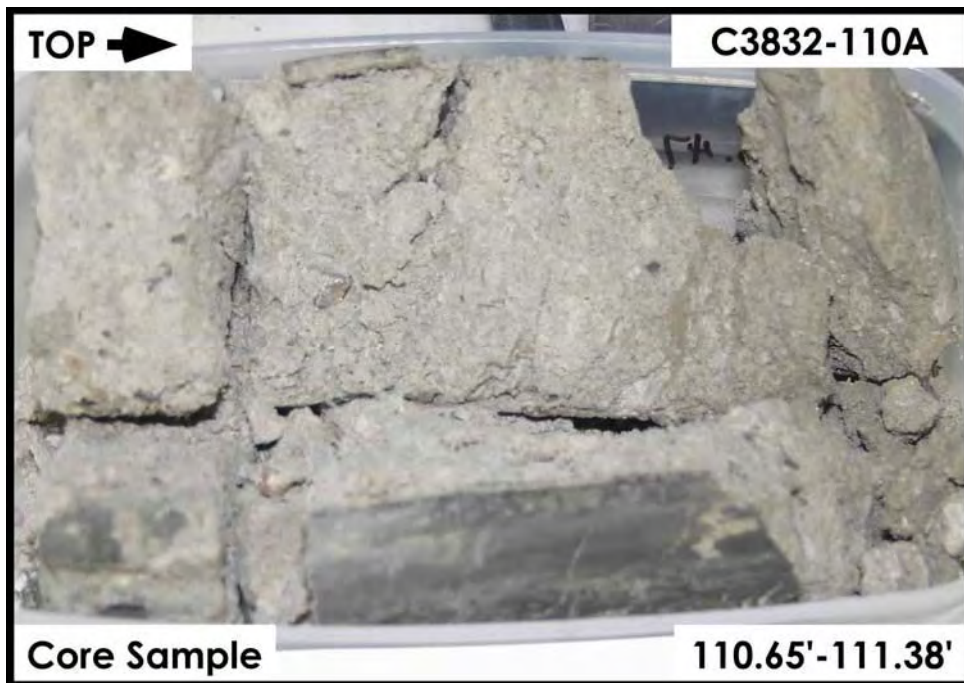
Figure A-4.34. Cold Creek Unit – Lower (CCU$_l$) 110.65 ft – 111.38 ft
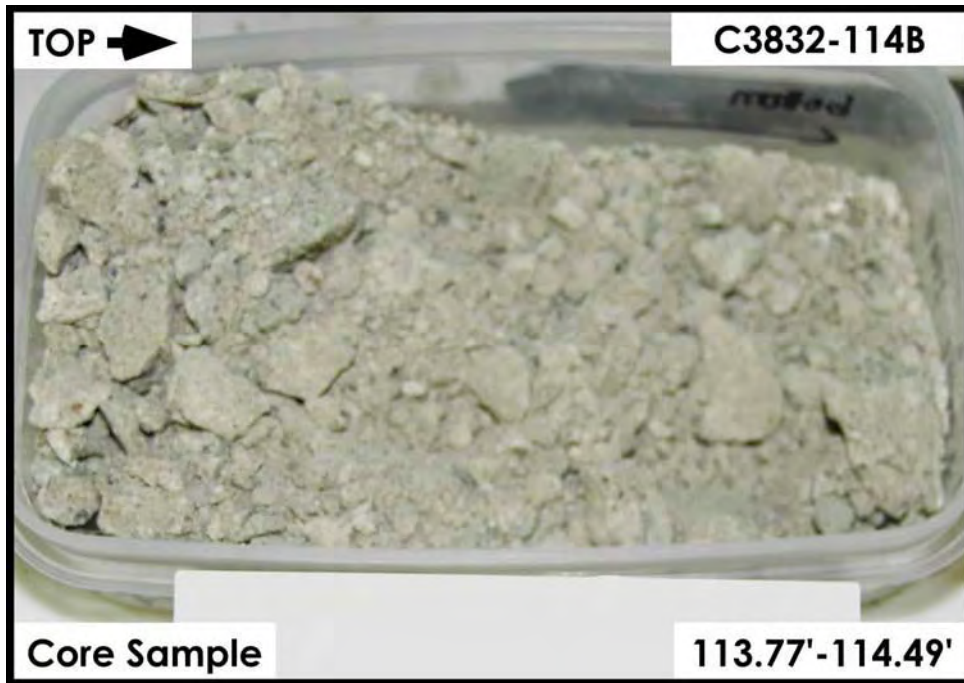
Figure A-4.35. Cold Creek Unit – Lower (CCU$_l$) 113.77 ft – 114.49 ft
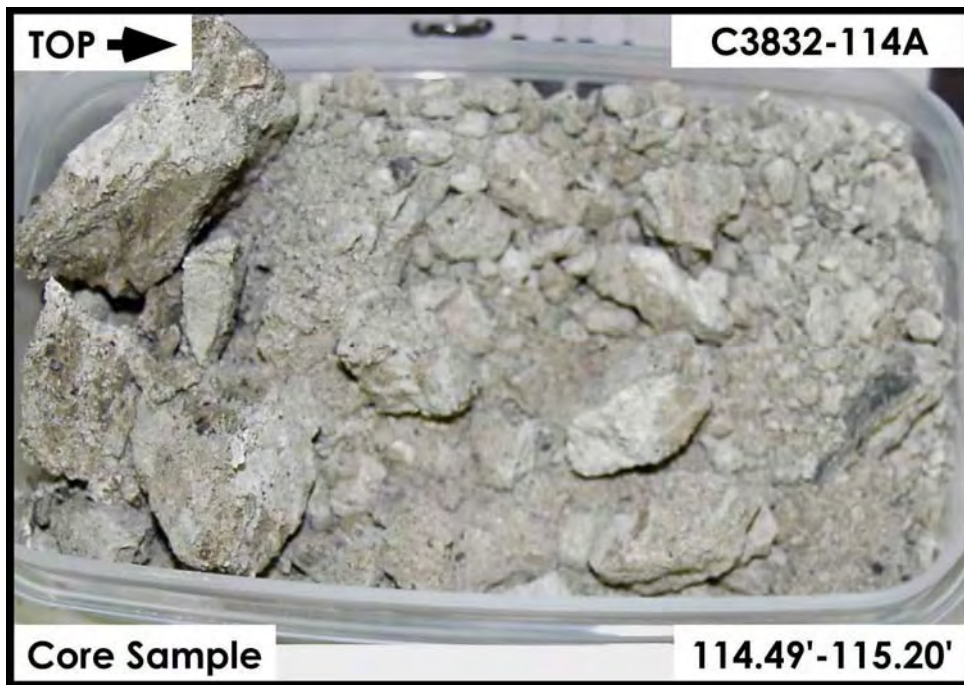
Figure A-4.36. Cold Creek Unit – Lower (CCU$_l$) 114.49 ft – 115.20 ft
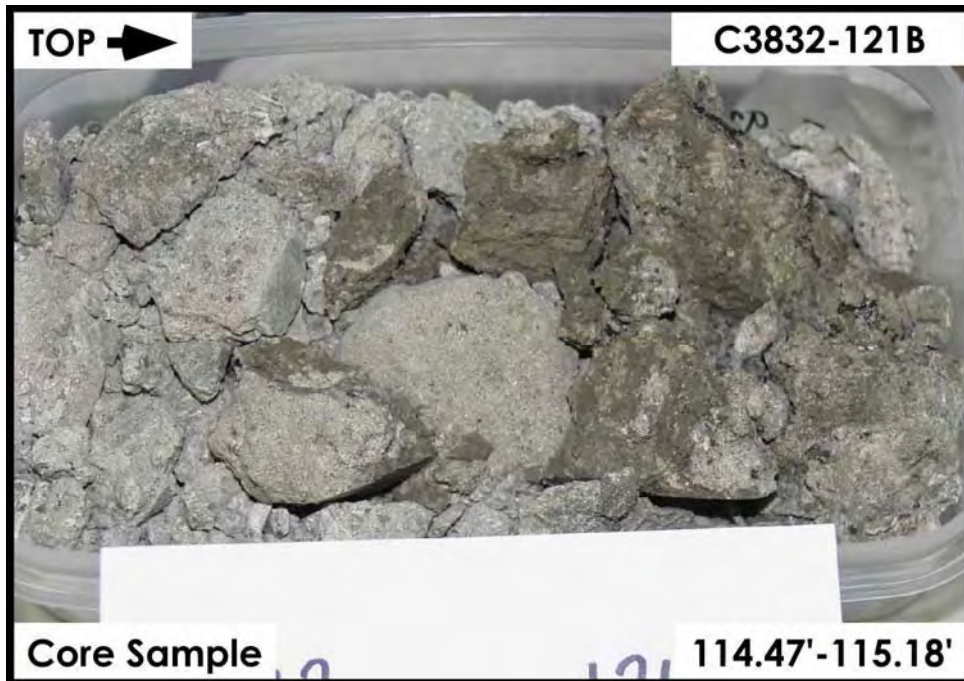
Figure A-4.37. Cold Creek Unit – Lower (CCU$_l$) 114.47 ft – 115.18 ft
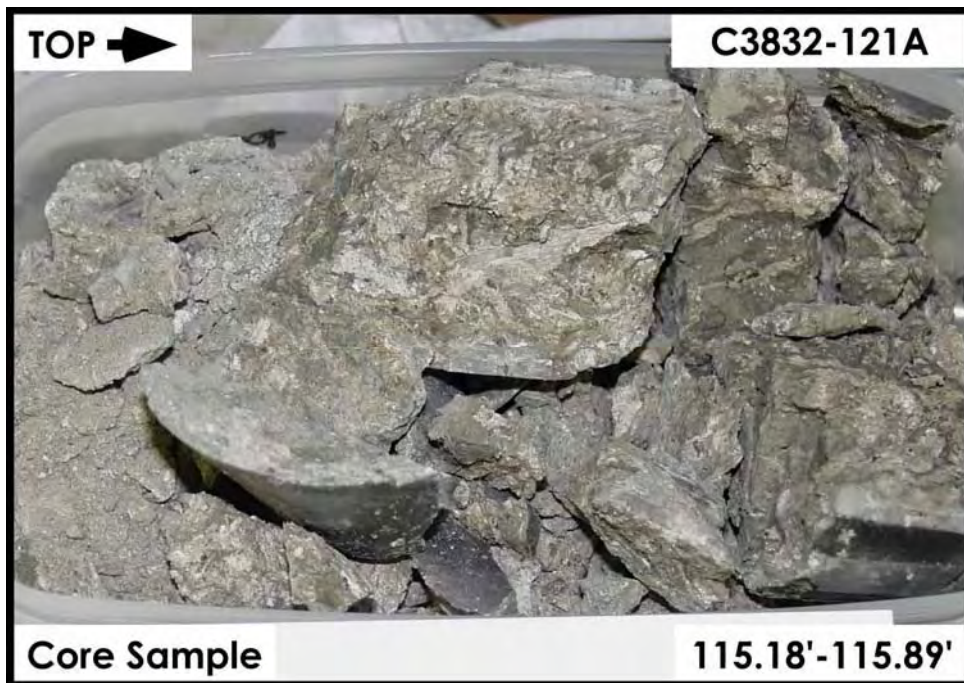
Figure A-4.38. Cold Creek Unit – Lower (CCU$_l$) 115.18 ft – 115.89 ft

APPENDIX B. CORE LOGS*

B.1   C3830

B.2   C3831

B.3   C3832

*Core Logs for 299-W10-27 are presented in Lindsey et al. (2001).

APPENDIX B.1

C3830 (TX-105)

GEOLOGIC DESCRIPTION OF CORE OBTAINED

DURING OPENING IN LAB

Contents

Pacific Northwest National Laboratory

DAILY BOREHOLE LOG

Boring/Well No __C3830__   Depth __14.96 - 42.49__   Date __10-16-02__

Location __TX-105__   Project __Vadose Zone__

Logged by __B N Bjornstad__

Reviewed by _____

Lithologic Class. Scheme _____

Steel Tape/E-Tape __/__   Field Indicator Equip. 1)   2)

Procedure _____   Rev _____   Date _____

Drilling Contractor _____

Driller _____

Rig/Method _____

Depth Control Point _____

DEPTH ( )	TIME	SAMPLES TYPE	ID NUMBER	CONTAMINATION INSTR READING	MOIS-TURE	GRAPHIC LOG C Z S G	LITHOLOGIC DESCRIPTION (particle size distribution, sorting, mineralogy, roundness, color, reaction to HCl, etc.)	H₂O ADDED	CASING	DRILLING COMMENTS (drilling rate, down time, blow counts, water level, drill fluid, etc.)
14.96		GP	14.96 B		M		few small pebbles, matrix sup. wk rxn w/ HCl, max ped. size = 5mm			GP = geoprobe
		GP	14.96 A				S, mostly fine, 7.5YR 4/2 (brown) well sorted, sl. compact, massive no rxn w/ HCl			Backfill
16.3							(gravelly)			
27.91		GP	27.91 B		SM		gS gravelly fn-crs sand poorly sorted, mod rxn w/ HCl wk lamination, max ped size = 20 mm, loose, brown some pulverization 10 YR 4/2			
		GP	27.91 A				dk. grayish brown, wk rxn w/ HCl toward bottom			
29.15										
40.93		GP	40.93 B		SM		gS pebbly fn-crs sand, mod. sorted, 10YR4/2 (dk. grayish brn.) mod-strng rxn w/ HCl, massive, max ped. size = 10 mm, fewer pebbles below			
		GP	40.93 A							
42.49										

W = Wet, M = Moist, D = Dry

Pacific Northwest National Laboratory

DAILY BOREHOLE LOG

Boring/Well No __C3830__

Location __TX-105__

Project __Vadose Zone__

Logged by __B N Bjornstad__

Reviewed by _____

Lithologic Class. Scheme _____

Steel Tape/E-Tape _____ 1

Procedure _____

Field Indicator Equip. 1) _____ 2)

Rev _____

Date _____

Drilling Contractor _____

Driller _____

Rig/Method _____

Depth Control Point _____

DEPTH	TIME	SAMPLES			CONTAMINATION		MOIS-TURE	GRAPHIC LOG				LITHOLOGIC DESCRIPTION (particle size distribution, sorting, mineralogy, roundness, color, reaction to HCl, etc.)	H₂O ADDED	CASING	DRILLING COMMENTS (drilling rate, down time, blow counts, water level, drill fluid, etc.)
		TYPE	ID NUMBER		INSTR	READING		C	Z	S	G				

DEPTH	TYPE	ID NUMBER	MOIS	Description	CASING	COMMENTS
46.2	GP	46.2 B	SM	gS pebbly fn-crs sand, mod sorted, massive, 10YR5/2 (grayish brn) mod. rxn w/ HCl, max part. size = 20 mm. sand = 20-30% mafic		Backfill
		46.2 A				
47.5		47.5 B	SM	(g)S slightly pebbly fn-crs sand mod-poorly sorted massive 2.5Y6/2 (dk grayish brn, mod-strg rxn w/ HCl, max part. size = 80 mm		
49.0		47.5 A		slough - (g)S massive		
52.98		52.98 B	SM	S fn-md, mod-well sorted laminated, 10YR6/2 (lt brnish gray), max part. size = md sand, sand = 20-30% md sand		Hanford Fm.
54.36		52.98 A		mafic, stratified at base- alternating layers of fine and medium sand. fine grained layers are 10YR6/3 (pale brown), mod-rxn w/ HCl, max part size = crs sand		

W = Wet, M = Moist, D = Dry

1098/DCL/PROC/DBL/001

Pacific Northwest National Laboratory

DAILY BOREHOLE LOG

Boring/Well No __C3830__   Depth __56.99 - 59.7__   Date __10-16-02__

Location __TX-105__   Project __Vadose Zone__

Logged by __B N Bjornstad__ _(Print)_ _(Sign)_

Reviewed by _____ _(Print)_ _(Sign)_   Date _____

Lithologic Class. Scheme _____   Procedure _____   Rev _____

Steel Tape/E-Tape __/__   Field Indicator Equip. 1) _____ 2) _____

Drilling Contractor _____
Driller _____
Rig/Method _____
Depth Control Point _____

DEPTH ( )	TIME	SAMPLES		CONTAMINATION		MOIS-TURE	GRAPHIC LOG					LITHOLOGIC DESCRIPTION (particle size distribution, sorting, mineralogy, roundness, color, reaction to HCl, etc.)	H₂O ADDED	CASING	DRILLING COMMENTS (drilling rate, down time, blow counts, water level, drill fluid, etc.)
		TYPE	ID NUMBER	INSTR	READING		C	Z	S	G					
56.99		GP	56.99 B			D	Sl		X			loose slough at top			Sl = slough
		↓	56.99A						X			S: fn sand, well sorted, laminated, 10YR7/2 (t. gray), sand = 10-15%, basalt drier and lighter colored compared to previous samples, mod rxn w/ HCl, max part. size = md sand, coarsens to md sand below			Hanford fm.
58.37		↓				→									
58.29			58.29 B			M	Sl					silty, sandy slough w/ plastic			X = sample location
						Sw	s		X			S: sand mostly medium grained, mod-well sorted, massive, loose sand: 20-30% mud, rxn w/ HCl, max part. size = cs. sand, 10YR5/2			
		↓	58.29A			→									
59.7		↓				→						(grayish brn). Two layers of silty fine sand, 10YR5/3 (brn) at bottom, well laminated, gradational contacts			

W = Wet, M = Moist, D = Dry

1988/DCL/PROC/DBL/001

DAILY BOREHOLE LOG

Pacific Northwest National Laboratory

Boring/Well No	C3830
Location	TX-105
Depth	66.06 - 78.35
Project	Vadose Zone
Date	10-16-02
Sheet	4 of 7

Logged by __BN Bjornstad__

Reviewed by _____

Lithologic Class. Scheme ____ Procedure ____ Rev ____

Steel Tape/E-Tape __1__   Field Indicator Equip. 1) ____ 2) ____

Drilling Contractor _____
Driller _____
Rig/Method _____
Depth Control Point _____

DEPTH ( )	TIME	SAMPLES TYPE	ID NUMBER	CONTAMINATION INSTR. READING	MOIS-TURE	GRAPHIC LOG	LITHOLOGIC DESCRIPTION (particle size distribution, sorting, mineralogy, roundness, color, reaction to HCl, etc.)	H₂O ADDED	CASING	DRILLING COMMENTS (drilling rate, down time, blow counts, water level, drill fluid, etc.)
66.06		GP	66.06 B		D	sl.	loose slough			sl = slough
			66.06 A			x	S, fn sand, well sorted, laminated, 10YR7/2 (lt. gray)			
							sand = 10-15% mafic, max.			
							pat. size = md. sand, sl.			
67.46							compact, mod rxn. w/ HCl			
							Bottom: md sand, loose.			
							max. pat. size = sm. pebble			
							w/klg laminated, mod rxn			
							w/ HCl			
71.95			71.95 B		D	sl.	S, fn-md sand, well-sorted, laminated, 10YR7/2 (lt.			
			71.95 A			x	gray) max pat size = md sand			
							sand = 10-20% basalt, mod			
73.3							rxn w/ HCl, interlaminated			
							fn and md sand at base			
76.98			76.98 B		D	s	loose			
			76.98 A		SM	x	S, fn sand, well sorted, laminated,			
							10YR7/2 (lt. gray), max pat.			
							size = fn sand, mod rxn w/			
							HCl, mostly md sand in lower			
78.35							half, 10YR8/2 (lt. brnish gray)			

W = Wet, M = Moist, D = Dry

1998/DCL/PROC/DBL/001

B-1.4

DAILY BOREHOLE LOG

Pacific Northwest National Laboratory

Boring/Well No __C3830__ Depth __80.91 – 100.5__ Date __10-16-02__

Location __TX-105__ Project __Vadose Zone__

Logged by __B N Bjornstad__ Drilling Contractor ___

Reviewed by ___ Date ___ Driller ___

Lithologic Class. Scheme ___ Procedure ___ Rev ___ Rig/Method ___

Steel Tape/E-Tape __/__ Field Indicator Equip. 1) 2) Depth Control Point ___

DEPTH ( )	TIME	SAMPLES		CONTAMINATION		MOIS-TURE	GRAPHIC LOG				LITHOLOGIC DESCRIPTION (particle size distribution, sorting, mineralogy, roundness, color, reaction to HCl, etc.)	H₂O ADDED	CASING	DRILLING COMMENTS (drilling rate, down time, blow counts, water level, drill fluid, etc.)
		TYPE	ID NUMBER	INSTR. READING			C	Z	S	G				
80.91		GP	80.91 B			D	si		X		S, fn-md sand, mod. sorted, laminated 10YR7/2 (lt-gray) max. part. size = crs sand, mod-strng rxn w/ HCl sand = 10-20% mafic			Si = slough
			80.91 A											
82.21														
86.11			86.11 B			SM	si		X		S, md-crs sand, laminated, s = 20-30% mafic, mod sorted, max part. size = sm. pebble, mod-strng rxn w/ HCl, 10YR5/2 & (grayish brn)			X = sample location
			86.11 A						X		2S, 2.5Y 6/6 & olive yellow), silty w/fn sand, laminated, v. well sorted, mod-strng rxn w/ HCl			
87.41														
											loose slough at top			
98.91			98.91 B			SM	si		X		S, fn-md sand, mod sorted, laminated, sand = 10-20% mafic, max part. size = md sand 10YR 6/2 (lt. brnish gray), mod-strng rxn w/ HCl			
			98.91 A						X		mostly crs sand at base, 30-40% mafic			collected from nose cone below A sleeve
100.36											2 fn sand 10YR5/4 (yell brn), mod-strng rxn w/ HCl			Contact w/ CCUz @ ~100.4'
100.5							CCUz?							

W = Wet, M = Moist, D = Dry

B-1.5

Pacific Northwest National Laboratory

DAILY BOREHOLE LOG

Depth 100.32 - 104.44   Date 10-16-02.   Sheet 6 of 7

Boring/Well No __C-3830__   Project __Vadose Zone__

Location __TX-105__

Logged by __BN Bjornstad__

Reviewed by

Lithologic Class. Scheme __1__

Steel Tape/E-Tape __1__   Field Indicator Equip. 1)   2)

Procedure ___ Rev ___   Date ___

Drilling Contractor
Driller
Rig/Method
Depth Control Point

DEPTH ( )	TIME	SAMPLES TYPE	SAMPLES ID NUMBER	CONTAMINATION INSTR. READING	MOIS-TURE	GRAPHIC LOG (C Z S G)	LITHOLOGIC DESCRIPTION (particle size distribution, sorting, mineralogy, roundness, color, reaction to HCl, etc.)	H₂O ADDED	CASING	DRILLING COMMENTS (drilling rate, down time, blow counts, water level, drill fluid, etc.)
100.32		GP	100.32 B		SM	s	slough = gray, poorly sorted, massive, compact			sharp contact w/ silt below
						x	zS, silty fn sand, well sorted, laminated, 10YR 4/3 (brown)			CCU silt
			100.32A		m	x	coarsens to fn sand below			X = sample location
101.72							compact, mod-strng rxn w/ HCl, max pclst sized = fn sand			
							Interlaminated silty fn sand and fn sandy silt, compact, well sorted, 10YR4/3 (pale brn), strng rxn			
							silt, 10YR5/4 (yellowish brn), v well sorted			
							laminated, strng rxn w/ HCl, v compact/cohesive			
102.99			102.99B		SM	GI	S, fn-crs, loose, poorly sorted, MSV = slough			CCU silt
						x				sl = slough
			102.99A		M	x	sZ, fn sand y silt, laminated, compact, 10YR5/4 (yell. brn), mod-strng rxn w/ HCl, more massive and silty toward bottom			
104.44										

W = Wet, M = Moist, D = Dry

1988/DCL/PROC/DBL/001

Pacific Northwest National Laboratory

DAILY BOREHOLE LOG

Boring/Well No **TX-105**

Location _____

Depth **107.9 - 115.0** Date **10-16-02**

Project **Vadose Zone**

Logged by **B N Bjornstad**

Reviewed by _____

Lithologic Class. Scheme _____

Steel Tape/E-Tape _____ 1

Drilling Contractor _____

Driller _____

Rig/Method _____

Depth Control Point _____

Procedure _____ Date _____

Field Indicator Equip. 1) _____ 2) _____ Rev _____

DEPTH ( )	TIME	SAMPLES		CONTAMINATION		MOIS-TURE	GRAPHIC LOG					LITHOLOGIC DESCRIPTION (particle size distribution, sorting, mineralogy, roundness, color, reaction to HCl, etc.)	H₂O ADDED	CASING	DRILLING COMMENTS (drilling rate, down time, blow counts, water level, drill fluid, etc.)
		TYPE	ID NUMBER	INSTR.	READING		C	Z	S	G					
107.84		GP	107.84 B			SM			S		loose			CCU silt
			107.84 A						X		s₂, fine sandy silt, compact massive strong rxn w/ HCl 10YR 6/3 (golfboro), well sorted uniform			S1 = slough
109.14									X					
113.55			113.55 B			SM			s₁?		s₂ as above globby caliche cemented and mottled sand, silt, and clay violent rxn w/ HCl, v. poorly sorted, tightly cemented and difficult to remove from liner. pebbles mostly angular basalt, v. poorly sorted 7.5YR 6/2 pinkish gray			CCUz in contact w/ CCU caliche @ ≈ 113.8' x = sample location
			113.55 A											
115.0														

W = Wet, M = Moist, D = Dry

1998/DCL/PROC/DBL/001

B-1.7

APPENDIX B.2

C3831 (TX-107)

GEOLOGIC DESCRIPTION OF CORE OBTAINED

DURING OPENING IN LAB

Contents

DAILY BOREHOLE LOG

Pacific Northwest National Laboratory

Boring/Well No **C 3831**   Location **TX-107**   Depth **14.93 – 46.39**   Date **8-14-02**

Logged by **BN Bjornstad**
Reviewed by _____
Lithologic Class. Scheme _____
Steel Tape/E-Tape _____

Procedure _____   Rev _____   Date _____
Field Indicator Equip. 1) _____   2) _____

Project _____
Drilling Contractor _____
Driller _____
Rig/Method _____
Depth Control Point _____

DEPTH ( )	TIME	SAMPLES TYPE	ID NUMBER	CONTAMINATION INSTR. READING	MOIS-TURE	GRAPHIC LOG (C Z S G)	LITHOLOGIC DESCRIPTION (particle size distribution, sorting, mineralogy, roundness, color, reaction to HCl, etc.)	H₂O ADDED	CASING	DRILLING COMMENTS (drilling rate, down time, blow counts, water level, drill fluid, etc.)
14.93–		S.S.	C3831-15B		D		msG, dk rxn w/ HCl, 2.5Y4/2 (dk gray) top/bottom			Backfill
16.31			-15A		SM		half is compact, max. particle size = 2cm, poorly sorted			1.38' = length of core
20.8–		S.S.	-21B		SM		msG, dk rxn w/ HCl, poorly sorted, loose, dk gray, sand/gravel			Backfill
22.3			-21A		↓		top has max part size = 5cm, 2.5Y4/2 (dk grayish brn)			1.5' length
							mod rxn w/ HCl (bottom)			
27.96–		S.S.	-28B		SM		msG, mod rxn w/ HCl, 2.5Y4/2 (dk grayish brn)			Backfill?
29.21			-28A		↓		v. poorly sorted, max part size = 2cm (mod rxn w/ HCl)			1.25' length
45.06–		S.S.	-45B		SM		msG, slough, oxygen tubing fragment, is backfill? 2.5, well sorted, laminated, 2.5Y4/4 olive brn			1.33' length Backfill
46.39					M		95+ nail/metal-rust coated, 2.5Y5/2 (grayish brn)			
			-45A		SM		poorly sorted, iron oxide concretions/coatings, max part size = 3cm, strong rxn w/ HCl			X = sample location

W = Wet, M = Moist, D = Dry

1998/DCL/PROC/DBL/001

Pacific Northwest National Laboratory

DAILY BOREHOLE LOG

Boring/Well No __C3831__ Depth __51.01 - 60.24__ Date __8-14-02__

Location __TX-107__ Project _____ Sheet __2__ of __7__

Logged by __B. N. Bjornstad__

Reviewed by _____ Date _____ Rev _____

Lithologic Class. Scheme _____ Procedure _____

Steel Tape/E-Tape _____ Field Indicator Equip. 1)_____ 2)_____

Drilling Contractor _____

Driller _____

Rig/Method _____

Depth Control Point _____

DEPTH ( )	TIME	SAMPLES TYPE	ID NUMBER	CONTAMINATION INSTR.	READING	MOIS-TURE	GRAPHIC LOG	LITHOLOGIC DESCRIPTION (particle size distribution, sorting, mineralogy, roundness, color, reaction to HCl, etc.)	H₂O ADDED	CASING	DRILLING COMMENTS (drilling rate, down time, blow counts, water level, drill fluid, etc.)
51.01 - 52.36		S.C.	C3831-51B			SM		mS, loose, poorly sorted, 2.5Y6/2, lt. brnish gray, wk rxn w/ HCl			1.35' length
			-51A			M		mSG, similar to above except more gravel 2-4cm S, 2.5Y6/4 (lt. yell-brn), well sorted, wk rxn w/ HCl, msv, compact			Base of backfill? Top of Hanford fm ~52.3'
52.16 - 53.51		S.S.	-52B			D		mSG, poorly sorted 2.5Y5/2 (grayish brn), max part. size = 2-3cm, wk rxn w/ HCl, slough			~1.35' length - 0.2 overlap w/ core above slough
						SM		S, md-crs, well sorted 2.5Y5/2 (grayish brn), wk rxn w/ HCl			
58.04 - 60.24		S.S.	-54B			SM		S, md, 2.5Y6/2 (lt. brnish gray) well sorted, mod. rxn w/ HCl, upper part shows partings (compaction during drilling?) max part. size = 5mm			Length = 1-2'
			-54A			M		Fines downward into silty fn sand w/ some rusty mottling, well sorted, msv, 2.5Y5/2D (grayish brn) mod. rxn w/ HCl, compact			

W = Wet, M = Moist, D = Dry

Pacific Northwest National Laboratory

DAILY BOREHOLE LOG

Boring/Well No __C3831__   Depth __60.08-69.98__   Date __8-14-02__

Location __TX-107__   Project ____

Logged by __BN Bjornstad__   Drilling Contractor ____

Reviewed by ____   Driller ____

Lithologic Class. Scheme ____   Rig/Method ____

Procedure ____ Rev ____ Date ____   Depth Control Point ____

Steel Tape/E-Tape ____   Field Indicator Equip. 1) ____ 2) ____

DEPTH	TIME	SAMPLES TYPE	SAMPLES ID NUMBER	CONTAMINATION INSTR. READING	MOIS-TURE	GRAPHIC LOG	LITHOLOGIC DESCRIPTION (particle size distribution, sorting, mineralogy, roundness, color, reaction to HCl, etc.)	H₂O ADDED	CASING	DRILLING COMMENTS (drilling rate, down time, blow counts, water level, drill fluid, etc.)
60.08- 61.50		s.s.	C3831-60B		M	x·B	Clastic dike - vertically lam. sand, silt and clay. Few SM.			Length = 1.42 Some overlap w/ previous core
			-60A		SM	A	poorly to v. poorly sorted, dk. gray sand to grayish brn sand and silty sand, compact, cohesive, mod rxn w/HCl			Hanford Fm.
							S. mostly md-crs, salt and pepper, well sorted, loose, 2.5Y5/2 (grayish brn), max part. size = v.crs sand, wk rxn w/HCl			
67.19- 68.54		s.s.	-67B		SM	x·B	S. mostly fn-md, uniform, well sorted wkly lam. 2.5Y6/2 (lt. grayish brn)			1.35' length
			-67A		M	A	mod d rxn w/HCl, max part size = md sand 2 fn S, laminated, well sorted, cohesive, mod rxn w/HCl, 2.5Y5/4 (lt. olive brn)			
68.43- 69.98		s.s.	-69B		SM	x·B	S. fn-crs, v. poorly sorted, compact, msv, 2.5Y5/2 (grayish brn) mod. rxn w/HCl			Length ≈ 1.55 0.1' overlap w/ previous core
			-69A		M	A	S. mostly md-crs, laminated, well sorted, loose, max part. size = crs sand, 2.5Y5/2 (grayish brn) mod rxn w/HCl, silty fn sand bd w/0.5 cm thick heterogeneous coarse sand beds			

W = Wet, M = Moist, D = Dry

B-2.3

Pacific Northwest National Laboratory

DAILY BOREHOLE LOG

Boring/Well No __C3B31__   Depth __74.04-79.04__   Date __8-14-02__   Sheet __4 of 7__

Location __TX-107__   Project ___

Logged by __B N Bjornstad__

Reviewed by ___   Date ___

Lithologic Class. Scheme ___   Procedure ___   Rev ___

Steel Tape/E-Tape __/__   Field Indicator Equip. 1) ___   2) ___

Drilling Contractor ___

Driller ___

Rig/Method ___

Depth Control Point ___

DEPTH	TIME	SAMPLES		CONTAMINATION	MOIS-TURE	GRAPHIC LOG	LITHOLOGIC DESCRIPTION (particle size distribution, sorting, mineralogy, roundness, color, reaction to HCl, etc.)	H₂O ADDED	CASING	DRILLING COMMENTS (drilling rate, down time, blow counts, water level, drill fluid, etc.)
		TYPE	ID NUMBER	INSTR. READING		C Z S G				
74.04		S.S.	C3B31-74B		D		S, mostly fn-md, 2.5Y6/2 (lt brnish gray) loose to compacted. Well sorted, wk-mod rxn w/ HCl			Length = 1.26 Fractured Fm.
75.3			-74A		SM		~5cm silty fn sand bed, sharp upper contact. compact			
							Well laminated, 2.5Y6/4 (lt. yellowish brn), v. well sorted, med rxn w/ HCl			
76.73		S.S.	-77B		D		msv, poorly sorted sand, loose			Length = 1.25'
77.98							S, mostly fn-crs, mod-well sorted, laminated to compacted mod.			
			-77A		SM		rxn to HCl, multiple layers, ~lower half w/ in several layers of crs md and fine			
							sand, ~ md silty fn sand. mod rxn w/ HCl 2.5Y5/4 (lt olivebrn) to 2.5Y5/2 (grayish brn)			
77.76		S.S.	-78B		W		S, fn-crs mod-well sorted, 2.5Y4/2 (dk grayish brn), lower part laminated, upper part			Length = 1.3'
79.04			-78A		SM		slough?, mod rxn w/ HCl two grad strias between 2 fn sand to fn-md sand			

W = Wet, M = Moist, D = Dry

B-2.4

Pacific Northwest National Laboratory

DAILY BOREHOLE LOG

Boring/Well No _C3831_   Depth _85.05 - 89.75_   Date _8-14-02_

Location _TX-107_   Project _____   Sheet _5_ of _7_

Logged by _BN Bjornstad_

Reviewed by _____   Date _____

Lithologic Class. Scheme _____   Procedure _____   Rev _____

Steel Tape/E-Tape _____/_____   Field Indicator Equip. 1) _____   2) _____

Drilling Contractor _____
Driller _____
Rig/Method _____
Depth Control Point _____

DEPTH ( )	SAMPLES		CONTAMINATION		MOIS-TURE	GRAPHIC LOG				LITHOLOGIC DESCRIPTION (particle size distribution, sorting, mineralogy, roundness, color, reaction to HCl, etc.)	H₂O ADDED	CASING	DRILLING COMMENTS (drilling rate, down time, blow counts, water level, drill fluid, etc.)
	TIME	TYPE	ID NUMBER	INSTR. READING		C	Z	S	G				
85.05-		S.S.	C3831-85B		SM					S, mostly fn-md, laminated, mod-well sorted, 2.5Y4/2 (grayish brn) mod rxn w/HCl			Length = 1.25'
86.30			-85A		M→					Silt to silty sand at base B, liner, flame structure and ball and pillow type structure			
					SM					2.5Y5/4 (lt. olive brn) mod rxn w/HCl, laminated, silt is stiff and cohesive at base B liner. A liner consists of multiple thin gradations between fn sandy silt and fn sand and silt-fn sand mod-strng rxn w/HCl, mostly 2.5Y5/4 (lt. olive brn)			
88.3-		S.S.	-88B							S, fn-md, 2.5Y5/2 (grayish brn) mod-well sorted, loose			Length = 1.45'
89.75			-88A							msv mod rxn w/HCl, slightly finer toward bottom 5Y5/2 (olive gray)			

W = Wet, M = Moist, D = Dry

B-2.5

DAILY BOREHOLE LOG

Pacific Northwest National Laboratory

Boring/Well No: **C3831**
Location: **TX-107**
Depth: **93.05 - 101.65**
Date: **8-14-02 / 8-15-02**
Sheet **6** of **7**

Logged by: **B N Bjornstad**
Reviewed by: _____
Lithologic Class. Scheme: ____
Steel Tape/E-Tape: **1**
Field Indicator Equip. 1) ____ 2) ____

Procedure ____ Rev ____ Date ____

Drilling Contractor ____
Driller ____
Rig/Method ____
Project ____
Depth Control Point ____

DEPTH ( )	TIME	SAMPLES		CONTAMINATION		MOIS-TURE	GRAPHIC LOG C Z S G	LITHOLOGIC DESCRIPTION (particle size distribution, sorting, mineralogy, roundness, color, reaction to HCl, etc.)	H₂O ADDED	CASING	DRILLING COMMENTS (drilling rate, down time, blow counts, water level, drill fluid, etc.)
		TYPE	ID NUMBER	INSTR.	READING						
93.05-		S.S.	C3831-93B			SM		S, mostly fn-md 2.5Y6/2 (.lt. brinish gray) water past. loose (slough?) wkly laminated, mod. rxn w/ HCl. Well sorted, few small Froxide blebs at bottom			Length = 1.25'
94.3											X = sample location
97.14-		S.S.	1-97B			D SM		S, fn-md 2.5Y5/2 (grayish brn) mod rxn w/ HCl, mod-well sorted, loose to compacted, msv to wkly laminated. lower-half consists of fn-md sand (like above) inter-			Length = 1.25'
98.38			-97A								Hanford Fm.
100.2-		S.S.	-100B			SM		bedded with layers of silt to silty fn sand, well laminated, cohesive, mod rxn w/ HCl. S, 2.5Y5/2 (grayish brn) mostly fn-md, well sorted, mod-strong rxn w/ HCl, laminated.			Length = 1.95'
101.65			-100A								Hanford Fm.
								Silty fn sand beds, well laminated, mod-strong rxn w/ HCl 2.5Y5/4 (lt. ol br brn)			

W = Wet, M = Moist, D = Dry

1008/DCI/PROC/OBL/001

Pacific Northwest National Laboratory

DAILY BOREHOLE LOG

Boring/Well No _C3831_

Location _TX-107_

Depth _101.63 – 115.37_ Date _8-15-02_

Project _____

Logged by _B N Bjornstad_

Reviewed by _____

Lithologic Class. Scheme _____

Procedure _____ Rev _____ Date _____

Field Indicator Equip. 1) _____ 2) _____

Steel Tape/E-Tape _____

Drilling Contractor _____

Driller _____

Rig/Method _____

Depth Control Point _____

DEPTH ( )	TIME	SAMPLES TYPE	ID NUMBER	CONTAMINATION INSTR. READING	MOIS-TURE	GRAPHIC LOG C Z S G	LITHOLOGIC DESCRIPTION (particle size distribution, sorting, mineralogy, roundness, color, reaction to HCl, etc.)	H₂O ADDED	CASING	DRILLING COMMENTS (drilling rate, down time, blow counts, water level, drill fluid, etc.)
101.63-		S.S.	C3831-102B		SM		S mostly f grnd w/ couple thin lenses of silty fn sand, lower part laminated, strng rxn w/ HCl, 2.5Y6/2 (lt. brnish gray) well sorted			Length = 1.35'
102.98			-102A				2 fn sand wkly lam, somewhat cohesive, 1wk sorted 2.5Y8/4 (lt. yellowish brn.) strng rxn w/ HCl			Hanford Fm? or CCU silt?
114.12-		S.S.	-114B		SM		(g)zS, poorly sorted, mod. consolidated, few small pebbles (basaltic) and CaCO₃ nodules, poorly sorted, 55% rk md 0s. 35% silt 5% sm. pebbles 2.5Y6/4 (lt. yellowish brn) msv. to wkly lam. at base, strng rxn w/ HCl mod consolidated, fines amsmts matrix supported angular basalt fine pebbles abundant CaCO₃ nodules and stringers mottled with 2.5Y7/2 (lt sray) and 2.5Y6/2 (lt. brnish gray) v. strng rxn w/ HCl			Length = 1.25' Cold Creek Unit caliche
115.37			-114A							

W = Wet, M = Moist, D = Dry

B-2.7

Appendix B.3

C3832 (TX-104)

GEOLOGIC DESCRIPTION OF CORE OBTAINED

DURING OPENING IN LAB

Contents

Logged by __BN Bjornstad__   Sign

Reviewed by ____   Print   Sign   Date

Lithologic Class. Scheme ____   Procedure ____   Rev ____

Steel Tape/E-Tape __1__   Field Indicator Equip. 1) ____   2) ____

Drilling Contractor ____

Driller ____

Rig/Method ____

Depth Control Point ____

DEPTH ( )	SAMPLES		CONTAMINATION		MOIS-TURE	GRAPHIC LOG				LITHOLOGIC DESCRIPTION (particle size distribution, sorting, mineralogy, roundness, color, reaction to HCl, etc.)	H₂O ADDED	CASING	DRILLING COMMENTS (drilling rate, down time, blow counts, water level, drill fluid, etc.)
	TYPE	ID NUMBER	INSTR.	READING		C	Z	S	G				
16.21	SS	15 B			SM					zSG, wk rxn to HCl, 2.5Y4/2 dk grayish brn (moist), 60% G, 30% S, 10% Z, loose			Backfill to w/B'
17.61	SS	15 A ↓			SM					sand mostly fn-md grained, highly pulverized. Grains more fines toward top. unbroken clasts are subangular to subrounded v. poorly sorted			All colors are based on whatever moisture naturally present - no H₂O added!!
28.09	SS	28 B			SM					zSG, 50% G, 35% S, 15% Z, wk mud rxn w/HCl, 2.5Y4/2 dk grayish brn (moist) max. particle size = 4cm (fine pebble) unbroken clasts are subangular to subrounded loose, highly pulverized			
29.49	SS	28 A ↓			SM					v. poorly sorted. >75% Basalt			

W = Wet, M = Moist, D = Dry

B-3.1

DAILY BOREHOLE LOG

Pacific Northwest National Laboratory

Boring/Well No	C3832
Location	TX-104
Depth	36.09 - 52.58
Date	6-11-02
Project	TX-104 Vadose Zone
Sheet	2 of 10

Logged by: BN Bjornstad

Reviewed by: _____

Lithologic Class. Scheme: _____

Steel Tape/E-Tape: / _____

Field Indicator Equip. 1) _____ 2) _____

Procedure: _____ Rev: _____ Date: _____

Drilling Contractor: _____
Driller: _____
Rig/Method: _____
Depth Control Point: _____

DEPTH ( )	TIME	SAMPLES		MOIS-TURE	GRAPHIC LOG (C Z S G)	LITHOLOGIC DESCRIPTION (particle size distribution, sorting, mineralogy, roundness, color, reaction to HCl, etc.)	H₂O ADDED	CASING	DRILLING COMMENTS (drilling rate, down time, blow counts, water level, drill fluid, etc.)
		TYPE	ID NUMBER	CONTAMINATION INSTR. READING					
36.09		S.S.	37B →	SM	0.0 0.0 0.0	sG, 60% v.fn-fn pebble 30% mod-crs sand, 10% fn sand >75% basalt, v. poorly sorted, unconsolidated, 2.5y04/2 dk grayish brn, wk-mod rxn w/ HCl			Backfill material
37.49		S.S.	37A →	SM	0.0 0.0 0.0				
44.14		S.S.	44B →	W		sS, 50% sand, 50% silt sand= vf-f sand, v. little basalt v.crs sand strong rxn to HCl, 2.5y04/2 to 3/2, well sorted one v.fn rtzite sorted, friable, consolidated			Bottom of backfill?
45.54		S.S.	44A →	M					
51.18		S.S.	52B →	SM		S, 100% sand, wk horiz. lamination, mod-well sorted, 70% md sand, 10% crs 10% fn sand, wk/y consol. mod-stng rxn 2.5Y 6/2 lt brnish gray (SM) poorly sorted dk silty sand mixed w/ gravel (slough) in top half of 40pp liner			Hanford H2 Unit
52.58		S.S.	52A →	SM					

W = Wet, M = Moist, D = Dry

1998/DCL/PROC/DBL/001

DAILY BOREHOLE LOG

Boring/Well No __C3832__   Depth __53.08 - 61.52__   Date __6-11-02__

Location __TX-104__   Project __TX-104 Vadose Zone__   Sheet __3__ of __10__

Logged by __B N Bjornstad__

Reviewed by ____

Lithologic Class. Scheme ____

Steel Tape/E-Tape __/__

Procedure ____   Date ____   Rev ____

Field Indicator Equip. 1) ____   2) ____

Drilling Contractor ____

Driller ____

Rig/Method ____

Depth Control Point ____

DEPTH ( )	SAMPLES		CONTAMINATION		MOIS-TURE	GRAPHIC LOG				LITHOLOGIC DESCRIPTION (particle size distribution, sorting, mineralogy, roundness, color, reaction to HCl, etc.)	H₂O ADDED	CASING	DRILLING COMMENTS (drilling rate, down time, blow counts, water level, drill fluid, etc.)
	TIME	TYPE	ID NUMBER	INSTR	READING		C	Z	S	G				
53.08		s.s.	53 B			SM					S, sand, 60% med, 30% crs, 10% fn, 2.5Y5/2, mod rxn w/ HCl wk horiz lam, mod sorted			
			↓			M					↑25 2 fn sand, mod. sorted, mod calc. 2.5Y4/4 olive brn			Samples taken @ finer material for geochem
54.43		s.s.	53 A			SM					Md-crs sand, mod. sorted, mod-strg rxn w/ HCl similar to 52.5 to 53.0 ft sample			
			↓								broken pebble @ 53.6' 5cm diameter			
60.12		s.s.	61 B			SM					S, 100 % sand, 50% md, sand, 40% crs sand, 10% fn sand, wk horiz lam.			
			↓								~30% basalt 2.5Y5/2			
61.52		s.s.	61 A			SM					grayish brn., wk-mod rxn w/ HCl, mod. sorted laminar structure toward top probably drilling induced			

W = Wet, M = Moist, D = Dry

1998/DCL/PROC/DBL/001

Pacific Northwest National Laboratory

DAILY BOREHOLE LOG

Boring/Well No **C3832**   Location **TX-104**

Depth **61.76 - 70.31**   Date **6-11-02**

Project **TX-104 Vadose Zone**

Sheet **4** of **10**

Logged by **B N Bjornstad**

Reviewed by _____ Date _____ Rev _____

Lithologic Class. Scheme _____ Procedure _____

Steel Tape/E-Tape ____1____   Field Indicator Equip. 1) ____ 2) ____

Drilling Contractor _____

Driller _____

Rig/Method _____

Depth Control Point _____

DEPTH	TIME	SAMPLES TYPE	ID NUMBER	CONTAMINATION INSTR. READING	MOIS-TURE	GRAPHIC LOG C/Z/S/G	LITHOLOGIC DESCRIPTION (particle size distribution, sorting, mineralogy, roundness, color, reaction to HCl, etc.)	H₂O ADDED	CASING	DRILLING COMMENTS (drilling rate, down time, blow counts, water level, drill fluid, etc.)
61.76		SS	62 B		M		S, 100% sand, 50% crs sand, 46% med, 10% fn sand, loose, mod. sorted			sharp contact @ 62.4' between 2 Sand S
63.36		SS	62 A		SM		30-40% basalt, 2.5Y5/2, grayish brn, HK-mod, rxn b/ HCl max flat size 20mm = v.crs sand			
							2S, silt fn sand, well laminated, 2.5Y4/4 olive brn, mod-strng rxn w/ HCl, compact, well sorted, max flat size = fn sand, 50% silt, 50% fn-vfn sand			
68.01		SS	68 B		SM		S, 70% md sand, 20% crs sand, 10% fn sand, horiz. lam., mod. sorted, 10YR6/2 lt brnish gray, max ped. size = crs sand, mod-strng rxn w/ HCl			
70.31		SS	68 A		M		2S, silt fn sand, v. well laminated, compact, well sorted, organics or Mn oxide staining, 10% silt, 90% sand, mod rxn w/ HCl, 2.5Y5/4 lt olive brn.			

W = Wet, M = Moist, D = Dry

B-3.4

Pacific Northwest National Laboratory

DAILY BOREHOLE LOG

Boring/Well No __C3832__   Depth __75.99-80.31__   Date __6-11-02__

Location __TX-104__   Project __TX-104 Vadose Zone__

Logged by __BN Bjornstad__

Reviewed by ____   Date ____   Rev ____

Lithologic Class. Scheme ____   Procedure ____

Steel Tape/E-Tape __/__   Field Indicator Equip. 1) ____   2) ____

Drilling Contractor ____

Driller ____

Rig/Method ____

Depth Control Point ____

DEPTH	TIME	SAMPLES TYPE	ID NUMBER	CONTAMINATION INSTR. READING	MOIS-TURE	GRAPHIC LOG	LITHOLOGIC DESCRIPTION (particle size distribution, sorting, mineralogy, roundness, color, reaction to HCl, etc.)	H₂O ADDED	CASING	DRILLING COMMENTS (drilling rate, down time, blow counts, water level, drill fluid, etc.)
75.99		S.S.	76B				S, 80% md, 10% crs, 10% fn, hor. lam., decomposed organic matter at top. Single pebble. Max part size = 4 cm, strg brxn w/ H= 2.5Y5/2			
		S.S.	76A		M		c=S, silt, fn sand, 80% fn sand 20% silt, well lam., compact			
77.39					SM		Mod-strg rxn w/ HCl, 2.5Y5/4 lt olive brn, max part size = fn sand			
							S 60% crs 40% mud sorted, loose, 30-40% basalt wk-mod rxn w/ HCl, max part size = v. crs. sand			
78.29		S.S.	79B		M		S2 fine sandy silt, 1" thick strng rxn w/ HCl, 2.5Y5/2 grayish brn			
80.31		S.S.	79A		M		S grades from mostly md-crs sand at base to fn sand then coarse again. Well laminated, 2.5Y5/4 lt olive brn (moist) above to 2.5Y5/2 lt brnish gray below, crs sand = mod rxn w/ HCl, fn sand = mud- strng rxn. max part size = crs sand, mod. sorted			Grades sand from finer material

W = Wet, M = Moist, D = Dry

1998/DCL/PROC/DBL001

DAILY BOREHOLE LOG

Depth 82.99–88.41   Date 6-12-02   Sheet 6 of 10

Boring/Well No C2832   Project TX-104 Vadose Zone

Location TX-104

Logged by B N Bjornstad (Sign)

Reviewed by _____ (Print) _____ (Sign)   Date _____

Lithologic Class. Scheme _____   Procedure _____   Rev _____

Steel Tape/E-Tape _____   Field Indicator Equip. 1) _____ 2) _____

Drilling Contractor _____
Driller _____
Rig/Method _____
Depth Control Point _____

DRILLING COMMENTS
(drilling rate, down time, blow counts, water level, drill fluid, etc.)

DEPTH ( )	TIME	SAMPLES TYPE	ID NUMBER	CONTAMINATION INSTR. READING	MOIS-TURE	GRAPHIC LOG C Z S G	LITHOLOGIC DESCRIPTION (particle size distribution, sorting, mineralogy, roundness, color, reaction to HCl, etc.)	H₂O ADDED	CASING	DRILLING COMMENTS
82.99		s.s.	83B		SM		S, 60% crs, 40% md, laminated, mod rxn w/ HCl, 2.5Y 6/2. It brnish gray, max part size = crs sand, mod. to poorly sorted. Interlam. sand to silty sand. 2.5Y 5/4 to 2.5Y 5/2, d max part size = md sand, well laminated, beds 1–5 cm thick			Sample from this depth
		s.s.	83A		M		zS silty fn sand, 40% silt, 60% fn sand, compact, reddish (oxidized) 2.5Y 5/4. It olive brn, strog rxn w/ HCl. Well sorted			
84.34										
86.99		s.s.	87B		M		S, 50% crs, 50% md, mod sorted, 2.5Y 5/2 grayish brn, 2 fn sand, bed of very laminated, max part size = crs sand. zS lam., 2.5Y 4/4 olive brn, poorly sorted lam.			X = Sample interval fn fr geochem ↓
		s.s.	87A		SM		Sand, 60% crs, 40% md, laminated, wk rxn w/ HCl 2.5Y 5/2 grayish brn. Single lamina of v.fn. pebbles mod. sorted, max part size = v.fn pebble			X = Sample interval fn fr geochem
88.41										

W = Wet, M = Moist, D = Dry

1998/DCL/PROC/DBL001

DAILY BOREHOLE LOG

Pacific Northwest National Laboratory

Depth 92.99-97.04   Date 6-12-02

Boring/Well No C3832   Project TX-104 Vadose Zone

Location TX-104

Logged by BN Bjornstad

Reviewed by _____ Date _____

Lithologic Class. Scheme _____ Procedure _____ Rev _____

Steel Tape/E-Tape ___1___   Field Indicator Equip. 1) ___ 2) ___

Drilling Contractor _____

Driller _____

Rig/Method _____

Depth Control Point _____

DEPTH ( )	TIME	SAMPLES		CONTAMINATION INSTR. READING	MOIS-TURE	GRAPHIC LOG (C Z S G)	LITHOLOGIC DESCRIPTION (particle size distribution, sorting, mineralogy, roundness, color, reaction to HCl, etc.)	H₂O ADDED	CASING	DRILLING COMMENTS (drilling rate, down time, blow counts, water level, drill fluid, etc.)
		TYPE	ID NUMBER							
92.99		S.S.	93B		D	slough	loose, powdery, dry sand = slough?			
					SM		zS, hard, compact, more moist, poorly sorted			mod rxn w/ HCl, 2.5Y5/2, grayish brn
		S.S.	93A		D		S, 50% crs 50% md, mod.			
94.40					SM		sorted, well laminated (horiz.), max part. size = crs sand, 2.5Y5/2 grayish brn, vk rxn w/ HCl			
95.04		S.S.	96B							
					SM		S, 70% crs-v.crs sand, 30% md sand, loose, 40-50% basalt, max part. size = v. crs sand, mod. sorted, mod. rxn w/ HCl, 2.5Y 4/2, dk grayish brn			
97.04		S.S.	96A							

W = Wet, M = Moist, D = Dry

Pacific Northwest National Laboratory

DAILY BOREHOLE LOG

Boring/Well No __C3832__   Depth __95.64-105.36__ Date __6-12-02__

Location __TX-104__   Project __TX-104 Vadose Zone__   Sheet __8__ of __10__

Logged by __B N Bjornstad__

Reviewed by ____   Print ____ Sign ____   Date ____

Lithologic Class. Scheme ____   Procedure ____   Rev ____

Steel Tape/E-Tape __1__   Field Indicator Equip. 1) ____ 2) ____

Drilling Contractor ____
Driller ____
Rig/Method ____
Depth Control Point ____

DEPTH ( )	TIME	SAMPLES TYPE	SAMPLES ID NUMBER	CONTAMINATION INSTR. READING	MOIS-TURE	GRAPHIC LOG C Z S G	LITHOLOGIC DESCRIPTION (particle size distribution, sorting, mineralogy, roundness, color, reaction to HCl, etc.)	H₂O ADDED	CASING	DRILLING COMMENTS (drilling rate, down time, blow counts, water level, drill fluid, etc.)
95.64		S.S.	96B							
		S.S.	96A		SM		2 S and S interbedded sand beds = 30% crs 70% m-g sand. Wavier laminations. Mod-well sorted. 2.5Y5/2 grayish brn. Max part size = crs sand. Mod rxn w/ HCl			Hanford formation H2 Unit
97.04							silt fn sand beds are 20% silt 80% fn-v.fn sand, compact 2.5Y5/2 grayish brn, decomposed plant remains in clod ~3 cm long at top of core liner in 2 fn sand			
							~mottled w/ fn sandy silt			
103.94		S.S.	104B		D SM		2 S, silty fn-v.fn sand well sorted. Massive to wkly mottled. yellowish 80% fn-v.fn sand 20% silt 2.5Y6/4 lt. yellowish brn, mod-strg rxn w/ HCl, compact, 1cm thick silt lens and laminated towards top, dry poorly sorted slough at v. top			Cold Creek Unit silt 104B liner only 3/4 full
105.36		S.S.	104A							

W = Wet, M = Moist, D = Dry

1998/DCL/PROC/DBL001

DAILY BOREHOLE LOG

Pacific Northwest National Laboratory

Boring/Well No __TX-104__   Depth __109.91-115.2__ Date __6-12-02__

Location __TX-104__   Project __TX-104 Vadose Zone__

Logged by __BN Bjornstad__

Reviewed by _____

Lithologic Class. Scheme _____   Procedure _____ Date _____ Rev _____

Steel Tape/E-Tape __1__   Field Indicator Equip. 1) _____ 2) _____

__C3832__

Drilling Contractor _____

Driller _____

Rig/Method _____

Depth Control Point _____

DEPTH	SAMPLES			CONTAMINATION	MOIS-TURE	GRAPHIC LOG				LITHOLOGIC DESCRIPTION (particle size distribution, sorting, mineralogy, roundness, color, reaction to HCl, etc.)	H₂O ADDED	CASING	DRILLING COMMENTS (drilling rate, down time, blow counts, water level, drill fluid, etc.)
	TIME	TYPE	ID NUMBER	INSTR. READING		C	Z	S	G				
109.91		S.S.	110 B		SM					2S, silty fu sand, 60% fn-vf sand 40% silt, compact, horiz laminations, well sorted			Cold Creek Silt
		S.S.	110 A							2.5Y4/4 olive brown, strng rxn w/ HCl			contact @ 110.4' = sharp
110.4										(g)mS, slightly pebbly, clayey silty sand, v. poorly sorted. compact and cemented with CaCO₃. 5% v. fn pebble = max pbl. size, carbonate nodules abundant, pebbles mostly well rounded and highly weathered/altered 2.5Y4/4 olt. how/old salt, yellowish brn, violent rxn w/ HCl			Cold Creek caliche
111.30													
113.77		S.S.	114 B		SM					gsM, pebbly sandy mud, 10% pebbles, 40% sand, 50% silt + clay, mottled to massive, v. compact and cemented with CaCO₃, v. poorly sorted, 10YR6/3 pale brn, mottled to			Cold Creek caliche highly cemented - extruder doesn't work - have to bang out with hammer
115.2		S.S.	114 A		SM								

W = Wet, M = Moist, D = Dry Some secondary porosity, locally

1998/DCL/PROC/DBL001

B-3.9

Pacific Northwest National Laboratory

DAILY BOREHOLE LOG

Boring/Well No **C3832**
Location **TX-104**

Depth **114.47 - 115.89** Date **6-12-02**
Project **TX-104 Vadose Zone**

Logged by **BN Bjernstad** _Sign_
Reviewed by _____ _Sign_ _Print_ _____ Date _____
Lithologic Class. Scheme _____ Procedure _____ Rev _____
Steel Tape/E-Tape _____ Field Indicator Equip. 1) _____ 2) _____

Drilling Contractor _____
Driller _____
Rig/Method _____
Depth Control Point _____

DEPTH	TIME	SAMPLES			CONTAMINATION		MOIS-TURE	GRAPHIC LOG				LITHOLOGIC DESCRIPTION (particle size distribution, sorting, mineralogy, roundness, color, reaction to HCl, etc.)	H₂O ADDED	CASING	DRILLING COMMENTS (drilling rate, down time, blow counts, water level, drill fluid, etc.)
		TYPE	ID NUMBER		INSTR	READING		C	Z	S	G				
114.47		s.s.	121 B				SM					Same as 114 A & B			Liners stuck in core barrel - have to bang out /pry sample from core barrel
		s.s.	121 A									White and olive bedding/swirling laminations, more clay/silt at base of this core 10 YR 6/2 14. brownish gray strong rxn w/HCl			
115.89															

Distribution

No. of
Copies

No. of
Copies

44 OFFSITE

Steve Airhart
Freestone Environmental Services
1933 Jadwin Ave.
Suite 135
Richland, WA 99352

Dr. Harry Babad
2540 Cordoba Court
Richland, WA 99352-1609

Pat Brady
Geochemistry Department, 6118
Sandia National Laboratories
P.O. Box 5800
Albuquerque, New Mexico 87185-0750

Charles R. Bryan
Sandia National Laboratories
4100 National Parks Highway
Carlsbad, N.M. 88220

Susan Carroll
Lawrence Livermore National Laboratory
Mail Stop L-219
Livermore, CA 94550

John N. Christensen
Center for Isotope Geochemistry
Lawrence Berkeley National Laboratory
1 Cyclotron Road Bldg, Mail Stop 70A4418
Berkeley, CA 94720-8179

Jon Chorover
Associate Professor – Environmental
  Chemistry
Department of Soil, Water and
  Environmental Science
Shantz 429, Building #38
University of Arizona
Tucson, AZ 85721-0038

Dave G. Coles
Coles Environmental Consulting
750 South Rosemont Rd
West Linn, OR 97068

Mark Conrad
Department of Earth and Planetary Sciences
University of California Berkeley
Berkeley, CA 94720

Dr. James A. Davis
U.S. Geological Survey
MS-465
345 Middlefield Rd.
Menlo Park, CA 94025

Donald J. DePaolo
Geology & Geophysics Dept., MC4767
University of California
Berkeley, CA 94720-4767

Dirk A. Dunning
Oregon Office of Energy
625 Mariona St. N. E.
Salem, OR 97301-3742

Mark Ewanic
MSE Technology Applications, Inc.
200 Technology Way
Butte, MT 59701

Markus Flury
Department of Crop and Soil Sciences
Washington State University
Pullman, WA 99164

Amy P. Gamerdinger
2122 E. Hawthorne
Tucson, AZ 85719

No. of
Copies

Jim Harsh
Department of Crop & Soil Sciences
Washington State University
Johnson Hall - Room 249
Pullman WA 99164-6420

Victoria Johnson
Kennedy/Jenks Consultants, Inc.
1020 N. Center Parkway, Suite F
Kennewick, WA 99336

Dr. Cliff Johnston
Soil Chemistry and Mineralogy
1150 Lily Hall
Purdue University
West Lafayette, IN 47907-1150

Dr. Daniel I. Kaplan
Westinghouse Savannah River Company
Bldg. 774-43A, Rm 215
Aiken, SC 29808

Dr. Peter C. Lichtner
Los Alamos Natl. Lab
P.O. Box 1663
Los Alamos, NM 87545

Kevin A. Lindsey
Kennedy / Jenks Consultants, Inc.
1020 N. Center Parkway, Suite F
Kennewick, WA 99336

Patrick Longmire
Los Alamos National Laboratory
Mail Stop J534
P.O. Box 1663
Los Alamos, NM 87545

Kate Maher
The Center for Isotope Geochemistry
301 McCone Hall
University of California, Berkeley
Berkeley, CA 94702-4746

John M. Matuszek
82 McGuffey Lane
Delmar, NY 12054

Melanie A. Mayes
Environmental Sciences Division
Oak Ridge National Laboratory
P.O. Box 2008
[*Bethel Valley Road for FedEX/UPS
  delivery*]
Oak Ridge, TN 37831-6038

Jean Moran
Isotopic Tracers and Transport Group
Analytical and Nuclear Chemistry Division
Lawrence Livermore National Laboratory
L-231, P.O. Box 808
Livermore, CA 94550

Dr. Kathryn L. Nagy
Department of Earth and Environmental
  Sciences
University of Illinois at Chicago (MC-186)
845 West Taylor Street
Chicago, IL 60607-7059

Heino Nitsche
Director, Center for Advanced
  Environmental and Nuclear Studies
Lawrence Berkeley National Laboratory
1 Cyclotron Road
MS 70A-1150
Berkeley, CA 94720

Phil Reed
U.S. Nuclear Regulatory Commission
Office of Nuclear Regulatory Research
Division of Systems Analysis and
  Regulatory Effectiveness
Radiation Protection, Env. Risk and Waste
  Management Branch
Mail Stop: T9-F31
Washington, DC 20555-0001

No. of
Copies

No. of
Copies

Richard J. Reeder
Dept. of Geosciences
State University of New York at
  Stony Brook
Stony Brook, NY 11794-2100

Al Robinson
68705, E 715 PRNE
Richland WA, 99352

Phil Rogers
13 Mountain Oak
Littleton, CO 80127

Sherry D. Samson
Research Assistant Professor
Department of Earth and
  Environmental Sciences
University of Illinois at Chicago (MC186)
845 W. Taylor St.
Chicago, IL 60607-7059

Dawn A. Shaughnessy
Glenn T. Seaborg Center
Lawrence Berkeley National Laboratory
1 Cyclotron Road
MS 70A-1150
Berkeley, CA 94720

Doug Sherwood
Rivers Edge Environmental
1616 Riverside Drive
West Richland, WA 99353

David K. Shuh
Lawrence Berkeley National Lab
1 Cyclotron Road
Mail Stop 70A-1150
Berkeley, CA 94720

James "Buck" Sisson
Idaho National Engineering and
Environmental Laboratory
P.O. Box 1625, MS-2107
Idaho Falls, ID 83415-2107

Robert W. Smith, Ph.D.
Professor of Subsurface Science
Adjunct Professor of Geological Sciences
University of Idaho at Idaho Falls
1776 Science Center Drive
Idaho Falls, ID 83402

Stan Sobczyk
242 N. Laurel St.
Genesee, ID 83832-9760

Carl I. Steefel
Earth Sciences Division
Lawrence Berkeley National Laboratory
1 Cyclotron Road, Mail Stop 90R1116
Berkeley, CA 94720

Dr. Samuel J. Traina, Director
Sierra Nevada Research Institute
University of California, Merced
P.O. Box 2039
Merced, CA 95344

Dr. T. T. Chuck Vandergraaf
P.O. Box 857
Pinawa, Manitoba ROE 1LO
Canada

Dr. Jiamin Wan
Lawrence Berkeley National Laboratory
1 Cyclotron Rd. MS 70-0127A
Berkeley, CA 94720

Mr. Ronald G. Wilhelm
Office of Radiation and Indoor Air
401 M Street, S.W.,
Mail Code 6603J
Washington, D.C. 20460

W. Alexander Williams
U.S. Department of Energy
Office of Environmental Restoration
EM-33
19901 Germantown Road
Germantown, MD 20874-1290

No. of
Copies

ONSITE

4 **DOE Office of River Protection**

P. E. LaMont	H6-60
R. W. Lober	H6-60
S. A. Wiegman	H6-60
R. B. Yasek	H6-60

8 **DOE Richland Operations Office**

B. L. Foley	A6-38
J. P. Hanson	A5-13
R. D. Hildebrand	A6-38
K. A. Kapsi	A5-13
J. G. Morse	A6-38
K. M. Thompson	A6-38
DOE Public Reading Room (2)	H2-53

Bechtel Hanford, Inc.

K. R. Fecht	H0-02

22 **CH2M HILL Hanford Group, Inc.**

A. Amonette	
Technical Writer's Ink	E6-35
F. J. Anderson	E6-35
R. Calmus	H6-05
M. P. Connelly	E6-35
J.G. Field	H6-62
T. E. Jones (2)	E6-35
A. J. Knepp	H6-60
S. L. Lambert	
Lambert Engineering	E6-35
J. E. Laurenz	H6-62
F. M. Mann (5)	E6-35
W. J. McMahon	E6-35
C. W. Miller	H6-35
D. A. Myers (3)	E6-35
G. Parsons	H6-19
T. L. Sams	H6-05

No. of
Copies

3 **Duratek Federal Services, Inc.,**
Northwest Operations

M. G. Gardner	H1-11
K. D. Reynolds	H1-11
D. E. Skoglie	H1-11

2 **Environmental Protection Agency**

N. Ceto	B5-01
D. A. Faulk	B5-01

2 **Fluor Federal Services**

R. Khaleel	E6-17
R. J. Puigh	E6-17

6 **Fluor Hanford, Inc.**

M. W. Benecke	E6-35
T. W. Fogwell	E6-35
B. H. Ford	E6-35
J. G. Hogan	H1-11
V. G. Johnson	E6-35
M. I. Wood	H8-44

72 **Pacific Northwest National Laboratory**

S. R. Baum	P7-22
B. N. Bjornstad (3)	K6-81
T. M. Brouns	K9-69
C. F. Brown	P7-22
R. W. Bryce	E6-35
K. J. Cantrell	K6-81
R.. E. Clayton	P7-22
W. J. Deutsch	K6-81
P. E. Dresel	K6-96
K. M. Geisler	P7-22
M. J. Fayer	K9-33
A. R. Felmy	K8-96
V. L. Freedman	K9-36
M. D. Freshley	K9-33
J. S. Fruchter	K6-96
G. W. Gee	K9-33
D. G. Horton (3)	K6-81

No. of **Copies**		**No. of** **Copies**	
J. P. Icenhour	K6-81	M. Valenta	P7-22
C. T. Kincaid	E6-35	T. S. Vickerman	P7-22
K. M. Krupka	K6-81	A. L. Ward	K9-33
I. V. Kutnyakov	P7-22	B. A. Williams	K6-81
G. V. Last (2)	K6-81	S. B. Yabusaki	K9-36
V. L. LeGore	P7-22	J. M. Zachara	K8-96
M. J. Lindberg	P7-22	F. Zhang	K9-33
C. W. Lindenmeier (2)	P7-22	Information Release Office (2)	
W. J. Martin	K6-81		
S. V. Mattigod	K6-81	**S.M. Stoller**	
B. P. McGrail	K6-81		
P. D. Meyer	BPO	R. G. McCain	B2-62
C. J. Murray	K6-81		
S. M. Narbutovskih	K6-96	6 **Washington State Department of Ecology**	
R. D. Orr	K6-81		
E. M. Pierce	K6-81	S. Dahl-Crumpler	HO-57
Nik Qafoku	K3-61	J. A. Caggiano	HO-57
S. P. Reidel	K6-81	F. Hodges	HO-57
R. J. Serne (20)	P7-22	A. D. Huckaby	HO-57
H. T. Schaef	K6-81	B. Rochette	HO-57
W. Um	P7-22	J. Yokel	HO-57